LA-3556 REVISED

LOS ALAMOS SCIENTIFIC LABORATORY
of the
University of California
LOS ALAMOS • NEW MEXICO

Ultra High Temperature Reactor Experiment (UHTREX) Facility Description and Safety Analysis Report

UNITED STATES
ATOMIC ENERGY COMMISSION
CONTRACT W-7405-ENG. 36

This report expresses the opinions of the author or authors and does not necessarily reflect the opinions or views of the Los Alamos Scientific Laboratory.

Printed in the United States of America. Available from
Clearinghouse for Federal Scientific and Technical Information
National Bureau of Standards, U. S. Department of Commerce
Springfield, Virginia 22151
Price: Printed Copy $3.00; Microfiche $0.65

DISCLAIMER

LA-3556 Revised
UC-80, REACTOR
TECHNOLOGY
TID-4500

LOS ALAMOS SCIENTIFIC LABORATORY
of the
University of California
LOS ALAMOS • NEW MEXICO

Report written: September 1966
Report revised: February 1967
Revision distributed: April 1967

Ultra High Temperature Reactor Experiment (UHTREX) Facility Description and Safety Analysis Report

Prepared by

K Division

Work done by

CMB, GMX, H, J, K, T, and W Divisions
and the Engineering Department

ABSTRACT

Intended to advance the technology of gas cooled reactors, the Ultra High Temperature Reactor Experiment (UHTREX) is designed for the operation of a graphite-moderated, helium-cooled reactor at a thermal power of 3 MW and a maximum gas temperature of 2400°F. The small graphite fuel elements containing enriched uranium operate in direct contact with the coolant and can be loaded or unloaded while the reactor is operating.

The UHTREX facility design and operating plans are described. From analyses of postulated accidents and evaluation of safety features, it is concluded that the UHTREX facility can be safely operated.

CONTENTS

	Page
ABSTRACT	3
1. INTRODUCTION AND SUMMARY	1-1
1.1 Principal Design Features	1-1
1.1.1 Site	1-1
1.1.2 Reactor	1-2
1.1.3 Fuel	1-2
1.1.4 Coolant System	1-3
1.1.5 Instrumentation and Control	1-4
1.1.6 Radioactivity Control	1-4
1.1.7 Utility Systems	1-5
1.2 Design Characteristics	1-5
1.3 Design Research and Development Programs	1-10
1.3.1 Reactor Components	1-10
1.3.2 Coolant System Components	1-12
1.3.3 Auxiliary System Components	1-12
1.3.4 Instrumentation and Control Components	1-13
1.4 Identification of Contractors	1-13
1.5 General Conclusions	1-14
2. SITE	2-1
2.1 Location	2-1
2.2 Layout	2-1
2.3 Population	2-9

CONTENTS (continued)

		Page
2.4	Meteorology	2-10
2.4.1	Winds	2-10
2.4.2	Inversions	2-10
2.4.3	Precipitation and Temperature	2-12
2.5	Hydrology and Geology	2-12
2.6	Seismicity	2-13
3.	FACILITY	3-1
3.1	Secondary Containment	3-1
3.1.1	Reactor and Recuperator Room	3-8
3.1.2	Helium Purification and Storage Rooms	3-8
3.1.3	Fuel Discharge Room	3-9
3.2	Operating and Control Areas	3-9
3.2.1	Fuel Transfer Cell and Lock	3-10
3.2.2	Remote Maintenance Corridor	3-11
4.	REACTOR	4-1
4.1	Mechanical Design	4-1
4.1.1	General Description	4-1
4.1.2	Pressure Vessel	4-4
4.1.3	Reactor Structure	4-12
4.1.4	Fuel Elements	4-27
4.1.5	Fuel Loader	4-30
4.1.6	Core Indexing Mechanism	4-34
4.1.7	Control Rod System	4-37
4.2	Nuclear Design	4-48
4.2.1	Nuclear Characteristics of Design	4-48
4.2.2	Nuclear Design Analysis	4-57
4.3	Thermal Design	4-75
4.3.1	Temperature Distribution Analyses	4-76
4.3.2	Coolant Flow Analyses	4-83

CONTENTS (continued)

		Page
5.	COOLANT SYSTEM	5-1
	5.1 Design Description	5-1
	5.1.1 Primary Coolant Loop	5-1
	5.1.2 Secondary Coolant Loop	5-27
	5.2 Design Analyses	5-32
	5.2.1 Reactor and Coolant System Dynamics Studies	5-32
	5.2.2 Piping Stress Analysis	5-54
	5.3 Testing	5-55
6.	FUEL HANDLING SYSTEM	6-1
	6.1 General Description	6-1
	6.1.1 New Fuel Introduction	6-2
	6.1.2 Loading Sequence	6-5
	6.1.3 Spent Fuel Removal from Drybox	6-8
	6.2 Design Details	6-9
	6.2.1 Cell Operating Area	6-9
	6.2.2 Fuel Transfer Lock	6-10
	6.2.3 Fuel Transfer Cell	6-10
	6.2.4 Drybox	6-11
	6.2.5 Secondary Gas Locks	6-12
	6.2.6 Conveyors	6-13
	6.2.7 Primary Gas Locks	6-14
	6.2.8 Primary Gas Lock Pressure Regulation System	6-17
	6.3 Control and Instrumentation	6-18
	6.3.1 Computer Functions	6-18
	6.4 System Design Analysis	6-19
	6.4.1 Primary Gas Locks	6-19
	6.4.2 Conveyors	6-22
	6.5 Testing	6-22

CONTENTS (continued)

		Page
7.	GAS CLEANUP SYSTEM	7-1
	7.1 General Description	7-1
	7.2 Design Details	7-4
	7.2.1 Filter	7-4
	7.2.2 Preheater	7-4
	7.2.3 Copper Oxide Bed	7-5
	7.2.4 Water-Cooled Heat Exchanger	7-7
	7.2.5 Decay Heat Exchanger	7-7
	7.2.6 Molecular Sieve Beds	7-8
	7.2.7 Glycol-Cooled Heat Exchanger	7-9
	7.2.8 Delay Beds	7-10
	7.2.9 Sidestream Adsorption Beds	7-11
	7.2.10 Blower Preheater	7-12
	7.2.11 Cleanup System Blower	7-12
	7.2.12 Auxiliary Systems	7-13
	7.3 Maintenance of Components	7-15
	7.4 Instrumentation and Control	7-17
	7.4.1 Analytical Instruments	7-17
	7.4.2 Radioactivity Instruments	7-21
	7.5 System Design Analysis	7-21
	7.6 Testing	7-23
8.	HELIUM STORAGE AND PRESSURE REGULATION SYSTEM	8-1
	8.1 General Description	8-1
	8.2 Design Details	8-2
	8.2.1 Low Pressure System	8-2
	8.2.2 High Pressure System	8-4
	8.2.3 Jacking Gas Systems	8-5
	8.3 Pressure Regulation Systems	8-6
	8.3.1 Primary Loop	8-6

CONTENTS (continued)

	Page
8.3.2 Secondary Loop	8-8
8.4 Design Analysis	8-8
9. CONTAINMENT	9-1
9.1 Structure Design	9-1
9.2 Penetrations	9-2
9.3 Secondary Containment Ventilation	9-6
9.4 Design Pressure Calculations	9-11
9.5 Testing	9-11
10. EMERGENCY ELECTRICAL SYSTEM	10-1
10.1 General Description	10-1
10.2 Design Details	10-3
10.2.1 Distribution System	10-3
10.2.2 Diesel Power Supply	10-4
10.2.3 Battery-Driven Power Supply	10-5
10.3 Tests and Inspections	10-6
11. INSTRUMENTATION AND CONTROL	11-1
11.1 General	11-1
11.1.1 Control Room	11-1
11.1.2 Instrumentation and Measurements	11-7
11.1.3 On-Line Process Computer	11-17
11.2 Reactor	11-25
11.2.1 Nuclear Instrumentation	11-25
11.2.2 Rod Drive Control Systems	11-32
11.3 Coolant System Controls	11-37
11.3.1 Coolant Blowers	11-37
11.3.2 Recuperator Bypass Valve	11-39
11.3.3 Secondary Loop Isolation Valves	11-40
11.3.4 Heat Dump	11-41

CONTENTS (continued)

		Page
11.4	Safety Systems	11-42
11.4.1	Primary Loop Loss of Coolant Emergency System	11-43
11.4.2	Secondary Loop Loss of Coolant Emergency System	11-46
11.4.3	Primary Loop Coolant Flow Monitor	11-46
11.4.4	Secondary Loop Coolant Flow Monitor	11-47
11.4.5	Reactor Inlet Pipe Temperature Monitor	11-47
11.4.6	Heat Exchanger Tube Temperature Monitor	11-48
11.4.7	Primary Loop Pressure Relief System	11-48
11.4.8	Secondary Loop Pressure Relief System	11-48
11.4.9	Secondary Loop Radiation Contamination Detection System	11-49
11.4.10	Heat Dump Air Flow Monitor	11-49
11.4.11	Annunciator System	11-49
11.5	Communications Systems	11-50
11.5.1	Telephones	11-50
11.5.2	Paging System	11-50
11.5.3	Audio Intercommunication System	11-50
11.5.4	Emergency Alarm System	11-50
11.5.5	Closed Circuit Television	11-51
12.	AUXILIARY SYSTEMS	12-1
12.1	Gas Sampling System	12-1
12.2	Cooling Water Systems	12-2
12.2.1	General Description	12-2
12.2.2	Design Details	12-4
12.2.3	Instrumentation	12-8
12.2.4	Design Analysis	12-8
12.2.5	Tests and Inspections	12-9

CONTENTS (continued)

		Page
12.3	Facility Ventilation Systems	12-9
	12.3.1 General Description	12-9
	12.3.2 Design Details	12-11
	12.3.3 Instrumentation	12-13
	12.3.4 Design Analysis	12-13
	12.3.5 Tests and Inspections	12-14
12.4	Compressed Air Systems	12-14
	12.4.1 General Description	12-14
	12.4.2 Design Details	12-14
	12.4.3 Design Analysis	12-15
	12.4.4 Tests and Inspections	12-15
12.5	Door Seal Vacuum System	12-15
	12.5.1 General Description	12-15
	12.5.2 Design Details	12-16
12.6	Contaminated Liquid Waste System	12-16
	12.6.1 General Description	12-16
	12.6.2 Design Analysis	12-17
12.7	Facility Service Systems	12-17
	12.7.1 Vacuum Cleaning System	12-17
	12.7.2 Breathing Air System	12-18
	12.7.3 Air Sampling System	12-18
13.	RADIOACTIVITY CONTROL	13-1
13.1	Fuel Handling	13-1
	13.1.1 New Fuel	13-1
	13.1.2 Spent Fuel	13-2
13.2	Liquid Wastes	13-3
13.3	Gaseous Wastes	13-3
	13.3.1 Dilution Factors for Stack Release	13-3

CONTENTS (continued)

		Page
13.3.2	Source Intensities	13-5
13.3.3	Gas Cleanup System Vent Gas	13-8
13.4	Primary Shielding	13-11
13.4.1	Reactor and Gas Cleanup Rooms	13-11
13.4.2	Other Areas Inside the Secondary Containment	13-13
13.4.3	Fuel Transfer Cell and Lock	13-14
13.4.4	Shielding Materials	13-14
13.4.5	Thermal Shield	13-14
13.5	Shielding of the Secondary Containment	13-16
13.6	Health Monitoring Systems	13-23
13.6.1	Area Monitoring System	13-23
13.6.2	Air Particle Monitoring System	13-28
13.6.3	Stack Monitoring System	13-28
13.7	Health Physics	13-33
13.7.1	Los Alamos Scientific Laboratory Radiation Safety Policies	13-33
13.7.2	Facility Layout	13-35
13.7.3	Personnel Monitoring	13-36
13.7.4	Protective Equipment	13-37
13.7.5	Monitoring Equipment	13-38
13.7.6	Routine Surveys	13-39
13.7.7	Bioassay	13-40
13.7.8	Medical Examinations	13-41
14.	CONDUCT OF OPERATIONS	14-1
14.1	Organization and Responsibility	14-1
14.1.1	Organization Structure	14-1
14.1.2	UHTREX Steering Committee	14-3
14.1.3	Operating Staff Qualifications	14-4

CONTENTS (continued)

		Page
14.2	UHTREX Operating Manual	14-4
14.2.1	Operating Standards	14-5
14.2.2	Standard Operating Procedures	14-5
14.2.3	Emergency Operating Procedures	14-6
14.2.4	Operating Plans	14-6
14.2.5	Instrumentation and Control	14-6
14.2.6	Maintenance and Repair	14-7
14.3	Training and Qualification Program	14-7
14.3.1	Classroom Review and Instruction	14-7
14.3.2	On-the-Job Training	14-8
14.3.3	Qualification	14-8
14.4	Records	14-9
14.4.1	Operations Log Book	14-9
14.4.2	Periodic Test and Inspection Record	14-9
14.4.3	Instrumentation Record	14-9
14.4.4	On-Line Computer Data File	14-10
14.4.5	Fuel Management Records	14-10
14.4.6	UHTREX Operating Manual Change Record	14-10
14.4.7	Facility Modification Record	14-10
14.4.8	Health Physics Record	14-10
14.4.9	UHTREX Steering Committee Meeting Minutes	14-10
15.	INITIAL TESTS AND OPERATIONS	15-1
15.1	Tests Prior to Reactor Operation	15-1
15.2	Initial Fueling and Low Power Tests at Ambient Temperature	15-2
15.2.1	Initial Fuel Loading	15-2
15.2.2	Low Power Tests	15-3
15.3	Initial Power and Temperature Ascension	15-4
15.3.1	Fuel Loading	15-7

CONTENTS (continued)

		Page
15.3.2	Initial Ascension	15-8
16. SAFETY ANALYSES		16-1
16.1	Safety in the Design	16-1
16.1.1	Reactor	16-1
16.1.2	Control Systems	16-2
16.1.3	Coolant Loops	16-3
16.1.4	Auxiliaries	16-4
16.2	Effects of Operational Errors	16-4
16.2.1	Reactivity Insertions	16-5
16.2.2	Coolant Blower Shutdowns	16-10
16.2.3	Opening of Recuperator Bypass Valve	16-13
16.2.4	Malfunctions in the Gas Cleanup System	16-15
16.3	Effects of Component Failures	16-16
16.3.1	Rupture of the Primary Coolant Loop	16-17
16.3.2	Rupture of the Secondary Coolant Loop	16-26
16.3.3	Failure in the Fuel Loader and Core Indexing Mechanisms	16-27
16.3.4	Failure in the Fuel Handling System	16-28

APPENDICES

A.	Meteorological Data for Los Alamos	A-1
B.	Geology and Hydrology of the UHTREX Site	B-1
C.	Manufacturing and Installation of UHTREX Pressure Vessel	C-1
D.	Results from UHTREX Critical Experiment	D-1
E.	Dose Rate Derivation	E-1
F.	Analysis of Primary Loop Rupture Accidents	F-1

CONTENTS (continued)

		Page
G.	Calculation of Radiation Doses Resulting from Double-Ended Pipe Rupture Accident	G-1
H.	Equilibrium Fission Product Inventory in UHTREX	H-1
I.	Answers to Questions of Division of Reactor Development and Technology, February 1, 1967	I-1

1. INTRODUCTION AND SUMMARY

1.1 Principal Design Features

The Ultra High Temperature Reactor Experiment (UHTREX) is being conducted by the Los Alamos Scientific Laboratory (LASL) to advance the state of technology applicable to gas cooled reactors. Consistent with this aim, the experiment is designed to take advantage of the intrinsically safe features of a graphite-moderated, helium cooled reactor that can operate at very high fuel and exit coolant temperatures.

1.1.1 Site

The UHTREX site is situated about 2½ miles from the town of Los Alamos, New Mexico, in a lightly populated region within an ~67-square-mile, Federally-owned tract controlled by the Atomic Energy Commission and used by LASL in its diversified technical programs. The principal structure is the reactor building, which has a gas-tight secondary containment enclosing the reactor, primary cooling system, and closely related systems. Other space in the building houses auxiliary equipment, fuel handling systems, utility systems, the control room, staff offices, and minor-maintenance laboratories. Ventilation systems provide appropriate atmospheric control of potentially contaminated spaces; contaminated liquid waste can be pumped to a nearby process plant. Storage, repair, or modification of clean or lightly-contaminated equipment is conducted in the reactor building. Access to the site, limited by a fence and the surrounding rugged terrain, is under the control of the reactor operating force.

1.1.2 Reactor

Designed exclusively for experimental use, the reactor produces 3 MW of heat which is dissipated through helium-filled coolant systems to the atmosphere. No power is produced; there are no availability requirements other than the desirability of continuous operation of the reactor for experimental purposes. The reactor is designed to operate for a minimum of three years at maximum design conditions.

The reactor's moderator, reflector, thermal insulation, and internal gas ducts are made of elemental carbon, the most highly refractory substance known. In the cylindrical core, graphite, which serves in the dual capacity of structure and moderator, contributes to the negative temperature coefficient, prevents sudden changes in moderation, and, because of its mass, restricts to a low rate the reactivity insertion due to cooling of the core.

Control rods are designed to resist the environments to which they are exposed when inserted into the operating reactor core. The rods, their drives, and the channels through which the rods enter the core are designed to ensure that the reactor always can be shut down safely. During full power operation all control rods are withdrawn.

1.1.3 Fuel

Fuel elements are small in size, simple in form, unclad in the usual sense, and can be loaded and unloaded while the reactor is operating at design conditions. When the reactor is operating at design power, fuel element temperatures are 2000-2900°F.

The fuel is UC_2 spheres coated with three layers of pyrolytic carbon and bound in a graphite matrix. There are 1248 elements in a full loading; each element represents a reactivity increment of only a few cents. The graphite matrix is refractory and strong and contributes to the negative fuel temperature coefficient. An objective of the reactor experiment is the study of effects on fuels and of various types of fuels; consequently, the fuel elements have no restricted design lifetime.

Some elements may be exposed to burnup as high as 50%, whereas others may be moved through the reactor on short exposure cycles. A remotely controlled fuel handling system is designed to move fuel elements to and from gas locks that pass the elements into and out of the reactor while coolant system integrity is maintained. Therefore, there is no need for excess reactivity to compensate for fuel burnup.

1.1.4 Coolant System

A primary and a secondary closed cycle helium loop operate in series at 500 psi to remove 3 MW of heat from the core and discharge it to the atmosphere. The primary loop, designed to contain fission products released from the unclad fuel, is separated from the secondary loop by a heat exchanger and is enclosed within the secondary containment portion of the facility structure. Under maximum design conditions, the coolant helium enters the reactor at 1600°F and leaves it at 2400°F.

A high degree of reliability and leak tightness is built into both coolant loops. The number of joints and welds is minimized, and there are no rotating shaft seals. Coolant in each loop is circulated by completely canned, centrifugal blowers with gas bearings. Blower power comes from on-site generators driven by dual electric motors supplied from either of two power lines.

The refractory nature and high heat capacity of the reactor core make unnecessary an auxiliary helium coolant system for emergency use. Decay heat moves out of the reactor vessel by radiation to wall panels served by a cooling water system with an emergency capability.

All components of the coolant systems are designed to withstand the effects of credible accidents without rupture of the primary loop. Both loops have undergone rigorous inspection and complete nondestructive testing during fabrication and installation and must pass helium leak-tightness tests at operating pressures.

A gas cleanup system, operating as a sidestream of the primary loop, maintains the purity of the coolant helium by continually removing fission

products emitted from the fuel and impurities outgassed from the carbon parts of the core and coolant system.

1.1.5 Instrumentation and Control

The reactor and its auxiliaries are designed to be operated from a control room that remains habitable under the conditions that arise from any credible reactor accident. To monitor and control the reactor there are 11 nuclear instrumentation channels: two neutron counting, two log power, two linear power, one log gamma flux, and four safety level channels. Highly reliable safety systems automatically shut down the reactor and take other appropriate actions when out-of-limit conditions are detected in coincidence by monitoring transducers. Ten other safety systems detect malfunctions in the coolant system and automatically take corrective action. The gas cleanup and fuel handling systems are under surveillance and control from the control room.

An on-line process computer, installed in the control room, is designed to collect data, monitor system operations, perform recurrent operating sequences, and generally assist the reactor operators.

Health physics systems monitor radioactivity levels throughout the site, report out-of-limit levels to the control rooms, and initiate alarms under high level conditions.

1.1.6 Radioactivity Control

Provisions have been made to accommodate very high levels of fission product contamination in the primary coolant system and thus allow for the possibility of high release rates from unclad fuel elements. The primary loop is well shielded, and a secondary containment system encloses the reactor, primary coolant loop, and associated auxiliaries to prevent the uncontrolled release of contaminated coolant leaked from the primary system. The secondary containment structure, made of reinforced concrete with a partial steel liner and gas-tight doors, has the demonstrated capability to withstand a 5-psig internal pressure, which is

greater than the pressure produced in any credible accident. Leak rate from the structure, in actual tests, was found to be 3% per day of the contained volume at 5-psig pressure. This leak rate would not produce an intolerable release of radioactivity if the primary loop fission product inventory were to be released inside the structure in an accidental rupture of the loop.

Because the fuel handling system can accommodate only single fuel elements, the assembly of a critical mass in the system is impossible. Fuel element storage facility designs preclude the occurrence of critical assemblies of either new or spent elements. Reprocessing of fuel will not be done at the reactor site. Shielded cells with remote handling fixtures and shielded casks for spent elements protect operators during fueling operation.

1.1.7 Utility Systems

Two independent power lines and two on-site generators ensure the availability of power for safe reactor shutdown. An unlimited supply of air cools the reactor. Auxiliary cooling water systems, normally on closed-cycle operation, can use water from Los Alamos mains under emergency conditions.

1.2 Design Characteristics

General

1.	Reactor type:	Experimental, high-temperature, helium-cooled, unclad fuel
2.	Nominal reactor power:	3 MW (thermal)

Reactor Physics

3.	Neutron energy and lifetime:	0.14 eV at 1350°C, lifetime 6.8×10^{-4} sec

4. Core parameters:

η = 1.95	ε = 1.00
f = 0.602	P = 1.00
k_∞ = 1.174	k_{eff} = 1.05
L^2 = 470 cm^2	τ = 350 cm^2

Thermal leakage factor:

Cold: 0.944

Hot: 0.902

Fast leakage factor: 0.995

5. Neutron flux (neutrons/cm^2-sec):

	Radial	Axial
Thermal ave.	3.7×10^{13}	3.5×10^{13}
Thermal max.	4.9×10^{13}	4.9×10^{13}
Fast ave.	2.7×10^{13}	2.7×10^{13}
Fast max.	3.1×10^{13}	3.1×10^{13}

6. Reactivity balance:

Max. built in (cold, clean): 13% $\frac{\Delta K}{K}$

To compensate for temperature: 10% $\frac{\Delta K}{K}$

Xe and Sm at rated power: 3% $\frac{\Delta K}{K}$

Core

7. Shape and dimensions: Hollow vertical cylinder, 23-in. i.d. x 70-in. o.d. x 39-in. high, mounted on plate that rotates

8. Number of channels and subassemblies: 312 radial channels, 1.1-in. diam, 23.5-in. long, each contains 4 fuel elements

9. Lattice: Radial channels at 15° intervals in 13 horizontal planes

10. Critical mass: 5.68 kg 93.6% enriched uranium

11. Core loading at design power: 11.0 kg 93.6% enriched uranium

12. Average specific power in fuel: 270 kW/kg enriched uranium

13. Average power density in core: 1.4 kW/liter

14. Burnup: 10% - 50%

15.	Fuel loading and unloading:	While reactor operates, fuel loaded and unloaded by loader fixed on side of vessel; core rotates to locate desired fuel channel at loader which inserts new element, displacing spent element. Remotely controlled conveyor system moves elements to and from loader.
16.	Irradiated fuel storage:	Fuel handling cells shielded for 100 spent elements
17.	Moderator:	Graphite core structure

Fuel Element

18.	Form and composition:	Hollow cylinders, 0.5-in. i.d. x 1.0-in. o.d. x 5.5-in. long; graphite matrix contains 93% enriched UC_2 spherical particles with triplex pyrolytic carbon coating
19.	Cladding:	None

Core Heat Transfer

20.	Heat transfer area:	224 ft^2
21.	Heat flux:	Inside and outside surface of fuel elements: 5×10^4 Btu/h-ft^2, ave.
22.	Fuel element temperatures:	Max fuel: 2880°F Ave. fuel: 2600°F Film drop: 625°F
23.	Heat transfer coefficients:	Central hole of fuel element: 135 Btu/ft^2-h-°F, ave. Annulus around fuel element: 45 Btu/ft^2-h-°F, ave.
24.	Coolant flow area and velocity:	Total area: 0.783 ft^2 Ave. velocities: Central hole in element: 75 ft/sec Annulus around element: 16 ft/sec

25. Coolant mass flow rate: 10,250 lb/h (nominal)

26. Coolant pressures and temperatures
Inlet: 473.5 psi, 1600°F
Outlet: 473 psi, 2400°F

27. Hot channel factor (calculated for center fuel channel):

Film drop:	1.035
Surface heat flux:	1.035
Coolant temperature rise:	1.070

28. Peak-to-average power ratio: 1.13

29. Shutdown heat removal: Heat moves by conduction to pressure vessel wall and radiates to water-cooled panels that cover reactor room walls and floor.

Control

30. Control rods:

8 central plug rods; 1.0-in. o.d. Nb tube enclosing 0.875-in. o.d. B_4C cylinders on central Nb rod; active length 40 in.

4 core rods; articulated assembly of 1% ^{10}B alloyed in Type 304 stainless steel, 1.44-in. o.d.; active length 40 in.

Total worth, plug rods: 14% $\frac{\Delta K}{K}$

Total worth, core rods: 8.5% $\frac{\Delta K}{K}$

Speed of plug rods:

Normal: 18 in./min =

$3.2 \times 10^{-4} \frac{\Delta K}{K}$/sec (max.)

Fast (in): 18.6 ft/sec (max.) =

$3.6 \times 10^{-2} \frac{\Delta K}{K}$/sec (ave.)

Speed of core rods:

Normal: 18 in./min =

$2.1 \times 10^{-4} \frac{\Delta K}{K}$/sec (max.)

31. Reactivity addition rate: $3.2 \times 10^{-4} \frac{\Delta K}{K}$/sec (max.)

32. Scram time and mechanism: 0.9 sec, plug rods in free fall

33. Sensitivity of auto control: On-off control with ±1% or better dead band

34. Temperature coefficients $\left(\frac{\Delta K}{K}\right)$:

	At 20°C	At 1440°C
Core moderator	-1.83×10^{-4}	-1.18×10^{-4}
Core fuel	-1.40×10^{-5}	-8.41×10^{-6}
Reflector	$+8.22\times10^{-5}$	$+1.28\times10^{-5}$

Reactor Vessel and Overall Dimensions

35. Form, material, and dimensions: Spherical, carbon steel, 13.5-ft diam, minimum wall thickness 1.75 in.

36. Working, design, and test pressures:
    - Working: 500 psi
    - Design: 550 psi
    - Test: 825 psi

37. Reactor size with shielding: 60 ft x 25 ft, 42 ft below grade

Reflector and Shielding

38. Reflector: Graphite and dense carbon, overall dimensions 104-in. o.d. x 72-in. i.d. x 78-in. high

    Thickness:
    - Sides: 6 in. graphite, 10 in. carbon
    - Top: 7 in. graphite, 15 in. carbon
    - Bottom: 6 in. graphite, 11 in. carbon

39. Radiation levels: 1 mrem/h in accessible areas outside secondary containment

40. Shielding:
    - Sides: 3.5 to 5 ft magnetite concrete
      2.5 to 7 ft ordinary concrete
    - Bottom: 4.0 ft magnetite concrete
    - Top: 5.0 ft magnetite concrete in removable slabs

40.	Shielding (Cont.):	Lead thermal shield, 2-in. thick, lines outside walls of reactor room to reduce energy current to concrete
		Water-cooled panels cover reactor room walls and floor.
		Ave. shield temperature 85-105°F

Containment

41.	Type and material:	Reinforced concrete structure, 60- x 51- x 81-ft high (42 ft underground), lined with welded steel plate
		Superstructure walls 1.5-ft thick
		Test pressure 5.0 psig
		Actual leakage 3.0% of total volume per day at 5.0 psig
42.	Surroundings:	2.5 miles SE of Los Alamos, population 16,000, no other towns within 3-mile circle which encompasses most Los Alamos Scientific Laboratory technical sites.

1.3 Design Research and Development Programs

Investigations were made of many of the UHTREX design features in the process of developing and proving the final designs. Research and development programs were carried out independently at LASL and in cooperation with contractors at their plants. The results of some of the major programs are described briefly below and in more detail in the relevant sections of this report.

1.3.1 Reactor Components

At the time the core structure was designed there were no empirical data for the prediction of radiation-induced dimensional changes in the UHTREX graphite, Union Carbide's Type CGL, and carbon. An irradiation program at Battelle Memorial Institute/Pacific Northwest Laboratories, demonstrated that the design assumptions were conservative.

Thermal characteristics of the core materials, particularly thermal conductivity, were measured in LASL experiments.

An extensive study[1] has been made of the corrosive effects on the UHTREX core of chemical contaminants in the helium coolant. In a corrosion test loop, a full-scale model of one fuel channel has been exposed, at UHTREX design temperatures and flow rates, to helium that contains various concentrations of the impurities expected to be outgassed from the core.

For experimental verification of the pressure vessel design calculations, an approximately 1/7-size scale model of the vessel was built and tested extensively under full pressure and moderately elevated temperatures. Strain gage measurements that were taken from the model were used in improving the design, particularly of the vessel cover, and in verifying that all stresses are within code limitations.

The adequacy of the fuel loader design was demonstrated in tests of full-scale mockups of the loader rams and drives, of the elevator, of the slot in the reactor plug through which the elements fall, and of the dislodger rod. A successful, long-term test was made of the core support bearing, in the reactor environment except for the radiation field.

Environmental tests confirmed the choice of materials for both sets of control rods. The ability of the articulated core rods to enter the displaced core was demonstrated in tests made with a full-scale mockup of the core and a core rod. Capabilities of the rod drives were demonstrated in long-term tests in which a prototype drive was operated through thousands of cycles that included free-fall drops.

The nuclear design of the core was proved in the UHTREX critical experiment, in which the actual UHTREX core, reflector, and fuel elements made up the critical assembly.

---

[1]P. G. Salgado, "Graphite Corrosion Studies for the Ultra High Temperature Reactor Experiment," Los Alamos Scientific Laboratory report LAMS-3063, March, 1964.

Coolant flow distribution through the core was improved by redesign after extensive experimentation with a flow model that is a half-scale, geometrical duplicate of the core, core plug, reflector inner surface, and exit nozzle. Electrical heaters simulated the fuel elements. With the exception of radiant heat transfer within the core, all similarity members were modeled for a thermal, as well as a flow, model.

1.3.2 Coolant System Components

To meet the temperature, pressure, and no-leakage requirements for operation in the coolant loop, a 60-hp, gas-bearing, centrifugal blower was developed in cooperation with Mechanical Technology, Incorporated. A prototype and all three of the final design blowers were subjected to analysis and proof tests in a blower test loop at LASL. In the same loop, proof tests were run on the recuperator bypass valve, the secondary loop blower bypass valve, and the coolant loop flowmeters.

The dynamic behaviour of the reactor, the primary coolant loop, and the secondary coolant loop, all acting together as a single system, was the subject of an intensive computational study. A mathematical model of the system was formed which has enough detail to make its use valid for predictions of the system stability and the time responses of system components to parameter changes.

1.3.3 Auxiliary System Components

When fuel elements pass into and out of the pressurized reactor, gas locks maintain the primary containment. The ball valves that make up the gas locks were developed in an extensive program performed in cooperation with the Controls and Guidance Division of Whittaker Corporation. After many proof tests of component designs, a prototype valve was designed, built, and subjected to a proof and endurance test program in which the actual gas lock environment was simulated, except for radiation fields. Included in the program were tests of the valve's ability to close tightly after temperature, pressure-shock, and differential-

pressure cycles; after the repeated introduction of abrasive dust; and after many impacts of falling fuel elements. The prototype valve survived the test program leak-tight and in good working condition.

The performance of the gas cleanup system was verified in pilot plant studies of the copper oxide bed, the molecular sieve beds, and the delay beds. Operating characteristics of each bed were predicted from the experimental data, and methods for controlling the system operations were worked out. Instruments to be used for chemical analysis of system streams were tested,and their performance characteristics were determined.

1.3.4 Instrumentation and Control Components

Performance tests for extended periods under simulated process conditions were run on instrumentation components that must satisfy the stringent sealing requirements and survive the extreme environments of UHTREX. Among the components tested were W5Re/W26Re thermocouples, acoustic thermometers, and strain gage differential and absolute pressure transducers.

In cooperation with Honeywell, an on-line process computer was developed to aid in the operation of the reactor, the reactor coolant loops, and auxiliary systems. A three-month reliability demonstration run of the computer system was made during which programs continually exercised and checked the system. Only three failures occurred, none of which were in the central processor.

1.4 Identification of Contractors

K-Division of LASL has the principal responsibility for the design of the UHTREX facility; for technical direction of facility construction; for supervision of equipment fabrication, inspection, and installation; and for performance or management of the design research and development programs.

Architect-engineer for construction of the UHTREX structure and site was W. C. Kruger and Associates Architects-Engineers Inc., Santa Fe, New Mexico, who worked from criteria developed by K-Division and the Engineering Department of LASL. The structure and site were built by Robert E. McKee General Contractor, Inc., Santa Fe, New Mexico.

Installation of equipment has been done by Los Alamos Constructors, Inc., a division of the Zia Company, local maintenance contractor to the AEC, from designs prepared by, and under the direction of, K-Division and the Engineering Department of LASL.

K-Division is responsible for facility operations, which will be performed by LASL staff members and technicians.

1.5 General Conclusions

The UHTREX reactor facility can be operated without undue risk to the health and safety of the public and of the operating personnel. In the design effort, accidents were postulated and the facility systems were designed to withstand the consequences. Research and development programs provided data for sound designs and proved the capabilities of prototypes. Rigorous inspection during facility construction and during equipment fabrication and installation ensures that design standards are met. Analyses of the complete facility show that it is protected by an adequate number of safety features.

2. SITE

2.1 Location

The UHTREX site, designated TA-52, is located within a Los Alamos area owned and controlled by the Atomic Energy Commission. The site is approximately 2-1/2 miles southeast of the city of Los Alamos, 22 miles northwest of the city of Santa Fe, shown in Fig. 2.1.1, and 2 miles southeast of the Administration Area of the Los Alamos Scientific Laboratory, designated TA-3 in Fig. 2.1.2. Most of the LASL technical area sites and much of the residential area of the city of Los Alamos lie within a three-mile circle centered on TA-52. However, none of the town sites and only five of the LASL sites lie within the 1-mile circle. Names and uses of the LASL technical areas that appear on Fig. 2.1.2 are listed in Table 2.1.1.

The nearest privately controlled land is occupied by a trailer court which lies slightly more than 1 mile to the northwest of TA-52. All of the land within the 1-mile circle is used exclusively by AEC contractors, principally LASL and the Zia Company, the Los Alamos area maintenance and construction contractor. Current plans of the AEC do not provide for the future use by individuals or private firms of the land in the vicinity of TA-52.

2.2 Layout

The site and adjacent areas appear in Fig. 2.2.1. In the lower right-hand corner of the figure is the reactor building, RD-1, which is discussed in detail in Chapter 3. To the northwest of RD-1, behind the stack, is

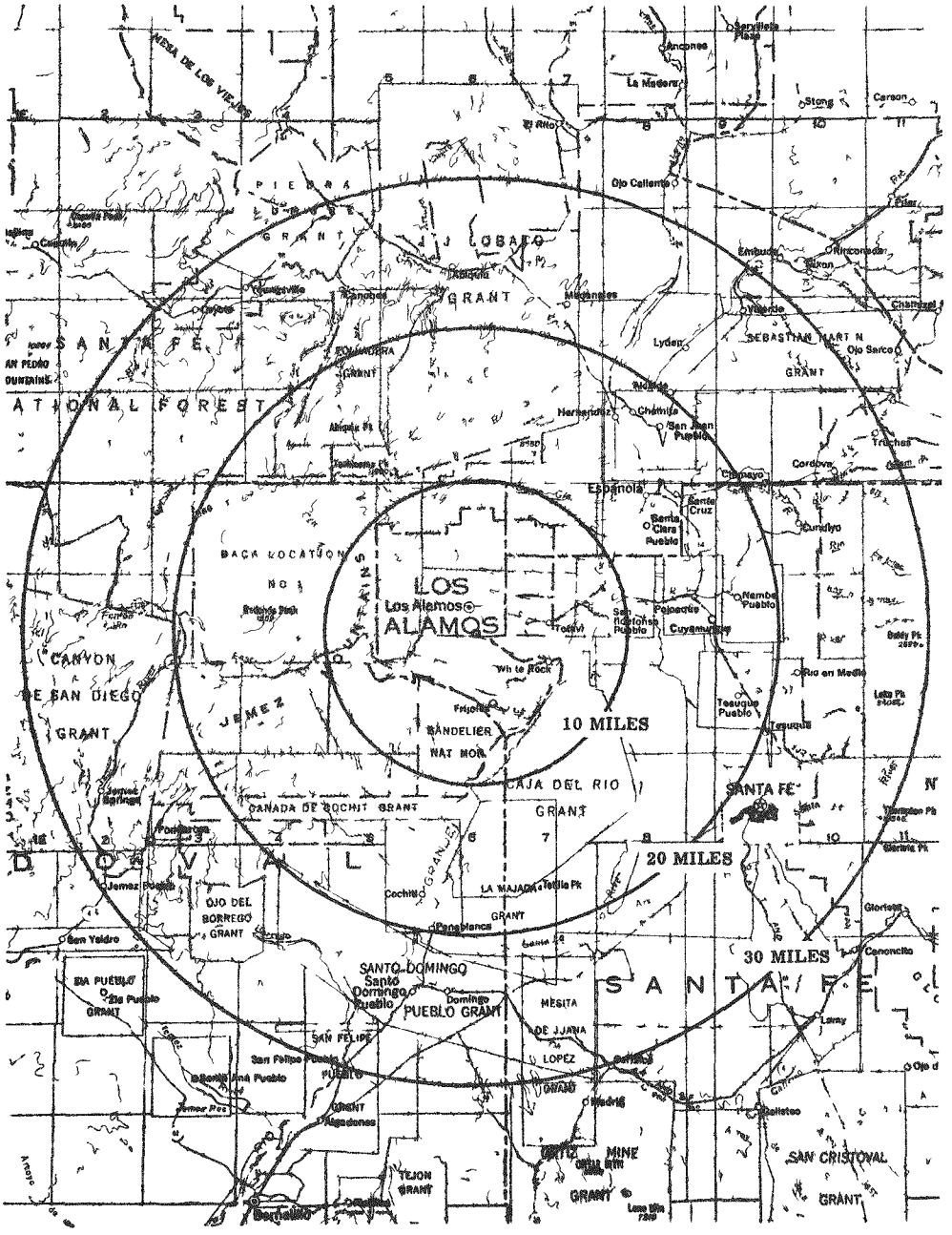

Fig. 2.1.1 Area surrounding Los Alamos

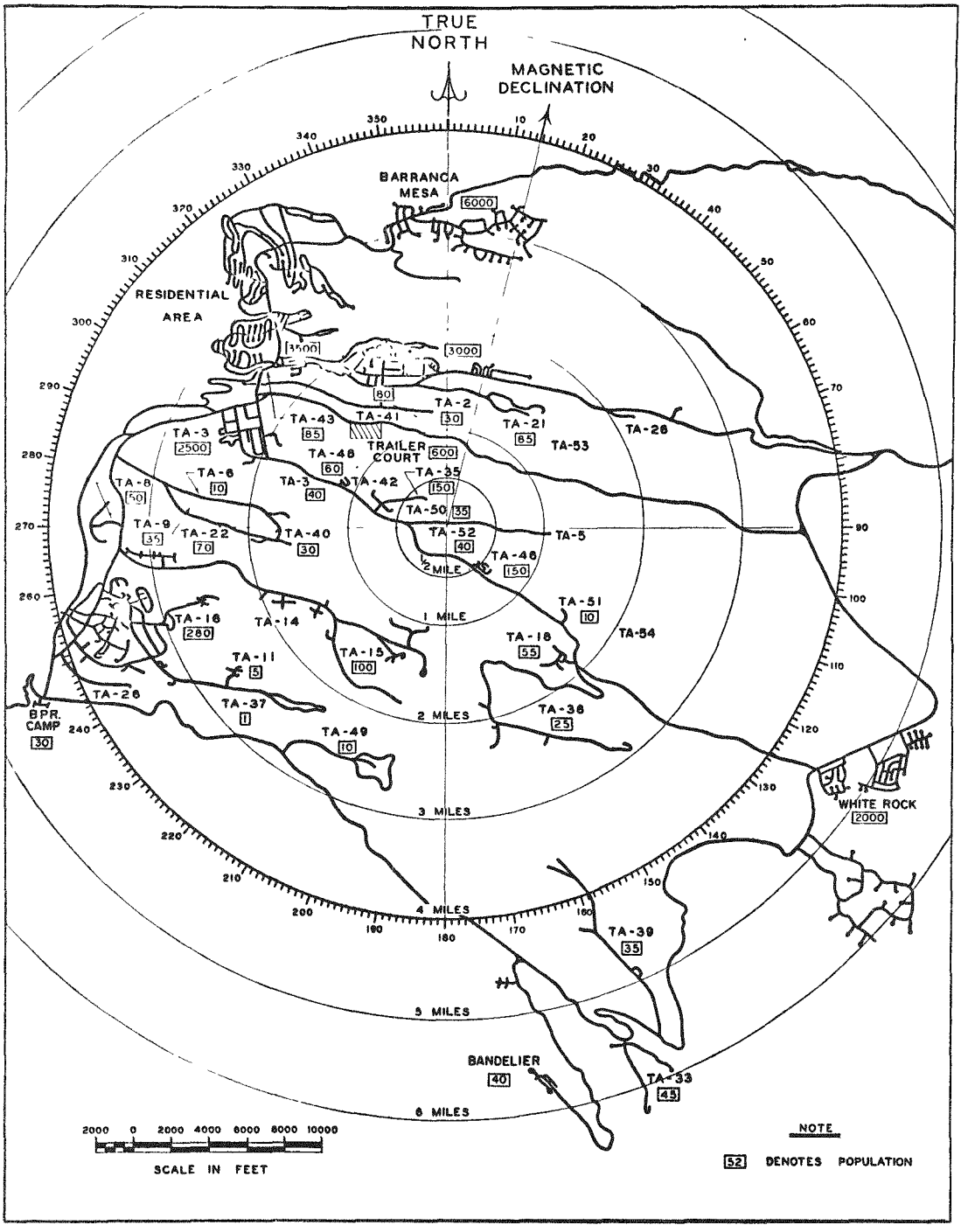

Fig. 2.1.2 Los Alamos townsite and Technical Areas. Boxes show local area population

TABLE 2.1.1

LASL TECHNICAL AREAS

Technical Area Number	Name	Facilities and Functions
TA-2	Omega Site	OWR, Water Boiler Reactor, Offices, Laboratories
TA-3	South Mesa Site (Main Technical Area)	Offices, Laboratories, Shops
TA-5*	Beta Site	Laboratories
TA-6	Two-Mile Mesa Laboratory	Offices, Laboratories
TA-8	Anchor Site West	Offices, Laboratories, Source for radiography
TA-9	Anchor Site East	Offices, Laboratories
TA-11	K-Site	Explosive testing
TA-14	Q-Site	Explosive firing
TA-15	R-Site	Offices, Laboratories, Explosive firing
TA-16	S-Site	Offices, Laboratories, Explosive plant
TA-18	Pajarito Laboratory	Offices, Laboratories, Critical assemblies
TA-21	DP-Site	Offices, Laboratories
TA-22	TD-Site	Offices, Laboratories, Explosive plant
TA-28*	Magazine Area A	Explosive storage
TA-33	HP-Site	Office, Laboratories
TA-35	Ten Site	Offices, Laboratories, Reactor development tests

* Site used occasionally, by fewer than 10 persons.

TABLE 2.1.1 (continued)

Technical Area Number	Name	Facilities and Functions
TA-36	Kappa Site	Offices, Laboratories, Explosive firing
TA-37	Magazine Area C (PMA)	Explosive storage
TA-39	AC-Site	Offices, Laboratories, Explosive firing
TA-40	DF-Site	Offices, Laboratories, Explosive firing
TA-41	W-Site	Offices, Laboratories
TA-42*	Incinerator Site	Incinerator
TA-43	Health Research Laboratory	Offices, Laboratories
TA-46	WA-Site	Offices, Laboratories
TA-48	Radiochemistry Site	Offices, Laboratories
TA-49	Frijoles Mesa Site	Laboratories
TA-50	Liquid Waste Plant	Offices, Laboratories
TA-51	Radiation Exposure Facility	Laboratories
TA-52	Reactor Development Site	UHTREX
TA-53**	Los Alamos Meson Physics Facility	Offices, Laboratories
TA-54*	MD-Site	Waste burial

* Site used occasionally, by fewer than 10 persons.

** Proposed.

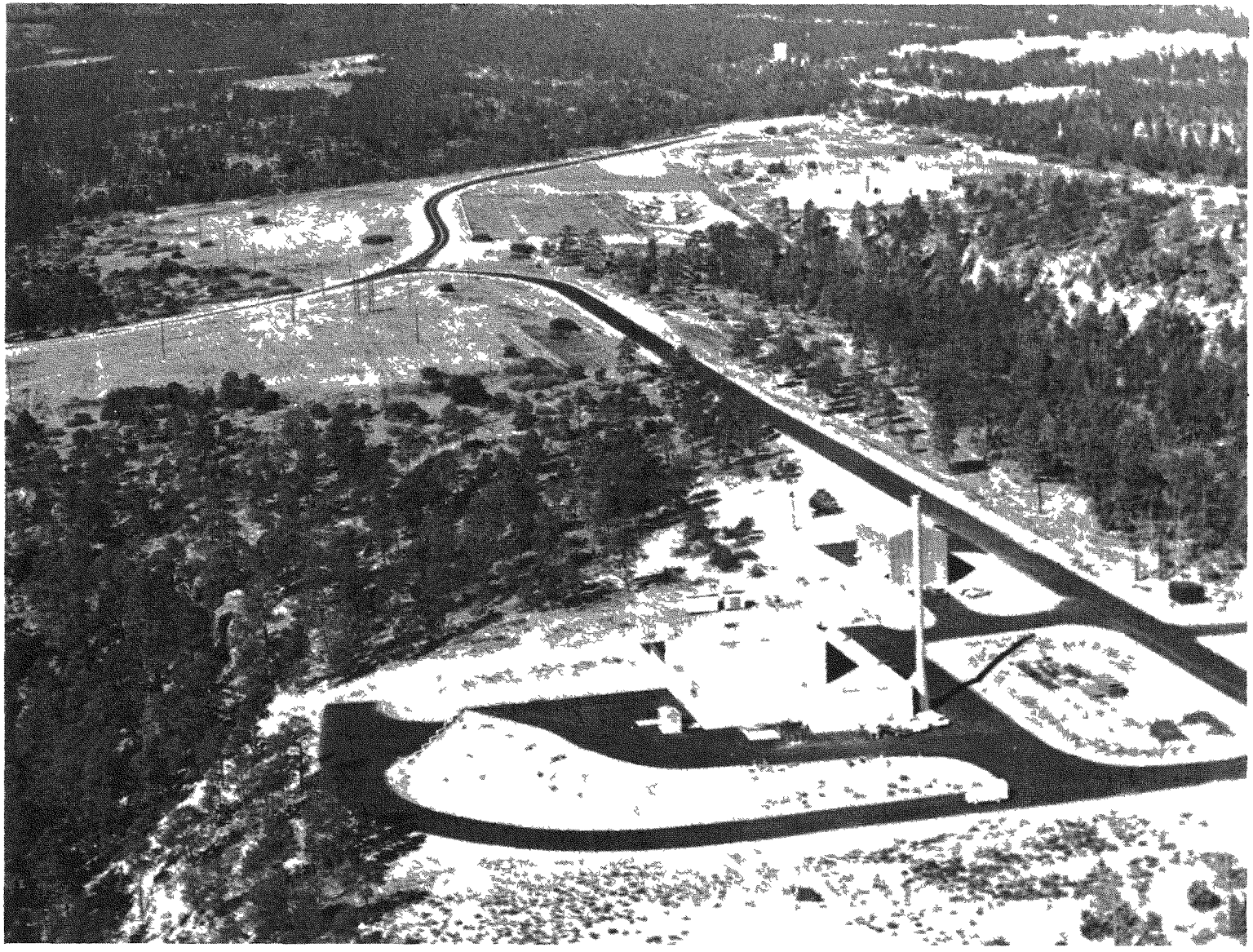

Fig. 2.2.1 UHTREX site

Building RD-11, where there are machine tools and other equipment used in the initial assembly of, and to be used for the maintenance and repair of, UHTREX system components. As a part of the UHTREX site, RD-11 is occupied and under the control of UHTREX operating personnel. To the right of RD-11 is Puye Road, the only site access route, which joins Pajarito Road at the top of the picture. To the left of the picture is Mortandad Canyon; to the right is Canyon del Buey. There is no private traffic on Puye Road, which extends 1 mile beyond the UHTREX site to Beta Site, a LASL facility used only on rare occasions. Pajarito Road, which skirts TA-52 to the south, is the principal route for general traffic between the city of Los Alamos and the residential areas around White Rock, 5 miles ESE of the site. The floors of Mortandad Canyon and Canyon del Buey, generally 200- to 300-feet below TA-52, are covered with large pine trees and are accessible only along rough roads that are posted by the AEC against trespassers.

Figure 2.2.2 shows the orientation of TA-52 with other nearby sites. Access to the TA-52 site is limited on the east and west by fences and on the other two sides by the precipitous edges of the mesa. The fence on the east, near Beta Site, is closed with a locked gate, under the control of the LASL group responsible for that site. All traffic to Beta Site must pass through the TA-52 entrance gate, located in the western fence across Puye Road.

When reactor operations are in progress at TA-52, movement through the site entrance gate is controlled from the reactor control room by means of a remotely operated latch. A telephone at the gate permits any unexpected visitor to call in. The movements of personnel into and out of the site are entered in a log by an operator in the control room.

When the reactor is not operating, the site entrance gate remains open during daytime working hours and is locked for the rest of each day. Keys to the gate lock are issued to persons employed at the site.

All activities at TA-52 are directly related to UHTREX and are under the control of the UHTREX operating group.

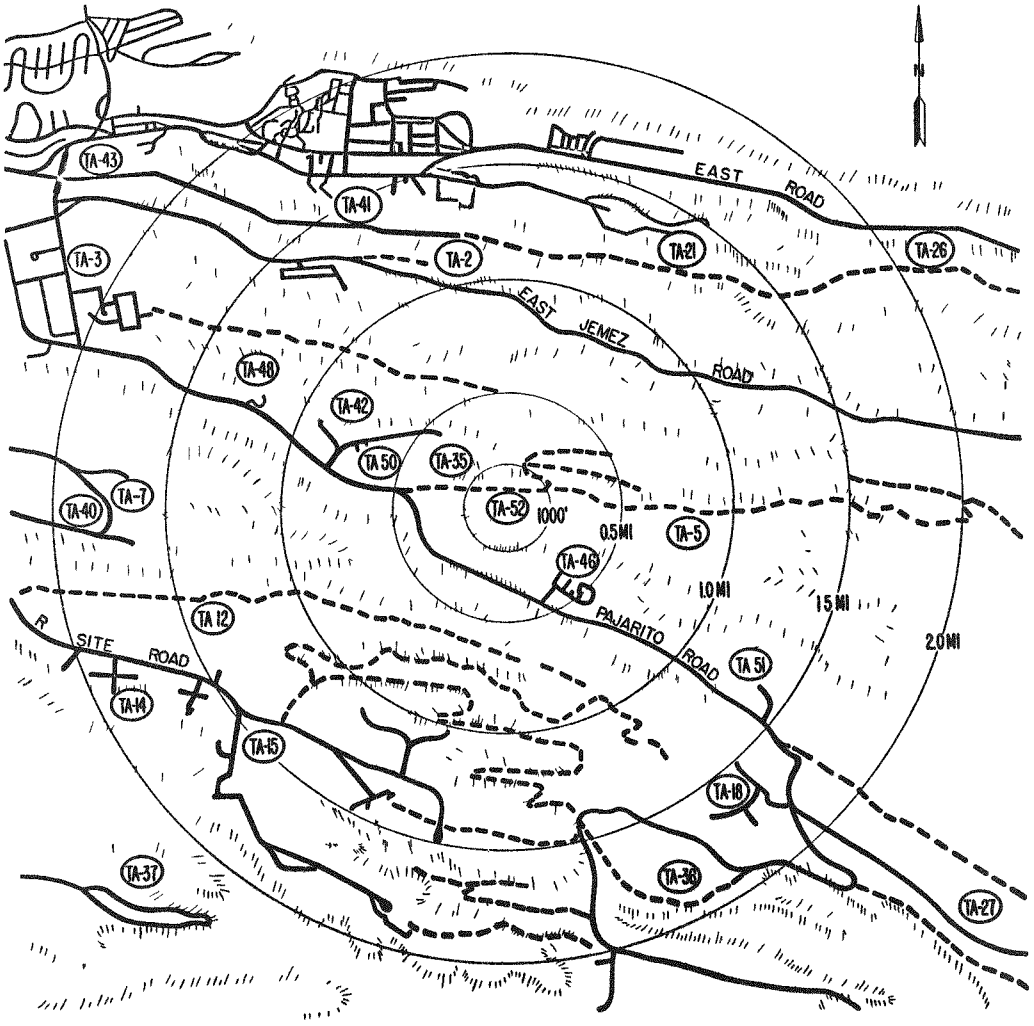

Fig. 2.2.2 UHTREX site and locality

2.3 Population

In the vicinity of the UHTREX site, the population is concentrated inside the LASL technical areas and within the Los Alamos townsite. The numbers of people to be found within each area are shown in boxes on Fig. 2.1.2 and summarized in Table 2.3.1. These numbers are not additive because 75% of the people listed for the technical areas are also listed for the residential areas. During working hours, there are a total of 19,000 people in the Los Alamos area.

TABLE 2.3.1

POPULATION WITHIN RADIAL ZONES

Zone Limits (Miles)	Los Alamos Areas Included	Number of People
0 - 0.5	Technical Areas	340
0.5 - 1.0	Technical Areas	35
1.0 - 2.0	Residential and central business district	3600
	Technical Areas	500
2.0 - 3.0	Residential	3500
	Technical Areas	2625
3.0 - 6.0	Residential	8070
	Technical Areas	445

Except for the city of Los Alamos, the area within a 10-mile circle around the UHTREX site is sparsely populated. There are few permanent residents at Frijoles, 5 miles SSE, but, during the summer, visitors to the Bandelier National Monument can raise the population to nearly 300. At White Rock, 5 miles ESE, homes are being built in several private residential areas that may house 3000 people within the lifetime of UHTREX. At San Ildefonso Pueblo, 9 miles to the ENE, there are approximately 400 people.

In the 10- to 20-mile zone, the total population is 20,000 with 6000

concentrated around Espanola, 15 miles to the northeast.

Between 20 and 30 miles away from the site, the total population is almost 40,000 with 85% of the people concentrated in the vicinity of Santa Fe, 22 miles to the southeast.

There are no other population centers within 50 miles of the site. Albuquerque, population 300,000, lies 53 miles to the south.

2.4 Meteorology

2.4.1 Winds

Surface movements of air at the UHTREX site are influenced strongly by its location on a mesa that slopes away from the Jemez Mountains on the west. The site is surrounded on the other three sides by deep canyons that drain eastward into the Rio Grande valley, 1500 feet below. After sunset, cooler air from the mountains flows across the mesas, and channels through the canyons to the river valley. The flow is reversed during the day.

Winds are generally light and southerly. The average wind speed is less than 10 mph about 75% of the time and reaches 30 mph only 0.1% of the time, usually in gusts. Over the entire year, average wind direction lies in the quadrant from south to west about 50% of the time. Surface wind roses based on data from 13 years' observations are shown in Fig. 2.4.1.1. Tabulations of average wind direction and speed for each month of the year are presented in Tables A.1 and A.2 of Appendix A.

While there are periods of strong, gusty winds during the spring months, no tornadoes have been observed during the past 55 years. Wind damage that has occurred is restricted to isolated breaking of poles and trees, and one instance of roof damage to a frame structure.

2.4.2 Inversions

In the Los Alamos area, inversions are almost always caused by surface cooling or frontal activity. Surface cooling inversions, by far the most common, can be expected to form during any night when the skies are

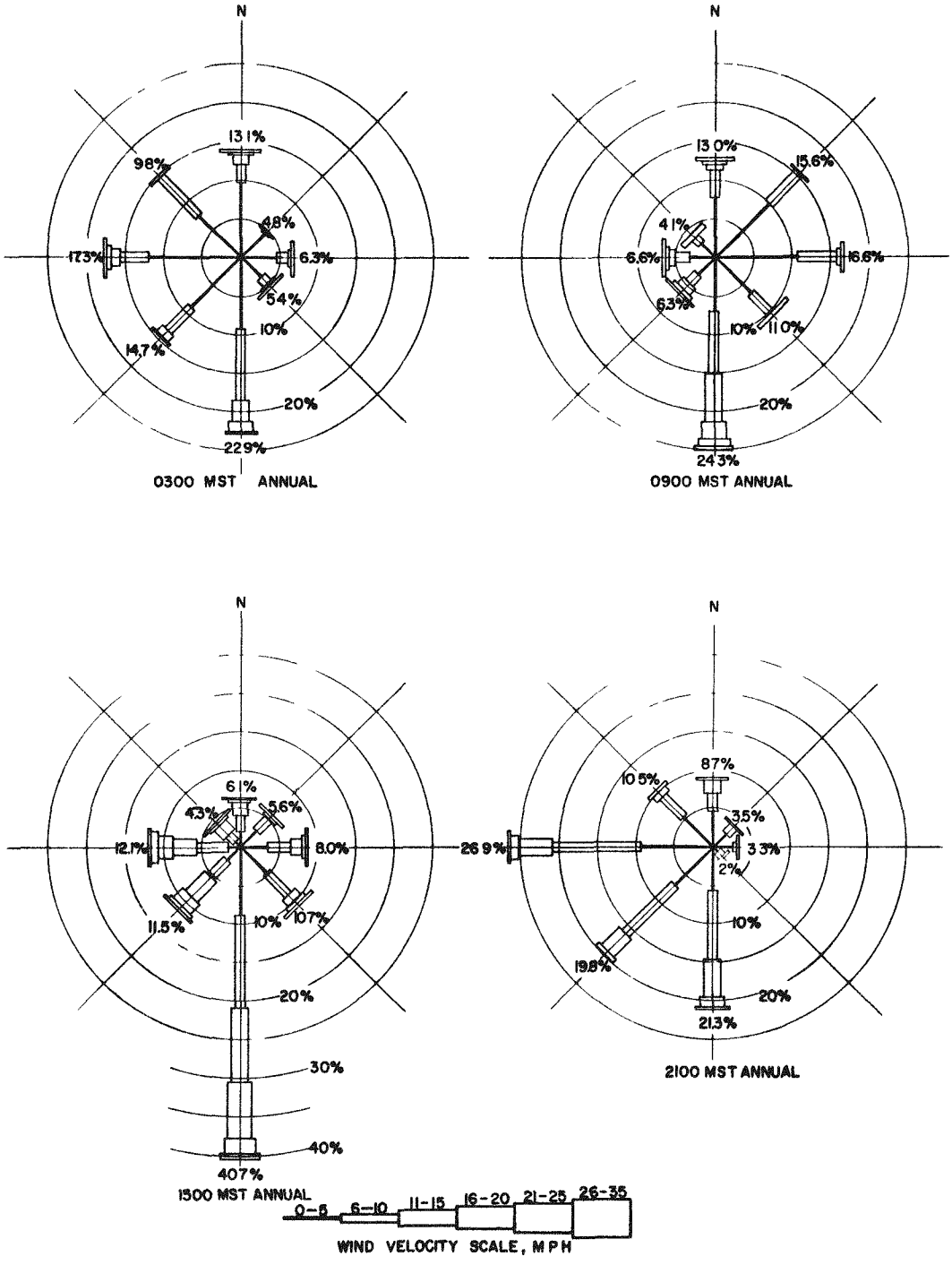

Fig. 2.4.1.1 Surface wind roses for Los Alamos. Directions are those from which the wind blows

generally clear and wind speeds are low. On the mesas, such inversions usually dissipate by midmorning. Inversions due to frontal activity are subject to considerable mixing caused by the moderate winds that usually accompany the fronts. Lateral mixing is reinforced by vertical mixing created by the mechanical turbulence of the winds flowing across the broken terrain.

Observations at the UHTREX site, made recently over a relatively short period of time, indicate that stable layers of air form during the night, but that they are disturbed by the drainage effect of air flowing into the adjacent canyons.

2.4.3 Precipitation and Temperature

Average precipitation data for Los Alamos are presented in Table A.3 of Appendix A, and Table A.4 lists the wind direction during periods when 0.01 in. or more of moisture was observed. Los Alamos is in an area where summer thunderstorms are common. As a consequence, the UHTREX facility and others in the area are well protected by lightning arresting systems.

Average temperature data are presented in Table A.5, Appendix A.

2.5 Hydrology and Geology

Theis[1] and Hale[2] describe the hydrology and geology of the Los Alamos area and of the UHTREX site in particular. UHTREX operations should have no effect on ground water since only gaseous wastes will be discharged under controlled conditions. There seems no credible mechanism for an accidental introduction of radioactive materials into the ground water.

---

[1] C. V. Theis, "Geologic Background of Waste and Water Supply Problems at Los Alamos," Paper No. 1, "Meeting of AEC Waste Processing Committee at Los Alamos, New Mexico," TID-460, October, 1950.

[2] W. E. Hale, Appendix B of this report.

2.6 Seismicity

The Los Alamos area, shown in Zone 2 on earthquake probability charts, lies on the Rio Grande structural trough near faults of large magnitude, and, hence, earthquakes might be expected to occur at any time. Further, the Los Alamos area might experience tremors from quakes originating in other parts of the trough. However, there is no geologic evidence to indicate that intensive earthquakes have occurred recently in the Los Alamos region.

According to S. A. Northrup*, in a region like New Mexico that is subject to a high frequency of shocks of moderate intensity, the frequent shocks act as a safety valve to relieve earth stress before it can accumulate in force to produce a violent shock. Northrup reports that of 575 earthquakes recorded in New Mexico during the century preceding 1949, 94% originated in a 75-mile section of the Rio Grande valley extending south from Albuquerque (53 miles south of Los Alamos) to Socorro. Only 2% of these shocks were of intensity VIII-IX on the Rossi-Forel scale. (Intensity VIII shocks cause walls to crack; an intensity X shock causes general disaster.) One of the strongest shocks, reported to be of intensity IX, originated near Cerrillos, 33-miles south of Los Alamos, on May 28, 1918. The resultant shock at Los Alamos presumably attained intensity VI. Another report[3] lists a brief shock of intensity V that occurred at Los Alamos on August 17, 1952.

Observations made by the Geological Survey** indicate that the area has been stable for hundreds and possibly thousands of years. Certain

---

*Collaborator in seismology for New Mexico, U.S. Coast and Geodetic Survey; and Head, Department of Geology, University of New Mexico.

[3]"Abstracts of Earthquake Reports for the Pacific Coast and the Western Mountain Region," MSA-75, July, August, and September, 1952, U.S. Coast and Geodetic Survey.

**Letter from Ronald Willden, Geologist, Branch of Crustal Studies, U.S. Geological Survey, Denver, Colorado, April 5, 1966.

geologic, archeological, and cultural features of the general area show evidence that strong earthquakes have not affected the area within the last 300 to 500 years. One geologic feature is a large number of pinnacles located in Rendija Canyon, just to the north of Los Alamos. The pinnacles, eroded from soft formations, are 10- to 50-ft high and are capped with boulders that are two to five times the diameter of the pinnacle neck beneath them. These pinnacles are unstable, and it is unlikely that they could survive a strong earthquake. Furthermore, ruins of Indian dwellings in the Los Alamos area have free-standing walls that, because they lack lateral strength, indicate an absence of severe ground shaking since the time of their construction, estimated to be between the fourteenth and sixteenth centuries. Cultural evidence for long-continued ground stability includes nearby Indian pueblos that have been occupied continuously since the late sixteenth century, surviving buildings in Sanda Fe constructed by the Spanish in the early seventeenth century, and an absence of references to earthquakes in the records that survive from the former Spanish and Mexican governments of New Mexico.

3. FACILITY

So that the reader may be oriented when he progresses through the report, this chapter presents a brief description of the UHTREX facility as a whole. Each subject treated here is expanded upon in chapters that follow.

A single, integrated, reinforced concrete structure, depicted in Figs. 3.1 through 3.6, houses the reactor and the associated experimental, operational, and support facilities. The building has two primary parts, separated by radiation shielding, gas-tight doors, and a gas-tight steel membrane. One portion of the building contains the reactor, the primary (contaminated) helium coolant loop, fuel handling systems, and the gas cleanup and storage systems, and serves as the secondary containment for volatile fission products carried in the helium coolant. The remainder of the building contains the control room, offices, fuel handling and gas sampling cells, utility distribution systems, and other auxiliary equipment.

3.1 Secondary Containment

The primary containment for volatile fission products consists of the reactor vessel and its attached auxiliaries, the primary coolant loop, and the gas cleanup and storage systems. To provide a second barrier to the uncontrolled release of fission products, a secondary containment is established. Its boundaries are the secondary coolant loop, the containment portion of the building, and the recirculating ventilation system that serves that part of the building.

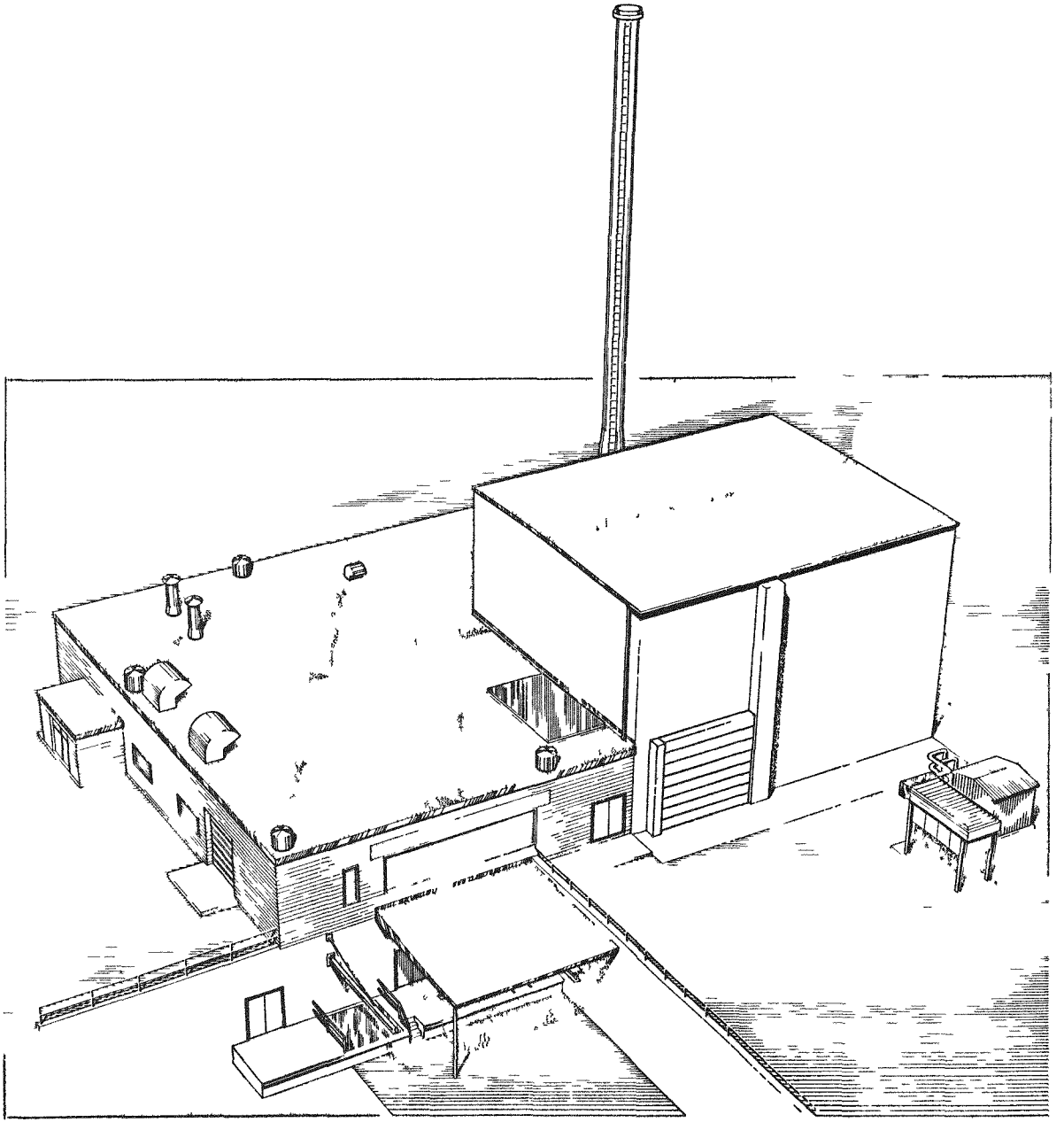

Fig. 3.1 General view of UHTREX facility

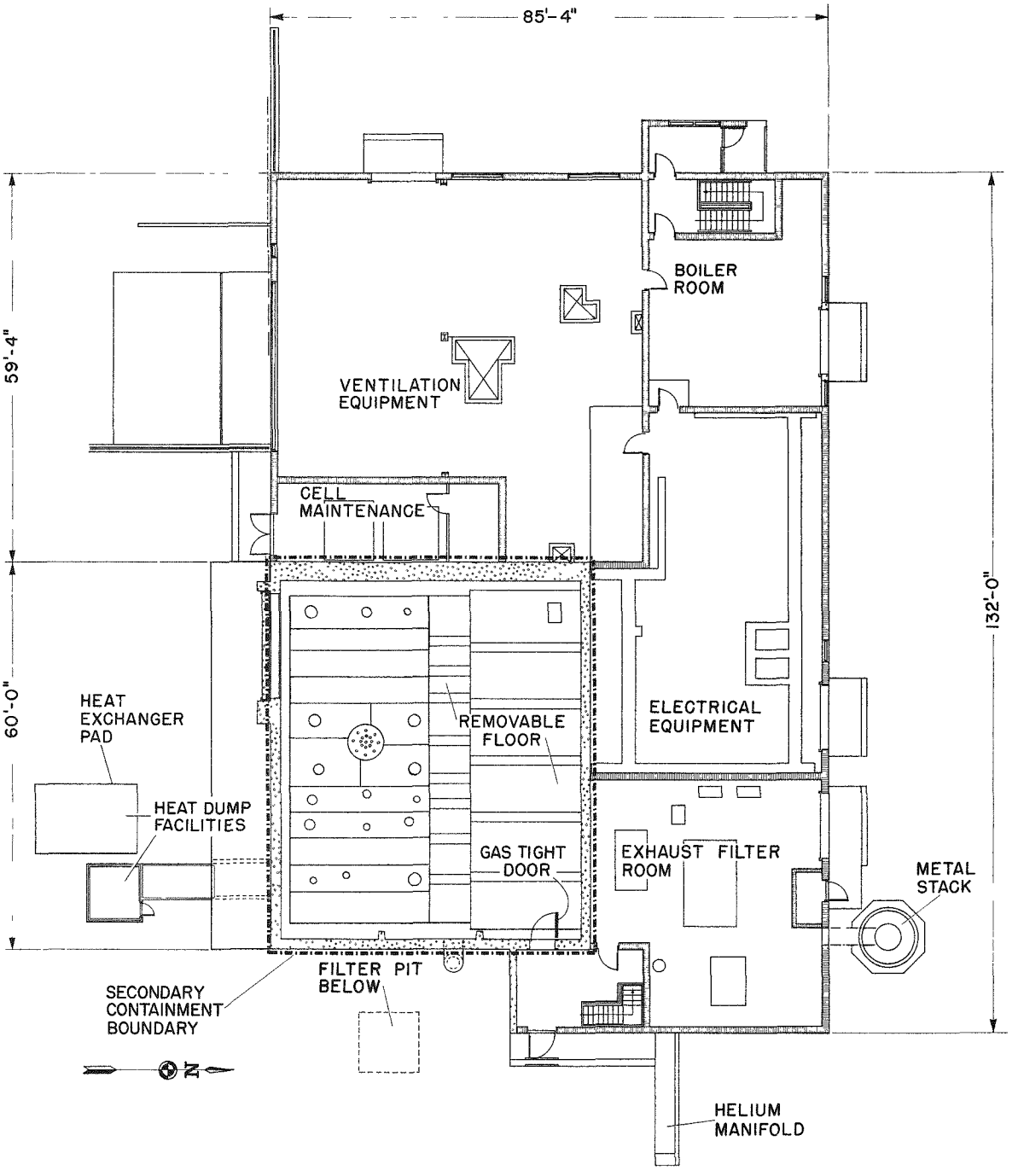

Fig. 3.2 Building floor plan, ground level

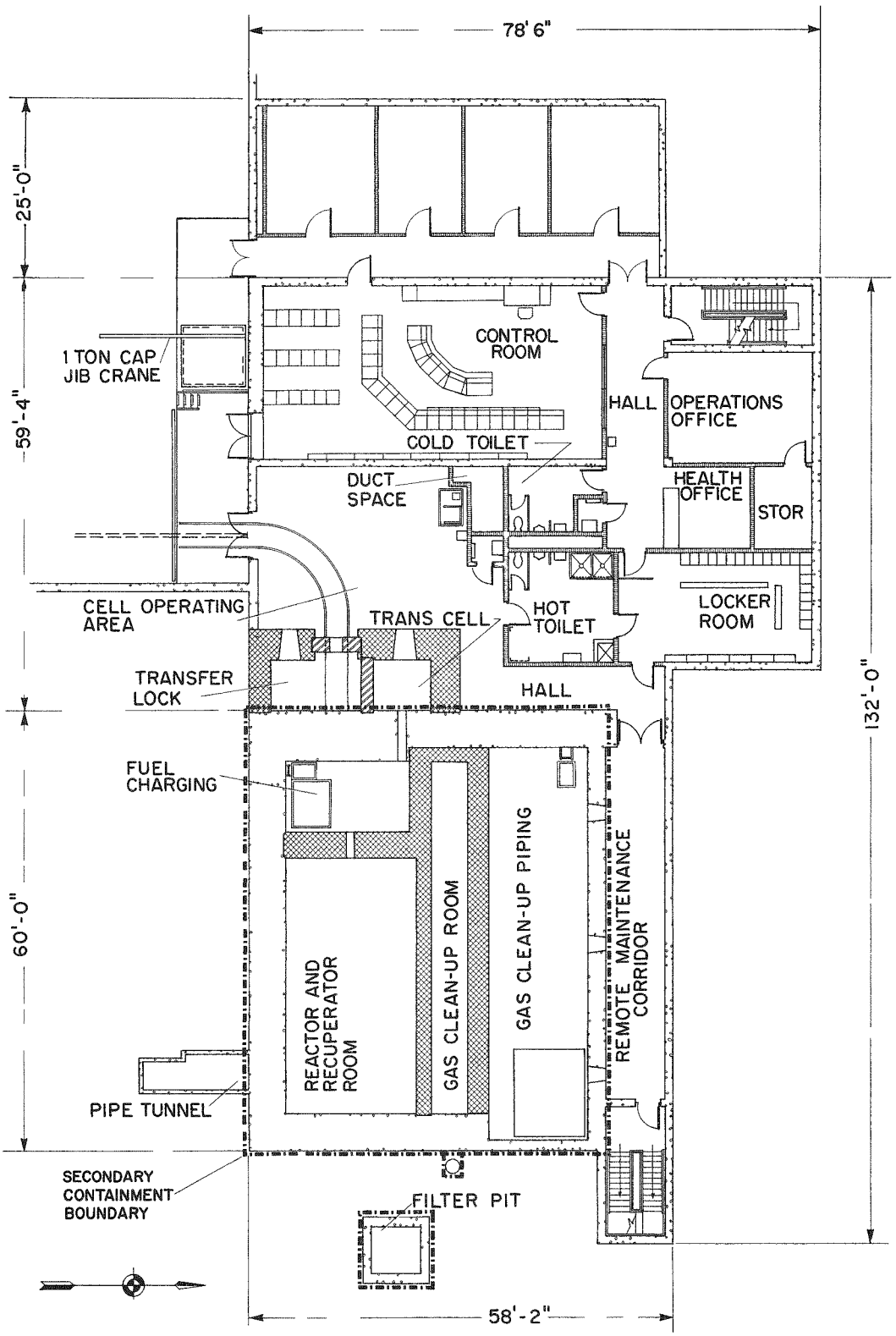

Fig. 3.3 Building floor plan, operating level

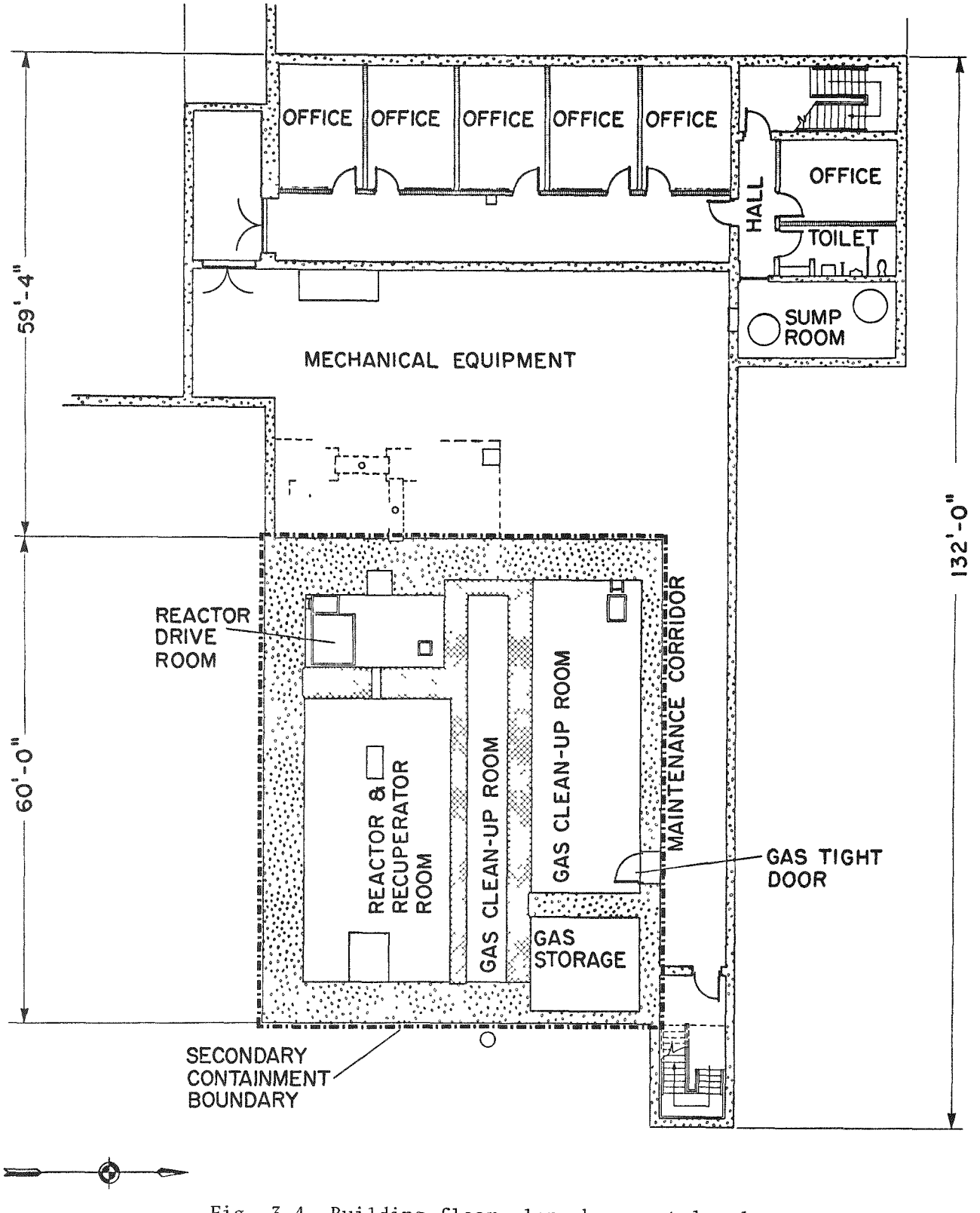

Fig. 3.4 Building floor plan, basement level

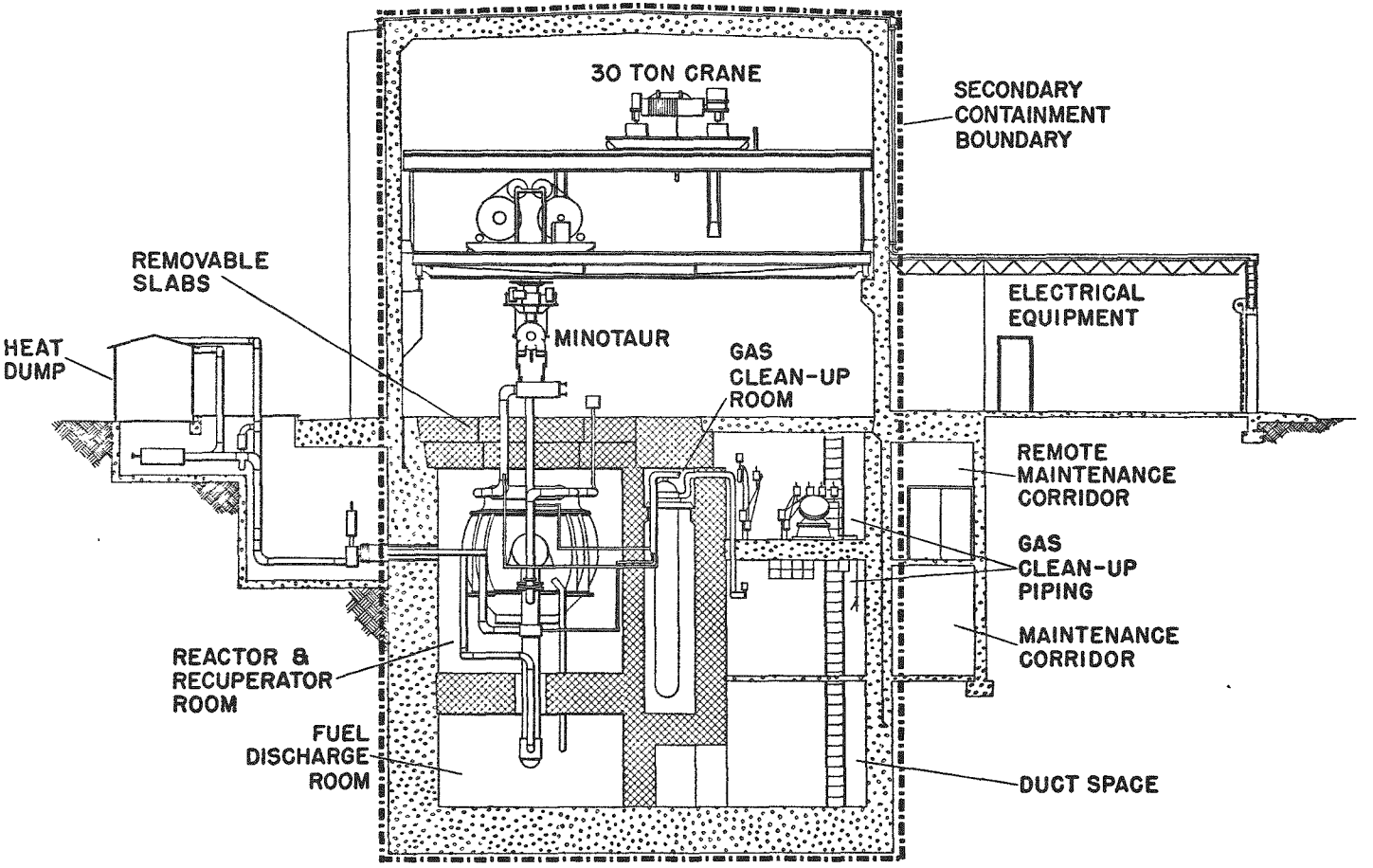

Fig. 3.5 Building section through reactor-recuperator room

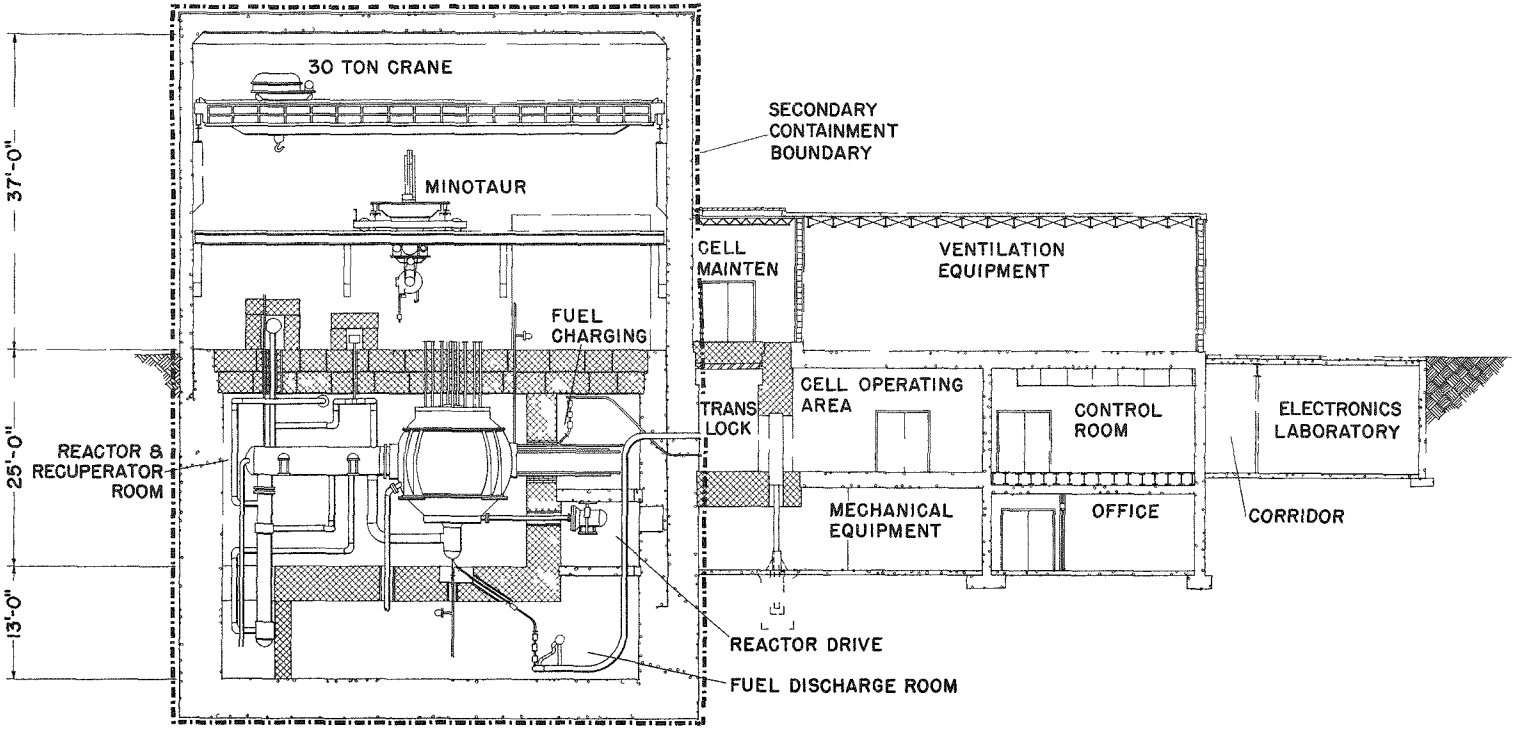

Fig. 3.6 Building section through control room

The major part of the containment portion of the building extends above grade in a superstructure that has inside dimensions of 46 ft x 56 ft x 37 ft high and encloses a free volume of 94,000 ft^3. This superstructure is designed to withstand the internal pressure that would be generated by a failure of the primary containment. To ensure gas tightness of the superstructure, a liner made of welded steel plate covers the inside walls and roof. Below grade, this steel membrane extends within the walls to the base of the building on the two sides adjacent to habitable portions of the structure and to 5 ft below grade on the two outside walls.

Operating within the superstructure are MINOTAUR, the remote maintenance machine described in Sec. 7.3 and a 30-ton bridge crane. Both machines can be controlled from within the secondary containment superstructure or from outside it, in the remote maintenance corridor.

3.1.1 Reactor and Recuperator Room

The reactor, primary coolant loop, and fuel loading equipment are located below grade in a shielded cell, approximately 18 ft x 48 ft x 38 ft deep, with a total free volume of 24,000 ft^3. The top of this cell consists of removable concrete shielding slabs that permit access to the reactor and coolant system. Penetrations in the shielding exist for control rod drives, nuclear instrumentation, sampling and survey ports, fueling apparatus, coolant lines, ventilation, and utilities. Near the reactor and primary coolant loop, the walls of the cell are covered with water-cooled panels that remove heat radiated from the surfaces of hot containment vessels.

3.1.2 Helium Purification and Storage Rooms

The gas cleanup system and the associated storage system are housed in three other below-grade rooms inside the secondary containment. Overall dimensions of these three rooms are 21 ft x 50 ft x 38 ft deep; total free volume is 30,000 ft^3. The gas cleanup room, a long, narrow pit with magnetite concrete walls and removable shielding slab covers, contains

suspended oxidation and adsorption units, heat exchangers, and storage tanks, all of which will accumulate deposits of fission products. Interconnecting piping extends over the edge of the pit to valve manifolds and compressors located in the upper gas cleanup piping room. MINOTAUR has access to the upper part of this region after cover slabs are removed with the 30-ton crane. In the lower piping room are located equipment, piping manifolds, and valves for clean helium, cooling water, refrigerant, and air systems. Contact maintenance work can be performed in this lower room while the reactor is shut down.

3.1.3 Fuel Discharge Room

Fuel elements discharged from the reactor drop through a line that penetrates the bottom floor of the reactor cell at an angle and enters the well-shielded fuel discharge room in the subbasement level of the reactor building. In this room, the elements pass through the outlet gas lock valves and enter a conveyor that travels up through the reactor drive room and the fuel charging room to the transfer cell.

Adjacent to the fuel discharge room are the duct space, through which ventilation conduits return to the filters, and the bottom of the pit in which rest the helium storage tanks.

Access to this entire region will be allowed only when the reactor is shut down and, even then, will be carefully controlled to limit exposure.

3.2 Operating and Control Areas

Building design provides for unlimited access to operating and control areas on three floors outside the secondary containment. On the gound floor, Fig. 3.2, are ventilation and electrical equipment rooms, a boiler room for site heating equipment, and the exhaust filter room of the operating and control areas ventilation systems.

On the first subgrade floor, the operating level, Fig. 3.3, comprises

a clean area and a control area. In the clean area are the control room, operations office, and maintenance laboratories. Access to the control area is through a hall that passes the health office to a locker room, where personnel must change clothes. From the locker room, personnel may enter the operating area serving the fuel transfer cell and the transfer lock, and continue on to the remote maintenance corridor. The corridor provides access to the exhaust filter room, on the upper level, during reactor operation. When the reactor is shut down, the stairway at the end of the corridor may be used to go to the basement and ground levels where gas-tight doors open into the secondary containment enclosure.

At the basement level, Fig. 3.4, unrestricted access, by way of the western staircase, is limited to the office and electrical equipment areas. The mechanical equipment and sump rooms, where the possibility of radioactive contamination exists, are accessible through the maintenance corridor by way of the eastern staircase, entered from the operating level only.

3.2.1 Fuel Transfer Cell and Lock

Fuel elements move into and out of the reactor through the fuel transfer lock and cell which are shown in Fig. 3.3. New fuel elements may enter, and spent elements leave, inside casks that travel on rails between a loading dock and the transfer lock. The casks pass through a 20-in.-thick cast Meehanite outer door that moves on hydraulic lift and locking mechanisms operated from the basement. When a cask is inside the lock and the outer door is pneumatically sealed, an inner door between the lock and cell can be opened. Manipulators move elements between cask and cell under the control of operators who work before viewing windows in the cell operating area. Sequential interlocks prevent the premature opening of cell doors, and special cell-ventilating systems prevent the spread of particulate matter outside the cell or lock when the doors are opened.

Inside a dry box in the transfer cell are the inlet and outlet of the fuel handling system, described in detail in Chap. 6.

3.2.2 Remote Maintenance Corridor

Along the inner walls of the remote-maintenance corridor are control stations for MINOTAUR and the 30-ton crane. Set into the walls are three viewing windows through which can be seen the interior of the gas cleanup piping room, where the gas cleanup system valve manifolds, compressors, and analytical instruments are located. From the corridor, operators can carry out, with the aid of MINOTAUR and a Model A master-slave manipulator, adjustments and minor repair of components while the cleanup system is operating and more extensive repairs when the system is down. Through combined operation of MINOTAUR and the crane, entire piping manifolds, process vessels, and instrument components can be removed and replaced without exposure of the operators.

4. REACTOR

4.1 Mechanical Design

4.1.1 General Description

The reactor, illustrated in Fig. 4.1.1.1, comprises a vertical, cylindrical core, surrounded by a reflector and insulation, encased in a spherical pressure vessel. Control rods enter the vessel from above. Fuel elements are charged through the side and discharge from the bottom. At full power, the reactor delivers 3 MW of heat to helium coolant flowing at the rate of 10,250 lb/h at 500 psia. Under maximum design conditions, the coolant enters the reactor at 1600°F and leaves at 2400°F.

Container for the reactor is a 13.16-ft-i.d. carbon steel pressure vessel. Its 1.75-in. wall thickness is designed for a maximum wall temperature of 650°F at a pressure of 550 psia.

The core, in which graphite serves as structural material and moderator, is a hollow vertical cylinder, 70-in. o.d. x 23-in. i.d. x 39-in. high. Fuel channels are 1.1-in.-diam radial holes bored through the cylinder wall at 15° intervals in 13 horizontal planes. The vertical separation of adjacent fuel channels is 3 in. center-to-center. Surrounding the core is the 16-in.-thick reflector, 4 in. of graphite and 12 in. of dense, ungraphitized carbon. Between the reflector and the pressure vessel is rigid, low-density carbon insulation. The hollow, axial region of the core is filled with a graphite plug, tapered from 22-in. diam at the top to 20-in. diam at the base of the core. The taper leaves a plenum between the plug and core, through

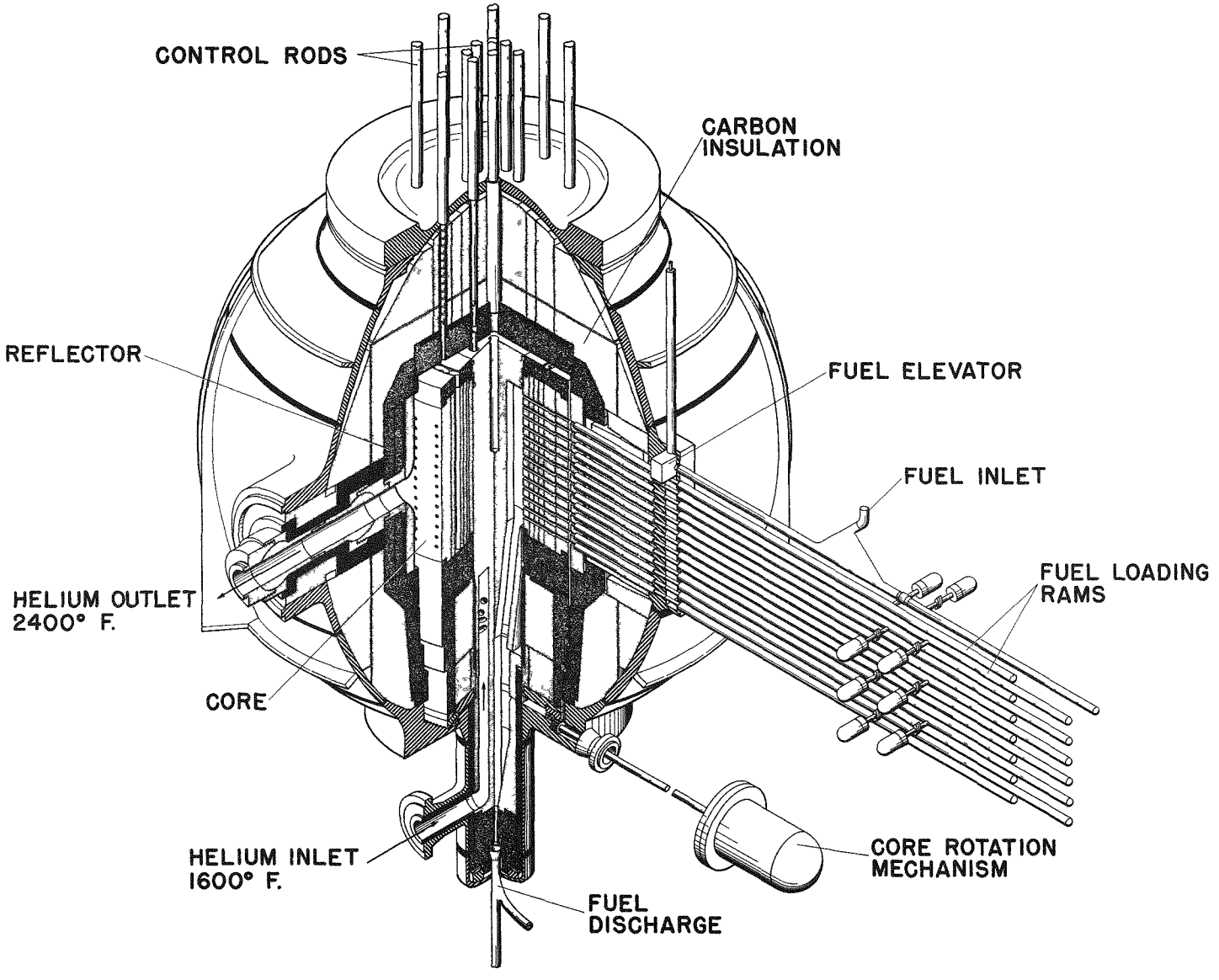

Fig. 4.1.1.1 UHTREX reactor

which the helium coolant enters the fuel channels. All of the core, together with portions of the reflector and insulation, can be rotated about the cylindrical axis to accomplish fuel loading and unloading. This movable portion of the reactor is mounted on a column of dense carbon that rests on a steel plate and thrust bearing at the bottom of the pressure vessel.

Fuel elements are unclad, hollow graphite cylinders, 1-in. o.d. x 0.5-in. i.d. x 5.5-in. long, loaded with highly enriched uranium. Four fuel elements rest end-to-end in each of the 312 fuel channels to make a total of 1248 elements in a complete core loading.

A fuel loader, mounted on the side of the pressure vessel, moves fuel elements into the core. The loader, essentially a vertically-aligned series of horizontal motor-driven rams, operates in conjunction with an indexing mechanism that rotates the core. While the reactor is operating, a particular fuel channel may be loaded by one of the 13 loading rams after the core is indexed to one of the 24 radial channel positions. As a new fuel element is charged, a spent element is displaced into a slot in the center of the core, falls out of the reactor, and is mechanically conveyed to a fuel-handling cell.

Two sets of control rods regulate the nuclear operation of the reactor. A central set of eight plug rods is arranged within the stationary central graphite plug in a circle whose diameter is 16.25 in., centered on the vertical axis of the core. The poison in the plug rods is boron carbide, compressed into disks that are strung on a central niobium rod and enclosed in an outer niobium tube. The second set of four core rods is arranged, equally spaced, in a concentric circle of 47-in. diam within the movable portion of the core. In order that the core rods can be inserted when, if ever, the core is not in proper alignment with the reflector, the rods are articulated and the core has 24 rod holes, each flared at the top. The core rods are machined from type 304 stainless steel alloyed with 1 wt/% of boron-10.

Helium coolant enters at the bottom of the reactor, flows up through a flow distributor into the plenum around the central plug, passes through the fuel channels, collects in an annular plenum around the outside of the movable core, and leaves the reactor through a graphite pipe at the side.

4.1.2 Pressure Vessel

A carbon steel sphere approximately 13.5 ft in diameter, the reactor pressure vessel contains the core, moderator, reflector, and associated insulation; it supports externally the fuel loader and unloader mechanisms and the control rod drives. The vessel and the units attached to it form a major part of the primary containment for the helium coolant, which enters the vessel through a nozzle at the side of the bottom appendage and leaves through the recuperator nozzle at the vessel's horizontal center line. Figures 4.1.2.1 through 4.1.2.3 depict the pressure vessel.

At the top of the vessel is an opening through which the reactor structure was inserted. The opening is closed by a forged top cover, bolted with 48 studs to a grooved flange and sealed with a C-section ring that is welded outside the bolt circle to both the cover and flange. Each stud is covered with a "bull plug," which screws into and is seal-welded to the top surface of the cover. Seventeen 3-in.-diam tubes are welded into the central part of the cover, but only 12 of them will be used to support the control rod drives. These tubes and the rod drive housings are leak-tight extensions of the primary containment, open at the reactor end to the primary coolant.

On one side of the pressure vessel, at its horizontal center line, is a 50-in.-o.d. nozzle to which the recuperator pressure vessel is connected by a bolted flange that is sealed with a C-section ring joint. The recuperator vessel, which rests on its own support, does not transmit a load to the reactor vessel.

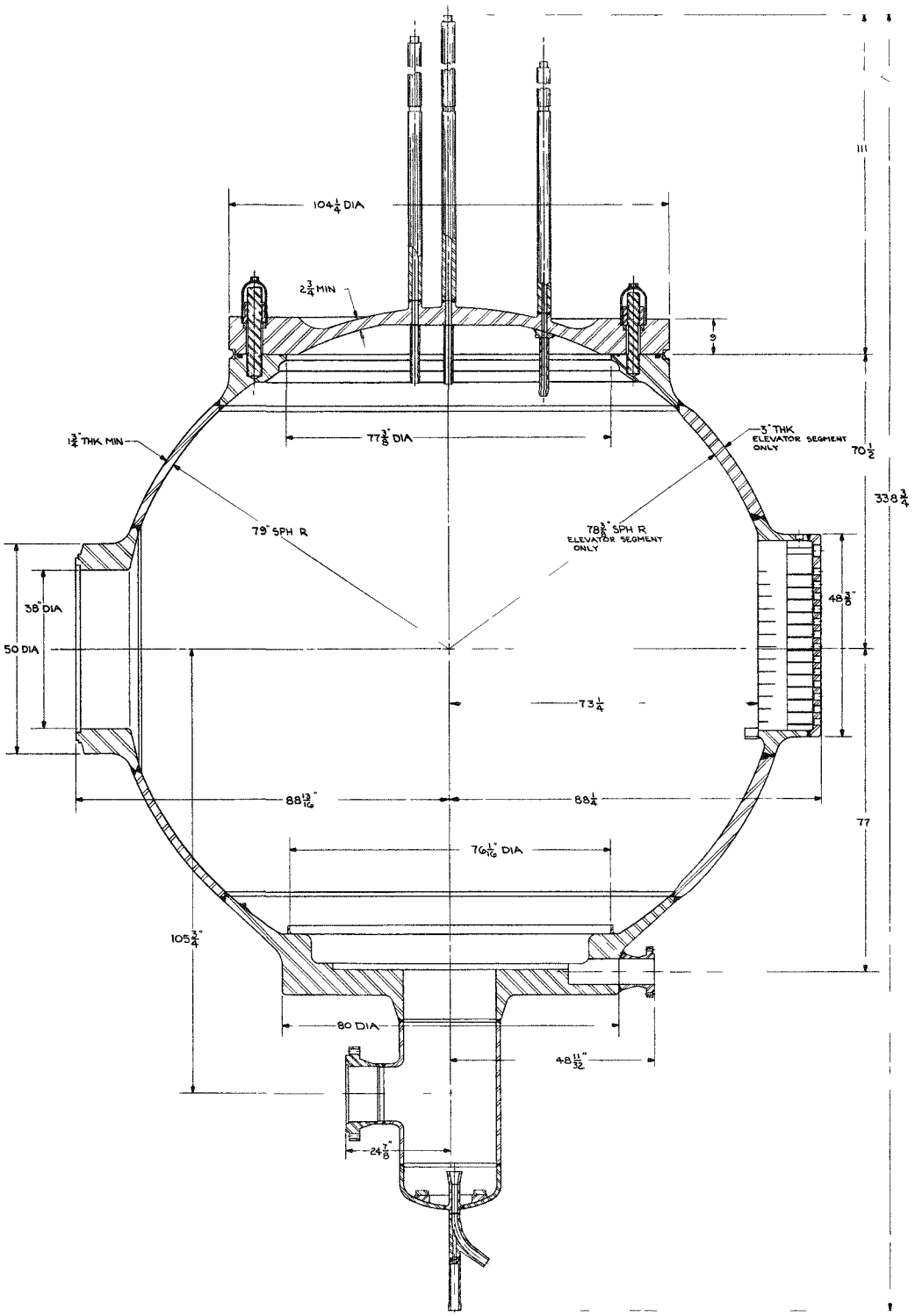

Fig. 4.1.2.1 Cross section of reactor pressure vessel

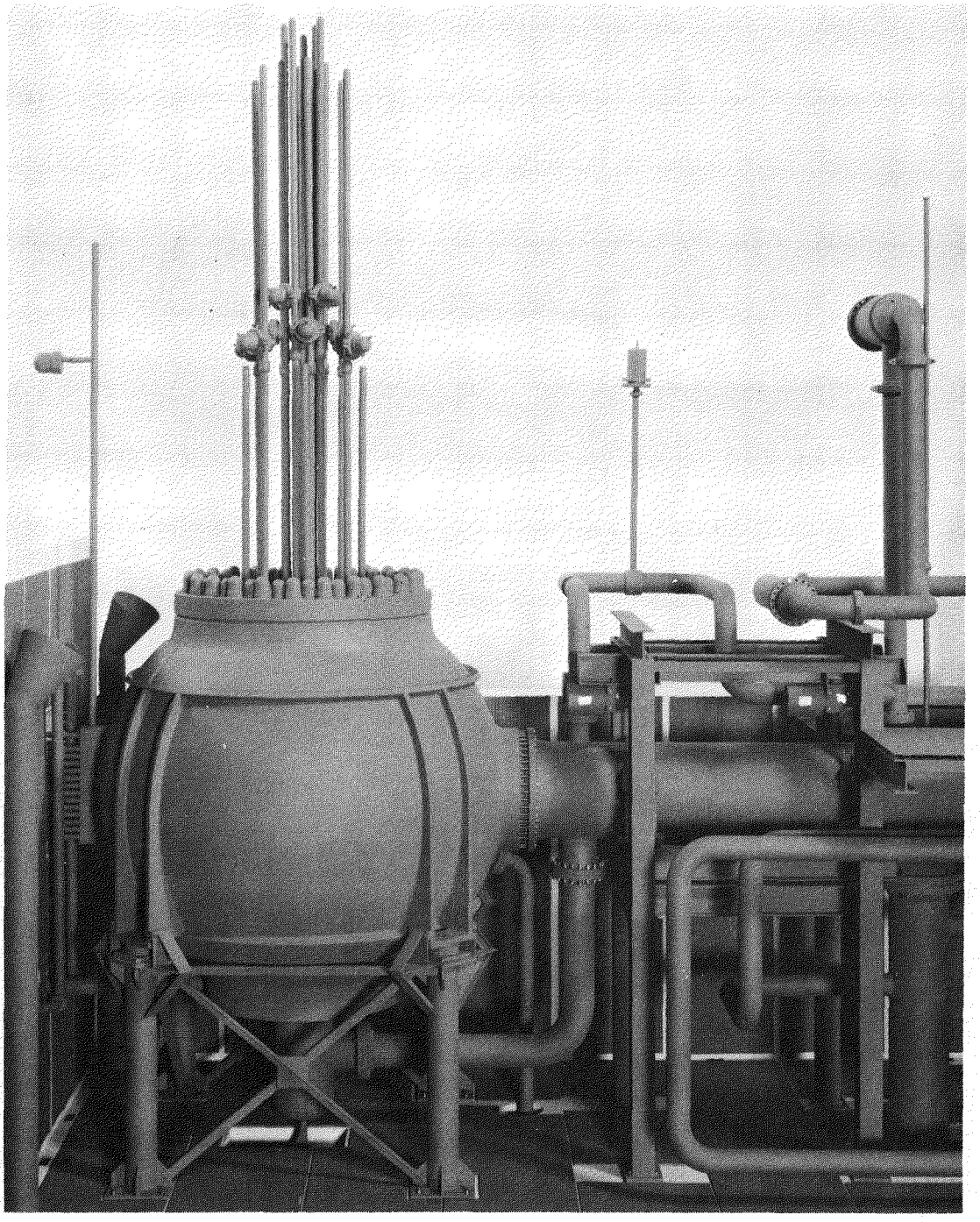

Fig. 4.1.2.2 Side view of reactor vessel, from model

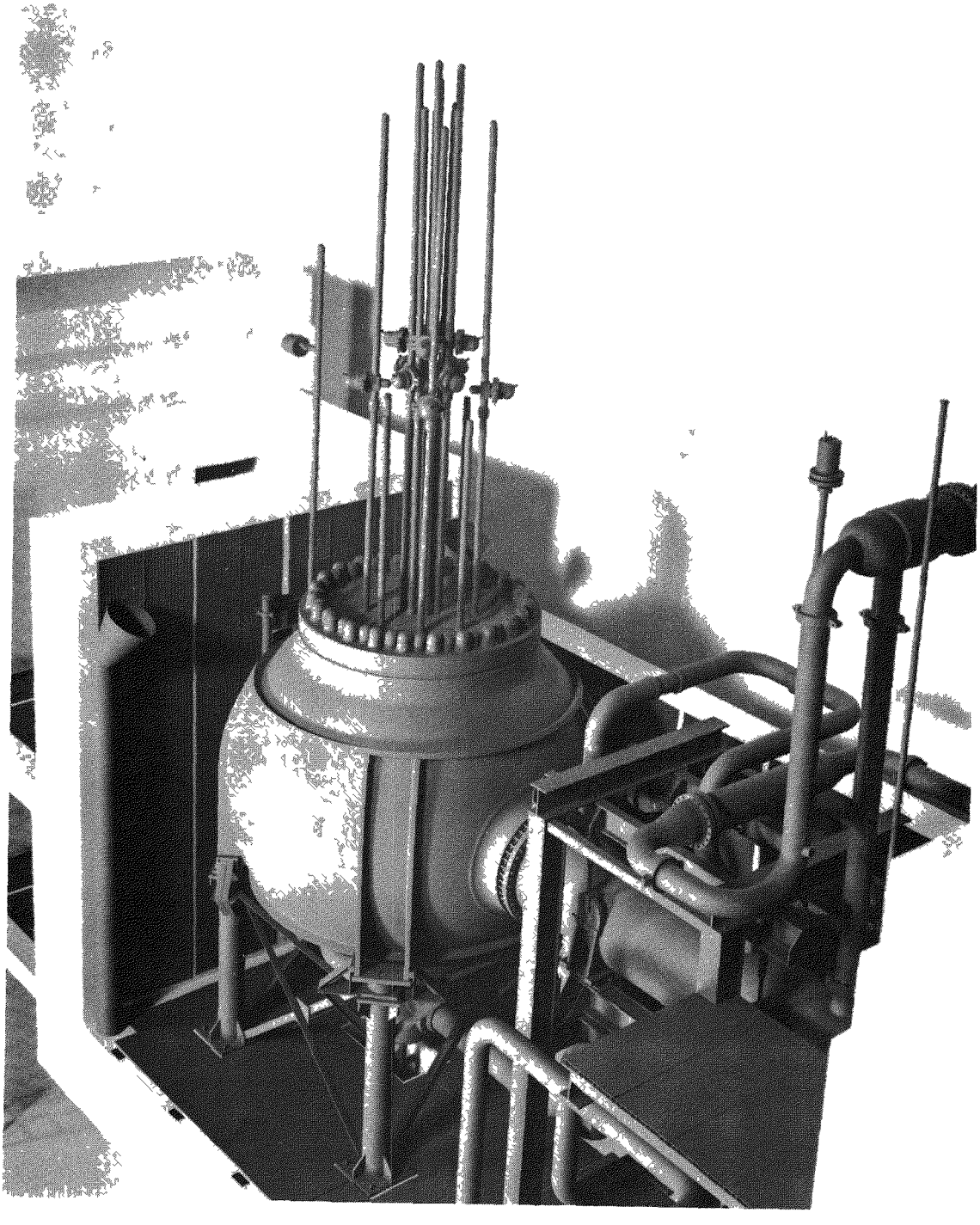

Fig. 4.1.2.3 Top view of reactor vessel, from model

Opposite the recuperator nozzle is the fuel elevator housing, a carbon steel forging welded into a segment of the pressure vessel, which is made of plate approximately twice as thick as that in the rest of the vessel. A tube that supports the elevator drive is threaded and seal-welded to the top of the elevator housing, and 14 tubes that support the fuel loader are threaded and seal-welded to the side. Like the control rod assemblies, the tubes and housings for the fuel loading mechanisms are a part of the primary containment.

At the bottom of the reactor vessel, the massive forging in which the core support bearing is mounted has two appendages. On the side is a nozzle terminated by the bolted, seal-welded flange which joins the indexing mechanism housing. At the bottom is a cylindrical extension, with a side nozzle joined to the helium inlet line and a dished bottom head penetrated by the fuel discharge pipe. The side nozzle joint is made with another set of bolted flanges with a seal weld.

The final penetration of the reactor vessel wall is made by a 6-in.-diam nozzle adjacent to and below the recuperator nozzle. Joined to the smaller nozzle is the pipe through which the thermocouple leads leave the reactor vessel. A bolted joint with a welded seal connects the pipe to the vessel.

The weight of the reactor vessel and the components it supports is borne on two horizontal support ribs and four sets of vertical support ribs, all welded to the vessel outer wall. The sets of vertical members terminate in brackets that rest on pads supported by four reactor support columns that are bolted to the reactor cell floor. The pads, which have spherical thrust bearings, are designed to allow relative movement between the column tops and the support brackets as the reactor vessel expands and contracts. Movement is restrained by bolts in oversize holes.

Design Basis - The reactor vessel was designed to conform with the requirements of the ASME Boiler and Pressure Vessel Code, Section

VIII, with revisions, addenda, and special cases, including 1270 N. The objective was to fabricate a reactor vessel with a useful life of 3 years under operating conditions specified below.

Design conditions for the vessel are listed in Table 4.1.2.1. Care was taken in the design and fabrication to minimize stress concentrations at changes in section or penetrations. Fillet radii are equal to at least half of the thickness of the thicker of the two sections being joined. No corrosion allowance was required.

Operating Conditions - Portions of the ASME code require that certain aspects of the vessel design be evaluated under the extreme operating conditions to be expected rather than under the general design conditions. The operating conditions used in the design analysis are defined below.

1. Hydrostatic and Pneumatic Pressure Tests - In addition to withstanding the shop hydrostatic pressure testing at 825 psia required by the Code, the vessel was designed to withstand a pressurization of 688 psia during the primary loop pneumatic test. This second test will be conducted at ambient temperature during the preoperational checkout of the assembled coolant system.

2. Startup and Shutdown Operation - The vessel was designed to withstand 1000 standard startup and shutdown cycles during which the power level ranges between 0% and 100%. It was assumed that steady state conditions exist before each startup or shutdown is initiated.

3. Pressure and Temperature Fluctuations at Steady State - According to the Code specification for A212 Grade B steel, used in the reactor vessel, a significant pressure fluctuation, during operation at design temperature and pressure, is defined as a pressure variation greater than that calculated from the following expression,

$$\text{Design pressure} \times 1/3 \times S/S_m$$

where S is the allowable amplitude of alternating stress intensity and S_m is the design stress intensity value. For the reactor vessel, this defined significant pressure fluctuation is 127 psi.

TABLE 4.1.2.1

REACTOR VESSEL DESIGN CONDITIONS

Pressure	
Internal	550 psig
External	0 psig
Temperature	steady state temperature distribution, See Fig. 4.3.1.4
Mechanical Loads	
Component Weights	
Reactor vessel	74,000 lb
Top cover	22,000 lb
Core parts	94,000 lb
Rod drives	2,500 lb
Recuperator, shared load	10,000 lb
1600°F pipe, shared load	3,500 lb
Total	206,000 lb
Bolt Prestress	
Top cover	28,000 psi
Recuperator nozzle	29,000 psi
Coolant inlet nozzle	12,000 psi
Pipe Reactions	
Horizontal component	8,403 lb
Vertical component	12,376 lb
Moment about horizontal axis	53,433 ft-lb

A significant temperature fluctuation is defined as one which exceeds that calculated from the expression

$$\frac{S}{2E\alpha},$$

where E is Young's modulus and α is the coefficient of thermal expansion. A significant temperature fluctuation for the reactor vessel is, thus, 30°F.

During steady state reactor operation, the pressure fluctuates 50 psi and the temperature fluctuates less than 20°F. Since neither of these fluctuations is considered significant, the vessel is considered capable of withstanding an infinite number of fluctuations without suffering any fatigue damage.

4. Fluctuations Produced by Transients - The conceivable transient that would have the most radical temperature effect on the reactor would be produced if the helium coolant flow rate in the primary loop were to be doubled. If, for purposes of analysis, the flow is doubled, the gas temperature at the reactor outlet shows an immediate increase of 150°F and the rise at the reactor inlet is 50°F. The corresponding temperature changes in the metal surrounding the outlet and inlet are 27°F and 12°F, respectively. Since these temperature fluctuations are below the 30°F "significant temperature fluctuation" defined for the material, an infinite number of transients of this type can be accommodated without damage to the vessel.

5. Temperature and Pressure Limits - During operation at design power, the maximum temperature of the reactor vessel is 600°F. Internal pressure is limited to 520 psia by a pressure regulation system that is backed up by a blowdown valve that opens at 550 psia. Sufficient helium storage capacity exists to allow an immediate reduction in primary coolant pressure to 140 psi.

6. Nil Ductile Transition Limit - In A212 Grade B steel, changes in the nil ductile transition temperature occur at 2×10^{18} nvt. At the point on the reactor vessel where the flux is greatest, the total

dose for neutrons above 0.9 MeV is 2 x 10^{17} nvt for 3 year's operation with 100% load factor. Since the calculated dose is approximately an order of magnitude below the damage limit, no plans have been made to continue the determination of nil ductile transition temperature past the tests used for quality ensurance on the vessel material during manufacture.

4.1.3 Reactor Structure

The many component parts of the reactor structure appear in Fig. 4.1.3.1, assembled inside the reactor pressure vessel.

The movable core, shown with its associated parts in Fig. 4.1.3.2, is a vertical graphite cylinder, 70-in. o.d. x 23-in. i.d. x 39-in. high, fabricated from six nested, concentric, hollow cylinders. The cylinders, designed to limit thermal stresses across each monolithic piece of graphite, are keyed to a dense carbon ring at the top and rest on a column of joined pieces of carbon. The column base bears on a stainless steel plate mounted on a large-diameter ball bearing in the bottom of the reactor vessel. Fuel channels drilled through each nested core cylinder are flared at the outer edge to accommodate vertical misalignment between cylinders.

The stationary plug in the center of the core, shown with the reflector in Fig. 4.1.3.3, is a single tapered piece of graphite slotted on one side to receive spent fuel elements and bored at the bottom for the coolant inlet channel. The plug rests on other fitted pieces of graphite that are bored to direct the fuel elements downward and to distribute the coolant laterally. These pieces are, in turn, supported inside a steel bell welded to the bottom of the reactor vessel. Graphite felt and crinkled metal foil insulation separate the hot graphite parts from the steel walls of the bell.

Graphite and dense carbon parts of the reflector (4 in. of graphite and 12 in. of carbon) are segmented to minimize stresses and facilitate assembly. A layer of graphite felt, visible in Fig. 4.1.3.3, limits

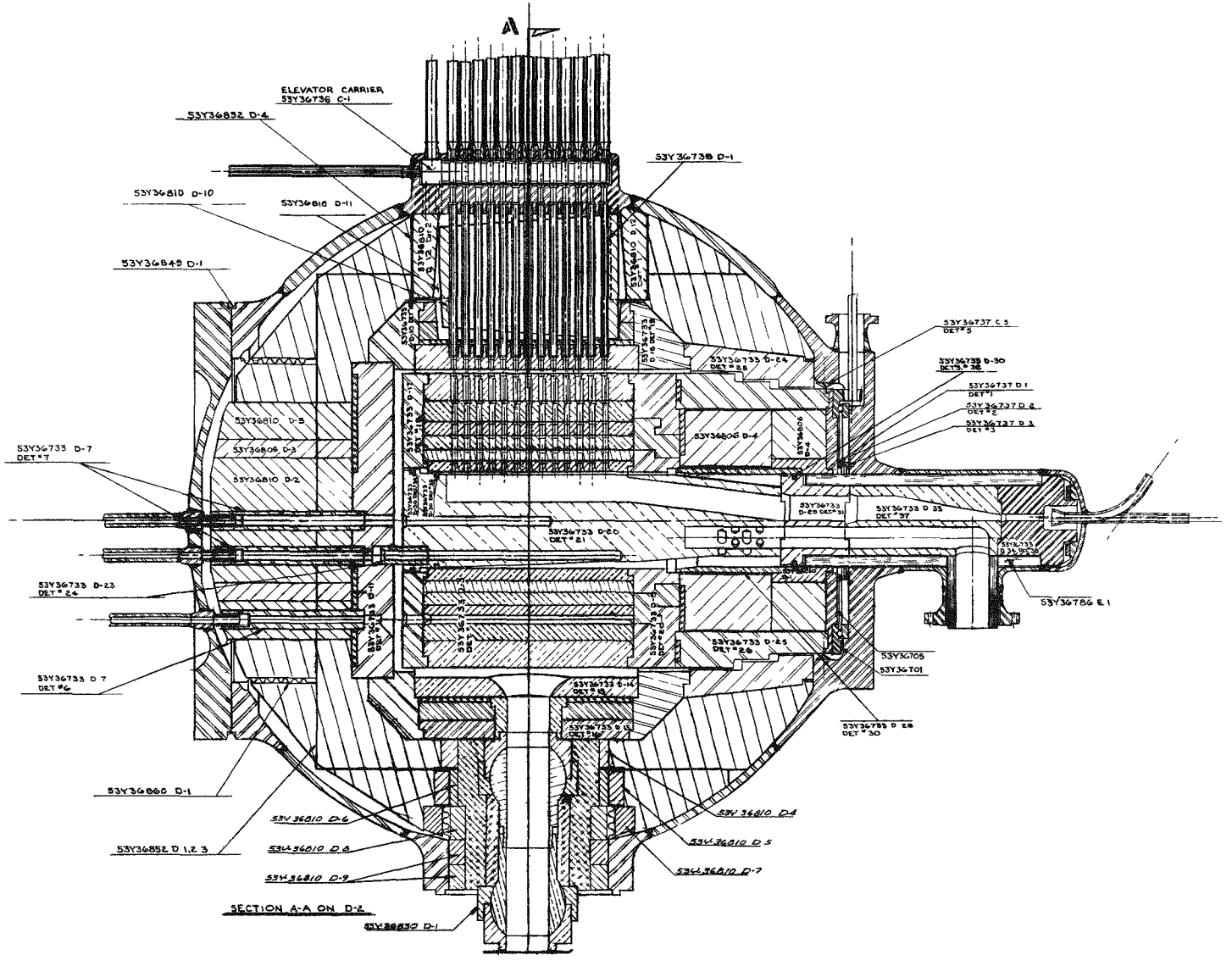

Fig. 4.1.3.1 Reactor core assembly

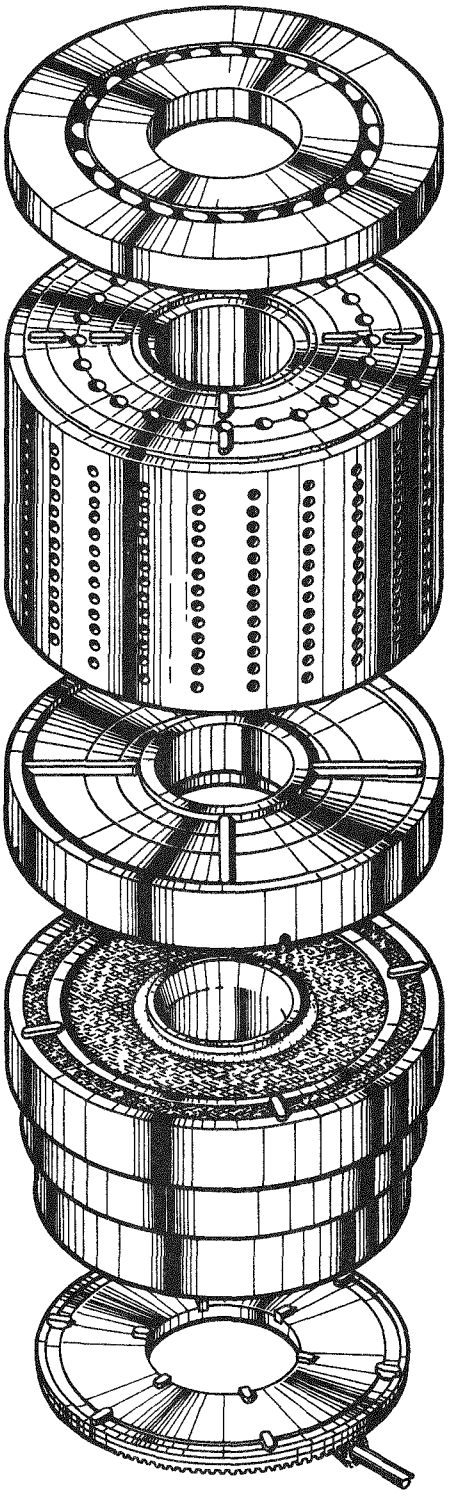

Fig. 4.1.3.2 Exploded view of core assembly

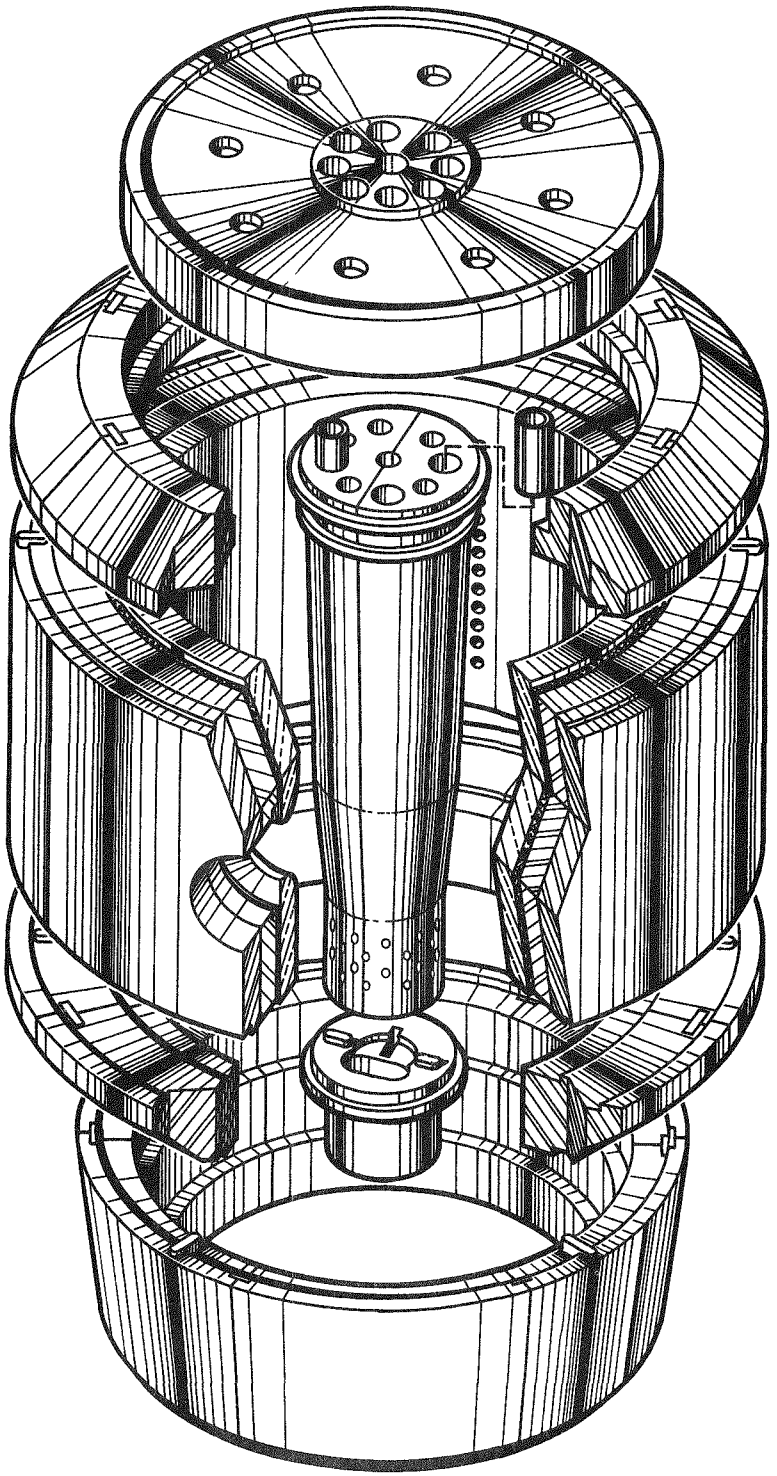

Fig. 4.1.3.3 Exploded view of core plug and reflector

the flow of heat past the innermost layer of the reflector. The segments bear directly on the pressure vessel at the bottom and are supported by porous carbon bricks supported by the top reflector. Ample clearance exists between the carbon bricks to prevent the transmission of expansive forces to the pressure vessel.

Mechanical Design Analysis - Graphite is an effective moderator, and it has adequate mechanical strength at high temperatures. However, the use of graphite and carbon as structural materials introduced problems in material selection, structural integrity, and coolant flow control. Each set of problems was solved, and the solutions are described below.

1. Materials - Three characteristics were required of the graphite and dense carbon parts that make up the core and reflector: a low concentration of neutron absorbing impurities, high density, and a high degree of isotropy.

Since neutron economy is not so stringent a requirement in UHTREX as in power producing reactors, the maximum boron content in the graphite and dense carbon was set at 1.5 ppm, and ash content was limited to 0.7 wt/% for the graphite or 2.0 wt/% for the carbon. The material, Union Carbide's Type CG-L, was manufactured under these standards at a price lower than that for the usual, higher purity, nuclear grade materials, but according to the nuclear grade manufacturing procedures. Final analysis of molded graphite stock showed boron concentrations over the range of 0.9 to 1.5 ppm, and ash contents ranged between 0.12 and 0.56 wt/%.

The use of graphite and dense carbon for neutron moderation and reflection, as well as for structural materials, demanded high density in both materials. A minimum bulk density of 1.65 g/cm^3 was required, and the following density ranges were produced: 1.73 to 1.80 g/cm^3 for the graphite stock and 1.72 to 1.78 g/cm^3 for the dense carbon stock.

Isotropy in graphite and dense carbon can be improved by proper choice of the size and shape of the carbon particles from which the stock pieces are made, and by the use of molding rather than extrusion processes to form the stock pieces. The base material for UHTREX stock was petroleum coke, selected for its random distribution of particle shapes and screened to produce a maximum particle size of 0.032 in. for graphite pieces and 0.065 in. for carbon pieces. After the stock pieces were molded and baked, reactor components were machined from the stock to yield finished pieces whose vertical axes, when assembled into the reactor, coincide with the direction of molding force application to the stock pieces. As a result of this care in preparation, all pieces made from the same material have a reasonably uniform coefficient of thermal expansion in the radial direction and also in the vertical direction, although the two directional coefficients are slightly different.

The nuclear requirement for high density is compatible with mechanical requirements for strength; the two properties are directly related. To insure uniform, high strength in the finished pieces, material specifications required that test specimens be taken, both with the grain and against it, from each end of each stock piece. Before a stock piece was accepted, its samples passed a flexure test with minimum strength requirements of 1350 psi for graphite and 1700 psi for dense carbon. Flexural strength, which can be tested more readily in carbonaceous samples, is directly related to tensile strength. For the UHTREX tests the ratio of flexural to tensile strength was very near 1.5. Therefore, minimum ultimate tensile strengths were taken to be 900 psi for graphite and 1300 psi for dense carbon. Compressive strengths, which are known to be two to three times the tensile strengths in these materials, are not limiting in any of the components.

At the time that the core design was prepared, there were no empirical data for a prediction of the radiation-induced dimensional changes in UHTREX graphite and carbon. Therefore, a contraction of 1.5% was defined for design use. Subsequently an irradiation program at Battelle Memorial

Institute/Pacific Northwest Laboratories produced data[1] which indicate that a contraction of 1.2% in the carbon components and 0.3% in the graphite may be expected.

2. Structural Integrity - To accommodate the moderate physical strength of the graphite and carbon parts, to allow for their relative movement during thermal cycles, and to compensate for radiation-induced dimensional changes, the reactor design uses many massive pieces held together by keys in slots, pins in holes, and bosses in counterbores, many of which appear in Figs. 4.1.3.2 and 4.1.3.3.

By careful design, advantage was taken of the differences in thermal expansion coefficients between the reactor and pressure vessel materials. In the central regions of the core, where the temperatures reach the highest levels, the thermal coefficients of the materials are the lowest, and, moving away from the center, the coefficients increase as the temperature drops. As a net result, the expansion of the reactor along its vertical axis very nearly matches the expansion of the steel pressure vessel in the same direction. Furthermore, in the radial direction, the displacement of the control rod holes in the core very nearly equals that of the matching holes in the upper carbon reflector and the vessel top cover. Nevertheless, generous allowances were made in the design to accommodate relative movement between reactor and vessel. As an example, the fuel loader can function despite a vertical displacement of ± 2 in. between the core and the loader housing in the vessel wall. The Graph-i-tite G guide tubes and the carbon housing that surrounds them, can pivot as the differential movement occurs. In the radial direction, the dimension between the core and vessel wall can change ± 1 in. without interference in the loader operation. Another critical connection between core and vessel exists at the coolant exit pipe. There, a double, spherical, ball joint easily accommodates a ± 1-in. radial displacement and can contract or expand 2 in. from the cold position.

---

[1]J. W. Helm, "Effect of Neutron Irradiation on UHTREX Graphite and Carbon," BNWL-191, February 1966.

The simplest design for the core would have been a single, massive, hollow cylinder, but the high thermal stresses that would develop in a monolithic core forced the use, instead, of six concentric, nested cylinders. For the same reason, the cylindrical portions of the outer reflector and of the lower reflector are divided into three concentric cylinders. In each of these components, mating diameters were sized to allow for thermal and radiation-induced changes in dimensions plus, in some instances, additional clearances that allow for the bending that is induced by thermal gradients.

Because the overall size of many of the cylindrical components exceeded both the size of commercially available stock pieces and the size of the opening into the vessel, the components were divided into segments. The vertical joints between the segments that make up a cylinder are made with single-piece keys, I-shaped in cross section, that fit into slots milled along the adjoining faces of the segments. The keys limit relative motion between segments to a maximum of 1/8 in., but permit the relief of constraint stresses.

Each piece of carbon and graphite is joined to the component upon which it rests by means of a locating boss and counterbore. (Typical joints can be seen in Fig. 4.1.3.2.) Adequate clearances accommodate thermal expansion and radiation-induced dimensional changes. In some instances, the clearance is large enough to permit the eccentric movement of a cylindrical piece with respect to its mating piece. To keep the components concentric and to prevent relative lateral movement, close fitting radial keys are employed. The keys fit into slots milled into the adjoining component faces. When heat causes components to expand, the radial keys direct the movement uniformly about the geometric center of the core.

Features of the reactor design ensure that the control rods can always enter the core from the rod housings that are mounted on the reactor vessel cap. Both sets of rods move inside oversize, dense-carbon tubes through the insulating carbon blocks above the reflector.

At their upper ends, the tubes connect to the rod openings in the vessel with bellows, which allow relative movement. At their lower ends, the tubes are inset in the reflector. Three other tubes made of graphite join the reflector to the central core plug, where the plug rods come to rest. To guide the core rods into place, if the core should be displaced from its normal, registered position, funnel-shaped openings are machined into the bottom face of the reflector and the top face of the core. The configuration of a core rod (described in Sec. 4.1.7) as it enters the displaced core appears in Fig. 4.1.3.4. The funnels on the top of the core, which feed into 24 holes that can receive the rods, join each other in a sharp ridge. When the rounded end of a core rod reaches the core, it comes into contact with the side of one of the funnels and is directed into a hole. If the core is in the worst possible position for rod insertion, the spherical rod end contacts the sharp ridge between funnels and is deflected into either one or the other of the corresponding holes which are too far removed from the next control rod position to have already accepted a rod. Tests run on a mockup of the core and a core rod demonstrated, in thousands of cycles, that a rod impacting on the ridge invariably enters a hole. During the tests, the rod was dropped from a position that was misaligned 7/8 in. radially, an inconceivable occurrence in the reactor, but the rod continued to enter a hole. Tests also demonstrated that the core can be moved 18° with a core rod in place before the rod segments began to bind against the sides of the core hole.

The core and reflector assemblies stand on the core bearing plate and on the bottom of the reactor vessel. Between these assemblies and the walls of the vessel, wedge-shaped bricks of insulating carbon are fitted in uncemented layers of concentric rings. The joints in alternate layers are staggered. In the lower two-thirds of the reactor, the bricks fit closely between the inner assemblies and the wall but do not transmit forces between them. Above the core, gaps between the bricks

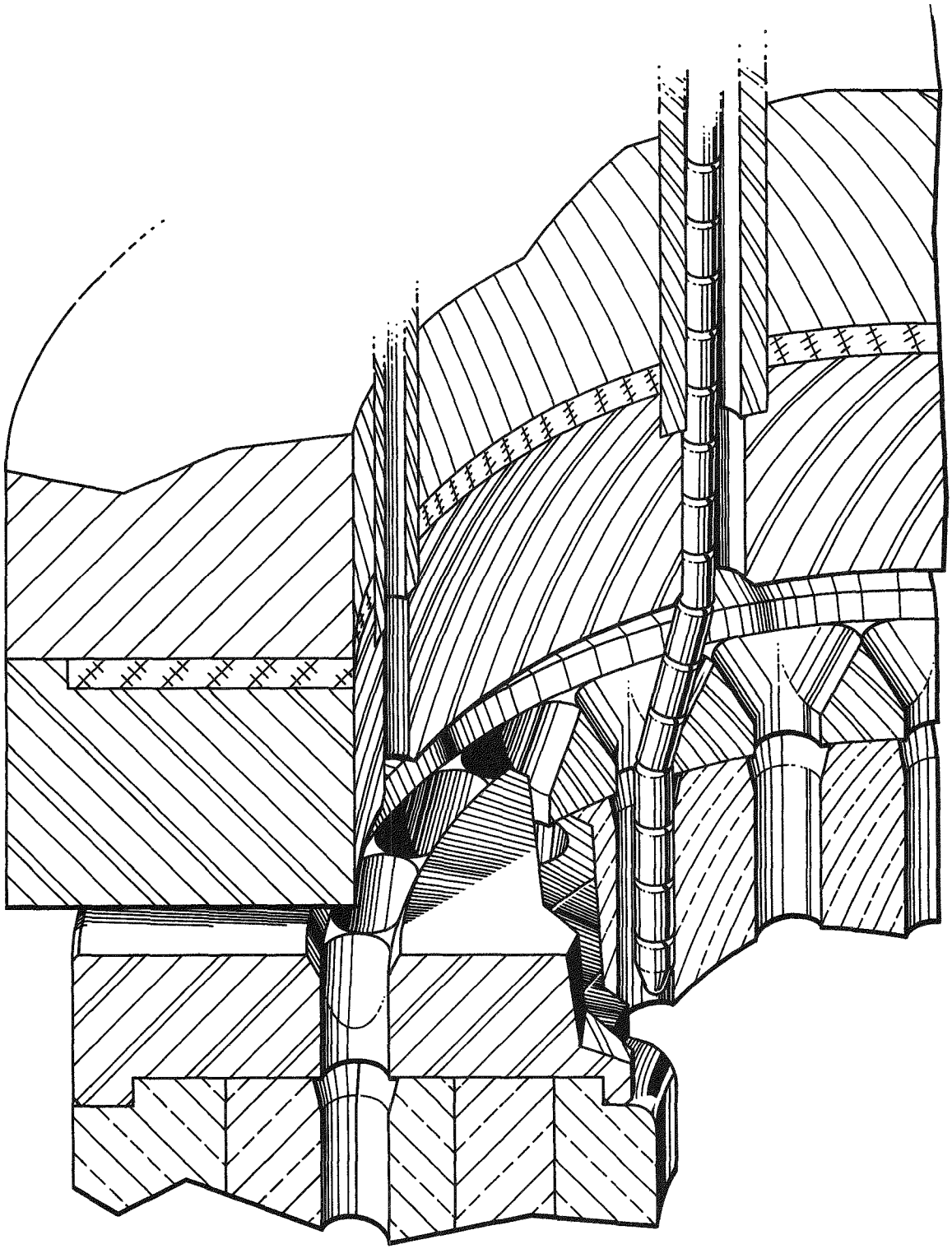

Fig. 4.1.3.4 Core rod in displaced core

and the vessel allow relative movement to occur as the core heats up more rapidly than the vessel.

The dimensions of the core and reflector assemblies were checked twice before they were finally installed in the reactor. During the second preinstallation assembly, made at the time of the UHTREX critical assembly experiment, keys were machined and installed for precise alignment of the parts. Dimensional checks showed that the top surfaces of the core and the top reflector were parallel to the bearing plane within 0.004 in./ft, and that the core run-out during rotation was a maximum, at the top, of 0.048 in. total. Alignment of the fuel channel holes, drilled through the six nested cylinders of the core, was checked with straight gauge rods. The six, individual, 1.100-in.-diam holes that make up each channel were found to have the same centerline within 0.015 in.

Although the reactor design minimizes the probability of a component failure, the possibility exists and was recognized by the designers. The most probable mode of failure is the propagation of a crack through a line of fuel channel holes in a core cylinder or between the upper and lower keyways in other components. If an inside core cylinder should crack, pieces would be confined by the adjacent cylinders. Should either the inner or outer core cylinder break, it is unlikely that any sizeable pieces would move, because the ends of both cylinders are confined inside the rims on the reflector base and top piece. In either case, the crack would merely effect the relief of the stresses that caused it.

Confinement within other parts would fix the positions of most of the other components if they were to fail. However, a few parts, e.g., the control rod guide tubes and the fuel element tubes between the loader housing and the reflector, are protected only by clearances that are more than adequate to accommodate credible conditions.

3. Coolant Flow Control - There could be two serious effects if coolant helium streams were to leave their normal paths and pass through the joints between reactor components: (1) the core could be cooled inefficiently or unevenly, and (2) the pressure vessel could be overheated

by streams of hot helium. To direct the coolant through its proper channels, three types of seals are employed: a labyrinth seal between the core bearing plate and the bottom of the pressure vessel; three graphite, split-ring seals around the core plug; and a stainless steel membrane around the outside of the reflector. Locations of the seals are shown in Fig. 4.1.3.5.

As the coolant stream moves through the core, from A to D in the figure, the pressure drops that develop along the normal flow paths are the driving forces for bypass flow. These pressure drops, all relatively low, are listed in the figure. Before flow can develop, a path must be open between two regions where the pressure difference is great enough to force the movement of gas. Throughout the reactor, care has been taken to ensure that at least two solid barriers exist between regions of significantly different pressures, and that at least one barrier separates regions of nearly equal pressure where bypass flow could occur. The net result is that significant bypass flow in the reactor is prevented.

The three split-ring seals, two at the top of the core plug and one just below the radial helium distribution ports near the bottom of the plug, confine the incoming helium stream and force it to flow out through the fuel channels. Each of the graphite seal rings, fitted into a groove in the plug, springs outward against the opposing face of the movable core or core support, and moves with the core. The clearance between the moving ring and the stationary groove in the core plug is a total of 0.010 in., top and bottom. If the ring makes contact with one side of the groove, the ring moves up or down on the core surface.

At the top of core plug, leakage past the two seals would allow some coolant to bypass the core without cooling the fuel elements, but the bypass stream would not be deflected to the pressure vessel wall.

At the bottom of the core plug, the split-ring and labyrinth seals interrupt a flow path, shown schematically in Fig. 4.1.3.6, from the core plug plenum, down through the open space around the core support bearing, past the ring gear, and upward into the plenum between the core and the

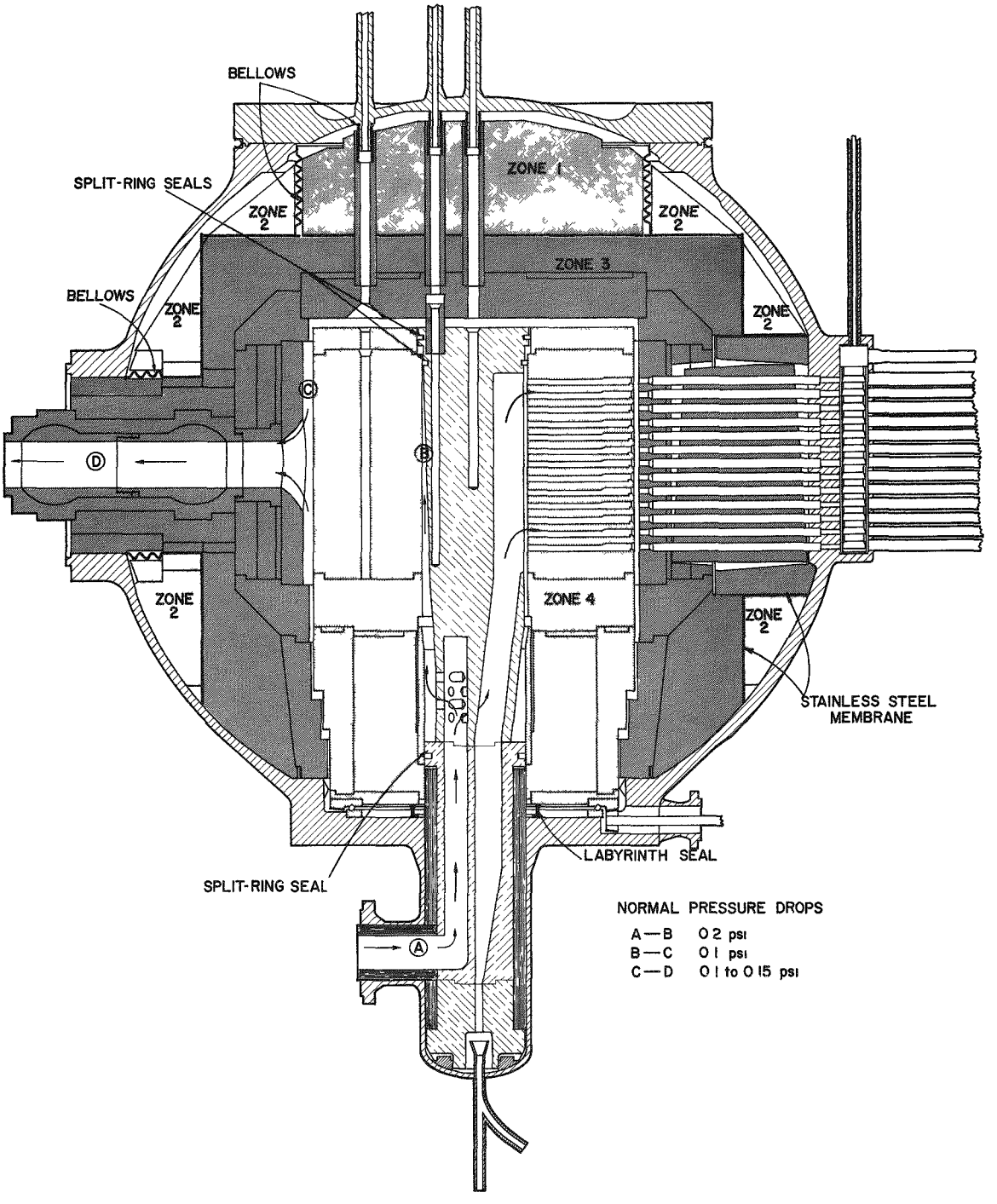

Fig. 4.1.3.5 Coolant flow control seals

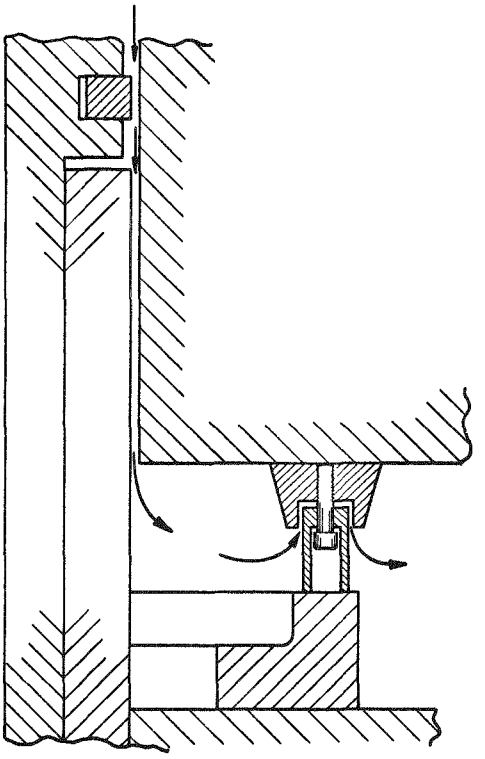

Fig. 4.1.3.6 Flow path from base of core plug to bearing cavity

reflector. Helium flowing along this path would not only bypass the core, it would heat the bottom of the pressure vessel. However, such a flow cannot develop under credible conditions. If, by some hypothetical means, the split-ring seal were to break into small pieces and fall away, helium could flow past the labyrinth seal, but the combined effects of the low driving force, 0.3 psi (A-C), and the tortuous path would limit this bypass flow to 18 lb/h. The result would be a rise of 10-30°F in the temperatures of the pressure vessel wall and a resultant increase of about 2000 psi in combined wall stress, which would remain much less than the allowable for primary membrane and primary bending stresses.

Bypass flow paths through the joints in the insulating carbon bricks are closed by a membrane, made of 0.062-in.-thick, Type 316 stainless steel, that encloses the reflector assembly (see Figs. 4.1.3.7 and 4.1.3.8). The cylindrical membrane, welded to the pressure vessel at

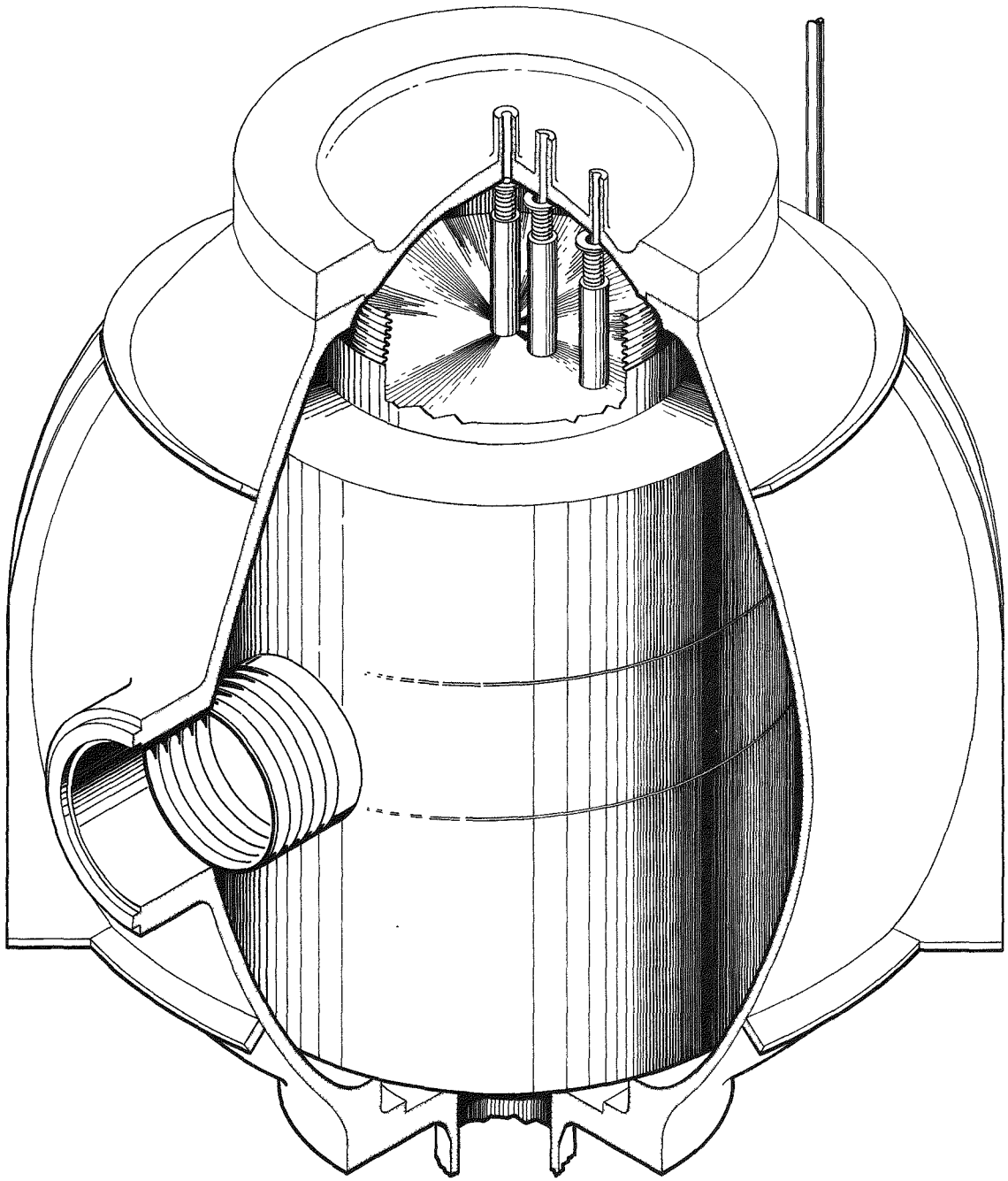

Fig. 4.1.3.7 Coolant flow control membrane, recuperator nozzle side

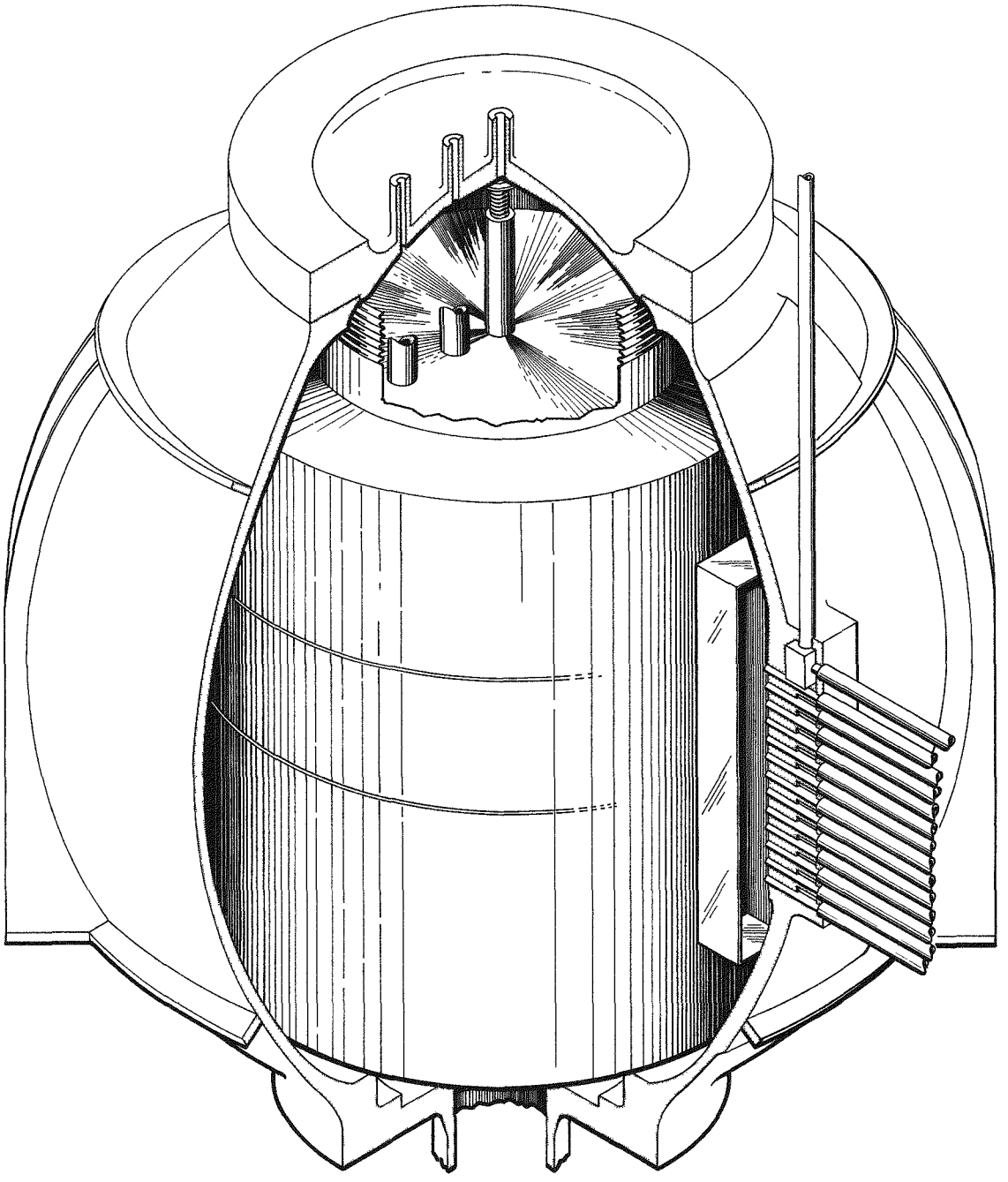

Fig. 4.1.3.8 Coolant flow control membrane, fuel loader side

the bottom, rises vertically through the carbon bricks and extends about 8 in. above the top reflector. A flat plate extends across the membrane at that level to close the top. Around the central zone of the top plate (see Zone 1 in Fig. 4.1.3.5), where there are numerous holes for control rods, a bellows joins the membrane to the edge of the top opening into the vessel. Individual bellows also extend from the vessel cap into the control rod guide tubes, to interrupt flow paths through the tubes. Another bellows joins the membrane to the side nozzle where the helium coolant leaves the reactor. At the other side, the membrane extends to the vessel wall to close off the loader housing.

In general, with reference to Fig. 4.1.3.5, the membrane isolates Zone 3 from Zones 1 and 2, preventing the flow of hot helium along sneak paths past the walls of the pressure vessel. To allow the equalization of pressures on both sides of the membrane, there are horizontal slip joints in the vertical walls of the membrane.

Temperatures inside and outside the reactor are monitored with thermocouples. The locations of thermocouples on the surfaces of the pressure vessels are shown in Fig. 4.1.3.9. Figure 4.1.3.10 is a diagram of the locations, inside the reactor vessel, of thermocouples that were installed specifically to detect abnormal temperatures that would develop if bypass flow were to occur. During reactor operations, all of the surface and most of the interior thermocouple outputs are scanned every 15 sec by the computer and compared with high limit alarm set points. For the initial power and temperature ascension, described in Sec. 15.3, all pertinent thermocouple data will be examined at every temperature plateau, and comparisons will be made with the results of calculations to detect incipient hot spotting.

Thermal Stress Analysis - An extensive series of calculations were made to predict the thermal stresses induced in the graphite parts of the reactor core during operation of the reactor at design conditions. The results of the calculations indicate that the core can withstand the highest predicted stresses.

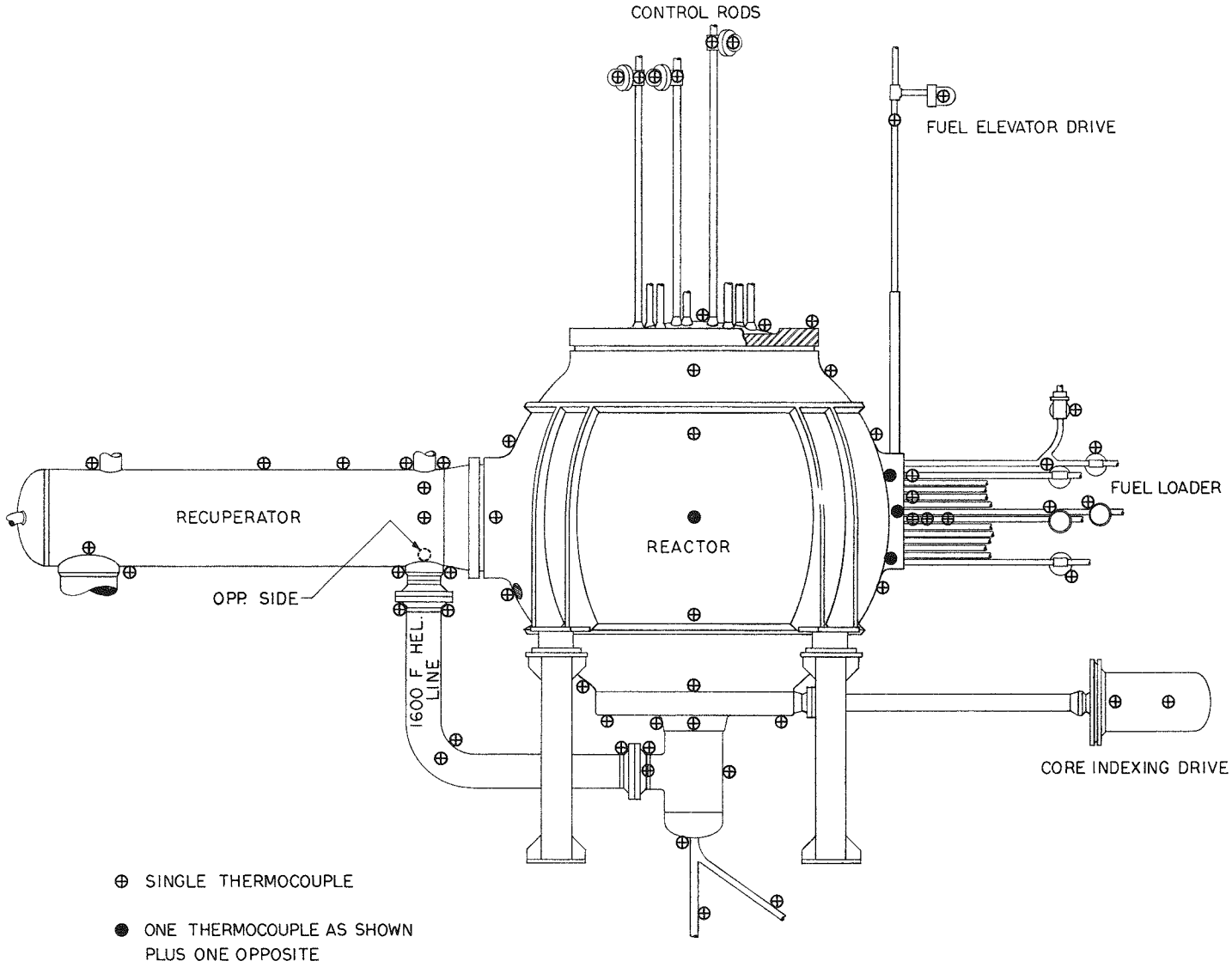

Fig. 4.1.3.9 Locations of surface thermocouples on reactor and recuperator pressure vessels

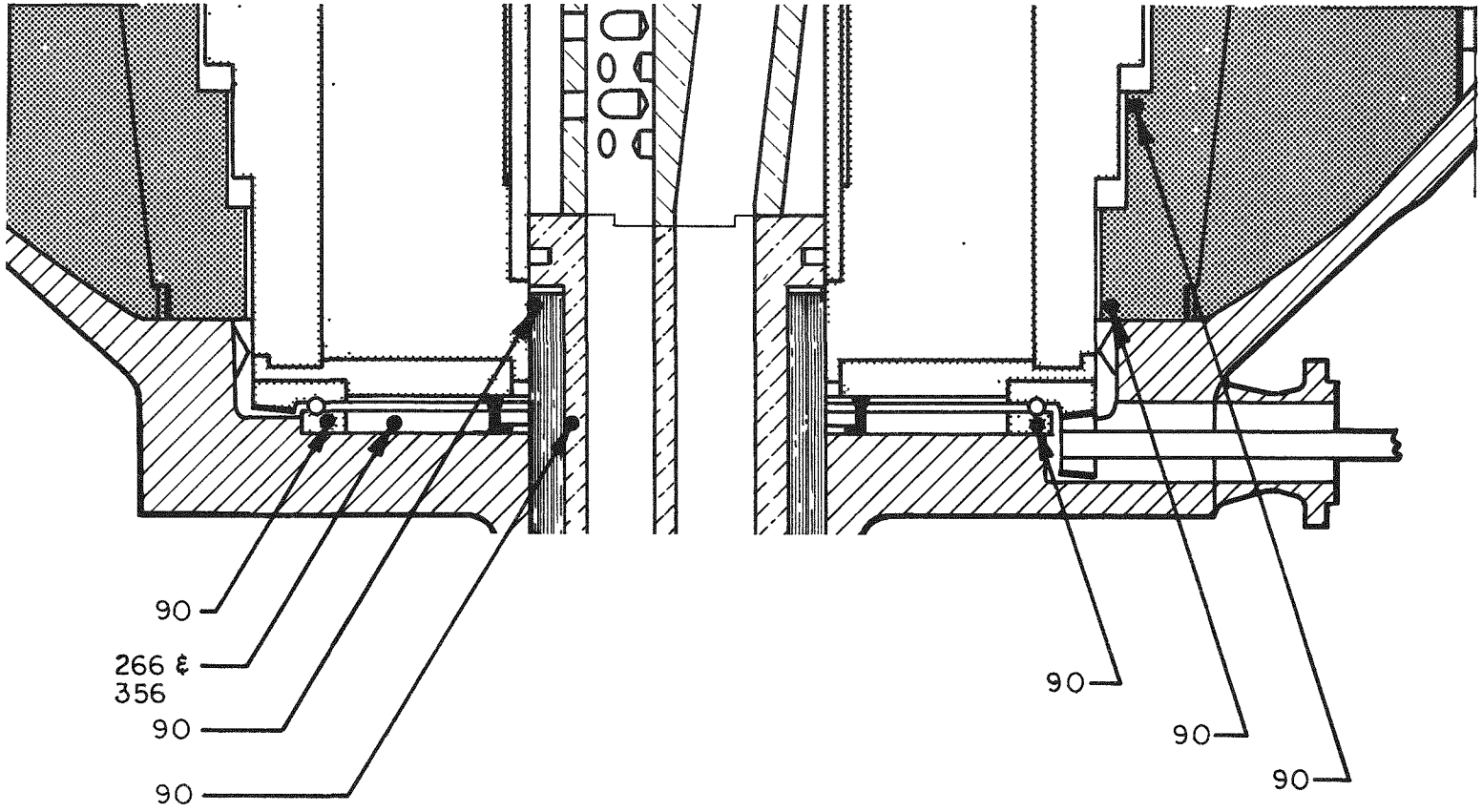

Fig. 4.1.3.10 Locations of internal thermocouples at base of reactor

For design purposes, the maximum tolerable stresses for UHTREX graphite parts were established to be 650 psi in tension and 1200 psi in compression. A set of calculations based on thin-wall theory predicts that, for operation at design conditions, the highest principal stresses will exist as axial and circumferential stresses on the inside surface of the innermost one of the nested cylinders that make up the core. The calculated value for both sets of maximum stresses is 450 psi in tension. When stress concentrations around fuel channel holes were taken into consideration, through the use of thick-wall theory, the calculations predicted that maximum stresses at the same inner surface will reach 610 psi in tension, both in axial and circumferential directions. For all other points in the core, the thick-wall theory calculations yielded lower stresses.

Thermal stress calculations were based on the temperature distributions described in Sec. 4.3.1 of this report. The temperature distributions were used as input to the RASH code, a LASL modification of the SAD[2] code, which uses thin-shell theory to calculate axial and circumferential stresses in the six hollow cylinders of the core. Another LASL code, CYLSTR, produced calculations, based on thick-wall theory,[3] which included the effect of stress-concentration factors.[4]

Plots of the axial and circumferential stresses at the inside and outside walls of the innermost core cylinder appear in Figs. 4.1.3.11 and 4.1.3.12. The plotted results were produced by the RASH code for the reactor operating at design conditions with a fuel loading whose mass and distribution accord with the results of the UHTREX critical experiment (see Appendix D). Similar plots were made for the other core cylinders, none of which had stresses as high as the innermost ones.

---

[2]P. P. Radkowski, et al., "A Numerical Analysis of the Equations of Thin Shells of Revolution," American Rocket Society 15th Annual Meeting, Washington, D. C., 1960 paper 1580-60.

[3]S. Timoshenko and J. N. Goodier, Theory of Elasticity, 2nd Ed., McGraw-Hill, New York, 1951.

[4]R. E. Peterson, Stress Concentration Design Factors, Wiley, New York, 1953, p. 196.

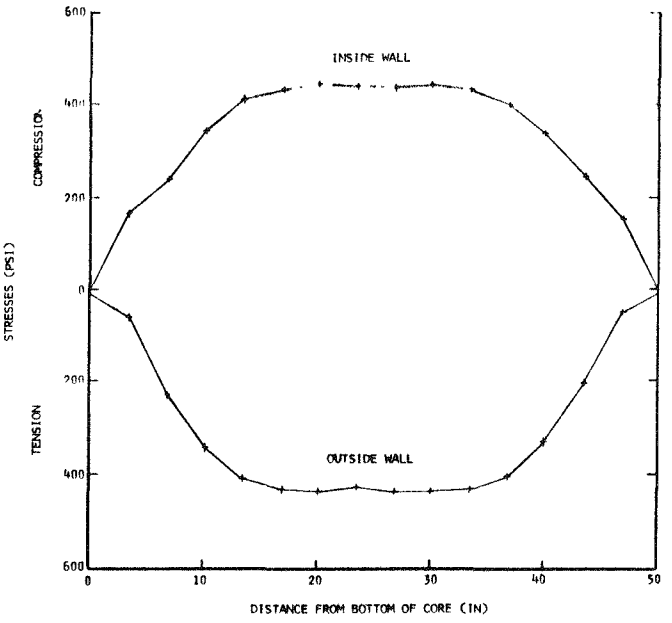

Fig. 4.1.3.11 Axial thermal stresses, innermost core cylinder. Positive values are stresses in compression; negative values are stresses in tension.

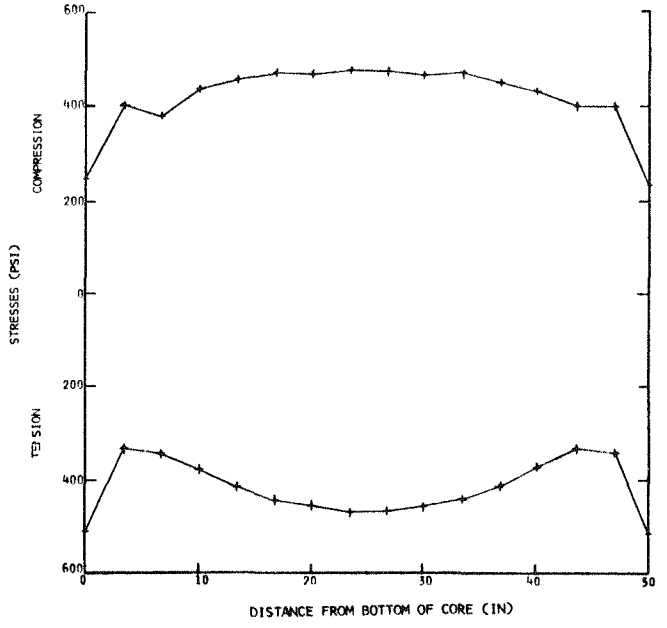

Fig. 4.1.3.12 Circumferential thermal stress, innermost core cylinder. Positive values are stresses in compression.

4.1.4 Fuel Elements

A full fuel loading for the reactor consists of 1248 fuel elements, each one a hollow cylinder 1-in. o.d. x 0.5-in. i.d. x 5.5-in. long (see Fig. 4.1.4.1). Structural material for the elements is graphite. Contained within the graphite matrix is the uranium fuel, enriched to 93.15% ^{235}U. The mass of uranium in each type of element and the method of manufacture of the various types of elements are described in the design subsection that follows.

Fig. 4.1.4.1 UHTREX fuel element

Four of the elements rest, end to end, directly on the moderator graphite in each of the 312 fuel channel holes. Since there are no centering splines or other supports on the elements, an eccentric annulus is formed between the outer surface of each element and the wall of the fuel channel. The cross sectional area of the flow channel through the annulus is 0.160 $in.^2$, whereas the channel through the 0.50-in.-diam central hole is 0.196 $in.^2$ in area. However, because of the smaller equivalent diameter of the eccentric annulus, 85% of the coolant flows through the hole, where the major portion of the heat from the element transfers to the coolant. The flowing helium creates a force of 0.1 lb f, in the direction of the flow, against the four elements, which are restrained from moving by their frictional force against the channel and by a 3/16-in.-high step at the outer end of the flow channel.

When the reactor is operating at its design power of 3 MW, the average power generation per fuel element is 2.40 kW, the maximum power for any one element is 2.75 kW, and the fuel element temperatures are 2000 - 2900°F.

Since UHTREX is to be used for testing a number of types of fuel elements which can be loaded or unloaded at power, there is no specific design lifetime for elements, but the elements are expected to endure to at least 50% burnup. The usual restrictions on fission product release from fuel elements do not apply to UHTREX, which is designed to use unclad elements.

Element Design - Although the UHTREX reactor and its coolant and containment systems were designed to operate safely with fuel elements that release fission products to the coolant stream, the elements of the first fuel loading, to be used during the startup and early investigation phases of the experiment, contain barriers to fission product release. The fuel is in the form of uranium dicarbide (UC_2) spheres, about 150-μ diam, coated with about 100 μ of pyrolytic carbon, in three layers. The spheres are bound together in a graphite matrix to

form the elements, all with the same exterior dimensions. Nine groups of elements were prepared, each group different from the others in the amount of contained fuel. Table 4.1.4.1 presents the masses and densities of the uranium, enriched to 93.15% ^{235}U, that are loaded in each group of elements.

TABLE 4.1.4.1

URANIUM LOAD IN ELEMENTS, FIRST UHTREX LOADING

Group	Mass (grams U/element)	Density (mgU/cm^3)
1	3.5	68
2	4.2	79
3	4.8	93
4	5.7	108
5	6.6	127
6	7.7	148
7	9.0	173
8	10.5	202
9	12.3	237

The spherical, pyrolytic carbon-coated UC_2 particles, manufactured by General Atomic at San Diego, California, have the following characteristics.

Uranium (93.15% enriched) (wt/%)	36
UC_2 core diameter (μ)	147-208
Particle density (g/cm^3)	2.46
Exposed U (%)	0.01
Coating thickness (μ)	
Buffer layer (innermost)	26.8
Isotropic layer	40.4
Granular layer (outermost)	35.4

Total thickness	102.6
Coating density (g/cm^3)	
Buffer layer	1.1
Isotropic layer	1.39
Granular layer	1.92

Taub and Bard[5] have reported, in detail, the UHTREX fuel element manufacturing process; a brief description of the process follows. In the first step, coated particles were leached in nitric acid to reduce the exposed uranium to 0.01%. Then, a precise quantity of coated particles was mixed with dry carbon ingredients (85% graphite flour, 15% carbon black) and a polymerized furfuryl alcohol. The mix was extruded into nominal 1-in.-o.d. x 0.5-in.-i.d. x 57-in.-long pieces. These stock pieces were cured to a temperature of 480°F in air, baked to 1560°F in vacuum, and finally heated to 3090°F in helium. Each stock piece was embossed with a number that identified the piece and its uranium loading density. From one stock piece, 10 elements were machined, each of which was engraved with a serial number, based on the stock piece number, and a number that represented the loading. When each element was finished, it was leached, with 20% HCl gas in a helium atmosphere at 2910°F, to remove the uranium exposed during fabrication and machining. Finally, the loading in each element was verified by a gamma count, calibrated against a chemical analysis of a sample of the stock from which the element was made. The fuel elements are fabricated to the following tolerances: o.d., 0.993 ± 0.010 in.; i.d., 0.497 ± 0.005 in.; length, 5-1/2 ± 1/32 in.; bow in each element, < 0.010 in.

4.1.5 Fuel Loader

A fuel loader, attached to the side wall of the pressure vessel (see Fig. 4.1.5.1), moves fuel elements into the core. In the first

[5]J. M. Taub and R. J. Bard, "Coated Particle Fuel Elements for UHTREX," LA-3378, July 1965.

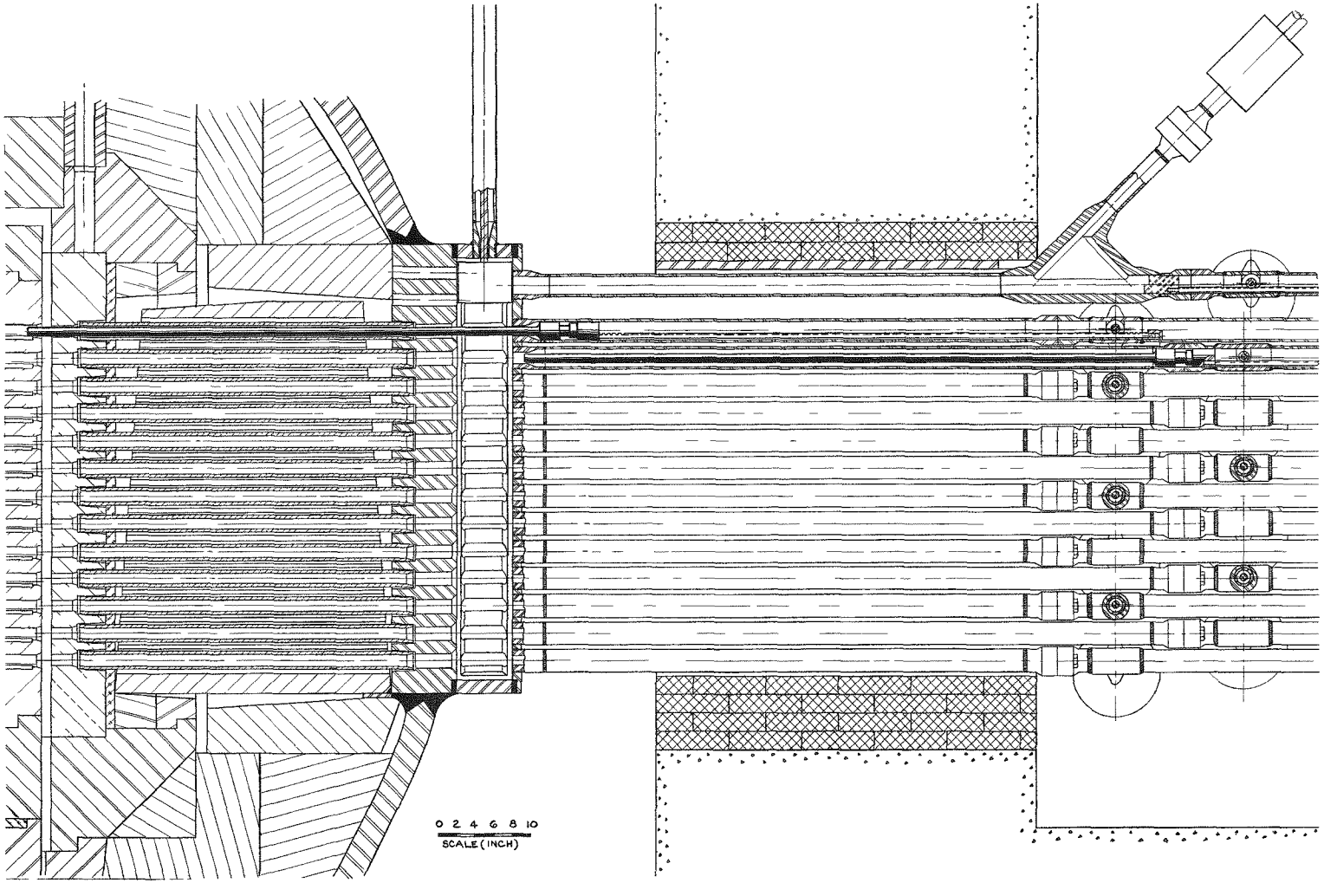

Fig. 4.1.5.1 Section through fuel loader

step of the loading operation, the fuel channel to be loaded is located by rotation of the core, which aligns the proper vertical row of channels with the loader, and by withdrawal to its rearmost position of the single loading ram that normally closes the entrance to the proper channel. Then a new fuel element drops through the gas lock at the top of the loader and stops on its side in front of a short steel ram. This ram moves the element through a tube to the fuel elevator, which is open on one side. In the elevator, the element moves slowly downward past slots in the loading tubes that are closed by the inactive Graph-i-tite G loading rams. When the element passes the slot opened by the withdrawal of a ram, the element drops out into the loading tube. The long, graphite loading ram then advances the element past the pressure vessel wall, through a graphite tube that extends to the graphite portion of the outer reflector, and into the core. In the core, the element, driven by the ram, displaces the old elements along the fuel channel. When the new element is in place, the ram withdraws to its idle position inside the stationary reflector.

Meanwhile, the innermost of the old elements, displaced into a vertical slot in the stationary central plug, drops down through a chute in the plug to the fuel discharge pipe at the bottom of the reactor vessel. The element, decelerated by contact with the discharge chute walls, comes to rest against the inlet valve to the bottom gas lock, where it can be held long enough to cool. Should the element become wedged in the discharge chute, a stainless steel dislodger rod is driven up the chute to free the element. After a controlled passage through the gas lock, the element drops into a mechanical conveyor, described in Chapter 6 where a complete description and analysis of the fuel handling system appears.

Rack and pinion drives with sealed electric motors actuate the rams, elevator, and dislodger rod. Position indicators, mounted on each drive, transmit to display instruments in the control room. These indicators are used in the loading operation to determine how far the

rams must be extended to position a new fuel element properly, since thermal expansion may change the insertion depth by as much as 5/16 in. In the first step of the procedure used to find the exact distance to the surface of the core, the indexing mechanism is operated through only half its cycle to position the blank core surface (between fuel channel rows) in front of the loader. Then a ram is extended until contact is made, and the indicator reading is noted. The correct insertion depth, then, is the distance indicated plus the maximum calculated distance to the step inside the core channel. An element will seat satisfactorily in a channel if the outermost end of the element lies between the step and a point 1/2 in. inside the step.

Design Analysis - Each fuel loader is designed to operate without maintenance through 15,000 load-and-retract cycles, over a 3-year period. Motive power for each loader ram is applied through a simple, reliable, rack and pinion, driven by an electric motor through a gear reducer. The two-phase induction motor has polyimide insulation and ball bearings with NRRG 159 lubricant. It is controlled with a servo system located in the control room, that receives a position indication signal from a multiturn potentiometer coupled to the pinion drive shaft. In a reliability test, a full-scale prototype fuel loader survived operation through 260,000 cycles over a period of 2 years.

The design of the loader and associated core parts accommodates misalignments due to manufacturing tolerances, thermal expansion, and radiation-induced dimensional changes. Loader operation can continue despite misalignments of 2 in. in the vertical plane, 1/2 in. horizontally, and 1/2 in. between core and reflector. Proper operation of the loader under these conditions has been verified in tests with full-scale mockups. In a reliability test, a full-scale Graph-i-tite G push rod was flexed 100,000 times through a 2-in. deflection without failure.

Housings for the fuel loaders are designed to operate at 0 to 650°F and 0 to 550 psig. They are made of low carbon steel, ASTM A-210,

seamless tubing; ASTM A-105 Grade II forgings; and ASTM A-212 Grade B plate. Each housing has two Conoseal joints that are designed for operation at 0 to 550 psig and 0 to 650°F with leakage of less than $5x10^{-8}$ std. cc/sec under the working pressure of 500-psig helium. All other joints have full penetration welds per NAVSHIPS 250-1500 with 100% radiographic inspection at the 2-1T quality level. All pressure containing materials undergo complete ultrasonic inspection at the quality level of a 3% notch, and a magnetic-particle or liquid penetrant inspection per MIL-STD-271C with all indications rejected or removed. All pressure containing structures meet the input requirements of paragraph N-332 of ASME Nuclear Vessels Code, Section III.

Electrical feedthroughs carry power and instrumentation leads through the fuel loader housings. Each feedthrough has two leak-tight, ceramic-insulated connectors with an intermediate buffer zone, monitored by a pressure switch for any leakage through the inside connector. The feedthroughs are designed for operation under 0- 500-psig helium at 0° to 300°F with leakage of less than $1x10^{-8}$ std cc/sec at 500 psig. Prototype feedthroughs survived an extensive series of reliability tests, including tests for conductor insulation against high voltages in a helium atmosphere, for current carrying capacity, and for leak tightness after pressure and temperature cycling. The test results demonstrate that the feedthroughs are capable of carrying at least twice the voltage and 10 times the surge amperage prescribed for the drive motors, and that the feedthroughs remain leak-tight after hundreds of cycles between ambient and operating temperatures and pressures. Each feedthrough undergoes visual inspection and leak tests before installation in a loader housing, and the assembled loader is tested through 250 cycles before installation on the reactor vessel. The buffer zone, between the inner and outer connectors of each feedthrough, is monitored with a pressure switch.

4.1.6 Core Indexing Mechanism

The rotating core of the reactor is mounted on a support plate, which in turn is supported by a combination ball-bearing gear that is

63-in. o.d. x 49-1/2-in. i.d. and rotates on 110, 1-1/4-in.-diam balls. The integral spiral bevel gear is at the edge of the top bearing race. Both the support plate and bearing gear are fabricated of 17-7 PH stainless steel. The bearing is coated with a dry film lubricant.

The core is rotated to each of the 24 radial fuel loading stations by an indexing mechanism which provides the necessary motion and positive index location. The indexing mechanism consists of a motorized reducer operating through a starwheel mechanism that rotates and locks the pinion drive shaft at 180° intervals. A 180° rotation of the pinion shaft, through the 12:1 ratio at the bearing gear, indexes the core one loading station. The time consumed in indexing the core from one station to the next is approximately 15 sec. To eliminate the necessity for a rotating helium seal, the complete mechanism is housed in a pressure vessel which is an integral part of the main helium containment. The mechanism extends outside of the reactor room and is accessible for maintenance when the reactor is shut down.

Design Analysis - The core support bearing, its size determined by mechanical stability considerations rather than by the weight of the core, is loaded to only a few per cent of theoretical capacity. To evaluate the accelerated wear that is known to occur in bearings operated in a pure helium atmosphere, a long-term bearing test was conducted with all operating conditions simulated except the radiation field. Results showed that even an unlubricated bearing would survive for the life of the experiment, and that the dry-film lubricated bearing will operate without significant wear.

For the tests, two identical sets of bearings were prepared with full-size balls and full-scale races but a scaled-down total bearing diameter. One set was tested without lubricant, the other with a coating of molybdenum disulfide in a sodium silicate binder. The tests were run with the bearings under a ball load equivalent to the weight of the core on the full-size bearing. Heaters maintained the bearings at 650°F in a helium atmosphere. The bearings were operated every 15 min,

through a cycle equivalent to indexing the core through two loading positions, until the accumulated bearing movement was equal to 600 revolutions of the core.

At the end of the tests, the unlubricated bearing showed an accumulation of metal on the races and a roughening of the surface finish on the balls from 4 rms to 140 rms. Despite the change, the bearing rotated freely, with no significant increase in its drive torque, at the end of the test. The lubricated bearing was free of wear or galling, and the coating of lubricant on the balls and races was intact at the end of the test.

Design of the indexing mechanism is conservative. The torque available from the drive is 9000 in.-lb; the core rotates under a torque of 120 in.-lb. Tests of the indexing accuracy of the mechanism indicate a ± 15 min variation in the 180° rotation. The starwheel mechanism locks after each rotation, and its drive gears disengage to eliminate the accumulation of indexing errors.

The pinion gear that drives the gear on the core support plate was successfully tested, with the associated drive shaft and bearings, under severe loads and in the operating environment, except for the radiation field. In a helium atmosphere at 650°F, the pinion gear assembly transmitted torque loads of 2250, 4500, and 7200 in.-lb. The duration of the test at each torque level was 6000 revolutions, which is equivalent to 500 revolutions of the core. At the end of the two successive, lower torque level tests, there were no visible signs of wear. After the subsequent test at 7200 in.-lb, some of the dry film lubricant had worn from the pinion, and the teeth of the driven gear were scored, but the bearings were in satisfactory condition. It is not probable that the drive gear on the core support plate would show wear under similar conditions, because there are 12 times as many teeth on the actual gear as on the test gear.

In case of a failure in the indexing mechanism or pinion drive shaft assembly, the indexing mechanism and the pinion drive shaft

assembly can be removed and replaced without entering the reactor room. If the core support bearing or core should become jammed, there is enough drive torque available to slide the bearing with the balls locked or to shear off core obstructions, such as a jammed fuel element or graphite seal. The latter capability was demonstrated during the UHTREX critical experiment, when two protruding fuel elements were sheared by the moving core. Damage was confined to chipping at the edge of the fuel discharge slot in the core plug.

4.1.7 Control Rod System

Rods - A total of 12 control rods regulate the UHTREX reactor. Two sets of rods are arranged, with their axes parallel to the core axis, in two circles concentric with the core. Around the 16.25-in.-diam inner circle are eight plug rods that move in and out of the stationary central core plug. The outer set of four core rods, equally spaced around a circle with a 47-in. diameter, enters holes in the movable core.

The central set of plug rods is used for power regulation, emergency shutdowns, the initiation of planned shutdowns, and the completion of restarts after shutdown. In emergency shutdowns, the plug rods fall freely into the core plug. For a planned shutdown, the plug rods are driven in at a measured rate. After the reactor is shut down and starts to cool, core rods from the outer set are inserted to compensate for the increase in reactivity. On a restart, the core rods are withdrawn first, and then the reactor is brought up to power on the plug rods. Because fuel can be added or discharged from the reactor at power, there is no need for shim rods; the control rods can be withdrawn completely from the core at any power level.

Since the two sets of rods have different functions and environments, each set has a distinctive design.

The plug rods, which experience temperatures above 2400°F in a carbonaceous environment, use a temperature resistant poison, boron

carbide. As depicted in Fig. 4.1.7.1, the B_4C is in the form of hollow cylinders, each 0.875-in. o.d. x 0.410-in. i.d. x 2-in. long. The carbide, made from normal boron, is hot pressed to 97% of theoretical density. Twenty of the cylinders are strung on a central rod, 0.375-in. diam x 79.5-in. long, that is machined from a niobium forging. The cylinders rest on a niobium end piece and are in contact at the top with a niobium tube and ring assembly. Above the ring, a 4-in.-long spring made of Haynes 25 alloy is compressed against the top of the rod case. The spring restrains the movement of the poison assembly along the central rod which screws into, and is pinned to, the top piece. Enclosing the poison is a niobium case, made from a 1.000-in.-o.d. x 0.900-in.-i.d. tube formed over machined end pieces. There is an expansion gap between the poison support rod and the lower end piece of the case.

At the upper end, the top piece screws into a Type 316 stainless steel connector that is either 48- or 33-in. long. (The difference in length allows the vertical displacement of adjacent rod drive housings in the congested central area above the core.) On the top end of the connector is a knob that fits into a side-opening slot in a coupling mounted at the lower end of the rod drive rack. The coupling is made secure by a sleeve that slides down over it and is detained by a spring plunger. The total length of the four longer control rods is 139 in.; the other four are 124-in. long.

Each of the four core rods, shown in Fig. 4.1.7.2, is an articulated assembly of 14 segments, each 1.438-in. diam x 4-in. long, with a 0.720-in.-diam ball at one end and a 0.750-in. socket at the other end. A bolted insert in the side of each segment closes an opening through which the ball of one segment is inserted into the socket of the next segment. The bottom segment has, instead of a socket, a tapered end that guides the assembled rod into a hole in the movable core. The 10 lower segments, machined from an alloy of 1 wt/% ^{10}B in type 304 stainless steel, constitute the 40-in. effective length of the rod.

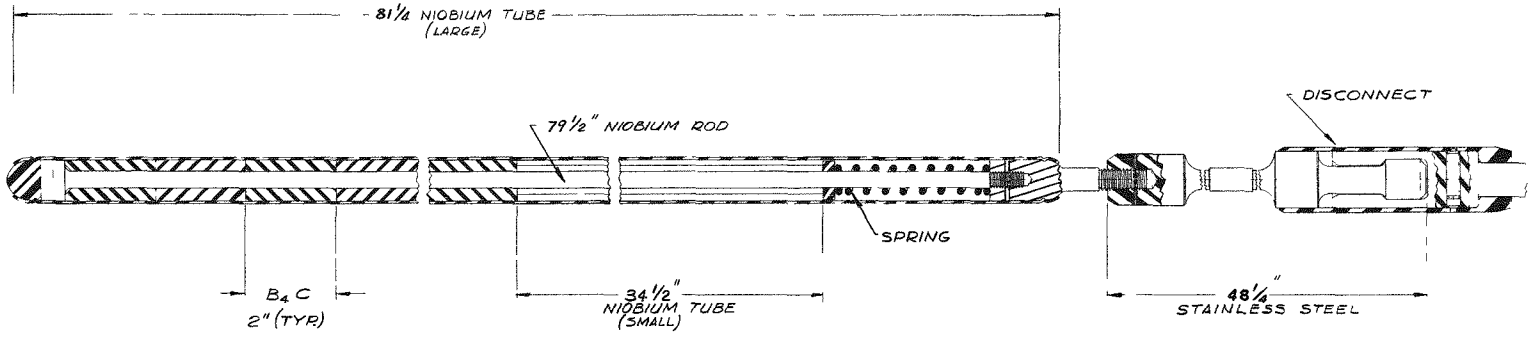

Fig. 4.1.7.1 Cross section of plug rod

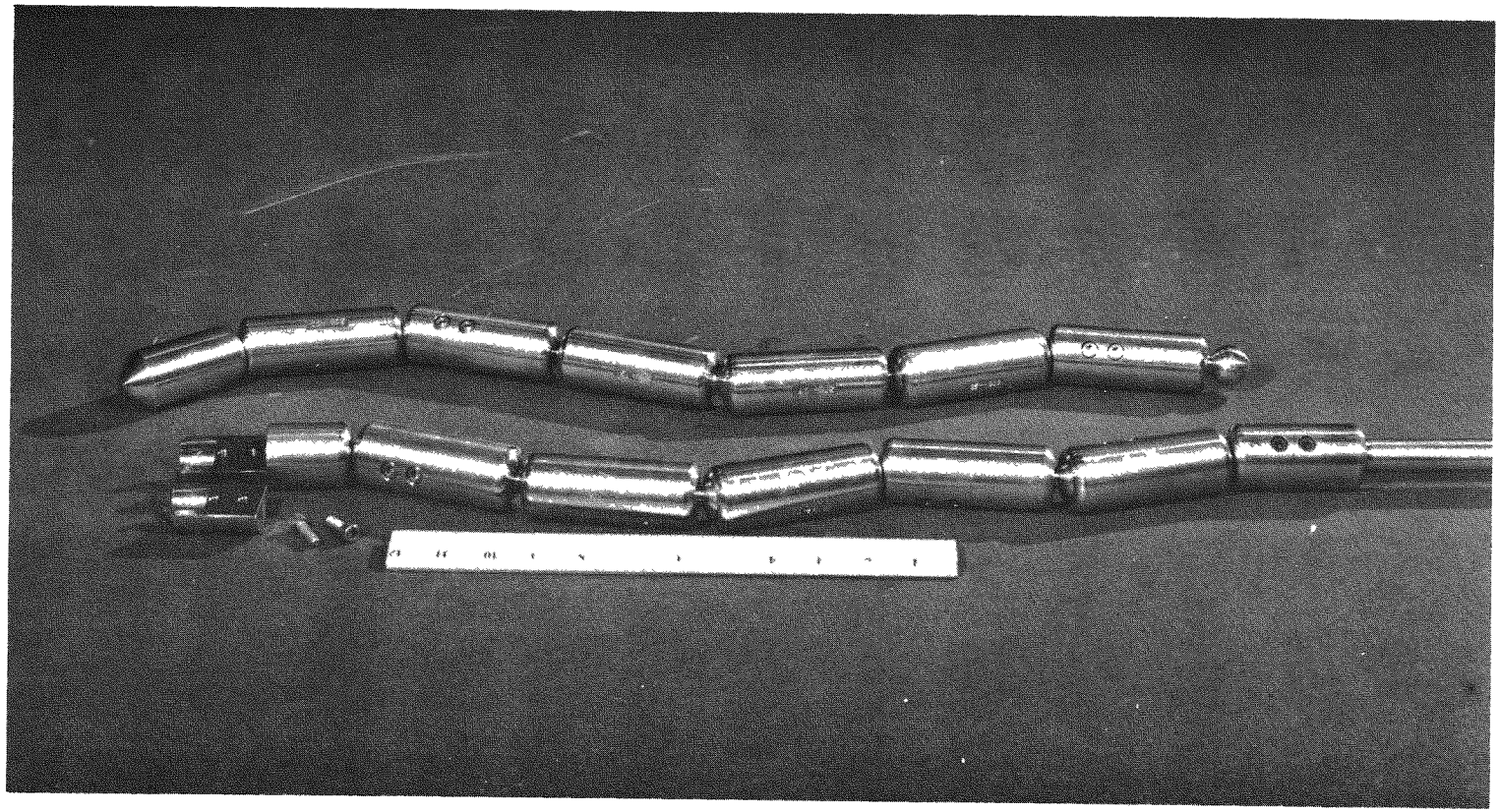

Fig. 4.1.7.2 Articulated core rod

The four segments at the upper end of the rod are identical to the active segments, but are made of standard Type 316 stainless steel. At the top of the rod, the terminal ball fits into a socket at the lower end of a Type 316 stainless steel connector, which is coupled to a rod drive rack by the same device used on the control rods. The overall length of a core rod is 98.25 in.

Rod Design Analysis - Two sets of operating conditions established the design features for the two sets of control rods. The plug rods must be capable of withstanding temperatures near 2400°F after the rods are inserted into the core plug while the reactor is at design temperature. However, the plug rods remain outside the core while the reactor is running, except for short periods during startup. Core rods, which do not enter the core until it has cooled to 1000°F or lower, must be capable of insertion into rod holes in the core which are displaced from the corresponding rod holes in the top reflector.

The materials used in the design of the plug rods were chosen for mechanical strength at high temperatures and for resistance to reaction at high temperatures with carbon, with contaminants in the helium coolant, and with other control rod materials. Compatibility tests to verify the suitability of the rod materials were run in out-of-pile rigs that simulated reactor conditions.

Corrosion resistance of niobium was demonstrated by specimens exposed at 2400°F to impure helium inside a graphite tube furnace. Impurity levels in the 11.5-psia exit helium stream from the furnace were 50 ppm CO_2, 4000 ppm CO, 200 ppm O_2, 3000 ppm N_2, and 2000 ppm H_2. All specimens were made from reactor grade niobium that had been re-crystallized by heating for 1 h at 2500°F in a vacuum. After furnace exposure, each specimen exhibited a lavender color, attributed to the formation of a NbC case by reaction of the Nb with CO. The Vickers (DPH) hardness of the specimen surfaces increased from 70 to 700 over a 155-day exposure span, rapidly at first, but more slowly as exposure periods lengthened. After 212 days in the furnace at 2400°F, the

carbide case on a 1/4-in.-diam specimen was 0.007-in. thick and strongly adherent. During tensile tests, the yield points of specimens were reached before their carbide cases began to flake off. Dimensional changes were small. After 41 days exposure, a typical cylinder gained 0.85% of its original weight and increased in length by <1%.

Eleven tensile test specimens were exposed in the furnace for various periods, and then their physical properties were determined for comparison with those of identical unexposed specimens. Yield strength of the specimens, 17,000 psi with no exposure, reached a maximum of 54,000 psi after 35 days, and then declined to a stable 43,000 psi. Per cent elongation began at 35%, dropped to 20% after 10 days exposure, and remained there as exposure time increased.

In total, the exposure tests demonstrated that niobium will retain its dimensions, tensile strength, and ductility in the plug rod environment, despite some surface embrittlement due to carbide formation.

Compatability of the B_4C poison in the plug rods with the niobium case was shown by the results of another series of graphite tube furnace tests. A hot-pressed B_4C disk was sealed inside a niobium tube, which was then heated to 2400°F in the furnace and held at that temperature for 400 h in an impure helium atmosphere. The effect of the exposure on the tube was the usual formation of a NbC case and a gain in weight of 0.3%. For the B_4C disk, the weight change was a 0.3% loss, with no alteration in the color or other dimensions of the disk.

Although the environment of the core rods is less severe, the accumulation of corrosion products could limit mobility of the segments. Tests in simulated environments demonstrated the adequacy of the design and the materials.

A prototype core rod, made of Type 304 stainless steel alloyed with 1.9 wt/% boron, was subjected to 1277 temperature cycles between 150 and 1000°F, to simulate the movement of the rod in and out of the core. The rod was run into and withdrawn from a graphite tube furnace,

with a 1-h soak period at the in and out positions where the temperature extremes occurred. After 38 cycles, an inspection of the rod revealed the formation of a blue color on the rod surface and a slight stiffening in the action of the ball joints. However, the joints were still loose enough to allow the rod to resume its vertical position after being flexed. On inspection after another 1239 cycles, the appearance and flexibility of the rod had not changed.

To verify the corrosion resistance of the boron-stainless steel rod material, tensile test specimens were checked after exposure to contaminated helium at 1600°F for various periods of time. After the maximum exposure time of 140 days, the yield strength of a specimen had decreased 10%, but there were no changes in per cent elongation or hardness.

Drives - All 12 of the rod drives are linear, vertical actuators of the rack and pinion type, driven by an electric motor through a planetary gear speed reducer. The eight plug rod drives, one of which appears in Fig. 4.1.7.3, have two design features not found in the four core rod drives. The first feature, an electromagnet clutch that joins the drive motor and the pinion, permits the plug rods to fall freely into the core plug when the clutch current is interrupted. The second feature is a decelerator, mounted on the upper end of the rack to cushion its free fall. In the core rod drives, the motor shaft to pinion joint is made with a flexible coupling and there is no decelerator. Another difference between the two sets of drives lies in their stroke lengths, 72 in. for the plug rod drives and 96 in. for the core rod drives. The added length permits the retraction, that much farther from the hot core, of the less refractory core rods. All other design features are common to both types of drives.

Tubes that extend from the top of the reactor vessel cap, support the rod drives and enclose the rods. Extensions welded to the tubes terminate in a double-seal Conoseal joint, one-half of which is seal-welded to the rod drive housing, shown in Fig. 4.1.7.4. The entire

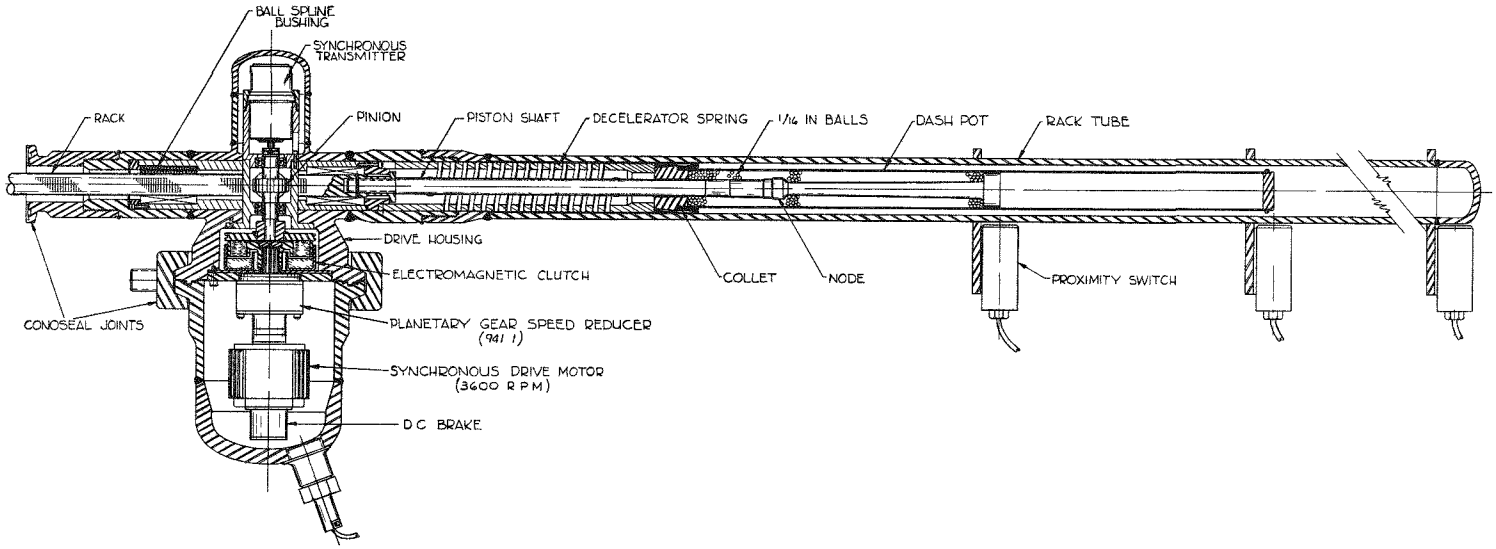

Fig. 4.1.7.3 Cross section of plug rod drive

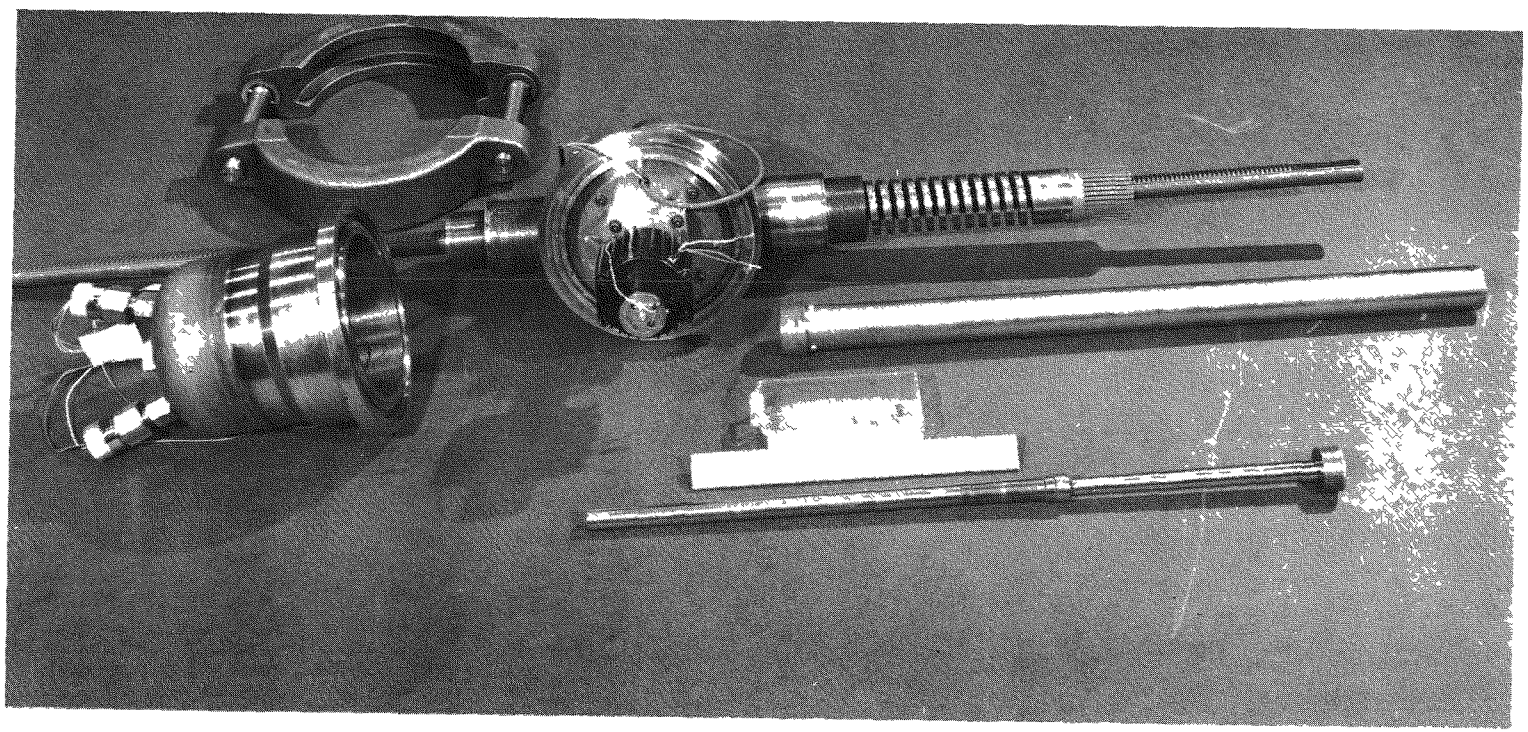

Fig. 4.1.7.4 Disassembled prototype plug rod drive

drive is contained in a leak-tight enclosure with two main parts, the motor train housing and the rack tube.

At one end of the motor housing is a removable bell with a double Conoseal joint. Enclosed in the bell is the synchronous drive motor and its dc brake. The motor is connected, in the plug rod drives, through a planetary gear speed reducer to a fixed field, electromagnetic clutch. The driven half of the clutch is coupled to the pinion shaft, which, at its other end, is connected to a synchronous transmitter, the sensor for the rod position readout system.

Geared to the pinion is the rack, a round shaft that has teeth machined along its surface between 2 of 3 vertical splines. The splines engage two ball spline bushings, one on either side of the pinion, that guide the rack as it moves up or down. At its lower end, the rack has the female half of the control rod coupling, described above.

Joined to the other end of the rack, in the plug rod drives, is the decelerator, a dashpot device that uses 1/16-in.-diam steel balls as the fluid medium. As a rod is raised, the dashpot piston, on the end of a shaft joined to the rack, moves up with the rack; an intermediate node on the same shaft moves through the balls in the dashpot; and the piston raises the dashpot to its "cocked" position at the top of the stroke. If the rod is then scrammed, the dashpot and piston shaft move downward together, until the lower end of the dashpot comes in contact with the upper end of the decelerator spring, a tube with a 14-turn helix cut through its wall. Since the lower end of the spring is fixed to the drive housing, the dashpot comes to a stop. The initial deceleration shock is taken up in the spring, and then a decelerating force is transmitted, through the balls, from the dashpot to the piston shaft and from it to the rack. A smooth deceleration of the rack continues while the node on the shaft, in its downward movement, displaces the "fluid" balls. As a net result, the velocity of the falling control rod is reduced to zero without a damaging shock to rod or drive.

When the rack moves upward again, there is some tendency for the dashpot to move with the piston shaft before the node has displaced the balls in the upper part of the dashpot. To apply a restraining force on the dashpot while the piston "recocks," a 36-finger collet is machined into the upper end of the decelerator spring. The collet engages the lower end of the dashpot on a downward stroke and holds it with about 50 lb force.

Three magnetic proximity switches, mounted on the stainless steel rack tube, sense the positions of the steel decelerator components inside the tube. The lowest switch detects the dashpot piston at its lowest point to verify that the rod drive has moved to the "in" position; the center switch verifies that, on the upward stroke, the top of the dashpot does not move until the piston is in the cocked position; and the top switch detects the arrival of the dashpot top, to verify that the rod drive moved all the way to the "out" position.

Drive Design Analysis - Control rod drives are designed to withdraw either a plug rod, decelerator, and rack assembly, or a core rod and its rack assembly. In either case, the weight of the load is <50 lb, but the drive can transmit a minimum thrust of 318 lb. The additional capacity is designed to overcome forces that might bind a rod, e.g., friction of the wall of a core hole against a core rod that is being withdrawn after the core is rotated part way between indexing steps. Each drive has a minimum estimated, operational service life of 300 cycles, consisting of a full insertion and full withdrawal of a rod. For the plug rod drives, 150 of the insertions can be free-fall drops.

The position indication system for the rod drives has a demonstrated capability of indicating actual rod position within 0.030 in., and the drive can reproduce a rod position with equal accuracy.

To establish the reliability of the rod drive systems, a long-term test was made of a prototype plug rod drive, position indicating system, and associated power supplies. During the test, improvements

in the decelerator design were made and tested. The drive motor, shaft, pinion, brake, electromagnetic clutch, and rack survived, without damage, 3000 insert-withdraw cycles, including 800 free-fall drops, throughout the test. There were no failures or detectable signs of wear in any component during the test, while three improvements were made in the decelerator design. The final, complete design was tested, with a simulated rod, through 1050 cycles, with 595 free-fall drops. In this final series, the rod drive operated in a dry helium atmosphere. To simulate the effects of the reactor environment, electric heaters maintained the drive housings at elevated temperatures.

Protection against radiation damage is afforded the drive motor and main gear train by the reactor shield slabs. However, the rack and pinion are exposed to neutron and gamma radiation through the tubes that penetrate the slabs, and therefore are coated with a dry film lubricant that can withstand the exposure.

During manufacture, the rod drives undergo the inspection described in Sec. 4.1.5 for the fuel loader housings. To ensure that the rod drives can function properly, each undergoes a preinstallation test of 30 operating cycles, which include 15 free-fall drops for plug rod drives.

4.2 Nuclear Design

4.2.1 Nuclear Characteristics of Design

Excess Reactivities and Shutdown Margin - Burnup compensation is achieved by refueling at power, and the rods are not used for flux shaping. Consequently, there is little or no excess reactivity, in the hot operating case, when xenon equilibrium is attained. Startup from room temperature will be conducted rather slowly so that departures from xenon equilibrium are minimized. The cold excess K, after xenon has decayed out, will be about 13.5% $\Delta K/K$. It is expected that the maximum ΔK that will be required to override xenon at room temperature will be about 2-3% $\Delta K/K$.

With eight rods in the plug ring and four rods in the core ring, the estimated total shutdown capability is 22.5% ΔK/K. With 13% ΔK/K required for temperature and xenon compensation, the estimated shutdown margin is thus 9% ΔK/K.

Numerous voids exist in the core assembly, e.g. control rod holes, coolant flow passages, and clearance spaces for thermal expansion. The total void worth might be as much as 5% ΔK/K, if graphite were used to fill the voids. Filling the voids with other common materials such as steel or water would cause large decreases in reactivity.

Coefficients of Reactivity - The isothermal temperature coefficients of reactivity for room temperature and at operating temperature are:

	293°K	1714°K
Core moderator coefficient	-1.83×10^{-4} ΔK/°K	-1.18×10^{-4} ΔK/°K
Core fuel coefficient	-1.40×10^{-5} ΔK/°K	-8.41×10^{-6} ΔK/°K
Reflector coefficient	$+8.22 \times 10^{-5}$ ΔK/°K	$+1.28 \times 10^{-5}$ ΔK/°K

These coefficients derive from the effects of temperature on neutron thermalization. In UHTREX, 90-95% of the fissions are induced by thermal neutrons; the neutron energy spectrum is, thus, well-moderated; and the neutrons in the thermal energy region are in near-equilibrium with the thermal energies of the moderating carbon atoms. As the temperature of the moderator increases, there is a corresponding increase in the average energies of the thermal neutrons. Both the effective fission and the effective capture cross sections decrease as the average thermal energy increases, but the decrease in the fission cross section is larger. Therefore, k_∞ decreases as the temperature increases.

Much larger effects on reactivity, however, are produced by the changes in thermal neutron leakage than by the changes in k_∞. As the temperature of the core rises, the rate of thermal neutron absorption decreases, and, as a result, the rate of leakage of thermal neutrons

from the core increases. This is the principal mechanism responsible for the strong negative core coefficients.

Concurrently, an increase in the reflector temperatures reduces thermal neutron absorption in the reflector, and thereby increases the rate of return of thermal neutrons from the reflector to the core. Reflector temperature coefficients are, therefore, positive.

The isothermal coefficients provide only a rough indication of the reactivity changes that occur under transient conditions. In any realistic excursion, the temperature changes are not uniform throughout the core. It is particularly unrealistic to consider the reflector regions in terms of a total isothermal coefficient. A discussion of the spatially distributed coefficients is presented in Sec. 4.2.2.

Thermal effects, other than those discussed above, are essentially negligible. Because of the small expansion coefficients of graphite, the effect of expansion on temperature coefficients of reactivity is at least an order of magnitude smaller than the thermalization effects. Moreover, Doppler coefficients are extremely small because of the absence of fertile material in the UHTREX core.

Like the moderator and reflector coefficients, the fuel coefficient derives mainly from the effect of variation in the fuel temperature on the thermalization of neutrons by the graphite in the fuel elements. Expansion effects are small. If the fuel alone expands, it must move toward the center of the core and plug assembly; outward motion of the four fuel elements in a channel is blocked by a restraining shoulder at the outer end of the channel. The reactivity due to fuel expansion inwards is negligible for reasonable temperature increases.

The fuel geometry produces complex self-shielding effects on thermal neutrons. First, there are the self-shielding effects associated with the coated particles. Since the particles are small compared to neutron mean-free paths, multiple collision processes may be neglected, and a simple first-flight attenuation theory may be used to derive self-shielding on the particles. There are complications, however,

due to the dependence of this self-shielding on neutron energy and particle sizes, both of which vary. When self-shielding of an entire fuel element is considered, multiple collision processes are important. Furthermore, the application of cell theory to the fuel element self-shielding is complicated by the cell geometry of the element. The basic cell is a segment of a cylindrical annulus, and there are four different cell sizes corresponding to the four different fuel element positions. Variations of the loading in fuel elements and of the temperature of the cell introduce more complications.

The self-shielding effects are listed below for the two extreme cases, room temperature and operating temperature. The loading of 5.68 kg (enriched to 93.1% in ^{235}U) is the estimated critical loading for the cold, clean case. The 11.0-kg loading is the estimated critical loading for design operating conditions at xenon equilibrium.

	Case	
	293 °K 5.68 kg	1714 °K 11.0 kg
Coated particle	2.09 % ΔK	0.92 % ΔK
Fuel element	3.48 % ΔK	2.62 % ΔK
Total	5.57 % ΔK	3.54 % ΔK

Control Rod Worths - Control rod worths, from calculations and from measurements made in the UHTREX Critical Experiment are listed in Table 4.2.1.1. The worths are for numbers of rods taken in combination as listed in the left column of the table.

The total worth of all the rods, i.e., the eight plug rods plus the four core rods, is 22.5% ΔK/K in the 11.0-kg loading at room temperature.

The rods, all heavily loaded with boron, are essentially black to thermal neutrons. Consequently, the rods cause strong local perturbations in the power and thermal flux. However, they are to be used only for startup, shutdown, scram, and for controlling xenon. There is no need to use the rods for flux shaping or for burnup compensation.

TABLE 4.2.1.1

CONTROL ROD WORTHS

(% ΔK/K)

Number of Rods	Case			
	293°K, 5.68 kg	293°K 11.0 kg		1714°K 11.0 kg
	Plug Ring	Plug Ring	Core Ring	Plug Ring
1	2.4	2.9	2.1	3.2
2	4.5	5.3	4.1	6.1
3	6.5	7.4	6.3	8.7
4	8.0	9.2	8.5	10.8
5		10.7		
6		12.0		
7		13.1		
8		14.0		

During normal operation, after xenon equilibrium is reached, the rods will be fully withdrawn to positions where there is little exposure to damaging radiations. If however, a plug rod were to be fully inserted at full power, 3 MW, the maximum burnup rate of the boron at the surface of the rod would be 5% per year. The primary reason for operating with the rods retracted is to limit the exposure of the rods to high temperatures in the core rather than to limit exposure to nuclear radiations. The thermal environmental effects on the rods are discussed in Sec. 4.1.7.

Maximum Controlled Reactivity Insertion Rates - The maximum rates of reactivity variation are produced by rod motions. To minimize these rates, the rods are interlocked to prevent the actuation of more than one rod at a time. In addition, the withdrawal speed for all rod drives is limited to 18 in. per min. A plot of the percentage of total rod worth withdrawn per second versus rod position is presented in Fig. 4.2.1.1. This plot was made from data obtained in UCX, the UHTREX

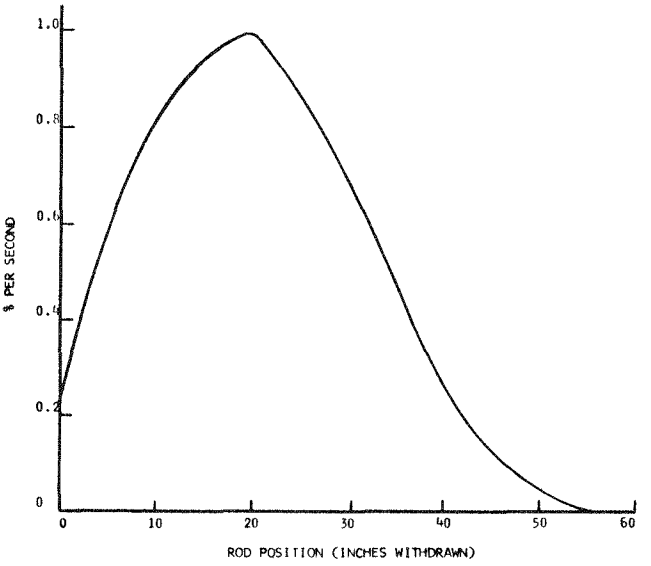

Fig. 4.2.1.1 Percent of total rod worth withdrawn per second

Critical Experiment (see Appendix D). At the zero position, the lower end of the rod is near the bottom of the core, and at 20 in. of withdrawal the bottom of the rod is near midheight. The maximum reactivity insertion rate occurs when rods are withdrawn about 20 in. At this position about 1% per sec of the total worth of any given rod is inserted as more of the rod is withdrawn.

The highest insertion rate that can be achieved occurs when there is just one plug rod at the 20-in. position in the loaded core, at operating temperature. From Table 4.2.1.1, the total worth of this rod is 3.2% $\Delta K/K$, and the maximum insertion rate when the rod is withdrawn, is therefore, 3.2×10^{-4} $\Delta K/K$ per sec, or about 4.7 ¢/sec.

Another high insertion rate occurs during startup after a shutdown. With the full loading of 11.0 kg of fuel, all 12 rods (8 plug and 4 core) will be fully inserted when the reactor is shut down. In starting up the reactor, at least two plug rods are retracted first, to provide scram. Then the four core rods are pulled in sequence before withdrawing the final six plug rods. Since the cold excess k is about 13.5%,

it is expected that criticality will be reached during the withdrawal of the last core rod. From Table 4.2.1.1, six plug rods are worth 12.0% and six plug rods plus one core rod are worth 14.1%. By difference, the worth of the last core rod is 2.1%, and, according to Fig. 4.2.1.1, the maximum reactivity insertion rate over the travel of the last core rod is 2.1×10^{-4} $\Delta K/K$ per sec, or 3.1¢/sec.

The maximum insertion rate during the initial loading of UHTREX at room temperature occurs during the brief interlude in the loading when the reactor is critical with only one plug rod inserted. The maximum insertion rate then is 2.9×10^{-4} $\Delta K/K$ per sec, or 4.2¢/sec.

Fuel Worth - UHTREX is designed for refueling at power. To accomplish on-line refueling, the fuel is divided into such a large number of increments (1248) that each fuel element represents only a small reactivity increment. In fact, the reactivity associated with the insertion of a single fuel element is so small that it is virtually undetectable. In UCX, the average reactivity change on inserting a fuel element was 1.8¢ per fuel element.

Other Worths - The worths of several of the voids in UHTREX were measured during UCX. The introduction of any materials from the UHTREX environment, other than fuel or graphite, into the voids causes reactivity reductions. Common materials such as steel or water act predominantly as poisons in the UHTREX core.

Power Distributions - Power profiles in UHTREX are plotted in Fig. 4.2.1.2. The individual profiles represent the variation in power from the bottom to the top of the core along a plane through the 13 channels in a vertical row. Channel numbers in a vertical row are on the J axis. One profile is plotted for each of the four radial positions, I, that an element may occupy inside one fuel channel. At the innermost position, I = 1. For the calculation of this profile, it was assumed that the core loading is 11 kg, the total reactor power is 3 MW, the reactor is at operating temperature, and xenon is at equilibrium.

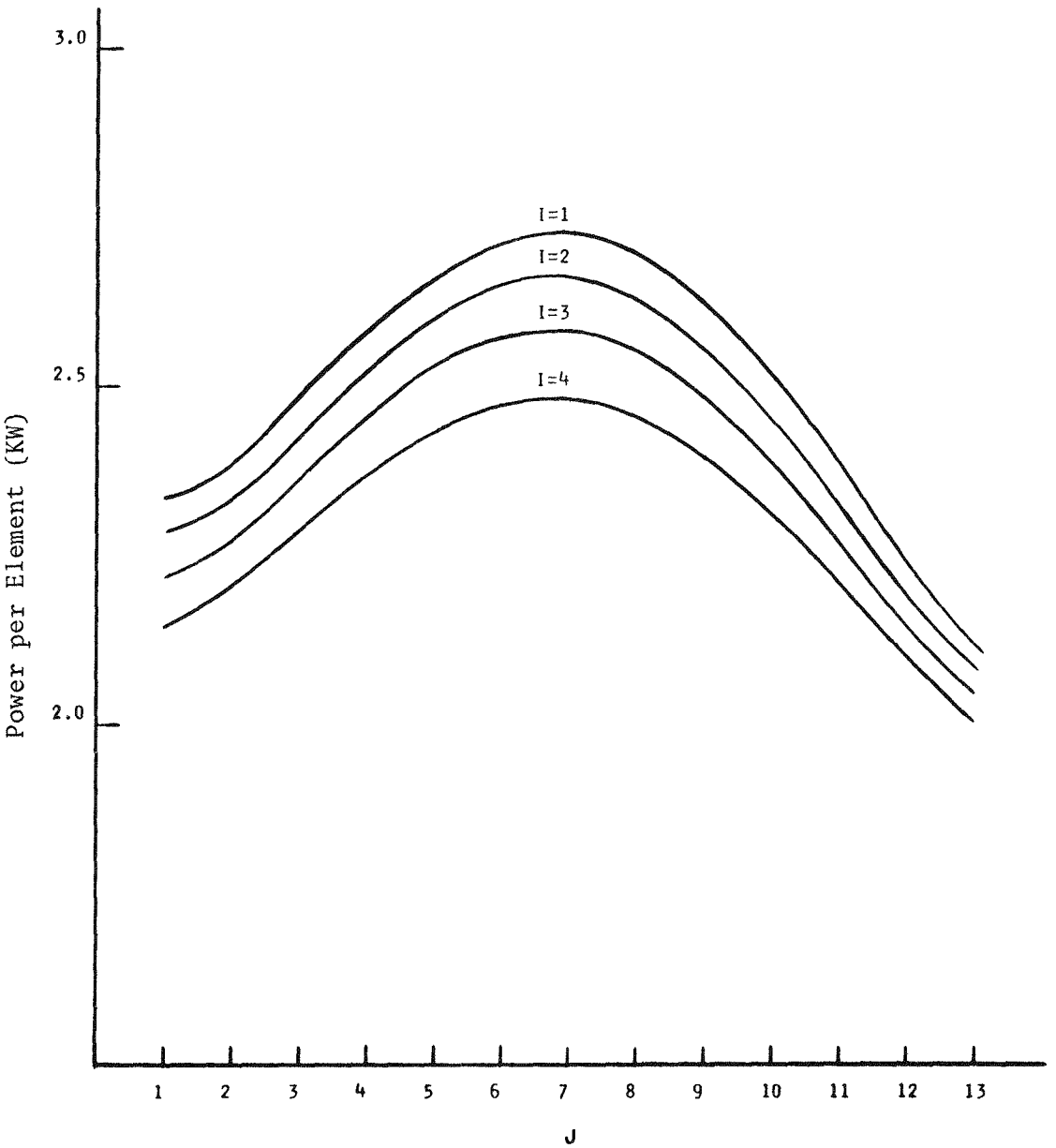

Fig. 4.2.1.2 Fuel element powers in UHTREX for 11-kg loading

The greatest variation of power with fuel element position occurs in the vertical direction. The power could be flattened by varying the fuel element loading pattern in the vertical direction, but this would complicate the loading program considerably and might have adverse effects. Stresses in the fuel elements are of no real concern, but the more important stresses in the bulk moderator and reflector structural components might be increased if the power were flattened vertically.

Flux measurements made during UCX indicate that significant local deviations from the profile shown in Fig. 4.2.1.2 are to be expected because of asymmetries that are not taken into account in calculations.

During startups of the reactor, a portion of one plug rod will remain inserted until xenon equilibrium is attained. The power in the innermost fuel elements will be reduced during this part of the operation.

Neutron Fluxes - Representative neutron fluxes in the UHTREX core and vessel are presented in Table 4.2.1.2 for the case of operation at 3-MW power, design temperatures, and xenon equilibrium. The fluxes are the nominal total numbers of neutrons/cm^2-sec in each energy range. The three listed positions all lie in a horizontal plane that bisects the core. Thermal flux is at a maximum at the reactor center, i.e.,

TABLE 4.2.1.2

NEUTRON FLUXES IN UHTREX AT 3 MW

	Flux (neutrons/cm^2-sec) at		
Energy Range	Reactor Center	Core Boundary	Vessel (Inside Surface)
Above 0.9 MeV	1.38×10^{12}	2.0×10^{12}	2.6×10^{9}
0.4 - 0.9 MeV	6.97×10^{11}	9.82×10^{11}	1.3×10^{9}
0.1 - 0.4 MeV	2.96×10^{12}	3.04×10^{12}	4.6×10^{9}
0.1 - 100 keV	5.84×10^{12}	4.23×10^{12}	1.7×10^{10}
Thermal - 100 eV	4.50×10^{12}	2.67×10^{12}	1.9×10^{10}
Thermal	4.90×10^{13}	2.40×10^{13}	9.7×10^{11}

the center of the core and plug assemblies. In the fuel, the maximum thermal flux, nominally 3.8 x 10^{13} neutrons/cm^2-sec, occurs in the innermost fuel elements that lie in channels at core midheight.

Power Decay Curve - Detailed measurements of rod drop times following a scram have been performed. Results for the scram of a plug rod at operating temperature are plotted in Fig. 4.2.1.3 in terms of the fraction of the total rod worth inserted versus the time in seconds after the scram is initiated. The coefficients for a sixth-order polynominal fit, in time, to the curve are listed in the figure.

Power decay curves resulting from the scram reactivity function described above are plotted in Fig. 4.2.1.4 for one, two, or three plug rods scrammed together from 3 MW. These curves were calculated with the kinetics code described in Sec. 4.2.2. The total decay energies are summarized in Table 4.2.1.3.

TABLE 4.2.1.3

SCRAM DECAY ENERGIES

Case	1 Rod	2 Rods	3 Rods
Worth (% ΔK)	3.2	6.1	8.7
Decay energy (MW-sec)	9.16	4.85	3.45

4.2.2 Nuclear Design Analysis

Nuclear characteristics of the UHTREX core were calculated according to the general methods described below. Results from these methods give good agreement with experimental data collected during the UHTREX Critical Experiment.[6] The simulation of the UHTREX core in UCX was exact, because the actual UHTREX core and reflector components were used. Therefore, wherever UHTREX characteristics have been evaluated solely by calculation, the UCX data provide a firm base for the extrapolations. In turn, the extrapolations will be

[6]Appendix D, this report.

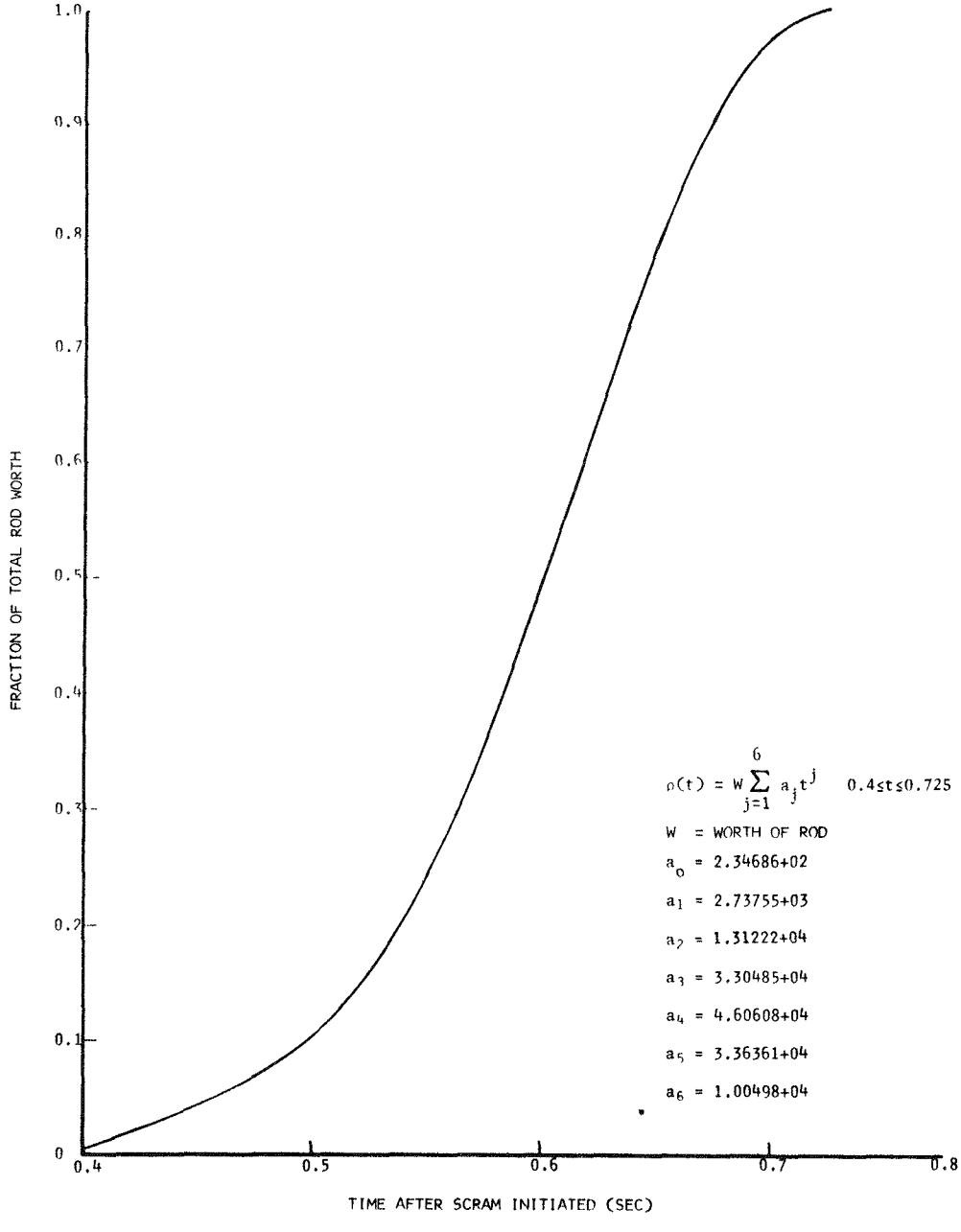

Fig. 4.2.1.3 Reactivity insertion on scram of one plug rod at operating temperature

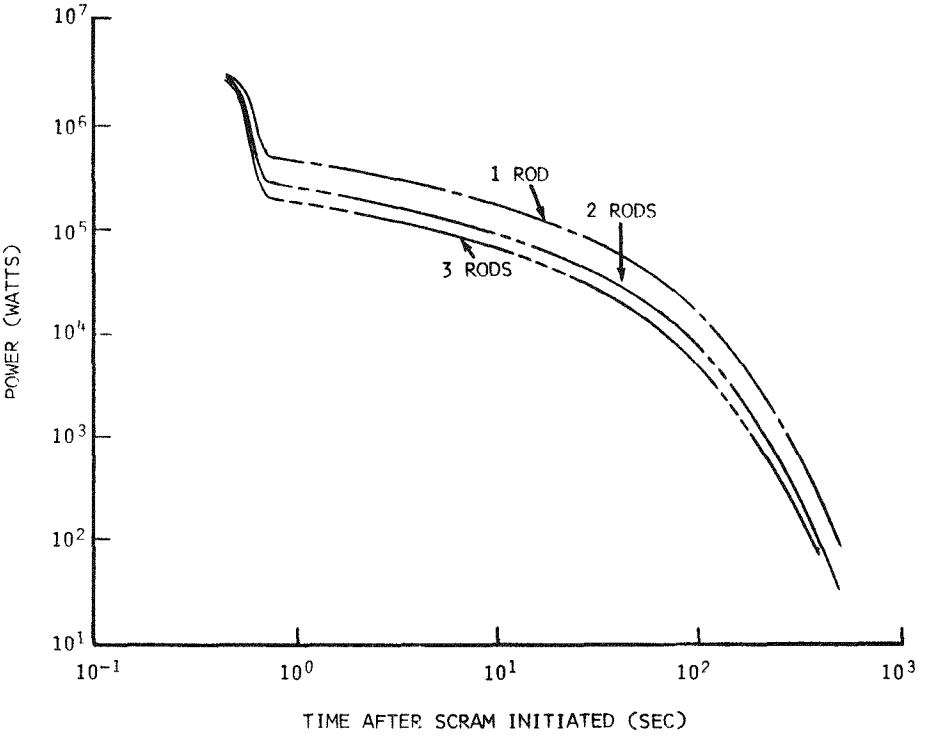

Fig. 4.2.1.4 Power decay from 3 MW after scram of 1, 2, or 3 plug rods

verified against the experimental data that will be collected during the UHTREX startup, discussed in Chapter 15. Calculations alone have been used in evaluating the effects on the core of its carbon insulation and pressure vessel, in extrapolating from UCX room temperature conditions to UHTREX operating temperature conditions, and in predicting reactor behavior under transient, normal, and extreme conditions.

Methods are described below for four sets of calculations, those used to determine critical mass, reactivity coefficients, control rod worth, and reactor kinetics. The critical mass calculations were made according to two-dimensional S_n transport theory, in cylindrical geometry, with an elaborate calculational model. Reactivity coefficients were calculated by perturbation theory methods using regular and adjoint

fluxes and currents from the two-dimensional S_n critical mass calculations. Control rod worths were determined by extensions of the method used by Scalletar and Nordheim[7] in one of the earliest estimations of the worth of a reactor control rod. In addition, selected calculational checks on rod worths were performed with two-dimensional S_n transport theory codes. Transient calculations were performed using a method which had not been previously applied to reactor kinetics problems. The method, called continuous analytic continuation,[8] is generally applicable to problems that require simultaneous numerical solutions to a set of differential equations. The unique advantage of the method is that upper limits on the numerical errors accrued in the course of a calculation are known and can be predetermined.

Critical Mass Calculations - The critical mass calculations are basically two-dimensional S_n transport theory calculations in cylindrical geometry. Since the leakage of neutrons from the UHTREX core is relatively high, the various graphite reflectors were mocked-up carefully in the calculational model, shown in Fig. 4.2.2.1, where voids in the core are represented by darkened areas. In the model, the core is split into four radial regions, each of which corresponds to a radial fuel element position. This model was used for determining the reference critical masses of 5.68 kg, at room temperature, and 11.0 kg at operating conditions. A simplified model, shown in Fig. 4.2.2.2, was used for the reference calculations of reactivity coefficients and control rod worths.

Neutron thermalization effects, complicated by the unusual fuel geometry, were treated in careful detail in terms of both spatial and energy variations. To handle these special thermal effects, a number of preliminary calculations were made to establish effective thermal cross sections for input to the finite geometry critical mass calculations.

---

[7]R. Scalettar and L. W. Nordheim, "Theory of Pile Control Rods," MDDC-42, June 1946.

[8]Harold T. Davis, "Introduction to Nonlinear Differential and Integral Equations," U. S. Government Printing Office 1961.

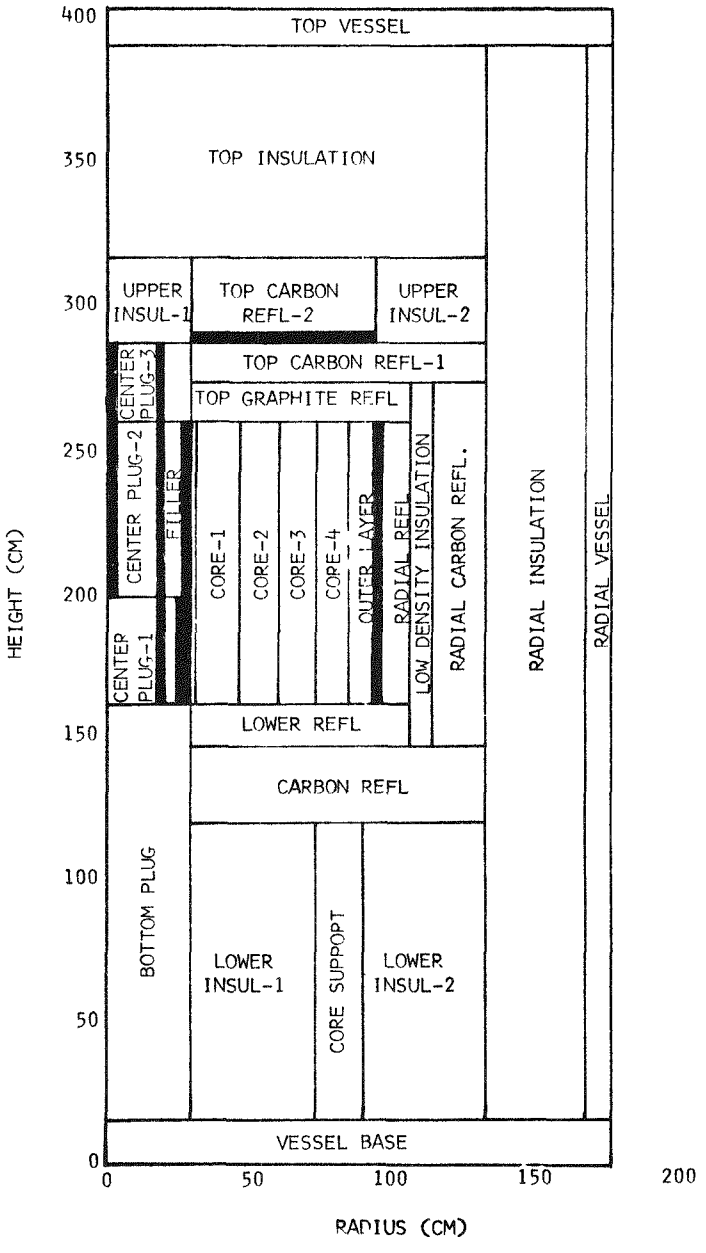

Fig. 4.2.2.1 Detailed, 37-region model used for critical mass calculations

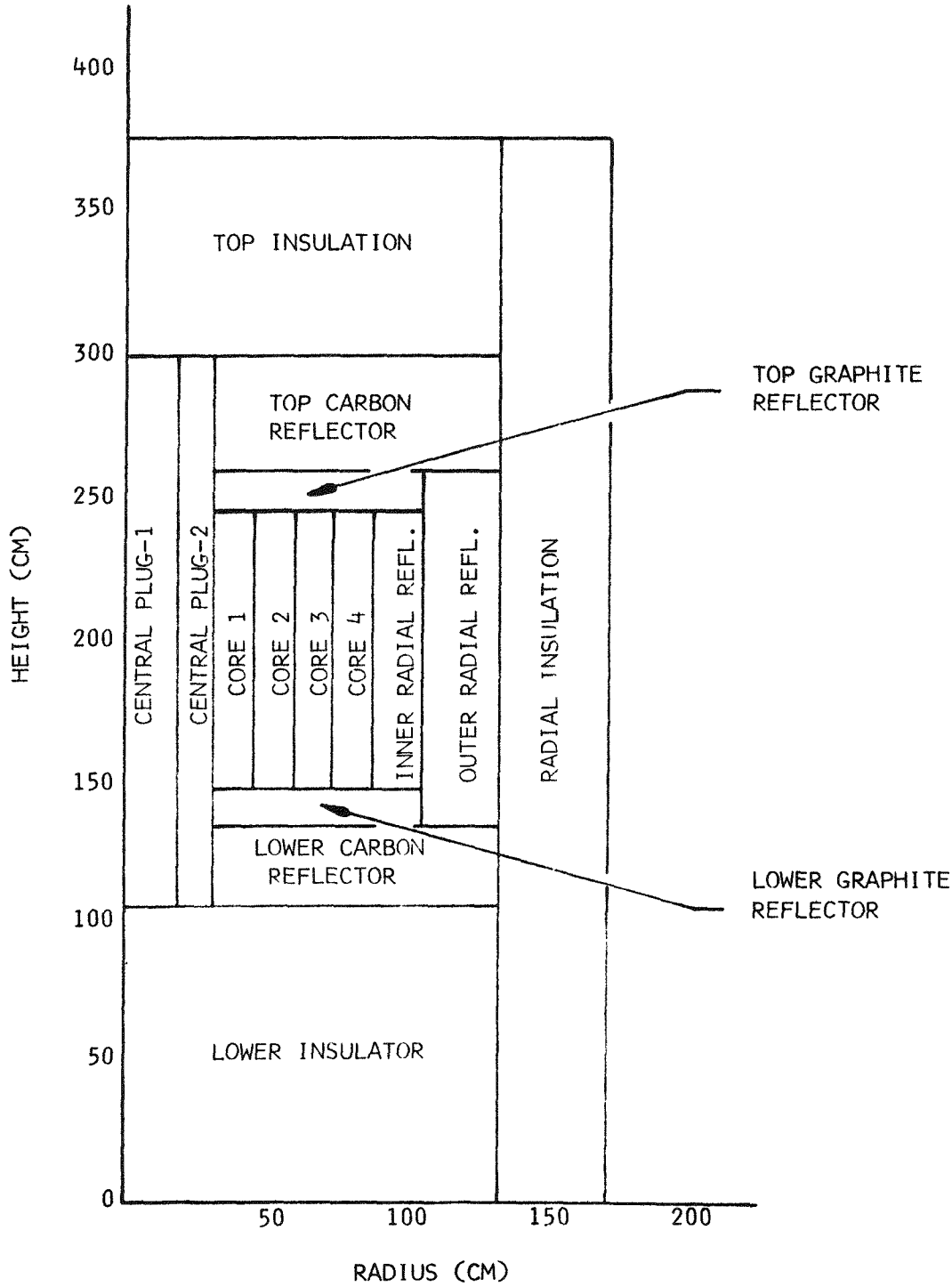

Fig. 4.2.2.2 Simplified, 15-region model used for reactivity and control rod calculations

The essential calculational steps used for accurate estimates of critical masses and effective multiplication constants for UHTREX configurations are enumerated below.

1. The carbon thermal neutron scattering matrix for each given temperature was calculated.

2. Coated particle self-shielding corrections to uranium, xenon, and samarium thermal cross sections were estimated.

3. Using results from (1) and (2), the thermal neutron spectra for the various media in UHTREX were calculated.

4. Spectrum averaged thermal neutron cross sections were obtained from results of (3).

5. With spectrum averaged cross sections, cell calculations were performed to obtain fuel element self-shielding factors.

6. Finally, the spectrum-averaged and cell-averaged cross sections were used in a two-dimensional neutron transport theory calculation for the UHTREX configuration.

In the first four steps of the critical mass calculation procedure, the thermal neutron spectral effects were treated, and in the last two steps the spatial problem was solved, on the assumption that the spatial and spectral problems were separable. This assumption is valid for most UHTREX problems, but for fuel temperature coefficient calculations it is not. The important effect in that case is the variation in the thermal neutron spectrum across the unit cell caused by the temperature differences between the fuel and bulk moderator. This fact is amplified in the detailed discussion of the calculational methods that follows.

Two properties of the moderating medium determine the thermal neutron spectrum. The first property is the temperature of the medium. In scattering interactions between neutrons and atoms, the exchange of energy between the two particles depends directly upon the thermal energy or temperature of the atoms. To take these effects into account for any

given temperature, the SUMMIT code[9] was used to generate a scattering group transfer matrix for 59 energy groups in the range 0-3 eV.

The second spectral determinant is the thermal neutron absorption. If the absorption is very low, neutrons, on the average, undergo many scattering collisions in the thermal energy range before they are absorbed, and their average energies approach the average thermal energy of the medium. On the other hand, if the absorption probability is high compared to the scattering probability, such as in a heavily fueled region or highly absorbing control rod, thermal neutrons may be virtually excluded.

For the computations, temperature and absorption effects were taken into account together by performing infinite medium transport calculations with the THERM code, a part of the SUMMIT code. In general, two types of media were considered: plain graphite or carbon mixtures, and mixtures of fuel and graphite. In the plain carbon mixtures, the absorption is low but nontrivial, and depends upon the contaminants present in the mixture. In the fuel mixtures, the absorption is controlled by the fuel and fission product poison concentrations.

In the infinite medium calculations, 59 group cross sections were first prepared for input to the THERM code. The scattering matrix that characterizes the assigned temperature of the medium was taken from SUMMIT results. Macroscopic group absorption cross sections were prepared for each of the constituent elements. For fuel mixtures of coated particles and graphite, the particle self-shielding factors were applied to the uranium and fission product poison adsorption cross sections.

In general, only a few neutron groups may be used in finite geometry calculations because of computing time limitations. This is particularly the case for two-dimensional calculations. To overcome this limitation, the infinite medium fluxes generated by THERM were applied to the 59

---

[9]J. Bell, "SUMMIT, an IBM-7090 Program for the Computation of Crystalline Scattering Kernels," General Atomics Report GA-2497, February 1, 1962.

group cross sections as weighting factors to obtain one-group effective thermal cross sections, which were then combined with a five-group set of fast cross sections for geometry calculations. The five-group set was derived from the Hansen-Roach 16-group set[10] using standard collapsing procedures.

Corrections for fuel element self-shielding effects were made before the core cross sections were used in finite geometry calculations of the UHTREX configuration. These corrections were obtained from S_n cell calculations with the DTF code.[11]

An UHTREX core cell is a segment of a vertical, cylindrical annulus. If the two ends of a fuel element are defined by the coordinates (R_1, θ_0, Z_0) and (R_2, θ_0, Z_0) in the cylindrical coordinate system of the core, then the surfaces of the associated cell are defined by

$$r = R_1, \; r = R_2,$$

$$\theta = \theta_0 \pm \pi/24,$$

and

$$Z = Z_0 \pm \Delta Z/2,$$

where ΔZ is the vertical distance between channels.

The cell calculations were performed in one-dimensional, infinite cylinder geometry, in which the volume fractions of fuel, moderator, and void were conserved. The actual cells can be represented somewhat more realistically in two-dimensional cell calculations, but comparisons

---

[10] G. E. Hansen and W. H. Roach, "Six and Sixteen Group Cross Sections for Past and Intermediate Critical Assemblies," LAMS-2543, November 1961.

[11] B. G. Carlson et al., "DTF Users Manual," Vols. I and II, UNC Phys/Math-3321, November 1963.

between one- and two-dimensional results were made, and it was found that the differences in the disadvantage factors were small.

In general, for any given UHTREX loading configuration, eight different cells are involved. Typically, two different channel loadings with four different cells are associated with the four fuel elements in each channel loading. A description of the loading procedures and configurations is presented in Appendix D.

In most of the cell calculations, one-group thermal cross sections were used. However, as mentioned before, lumping the thermal neutrons in one group is not adequate for calculations of the fuel temperature coefficient. Since the fuel element dimensions are not large compared to the mean-free paths of thermal neutrons, the variation in the thermal neutron spectrum across a cell must be taken into account. This was accomplished by using, in the DTF cell calculations, a 10-group representation of the thermal neutrons, combined with the five fast groups mentioned earlier. Only down-scattering in energy was considered for the fast groups. However, both up- and down-scattering were treated in the thermal groups, because the thermal neutrons gain energy as well as lose energy in collisions with the moderator nuclei. These so-called "speed up" calculations require considerable computer time; consequently, only one average cell for the entire core was considered.

From the spectrum and cell calculations a set of six-group cross sections was obtained for use in the two-dimensional DDK code[12] for S_n transport calculations of the overall UHTREX configuration. The model for these calculations was cylindrical and extended out to include the insulating porous carbon components and a cylindrical representation of the vessel. These outer regions were included because the insulating carbon's contribution to neutron reflection was found to be significant, and estimates of the fluxes in the vessel and in all the internal materials were needed for radiation damage evaluations.

---

[12]W. J. Worlton and B. G. Carlson, "The DDK Code," an unpublished Los Alamos Scientific Laboratory code.

For regions outside the core, the one-group thermal cross sections were spectrum averaged (with SUMMIT and THERM codes) to account for the temperatures and absorptions of these regions. Core thermal cross sections were cell-averaged, as well, to account for variations in the fuel element loadings.

The S_n transport code, DDK, was used in order to treat the voids in the assembly as realistically as possible. Otherwise, diffusion theory would have been adequate. The DDK code is a latter-day version of the series of S_n angular segmentation codes, SNG,[13] DSN,[14] TDC, etc., developed by B. G. Carlson and coworkers at Los Alamos.

Reactivity Coefficients - The reactivity coefficients were determined by perturbation methods using the Data Analysis Code (DAC) which has been developed recently at Los Alamos. Input to the code includes atom densities and dimensions defining the reactor model, cross sections of the elements contained in the reactor, changes in atom densities, cross sections, and dimensions that define the perturbations, and two-dimensional regular and adjoint fluxes and currents from the DDF code.

A summary of the integrated coefficients is given in Table 4.2.2.1.

Values for the effective delayed neutron fraction, β_{eff}, and the neutron lifetime, ℓ_{eff}, are also included in the table. These, as well as the reactivity coefficients, were obtained from perturbation theory. The effective delayed neutron fraction is only about 6% larger than the absolute delayed neutron fraction (0.00641) in UHTREX, and is not much different for the two cases tabulated. However, the prompt neutron lifetime is substantially lower at high temperatures. This effect is due to the increase in average velocities of thermal neutrons as temperatures are elevated.

---

[13] B. G. Carlson, "The S_n Method and the SNG Code," LAMS-2201, January 1958.

[14] B. Carlson, C. Lee, and W. J. Worlton, "The DSN and TDC Neutron Transport Codes," LAMS-2346, October 1959.

TABLE 4.2.2.1

INTEGRAL REACTIVITY COEFFICIENTS

Coefficient	Case 293°K, 5.68 Kg	Case 1714°K, 11.0 kg
Core moderator temp.	-1.83×10^{-4} ΔK/°C	-1.180×10^{-4} ΔK/°C
Core fuel temperature	-1.40×10^{-5} ΔK/°C	-8.41×10^{-6} ΔK/°C
Reflector temperature	$+8.22\times10^{-5}$ ΔK/°C	$+1.28\times10^{-5}$ ΔK/°C
Fuel element self-shielding	-3.48 % ΔK	-2.62 % ΔK
Coated particle self-shielding	-2.09 % ΔK	-0.922 % ΔK
β_{eff} (effective delayed neutron fraction)	0.00679	0.00676
ℓ_{eff} (neutron lifetime)	9.64×10^{-4} sec	6.76×10^{-4} sec

For each of the temperature cases cited in Table 4.2.2.1, the results were obtained using fluxes and currents from one regular and one adjoint two-dimensional S_n calculation. Unperturbed cross sections from spectrum and cell calculations were used in these reference calculations. To define the perturbations, separate spectrum and cell calculations were performed with the perturbation (temperature change, self-shielding change, etc.) included. The cross-section perturbations were then obtained by subtracting the unperturbed macroscopic cross sections from the perturbed cell-averaged and spectrum-averaged cross sections. These cross-section perturbations were processed by the DAC code to calculate the associated reactivities.

Spatially distributed temperature coefficients are plotted in Figs. 4.2.2.3 and 4.2.2.4, for the 11-kg loading at operating temperature (1714°K). The reactivity of each fuel element and its associated moderator, in units of cents per cm^3 of core per °C, appears in Fig. 4.2.2.3, where I and J represent the radial and vertical fuel element positions, as in the power plot of Fig. 4.2.1.2. The negative temperature coefficient is

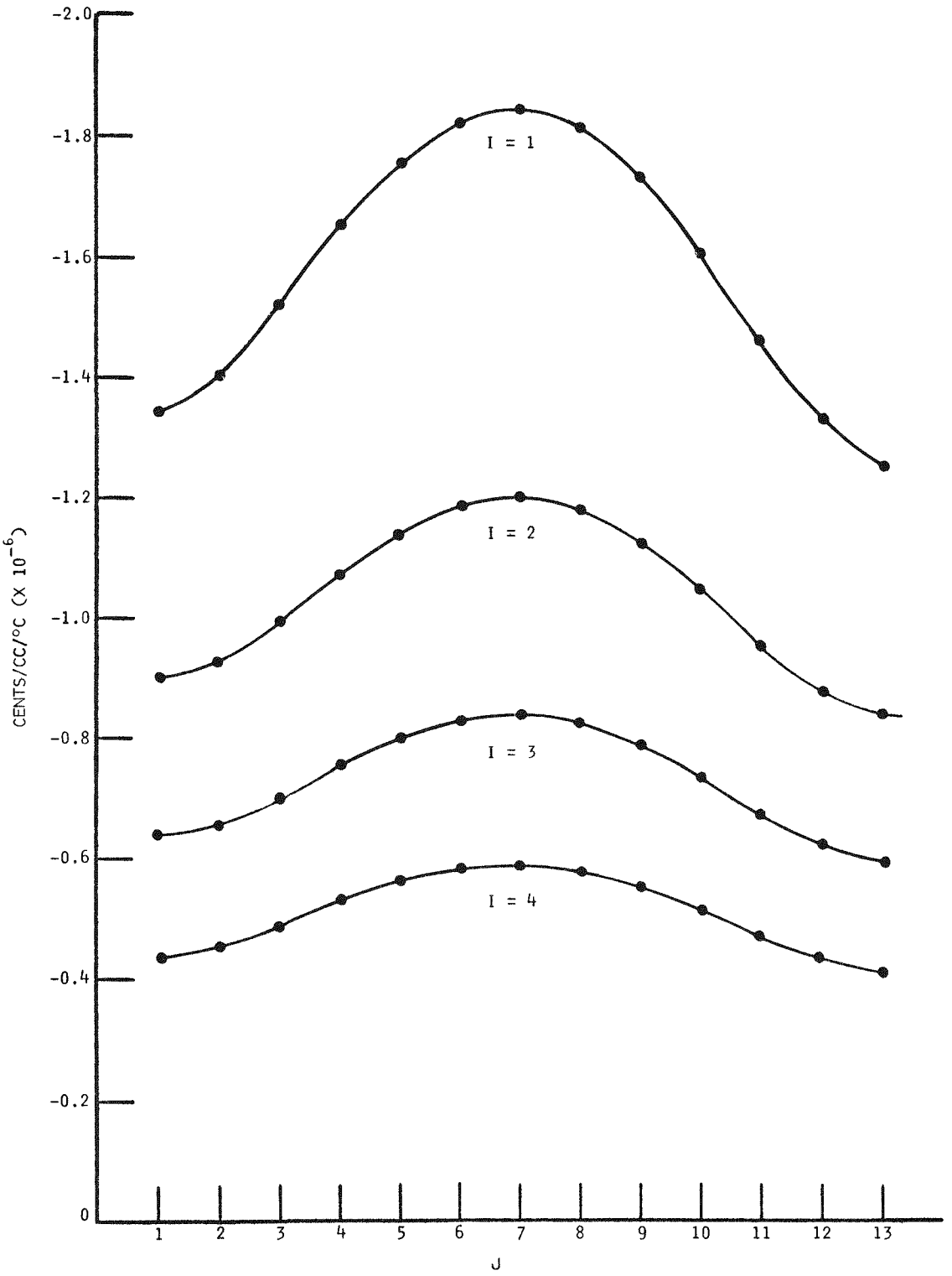

Fig. 4.2.2.3 Distributed moderator temperature coefficients for various radial positions (I) in core with 11.0-kg loading at 1714°K

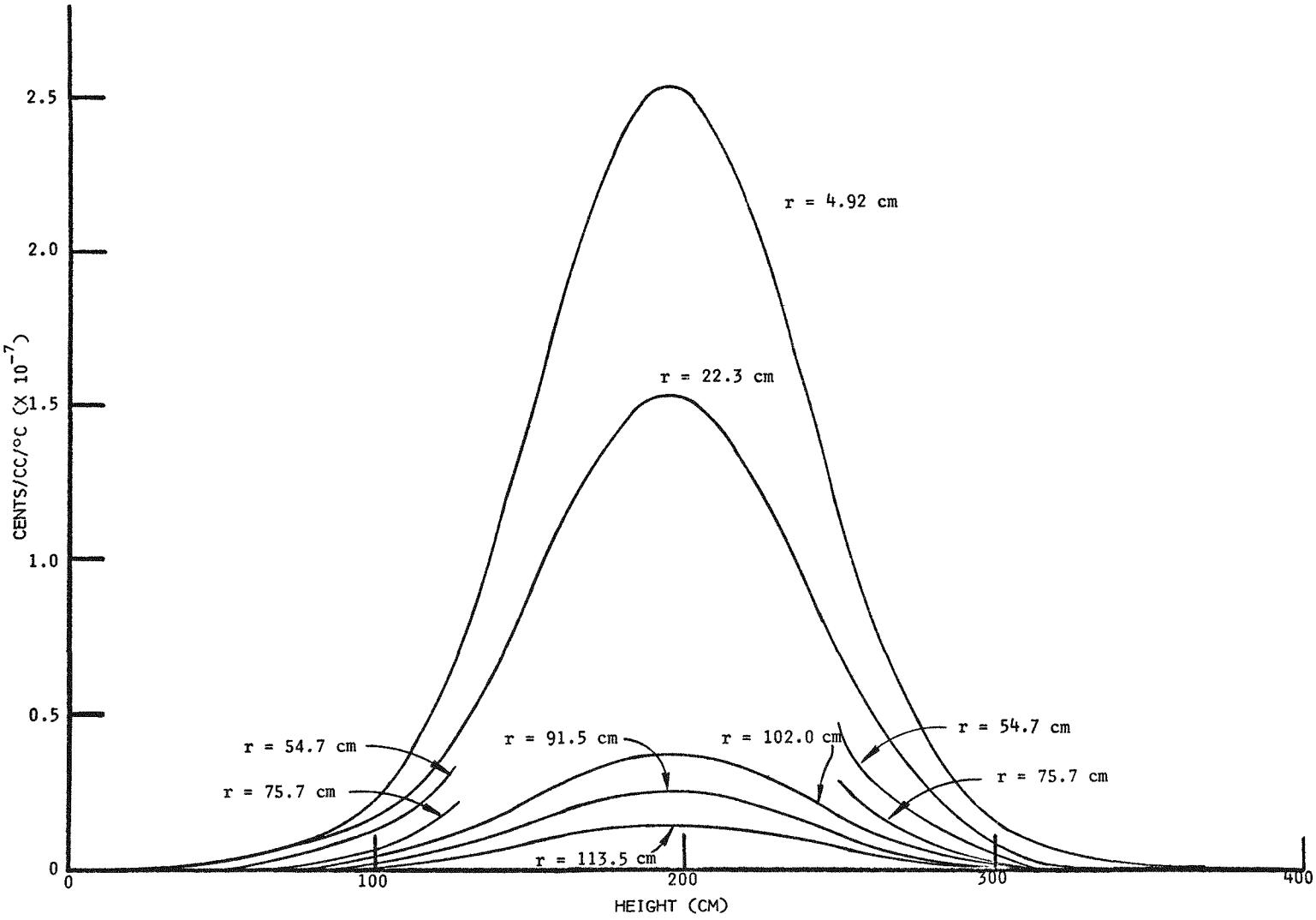

Fig. 4.2.2.4 Distributed reflector temperature coefficients at various radii in core with 11.0-kg loading at 1714°K

strongly peaked in core regions near the most centrally located fuel element (I=1, J=7). This characteristic is advantageous during fast transients, when the power in the central regions of the core might be more peaked than during steady-state operation.

The distributed reflector coefficients are plotted in Fig. 4.2.2.3. Each curve is a plot of the reactivity versus height at a specific radius in the calculational model of Fig. 4.2.2.2. Since the coolant flow in the core is directed radially outward, excursions in the core would cause relatively little heating of the central plug regions (r = 4.92 cm and r = 2.23 cm) where the positive coefficient is highest. The total coefficients for the reflector regions treated in Fig. 4.2.2.2 are listed in Table 4.2.2.2.

TABLE 4.2.2.2

REFLECTOR REGION TEMPERATURE COEFFICIENTS (¢/°K)

Region	Case	
	293°K, 5.68 kg	1714°K, 11.0 kg
Lower insulator	0.0290	0.011
Central plug-1	0.021	0.032
Central plug-2	0.170	0.026
Lower carbon reflector	0.097	0.017
Lower graphite reflector	0.118	0.014
Top graphite reflector	0.108	0.013
Top carbon reflector	0.087	0.013
Inner radial reflector	0.261	0.032
Outer radial reflector	0.110	0.018
Top insulation	0.013	0.005
Radial insulation	0.017	0.007
Total	1.212	0.189

Control Rod Calculations - The methods used in calculating control rod worths in UHTREX have been reported in detail.[15] The cell approach, which is currently used for control rod calculations in many large thermal reactor applications, could not be used because the rods are not distributed evenly over the core but are concentrated in two isolated rings. Instead, two other approaches were used, one analytical and one numerical. The analytical approach is a generalization of a method introduced by Scalettar and Nordheim.[7] Previously, the method had been applied only to the one-region, bare-core case, and to the two-region core plus single, external reflector case. For application to UHTREX, the method was extended to yield solutions for the worth of a control ring situated anywhere in a reactor composed of any number of regions.

In the analytic calculations, two-group, diffusion-theory, flux solutions were constructed which contain enough arbitrary constants to permit the satisfaction of boundary conditions at the regional interfaces of the reactor and at the surfaces of the cylindrical rods. The application of the boundary conditions provided a critical determinant that was used for calculating the K_{eff} of a system that contains a ring of control rods. A second calculation was made of the K_{eff} for the system without the rods. Comparison of the results of the two calculations yielded a ΔK_{eff} which was the ring worth.

The two-group, multiregion solution, which is well adapted to machine calculations, was incorporated in the RC3 code[15] for extensive use in UHTREX control ring problems. Savings in computing time, over strictly numerical, two-dimensional methods, made economically feasible the performance of extensive parametric surveys of ring worths. In the surveys, investigations were made of ring parameters, e.g., ring location and the number of rods contained in the ring, and rod parameters, e.g., rod diameter and rod extrapolation distances.

---

[15]B. M. Carmichael and R. J. LaBauve, "Control Rod Calculation Techniques with Applications to the UHTREX Reactor," LA-3194, November 1964.

The CRAM[16] diffusion code and the S_n transport theory codes, DTK and DDK, were used primarily to investigate the effects of the approximations and assumptions made in the two-group analytic study of control rod worths. The one-dimensional options in the codes were used first to establish appropriate input parameters for use in the two-dimensional calculations, where particular studies were made of the perturbations on the transverse or vertical neutron leakages caused by rod insertions. These effects had not been taken into account in the earlier two-group work.

The control ring numerical calculations were based upon applications of the r-θ options of the codes. A particular problem, however, arose in connection with the representation in the r-θ mesh of off-center cylindrical rods. In the UHTREX calculations, the off-center rod was represented by a single polar coordinate element with a radial increment, Δr, and an angular increment, $\Delta\theta$. Since the interaction of the thermal flux with the rod is primarily a circumferential effect, it was required that the circumference of the polar element and the actual rod circumference be equal. Under this condition, the cross-sectional area of the element is necessarily less than the actual rod area, but it was maximized to achieve 79% of the rod area through the use of the relation

$$\Delta r = a\Delta\theta = \pi c/2,$$

where a is the ring radius, and c is the rod radius. The use of more than one polar element to represent the rod was not adopted, because the discrepancy between circumference and area increases with the number of elements. Moreover, the number of space intervals increases rapidly, because of the fine structure required on each surface segment.

The general calculational procedure used in the ring calculations was as follows.

---

[16]A. Hassitt, "A Computer Program to Solve the Multigroup Diffusion Equations," UKAEA, TRG Report 229(R), 1962.

1. An r-θ problem was first run, using leakage cross sections from the zero-rod case. The geometry for a ring containing n rods was a pie-shaped cylindrical sector of angular width π/n. Fine structure in both the r and θ intervals was adopted near the rod surfaces.

2. Next, a series of one-dimensional cylindrical problems was run to define an annulus whose worth was equivalent to that of the ring of rods. In the calculations, the annulus was centered on the ring radius, and the width of the annulus was made equal to the radial increment, Δr, used to represent the rod in the r-θ calculation. Then, the boron concentration was adjusted to make the worth of the annulus equivalent to that of the ring.

3. The next step was an r-z calculation with an equivalent annulus that extended vertically through the core a distance equivalent to the actual lengths of the rods.

4. Finally, vertical leakage cross sections from the calculation of (3) and starting fluxes from the r-θ problem of (1) were used in a final r-θ calculation of the ring. The whole procedure was designed to take into account the three-dimensional end-leakage effects.

Results from the control rod calculations are given in Table 4.2.1.1.

Reactor Kinetics Calculations - A method for solving systems of non-linear differential equations known as continuous analytic continuation[8] was used in the UHTREX kinetics calculations. The method consists of expanding the dependent variables in Taylor series over successive overlapping analytic regions and is well suited for machine solution.

In the application of the point reactor kinetics equations

$$dN(t)/dt = \Lambda^{-1}[\rho(t) - \beta]N(t) + \sum_{i=1}^{6}\lambda_i C_i(t) + S \qquad (4.2.2.1)$$

$$dC_i(t)/dt = \Lambda^{-1}\beta_i N(t) - \lambda_i C_i(t) \qquad i = 1, \ldots, 6, \qquad (4.2.2.2)$$

the values of the dependent variables at $t = t_{j+1}$, such as the neutron and precursor populations or the system temperatures, are determined from those at $t = t_j$ by the Taylor expansion

$$f(t_{j+1}) = \sum_{n=0}^{K} f^{(n)}(t_j)(t_{j+1} - t_j)^n/n! \qquad (4.2.2.3)$$

The derivatives in Eq. (4.2.2.3) are obtained by differentiation of (4.2.2.1) and (4.2.2.2) and from the equation defining $\rho(t)$. The time step $t_{j+1}-t_j$ is obtained by requiring that the relative truncation error (determined by the remainder in the Taylor expansion) be $\leq\varepsilon$, where ε is an input parameter. By using a large-order K in the expansion, the time step can be made much larger than Λ. The relative error accumulation, E_n, after n time steps is given by $|E_n| \leq n\varepsilon$; i.e., the error accumulates, at most, linearly with the number of time steps.

The power decay curves in Section 4.2.1 and the rod withdrawal excursions in Sec. 16.2.1 were computed with a code based upon the above analysis technique. A one-lump, or point, model was used for treating the transient heat absorption and transfer in the core. It was assumed that 95% of the total fission energy is deposited in the fuel by the recoiling fission fragments, and that 5% of the energy from fission is deposited directly in the bulk moderator by neutron and gamma-ray energy absorption. Allowance was made for heat transfer from the fuel and bulk moderator by convection to the gas coolant, and for heat transfer from the fuel to the moderator by radiation. The reactivity function consisted of a driving term, due to rod insertion or withdrawal, and feedback terms derived from the fuel and moderator temperature coefficients.

4.3 Thermal Design

From the nuclear power distribution in the core, temperature distributions in the fuel elements and the core region were calculated. The

calculated core temperatures were then used to extend the temperature distribution analysis throughout the entire reactor, encompassing the outer reflector, insulation, and pressure vessel.

Flow analyses, based on the original core plug design, predicted flow imbalances and concomitant heat transfer problems. The solutions were found in an empirical investigation of the coolant flow through the core, and the plug was redesigned.

4.3.1 Temperature Distribution Analyses

Core - Two computer codes have been used to calculate the temperature distribution in the UHTREX core. One code computes both heat transfer and coolant flow distribution between the fuel element hole and the eccentric annulus for a single, isolated fuel channel. The other code calculates the temperature distribution in a seven-channel vertical wedge of the core for a certain flow and power distribution. The single-channel code, VAFLO, was written specifically for UHTREX and has considerable versatility in the selection of parameters that affect temperature and flow. The other is a LASL modification of the HEATING program that was prepared at ASTRA, Inc.[17] Both programs use a finite-difference technique to represent the conservation of energy equation and the Gauss-Seidel method for solving the simultaneous equations resulting from the implicit finite-difference representation. A detailed report of the computational methods and results has been published.[18] Brief discussions are presented below of the bases for the calculations and of the results most relevant to the final UHTREX core.

A power distribution was calculated for the radially tapered fuel loadings described in Appendix D of this report. The mass of fuel

---

[17]R. R. Liguori and J. W. Stephenson, "The HEATING Program," ASTRA, Inc., Raleigh, N.C., January 1, 1961.

[18]D. W. McEachern, "Ultra High Temperature Reactor Experiment -- Core Heat Transfer Calculations," LA-3136-MS, July 20, 1964.

contained in successive fuel elements in the same channel has the relationship c', c'x, c'x^2, c'x^3, where the innermost fuel element contains c' mass of fuel. The power distribution results presented here are for the studies corresponding to $x^3 = 1.6$. For a given value of x^3 the value of c' was the same for all fuel channels; i.e., there was no vertical tapering of the fuel loading.

For calculations made with the HEATING code, the helium coolant flow was considered to enter at the bottom of the inner annulus at 1600°F and flow upward in the inner annulus through the fuel channels and out through the outer annulus. The flow in each channel was taken to be 10,250/312 lbm/h, with 85% of the mass of helium passing through the element hole and 15% of the helium flowing through the fuel-channel annulus.

Heat transfer coefficients were assumed constant throughout the section under consideration. Their values for the various types of surfaces are as follows.

Type of Surface	Heat Transfer Coefficient (Btu/h-ft^2-°F)
Fuel element hole	135
Fuel element annulus	45
Inner annulus	85
Outer annulus	85

Transmission of heat by radiation was accounted for only by a simplified procedure. An "effective" conductivity, $_2K_1$, between two nodal points, which is linear in the temperature difference between the two points, was evaluated by estimating the temperatures of the two nodal points and by using the formula

$$_2K_1 = \frac{qA}{T_1 - T_2} = \frac{\sigma AF\left(T_1'^4 - T_2'^4\right)}{T_1' - T_2'} = \sigma AF\left(T_1'^2 + T_2'^2\right)(T_1' + T_2'),$$

where q is the heat flux, A is the heat transfer area, σ is the Stefan-Boltzmann constant, F is the view factor, and T' is absolute temperature.

Heat exchange by radiation was assumed to take place (1) between the core plug and the moderator across the inner annulus, (2) between the moderator and reflector across the outer annulus, and (3) between the fuel element and the moderator across the fuel channel annulus. In addition, it was assumed that heat exchange by radiation took place only between nodal points which were directly opposite one another. The values of view factor F used in each of the three regions named above were (1) across the inner annulus, F = 0.9; (2) across the outer annulus, F = 0.9; and (3) across the fuel channel annulus, F = 0.8.

In Figs. 4.3.1.1 through 4.3.1.3, temperature profiles are shown for a vertical segment of the core containing seven channels. Temperatures of the (1) coolant gas flowing through the fuel channel annulus, (2) coolant gas flowing through the fuel element hole, (3) moderator adjacent to the fuel element, and (4) fuel elements are shown for fuel loadings corresponding to $x^3 = 1.6$.

As would be expected, the channel temperatures increase as the center channel (channel 7) is approached. The values of maximum temperatures and the values of the temperature gradients do not indicate that there will be any difficulty with the operation of the UHTREX core because of excessive temperature or excessive thermal stress.

One important reason for making the analysis for the segment of the core was to find temperatures in the core which might be used as boundary temperatures in a heat transfer code that calculates the temperature distribution in the remainder of the reactor and in the pressure vessel. The code for this later computation, the results of which are discussed below, used the following calculated core temperatures as inputs. (1) Temperatures of the moderator adjacent to the fuel elements in the lowest fuel channel (channel 1), and (2) the temperatures of the reflector bordering on the outer annulus.

For a cross check, the temperatures of the nodal points located below the lowest fuel channel, which were calculated by the seven-channel HEATING code, were compared with the temperatures calculated for these

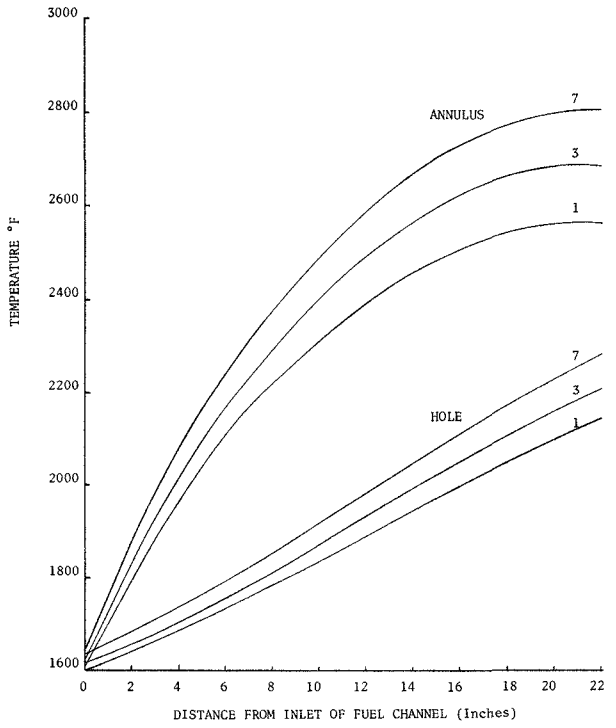

Fig. 4.3.1.1 Channel annulus and fuel element hole gas temperatures. curves for Channels 1, 3, 7 are shown, $x^3 = 1.6$

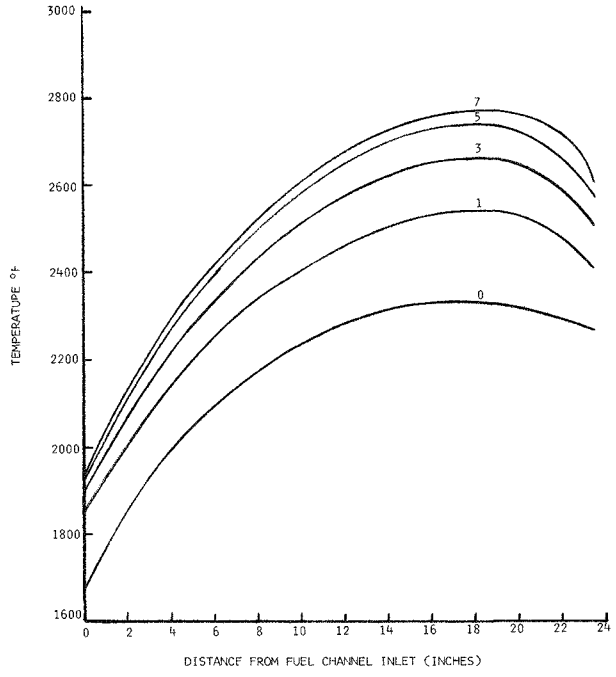

Fig. 4.3.1.2 Temperature of moderator adjacent to fuel elements. Channel numbers increase from bottom of core. Profile 0 is for bottom surfaces of core cylinders

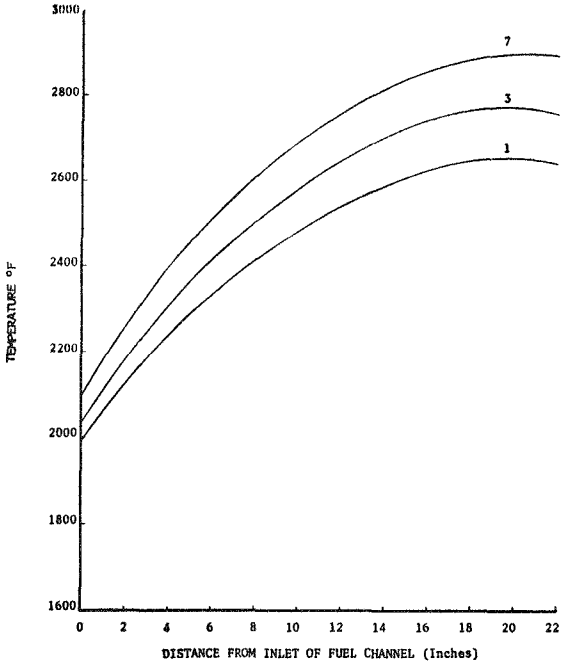

Fig. 4.3.1.3 Fuel element temperatures. Curves for Channels 1, 3, 7 are shown. $x^3 = 1.6$.

same points by the reactor heat transfer code, described below, which uses the boundary temperatures calculated by the HEATING code. The temperatures calculated by the two methods agreed within 3%.

Entire Reactor - An extensive analysis has been made of the temperature distribution in the entire reactor, including the reflector and insulation, and in the steel reactor pressure vessel. Representative results are plotted in Fig. 4.3.1.4 which shows temperatures in the symmetrical areas of the reactor and vessel. Although only one set of values is shown in the figure, many different cases were computed with various combinations of assumed thermal properties for the carbon materials. The final conclusion, drawn from the results of the entire analytical study, is that the pressure vessel, in general, will operate at temperatures well below its 650°F design temperature.

Temperature profiles in the reactor were calculated by relaxation methods using a generalized heat conduction code. The calculations were

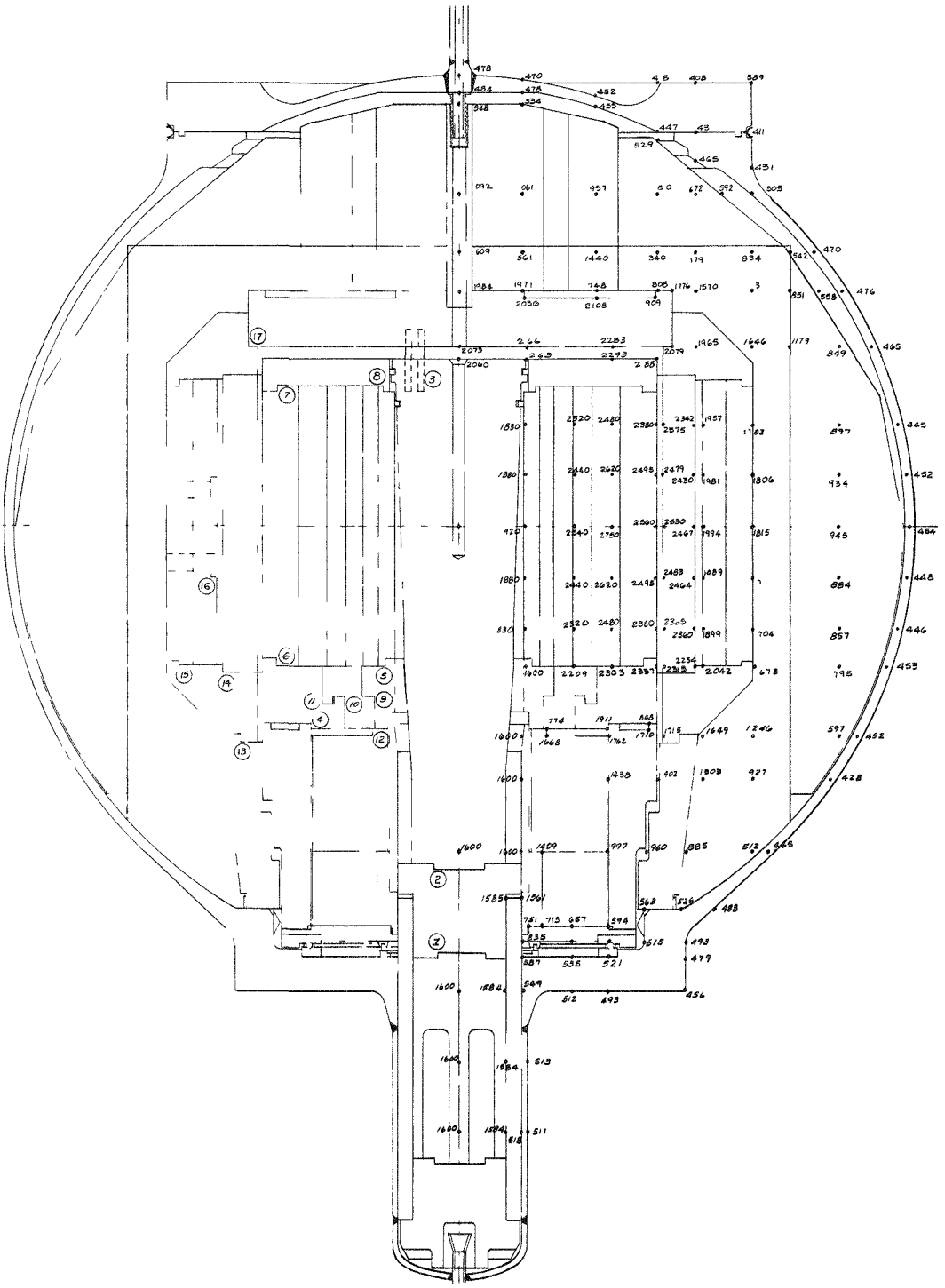

Fig. 4.3.1.4 Temperature distribution (°F) in reactor and pressure vessel

done separately for the top and bottom halves of the reactor with approximately 750 nodal points for each. For these problems, the temperatures and heat fluxes were computed on the basis of the following considerations.

1. Inlet helium temperature was taken to be 1600°F.

2. Core boundary temperatures were defined by the results of calculations of nuclear power profiles and heat transfer within the core. The consistency of the two sets of calculations was verified by extending the range of each set a short distance across the boundary.

3. Heat dissipation from the vessel was assumed to occur by radiation to 150°F cooling panels and by natural air convection with 200°F free air temperature. An emissivity of 0.70 was used for the vessel, and the convection coefficient was estimated to be 1.25 Btu/h-ft^2-°F under the prevailing conditions.

4. Thermal conductivities used in the calculations were:

Steel	24.0 Btu/h-ft^2-°F/ft
Graphite	24.0 Btu/h-ft^2-°F/ft
Dense carbon	6.0 Btu/h-ft^2-°F/ft
Porous carbon	2.0 Btu/h-ft^2-°F/ft
Graphite felt	0.3 Btu/h-ft^2-°F/ft.

Experimental measurements of the thermal conductivity of these materials in helium showed these values to be very conservative for the insulating material.

5. Except for the steel pressure vessel, neutron and gamma heating was not considered. It was estimated that 48 kW would be generated in the pressure vessel.

6. All contact resistance between carbon components and between the carbon components and vessel was neglected. Convection or radiation heat transfer in the outer coolant annulus was treated as conduction.

7. At the lower flange (bearing) and at the top of the reactor, an equivalent conductance was estimated to account for radiation plus convection heat transfer.

The asymmetric portions of the reactor, around the recuperator nozzle and the fuel elevator, were anlyzed in greater detail. Temperatures at the nozzle, presented in Fig. 4.3.1.5, are well within the design limits. However, at spots on the inner surface of the elevator housing, depicted in Fig. 4.3.1.6, temperatures exceed 700°F when the graphite loader ram is inserted with its tip at the inner edge of the reflector. In actual practice, the ram will be withdrawn to a dwell position outside the reflector to prevent overheating of the elevator housing.

4.3.2 Coolant Flow Analyses

Forces that arise from the flow of helium through the reactor core do not cause erosion, vibration of fuel elements, or other destructive kinetic effects. However, the asymmetry of the flow path does create an unequal distribution of flow among the fuel channels.

The only practical method of maintaining uniform flow is to shape the flow channels properly. For the inner annulus, a taper on the central core plug causes a decrease in the flow area as the gas flows upward. In the outer annulus, the core is oriented eccentrically to the reflector to create an increasing flow area as the gas moves around the core diameter toward the exit nozzle.

A rigorous mathematical analysis of the complicated flow path through the core would be impractical. Therefore, the flow distribution was determined experimentally with a flow model, a half-scale, geometrical duplicate of the core, central core plug, reflector inner surface, and exit nozzle. Electrical resistance heaters simulated the fuel elements in each fuel channel and the heat generation in the moderator. With the exception of the radiant heat transfer within the core, all similarity numbers were modeled for a thermal, as well as flow, model. Nitrogen at approximately 15 psia and at an inlet temperature of 100°F was the model fluid. Similarity numbers, e.g., N_{Re}, N_A, N_{Nu}, were modeled quantitatively for the design conditions of the prototype: 3 MW, 2.85 lb/sec helium flow, 500 psia, and 1600°F at the inlet.

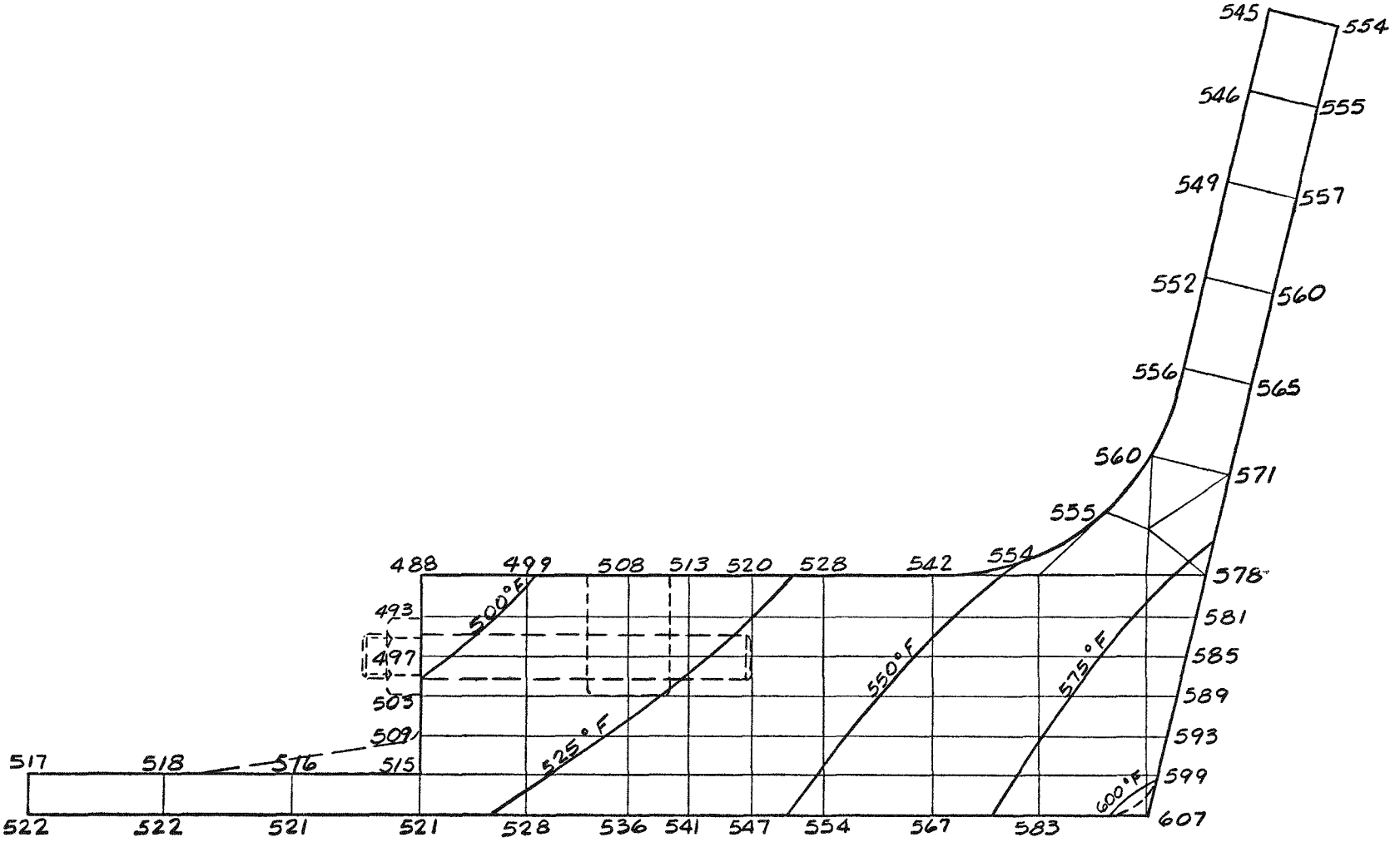

Fig. 4.3.1.5 Temperature profiles at reactor-recuperator nozzle

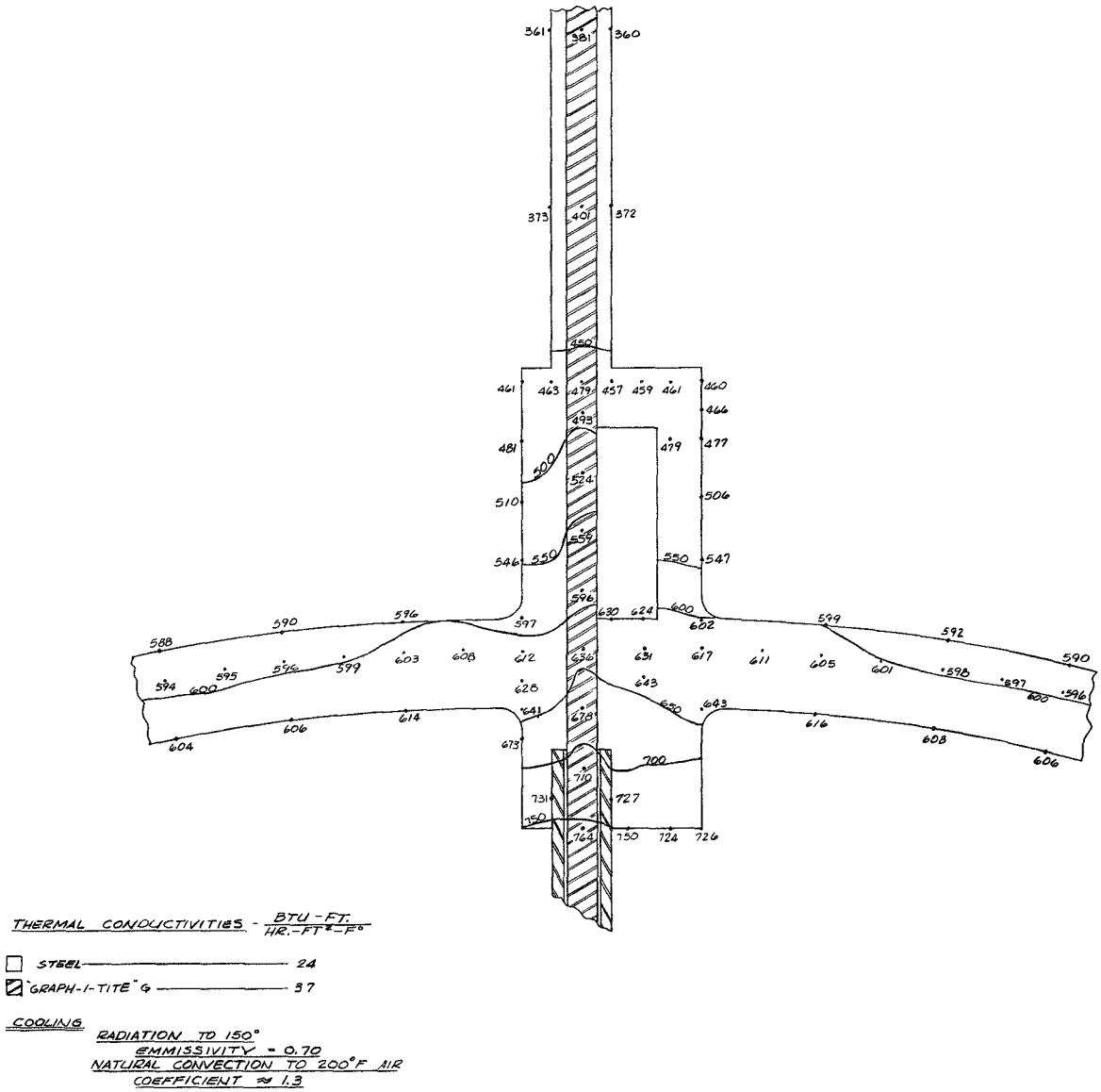

Fig. 4.3.1.6 Surface temperatures (°F) on fuel elevator housing

One vertical row of heated channels contained five sets of pressure taps and thermocouples, one set in every third channel, to measure static and kinetic pressures and gas and solid temperatures. The position, in relation to the exit nozzle and core plug fuel slot, of this row of instrumented channels was changed to measure the flow and temperature distributions at various positions around the azimuth.

The optimum geometric configuration for the inner and outer annular flow passages yielded the results presented in Figs. 4.3.2.1 and 4.3.2.2 which show a typical axial and azimuthal distribution of flow. The distribution through all instrumented channels, from a correlation of all data at the simulated prototype conditions, is presented in Table 4.3.2.1. Although the maximum flow in any channel remained 30% greater than the minimum, no further refinements were made because of the overriding effects of heat losses. Conduction and radiation losses from the core, and convection to the gas in the outer annulus had a stronger effect on temperature distribution in the core than did the remaining flow imbalance. Radial temperature profiles from model data agree with the temperature profile calculated with the HEATING code.

At the completion of the model study, the knowledge gained was applied in design modifications to the core plug and to the arrangement of the core within the reflector.

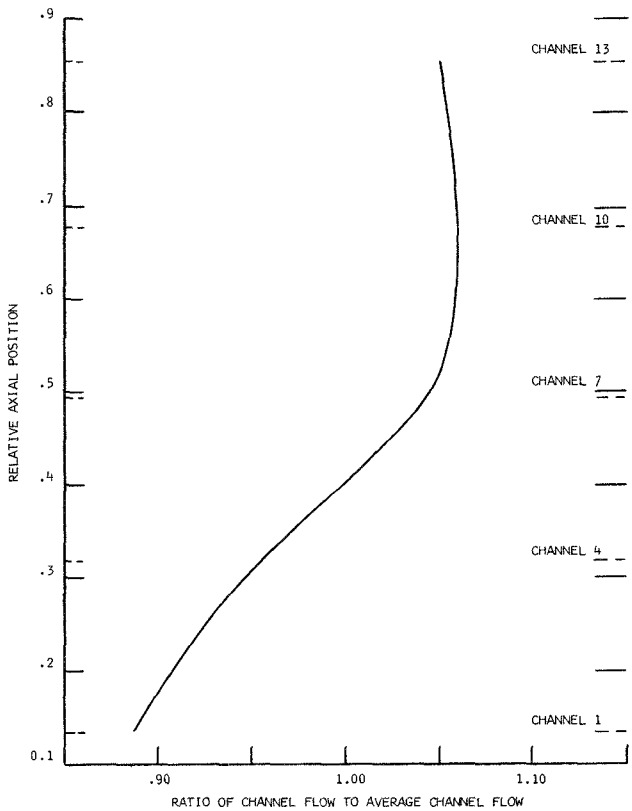

Fig. 4.3.2.1 Ratio of channel flow to average channel flow

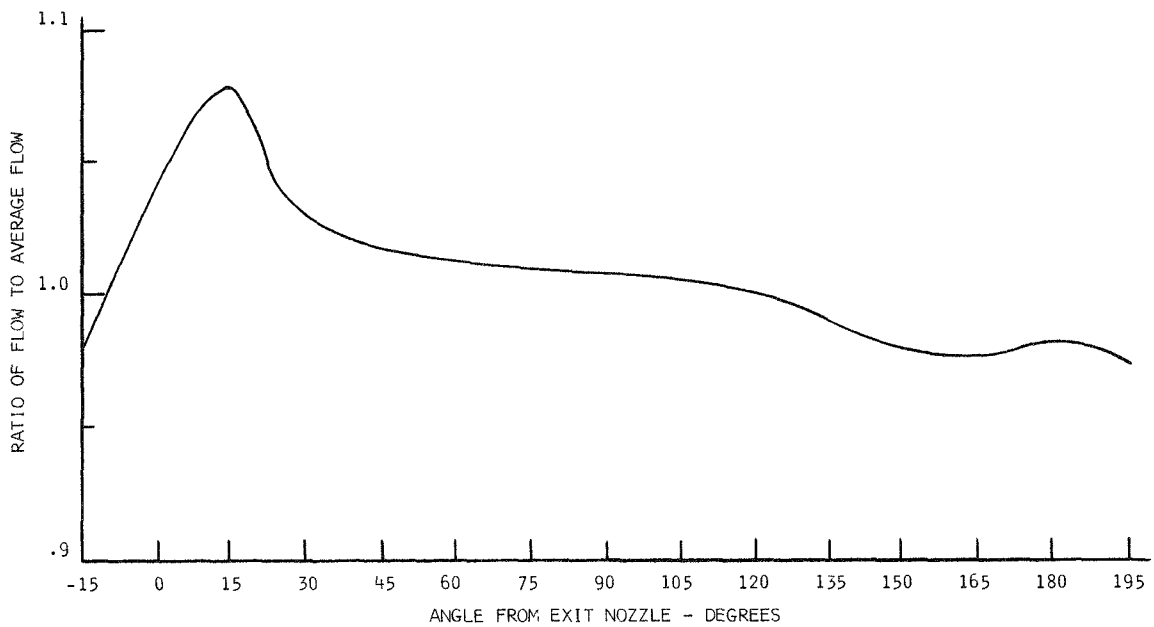

Fig. 4.3.2.2 Azimuthal flow distribution

TABLE 4.3.2.1

FLOW DISTRIBUTION IN CORE FLOW MODEL

Simulated Prototype Conditions:

Mass flow (lb/h) = 10,348 Reactor power = 3.0454 MW

Inlet temp (deg F) = 1600 Outlet temp = 2296°F

Reactor pressure = 500 psi

Flow Distribution At Position*	Channel 1	4	7	10	13	Mean
-15	0.862	0.950	1.086	1.048	0.958	0.981
0	0.911	1.011	1.086	1.112	1.054	1.035
15	0.955	1.090	1.109	1.146	1.084	1.077
30	0.917	1.018	1.057	1.083	1.054	1.026
45	0.915	0.990	1.044	1.066	1.059	1.015
60	0.907	0.974	1.045	1.065	1.062	1.011
75	0.899	0.960	1.048	1.072	1.065	1.009
90	0.891	0.969	1.041	1.076	1.069	1.009
105	0.883	0.949	1.034	1.065	1.066	0.999
120	0.881	0.956	1.048	1.068	1.069	1.004
135	0.854	0.931	1.028	1.048	1.064	0.985
150	0.817	0.893	1.041	0.997	1.015	0.953
165	0.815	0.862	1.035	0.984	1.005	0.940
180	0.907	0.867	1.022	1.034	1.084	0.983
195	0.877	0.863	1.027	1.048	1.056	0.974
Mean	0.886	0.952	1.050	1.061	1.051	

*Measured in degrees clockwise from exit nozzle.

5. COOLANT SYSTEM

5.1 Design Description

Under full-power conditions, two closed-cycle helium loops remove 3 MW of heat from the reactor core and dissipate it to the atmosphere. Figure 5.1.1 is a schematic diagram of the coolant systems and their nominal design temperatures. The primary coolant loop forms a closed system inside the secondary containment. Heat passes from the primary loop to a secondary cooling loop through the main heat exchanger. The secondary loop moves the heat to an air-cooled heat dump outside the reactor building. Under nominal conditions, helium flow rates in the two loops are matched; flow in the primary loop is 10,250 lb/h at 500 psia under full power conditions.

5.1.1 Primary Coolant Loop

The primary coolant loop components are illustrated in Figs. 5.1.1.1 and 5.1.1.2. Primary coolant helium enters the central plenum of the reactor at a temperature of 1600°F. As the coolant passes radially outward through the fuel channels, the helium gains heat and its temperature rises to 2400°F at the reactor outlet. The coolant stream then passes through the hot side of the recuperator, where the helium cools to 1400°F. From the recuperator, the helium flows to the main heat exchanger, where the stream temperature is dropped to 600°F by heat transfer to the secondary coolant loop. The coolant then passes through the blower, which can develop 8 psi pressure rise, and into the cool side

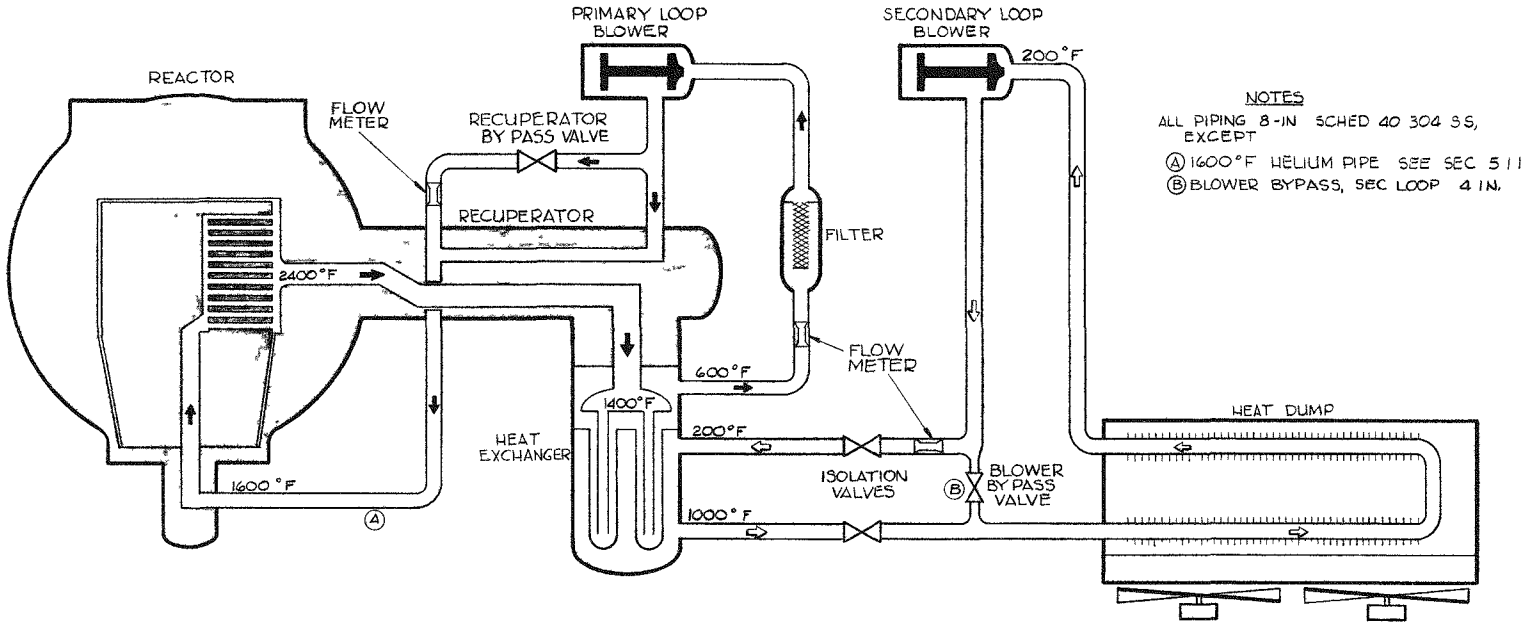

Fig. 5.1.1 Reactor coolant systems

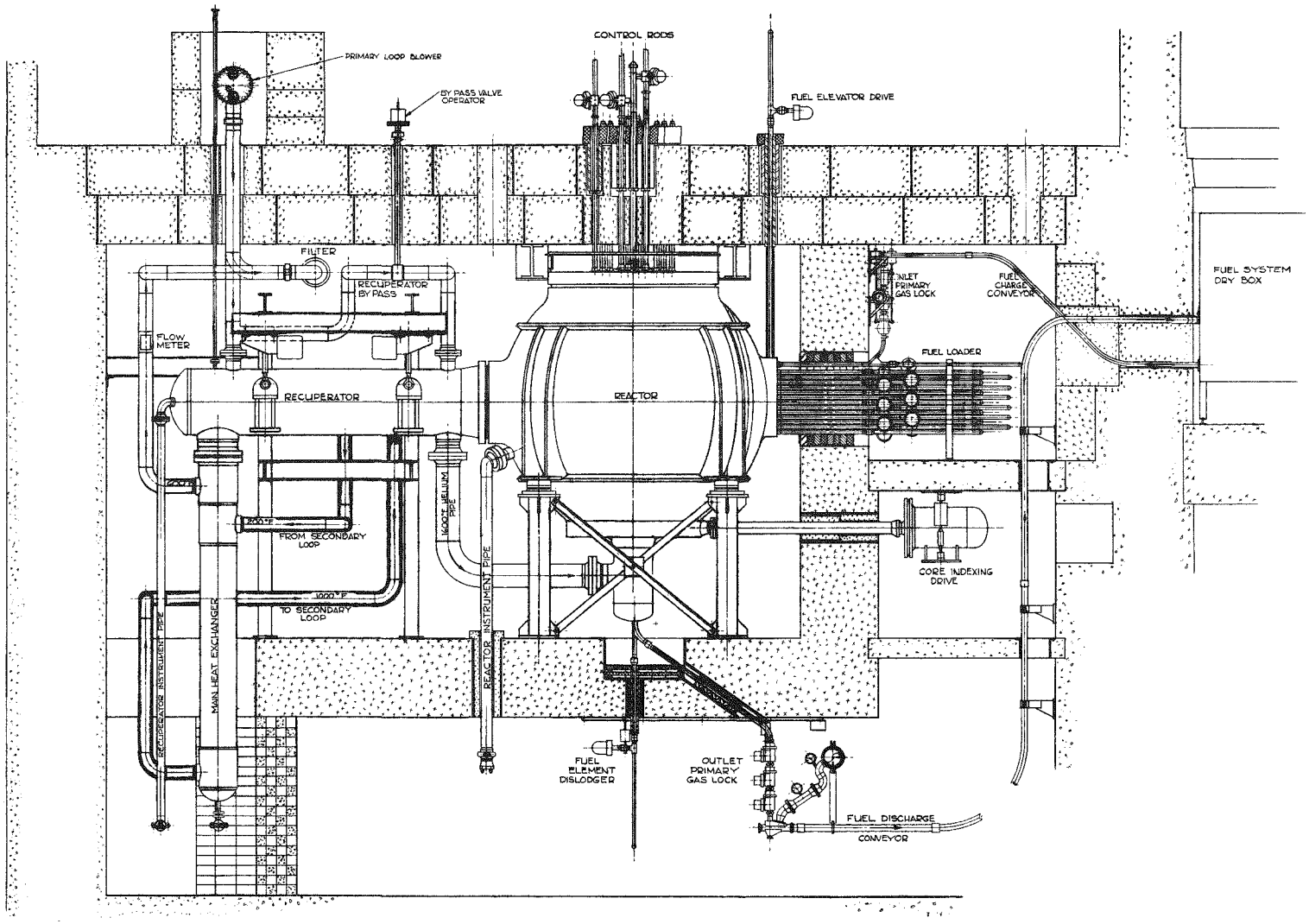

Fig. 5.1.1.1 Elevation of reactor and auxiliaries

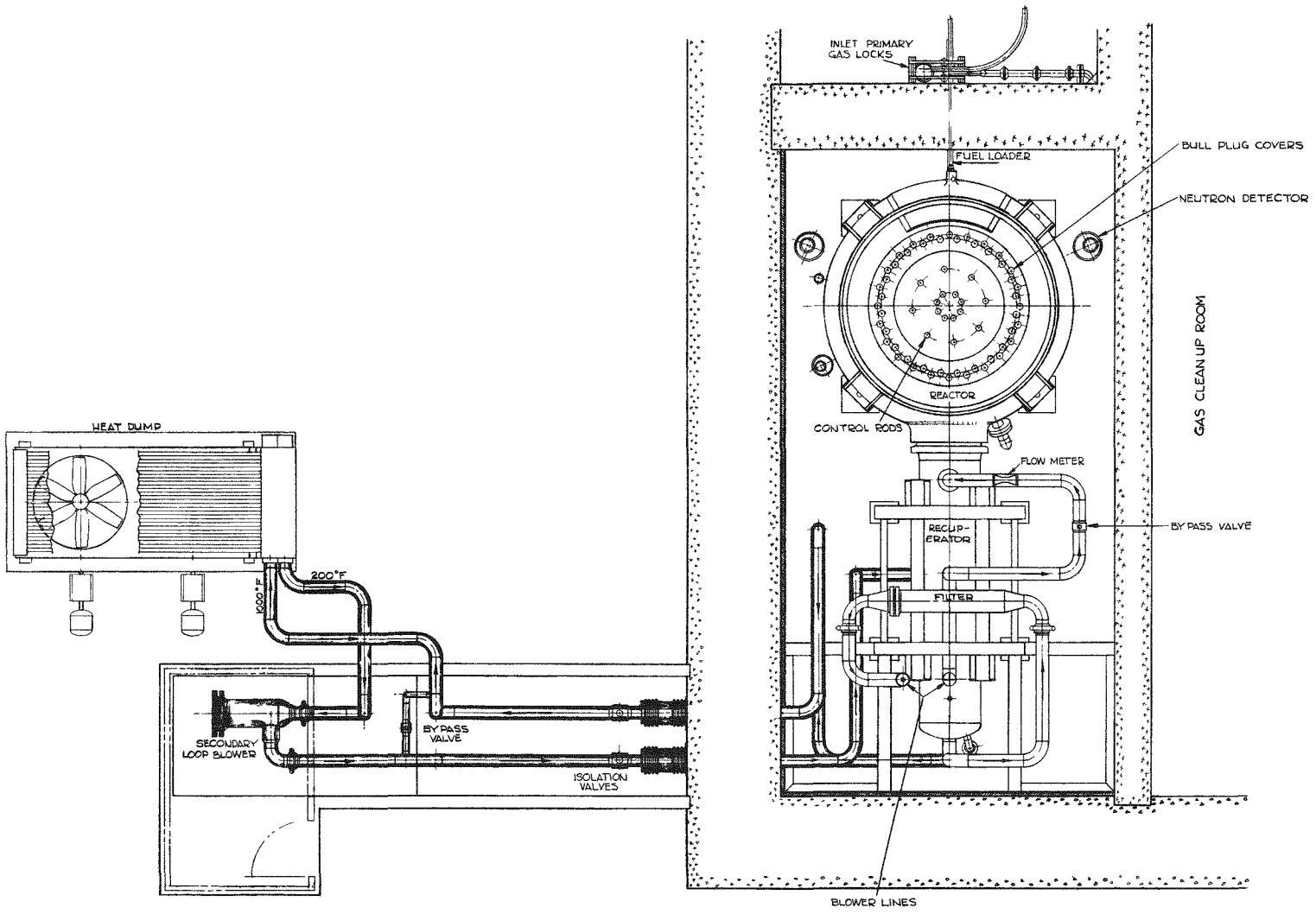

Fig. 5.1.1.2 Plan of reactor and auxiliaries

of the recuperator. Beyond the recuperator, the helium, its temperature restored to 1600°F, reenters the reactor to complete the loop.

Recuperator - An internally-insulated, regenerative heat exchanger, the recuperator reduces the helium coolant temperature from 2400°F, too hot for heat exchangers made of ordinary materials, to 1400°F, tolerable in the stainless steel main heat exchanger. At full reactor power, the recuperator exchanges 1.28×10^7 Btu/h between the hot, reactor-outlet helium and the cooler gas returning to the reactor. During operations, the cold-side flow rate is varied by means of bypass flow to obtain the desired hot-side heat exchange. The heat transfer area is overdesigned by about 25% to allow for uncertainties.

The recuperator, depicted in Figs. 5.1.1.3 through 5.1.1.6, consists of a graphite internal assembly wrapped in graphite felt insulation and supported on carbon blocks inside a carbon steel pressure vessel. Heat exchange occurs through the graphite walls between adjacent holes bored through the length of the five central heat exchanger blocks of the core. (See Fig. 5.1.1.5.) The 0.5-in.-diam holes, drilled on 15/16 centers, are arranged in 24 columns of 19 holes each. Through adjacent columns flow the hot, reactor outlet stream and the cool stream returning from the blower. At joints, between the core blocks and the headers at each end, graphite sleeves are cemented into the holes to make continuous flow channels and to maintain the alignment of the blocks.

Flows to and from the various columns of holes are distributed inside an inlet header, Fig. 5.1.1.4, and an outlet header, Fig. 5.1.1.6. The inlet header block is joined to the outlet of the reactor by a double, ball-and-socket connector that appears in Fig. 4.1.1.1. The socket of the recuperator half of the connector screws into the inlet header block. Its ball is inserted from the reactor side, after the reactor and recuperator are joined, and is held in place by a nut that engages the thread on the outer diameter of the recuperator socket piece. Internal passages within the header blocks are drilled holes, some of them plugged to form blind passages.

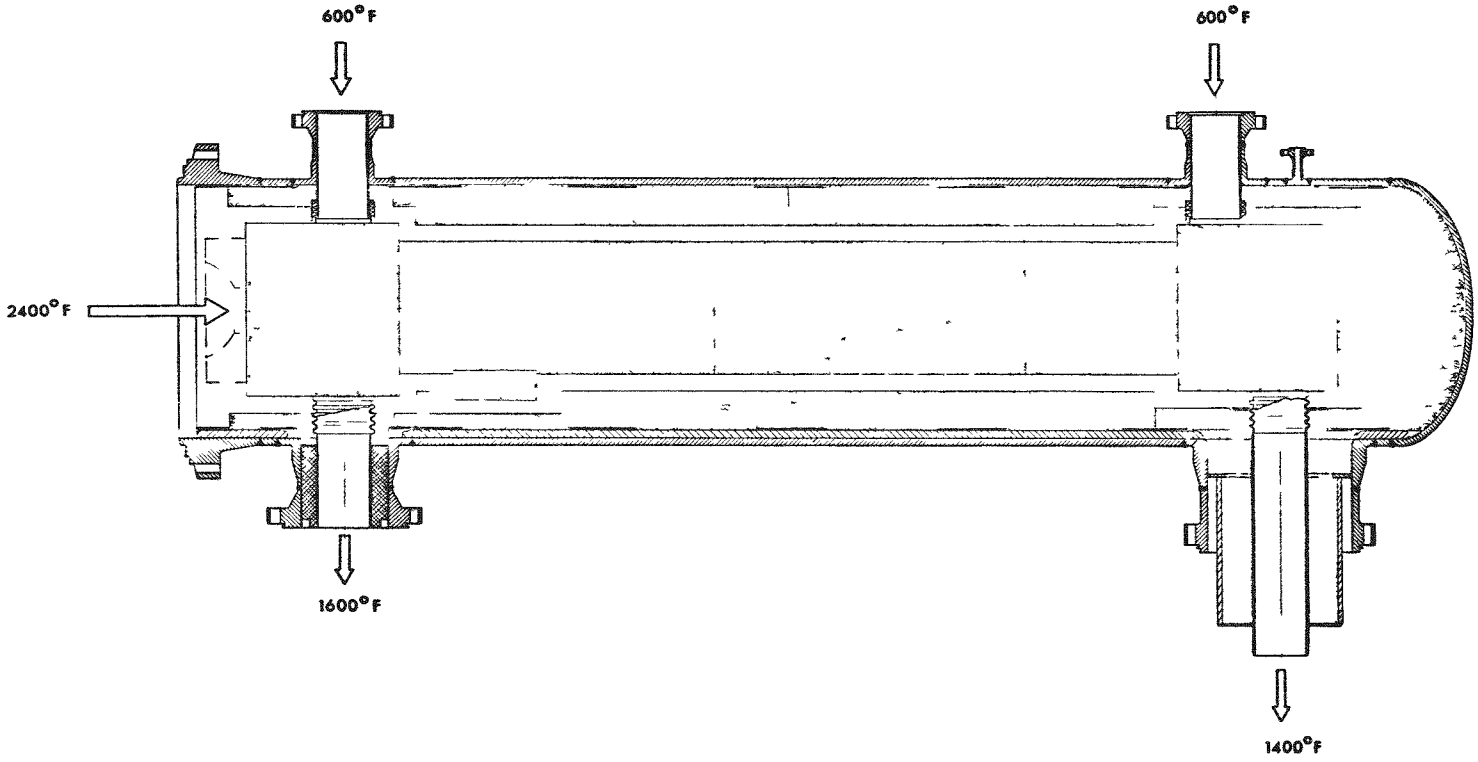

Fig. 5.1.1.3 Recuperator assembled in pressure vessel

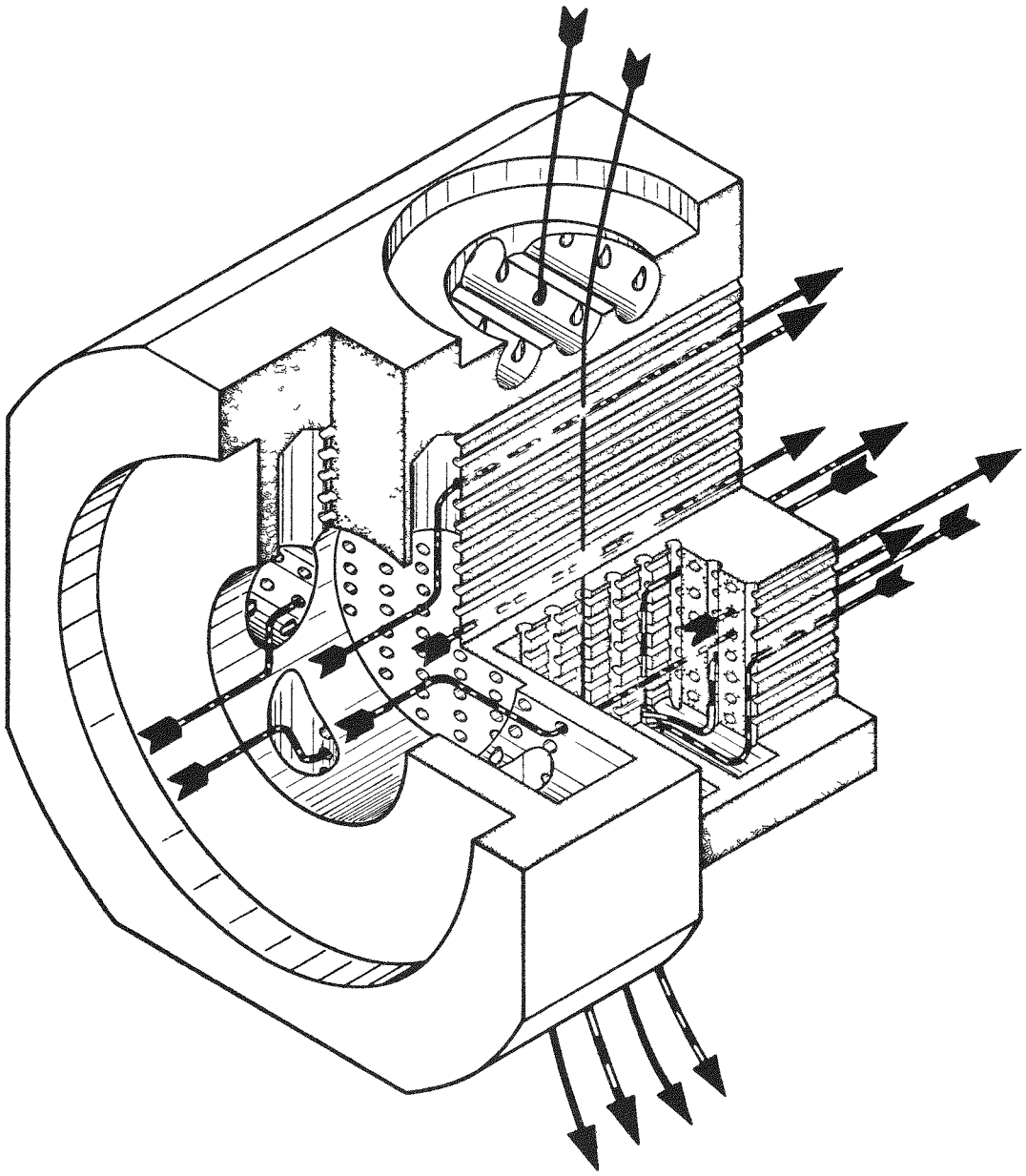

Fig. 5.1.1.4 Recuperator inlet header block

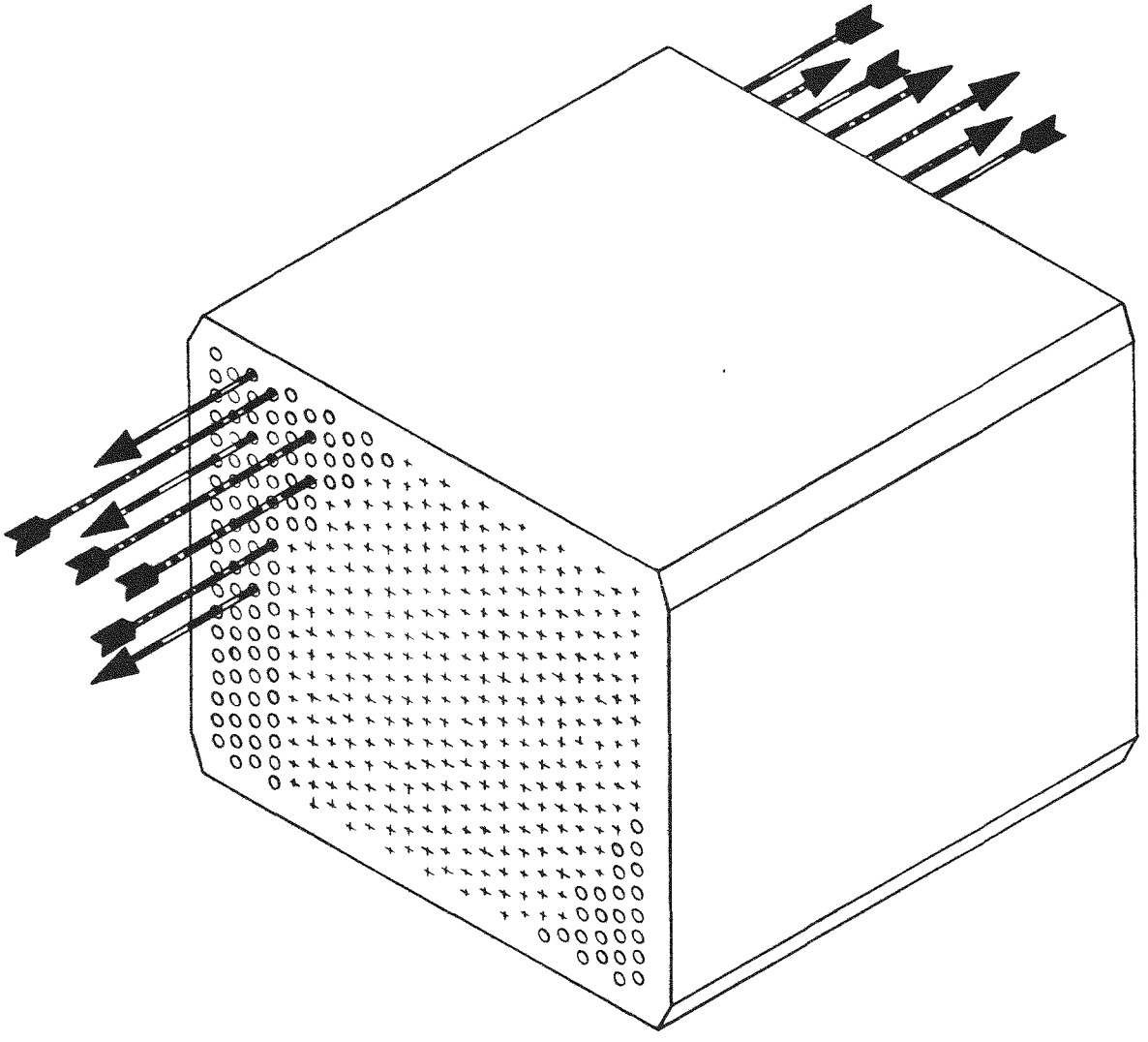

Fig. 5.1.1.5 Typical recuperator heat exchanger block

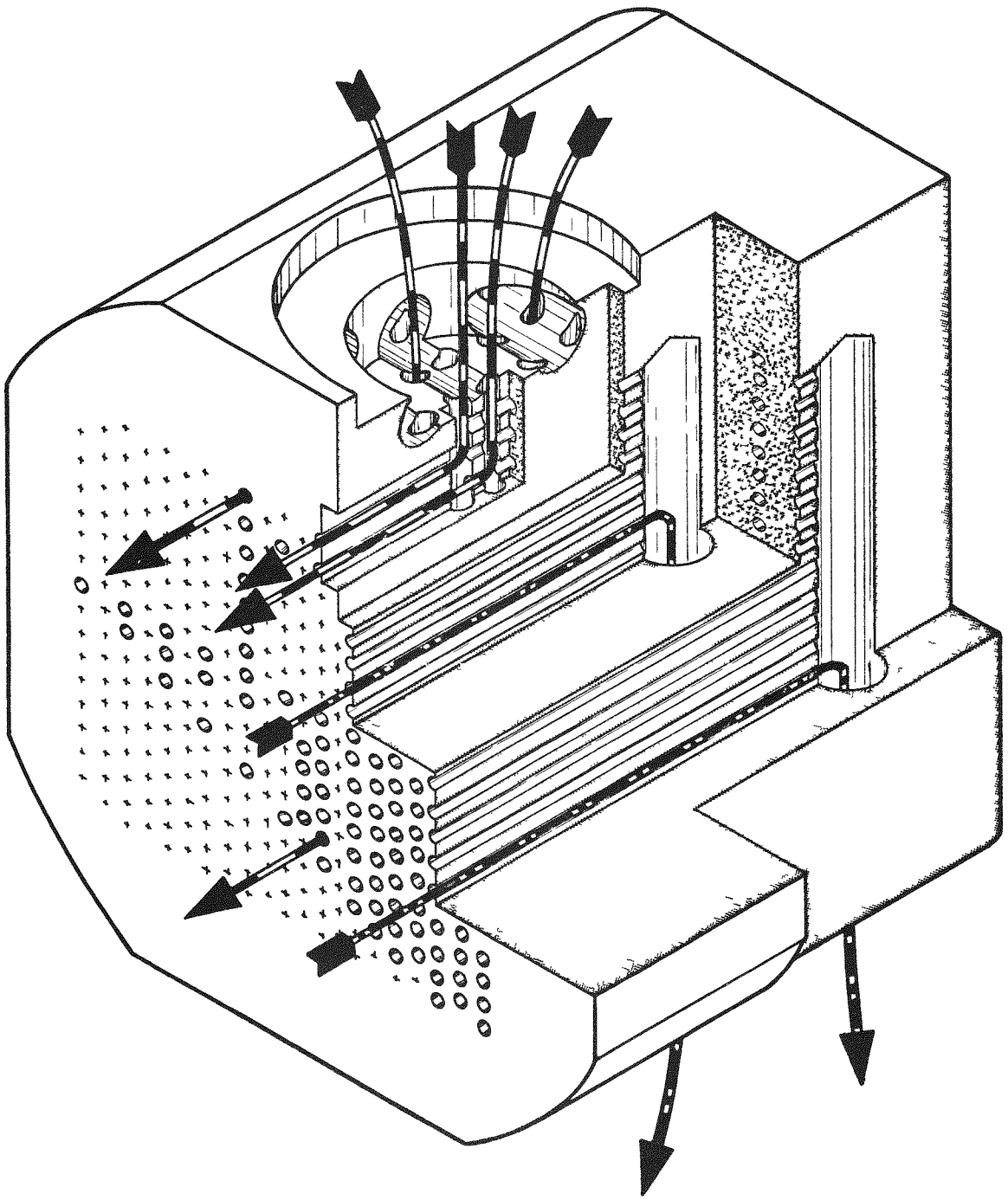

Fig. 5.1.1.6 Recuperator outlet header block

Hot helium leaves the reactor at 2400°F and flows directly through the inlet header and through the central core pieces, where its temperature drops to 1400°F, and then is directed downward in the outlet header to pass into the main heat exchanger. The outlet nozzle for the 1400°F helium is protected by an internal insulation assembly that extends inside the top flange of the main heat exchanger.

The returning 600°F helium stream enters through the top nozzle at the end of the recuperator away from the reactor. Passages inside the outlet header block direct the stream, around a right angle, back through the central core pieces and into the inlet header. There, the return flow, now heated to 1600°F, moves out the bottom nozzle to the metal foil insulated pipe that returns the coolant stream to the bottom of the reactor.

As much as 80% of the returning coolant stream can be bypassed around the recuperator to enter it at the top nozzle nearest the reactor. Passages joined to this nozzle allow the bypass flow to move directly through the inlet header block to the 1600°F outlet nozzle.

The graphite core and header assembly is wrapped in 2-3/4 in. of graphite felt, which is enclosed in machined, carbon liner blocks that make the transition in shape between the rectangular core and the round pressure vessel. The weight of the core assembly is borne on porous carbon feet, which rest on the liner blocks that, in turn, bear on the pressure vessel.

Keys restrain relative movement between the recuperator and its vessel. Movement around the long axis of the vessel is prevented by a steel key, welded to the vessel, that fits a slot machined in the liner blocks. Another steel key at the flange end of the vessel holds against movement along the axis. Relative movement between the core and the liner is restrained by a porous carbon key bonded to the core near the inlet block. This key fits into a slot in a liner block, but is separated from it by graphite felt insulation to prevent the transmission of heat. Therefore, the core "floats" on graphite felt insulation, except where the insulation feet contact the liner, but is not free to move.

Bellows assemblies, made of Type 316 stainless steel, connect the two top vessel nozzles to the graphite core. A flange on the bottom of each bellows fits into a socket in the top surface of the header block. The flange is loosely held in the socket by a graphite retainer ring, which screws into the block and is pinned to it. From the top of the bellows, a light-gauge liner pipe extends inside the vessel nozzle to within 1/8 in. of the face of the flange. The liner is welded to the surface of a step machined on the inside of the flange face.

The same sort of connection is made at the core end of the other two bellows assemblies, but the nozzle ends are different. On the heat exchanger nozzle bellows assembly, the liner pipe extends inside a large collar of graphite felt insulation, which is bolted inside the recuperator vessel nozzle and projects down into the upper part of the main heat exchanger. Inside the recuperator vessel nozzle that connects with the 1600°F pipe to the reactor, the liner pipe is butt-welded to a metal foil assembly that lines the nozzle and joins the metal foil liner in the 1600°F pipe.

Twelve thermocouples, all chromel-alumel, measure temperatures inside the recuperator. There are duplicate thermocouples in the header block ports to monitor the 1600°F outlet stream to the reactor, the 1400°F outlet stream to the main heat exchanger, the 600°F inlet stream from the blower, and the 600°F inlet bypass stream. A thermocouple is located inside a graphite piece that projects into the 2400°F inlet stream. Three others measure temperature at the front and rear faces of the inlet header block and at the rear face of the outlet header block. All of the thermocouple leads leave the recuperator through a 4-in. nozzle in the ellipsoidal head of the vessel. This nozzle connects to the recuperator instrument pipe which projects into Room 402, where the pipe terminates in a pressure-tight pass-through flange.

Near the 600°F inlet stream nozzle is a 1-in. nozzle through which passes the fission product deposition sample wire. This wire, whose function is described in the Main Heat Exchanger section below, traverses the recuperator in a hole drilled through the outlet header block.

The carbon parts of the recuperator are contained in a pressure vessel made of ASTM A-212 Grade B carbon steel, with forged nozzles made of ASTM A-105 Grade II carbon steel. All of the nozzles have bolted flanges modified for welded seals. The vessel is joined directly to the reactor vessel at one end and to the main heat exchanger at the other. Direct connection with seal-welded flanges eliminates the need for any 2400°F or 1400°F helium piping, conserves space, and increases structural integrity. Weight of the recuperator and main heat exchanger is borne on spring-loaded hangers, supported on a steel frame that rests on the cell floor. Temperature of the vessel walls is maintained below 600°F by radiant heat transfer to water cooled panels along the walls and floor of the reactor-recuperator room.

A summary of the operating conditions and mechanical characteristics of the recuperator appears in Tables 5.1.1.1 and 5.1.1.2.

TABLE 5.1.1.1

RECUPERATOR OPERATING CONDITIONS

Hot Side	
Flow rate	10,250 lb He/h
Inlet temperature	2400°F
Outlet temperature	1400°F
Inlet pressure	504 psia
Cold Side	
Flow rate	10,250 lb He/h
Inlet temperature	600°F
Outlet temperature	1600°F
Inlet pressure	507 psia
Pressure drop	4.0 psi total (sum of cold side and hot side)
Heat load	12,800,000 Btu/h (3.75 MW)
Over capacity	25% (increase in length by 25%)

TABLE 5.1.1.2

RECUPERATOR MECHANICAL CHARACTERISTICS

Core	Graphite block 2 ft x 20 in. x 9 ft, 7 in.
Holes (hot and cold sides)	451 - 0.50 in. diam
Heat transfer area	282 ft^2
Flow area	0.307 ft^2
Overall heat transfer coefficient	75 Btu/h-ft^2-°F
Heat transfer coefficients	
Hot side	202 Btu/h-ft^2-°F
Cold side	150 Btu/h-ft^2-°F
Graphite (per ft^2 of hole surface)	530 Btu/h-ft^2-°F
Coolant velocity	
Hot side (average)	119 ft/sec
Cold side (average)	77 ft/sec
Core weight (including header)	4450 lb

Main Heat Exchanger - Joined directly to the recuperator and supported by it, a shell-and-tube heat exchanger transfers heat from the primary to the secondary coolant loop. This main heat exchanger maintains primary containment of the helium stream that may be contaminated with fission products by direct contact with the core. The entire exchanger is austenitic stainless steel; all pressure-containing parts are Type 316. On the tube side of the exchanger, the primary coolant stream drops in temperature from 1400°F to 600°F, a level compatible with the operation of electric blowers. In the shell, the temperature of the secondary coolant stream, in counter-current flow, rises from 200°F to 1000°F.

Helium enters the main heat exchanger directly from the recuperator through an 8.656-in.-i.d. duct inside a 22-in.-i.d. flange, shown at the right side of Fig. 5.1.1.7. The flange, and its mate on the recuperator,

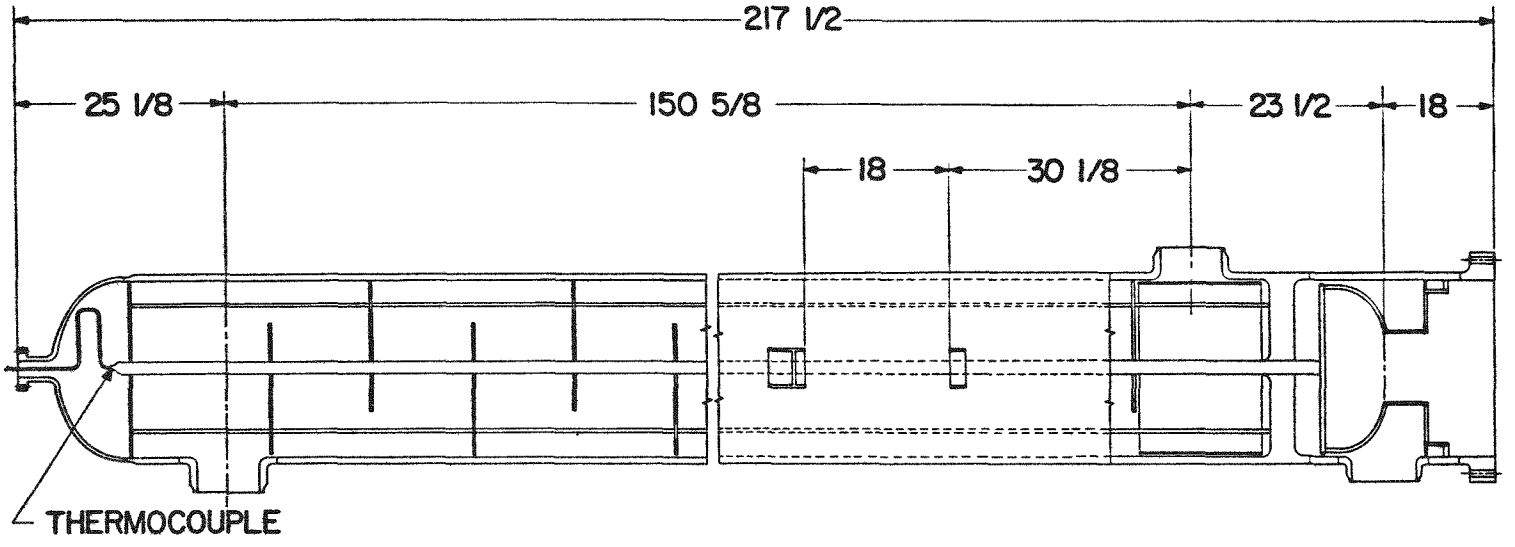

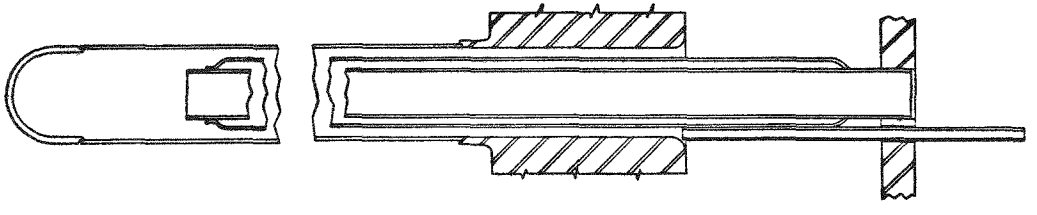

SECTION THRU TUBE SHOWING
GUIDE TUBE FOR WIRE SAMPLING DEVICE

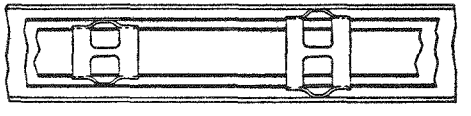

TUBE SPACER CLIPS

Fig. 5.1.1.7 Main heat exchanger cross section and details

are protected against the 1400°F helium stream by graphite felt internal insulation. At the top of the main heat exchanger, the entry duct opens into a dome that is joined to a floating tube sheet. Exhaust helium, cooled to 600°F in the tubes and discharged through a nozzle adjacent to the dome, prevents overheating of the shell at the top of the exchanger.

Welded to the inlet tube sheet are 96 sets of bayonet tubes with insulated core tubes, shown in detail on Fig. 5.1.1.7. The core tubes, 0.750-in. o.d. x 0.020-in.-thick wall, are rolled into and seal-welded to the inlet tube sheet. Inlet helium, at 1400°F, flows down through the core tubes, reverses direction at the bottom, and returns in the annular space between the core and outer tubes, 1.500-in. o.d. x 0.072-in.-thick wall (No. 15 B.W.G.). To control the flow of heat from the descending gas, the core tubes are enclosed in insulating tubes, 1.063-in. o.d. x 0.020-in.-thick wall, which are separated from the core tubes by spacer clips. Similar clips separate the insulating and outer tubes. The outer tubes, which maintain the separation between the primary and secondary loops, are joined to the fixed, lower tube sheet by machine-made, crevice-free welds, designed for and subjected to 100% radiographic inspection.

Heat from the primary loop coolant passes through the outer tube walls to the secondary loop coolant in the shell, as the primary helium moves upward. After cooling to 600°F, the primary coolant discharges above the fixed tube sheet, flows around the entry tube sheet and dome, and leaves the main heat exchanger through the uppermost side nozzle.

Helium, cooled in the secondary loop to 200°F, enters the shell of the exchanger through the side nozzle just below the tube sheet and flows past the baffled tube bundle. A thermal shield at the inlet nozzle reduces to a tolerable level the temperature gradient across the fixed tube sheet. The baffles are supported by tie bars from the fixed tube sheet. Antibypass bars hang against the shell from the baffles. The secondary loop coolant discharges through the lowest side nozzle.

In the outer annulus of one of the center bayonet tubes is a wire that collects on its surface a sample of the fission products deposited in the tubes. The wire is inserted through a 1/8-in.-i.d. guide tube, shown in a detail of Fig. 5.1.1.7, after passing through a hole in the recuperator.

Eight thermocouples, in 1/8-in.-o.d. stainless steel sheaths, pass out of the heat exchanger through the bottom flanged nozzle to an instrument pipe of the same type used on the reactor. The thermocouple measuring junctions are mounted on three of the outer tube caps (which reverse the primary coolant flow), on the side of one outer tube just below the tube-to-tube sheet weld, in duplicate at a point just inside the shell where the secondary coolant enters, and in duplicate at a point inside the thermal shield where the secondary coolant discharges.

The main heat exchanger is designed for operation over a period of at least 5 years under the normal conditions prescribed in Table 5.1.1.3. To allow for the differential thermal expansion and stress relief that may occur naturally at the higher operation temperatures, the exchanger design includes the assumption that the exchanger may be subjected to 1000 temperature cycles, any one of which might have a range as large as the difference between ambient and the maximum operating temperature. These individual cycles occur slowly (less than 100°F/h) in heating and cooling, and the pressure differential between the hot and cold sides of the exchanger does not exceed 50 psi during the cycle. Additional design characteristics ensure that the heat exchanger will survive at least five events of an accidental, nonroutine nature under circumstances in which the conditions in Table 5.1.1.4 prevail (i.e., sudden accidental loss of secondary loop coolant).

To allow for various modes of operation, the heat exchanger is capable of operation under a variety of conditions in which the maximum coolant temperatures may be as high as 1400°F at the hot side inlet, 600°F at the hot side outlet, 600°F at the cold side inlet, and 1100°F at the cold side outlet. Design temperature for the shell is 1100°F. In

TABLE 5.1.1.3

MAIN HEAT EXCHANGER

NOMINAL OPERATING CONDITIONS FOR CONTINUOUS SERVICE

Hot Side	
Fluid	Helium containing fission products and probably some graphite powder or particles in suspension
Inlet temperature	1400°F
Inlet pressure	502 psia
Outlet temperature	600°F
Flow rate	10,250 lb/h
Allowable pressure drop	2.0-psi maximum including loss through entrance and exit nozzles
Cold Side	
Fluid	Clean helium (no solids content anticipated)
Inlet temperature	200°F
Inlet pressure	508 psia
Outlet temperature	1000°F
Flow rate	10,250 lb/h
Allowable pressure drop	2.5-psi maximum including loss through entrance and exit nozzles
Heat load	10,250,000 Btu/h

TABLE 5.1.1.4

MAIN HEAT EXCHANGER
MAXIMUM EMERGENCY CONDITIONS

Hot Side	
Fluid	Helium containing fission products and probably some graphite powder or particles in suspension
Inlet temperature	1400°F
Inlet pressure	About 500 psia initially. Falls to 200 psia within 1 min, then reduced to atmospheric in 5 h
Outlet temperature	600°F, increasing toward 1400°F
Flow rate	Initially 10,250 lb/h. Reduced to about 2000 lb/h in 10 sec and to zero flow in about 60 sec total
Cold Side	
Fluid	Helium (no solids content anticipated)
Inlet temperature	200°F initially
Inlet pressure	About 505 psia initially, assumed rapid decompression to ambient pressure (12 psia)
Flow rate	10,250 lb/h initially, decreasing to zero with decompression

calculating the required heat exchanger area, a fouling factor of 0.0018 h-ft^2-°F/Btu was used.

Design pressure is 550 psi. The main heat exchanger can operate continuously with an unbalance of 50-psi pressure across the two sides of the exchanger, with the cold side at the higher pressure.

Filter - Between the main heat exchanger and the blower is a filter with eight woven-wire mesh elements. The primary function of the filter, illustrated in Fig. 5.1.1.8, is the removal from the flowing helium

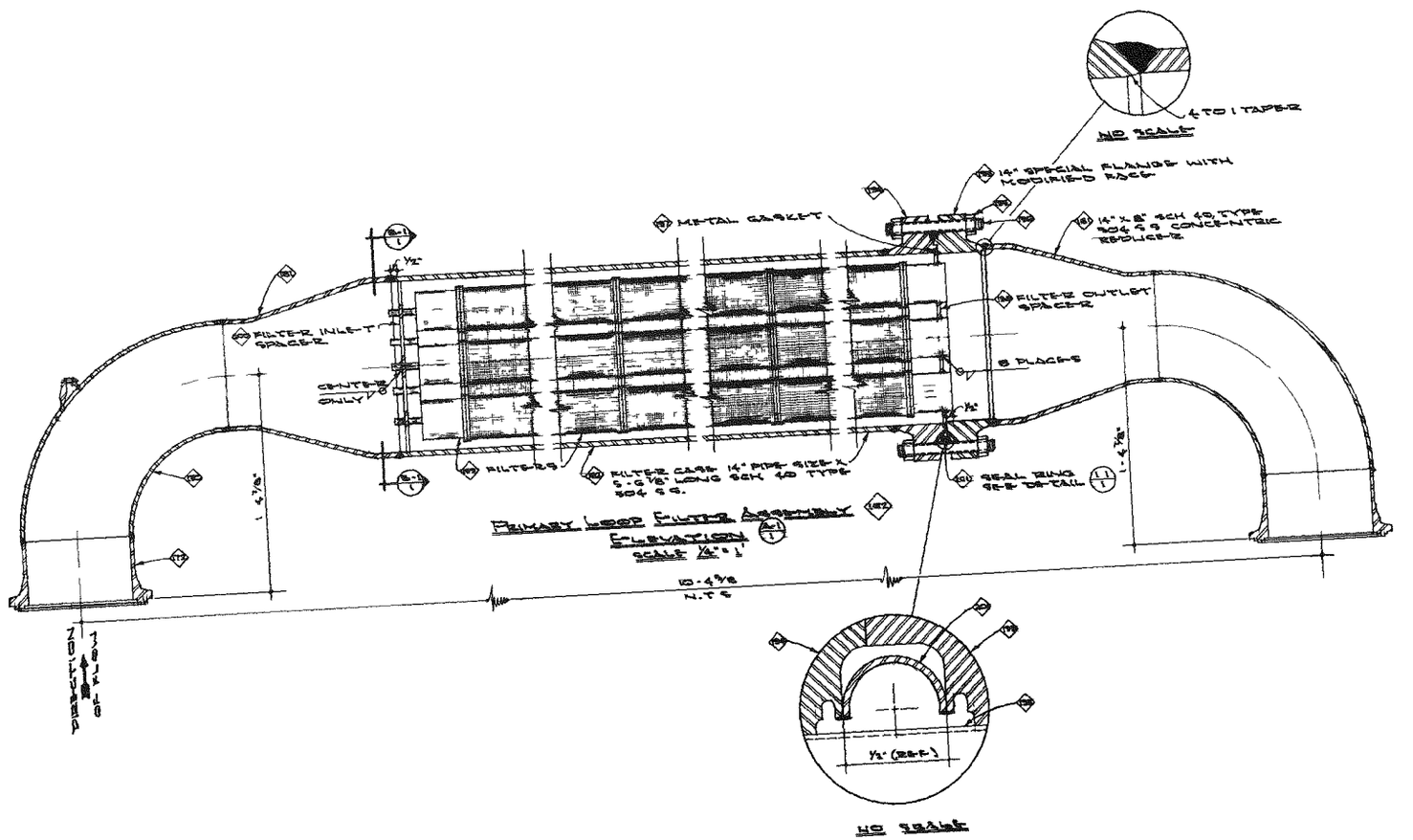

Fig. 5.1.1.8 Primary loop filter

coolant of particles of structural carbon and graphite. Its elements are rated for 98% removal of 2μ particles and 100% removal of 6μ and larger particles. If the filter elements become blinded or damaged, the entire filter assembly will be removed and replaced.

The filter medium is wire mesh made of Type 304L stainless steel filaments, woven in a Dutch twill pattern and annealed to fix the size of mesh openings. The fine wire mesh is supported on a No. 200 U.S.S. backup mesh, and the combination is formed into pleated cylinders, with the pleats parallel to the longitudinal axis. Each pleated cylinder is 3-5/8-in. o.d. x 21-in. long. Three cylinders are welded, end to end, over a 3-in.-o.d. perforated core tube to make one filter element. At its upstream end, each element is closed with a round plate that has at its center a guide pin. The center element's guide pin is welded to a spider plate that has seven holes, equally spaced on an 8.75-in. circle, into which the other elements' guide pins fit loosely enough to allow differential movement of the elements. The downstream, open, end of each element is welded into a tube sheet. Flow through the elements is from the outside, into the core tube, and out through the tube sheet.

A pressure vessel made of 14-in., Schedule 60 pipe encloses the filter elements. The element-tube sheet assembly slides into position through a flange to which the tube sheet is sealed with a metal gasket. A mating flange is bolted tight to close the vessel, and a welded C-section seal makes the joint leak-tight. A double Conoseal joint at each end of the pressure vessel connects the filter into the primary loop piping.

Characteristics of the filter design are summarized in Table 5.1.1.5.

Blower - The primary loop blower, shown in Fig. 5.1.1.9, is a horizontally-mounted, variable speed, single-stage, centrifugal blower. Under nominal conditions, it takes in a flow of 10,250 lb/h of He at 600°F and 500 psia and circulates it against an 8-psi head. The blower and its integral motor run on hydrodynamic bearings inside a case that has no rotating or stationary shaft seals.

TABLE 5.1.1.5

PRIMARY LOOP FILTER DESIGN CHARACTERISTICS

Fluid	Helium, 10,250 lb/h at 600°F, 500 psia
Filter rating	98% removal of 2μ particles 100% removal of 6μ particles
Filter area	300 ft^2
Fluid velocity, inside element	$\bar{<}$ 50 ft/sec
Fluid velocity, inside shell	$\bar{<}$ 55 ft/sec

Motive power for the coolant is developed by an 11-5/8-in.-diam, unshrouded, 19-vane impeller which rotates at a maximum speed of 12,000 rpm and discharges to a radial outlet diffuser. The impeller vanes are overhung at their tips to reduce thrust loads. Flow of the 600°F helium stream into the motor compartment is restricted by an 8-step, radial, labyrinth seal between the case at the rear of the impeller and the impeller shaft.

The impeller is driven by a 60-hp, 2-pole, 60- to 200-cycle, 3-phase. 133- to 440-V, continuous duty, squirrel cage motor, whose rotor is an integral part of the blower shaft. Motor speed can be controlled between 4000 and 12,000 rpm by changing the frequency of the input power, produced by a 75-hp, 200-cycle, ac generator. The output frequency of the generator is a direct function of the speed at which it is driven by two ac motors on a common shaft. These motors operate at constant speed, but are coupled to the generator by an eddy current clutch. Slippage in the clutch, and, thus, the generator speed is controlled by the excitation current to the clutch. As a net result, the blower speed changes when the excitation current to the generator clutch is changed.

Each of the two motors that drive a blower supply generator is capable of carrying the generator load for 30 min, and each is connected to a separate power line. In case of failure on one line, the blower can

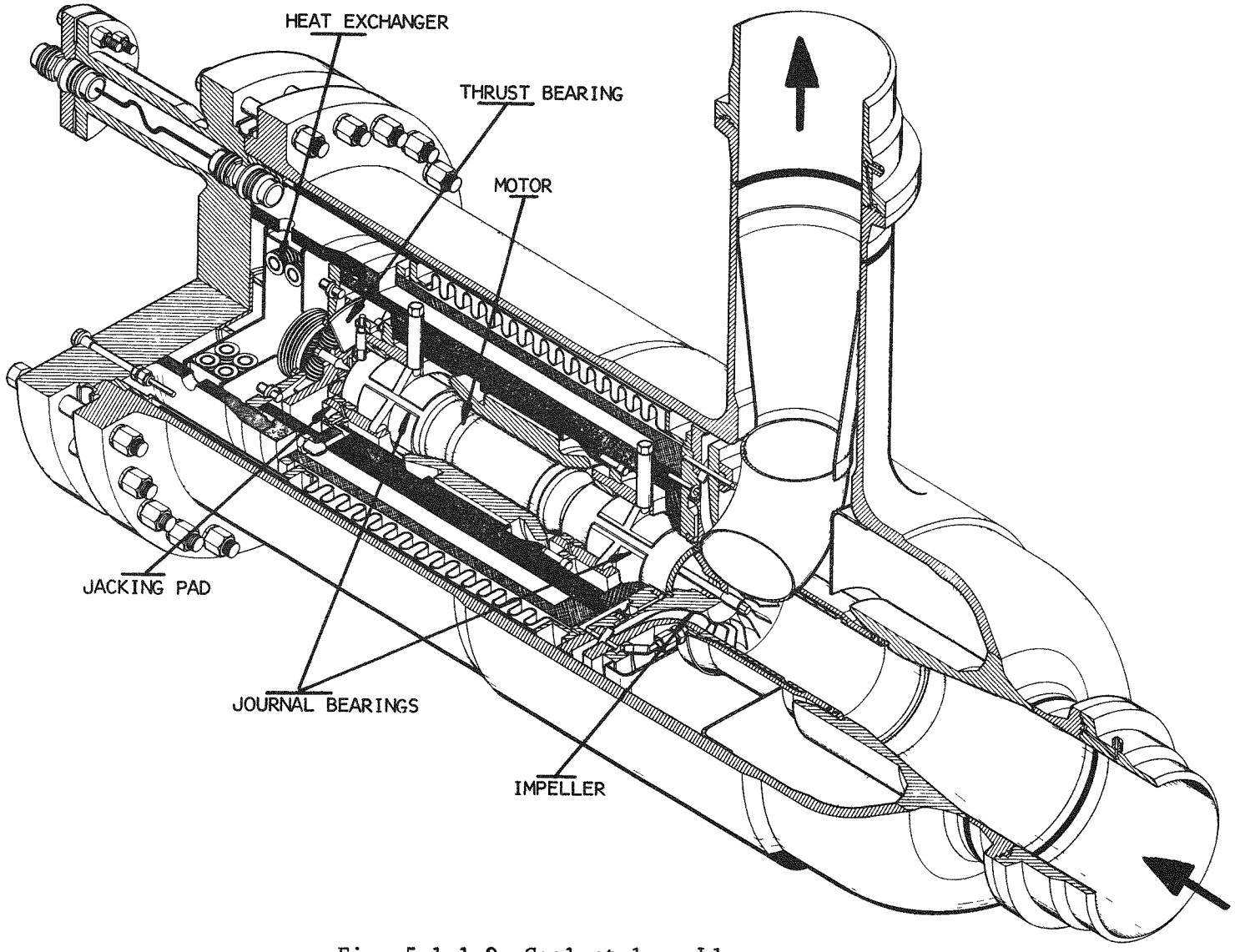

Fig. 5.1.1.9 Coolant loop blower

continue to run while a switch gear transfers the idled generator motor to the active line.

Two self-acting, hydrodynamic journal bearings and a hydrodynamic thrust bearing support the blower rotating assembly, which includes the main impeller, bearing journals, motor rotor, and thrust runner, all on one shaft. The bearings are lubricated by a film of loop coolant stream helium. There are no rotating or stationary shaft seals. Each journal bearing has four, segmented, pivot-mounted pads. Jacking gas (helium at >550 psi) is injected through hydrostatic jacking pads to lift the rotating assembly off the two journal bearings when the blower is started, stopped, or running at speeds less than 4000 rpm. The jacking pads, adjacent to each journal bearing, are 3/4-in. long and encompass a 120° arc. Seven 1/16-in.-diam gas holes admit the jacking gas.

In the thrust bearing, two fixed pads, pivoted on a gimbal ring, oppose the thrust runner plate mounted on the blower shaft. On the opposite side of the runner, a fixed-plate, Whipple groove bearing made of Graphalloy acts to restrain axial movement of the shaft on startup and during slow speed operation.

A finned tube heat exchanger is located at the rear of the case to cool the motor compartment and carry away motor heat. The cooling medium is 100°F water, flowing at 6 gpm from an isolated water system. An auxiliary helium fan located on the end of the thrust runner circulates helium in the motor compartment at 1500 lb/h past the finned coils of the heat exchanger. For added thermal protection of the motor insulation, a heat shield made of metal foil insulation is mounted directly behind the impeller.

The entire blower assembly slides into the case through a flanged opening that is bolted tight and sealed with a C-section ring joint. All instrumentation and power leads, the water lines, and the jacking gas line enter the case through the cover. Double Conoseal joints connect the case into the primary loop.

Recuperator Bypass Valve - For controlling the reactor helium inlet temperature, a butterfly valve operates in a bypass line around the low temperature side of the recuperator. The valve and its electric motor operator form a single leak-tight enclosure. There is no high pressure, rotating seal. Bolted, seal-welded flanges join the operator housing to the upper end of the extended valve bonnet and join the bonnet and lower cap to the valve body. The bonnet and stem pass through the reactor shield slabs to make the motor operator accessible while the reactor is shut down. A Conoseal joint below the operator housing permits the removal of the operator, while stem packing just below the joint prevents escape of volatile fission products.

The function of the valve is to control flow, not to completely block it. Therefore, there is no seat for the butterfly disk, which can rotate 360° inside the valve body. A selsyn geared to the valve stem senses the valve position.

Flowmeters - The primary loop has two flowmeters; one measures total system flow, and the other recuperator bypass flow. The flowmeters are Gentile flow tubes, located upstream of the primary helium filter and downstream of the recuperator bypass valve.

Piping - Since the primary coolant loop is a part of the primary containment for fission products volatilized from the fuel elements, a high degree of reliability and leak tightness is built into the components. The number of joints and welds was reduced to a minimum and, wherever possible, piping assemblies were prefabricated to minimize the number of field welds. All welds were radiographically inspected.

The major part of the loop piping is 8-in., Schedule 40, Type 304 stainless steel, seamless drawn pipe. Between the recuperator and the reactor inlet, the 1600°F helium pipe is 14-in., Schedule 40, Type 106 carbon steel, internally lined with stainless steel foil, reflective insulation (Solami). The remainder of the piping has conventional, external, calcium silicate insulation. Two views of the piping arrangement are shown in Figs. 5.1.1.10 and 5.1.1.11.

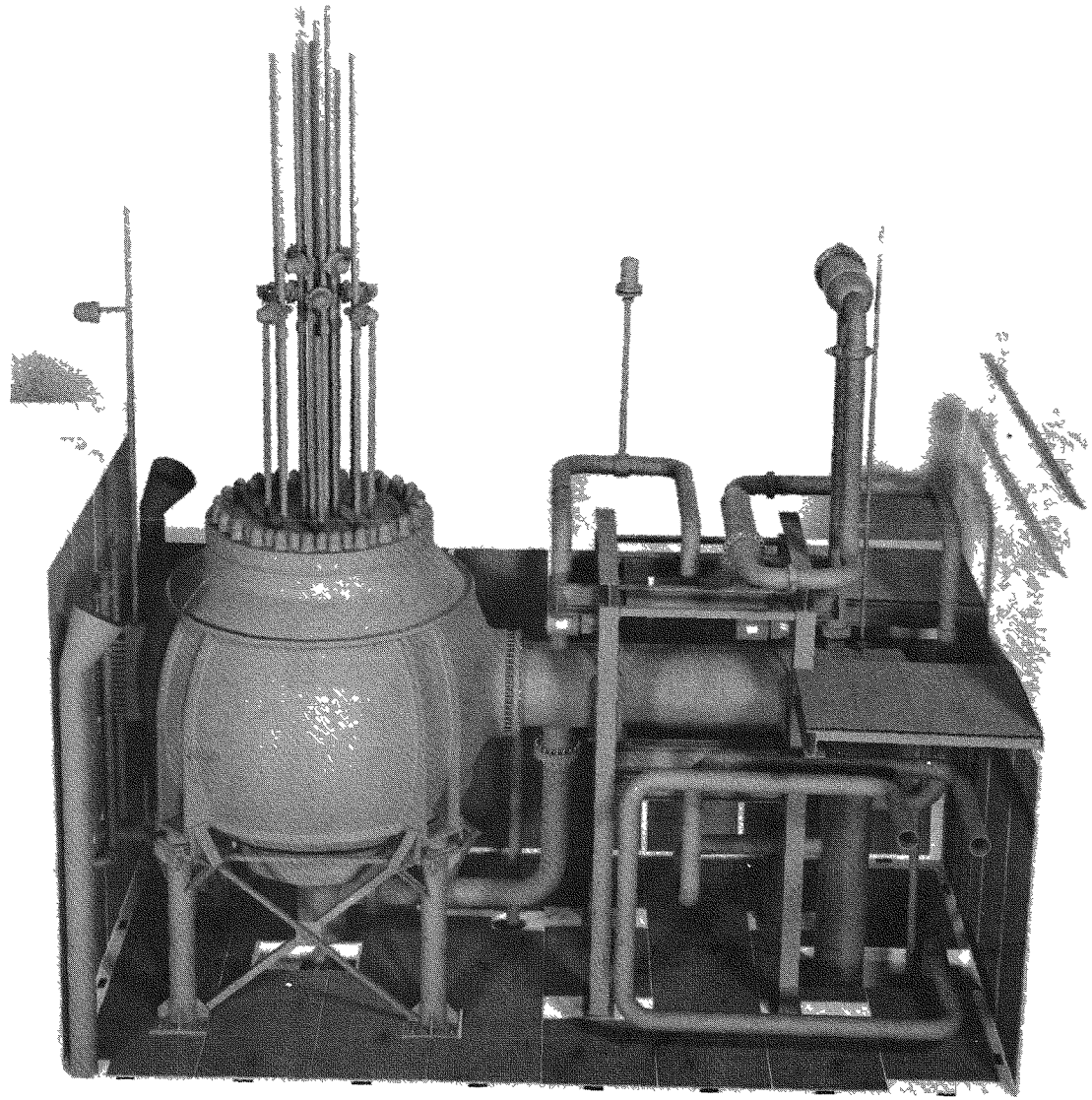

Fig. 5.1.1.10 Primary coolant loop piping, from model

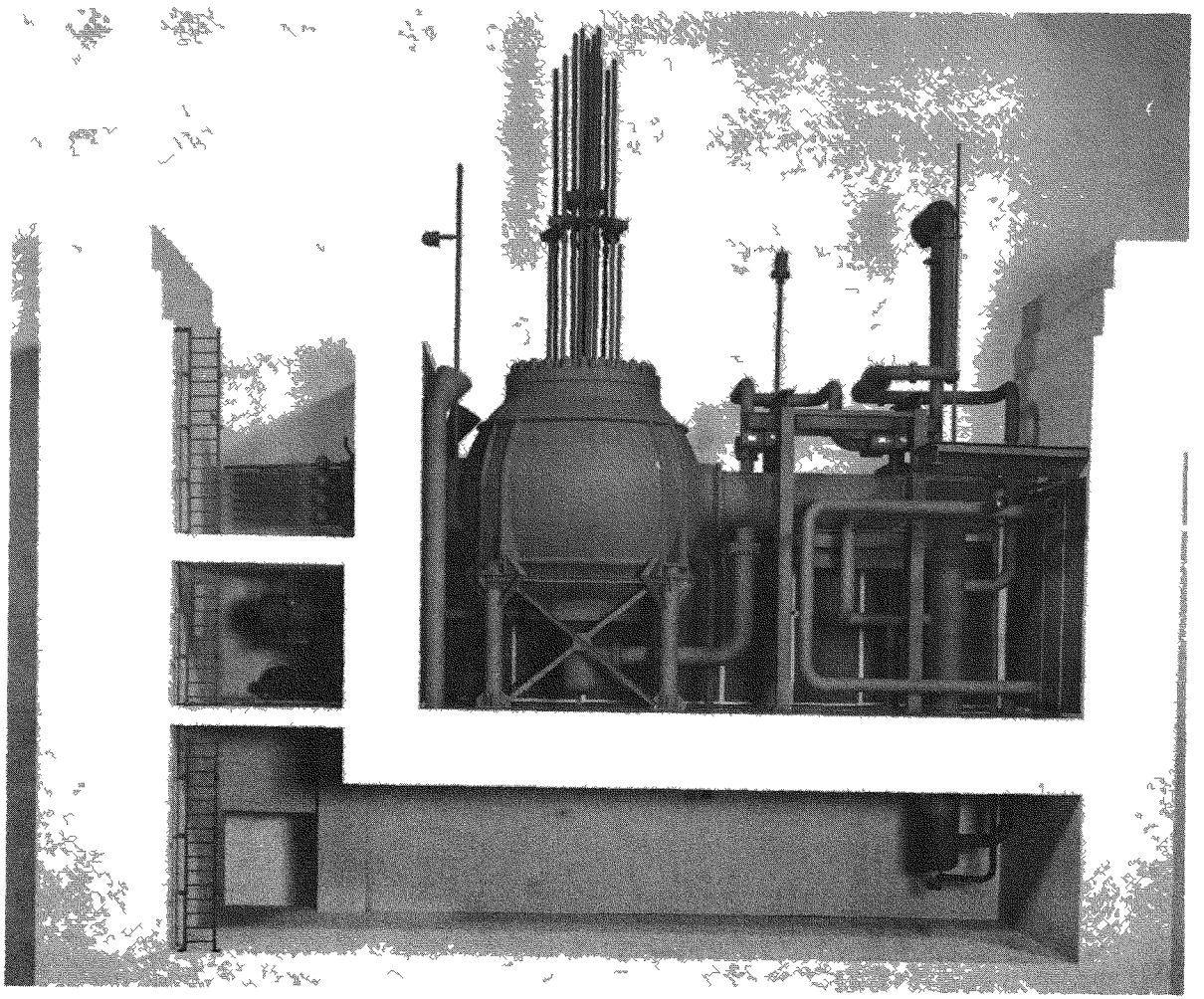

Fig. 5.1.1.11 Primary coolant loop piping, from model

To accommodate thermal expansion of the piping and pressure vessels, all primary loop components outside the reactor are suspended on spring-loaded hangers that effectively permit translational motion in any direction without introducing excessive stresses. In piping flexibility analyses, made according to a tensor analysis treatment of Castigliano's theorem, the center of the reactor was considered to be fixed in relationship to the other components. All calculated stresses, under the anticipated operating conditions, fall well within permissible limits.

External Cooling of Components - Water-cooled steel panels cover all four walls and the floor of the reactor-recuperator room, and one panel is supported on the reactor cover. These panels, see Fig. 5.1.1.12, form cool surfaces that increase the efficiency of radiant heat transfer from the steel vessel walls of components that are internally insulated and from the concrete walls of the cell. The panels have no material effect on the temperature of the air circulated in the cell. Cooling of vessels is effected primarily by radiation to the bare panel surfaces maintained at 100°F by flowing water. The vessels are cooled to prevent surface temperature rises above 600°F, where allowable stresses in mild steel begin to decrease rapidly, and to minimize the thermal stresses that develop between components that operate at different temperatures. Provision of a heat sink for the cell walls limits their ultimate temperature to a level lower than could be achieved by conduction of the deposited heat to the cool outer surfaces of the walls.

The water panels are designed to remove, at safe component surface temperatures, the total heat leak from the reactor and primary coolant loop. This design is conservative because 20% of the heat leak is normally removed in the air circulated by the ventilating system. Consideration was given to the removal of all of the heat leak with circulated air, but equipment reliability and fail-safe requirements raised more problems in an air system than in the water panels. Each panel has an individual flow monitor which warns the control room operator of flow abnormalities. The water systems are discussed in Section 12.2.

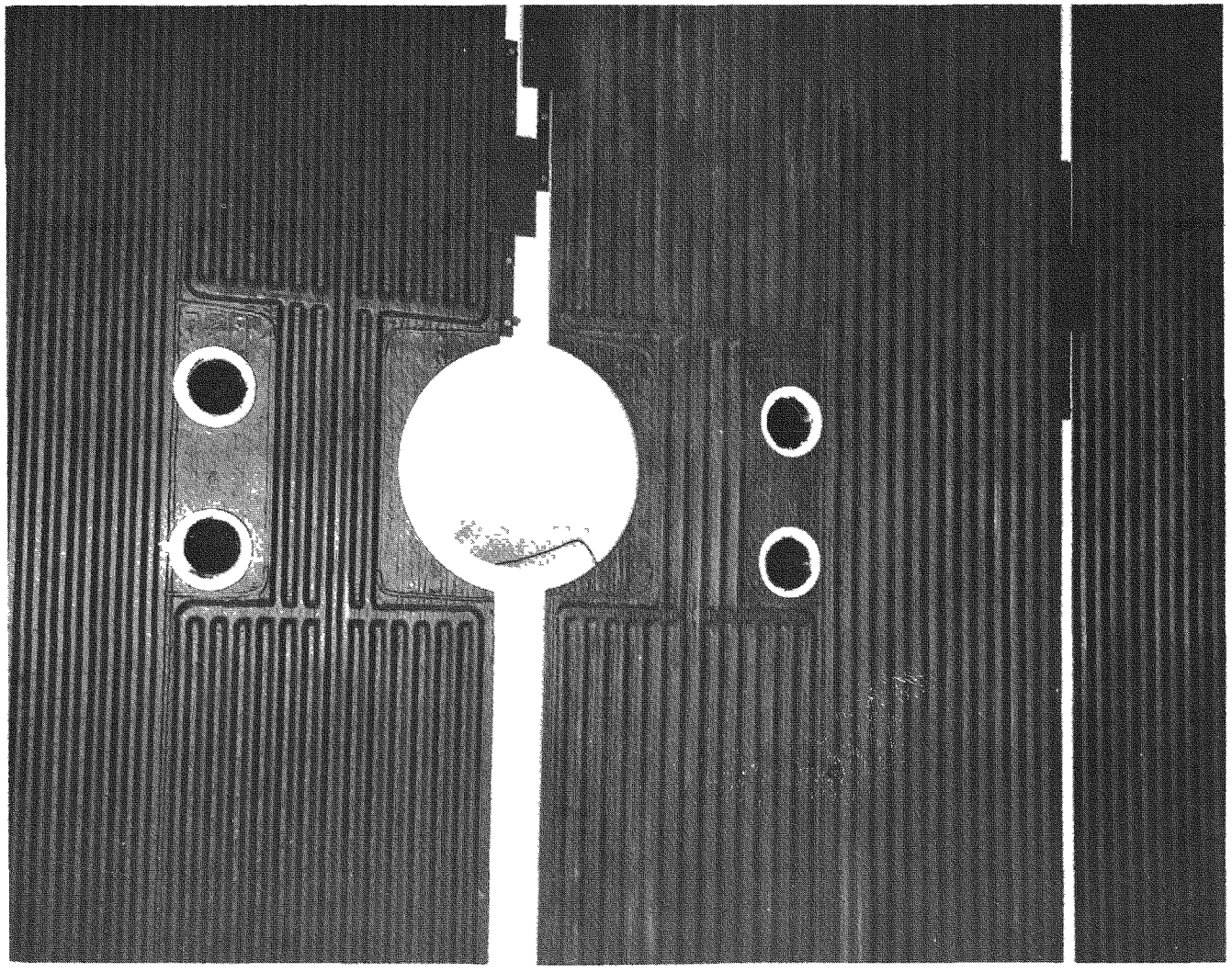

Fig. 5.1.1.12 Water-cooled panels in reactor room

5.1.2 Secondary Coolant Loop

In the secondary coolant loop, clean helium, circulated by a blower through 8-in. stainless steel lines, carries heat from the main heat exchanger to the heat dump, where the thermal energy developed in the reactor is finally discharged to the atmosphere. The flow rate of helium in the secondary loop is matched with the primary loop flow rate, 10,250 lb/h at maximum reactor power. Secondary loop helium pressure is 495-545 psia, at maximum power, to ensure that any leakage in the main heat exchanger flows inward to the primary loop, operated at 475 psia. Barring equipment failures, the secondary loop helium contains no radioactive contaminants. Should a rupture occur in the primary coolant loop, the secondary loop serves as secondary containment. Therefore, all components in the secondary loop are built to the same standards as were specified for the primary loop.

Heat Dump - From the shell side of the main heat exchanger, helium flows, at a maximum temperature of 1000°F, to the heat dump, an air-cooled heat exchanger designed to dissipate heat to the atmosphere at a maximum rate of 3 MW. Within the heat dump, illustrated in Fig. 5.1.2.1, the temperature of the helium stream drops to 200°F.

Heat is dissipated in a four-pass exchanger with 56 finned tubes, each 1.000-in. o.d. x 0.870-in. i.d., with seven 2.000-in.-o.d. fins per in. The seamless tubes are made of Type 304 stainless steel. The fins are 4-6% Cr/0.5% Mo steel helices, 0.03-in. thick, that are knurled into plowed grooves in the tubes. Tube banks terminate at 6-7/8-in.-i.d. manifold headers machined from Type 304 stainless steel forgings. The tubes are joined to machined bosses on the manifold faces with butt welds that were 100% radiographically inspected. A 67-in.-wide x 12.75-ft-long x 18-in.-high shroud encloses the tube banks.

The heat exchanger rests, 9 ft above the ground, on top of a 5-ft x 12-ft x 2.5-ft forced draft enclosure that is supported on 77-in. legs. Under the draft enclosure, inside shroud rings, are two 63-in.-o.d., fixed-pitch, six-bladed fans driven at variable speed by individual drive motors. Above the heat exchanger is a 17-blade shutter.

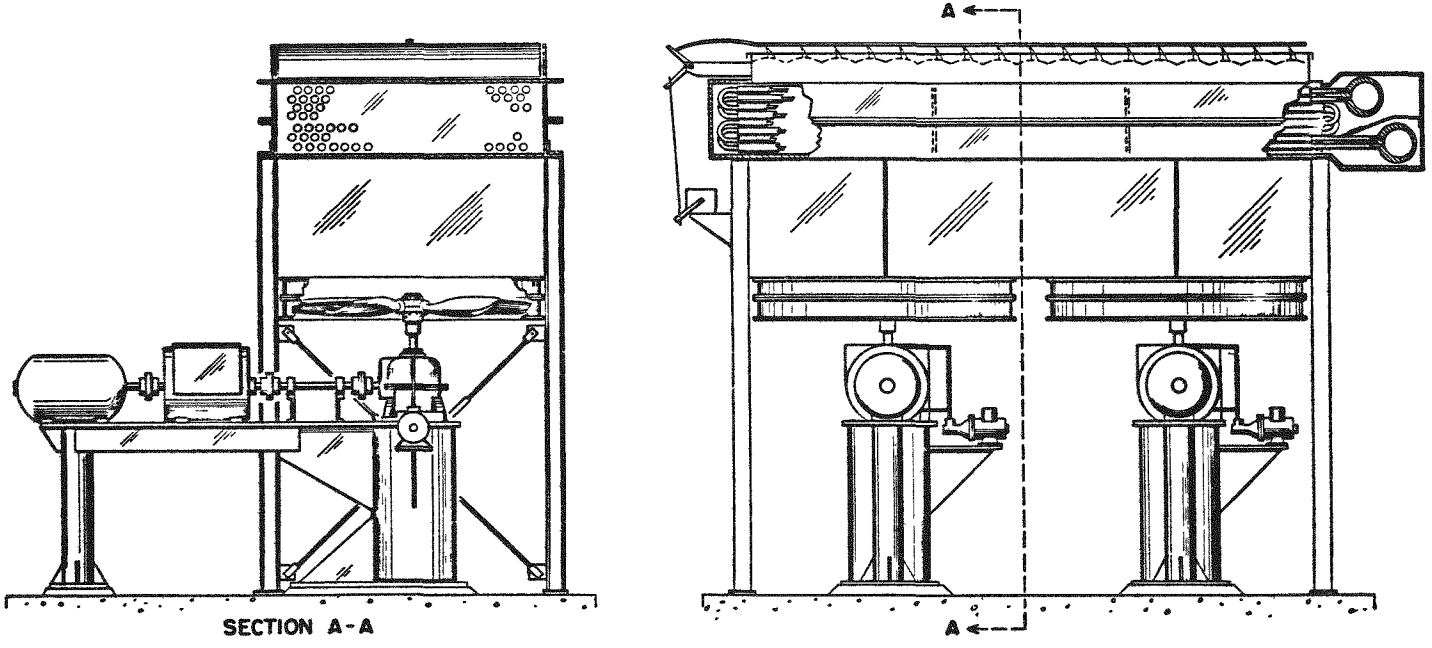

Fig. 5.1.2.1 Heat dump assembly

A maximum air flow of 154,000-lb/h is forced through the heat exchanger by the fans, turned, through magnetic drives and 2:1 reduction, 90° speed reducers, by individual 25-hp, 3-phase, 440-V, 1800-rpm, continuous duty motors. Fan speed can be controlled between 100 and 900 rpm by variations in the current to the drives. An auxiliary oil pump supplies lubricant to the speed reducers when the fans operate at low speeds.

Fine control of the air flow is achieved by adjustment of the pitch of the shutter blades, through a drive motor connected to a proportional controller.

Characteristics of the heat dump exchanger are summarized in Table 5.1.2.1.

Blower - After the 200°F helium leaves the heat dump, a centrifugal blower returns it to the main heat exchanger. This secondary loop blower is identical to the primary loop blower, and the standby motor generator set serves both. The blower is located outside the secondary containment in a pit under the heat dump building.

Isolation Valves - To maintain secondary containment if the secondary loop should be ruptured, there are automatically controlled isolation valves in the secondary loop lines, just outside the containment structure in the piping tunnel. These 8-in., normally open, plug valves have bellows seals on their stems and an auxiliary packing gland above the bellows. The isolation valves are closed by pneumatic operators triggered through a control system that senses a rapid decrease in secondary loop pressure, which would occur if the loop were to rupture. In addition to closing the isolation valves, the control system also opens a similar, normally closed valve in the 4-in. bypass line around the secondary loop blower, which would be damaged if flow were to cease suddenly.

Two pneumatic cylinders operate in tandem to open and close each isolation valve, and a single cylinder actuates the bypass valve. Each cylinder has a double-acting piston. Pneumatic circuits, diagrammed in Fig. 5.1.2.2, control the flow of compressed nitrogen into and out of the

TABLE 5.1.2.1

HEAT DUMP EXCHANGER

Operating Conditions

Hot Side (Tubes)	
Fluid	10,250 lb/h clean He
Inlet temperature	1000°F
Inlet pressure	505 psia
Outlet temperature	200°F
Allowable pressure drop	2.0 psi
Cold Side (Shroud)	
Fluid	154,000 lb/h air
Inlet temperature	100°F
Outlet temperature	377°F
Ambient pressure	12 psia
Heat load	10,250,000 Btu/h

Mechanical Design

Tube banks	Four passes, 56 tubes, No. 16 BWG, each 645-in. long, with seven 2.000-in.-o.d. fins per inch
Heat transfer surface	8,000 ft^2
Flow area, tubes	33.3 in^2
Overall heat transfer coefficient	4.75 Btu/h-ft^2-°F
Helium velocity, inlet	95.3 ft/sec
outlet	43.3 ft/sec
Tube side pressure loss	1.55 psi
Shroud side pressure loss	1.34 in. w.g.

cylinders. The source of nitrogen is a bank of gas cylinders located near the heat dump.

Normally, the isolation valves are held open, against a spring in the operator cylinder, by 30-psi nitrogen pressure fed from a pressure regulator at the nitrogen bank. The blower bypass valve is held closed against a spring by 40-psi nitrogen supplied from another regulator.

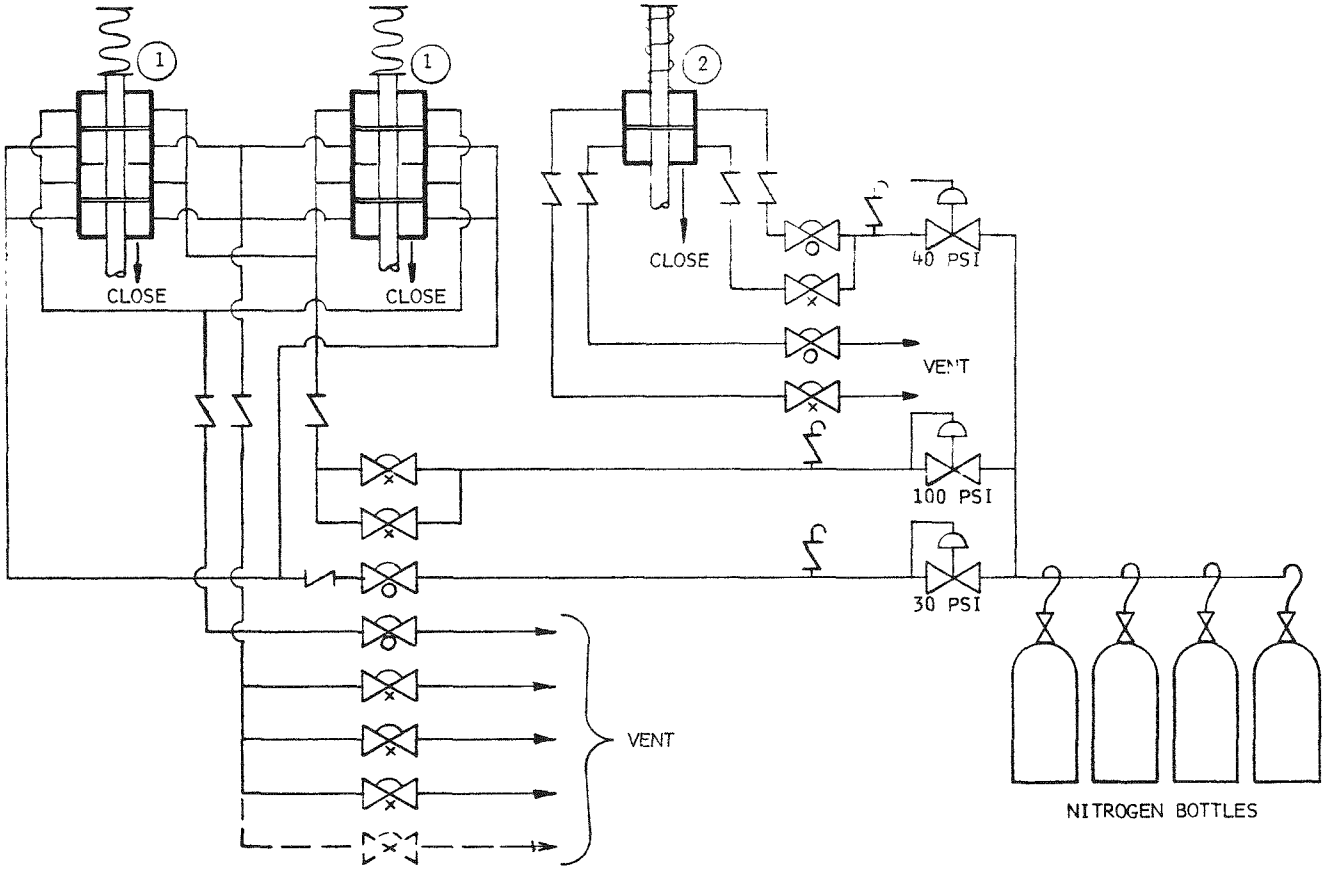

Fig. 5.1.2.2 Penumatic circuits for secondary loop valve operation

When the control circuit, described in Sec. 11.3.3, is triggered, squib valves operate to vent the pressure from the cylinders and to isolate the 30-psi source. Simultaneously, other squib valves connect 100-psi nitrogen to the tops of the isolation valve cylinders and 40-psi nitrogen to the bottom of the bypass valve cylinder. The isolation valves are closed within 270 msec after the control circuit is triggered. Opening time for the bypass valve is 140 msec. Operation of the squib valves is immediate, irreversible, and highly reliable.

Piping - The secondary coolant loop components are connected with Schedule 40, Type 304 stainless steel, seamless pipe. The main system piping is 8-in., and the bypass around the blower is 4-in. Where the loop penetrates the secondary containment wall, the pipes are enclosed in 3-ft-long, 16-in.-diam, tandem, combination end bellows, made of stainless steel. A flange at one end of each bellows is bolted to the pipe sleeve, cast into the wall, through which the coolant pipe passes. The other end of each bellows is welded to the coolant pipe.

Although stresses in the secondary loop piping are mild, the pipes are supported on spring hangers. Conventional external insulation is applied to the pipes, principally to protect personnel against contact with the hot pipes. Figures 5.1.2.3 and 5.1.2.4 show the piping.

5.2 Design Analyses

5.2.1 Reactor and Coolant System Dynamics Studies

An intensive computational study[1] was made of the dynamic behavior of the reactor, the primary coolant loop, and the secondary coolant loop, all acting together as a single system. A mathematical model was formed from about 200 basic equations that describe the components and phenomena of the system. The model has enough detail to make its use valid for

[1]H. B. Demuth, K. H. Duerre, F. P. Schilling, and C. E. Stiles, "System Dynamics Study for Ultra High Temperature Reactor Experiment," LA-3561, November, 1966.

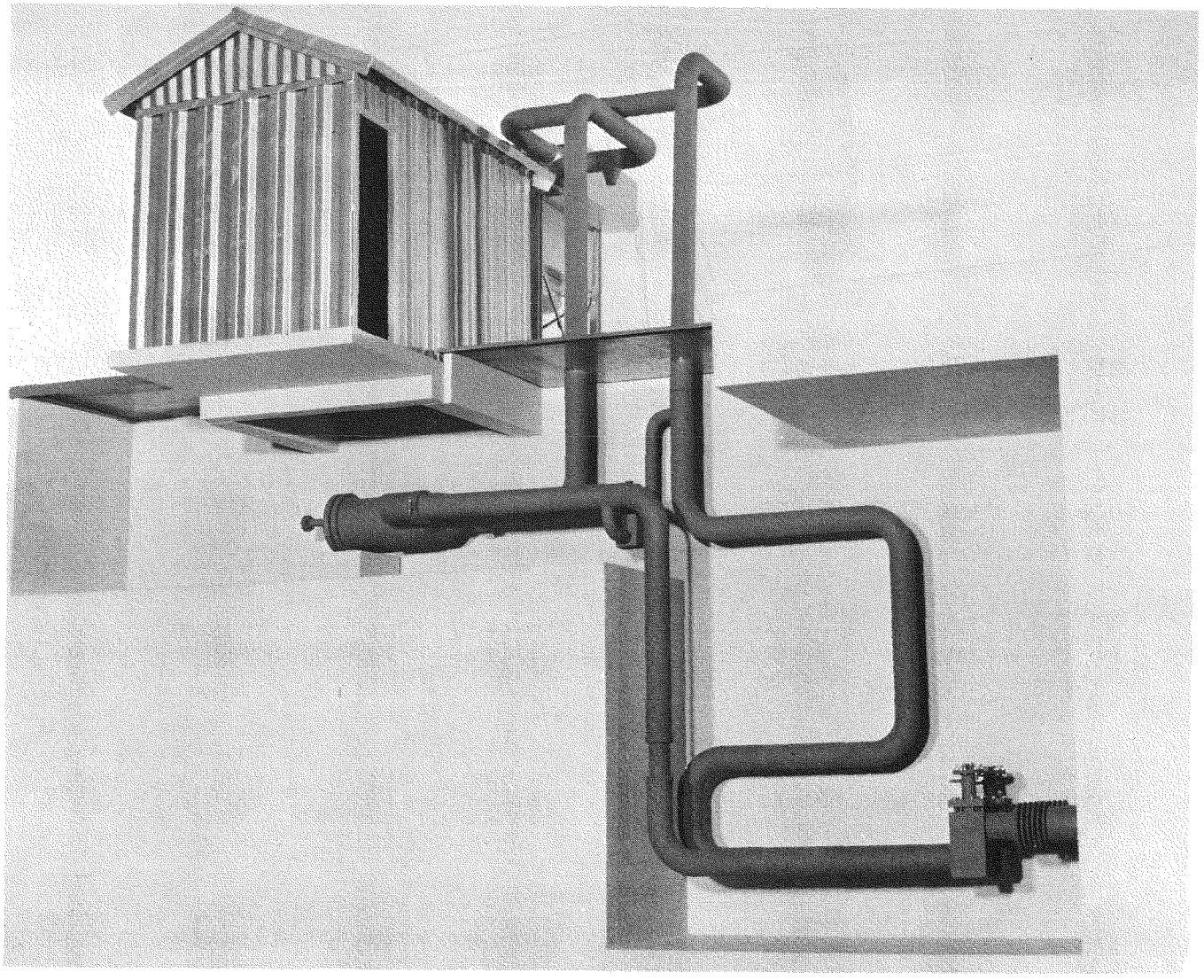

Fig. 5.1.2.3 Secondary coolant loop piping, from model

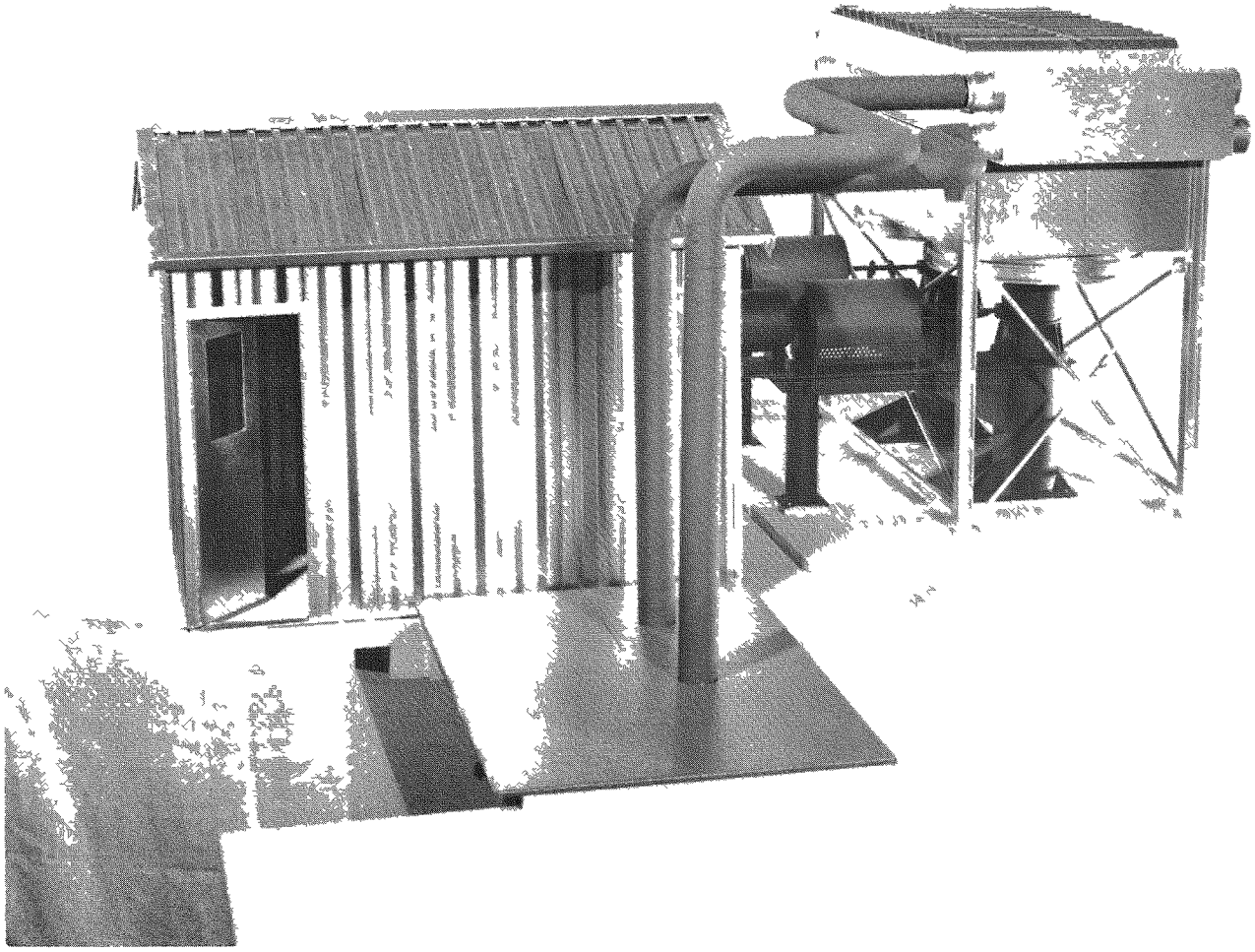

Fig. 5.1.2.4 Secondary coolant loop piping, from model

calculations of the system stability and of the time response of reactor power, gas flow rates, inlet and outlet gas temperatures, gross average solid temperatures, etc., to changes in blower speed, reactivity, and bypass setting.

During the early stages of the study, an IBM-7094 digital computer program (UHXCOM) that solves the system equations was written and used to simulate system behavior in the time domain. Then, a set of system transfer functions was derived from the UHXCOM-calculated transient responses of the system to small step changes. For comparison, another set of transfer functions was obtained directly, after the system equations were linearized, Laplace transformed, and solved with digital computer frequency domain programs. Finally, the transfer functions obtained from the frequency domain programs were checked against the transfer functions obtained from the time domain simulation program. Agreement between the two sets showed that there are no basic errors in any of the programs, and that accurate numerical methods are used to solve the system differential equations in the time domain program.

Results of the UHXCOM-calculated simulation runs show that the UHTREX system will operate stably and can achieve the maximum design conditions without exceeding any design limitation on the system. A number of simulation runs are described below. In all of the runs, the independent and controllable variables are the blower speeds and pressures in the primary and secondary coolant loops, the rate of air flow through the heat dump, the fraction of primary flow bypassed around the recuperator, and the reactivities of the fuel and control rods. All desired reactor operating conditions were achieved by manipulation of these eight variables. Abbreviations used in the studies are defined in Table 5.2.1.1.

For the UHXCOM runs, a set of reasonable operating conditions were defined that are, on the whole, less rigorous than the nominal design conditions set forth in Fig. 5.1.1 and the design descriptions. The UHXCOM conditions are presented in Fig. 5.2.1.1. Note that the secondary

TABLE 5.2.1.1

ABBREVIATIONS USED IN UHTREX SYSTEM DYNAMICS STUDIES

BS_1	Primary loop blower speed
BS_2	Secondary loop blower speed
F°	Degrees Fahrenheit
FB	Fraction of primary flow bypassed around recuperator
HP_1	Primary blower horsepower
HP_2	Secondary blower horsepower
P_1	Primary loop coolant pressure
P_2	Secondary loop coolant pressure
Q_d	Heat dump thermal power
Q_n	Reactor neutronic power
Q_t	Reactor thermal power
°R	Degrees Rankine
T_{air}	Heat dump inlet air temperature
T_{avg}	Average reactor solid temperature
T_{dci}	Heat dump cold inlet air temperature
T_{dco}	Heat dump cold outlet air temperature
T_{dhi}	Heat dump hot inlet coolant temperature
T_{dho}	Heat dump hot outlet coolant temperature
T_i	Reactor inlet coolant temperature
T_o	Reactor outlet coolant temperature
T_{pli}	Pipe No. 1 inlet coolant temperature
T_{plo}	Pipe No. 1 outlet coolant temperature

TABLE 5.2.1.1 (continued)

T_{p2i}	Pipe No. 2 inlet coolant temperature
T_{p2o}	Pipe No. 2 outlet coolant temperature
T_{rci}	Recuperator cold inlet coolant temperature
T_{rco}	Recuperator cold outlet coolant temperature
T_{rhi}	Recuperator hot inlet coolant temperature
T_{rho}	Recuperator hot outlet coolant temperature
T_{xci}	Heat exchanger cold inlet coolant temperature
T_{xco}	Heat exchanger cold outlet coolant temperature
T_{xhi}	Heat exchanger hot inlet coolant temperature
T_{xho}	Heat exchanger hot outlet coolant temperature
$\mathring{\omega}_1$	Primary loop coolant flow rate
$\mathring{\omega}_2$	Secondary loop coolant flow rate
$\mathring{\omega}_3$	Heat dump air flow rate
X_b	Recuperator bypass stem position
ΔP_{21}	Pressure difference between primary and secondary loops
ρ	Net reactivity
ρ_r	Rod reactivity
ρ_t	Temperature reactivity
ρ_s	Shutdown reactivity
ϕ_1	Primary blower flow coefficient
ϕ_2	Secondary blower flow coefficient

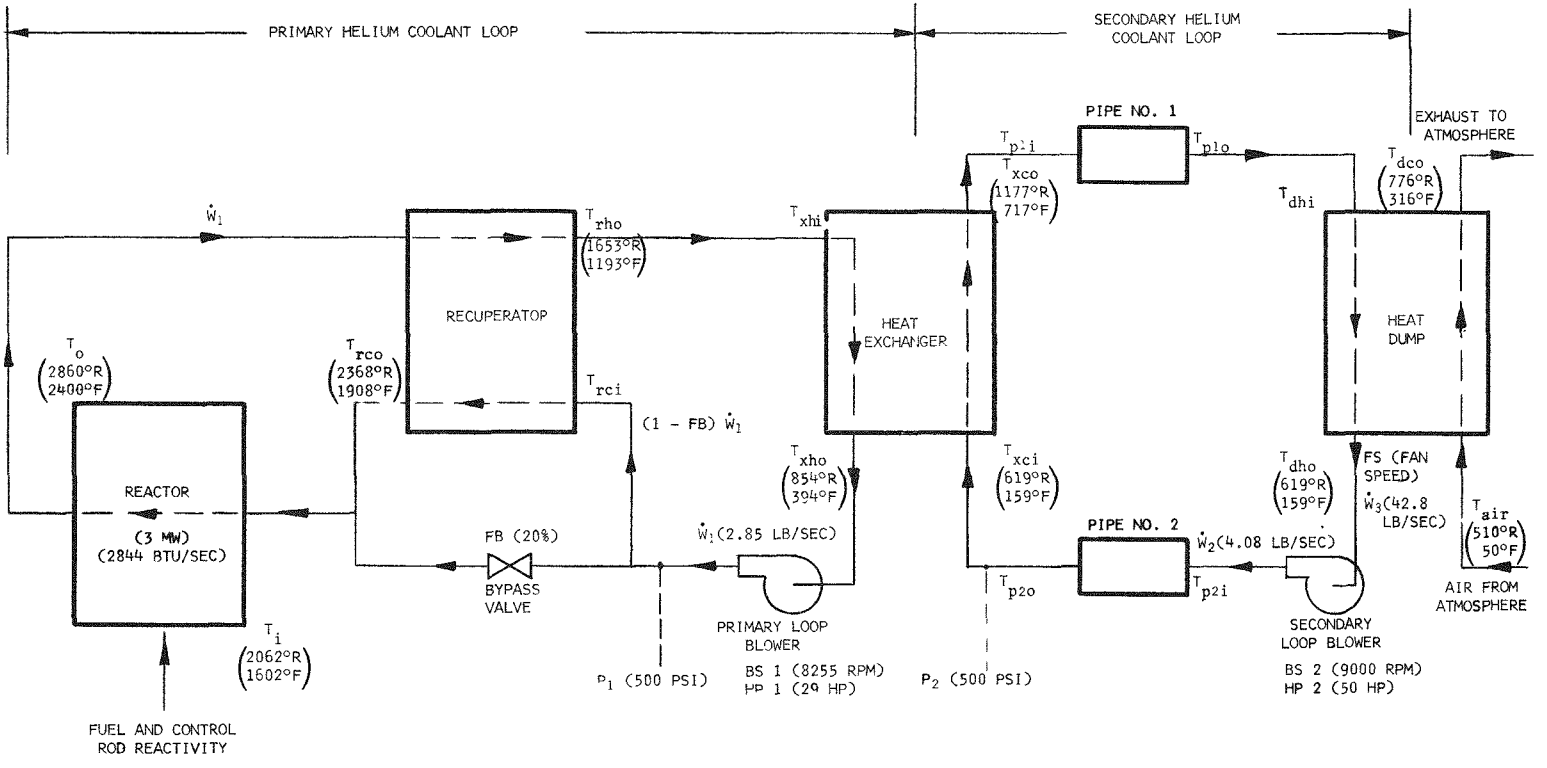

Fig 5.2.1.1 Full power, steady state for UHXCOM studies

loop flow rate is higher than that in the primary loop and that the temperatures at the main heat exchanger are lower than the design temperatures.

Full Power Steady-State Operations - An UHXCOM simulation run was made to determine overall system conditions under full power, i.e., when the reactor neutronic power is 3 MW, the reactor outlet gas temperature is 2400°F, and the primary flow rate is 2.85 lb/sec (10,250 lb/h). In this run, calculational closed loops were used to obtain the 3-MW, 2400°F, and 2.85-lb/sec values. Specifically, the following variables were adjusted to obtain the desired values.

	Variables	Desired Values
1.	Reactor bypass FB	Reactor power Q = 2845 Btu/sec
2.	Reactivity TAMB	Reactor outlet gas temperature T_o = 2400°F
3.	Primary loop blower speed BS_1	Primary flow rate $\mathring{\omega}_1$ = 2.85 lb/sec

Secondary loop blower speed was 9000 rpm, and the heat dump air flow rate was 42.8 lb/sec (154,000 lb/h).

Results of this run, shown in Fig. 5.2.1.1, demonstrate that there is at least one way of operating the system at full power so that the system limitations of Table 5.2.1.2 are satisfied. The conclusion is, in fact, by no means obvious, and can be based on nothing less than a complete steady state solution of the equations.

The conditions of Fig. 5.2.1.1 represent only one possible way of operating the system, and are not the final or design conditions for the system. For convenience, the conditions of Fig. 5.2.1.1 will be referred to as the "standard operating conditions." These standard conditions are used as the initial conditions in all simulation runs reported here except where other conditions are stated.

Off-Design Operation - A variety of steady-state simulation runs were made in operating regions close to the standard conditions to assess

TABLE 5.2.1.2

SYSTEM LIMITATIONS

System Variable	Abbreviation	Limits	Comments
Primary loop blower speed (rpm) Secondary loop blower speed (rpm)	N_1 N_2	$4000 < N_1 < 12{,}000$ $4000 < N_2 < 12{,}000$	Gas bearings not adequate at lower speeds without gas jacking. Upper speed limitation is fixed by limit on frequency output of alternator.
Primary blower motor power (hp) Secondary blower motor power (hp)	HP_1 HP_2	$HP_1 < 65$ $HP_2 < 65$	Motor powers limited by balance of losses, heat transmitted to motor via drive shaft, and cooling.
Heat dump air flow rate (lb/sec)	$\mathring{\omega}_3$	$\mathring{\omega}_3 < 50$	Approximate maximum design value for heat dump fans.
Reactor inlet gas tempeature (°R)	T_i	$T_i < 2060$	Design limit for piping at reactor inlet
Recuperator hot outlet coolant temp (°R)	T_{rho}	$T_{rho} < 1860$	Maximum design temperature for heat exchanger inlet.
Heat exchanger cold outlet coolant temp (°R)	T_{xco}	$T_{xco} < 1560$	Temperature rating of heat exchanger shell.
Heat exchanger tube temperature (°R)	T_{xt}	$T_{xt} < 1660$	Temperature rating of tubes.
Heat exchanger hot outlet coolant temp (°R) Heat dump hot outlet coolant temp (°R)	T_{xho} T_{dho}	$T_{xho} < 1060$ $T_{dho} < 1060$	Maximum design temperatures for steady state operation of coolant blowers.
Primary loop helium pressure (psia) Secondary loop helium pressure (psia)	P_1 P_2	$P_1 < 550$ $P_2 < 550$	Design limit of pressure vessels.
Secondary loop pressure-Primary pressure (psia)	P_2-P_1	$0 < (P_2-P_1) < 50$	Design limit of heat exchanger.
Fraction of primary flow bypassed around recuperator	FB	$0.01 < FB < 0.8$	Both limits are established by bypass valve and recuperator ΔP characteristics.

Rod System Limitations:

a. Articulated rods cannot be inserted when core temperature in the vicinity of their receiving holes exceeds 1660°R.
b. Rods can be run in and/or out at a maximum speed of 18 in./min. Scram time is ~ 0.6 sec.
c. Total rod worth of the whole rod system is approximately $30.
d. All rods are to be fully withdrawn, if possible, at and around full power design conditions.

Reactor Temperature Cycling:

Reactor temperature cycles from room temperature to design temperature should be minimized.

the effects of changes in bypass setting, blower speed, etc. The results are plotted in Figs. 5.2.1.2 through 5.2.1.7.

Each figure contains five curves, each of which shows how the dependent (ordinate) variable changes when only one of the independent (abscissa) variables is changed. The other four independent variables are held constant. Thus, curve FB in Fig. 5.2.1.2 shows that, when BS_1, BS_2, and $\mathring{\omega}_3$ are held constant at their standard condition points and FB is changed from 0.2 to 0.1, the reactor power decreases to about 2.8 MW. Each figure is discussed below.

Fig. 5.2.1.2 Reactor Power - A rise in reactor power occurs when the recuperator bypass flow is increased, when system reactivity is increased, or when the flow in any of the three coolant loops is increased. (Flows $\mathring{\omega}_1$ and $\mathring{\omega}_2$ are increasing functions of blower speeds BS_1 and BS_2 as shown in Figs. 5.2.1.6 and 5.2.1.7.) BS_1 and FB have considerably more effect than $\mathring{\omega}_3$ or BS_2. The heat dump air flow, $\mathring{\omega}_3$, has little effect on power in the range shown.

Fig. 5.2.1.3 Reactor Coolant Temperatures - The reactor inlet and outlet coolant temperatures are more sensitive to changes in bypass flow and reactivity than to changes in blower speed and flow rate. Both temperatures decrease when the flow bypassed around the recuperator is increased, or when the reactivity is decreased. The reactor inlet coolant temperature is particularly sensitive to changes in bypass flow and reactivity.

Fig. 5.2.1.4 Heat Exchanger, Primary Loop Coolant Temperatures - The heat exchanger hot inlet coolant temperature is quite sensitive to changes in bypass flow; an increase in bypass flow results in higher coolant temperatures. Temperature rises in the primary loop side of the main heat exchanger also accompany increases in ρ or BS_1. The essential result of an increase in FB, ρ, or BS_1, is a rise in power, accompanied by the elevation in temperatures.

Fig. 5.2.1.5 Heat Dump, Secondary Loop Coolant Temperatures - An increase in bypass flow, reactivity, or primary blower speed yields an

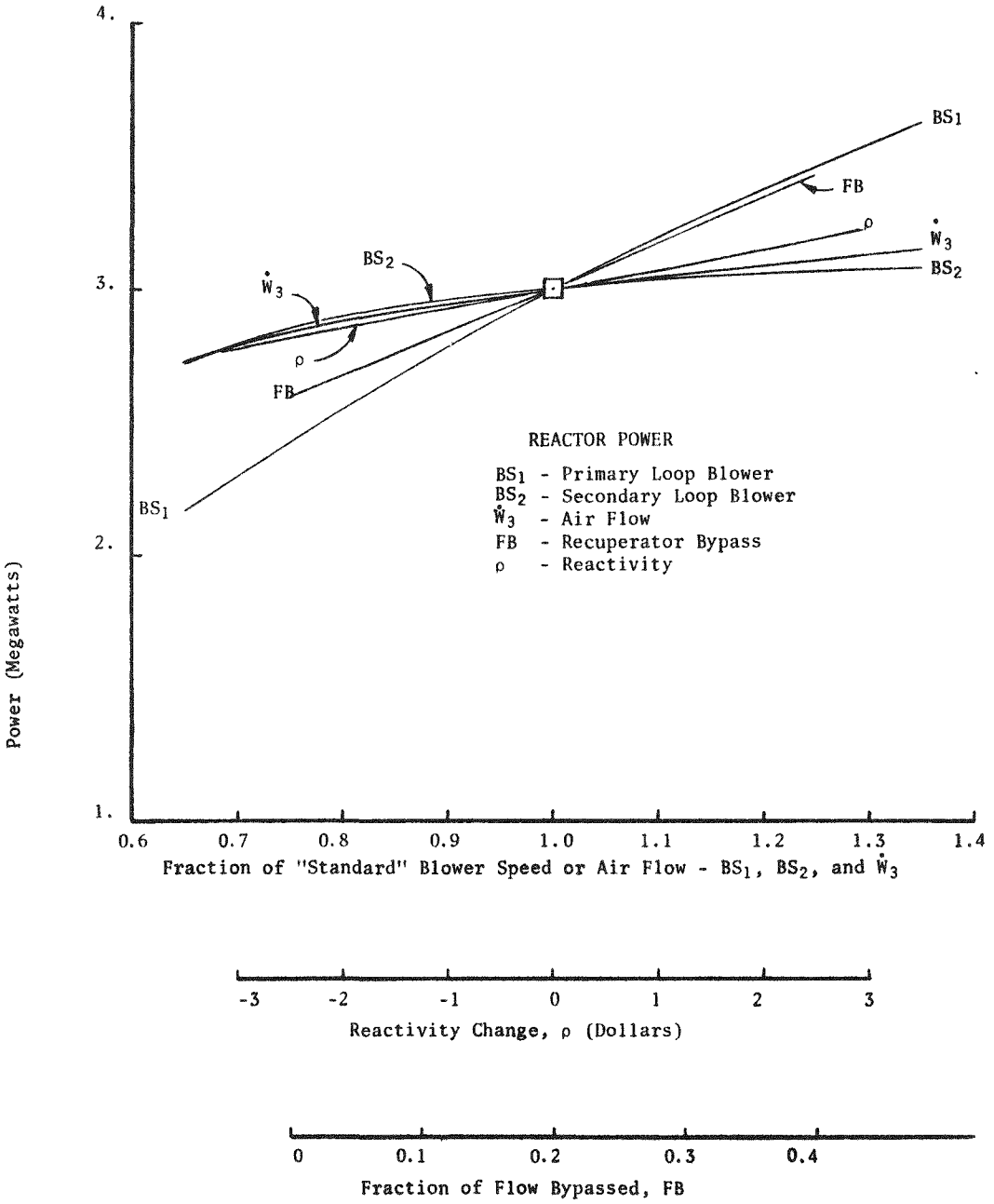

Fig. 5.2.1.2 Reactor power as a function of blower speeds, air flow, and recuperator bypass

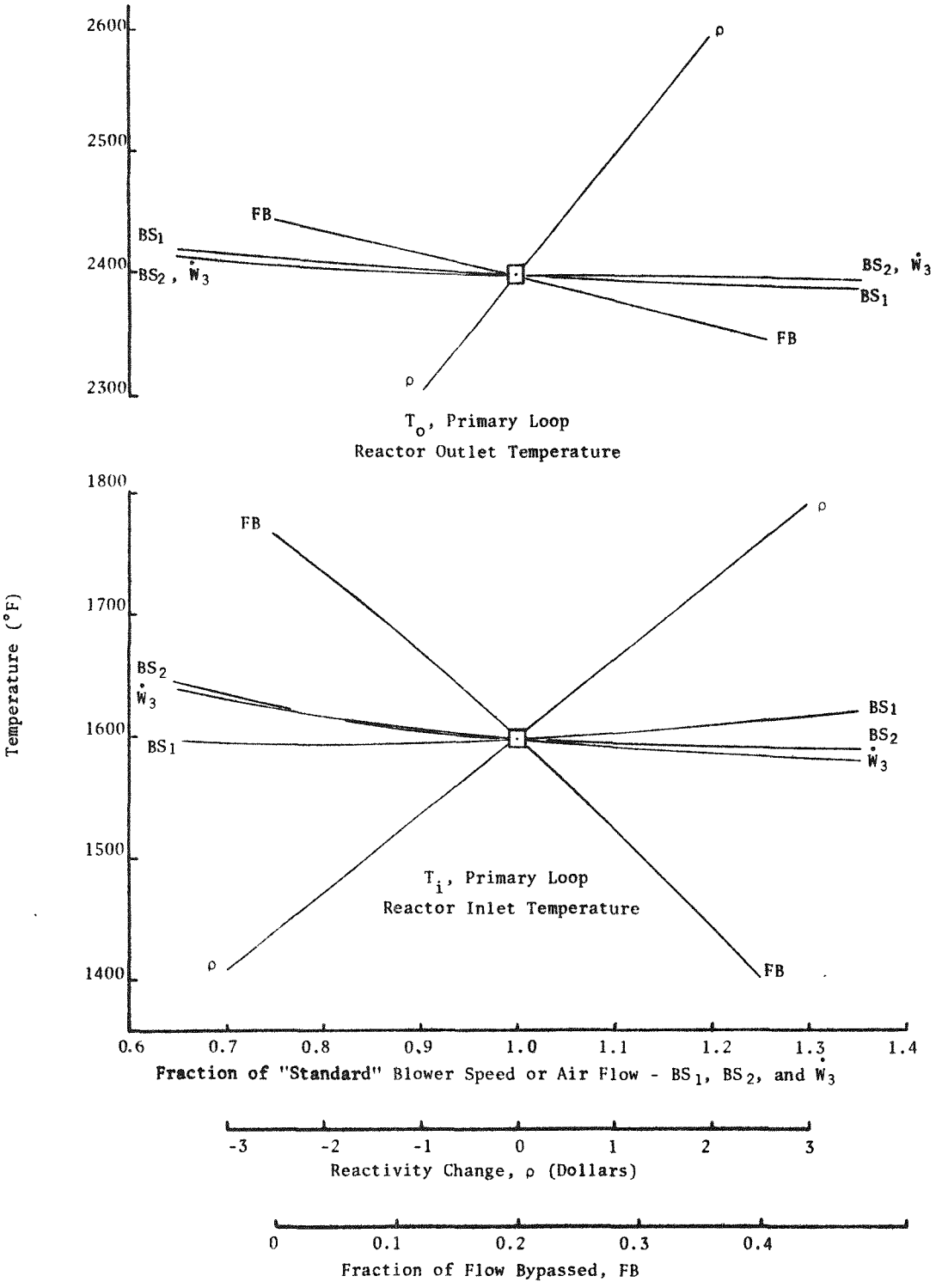

Fig. 5.2.1.3 Reactor inlet and outlet coolant temperature variations

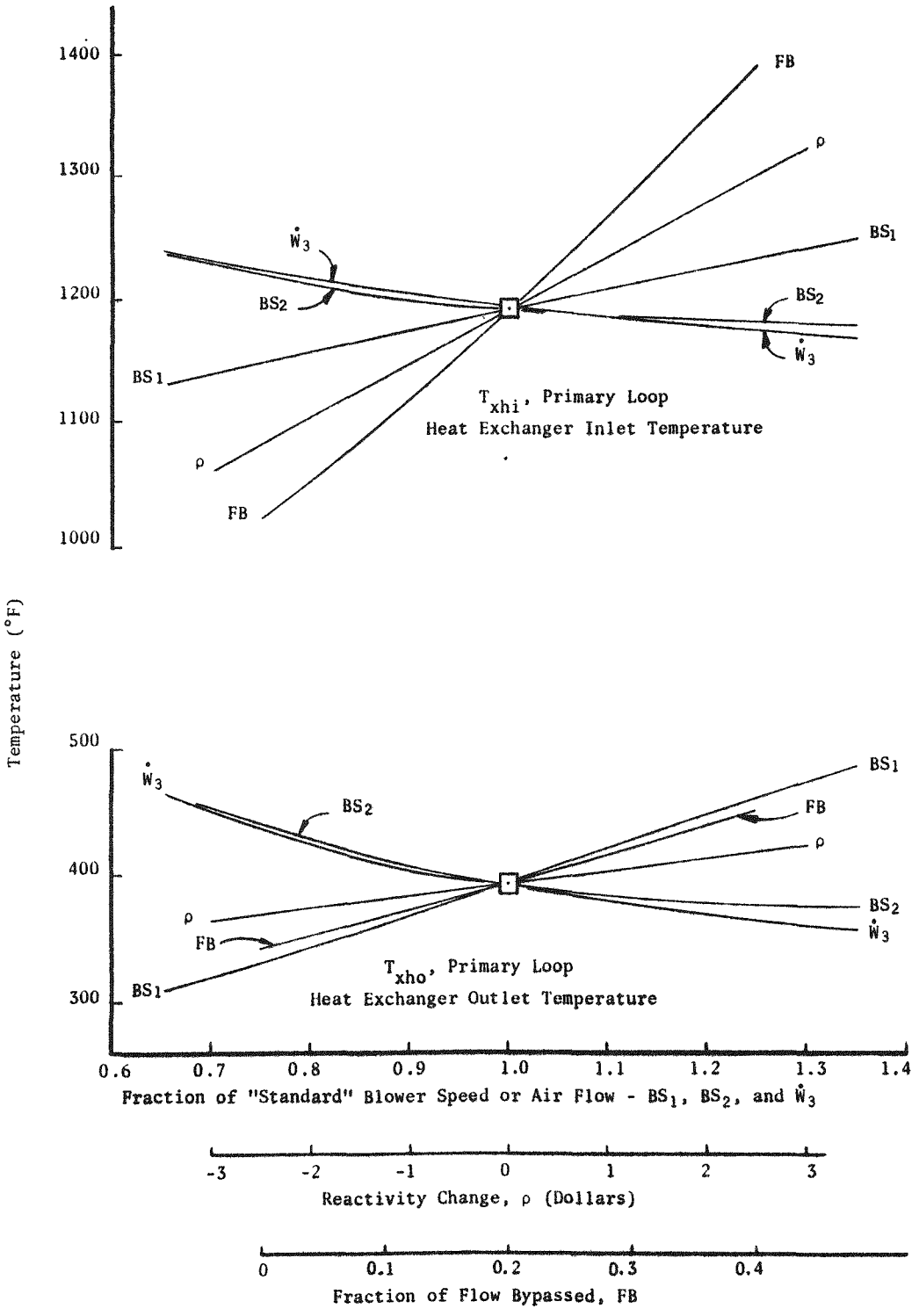

Fig. 5.2.1.4 Heat exchanger inlet and outlet coolant temperature variations

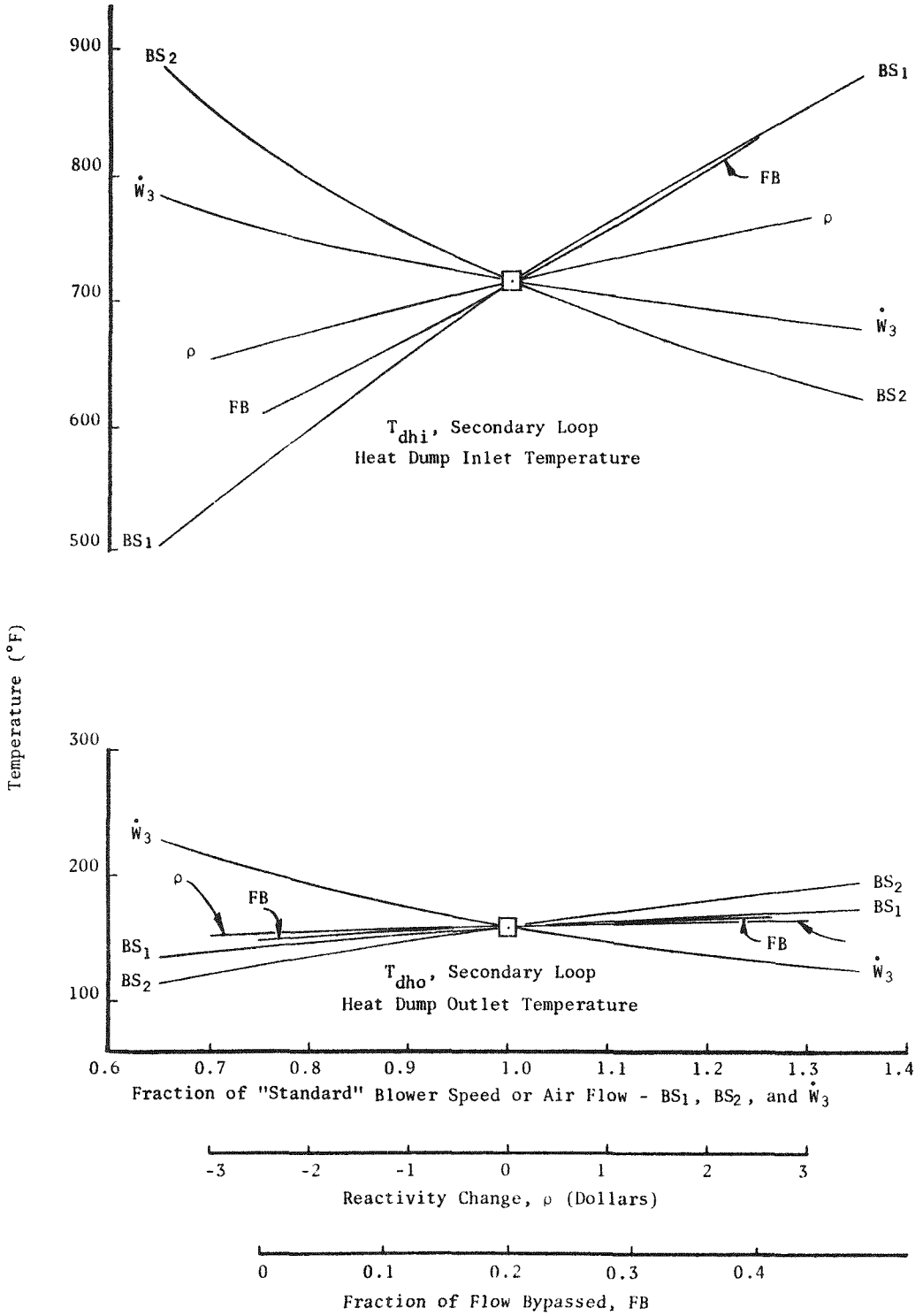

Fig. 5.2.1.5 Heat dump inlet and outlet coolant temperature variations

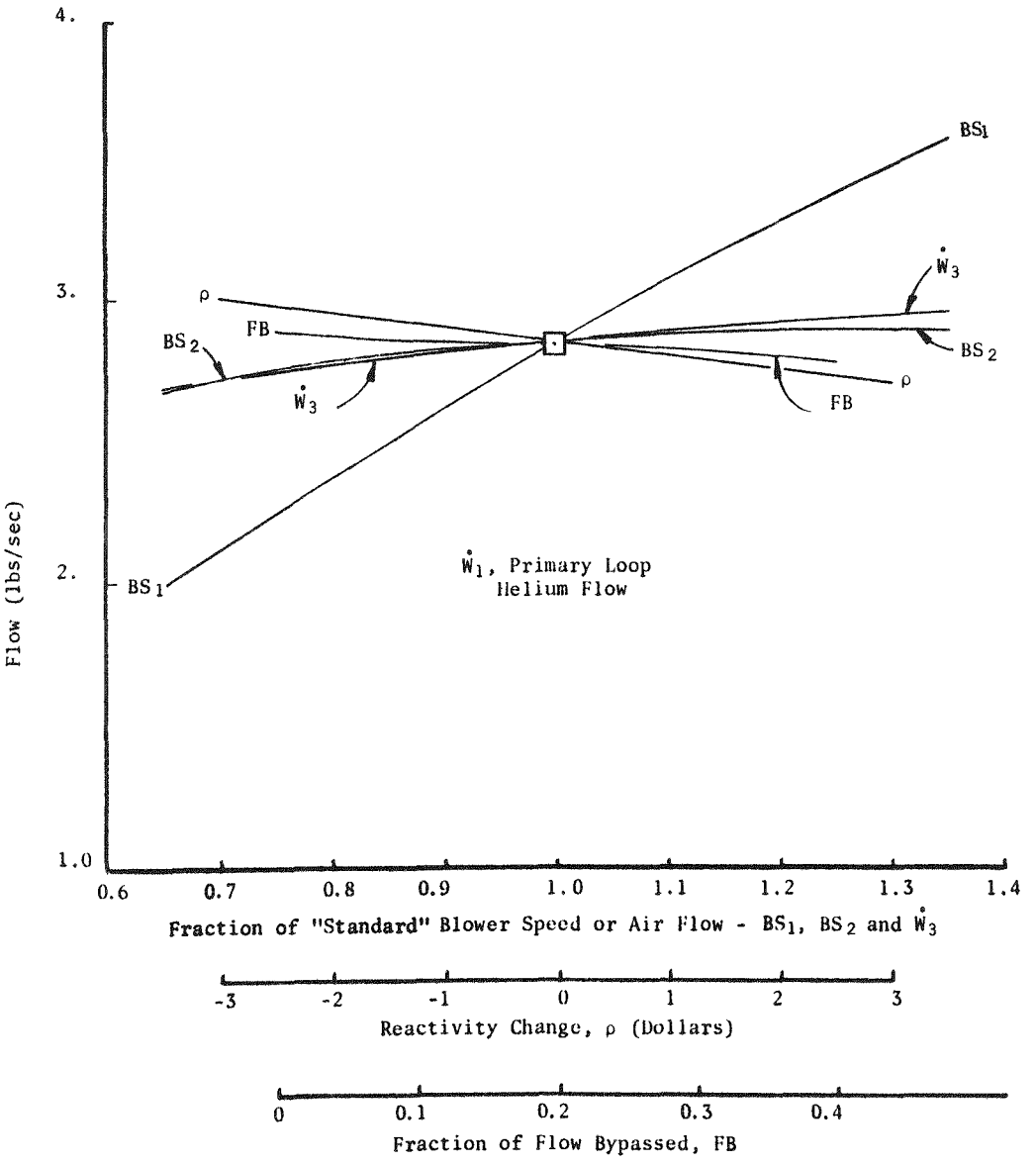

Fig. 5.2.1.6 Primary coolant loop flow rate variations

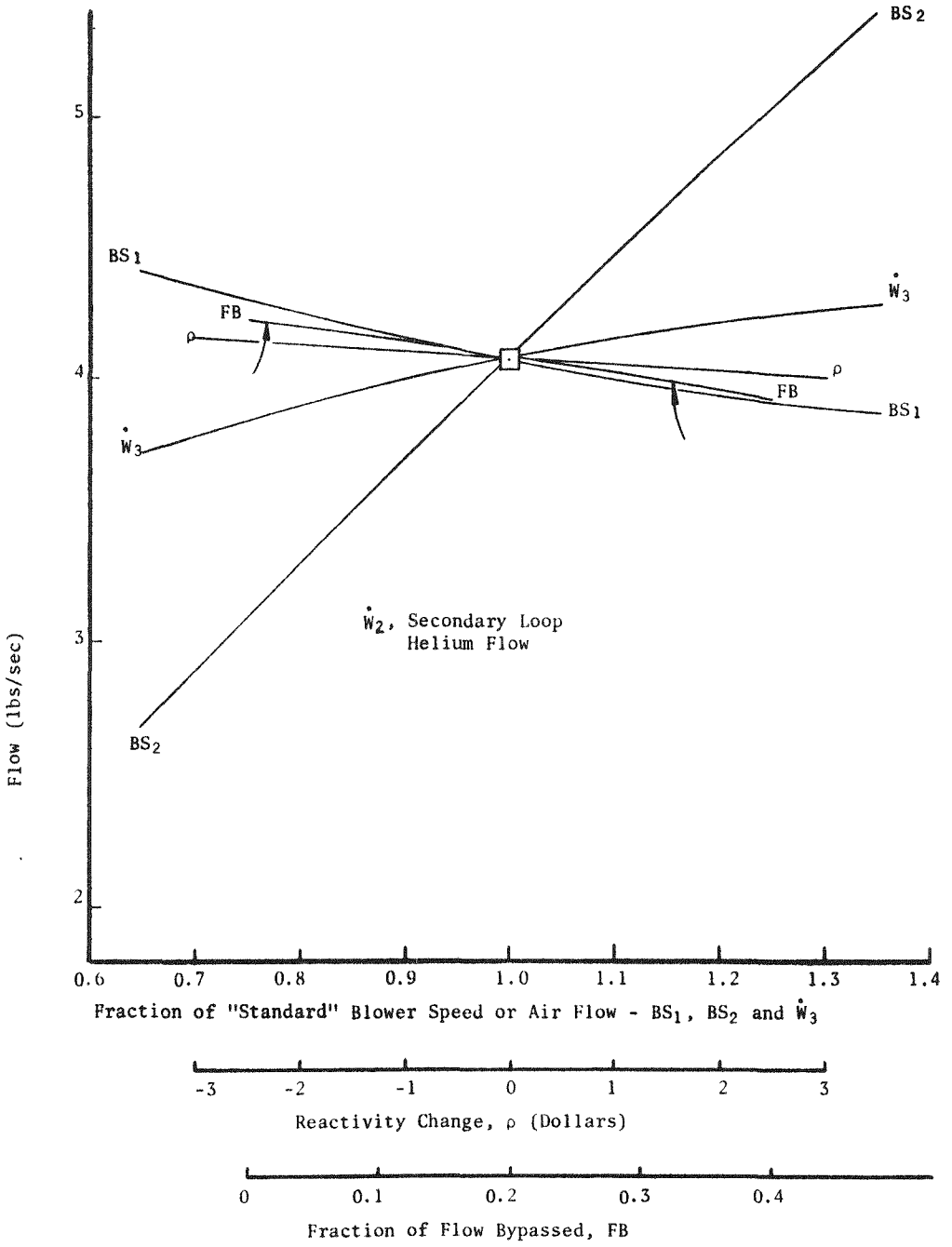

Fig. 5.2.1.7 Secondary coolant loop flow rate variations

increase in the heat dump inlet coolant gas temperature. The heat dump outlet coolant temperature is relatively insensitive to changes in operating variables.

Figs. 5.2.1.6 and 5.2.1.7 Primary and Secondary Loop Flow Rates - Primary and secondary loop flow rates increase with the speed of their respective blowers, but are relatively insensitive to changes in other independent variables.

Approximate results for cases in which two variables are changed can be determined from Figs. 5.2.1.2 through 5.2.1.7. For example, the effect of a change in BS_1 on T_{xhi} can be estimated for the case in which FB is concurrently changed to maintain constant power. In the first step of the estimation process, an arbitrary assumption is made that BS_1 increases to 1.2 times its standard value. From Fig. 5.2.1.2, it can be seen that to keep the power constant, the value of FB must be decreased to about 0.02. From Fig. 5.2.1.4, the effect of the change in BS_1 from 1 to 1.2 times its standard value is a rise in T_{xhi} of about 35°R, whereas the effect of decreasing FB to 0.02 is a decrease in T_{xhi} of about 155°R. The combined effect of the two changes, then, is a decrease in T_{xhi} of about 120°R. These results are only approximate because the system is not linear and the results of independent changes in FB and BS_1 cannot be superimposed with perfect accuracy. However, such superposition is adequate for useful estimates, as long as the departure is not too far from standard conditions. The conclusion reached above, that T_{xhi} decreases with an increase in BS_1 if the power is held constant, agrees with intuitive results.

In total, the simulation runs show that reactor power and most system gas temperatures are relatively insensitive to changes in the rates of flow of secondary coolant and heat dump air. However, bypass flow, reactivity, and primary blower speed have a considerable effect on power and, consequently, on gas temperatures. It is also apparent that critical system temperatures decrease with increasing secondary and heat dump flow rates and with an increase in primary flow rate, as long as the reactor power is held constant.

The runs predict that, at and near full power, five system independent variables can be manipulated to obtain desired values of other system variables. The relationships of 12 variables for control uses are shown in Table 5.2.1.3. For example, BS_1 can be adjusted to obtain a particular value of BS_1, or a desired $\mathring{\omega}_1$, or a desired Q_t. Such an adjustment could be made by an operator or by appropriate closed-loop control equipment.

TABLE 5.2.1.3

RELATIONSHIP OF SYSTEM VARIABLES FOR CONTROL USES

Changes Can Be Made in These Independent Variables	To Effect Desired Changes in These Variables
ρ	T_o
X_b	X_b or T_i
BS_1	BS_1, $\mathring{\omega}_1$ or Q_t
BS_2	BS_2, $\mathring{\omega}_2$ or T_{xco}
FB	FB or T_{xho}

Open Loop Dynamic Response to Modest Changes in Independent Variables - A series of simulation runs were calculated for the case where a modest change is made in the value of an independent variable and the system responds in a manner unlimited by any corrective action of the sort that would be taken by an operator or by a closed-loop control circuit external to the basic system.

The sizes and rates of changes in independent variables were selected to correspond roughly to physical changes that might be introduced through routine operator actions or by a radical change in the weather. When, for example, the blower speeds were varied, the change was made on a 5-min ramp rather than in an abrupt step, because the slow change would be the usual occurrence.

Figure 5.2.1.8 shows the system power responses to a +5¢ reactivity step. This step corresponds roughly to loading in a fuel element that does not displace another fuel element from the center of the core. The neutronic power rose about 20% to a peak 36 sec after the step, displayed two oscillations that have a period of 276 sec, and approached steady state in 10 min. Reactor thermal power, shown in the same figure, exhibited a minor oscillation, but the heat dump thermal power did not change at all. The average core temperature, not shown, rose a few degrees to nullify the +5¢ step. A low amplitude oscillation appeared in the net system reactivity, but reduced to less than 2¢ in 3 min. Temperature responses were moderate. Reactor exit coolant temperature rose < 50°R during the excursion, fuel elements rose 50°R in the first minute but returned to initial temperature within 10 min, and the moderator showed little change. However, nearly all of the temperature reactivity change was due to the change in moderator temperature rather than to fuel element temperature changes. The inverse period was less than 10^{-3} in 3 min. The recuperator outlet temperature showed a 40°R peak for about 2 min. Other system components showed no response. In summary, the results of the 5¢ step analysis demonstrate that, except for a modest power oscillation, there is no significant response. However, to avoid unnecessary shutdowns, the power oscillation must be kept in mind when power level scrams are set during fuel loading operations.

The system's behavior toward a 5¢ reactivity perturbation is typical: a disturbance at the reactor "end" of the UHTREX system is delayed and attenuated as it travels toward the heat dump. Similarly, at the other end of the system, heat dump disturbances are delayed and attenuated before they reach the reactor.

Another simulation run was made to determine the system response to a change in the quantity of coolant bypassed around the recuperator. For the run, the ratio of bypass flow to total coolant flow was decreased from 0.2 to 0.1 on a 5-min ramp. As expected, the reactor inlet and outlet gas temperatures rose during the ramp and then settled to new

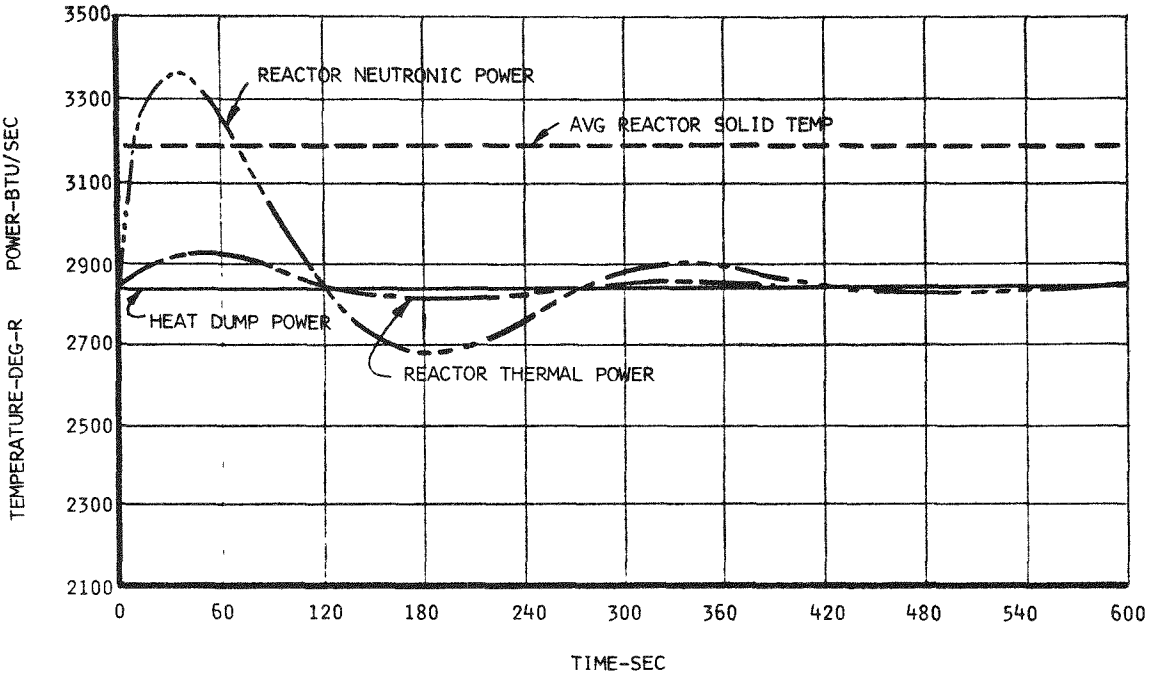

Fig. 5.2.1.8 Reactor power response to a 5¢ reactivity step

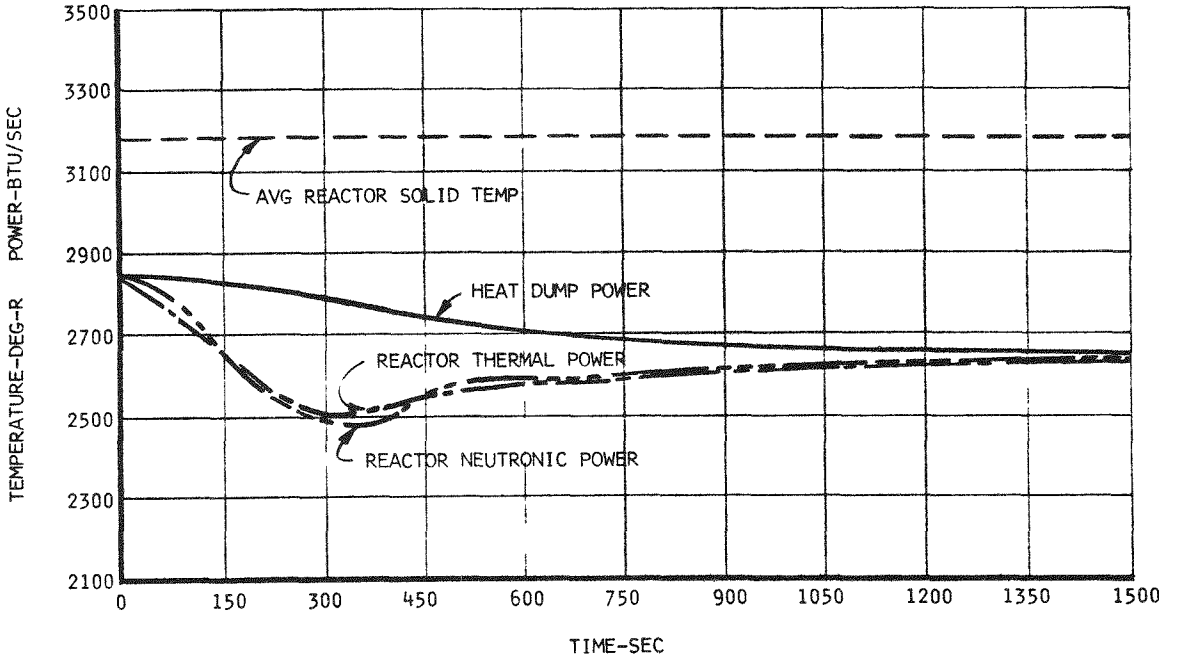

Fig. 5.2.1.9 Reactor power response to a change from 0.2 to 0.1 in ratio of bypass to total coolant flow

equilibrium values, 100°R higher at the inlet, 40°R higher at the outlet. The reactor solid temperatures rose enough to lower the reactivity by about 1¢, and the reactor neutronic power changed as shown in Fig. 5.2.1.9. The thermal power and neutronic power responded together in this case, because it is the gas temperature change that causes the neutronic power change, and the whole process proceeds fairly slowly. The heat dump thermal power change lagged considerably, however. Recuperator and heat exchanger gas temperatures changed by less than 100°R.

For the next run, the primary loop blower speed was decreased by 20% on a 5-min ramp. In response, the primary flow rate decreased by about the same percentage while the secondary flow rate rose slightly. System pressure drops and blower powers changed in proportion. Reactor neutronic and thermal power responses were similar to those produced by a bypass decrease, but the power changes were somewhat larger. Figure 5.2.1.10 shows the power changes on an expanded time scale. The heat dump thermal power change did not lag quite so much as it did in the bypass case.

The secondary loop blower speed was reduced 20% in 5 min for another run. The secondary loop flow rate, pressure drop, and blower power decreased the same percentage, but the corresponding variables in the primary loop fell only slightly. The heat exchanger hot outlet temperature rose about 140°F. Heat dump thermal power fell rapidly during the term of the blower ramp, and then stabilized, in about 15 min, at a value about 4% below the full power level. Reactor thermal and neutronic powers dropped slowly and finally reached the heat dump thermal power level.

When, for the next run, the heat dump air flow rate was decreased 20%, the three dependent heat dump gas temperatures slowly rose less than 50°R. System pressure drops and blower powers decreased by less than 5%, and the reactor powers dropped about 4% in 25 min.

To simulate what would happen during an extreme air temperature change, a run was made in which the heat dump air inlet temperature was

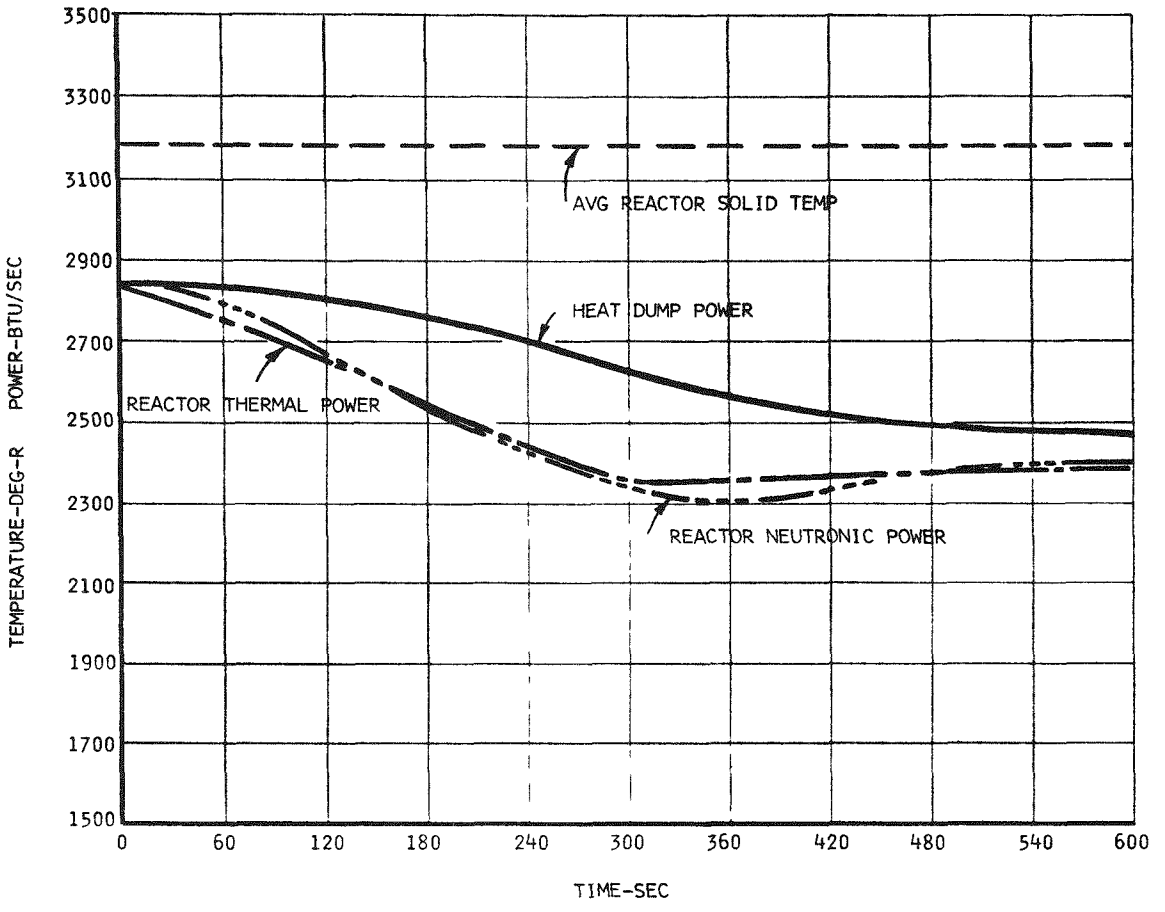

Fig. 5.2.1.10 Reactor power response to a 20% decrease in primary blower speed

decreased 40° on a 5-min ramp. In response, system flow rates and pressure drops rose by approximately 5%, the reactor gas temperatures decreased about 25°R, and the reactor powers increased slowly to about 4% above their initial values. About 2-1/2 min passed before the reactor powers started changing. The minimum period was about 1000 sec.

In summary, the entire system behaves in a very stable manner when disturbed by changes of the kind discussed in this section. Reactor power is almost the only physical variable of interest that responds quickly or with appreciable overshoot, and the effects of its changing are hardly felt elsewhere in the system.

Sensitivity of Calculated Results to Assigned Values of Parameters - It is obvious that the results of studies made with a mathematical model depend on the values assigned to the parameters treated in the model. In UHXCOM, the majority of the parameters can be defined with certainty and evaluated accurately. However, others, of which heat transfer coefficients are the most important, can be calculated with only limited accuracy and may change with time as the system operates; e.g., deposits on tube walls can change heat transfer coefficients in the heat exchanger. To assess the effects on calculated results of inaccurate or changing values of parameters, a series of UHXCOM simulation runs were made in which the less well-defined parameters were assigned a range of values.

The results of the runs showed that the validity of the UHXCOM analyses does not depend on precisely defined parameter values. Table 5.2.1.4 summarizes the system responses, which are discussed below.

For the parametric studies, the basic problem was the system response to a 5¢ step in reactivity, described above for the case in which standard parameter values were used. A change in the value of a single parameter was made for each run, and the results of the run were compared with the results of the standard run.

The effects of variation in the value of the reactor temperature coefficient of reactivity, ρ_t, were studied in runs 1, 2, and 3. In run 1 the value of ρ_t was reduced by 50%, and for run 3 it was increased by 50%, relative to the standard value, used in run 2. As was to be expected, the dynamic behavior of the system was strongly dependent on ρ_t, but the system responses remained stable and within tolerable limits. As the value of ρ_t decreased there were two responses: an increase in the size of the power overshoot that results from the reactivity step, and an increase in the period of the power oscillation.

Runs 4, 5, and 6 were made to evaluate the sensitivity of the calculated results to heat transfer coefficients. An arbitrary 50% increase in the recuperator heat transfer coefficient yielded results similar to a decrease in bypass flow: the reactor inlet and outlet

TABLE 5.2.1. 4

UHTREX SYSTEM RESPONSE TO PARAMETER CHANGES

Run	Parameter Varied	Change	Power Overshoot Max Q_n / Initial Q_n	Period of Power Oscillation (sec)	Q_t (Btu/sec)	Reactor Gas Temp. (°R) T_i	Reactor Gas Temp. (°R) T_o	Heat Exchanger Gas Temp. (°R) T_{xhi}	Heat Exchanger Gas Temp. (°R) T_{xho}	Heat Exchanger Gas Temp. (°R) T_{xci}	Heat Exchanger Gas Temp. (°R) T_{xco}	Maximum Heat Exchanger Tube Temp. (°R)
Standard conditions					2844	2062	2860	1653	854	619	1177	1241
Design Limits						2060	2860	1860	1060	1060	1560	1660
Run 1	Reactor temp. coefficient of reactivity	-50%	1.26	400	2851	2068	2870	1657	855	619	1179	1244
Run 2	Reactor temp. coefficient of reactivity	0%	1.18	276	2847	2065	2865	1655	855	619	1178	1243
Run 3	Reactor temp. coefficient of reactivity	+50%	1.14	172	2846	2063	2862	1654	855	619	1177	1242
Run 4	Recuperator heat transfer coefficient	+50%	1.14	280	2713	2129	2878	1586	837	615	1141	1202
Run 5	Heat exchanger heat transfer coefficient on shell side	-33%	1.14	280	2735	2079	2867	1673	885	616	1147	1262
Run 6	Heat dump heat transfer coefficient on tube side	-33%	1.08	284	2589	2104	2877	1702	929	691	1250	1308

Note: All runs include an initial +5¢ reactor reactivity step.

temperatures increased, the heat exchanger inlet and outlet temperature decreased, and power level dropped. A 33% reduction of the heat transfer coefficient in the shell side of the heat exchanger showed very little effect. A 33% reduction in the heat dump coefficient reduced power about 9% and increased temperatures in the primary and secondary loops as much as 80°R. As a general observation, large changes in the heat transfer coefficient of individual components do not seem to cause serious problems.

5.2.2 Piping Stress Analysis

The structural adequacy of the primary and secondary loop piping was evaluated for the following conditions:

1. Steady-state pressure
2. Steady-state thermal deflection
3. Equipment and piping weight loads.

The general design criteria follow the provisions of the "Code for Pressure Piping," American Standard ASA-B31.1-1955, Section 1. Stresses were calculated by means of a computer program[2] that uses a tensor analysis treatment of Castigliano's theorem. The computer program, a version of the Mare Island Naval Shipyard program, is capable of calculating closed-loop configurations and includes the effects of thermal expansion, concentrated loads, and uniform loads.

The highest stress (S_E) in the primary loop, 14,532 psi, occurs at 600°F, adjacent to the recuperator bypass valve, and arises from the effects of pipe loads, concentrated loads, and thermal expansion. The highest stress in the secondary loop, 16,782 psi, occurs at 1000°F in the elbow above the 4-in. bypass line connection. The allowable stress (S_A) for expansion of Type 304 stainless steel pipe at a temperature of 600°F is 23,100 psi, and at a temperature of 1000°F is 22,813 psi.

---

[2]J. H. Griffin, "A Piping Flexibility Analysis Program for the IBM-7090 and 7094," LA-2929, July 1963.

5.3 Testing

The coolant loops and all other helium containment systems in UHTREX were fabricated and installed according to written specifications that call for rigorous inspection and nondestructive testing of materials, components, and systems. In particular, all pressure system materials have passed ultrasonic inspections, all structural welds have been radiographically inspected for 100% penetration, and all completed systems will undergo helium leak tests at operating pressures.

Upon completion, the coolant loops will undergo code pressure tests, helium leak tests, and then a series of function tests before reactor startup. The first phase of functional testing will involve calibration and circuit testing of system transducers and controls and of the loop auxiliary systems, i.e., the pressure regulation and safety systems. Then, the loops will be pressurized and operational tests of each component and auxiliary system will be made. Finally, cold flow tests will be made of both loops, singly and together, and of all auxiliary systems. Concurrently, the on-line computer's programs will be exercised in calculations of blower characteristics, loop flow rates, and other parameters derived from loop instrumentation output data.

6. FUEL HANDLING SYSTEM

Fuel elements move inside a fuel handling system between a drybox in the fuel transfer cell, and the reactor vessel. The functions of this fuel handling system are described here. Information about the fuel elements, the fuel loader, and related equipment inside the reactor vessel is presented in Secs. 4.1.4 through 4.1.6 of this report.

The fuel handling system was designed to operate under the rigorous conditions that exist when the reactor is operating at design power and the fuel elements have experienced significant burnup. Therefore, in the descriptions of system design and operating procedures that appear below, design conditions are presumed. However, simplified procedures can be used when operating conditions are less severe, e.g., during initial loading, or during fuel substitution operations that take place while the reactor is depressurized and before fission products inventories are significant. These simplified procedures shall be reviewed and approved by cognizant groups before use.

6.1 General Description

Fuel elements can be charged into and discharged from the reactor while it is operating at design conditions. To accomplish this task safely, the fuel handling system must be operated rapidly and in precise sequence through many steps. Therefore, the fuel loading operation is controlled primarily by the on-line computer in the control room. However, each loading sequence begins and ends at the drybox, under the manual control of the cell area operator.

6.1.1 New Fuel Introduction

Fuel elements arrive at the facility in safe-geometry transport containers, described in Sec. 13.1.1. From the containers, the individual elements, which can be handled manually without hazard, are loaded into an alpha can inside a helium-filled glove box. As a part of the glove box procedure, the elements, the can, and a basket that fits inside the can are passed through an air lock that excludes the atmosphere. After as many as 21 elements are loaded into a can, its cover is fitted in place, and the helium-filled can and its contents are removed through the air lock. The elements are now ready to enter the fuel handling system, a schematic diagram of which appears in Fig. 6.1.1.1.

New elements on the way to the reactor and spent elements returning from the core move through a drybox in the fuel handling cell, shown in Fig. 6.1.1.2. To protect the hot, spent elements from oxidation as they leave the core and to prevent the entry of oxygen into the core with the new elements, the atmosphere is helium in the drybox and in the conveyors leading to and from it. The drybox window adjoins the lead glass window in the west wall of the fuel transfer cell. A pair of master-slave manipulators allow operators standing in the cell operating area to handle fuel elements inside the drybox.

If there are no spent fuel elements in the drybox, an operator can open both shield doors and load alpha cans directly into the transfer mechanism mounted under the drybox. Otherwise, he can open the outer door, set the cans inside the fuel transfer lock, close the outer door, open the inner door, and move one can at a time with the lock manipulator into the transfer mechanism. In either case, the mechanism moves the alpha can beneath the drybox, seals the can against an opening in the bottom of the drybox, and removes the can's cover. From the open can, an operator lifts out the basket of elements with the manipulators, removes a single element, and places it into a loading chute at the inlet end of the charge conveyor. Before an element is inserted into the charge conveyor, the operator reads the serial number engraved on the element and compares it with the loading list.

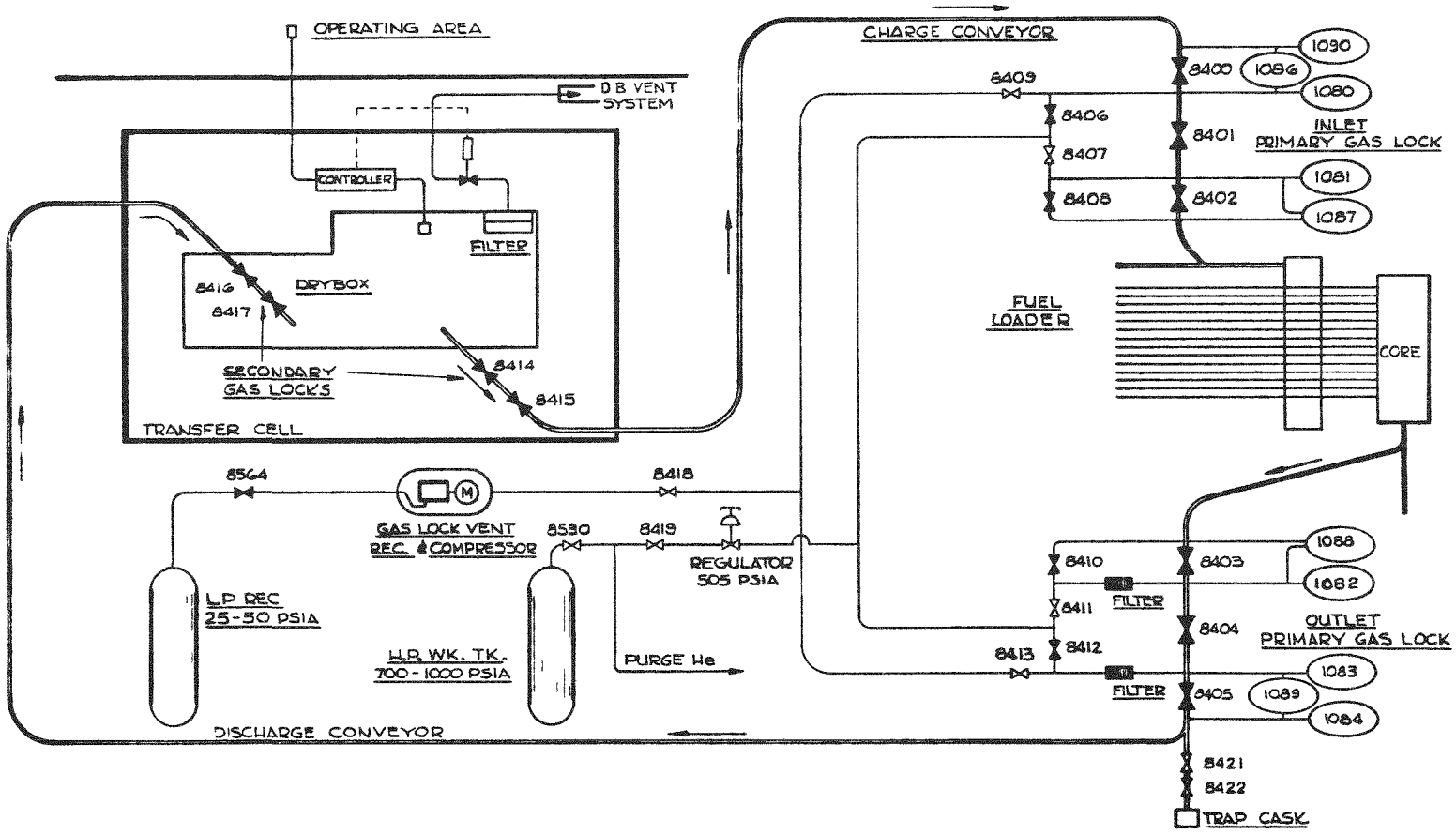

Fig. 6.1.1.1 Fuel handling system

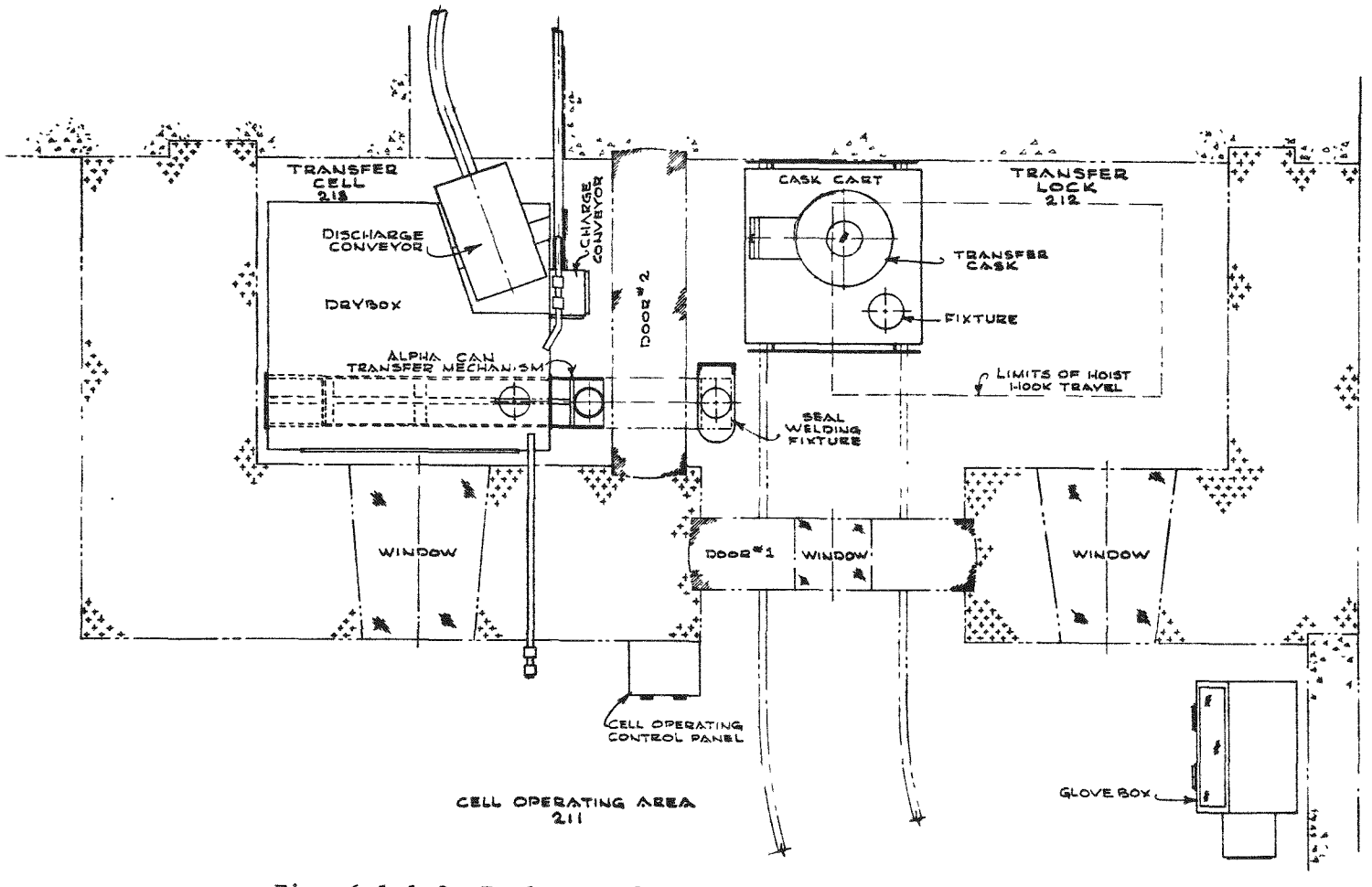

Fig. 6.1.1.2 Fuel transfer cell, lock, and operating area

In the charge conveyor, the new element slides into contact with the outer ball valve of the secondary gas lock. The cell operator then tells the control room operator to initiate the computer-controlled operation of the fuel handling system. The first step in the computer program is the entry by the control room operator of the fuel element's identification into the computer. When the fuel element data have been dialed in at the computer console, the computer prints out a log of the data for verification by the operator and then proceeds with the loading sequence.

6.1.2 Loading Sequence

In the first step of the loading sequence, the computer opens the outer valve of the charge conveyor's secondary gas lock, after checking that the inner valve is closed. The fuel element falls by gravity to the inner valve and rests there until the computer closes the outer valve. With secondary containment again established behind the fuel element, the inner valve opens and the fuel element falls into the conveyor boat, which can accept only one fuel element. Next, the computer starts a drive motor, which pulls a continuous cable attached to the boat. The boat moves through the conveyor tube to a position directly over the inlet primary gas lock valve, pivots on a cam surface, and dumps the fuel element into the primary gas lock.

The fuel element moves through the primary gas lock under the force of gravity, its movement controlled by the gas lock valves. A computer program job list that describes the steps in the primary gas lock operation appears in Table 6.1.2.1. As the element moves from the near atmospheric pressure of the conveyor to the high pressure environment of the reactor, a pressure regulation system adjusts the intervalve pressures inside the gas lock. Number groups, e.g., V8409, in Table 6.1.2.1 refer to valves that are a part of the pressure regulation system, which is shown schematically in Fig. 6.1.1.1 and is described in more detail in

TABLE 6.1.2.1

JOB LIST FOR INLET PRIMARY GAS LOCK OPERATION

Step No.	Action		Reason for Action
1.	Close	V8409	To prevent the venting of helium in the gas lock vent receiver line to the conveyor tube or drybox.
2.	Open	V8400	To allow the fuel to fall through the first gas lock valve.
3.	Wait	2 sec	To allow the fuel element to pass clear of V8400 before it closes.
4.	Close	V8400	
5.	Open	V8406	To equalize pressure across V8401.
6.	Wait	5 sec	To allow time for pressure equalization.
7.	Open	V8401	
8.	Wait	2 sec	To allow the element to fall completely through V8401 before it closes.
9.	Close	V8401	
10.	Close	V8406	To isolate the high pressure He supply from the low pressure receiver line.
11.	Open	V8409	To reduce the pressure between V8400 and V8401 to near atmospheric.
12.	Close	V8407	To prevent contamination of clean He supply by He from the reactor vessel.
13.	Open	V8408	To equalize pressure across V8402.
14.	Wait	5 sec	
15.	Open	V8402	To allow the element to drop into the preloader.
16.	Wait	2 sec	
17.	Close	V8402	
18.	Close	V8408	To close the bypass path around V8402.
19.	Open	V8407	To reapply clean He at pressure slightly above primary loop pressure.

Sec. 6.2.8. At each step of the primary gas lock operation, computer interlocks prevent the opening of a leakage path for the flow of helium out of the reactor.

From the primary gas lock, the fuel element slides into the fuel loader. The computer then returns the conveyor boat to the drybox and operates the fuel loader through the sequence described in Sec. 4.1.5.

After the spent element falls out of the core and slides down the discharge pipe, it comes to rest at the first valve in the outlet primary gas lock. As it did on entering the reactor, the fuel element falls through a primary gas lock, under the control of the computer, in a sequence of steps similar to that described in Table 6.1.2.1. However, because the newly discharged element is at a high temperature, the operating sequence for the outlet gas lock includes cooling steps, during which the element is held above each valve for a time and gives up heat to the cool walls of the gas lock.

The spent fuel element, cooled to about 700°F, leaves the gas lock and drops into the boat in the discharge conveyor. If fragments or dust fall past the boat, they collect in the trap cask below the conveyor tube. Once in the boat, the element moves back to the drybox under computer control. At the drybox the boat dumps the fuel element into the secondary gas lock, through which it falls into the drybox. The whole load-unload sequence, which takes about 15 min, terminates with the arrival of the discharged element in the drybox. However, if a fuel element fails to appear, the operator at the fuel cell window reports the fact and the operator at the computer initiates an alternate program which operates the fuel element dislodger rod to clear the slot in the reactor core plug where the element is probably lodged. The freed element then falls into the outlet gas lock, and the computer performs the remainder of the sequence to deliver the element to the drybox.

Throughout the loading sequence, the computer is directed by limit switches that indicate the positions of the valves, conveyor boats, loader rams, and elevators. For example, a limit switch is operated by

contact with the conveyor boat when it arrives at the discharge secondary gas lock. The switch signals the computer to start the next step, which is a time delay to allow the element to slide into the gas lock, followed by the opening of the outer gas lock valve. A limit switch on the valve then informs the computer that the valve is open, and the system is ready for the next step. The computer responds by pausing long enough to allow passage of the element through the valve, and then closes the valve. Again, a limit switch signals closure of the valve, and the computer advances to the next step, which is the operation of the second valve in the gas lock.

Each load-unload sequence starts with the insertion of a fuel element in the charge conveyor by a manually controlled manipulator and ends with the closing of the discharge secondary gas lock. The control room operator does not start another sequence until the cell operator has seen the spent element fall into the drybox and is ready to insert a new element.

6.1.3 Spent Fuel Removal from Drybox

When a radioactive, spent element reaches the drybox, the cell operator, looking through the cell window, can examine the element and return it to the reactor, or he can prepare the element for transportation away from the facility. In the latter case, he loads as many as 21 elements into an alpha-can basket and places the basket in its can. Next, he opens the inner shield door to the fuel transfer lock. Then he actuates the alpha-can mechanism, which closes the can with a cover, moves it into the lock, and elevates it into a seal-welding fixture. The fixture welds the cover to the alpha can, which is now ready to be removed from the transfer lock.

With the transfer lock manipulator, controlled from outside the lock, the operator removes the can from the weld fixture and inserts it into a basket suspended below the Meehanite cover of a transportation cask. Then he inserts the cover and can into the cask, which is waiting

on a cask cart. Before moving the cask cart, however, he must close the intercell door and monitor the fuel transfer lock for contamination. If all is well, he opens the outer lock shield door and moves the remotely controlled cart on rails to the truck loading dock. At the dock, a crane lifts the cask to a truck for removal to another LASL facility, where fuel inspection and recycle experiments can be performed.

6.2 Design Details

6.2.1 Cell Operating Area

The operator who loads and unloads the fuel handling system works in Room 211, the cell operating area, shown in plan view in Fig. 6.1.1.2. In this room are the glove box for loading new elements into alpha cans, the master ends of the fuel cell manipulators, and the controls for the cell door, crane, and motor-driven manipulator. Four-ft-thick shield walls of magnetite concrete and a 20-in.-thick Meehanite shield door are adequate protection for the operator against the radiation from at least 100 spent fuel elements, delivered to the fuel transfer cell at the maximum discharge rate from the reactor. Lead glass windows permit the operator to view the interiors of the cells. An intercom station provides for direct communication with the control room.

A control area, Room 211 can be entered only through the monitored change room while operations are in progress that could result in the release of contamination. Two gamma area monitors and one air particulate monitor, with local readout and alarm, continuously measure radiation levels. An independent ventilation system serves the area and moves the air from the operating area directly to filter banks, or when the cell door is opened, into the cells. Inflatable gaskets make airtight seals around the closed shield doors.

The cell operating area contains work benches and space where contaminated equipment can be maintained or repaired.

6.2.2 Fuel Transfer Lock

The fuel transfer lock, Room 212, is a heavily shielded buffer zone between the operating area and the fuel transfer cell. Access to the lock is through a vertically sliding shield door mounted on a hydraulic lift. Another shield door separates the lock from the transfer cell. When the intercell door is closed, an operator can open the outer door and move the cask cart in or out of the lock. The lock is shielded well enough against spent fuel in the cell and against the reactor that an operator can enter the lock safely, after checking the activity level reported by the gamma area monitor inside the cell.

Remotely controlled equipment in the lock allows the operator to handle spent fuel from his station in the cell operating area. The cask cart moves in and out on rails. An overhead, 1-ton bridge crane handles the cover of the fuel cask. A bridge-mounted, PaR Model 3000 manipulator, with 100-lb lifting capacity, moves the alpha cans between cask and transfer mechanism. The can welding fixture stands near the intercell door.

In the south end of the lock is the primary gas sampling system (see Sec. 12.1), operated with a set of master-slave manipulators mounted above the lead glass window.

6.2.3 Fuel Transfer Cell

A drybox, with the fuel conveyor and alpha-can transfer mechanisms attached to it, completely fills the fuel transfer cell. Conveyor tubes that penetrate the rear cell wall are welded to a steel plate that maintains the integrity of the secondary containment structure, and are surrounded by shielding that fills in the opening into the fuel charging room behind the cell. The front wall of the cell contains a lead glass window, a set of master-slave manipulators, and a tube with a double-valve gas lock through which a single fuel element can be dropped into the drybox. When the intercell door is open, the alpha-can transfer mechanism can move cans between the cell and the transfer lock.

The area ventilation system forces air to flow from the operating area to the cell. In the cell, the pressure is maintained below the cell operating area pressure by an independent set of two blowers and a filter bank. A third independent blower and filter bank set receives, directly, the exhaust from the drybox. A high range gamma monitor in the cell measures the radiation level there and indicates it on a meter in the cell operating area.

6.2.4 Drybox

Fuel elements enter and leave the fuel handling system inside the helium-filled drybox. Made from welded, 1/4- and 1/8-in. stainless steel plate, the drybox is the barrier against the spread of contamination from irradiated fuel elements. Its helium atmosphere is maintained at a pressure above the cell atmosphere by a control system that feeds helium from a bottle rack in the cell operating area or discharges helium to the drybox exhaust ventilation system. Small volumes of helium, discharged from the outer gas lock valves, enter the drybox through the conveyor systems, and are vented by the pressure control system. The vent helium passes through a bank of charcoal filter canisters, which can be replaced with the manipulators and inserted inside alpha cans for disposal. At the front of the drybox is a 1/2-in.-thick Homolite CR-39 window. Master-slave manipulators can reach all areas inside the box.

Cylindrical alpha cans, made of spun stainless steel, contain the fuel elements as they enter or leave the drybox. The cans have snug-fitting, inset covers that are sealed to the can with an O-ring. A flanged edge on the cover can be welded to the top of the can to close it tightly when it contains spent fuel elements. A removable basket, with 21 vertical pins on which the fuel elements are supported, fits inside each can.

A transfer mechanism, mounted on the bottom of the drybox, moves the cans inside the cells to and from the box. In its extended position,

the mechanism reaches into the fuel transfer lock (see Fig. 6.1.1.2). There, an operator can place a can in the mechanism and then actuate it from the control panel outside the lock. The mechanism retracts inside the transfer cell, elevates the can against a flanged, circular opening in the bottom of the drybox, and seals the top, outer edge of the can against a gasket. Inside the drybox, sealed against the top edge of the flanged opening, is a pneumatically actuated device which keeps the opening closed until a can is in place, at which time the device retracts and removes the can cover. The interior of the can is then accessible to the slave manipulators.

To remove an alpha can from the drybox, the operator actuates the can cover handling device, which descends, replaces the can cover, and seals the top edge of the flanged opening. The operator can then operate the transfer mechanism to move the can into the fuel lock. If the can contains spent fuel, the operator actuates the seal-welding fixture which welds the cover to the can. The can is then ready to be placed in a cask for removal from the transfer lock.

To maintain the helium atmosphere in the drybox, new elements are loaded into the alpha cans inside a helium-filled glove box in the cell operating area, and the can handling mechanisms prevent the entry of air at the drybox as cans are coupled to or disconnected from the box.

6.2.5 Secondary Gas Locks

Fuel elements pass between the drybox and the conveyors through the secondary gas locks, each a pair of remotely operated, motor-driven ball valves. The secondary locks maintain secondary containment in the conveyor systems. They are operated in sequence, only one open at a time. The secondary lock in the charge conveyor is outside the drybox, mounted in a tube which passes through, and is welded to, the drybox wall. For the discharge conveyor, the secondary lock is mounted inside the box on a tube that is welded to the drybox and connected to the discharge conveyor with a Conoseal tube joint. Limit switches on the valves indicate open and closed positions.

6.2.6 Conveyors

Two conveyors move the fuel elements between the drybox and the primary gas locks. Each has a boat that carries one element at a time through a pressure-tight, stainless steel conveyor tube. The boats are connected at each end to a continuous Teleflex cable that circles around a drive unit at one end of the conveyor and an idler sheave at the other end.

Each conveyor system is contained in a gas-tight enclosure which terminates in a Conoseal joint at the reactor end and in a secondary gas lock at the drybox end. The enclosure includes the conveyor drive unit, the main tube through which the boat moves, the idler at the reactor end of each conveyor, and the conduit through which the Teleflex cable returns from the idler to the drive unit. As the outer chamber of either gas lock opens, a small amount of relatively clean helium vents into the connected conveyor. In ordinary circumstances, the helium causes a small pressure rise inside the conveyor, which is vented to the drybox through the secondary gas lock. However, if a leak develops in the primary gas lock and a substantial quantity of helium is released, the pressure inside the conveyor rises, because the secondary gas lock maintains secondary containment. Should the internal conveyor pressure rise to 10 psi, a rupture disk near the primary gas lock vents the conveyor to the secondary containment ventilation system.

For the charging conveyor system, the main tube is made of 11-gauge, 2-1/2-in.-square, Type 304 stainless steel tubing. An open-topped, pivoted boat, which carries a single fuel element, is pulled back and forth inside the main tube by a continuous Teleflex cable. At the drybox end, the cable passes through a drive unit powered by a 1/4-hp gear motor through a mechanical slip clutch. An idler sheave at the reactor end of the conveyor keeps the cable taut and feeds it into a conduit that returns to the drive unit.

The main tube for the discharge conveyor is 11-BWG, 4-in.-o.d., Type 304 stainless steel. Inside it travels a cradle to which the fuel

element boat is pivoted. The boat is a tube, open at one end, which can contain a single element. At the reactor end of the conveyor, the boat pivots under the force of gravity to an upright position. After it has received an element, the boat is pulled into the main conveyor tube, which rotates the boat inside the cradle until the boat is horizontal and its open end is closed against the cradle. At the drybox end of the conveyor, cam surfaces turn the boat upside down to discharge its contents. The Teleflex mechanism that moves the discharge boat closely resembles the charging conveyor drive.

6.2.7 Primary Gas Locks

Two sets of gas locks maintain the integrity of the primary containment as a fuel element passes into or out of the reactor. Each gas lock consists of three valves, one of which is depicted in Fig. 6.2.7.1, coupled directly to one another with Conoseal joints. The outermost valve in each set connects to a fuel conveyor, the innermost connects to the fuel loader or to the fuel discharge pipe, both of which are joined directly to the reactor vessel.

When a fuel element drops into a primary gas lock valve, the element contacts a scissors-action gate that blocks the upper valve entrance and protects the polished valve ball against impacts. Before the element can pass through the valve, a certain sequence of events must occur. First, the pressure differential across the valve is reduced by operating the auxiliary gas valves according to a procedure described in Table 6.1.2.1. Then, the gas lock valve actuator motor starts to rotate the operating cam, which first retracts the seal away from the valve ball. This action prevents abrasion of the polished ball by fuel element dust. As the cam continues to operate, it engages a geneva lock mechanism that rotates the ball into the open position. The turning ball is cleaned by wipers on either side of the seal. When the ball has rotated to the open position, the geneva mechanism disengages and the still-turning

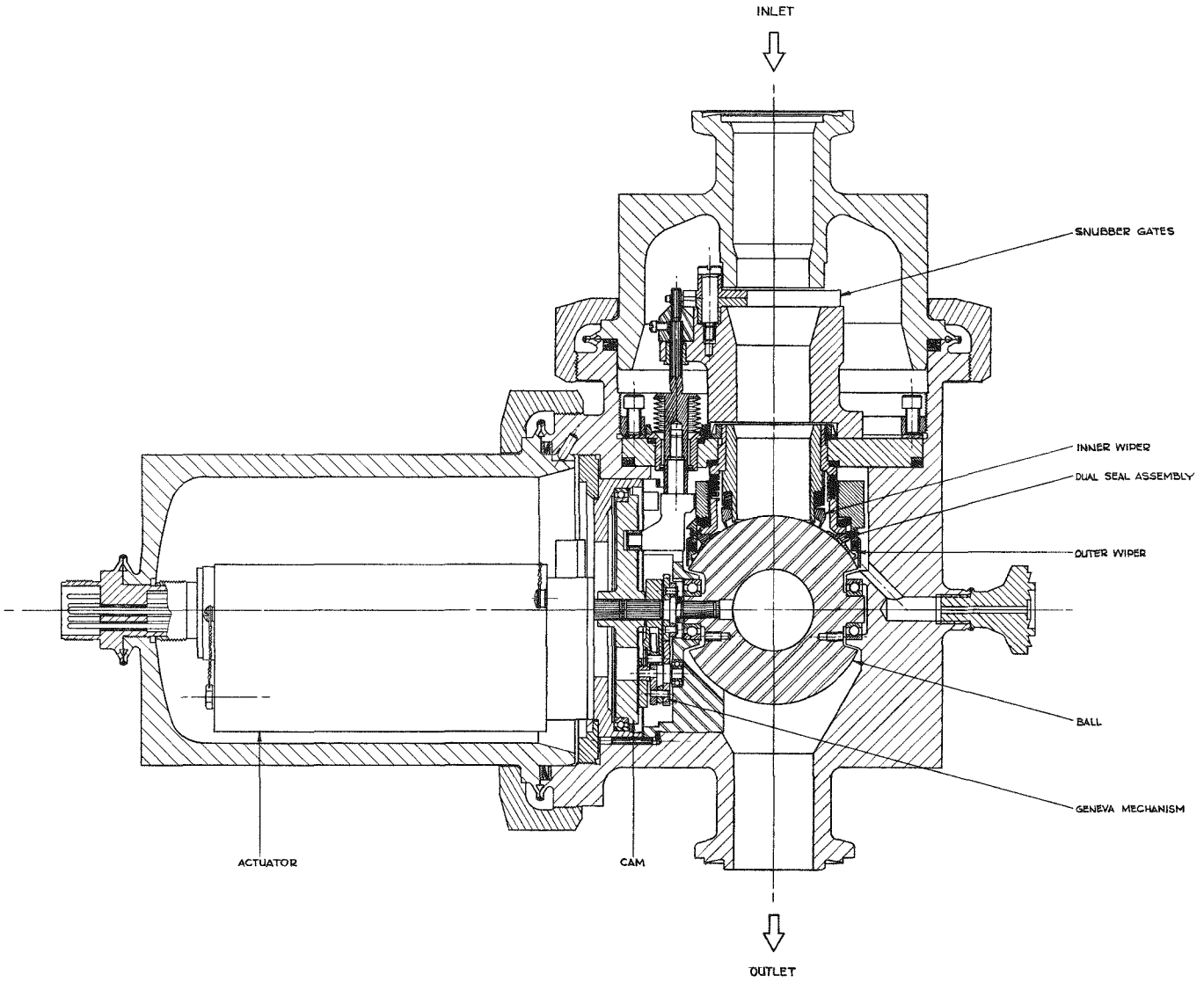

Fig. 6.2.7.1 Cross section of primary gas lock valve

cam opens the gate on which the fuel element is resting. Then, limit switches in the actuator stop the motor.

After the gate opens, the fuel element drops through the opening in the valve ball and falls out of the valve. The actuator motor, under computer control, then reverses direction, and the valve operation sequence is repeated in reverse order.

Valve bodies are made of Type 304 stainless steel with Conoseal flanges on the fuel inlet, fuel outlet, and helium port. The inlet and actuator housings, attached with union-type nuts, are sealed with static metal-to-metal seals and a seal weld. Power and instrumentation leads enter the actuator housings through double ceramic bead seals in a bulkhead-type feedthrough which is seal-welded in place. The valves were proof tested at 2500 psig with no measurable permanent deformation. All sealing surfaces were inspected according to the liquid penetrant method of MIL-STD-271. Complete valves were leak tested using a mass spectrometer. Observed leak rates were less than 1×10^{-8} std cc/sec at 500-psig internal helium pressure.

The ball in each valve is made of vacuum melted, Type 400 C stainless steel that was heat treated and stabilized at -120°F and drawn to a Rockwell hardness of 60 to 61. After heat treatment, each ball was ground and then lapped until spherical within 20 μin., with a surface finish better than 2 μin. rms. The metal seal that bears on the ball is made of Inconel X, with a hard chrome plating for wear resistance on the sealing edges. An integral, machined bellows makes it possible to retract the seal away from the ball before rotating the ball to open the valve. Each seal has inner and outer sealing surfaces that are flexible, conical disks with line contact edges. Both sealing edges are finish lapped, after chrome plating, to the same specifications as the ball. The flexibility of the seal, close tolerances, and fine surface finish ensure intimate contact with the ball; line contact gives the required high unit loading for sealing; and the hard chrome plating provides wear resistance.

To operate the valve, a 3-phase, 115-V, 400-cycle, 6,000 rpm induction motor drives a 556:1 speed reducer connected to a mechanical bar clutch that has positive stops to limit motion. The clutch turns the valve operating cam through an output shaft whose position is monitored by limit switches. Output of this actuator assembly is 270-in.-lb torque at 9 rpm; the torque needed to operate the valve is approximately 150 in.-lb. The electric motor has polyimide insulation and an armature mounted in ball bearings lubricated with NRRG-159 nuclear radiation resistant grease. All four stages of gears in the speed reducer are coated with a dry film lubricant, molybdenum disulfide with a sodium silicate binder, and NRRG-159 grease. All rotating elements are mounted on ball bearings lubricated with NRRG-159 grease.

6.2.8 Primary Gas Lock Pressure Regulation System

When fuel elements move through the primary gas locks, a pressure regulation system operated by the on-line computer sequentially vents and pressurizes the inter-valve spaces to prevent the escape of primary coolant from the reactor. The components of the system appear in Fig. 6.1.1.1. Each of the gas locks is served by the system in a similar manner; the functioning of the system in conjunction with the inlet gas lock is described in Table 6.1.2.1.

In addition to the 10 valves, numbered 8406-8413 and 8418-8419 in Fig. 6.1.1.1, the system includes 10 pressure and differential pressure transducers, numbered 1080-1090, which supply data to the computer. The system shares with the other helium systems the use of the low pressure receiver and the high pressure working tank, one to receive vented helium and the other to supply clean helium pressure.

Unique to the gas lock pressure system are the gas lock vent compressor and receiver. The compressor, an electric motor-driven piston machine, raises the pressure of helium vented from the gas locks at atmospheric pressure to the 25- to 50-psia operating range of the low pressure receiver. To maintain system integrity, the compressor is

enclosed in a 500-psia design pressure vessel that also serves as a receiver to limit on-off cycling of the compressor. A pressure switch on the receiver produces a signal to actuate an automatic control circuit that starts the compressor when receiver pressure reaches 0.5 psig and stops the compressor at 0 psig.

6.3 Control and Instrumentation

A crew of technicians operates the fuel handling system. One operating station is at the cell operating area where the fuel elements are moved into and out of the system. The other station is in the control room, where operators enter fuel information on the computer console, initiate computer controlled sequential operations, and observe the system performance. People at the two stations talk to each other over the facility communications system. The cell area operator observes his part of the operations through the cell windows. In the control room, the operators watch a graphic panel which indicates the status of each system component and the location of fuel elements as they move through the handling system. Switches for operating system components are mounted in the graphic panel.

6.3.1 Computer Functions

In fuel loading operations the on-line computer has two main functions: (1) maintaining the fuel element inventory record and individual fuel element burnup histories, and (2) sequencing the system hardware through the loading and unloading programs. Before an element is loaded, its serial number and loading and the fuel channel coordinates are transmitted to the computer through the console. From the signals of system and reactor instrumentation, the computer keeps track of each element's core position and integrates its estimated burnup. Fuel element data can be displayed on request. When a fuel element is discharged, its irradiation history is logged on a typewriter.

Once an operator starts a loading operation, the computer automatically moves fuel elements through the handling system according to a fuel loading sequence routine. Before any hardware component (valve, load ram, elevator, etc.) is actuated, the position of every other hardware component in the system is compared with an expected status list. Any disagreement results in the termination of the loading sequence and the typing of a termination message. For a hardware component that is involved in computer interlock logic, actuation is contingent on satisfying a set of interlock equations. If actuation would create an interlock violation, the loading sequence is halted.

Provision is made for an operator to halt a sequence at will and to restart a computer-terminated sequence if the condition that resulted in the termination has been corrected. By appropriate setting of mode switches, the operator may cause the computer to halt a sequence automatically at one or more intermediate points and pause before proceeding until the operator signals concurrence.

Manual control is provided sufficient only to render the system safe (all gas locks closed) in the event of computer stall or stop. Each valve may be opened (1) if the operator demands the opening of the valve and the computer agrees that the action is in proper sequence, or (2) if the valve is placed in computer control by the operator and the computer demands its opening as part of the charging sequence. The valve may be manually closed at any time.

6.4 System Design Analysis

6.4.1 Primary Gas Locks

For loading and unloading fuel elements while the reactor is operating, the primary gas lock valves must operate in a dry helium atmosphere at 500 psi, at temperatures between 60° and 300°F, and in a radiation field created by the reactor and intensified by intermittent exposure to fuel elements leaving the reactor.

After a preliminary screening of standard ball valves, it became evident that only a metal-to-metal seal could satisfy the leak tightness and environmental requirements. To explore the feasibility of a metal-to-metal seal, many combinations of materials, surface finish, hardness, and seal loading were tested for helium leak tightness and endurance under simulated operating conditions except for the radiation environment. Data from the tests indicated that a hard metal with a fine surface finish and high unit loading would meet the requirements and would endure the service conditions if the fine surface finish could be protected. To shield the surface finish on the seal and ball, the seal is designed to retract away from the ball before the ball is rotated into the open position. Further protection is afforded by wipers, one on each side of the seal, which clean the ball as it is rotated, and by the gate, which stops the fuel element and keeps it from impacting on the ball surface.

A prototype valve, with all the final design features, was built and subjected to a long series of proof and endurance tests. In the test program, the actual valve environment was simulated, except for the radiation fields. To minimize the possibility of any adverse effects of radiation, care was taken in choosing resistant materials for valve construction. During the initial stages of the test program, the prototype valve withstood a helium-pressure proof test at 2500 psig, and tests of external and internal helium leakage at 500 psig. The leakage tests were run with the valve at 75°F and at 300°F, the operating temperature.

Following these tests, the prototype valve was heated to 300°F in an environmental chamber and was subjected to two series of endurance tests. In the first series the valve was filled with helium at 500 psig and operated through 5000 cycles, each of which consisted of an opening and closing of the valve with a differential pressure of 5 psi across the seat. After each full cycle the direction of the pressure differential was changed. At the end of the test series, the valve passed a leak test, allowing no more than 10^{-5} cc/sec of helium to pass at 500-psi pressure and 300°F.

The second set of endurance tests was designed to check the operation of the wipers and retraction system that protect the valve ball and seal surfaces from abrasion. For each test cycle, an unloaded graphite fuel element and 3 g of grit were placed in the valve inlet port, the valve was opened, the fuel element and grit dropped through, and the valve was closed. The grit was a mixture of 66% graphite particles, 22% carbon particles, and 12% abrasive particles, designed to simulate fuel element fragments. After 1000 cycles at 300°F, the valve was still leak-tight.

Next in the program was a test of the scissors gate design. To simulate the impact of a fuel element falling out of the reactor core, a dummy element was dropped 18 ft, through a 1-1/2-in.-i.d. tube, onto the gate at the valve inlet. Then the valve was opened, the element passed through, and the valve was closed. After 100 of these drop tests, the gate showed no signs of damage, and the valve was leak-tight.

The valve was then subjected to 100 pressure shock cycles at each port, inlet and outlet. For each cycle, helium pressure against the closed valve was increased from 0 to 500 psig within a 0.010-sec period, and then the pressure was relieved over the same time period. No damage was done to the valve.

Finally, the strength of the seal was tested in a series of 4000 operations of the valve under a differential pressure across the seal. First, the valve was operated 500 times under a 25-psi differential across the seal from the inlet to outlet direction. Then the direction of the differential was reversed for another 500 cycles. Next, the differential was increased to 50 psi, and the valve was operated 1000 times with the differential applied alternately in each direction. Finally, a 500-psi differential pressure was applied from the inlet end, the valve was operated 20 times, the direction of the pressure was reversed, and another 20 operating cycles completed the tests.

At the end of the entire test program, the valve was in good working condition and still leak-tight.

6.4.2 Conveyors

The principal aim in the design of the fuel conveyors was to produce systems that are safe and simple. Safety is served by the fact that neither conveyor can handle more than one fuel element at a time and that both systems maintain secondary containment. When only one fuel element is present in a conveyor, there is no possibility of the inadvertent assembly of a critical mass. The element passes to and from each conveyor by falling through a gas lock that is opened only when the gas lock at the other end of the conveyor is closed.

Simplicity adds to the safety of the conveyor system designs. The boats move under a positive force applied through continuous cables. If a conveyor cable or drive fails, the conveyor enclosure remains intact, and no hazard is created. Failure of a conveyor drive does not affect operation of the gas locks. The drives are accessible, in the fuel loading cell, for maintenance and repair.

6.5 Testing

In addition to the tests made on components and subsystems during fabrication and installation, the entire fuel handling system will undergo at least 100 cycles, while under computer control and transporting dummy fuel elements, before loaded elements are handled. During operations, the sensors which control computer functions continually monitor the entire system. Inspection of the gas lock valves is planned after 3000 operating cycles. Concurrently, the secondary gas locks and conveyor drives will be inspected. These inspections will be made while the reactor is shut down and depressurized.

7. GAS CLEANUP SYSTEM

7.1 General Description

To preserve the chemical inertness of the coolant and to reduce the level of long-lived, volatile, fission product contamination in the primary loop, a portion of the helium stream is continuously purified in the gas cleanup system, a sidestream of the primary loop. Fig. 7.1.1 is a simplified flowsheet for the gas cleanup and helium storage systems. In succeeding sections of this chapter, the design characteristics of system components are described and their functions under nominal design conditions are detailed. For the generation of performance data, the system and individual components can be operated at conditions that vary from the nominal, but are within the limits fixed by the design.

The mass flow rate of helium through the gas cleanup system is 102 lb/h, removed from the primary loop at a point near the downstream side of the primary loop blower and returned to the primary loop just upstream from the blower. An additional maximum flow of 10 lb/h of helium may enter the cleanup system from the low pressure storage system concurrently with the flow from the primary loop. This additional gas is pumped into the cleanup system at a point upstream from the filter.

In the cleanup system, metallic filters remove particulate matter from the stream, a copper oxide bed oxidizes chemical reducing agents, molecular sieve beds adsorb carbon dioxide and water, and cooled beds of activated carbon delay or trap volatile fission products. Tritium, produced in the primary coolant loop by the $^{3}He\ (n,p)\ ^{3}H$ reaction, is removed with the reducing agents by oxidation in the oxide bed and

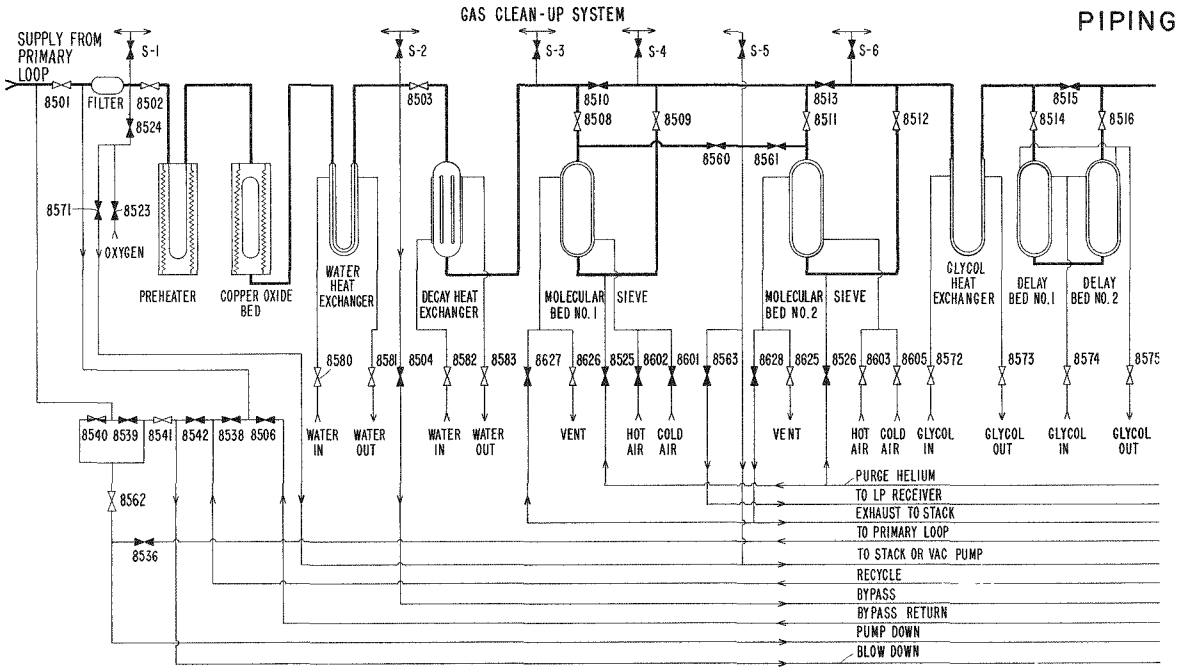

Fig. 7.1.1 Gas cleanup system flow diagram

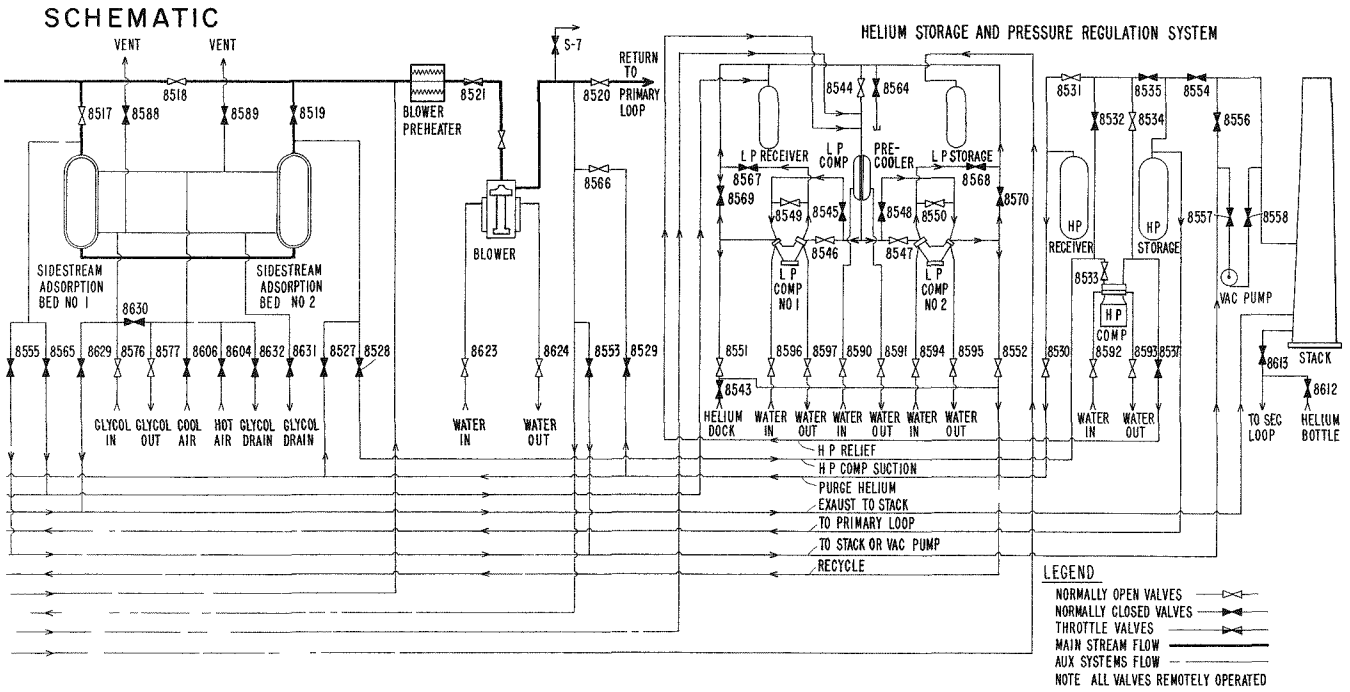
SCHEMATIC
HELIUM STORAGE AND PRESSURE REGULATION SYSTEM
VENT
VENT
8518
8517
8588
8589
8519
SIDESTREAM ADSORPTION BED NO 1
SIDESTREAM ADSORPTION BED NO 2
8630
8555
8565
8629
8576
8577
8606
8604
8632
8631
8527
8528
GLYCOL IN
GLYCOL OUT
COOL AIR
HOT AIR
GLYCOL DRAIN
GLYCOL DRAIN
BLOWER PREHEATER
8521
BLOWER
8566
8623
8624
WATER IN
WATER OUT
S-7
8520
RETURN TO PRIMARY LOOP
8553
8529
8544
8564
L P RECEIVER
L P COMP
PRE-COOLER
L P STORAGE
8567
8568
8569
8570
8549
8545
8548
8550
8546
8547
L P COMP NO 1
L P COMP NO 2
8551
8596
8597
8590
8591
8594
8595
8552
8543
HELIUM DOCK
WATER IN
WATER OUT
WATER IN
WATER OUT
WATER IN
WATER OUT
8531
8535
8554
8532
8534
8556
HP RECEIVER
HP STORAGE
8557
8558
8533
HP COMP
VAC PUMP
8530
8592
8593
8555
8613
STACK
8612
WATER IN
WATER OUT
TO SEC LOOP
HELIUM BOTTLE
H P RELIEF
H P COMP SUCTION
PURGE HELIUM
EXAUST TO STACK
TO PRIMARY LOOP
TO STACK OR VAC PUMP
RECYCLE
LEGEND
NORMALLY OPEN VALVES
NORMALLY CLOSED VALVES
THROTTLE VALVES
MAIN STREAM FLOW
AUX SYSTEMS FLOW
NOTE ALL VALVES REMOTELY OPERATED

adsorption in the sieve beds. Eventually, the tritium is vented to the stack, during sieve bed regeneration, without creating a radiation hazard.

The cleanup system is designed to accommodate the release, at a controlled rate, of all of the chemical impurities expected to be outgassed from the core and the release of fission products from a full loading of free-releasing fuel elements.

7.2 Design Details

7.2.1 Filter

Helium from the primary loop and low pressure and high pressure storage systems enters the gas cleanup system through a replaceable filter capable of removing particles as small as 1/2-μ diam. The filter has a single, 10-1/4-in.-long, 5-3/4-in.-diam., bellows-shaped element made of sintered Type 316 stainless steel. The total filter area is 10 ft^2. A vessel, made from a 20-in. length of 6-in., Schedule 40, Type 304 stainless steel pipe and two pipe caps, encloses the element. Helium enters the bottom cap through a pipe, passes through the outside of the filter element, collects in a central tube, and leaves through the upper cap in a pipe to which the element is welded.

Initially, pressure drop through the filter is low, but, as particles accumulate on the surface of the elements, pressure drop may rise to an intolerable level. If so, the system is depressurized and the filter is isolated between closed valves, the entire filter assembly is removed, and a spare unit is installed. The loaded filter is disposed of in accordance with established procedures for radioactively contaminated equipment. Design conditions for the filter are 550 psia at 600°F.

7.2.2 Preheater

After passing through the filter, helium enters the preheater at a temperature that ranges between the ambient level at startup and 600°F at full reactor power. In the preheater, the helium stream reaches 1000°F,

the operating temperature of the copper oxide bed. An electrical resistance heater that surrounds the preheater produces the heat. Power consumption at startup is 54 kW.

The preheater is fabricated from 40 ft of 1-in., Schedule XX, Type 316 stainless steel pipe formed into a flat, four-pass coil. A radiant heater with folded and formed, nichrome strip, electrical heating elements encloses the coil. The heater is insulated with 1 in. of fire-brick and 2-1/2 in. of calcium silicate blocks enclosed in a steel case. Design conditions for the coil are 550 psia at 1400°F.

The preheater is controlled by an instrument that senses the outlet helium temperature and then regulates the power to the electric heater. To protect the preheater, the controller is interlocked with the system helium flow meter, thermocouples on the pipe walls, and thermocouples inside the heater jacket. If helium flow is interrupted or hot spots develop, electrical power to the heater is interrupted. Two Burling thermoswitches inside the jacket back up the controller, to interrupt heater power if the controller fails.

7.2.3 Copper Oxide Bed

From the preheater, the helium flows at 1000°F into the copper oxide bed. In the bed, carbon compounds in the helium are oxidized to carbon dioxide, and hydrogen compounds to water. When the oxidation efficiency of the bed decreases, it is taken off-stream and regenerated with oxygen.

The bed is a 13-ft length of 8-in., Schedule 120, Type 316 stainless steel pipe with hemispherical heads at each end. It is packed with 818 lb of sintered CuO pellets, each 1/16-in. diam x 1/16-in. long, that react with oxidizable impurities in the helium stream and are reduced to copper.

For 12 ft of its length, the bed is enclosed in a cylindrical heating jacket similar in construction to the preheater jacket. Four thermocouples, inside wells that extend into the center of the bed, measure internal temperatures. One of the thermocouples is connected to a controller that regulates the heater power. Temperatures on the bed

surface are measured by seven thermocouples, which are connected to a recorder with a high temperature alarm. Ultimate protection against overtemperatures is the purpose of two Burling switches in the jacket. The bed is designed for operation at 1300°F and 550 psia.

Performance of the bed is continuously monitored by an infrared analyzer that determines the concentrations of carbon monoxide in the inlet and outlet streams. If carbon monoxide is detected in the outlet stream, the analyzer sounds an alarm to warn the operator that the bed is becoming depleted. Since the oxidation capacity of the bed is much greater than the amount of oxidizable impurities expected to be discharged into the helium stream, it is doubtful that the bed will become depleted during the life of UHTREX.

Should it become necessary, regeneration of the copper oxide bed can be delayed for a reasonable period after the initial warning, until it is convenient to shut down the gas cleanup system. At this time, the preheater and bed are maintained at 1000°F while system helium flow is bypassed directly to the blower from the outlet of the water-cooled heat exchanger. From the blower, the helium, instead of returning to the primary loop, flows back to the filter. Downstream from the filter, oxygen is fed to the helium stream until the concentration is 0.25% oxygen. The oxygen is carried by the helium stream into the copper oxide bed where the copper metal reacts to form CuO. Progress of the reoxidation can be traced by observing increases in the thermocouple readings as the exothermic reaction proceeds along the bed. During reoxidation, the part of the gas cleanup loop that contains oxygen is operated at a pressure below that of the remainder of the system to prevent leakage of oxygen-contaminated helium into the carbon beds and primary loop. When the reoxidation is complete, the oxygen-helium mixture is vented through the stack, the oxidation loop is purged with clean helium to remove traces of oxygen, and the loop is returned to the cleanup system.

7.2.4 Water-Cooled Heat Exchanger

After leaving the copper oxide bed, the helium stream enters a water-cooled heat exchanger where the helium temperature is reduced from 1000° to 100°F, the operating temperature of the molecular sieve beds. The heat exchanger is a counterflow, U-tube, double pipe exchanger with 35 ft of helium tube, constructed of 1-in., Schedule 160, Type 316 stainless steel pipe. The exchanger water jacket is 2-in., Schedule 40, carbon steel (A-53B) pipe, except in the 180° bend region where 3-in., Schedule 40 carbon steel pipe is used.

Operating duty of the heat exchanger is 153,000 Btu/h with a water flow of 30 gal/min. The cooler is designed for 550 psia at 1200°F on the helium side and 165 psia at 120°F on the water side. In the event that cooling water flow to the cooler is lost, a flow switch in the water line stops helium flow through the exchanger by de-energizing the cleanup system blower. A thermocouple senses the outlet helium temperature, which is displayed on an indicator with a high temperature alarm.

7.2.5 Decay Heat Exchanger

From the water-cooled exchanger, the process helium flows into the decay heat exchanger, a shell-and-tube exchanger with 12 tubes, each a 20-ft length of 4-in., Schedule 80 pipe. The tubes are packed with 525 lb of activated carbon, and cooling water circulates through the shell. In the tubes, the activated carbon, by gas chromatography, delays the passage of krypton and xenon and, by absorption, quantitatively removes any iodine or bromine that has not yet deposited elsewhere. The fixed halogens and the delayed noble gases undergo radioactive decay and liberate approximately 12 kW of heat when the reactor is loaded with free-releasing fuel. To aid in conducting the heat from the carbon to the walls of the tubes, 67 perforated aluminum baffles are spaced normal to the flow, on 2-1/4-in. centers, in the first two-thirds of the length of each tube.

Delay times in the bed are 1.2 h for krypton and 20 h for xenon.

Under maximum design conditions, the rate of decay heat production through the bed diminishes from about 13 kW to 1.4 kW, the latter heat due primarily to long-lived krypton. By delaying the fission products while they give up a major part of their decay heat, the decay heat exchanger protects both the molecular sieve and the delay beds against localized overheating. Six chromel-alumel thermocouples are spaced within wells along one of the 12 tubes to measure the temperature profile.

The decay heat exchanger shell, designed for 165 psia at 150°F, is fabricated from a cold-rolled, steel cylinder, 21-ft, 8-in. long x 27-3/4-in. in diam, closed with elliptical heads. The shell is not insulated and is designed for operation under pressures between full vacuum and 165 psia. The exchanger's operating duty is 40,000 Btu/h with 80°F inlet water flow of 100 gpm. Design pressure and temperature of the helium tubes is full vacuum to 550 psia at 50 to 150°F.

7.2.6 Molecular Sieve Beds

From the delay bed, the helium stream flows to one of two beds, each filled with 150 lb of Linde 4A molecular sieve. The sieve quantitatively removes water and carbon dioxide from the helium. (Krypton is not adsorbed in significant quantities; xenon cannot enter the sieve pores.) Concentrations in the outlet stream are reduced to low ppm levels of carbon dioxide and water. After 24 h onstream, at maximum outgassing rates in the reactor, the sieve bed becomes saturated and starts to pass carbon dioxide. During the latter part of the 24-h period, the two sieve beds are operated in series to prevent the liberation of carbon dioxide if premature breakthrough should occur in the upstream bed. An infrared analyzer detects the carbon dioxide, at <1-ppm levels, in the outlet stream and sounds a warning. The operator then valves off the saturated bed for regeneration.

To regenerate the sieve, the saturated bed is isolated from the system, evacuated, and heated to 600°F. Before heating starts, however, the bed is purged with clean helium to remove entrained krypton and xenon.

At a flow rate of 10 lb/h of helium, the purge period is 11 min. The purge gas passes to the low pressure receiver.

After the bed is purged, it is evacuated with the vacuum pump, and a flow of 800°F air is applied to the jacket. The bed is heated to 600°F over a 4-h period while the internal pressure is held $\leq$ 10 mm Hg. Then the bed is cooled, with air in the jacket, to 100°F in 10 h. At 100°F the bed is repressurized with helium to 500 psia and returned to service. Chilled air, at 50°F, can be circulated through the jacket to remove decay heat if the need arises.

The molecular sieve beds are designed for a pressure range from full vacuum to 550 psia in the vessel and vacuum to 165 psia in the jacket, over a temperature range of 50° to 800°F. Both vessels are fabricated from 9-ft, 2-in. lengths of 10-in., Schedule 40, Type 304 stainless steel pipe and pipe caps. The jackets, which enclose 6 ft of each vessel's length, are made from 12-in.-o.d. x 3/8-in.-thick, rolled, stainless steel cylinders.

Both vessels are instrumented with two internal thermocouples, in wells, and six surface thermocouples. The beds hang inside steel boxes that are filled with granular insulation.

7.2.7 Glycol-Cooled Heat Exchanger

After leaving the molecular sieve beds, the process helium flows through a counterflow, double-pipe, glycol-cooled heat exchanger. There the stream temperature is reduced from 100° to -20°F, the operating temperature of the delay beds. The cooling medium is a 40% water and 60% ethylene glycol mixture which is circulated through the heat exchanger shell at a temperature of -30°F.

The helium side of the exchanger is 80 ft of 12-BWG, Type 304 stainless steel tubing inside a shell made of 2-1/2-in., Schedule 40, Type 304 stainless steel pipe. The exchanger is designed for vacuum to 550 psia on the helium side and vacuum to 165 psia on the shell side, over a range of -30° to 120°F. The exchanger is insulated with 3 in. of "Foamglas" to

limit heat gain from the room to 150 Btu/h. The operating duty is 16,700 Btu/h.

To prevent overheating in the delay beds in case the heat exchanger does not function properly, there are two safety devices: a flow switch in the glycol inlet line sounds an alarm if the flow decreases below 50 gal/min, and a control circuit connected to a thermocouple in the outlet helium stream shuts down the cleanup system blower if the helium temperature rises above -20°F.

7.2.8 Delay Beds

At -20°F, the process helium enters two delay beds, connected in series, each 24-in. o.d. with a 16-ft active length. Each bed is packed with 1800 lb of activated carbon, maintained at -20°F by refrigerated ethylene glycol solution circulated in external jackets. In these two beds, krypton is delayed for 44 h (10 half-lives of ^{85m}Kr) and xenon for 1790 h (14 half-lives of ^{133}Xe). The beds, which remain onstream continuously at a constant temperature, are not regenerated.

The 17.5-ft-long vessels are welded cylinders, made from 5/8-in.-thick, Type 304 stainless steel plate and closed with 2:1 elliptical heads. Full-length jackets are rolled from 1/4-in., Type 304 stainless steel plate. Design conditions are full vacuum to 550 psia in the vessels and vacuum to 165 psia in the jackets, over a -30° to 120°F range.

The delay beds are covered with 4 in. of "Foamglas" insulation to limit heat gain from the room.

Under the most severe conditions, 0.6 kW of decay heat could be liberated in each bed. To obtain thermal gradient profiles of the beds, both longitudinally and radially, sets of four thermocouple wells are mounted at the top of each bed, and at points 1/3 and 2/3 down the bed length. The four thermocouples in each set are spaced at radial distances, from the wall, of 2, 5, 8, and 12 in. The thermocouple wells are accessible through hand holes in the vessel cooling jacket.

7.2.9 Sidestream Adsorption Beds

When the helium stream leaves the delay beds, its specific activity is so low that it has little effect on the overall activity of the primary loop to which the stream returns. However, the helium that is diverted from the delay beds to the high pressure storage system (during system pressure reductions or when make-up helium is added) should be clean. To remove the last traces of krypton and xenon, this sidestream helium passes through two adsorption beds, each packed with 155 lb of activated carbon. The beds, operated in series and cooled to -20°F by glycol solution circulated in external jackets, have the capacity to delay krypton for 44 h at a helium flow rate of 10 lb/h, the capacity of the high pressure compressor. As an alternative, the beds can purify the entire flow of the cleanup system for a period of 4 h before krypton breakthrough.

In normal operations, the adsorption beds receive helium from the delay beds periodically at a maximum flow rate of 10 lb/h and discharge to the high pressure system. When a radioactivity detector mounted on a line between the beds indicates that ^{85}Kr has broken through the first bed, both beds are regenerated at the first opportunity, i.e., during a period when no system pressure changes are planned or while the reactor is down for any reason. The saturated beds are regenerated by heating them to 500°F with hot air in the jackets and eluting the adsorbed gases with a clean helium purge. The purge helium can be discharged to the stack because it contains only low activity, long-lived isotopes that have already been delayed in the decay heat exchanger and the delay beds. After regeneration, the beds are cooled to -20°F and returned to service.

Each vessel was fabricated from a 12-ft, 9-in. length of 8-in., Schedule 40, Type 304 stainless steel pipe closed at each end with a welded pipe cap. The 12.5-ft x 9-5/8-in.-o.d. jackets were rolled from 1/4-in., Type 304 stainless steel plate. Design conditions for the vessels are full vacuum to 550 psia and for the jackets full vacuum to 165 psia, both over a range of -30° to 800°F. A total glycol flow of 20 gal/min moves through the jackets in parallel. For regeneration, the glycol in

the jackets is drained before hot air is introduced. On the cool-down cycle, room temperature air reduces the bed temperature to 100°F before the glycol is returned to the jackets. Both beds hang inside a steel box filled with granular insulation.

Two thermocouples inside wells measure internal bed temperatures, and three thermocouples mounted on the bed walls measure surface temperatures.

7.2.10 Blower Preheater

As the process helium stream leaves the delay beds, its temperature is -20°F. Before the stream enters the cleanup system blower, it is heated to 100°F in a length of pipe traced with electric strip heaters. Power to the heaters is controlled by a circuit that responds to a thermocouple in the outlet helium stream. An interlock prevents power flow to the heaters unless the blower is running. The blower preheater is designed to operate at 550 psia with a maximum temperature of 1000°F.

7.2.11 Cleanup System Blower

As the helium stream flows through the various cleanup system components, it experiences a total pressure drop of about 11 psi which is restored in a two-stage, centrifugal blower, the last item in the normal flow path through the system. From the blower, the purified helium reenters the primary loop at a point upstream from the primary loop blower.

The cleanup system blower uses hydrodynamic, gas-lubricated, journal and thrust bearings similar to those in the primary loop blower. The blower is capable of developing 16 psi at the maximum flow rate of 120 lb/h. The integral, 3-hp, squirrel cage, blower motor is driven with variable frequency electric power produced by a motor-generator set.

Two alternate methods are available for controlling the flow of helium through the blower: throttling the inlet stream to the blower, operated at constant speed; or regulating the speed of the blower by varying the frequency of the power supply. In either case, flow through the cleanup

system is measured by a Gentile flow tube whose output is used in an automatic controller that regulates the throttle valve or blower speed. An interlock in the flow control circuit interrupts power to the copper oxide bed preheater when the blower is shut down or if a flow stoppage should occur.

Performance of the blower is monitored by thermocouples that measure temperatures of the three bearings and motor windings, a magnetic detector for speed measurement, and a differential pressure transducer connected between the blower inlet and outlet lines. The thermocouples are wired to a recorder that alarms at 200°F, if the bearings make contact or the blower cooling system fails.

A water-cooled jacket, external to the pressure case, removes motor heat, which is carried to the cool wall by helium circulated inside the case by an auxiliary impeller on the blower shaft. The pressure case is closed by a cover bolted to a weld-seal flange. Through the cover pass the power and instrument leads, sealed on both sides of a buffer zone. The blower case was designed for operation at 550 psia and 100°F.

7.2.12 Auxiliary Systems

Three utility systems serve the cleanup system exclusively. They are described below.

Glycol Refrigeration System - Three of the cleanup system components, a heat exchanger, the delay beds, and the sidestream adsorption beds, are cooled by a stream of 60% ethylene glycol in water. The glycol is refrigerated in, and circulated from, a cooler unit located in the mechanical equipment room outside the secondary containment. The cooler unit, mounted in a single frame, contains two Freon 22 refrigeration units; two Freon-glycol heat exchangers; a 140-gal glycol supply tank; two 7-1/2-hp internal recirculation glycol pumps; and a 25-hp centrifugal pump that circulates the glycol to the vessels and heat exchanger. Total refrigeration capacity of the unit is 7.5 tons or 9.0×10^4 Btu/h. Glycol circulation rate is 150 gal/min at 80 psig.

The glycol piping system consists of a 3-in. supply and return header loop, and a 1-1/2-in. supply and return line to each component. All piping is Schedule 10, Type 304 stainless steel. Air-operated, block valves are installed in the component supply and return lines.

Process Air System - Air flows through external jackets on the molecular sieve and sidestream adsorption beds to heat and then cool them during their regeneration cycles.

For heating, a positive displacement blower in the mechanical equipment room takes in 150 ft^3/min of air, compresses it to 20 psig, and forces it through 2-in., Schedule 10, Type 304 stainless steel pipes to a heater in Room 307, within the secondary containment. Inside the heater, the air passes through a four-pass, double U-tube coil where the air is heated to 800°F by an external electric heater jacket constructed like that on the copper oxide preheater. The hot air temperature is regulated by an electric power controller that has a thermocouple sensor in the outlet air stream. The heated air, its movement controlled by air-operated valves, moves through the bed jacket and vents to the stack upstream from the particulate and carbon filters in the operating area ventilation system.

Air for cooling the beds moves from the blower through a water-cooled heat exchanger, enters the secondary containment, bypasses the air heater, passes through the bed jackets, and vents to the stack. Auxiliary cooling for the molecular sieve beds is produced by a centrifugal blower and glycol-cooled chiller mounted in Room 307. The blower takes in room air and forces it at 60 ft^3/min through the chiller where its temperature drops to 50°F. A throttling valve, actuated by a sealed-fluid temperature regulator, controls glycol flow to maintain the outlet air temperature. The chilled air enters the bed jacket and is discharged back to the room.

Helium leakage from a bed into the process air system could occur only from a molecular sieve bed after it had been repressurized and was being cooled with chilled air. The escaping helium would be exhausted inside the containment structure with the air. Remotely operated valves can be closed to isolate the process air piping that penetrates the secondary containment.

For pressure tests of the secondary containment, the process air blower supplies cooled air directly to Room 307.

Vacuum System - A standard, oil-sealed vacuum pump evacuates the molecular sieve beds during regeneration. The pump, driven by a 5-hp electric motor, has a rated capacity for 46 ft^3/min of free air. Located in Room 307, the pump is piped into a bypass loop in the vent line to the stack. An interlock on a pressure sensor in the vent line prevents opening of the vacuum pump valves until the pressure in the vent line is reduced to atmospheric. Since the molecular sieve beds are protected by the decay heat exchanger against solid fission product deposition, and are purged before evacuation to remove active gases, the vacuum pump will discharge only water, carbon dioxide, and clean helium to the stack. However, a radioactivity detector continuously monitors the gas that flows through the vent line to the vacuum pump.

7.3 Maintenance of Components

In anticipation of maintenance and repair problems, process units where radioactive isotopes may be concentrated are isolated behind substantial shielding, whereas process piping and valves are accessible. Valve actuators, which are expected to require the most servicing, are placed in positions that are as accessible as possible. A limited number of specially designed mechanical joints are included in the piping to facilitate the removal of pipe manifolds and process vessels.

Contact maintenance on parts of the system may be possible after waiting a reasonable time and flushing the system with clean helium. In order to provide a higher degree of ensurance that maintenance operations can be performed, a remote maintenance machine (MINOTAUR) was installed for work that must be done in radiation fields. The machine, shown in Fig. 7.3.1, is suspended from an overhead bridge crane on a telescoping vertical column. It includes two electromechanical manipulators, a small hoist on an extensible boom, closed-circuit television cameras, lights,

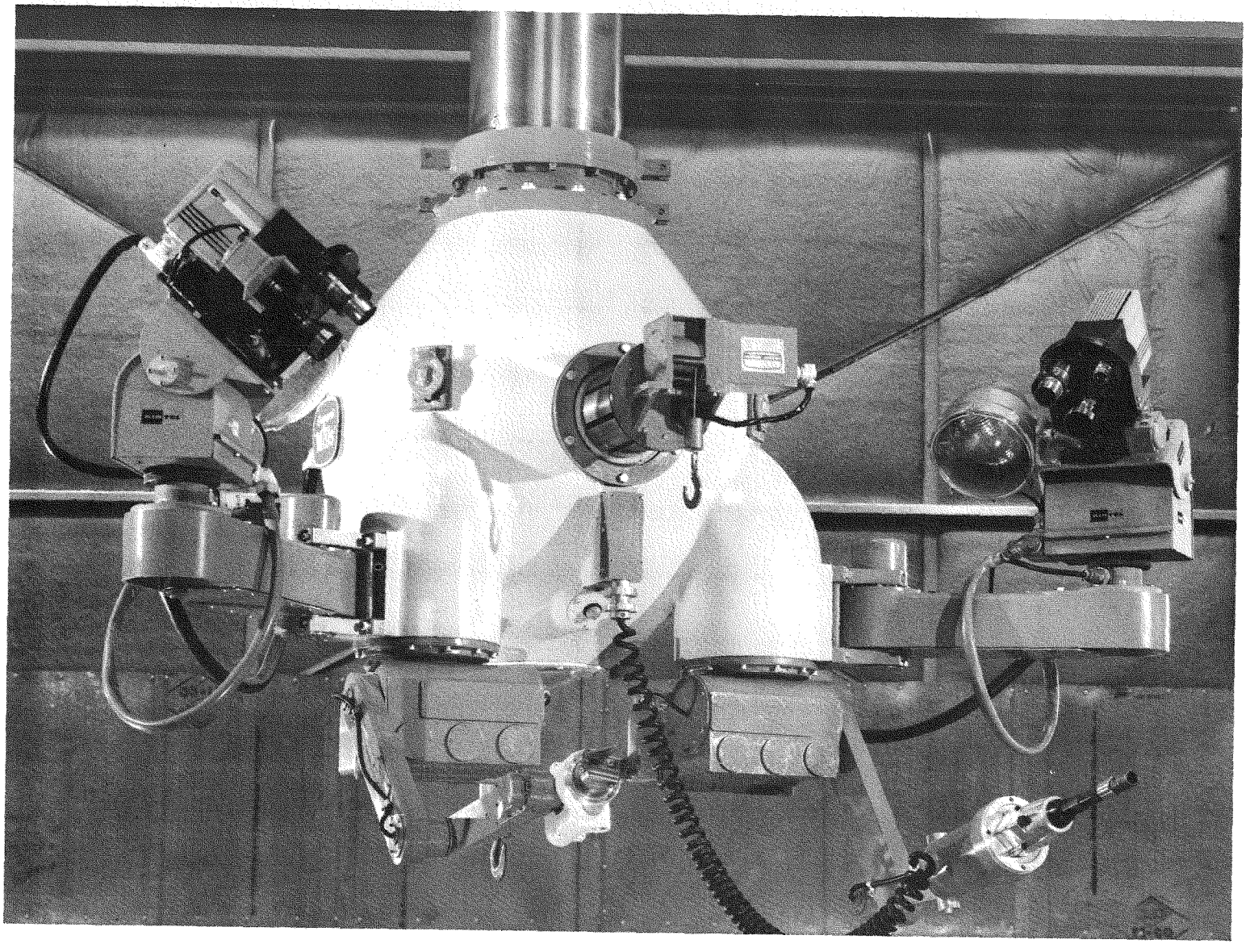

Fig. 7.3.1 MINOTAUR

and a microphone. The machine can be operated from either the reactor room or the remote maintenance corridor, which is shielded from, but has viewing windows into, the gas cleanup area.

7.4 Instrumentation and Control

Figures 7.4.1 - 7.4.3 are schematic diagrams of the gas cleanup system instrumentation. Related control functions are described in the preceding sections that treat individual components and in Sec. 11.1, which deals with operation of the cleanup system from the control room.

Temperature, pressure, and flow instrumentation in the cleanup system use the standard components described in Sec. 11.1. Many of the temperature and pressure instruments have no control functions; they are installed for the collection of experimental data. The instrumentation systems that are used in cleanup system process control are described below.

7.4.1 Analytical Instruments

Sample taps are installed at seven points in the cleanup system. The taps, closed with air-operated, bellows-sealed valves, are connected to analytical instruments with 1/4- and 1/8-in. stainless steel tubing.

Two infrared analyzers are used for process control. One analyzer monitors the CO concentration in the inlet stream to the copper oxide bed, over a 0- to 500-ppm range, and the outlet CO concentration over a 0- to 30-ppm range. The second infrared analyzer monitors the inlet stream to the molecular sieve beds for CO_2 over a 0- to 500-ppm range, and the outlet stream over a 0- to 30-ppm range. Sample streams from both analyzers discharge to the low pressure receiver.

A dual-column gas chromatograph, used for diagnostic and for experimental purposes, receives samples from any of the seven taps and analyzes them for 0- to 100-ppm concentrations of CO_2, O_2, N_2, CH_4, CO, and H_2. It has precut columns and automatic backflush to prevent the

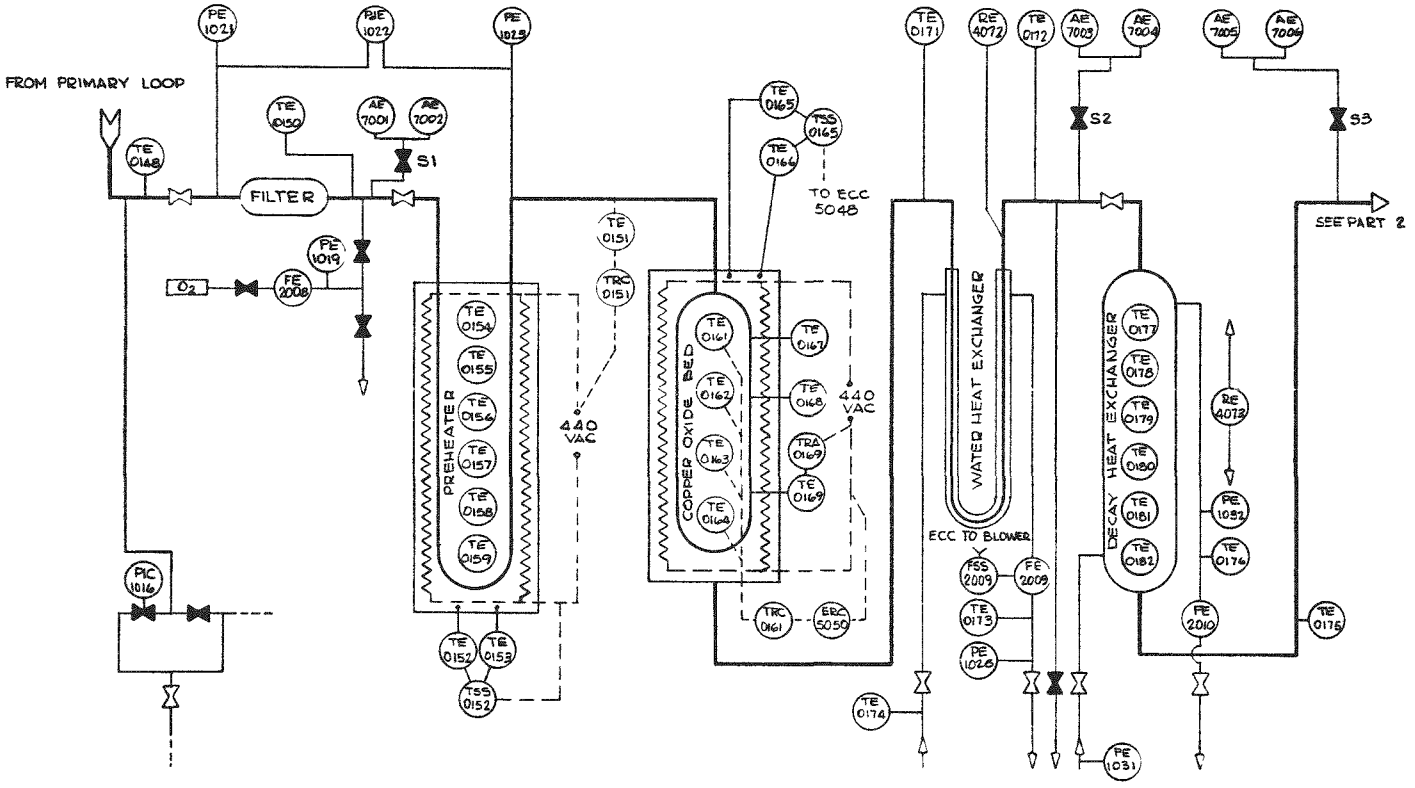

Fig. 7.4.1. Gas cleanup system instrumentation

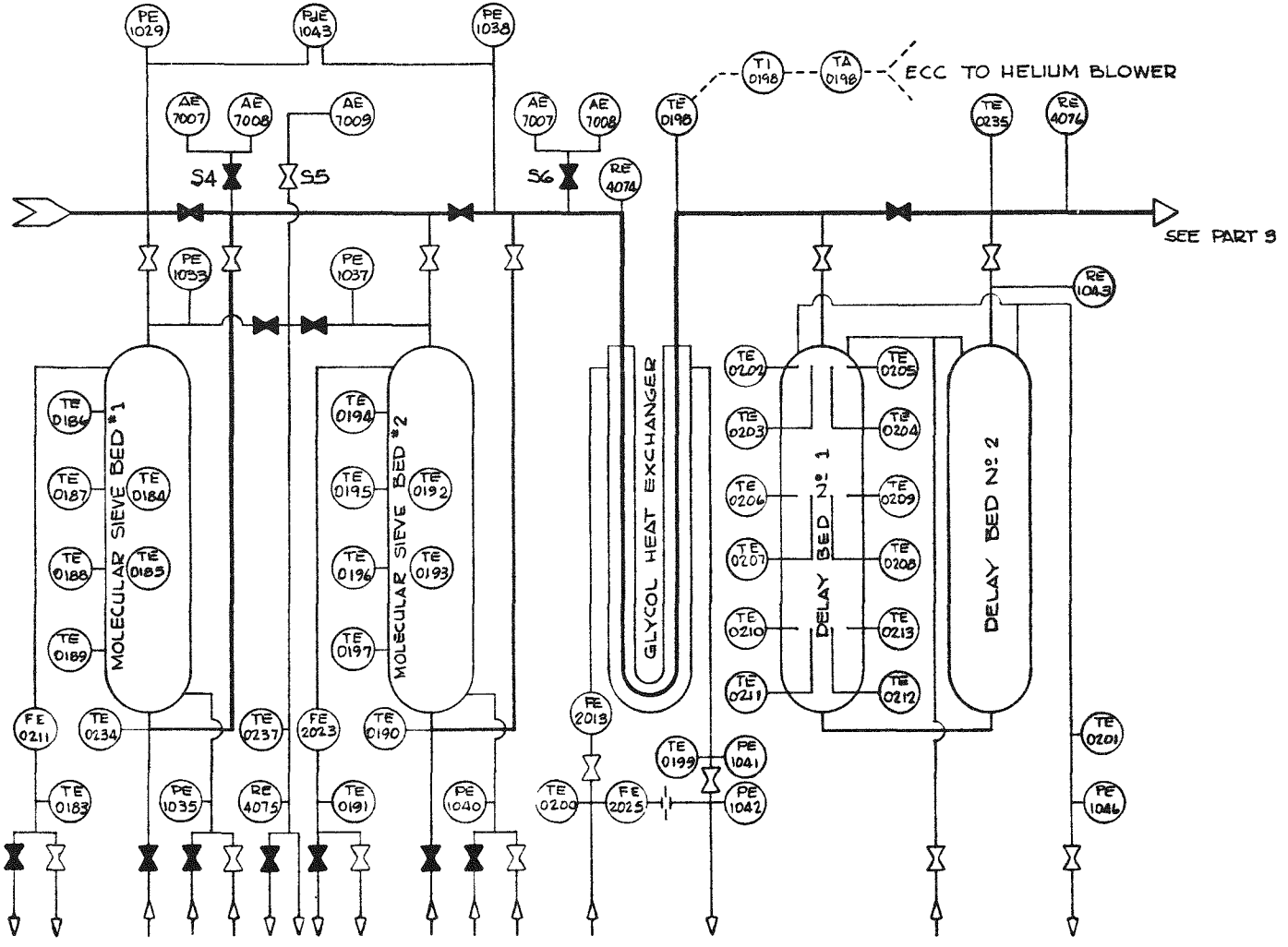

Fig. 7.4.2. Gas cleanup system instrumentation (continued)

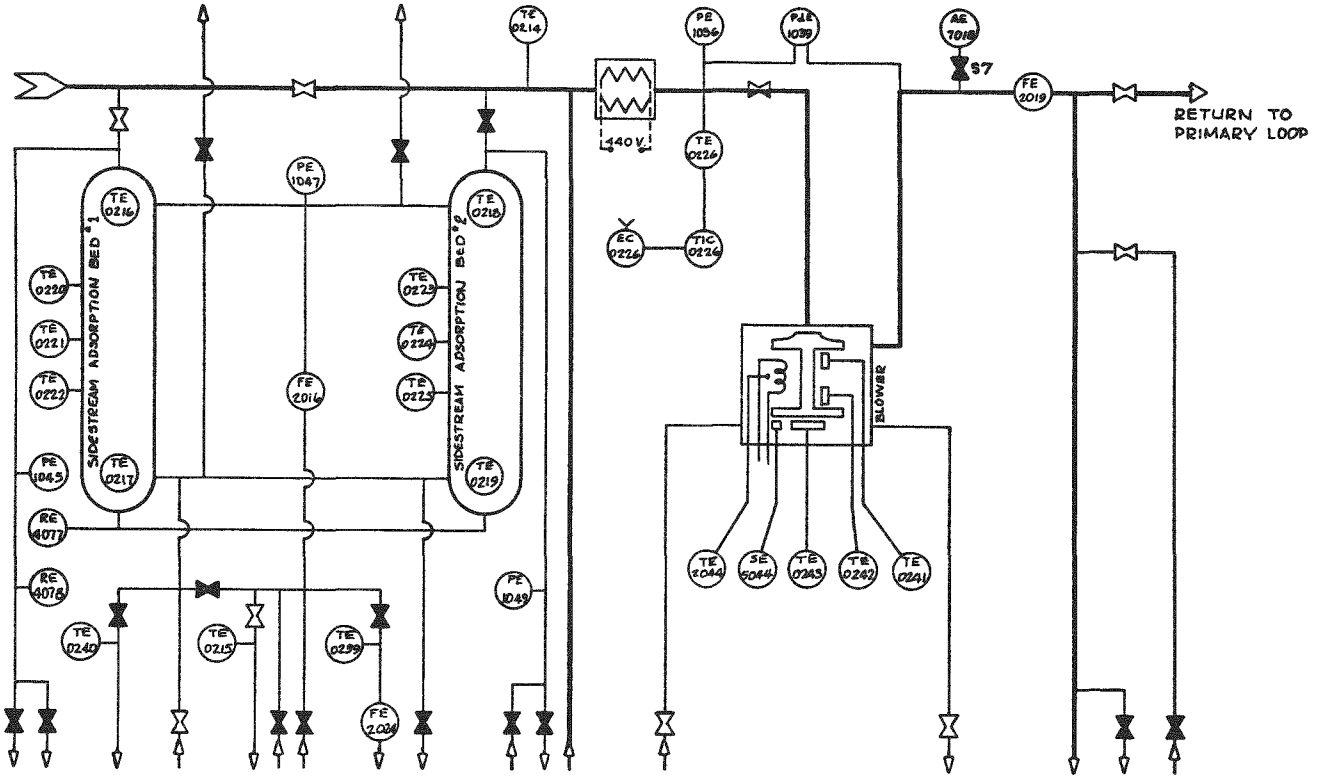

Fig. 7.4.3. Gas cleanup system instrumentation (continued)

entry of noble gases, acid gases, or halogens to the separation columns. Sample streams, other than from the detector, discharge to the low pressure receiver. The clean gas from the detector discharges to the stack.

Water concentrations in the inlet helium stream to the copper oxide bed are determined in the 0- to 1000-ppm range by an electrolytic hygrometer, which discharges to the low pressure receiver.

All of the control units and recorders for the analytical instruments are located in the control room. Only the infrared analyzers have control functions, described in Secs. 7.2.3 and 7.2.6. Minor adjustments to the analyzer units can be made with a master-slave manipulator mounted above the eastern viewing window in the remote maintenance corridor. All of the analyzers are installed in the gas cleanup piping room near the window.

7.4.2 Radioactivity Instruments

Breakthrough of radioactivity from the first sidestream adsorption bed is detected by a flow-through ion chamber mounted in the pipe between the two beds. The detector, which has the same electrical characteristics as a conventional gamma ion chamber, is contained in a case designed for internal helium flow at 550 psia. Another flow-through ion chamber is installed in the vent line through which process helium can flow to the vacuum pump or the stack.

Control units for both instruments are located on the cleanup system panels in the control room.

7.5 System Design Analysis

In the design of the gas cleanup system, the emphasis is on safety through simplicity in the construction of components and in their operation. As an extension of the primary loop, the cleanup system was built to satisfy the same mechanical code requirements and leak tightness standards.

All vessels in the cleanup system are simple cylinders with welded

seams, and all were designed and fabricated in accordance with the ASME Unfired Pressure Vessel Code. Facilities for heating or cooling the vessels are external to the pressure containing shell. Heat is applied from simple electrical heaters regulated by standard well-proved controllers, or by circulating low pressure, electrically-heated air through external jackets. Heat is removed in low pressure fluid streams that circulate through jackets. There are no penetrations through vessel walls. All thermocouples are contained in wells that are welded in place.

In all three heat exchangers, the helium is contained by welded joints. Both fluid-cooled exchangers have a simple, double-pipe design, with a single, continuous helium tube inside a pipe jacket. The shell-and-tube, decay heat exchanger contains the helium stream inside a floating tube sheet-welded to the top head. A bolted shell flange contains only the cooling water.

The pressure case for the blower has a bolted flange that is seal-welded for leak tightness. Penetrations into the case for power and instrumentation leads pass through two seals with a buffer zone between them. The blower cooling water flows inside a jacket external to the pressure case.

Process helium piping systems are joined by welds or Conoseals. In-line thermocouples are inside welded wells. Pressure transducers, contained in leak-tight cans, are welded to pipe taps. Radioactivity monitors are either external to the pipes or contained in pressure cases welded into the pipes. Flowmeters and orifices are machined from solid stock and welded into place.

Remotely operated, stainless steel globe valves control the flow in all process helium lines. Valve bodies are single pieces, machined from forgings; stems are sealed with bellows welded to the body and to the stems. Bonnets with secondary packing glands around the stems are designed to contain helium that could leak from failed bellows. The bonnet is monitored by pressure switches. All valve operators are pneumatic and readily removable without disturbing the valve body. The valves are welded into

manifolds that are connected together with Conoseal joints to form the piping system. If part of a valve, other than the actuator, should fail, the entire manifold of which the valve is a part is removed.

All pipes, valves, and process equipment in contact with the helium stream are made of stainless steel to limit the formation of dirt, which could collect in valves or small-diameter lines.

All major process components in the cleanup system are suspended in a heavily shielded pit. The inlet and outlet process and service lines for each component are brought to the top of the pit wall, where demountable joints are used to connect the component into the system piping manifolds. If a component should fail, it can be removed by lifting off the removable shielding overhead, breaking the Conoseal and other joints, and hoisting out the component and its attached lines.

For ease of access, the piping manifolds are hung on the outside face of the pit wall. No maintenance work will be done on actuators, valves, or lines, however, until the reactor is shut down, helium pressure is reduced to near atmospheric, and the piping manifolds are purged with clean helium.

7.6 Testing

All vessels in the gas cleanup system comply, as primary nuclear vessels, with the ASME Unfired Pressure Vessel Code, Section VIII, including Code Case Interpretations 1270N. Every vessel was pneumatically tested in accordance with the code. In addition, each vessel passed a leak test while pressurized with helium under the surveillance of a mass-spectrometer leak detector.

Piping system component tests follow the same procedures as the primary coolant piping tests described in Sec. 5.3.

The assembled system will undergo a preliminary leak test with nitrogen as the fluid, followed by a helium leak test at operating pressures.

Preoperational testing includes normal flow tests and calibration of

instrumentation and control devices. Inspection requirements beyond normal parameter monitoring capabilities and routine equipment inspection during shutdown periods are not anticipated.

8. HELIUM STORAGE AND PRESSURE REGULATION SYSTEM

8.1 General Description

As the reactor operates, the helium pressure in the primary and secondary loops is regulated to meet operating conditions. The source of helium added to increase primary loop pressure is the high pressure storage system, which also supplies the helium used for purging components of the gas cleanup and fuel handling systems. When helium is discharged to reduce the primary loop pressure, it goes to the high pressure storage system. The secondary loop is supplied directly from a bank of helium bottles. Figure 7.1.1 is a simplified flowsheet for the high and low pressure storage systems and the gas cleanup system.

When pressure must be vented rapidly from the primary loop, a blowdown valve opens, and the helium discharges directly to the low pressure storage tanks, which are maintained (at 12 psia) for such emergency use. The pressure in the primary loop falls rapidly to about 104 psia. The low pressure system compressor empties the remaining helium from the primary loop and discharges at 500 psia into the isolated gas cleanup system, from which the now clean helium enters the high pressure system compressor. This compressor discharges the helium (at a maximum pressure of 1000 psia) into the high pressure storage system. The high pressure storage tank is the ultimate storage place for helium emptied out of the primary loop.

After the primary loop is emptied, the gas from the low pressure storage tanks follows the same route as the primary loop helium to the high pressure storage tanks.

If the gas cleanup system should be inoperative, the low pressure

storage tanks could contain all of the primary loop helium. In this case, the compressor would evacuate the primary loop into the low pressure storage tanks which are designed to withstand a maximum operating pressure of 500 psia.

When the reactor is again ready for startup, the helium stored in the high pressure system is discharged into the primary loop under its own pressure until equilibrium is reached. Then the low pressure system compressor completes the evacuation of the high pressure system to build the primary loop pressure to 500 psia. The secondary loop is repressurized concurrently with new helium from bottles.

When a moderate, controlled pressure reduction is made in the primary loop, helium is discharged from the cleanup system into the high pressure receiver, not to one of the storage tanks. From the receiver, helium flows wherever it is needed to adjust pressures or to be used as a purge. During pressure reductions in the secondary loop, helium is discharged to the stack.

The low pressure receiver takes the small quantities of helium periodically discharged when various components are purged and the sample gas continuously discharged from analytical instruments. From the low pressure receiver, helium is returned to the gas cleanup system through a low pressure compressor and eventually is stored in the high pressure working tank.

8.2 Design Details

8.2.1 Low Pressure System

The system consists of two storage tanks, a receiver, and two 2-stage diaphragm compressors connected in parallel. General function of the system is the reception and temporary storage of helium that is, or could be, contaminated. The helium, which is generally received at pressures below the operating pressure of the coolant loops and the cleanup system, is returned to the gas cleanup system through one of the low pressure

compressors. System components are described below.

Low Pressure Storage - On blowdown, helium from the primary loop flows directly to two interconnected storage tanks, each with a 500-ft^3 capacity. The tanks rest, upright, on the floor of a shielded pit, Room 403, below the upper cleanup system piping room. Each tank has a 15-ft, 5-in.-long shell, rolled to 72-in. i.d. from 1-1/2-in., SA-212, Grade B carbon steel plate, and is closed with 2:1 elliptical heads. Design conditions are 550 psia at 650°F. The tanks are not insulated.

Low Pressure Receiver - Low pressure sample and purge streams flow to a bare 50-ft^3 receiver that hangs next to the sidestream adsorption beds in Room 308. For the 17-ft, 8-in.-long vessel shell, 5/8-in. plate of Type 304 stainless steel was rolled to 24-in. o.d. and closed with 2:1 elliptical heads, Design conditions are 500 psia at 650°F.

Low Pressure Compressors - Both of the low pressure compressors are Corblin, Model A4CV85, V-style, two-stage diaphragm compressors. They are connected in parallel through a valve manifold that has a single inlet and a single discharge line. Normally, one compressor is on-line, the other in standby. The control room operator can choose either compressor for on-line duty, or can run both simultaneously.

In ordinary operation, one compressor moves 10 lb/h of helium at an intake pressure of 25 psia and a discharge pressure of 500 psia. It starts automatically when the pressure on its intake side reaches 50 psia, and stops when the pressure drops to 25 psia. The compressor, normally connected on its intake side to the low pressure receiver, discharges into the gas cleanup system just upstream from the preheater. When the high pressure tanks are to be evacuated, the intake side is connected to a line from these tanks. After a blowdown, the intake side is connected to the blowdown line until the primary loop is evacuated, and then to the low pressure storage tanks. A double-pipe, water-cooled heat exchanger on the intake side reduces the temperature of the incoming gas to 80°F. Interstage and discharge heat exchangers remove heat of compression.

The compressors use single diaphragms made of 0.022-in.-thick sheets

of consumable electrode, vacuum-melt, Type 316 stainless steel ground to a No. 4 finish. Each diaphragm has been proved free of flaws in nondestructive tests and is seal-welded to the compressor head. In endurance tests of the actual compressors, the single, welded diaphragms survived 1000 h of operation without failure or the development of detectable flaws. As a precaution, a flow-through oil detector is located in the discharge line from each stage of the compressors. The detectors, photocell devices in weld-sealed pressure cases, have the demonstrated capability to respond to 5 cm^3 of compressor oil within a few seconds after it enters the helium stream.

8.2.2 High Pressure System

The system, which consists of a storage tank with a volume of 350 ft^3, a receiver of 50-ft^3 volume, and a single-stage compressor, has the general function of storing clean helium at pressures higher than the operating pressures of the coolant and cleanup systems.

High Pressure Storage Tank - A single, 350-ft^3 tank, mounted beside the low pressure storage tanks, is the ultimate storage place for all of the helium in the coolant and cleanup systems. The tank has a 17-ft, 10-in. shell, rolled to 58-in. i.d. from 2-in., SA-212, Grade B steel plate, and 2:1 elliptical steel heads. It is designed for 1000 psia at 650°F.

Ordinarily, with all helium systems operating at design conditions, the tank contains clean helium at 350 psia. If the coolant loops are operated at reduced temperatures or pressures, helium is added to or taken from the storage tank only when the working tank has insufficient capacity to accommodate the off-design condition. When all of the helium is removed from the coolant and cleanup systems, the helium pressure in the storage tank reaches 1000 psia. The tank receives clean helium from the cleanup system through the compressor, and discharges to the primary loop directly or through the low pressure compressor.

High Pressure Receiver - A reservoir for clean, process helium, the 50-ft^3 receiver hangs in Room 308 beside the low pressure receiver. The

24-in.-o.d. x 20-ft-long tank was made from 3/4-in., SA-212, Grade B carbon steel plate, and elliptical heads. It is designed for 1000 psia at 650°F.

Helium for the receiver comes from the high pressure compressor. The tank discharges to pipe manifolds that feed the cleanup purge, fuel lock pressure regulation, primary blower jacking gas, and primary loop pressure regulation systems. Regulation of the receiver pressure is one of the functions of the primary loop pressure regulation system described in Sec. 8.3.1.

High Pressure Compressor - The high pressure system uses a Corblin Model A2C250, single-stage, diaphragm compressor which receives a maximum of 10 lb/h of helium at 500 psia and discharges it at 1000 psia. The compressor uses a single, seal-welded diaphragm like those in the low pressure compressors. An oil detector monitors the discharged helium, which is cooled to 100°F in a double-pipe, water-cooled heat exchanger.

Operation of the high pressure compressor is controlled by the primary loop pressure regulation system.

8.2.3 Jacking Gas Systems

Helium at a pressure of 40 psi or more above the loop pressure must be supplied to the jacking bearings of the coolant loop blowers while the blowers are being started or stopped. (See Sec. 5.1.1.) This jacking gas flows to the blowers from two separate supply systems, one for the primary loop blower and one for the secondary loop blower.

Primary Loop Blower - The source of helium for jacking the primary loop blower is the high pressure receiver. From there, helium at 1000-psi maximum pressure is charged to a 1-ft^3 tank through a normally closed valve. When it is full, the tank, isolated from the high pressure receiver, contains enough helium for starting and stopping the blower five times. The tank pressure is monitored by a transducer that reads out on the blower control panel in the control room.

When a blower start or stop is initiated in the control room,

electrical circuits automatically open a feed valve in the line between the jacking gas tank and the blower. The feed valve remains open long enough for the blower to reach running speed or to coast to a stop. Then the valve closes. After five starts and stops, an operator must refill the jacking gas tank, the capacity of which is limited to prevent overpressuring of the primary loop if a control circuit failure were to allow the feed valve to remain open.

Secondary Loop Blower - Manifolded, size-H, gas bottles supply helium for jacking the secondary loop blower. The output of the bottle manifold, located near the heat dump outside the secondary containment structure, is regulated to 600 psia and monitored by a pressure transducer. A feed valve between the regulator and the blower is operated by a control circuit like that for the primary loop blower. Overpressures in the secondary loop in the case of a feed valve control failure are prevented by limiting the supply of available helium; the helium bottles contain only enough gas for five starts and stops.

8.3 Pressure Regulation Systems

8.3.1 Primary Loop

During normal operations, the operator at the main operations console controls the primary loop pressure, within the range of 445 to 495 psia, by opening and closing valves in the system depicted schematically in Fig. 8.3.1.1. To increase pressure, the operator opens valve 8529, allowing helium to flow from the high pressure receiver to the primary loop. To decrease pressure, the operator opens valve 8528, and helium is pumped from the primary loop to the high pressure receiver by the high pressure compressor. An automatic pressure relief operates if the system pressure rises to 505 psia. At that point, an annunciator alarm sounds, valve 8540 opens, and helium flows from the primary loop to the low pressure storage tanks until the loop pressure is decreased to 475 psia. If at any time the pressure is not decreased by the opening of either valve 8528 or

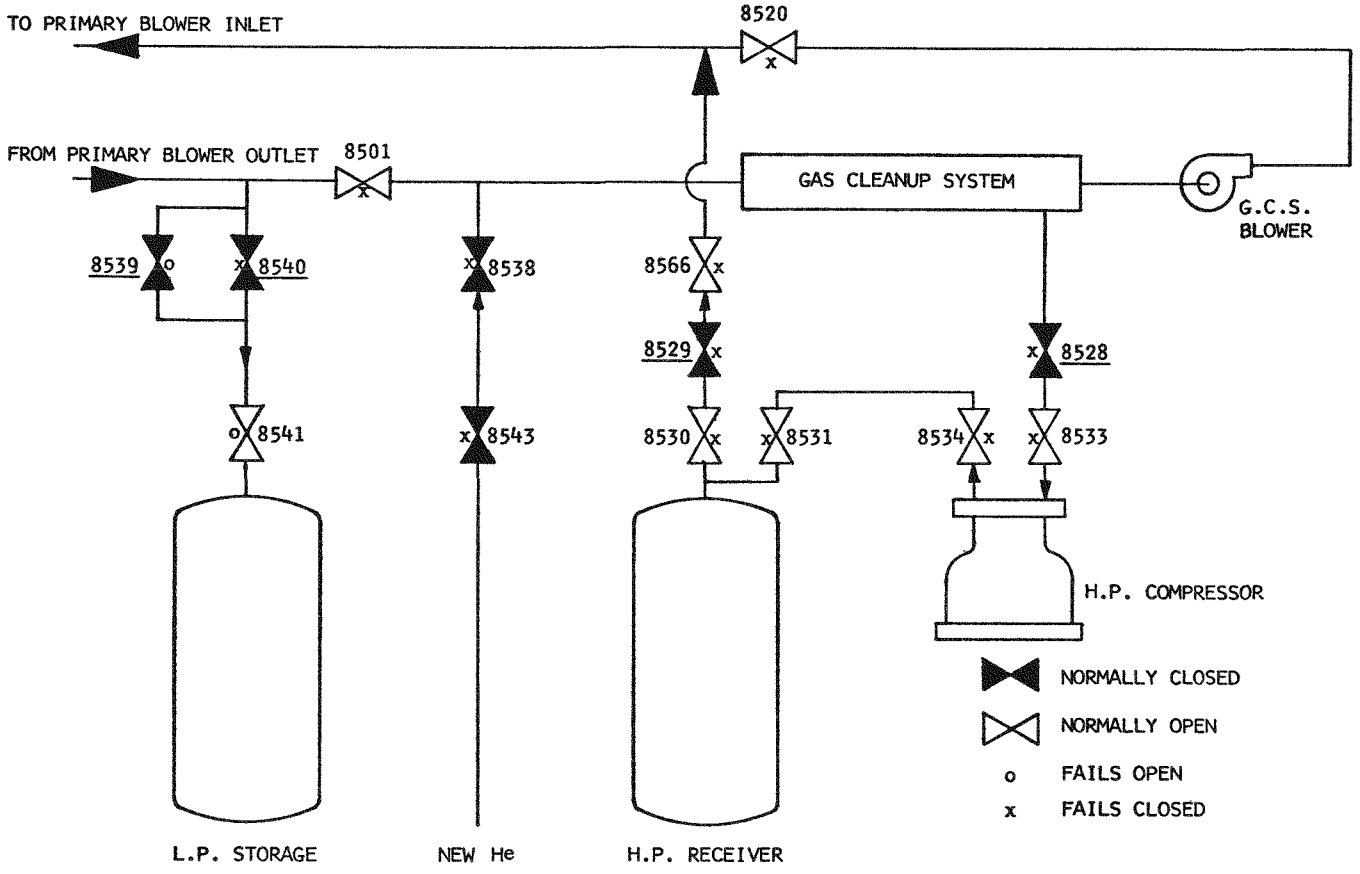

Fig. 8.3.1.1 Piping for primary loop pressure regulation system

8540, blowdown valve 8539 may be opened manually by the operator. Three transducers monitor the primary loop pressure. Two are located at the blower outlet, where system pressure is at its highest, and the third is located upstream of the blower.

8.3.2 Secondary Loop

Automatic controls maintain the secondary loop pressure within the range of 10 to 40 psi above the primary loop pressure. Figure 8.3.2.1 is a schematic diagram of the valves in the pressure regulation system. When the differential pressure decreases to 10 psi, valve 8612 opens, and helium flows from manifolded bottles to the secondary loop until the differential pressure is increased 20 psi. If the differential pressure rises to 40 psi during operations, valve 8613 opens and helium flows from the secondary loop to the stack until the differential pressure decreases to 30 psi. A safety circuit opens the relief valve, 8483, if the loop pressure rises to 545 psia, and helium vents to the stack until the pressure falls to 510 psia. The primary transducer for loop pressure control is a differential pressure element connected to a high side tap at the main heat exchanger cold side inlet and to a low side tap at the primary loop blower inlet. There is an installed spare for this transducer. For the pressure relief circuit, three pressure transducers are located at the heat exchanger.

8.4 Design Analysis

The two prime considerations in the design of the helium storage and pressure regulation system were system integrity and operational safety. The system was designed and built to the same standards of integrity as the gas cleanup system, discussed in Sec. 7.5. To achieve operational safety, the pressure regulation system was designed with these features:

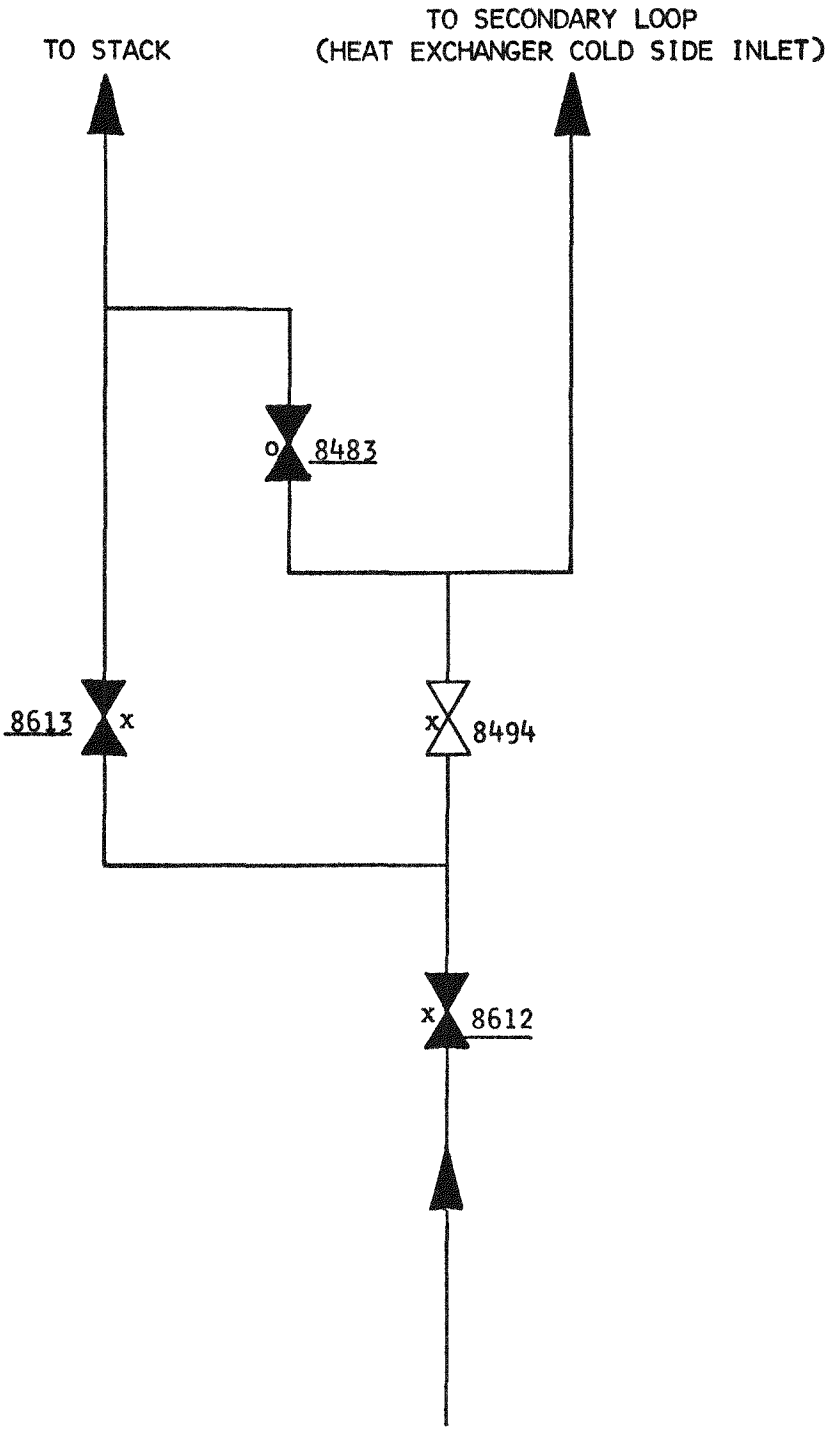

Fig. 8.3.2.1. Piping for secondary loop pressure regulation system

1. Helium flow rates into the coolant loops are always less than the capacity of the corresponding vent devices.

2. The volumes of helium available for high flow operations, e.g., jacking gas for the blowers, are limited to prevent overpressurization of the coolant loops.

Another characteristic of the coolant system adds to its safety: credible rates of temperature rise are not sufficient to cause excessive pressure rises.

Analyses of the effects on loop pressures of operations and accidents were made with the aid of the UHXCOM system dynamics computer code and with simulation studies on an analog computer. The results of the analyses are presented in Table 8.4.1. For each case, the initial pressures were assumed to be 475 psia in the primary loop and 495 psia in the secondary loop. The table is in two sections, one concerned with the effects of operations in the pressure regulation system, and the other with the effects of operations or accidents in the entire coolant system. Where "No pressure control" is listed in the remarks column, there was assumed to be no helium charged to or discharged from the system. For cases 1 through 6, only the primary loop was studied, and in cases 7 through 11, only the secondary loop.

TABLE 8.4.1

EFFECTS ON COOLANT LOOP PRESSURES OF OPERATIONS AND ACCIDENTS

Case	Action	Primary Loop				Secondary Loop				
	Pressure Regulation Effects	Maximum Helium Flow (lb/h)	Maximum Rate of Pressure Change (psi/sec)	Maximum Pressure (psia)	Final Pressure (psia)	Maximum Helium Flow (lb/h)	Maximum Rate of Pressure Change (psi/sec)	Maximum Pressure (psia)	Final Pressure (psia)	Remarks
1.	Open valve 8529	10	+0.02	495	495					Normal pressure increase
2.	Open valve 8528	10	-0.02	475	455					Normal pressure decrease
3.	Open valve 8540	700	-1.4	545	495					Automatic pressure relief
4.	Open valve 8539	1100	-2.2	475	104					Manual blowdown
5.	Primary blower jacking	22	+0.04	477	477					No pressure control
6.	Primary jacking valve sticks open	22	+0.04	479	479					No pressure control
7.	Open valve 8612					155	+1.0	535	535	Normal pressure increase
8.	Open valve 8613					155	-1.0	495	485	Normal pressure decrease
9.	Open valve 8483					310	-2.0	545	495	Automatic pressure relief
10.	Secondary blower jacking					22	+0.15	497	497	No pressure control
11.	Secondary jacking valve sticks open					22	+0.15	500	500	No pressure control
	System Effects									
12.	Reactor startup[1]	0	+0.004	495	475	0	+0.07	535	495	Manual primary loop control, automatic secondary loop control
13.	Reactor restart[2]	0	+0.03	480	480	0	-0.78	495	485	No pressure control
14.	Rec. bypass fails closed	0	+0.02	477	477	0	-0.02	495	470	No pressure control
15.	Rec. bypass fails open[3]	0	+0.02	477	477	0	+0.06	499	375	No pressure control, blowers in both loops are shut down after 60 sec.
16.	Secondary flow loss[3]	0	+0.12	482	482	0	-0.12	495	375	Safety circuit shuts down primary blower after 15 sec.
17.	Primary flow loss	0	+0.12	482	482	0	-0.42	495	385	No pressure control
18.	Heat dump air flow loss[3]	0	+0.03	515	515	0	+0.38	518	375	No pressure control, blowers in both loops are shut down after 60 sec.
19.	Primary loop rupture[3]	1.63×10^5	-100	475	13.5	0	-0.42	495	385	Automatic shutdown
20.	Secondary loop rupture[3]	0	+0.12	482	482	2.04×10^5	-600	495	11.4	Automatic shutdown

[1]Reactivity increase of 2¢/min starting from 100°F.
[2]Equilibrium after $2 scram, rods withdrawn until power of 30 kW, then blowers on at minimum speed.
[3]Safety circuits act to shut down reactor and blowers.

9. CONTAINMENT

A reinforced concrete structure, partially lined on the inside with steel plate, serves as the secondary containment. Descriptions and drawings of the structure appear in Section 3.1 and Figs. 3.2-3.6. Approximate overall dimensions of the containment structure are 60 ft x 49 ft x 81 ft. The contained free air volume is 150,000 ft^3.

The structure bears on welded volcanic tuff. Ground water was not encountered in a 300-ft-deep hole adjacent to the structure.

9.1 Structure Design

Design characteristics of the secondary containment are:

Maximum internal positive pressure	5 psi
Maximum internal negative pressure	0.5 psi
Measured leakage at 5 psi	3% of the contained volume per day
Wind loads, uplift	12 lb/ft^2
horizontal	20 lb/ft^2
Snow load	30 lb/ft^2
Seismic coefficient (Uniform Building Code for Zone II)	0.046

A gas-tight steel membrane, made from welded sheets of 9-gauge steel plate, lines the interior surface of the containment superstructure and, below grade, extends inside the walls to the base of the structure

on the north and west sides and to 5 ft below grade on the two outside walls. During construction, the steel liner plate was erected and all its seams were dye-penetrant inspected before forms were placed for the pouring of concrete. Form ties that passed through the liner were welded to the liner, and, after the forms were removed, were ground smooth at the liner face and inspected for cracks.

Wherever penetrations were made through the liner, the penetration enclosure was welded to the liner. Typical penetration installations are shown in Fig. 9.1.1. Each large rectangular opening, through which many cables pass, is closed with a 1/2-in.-thick steel plate that connects to the outer penetration flange with a bolted, gasket-sealed joint. Tapped holes in the penetration plates receive the cable connectors described below.

9.2 Penetrations

Walls of the secondary containment structure are penetrated in 392 places. The penetrations are listed in functional groups in Table 9.2.1.

TABLE 9.2.1

SECONDARY CONTAINMENT PENETRATIONS

Group	Number
Ventilation ducts	5
Fuel conveyor openings	2
Access doors	3
Shielding windows	3
Pneumatic tube boxes	114
Electrical conduits	235
Pipe sleeves	30
	392

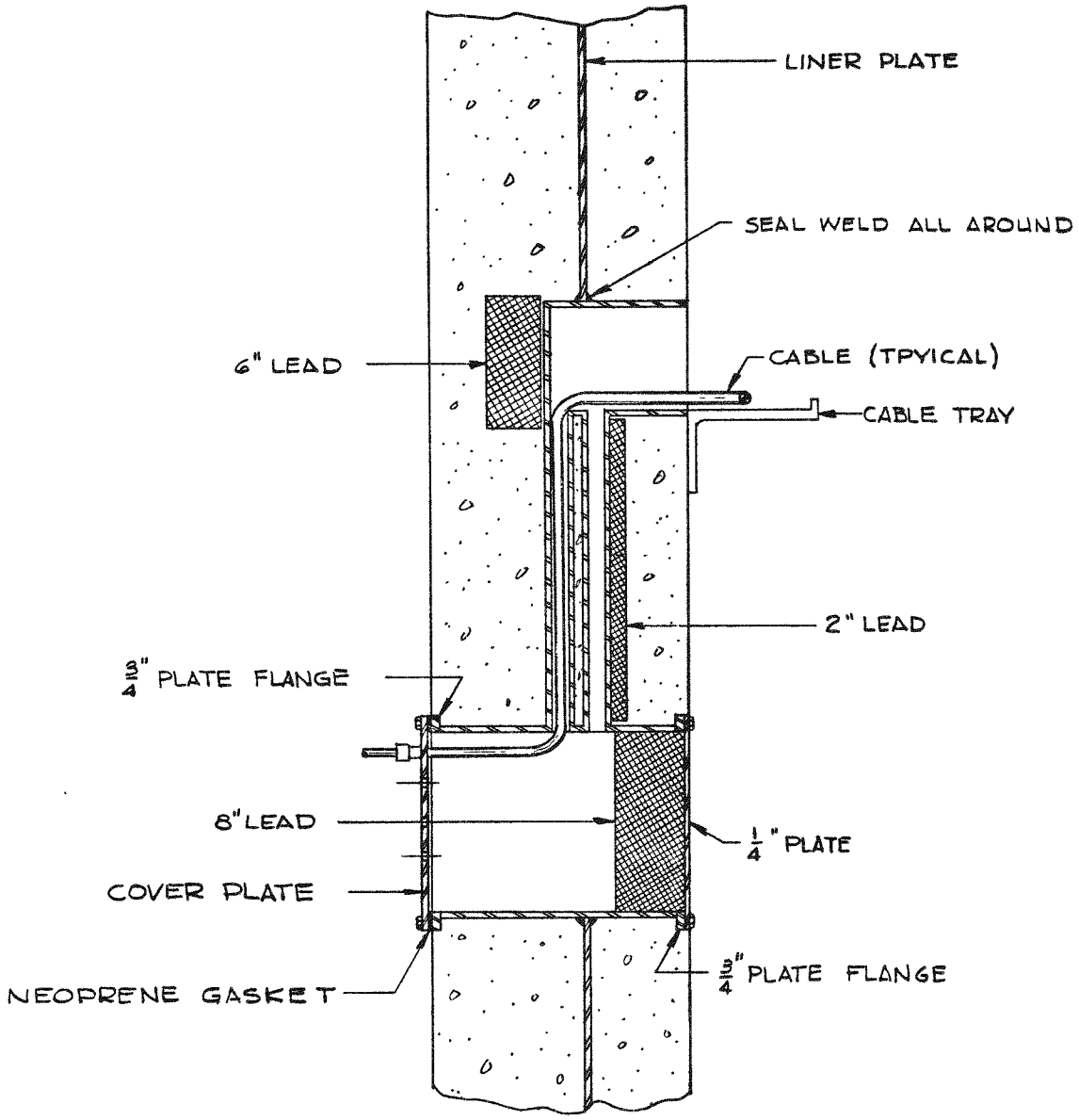

Fig. 9.1.1 Penetration enclosures

Closures that maintain the integrity of the secondary containment are discussed below for each group of penetrations.

Ventilation Ducts - Four of the ducts that penetrate containment walls are parts of the closed-cycle, air recirculation, ventilation system described in Sec. 9.3. The ducts, as extensions of the secondary containment, are included in the containment pressure and leakage test program. The fifth duct admits fresh air to the containment during open cycle ventilation periods when the reactor is shut down. A butterfly valve closes the duct during operating periods.

Fuel Conveyor Openings - Both fuel conveyor tubes are welded into a steel plate that is welded to the wall penetration sleeve on the inside of the fuel loader room. The sleeve is cast into the concrete wall. Pairs of secondary gas lock valves close the conveyor tubes, described in Sec. 6.2.6.

Access Doors - One door, 16 ft x 16 ft, is an opening at ground level for the passage of large equipment during the periods when equipment is installed. During operations, the opening is closed with a steel panel that is welded to the steel liner inside the containment structure. Concrete blocks, which are keyed together and to outside pilasters, slide in place behind the panel to reinforce it.

The other two doors, 3.5 ft x 7 ft are of the conventional, personnel access type used in air locks. Hand-operated dogs pull each door against a neoprene seal gasket, illustrated in Fig. 9.2.1. A door seal vacuum system, described in Sec. 12.5, maintains the low pressure in the buffer zone that holds the door tightly against the gasket.

Windows - Three standard, lead-glass, shielding windows penetrate the wall between the operating corridor and the upper gas cleanup room. Each window is sealed against a maximum overpressure of 10 psi by a gasketed seal plate.

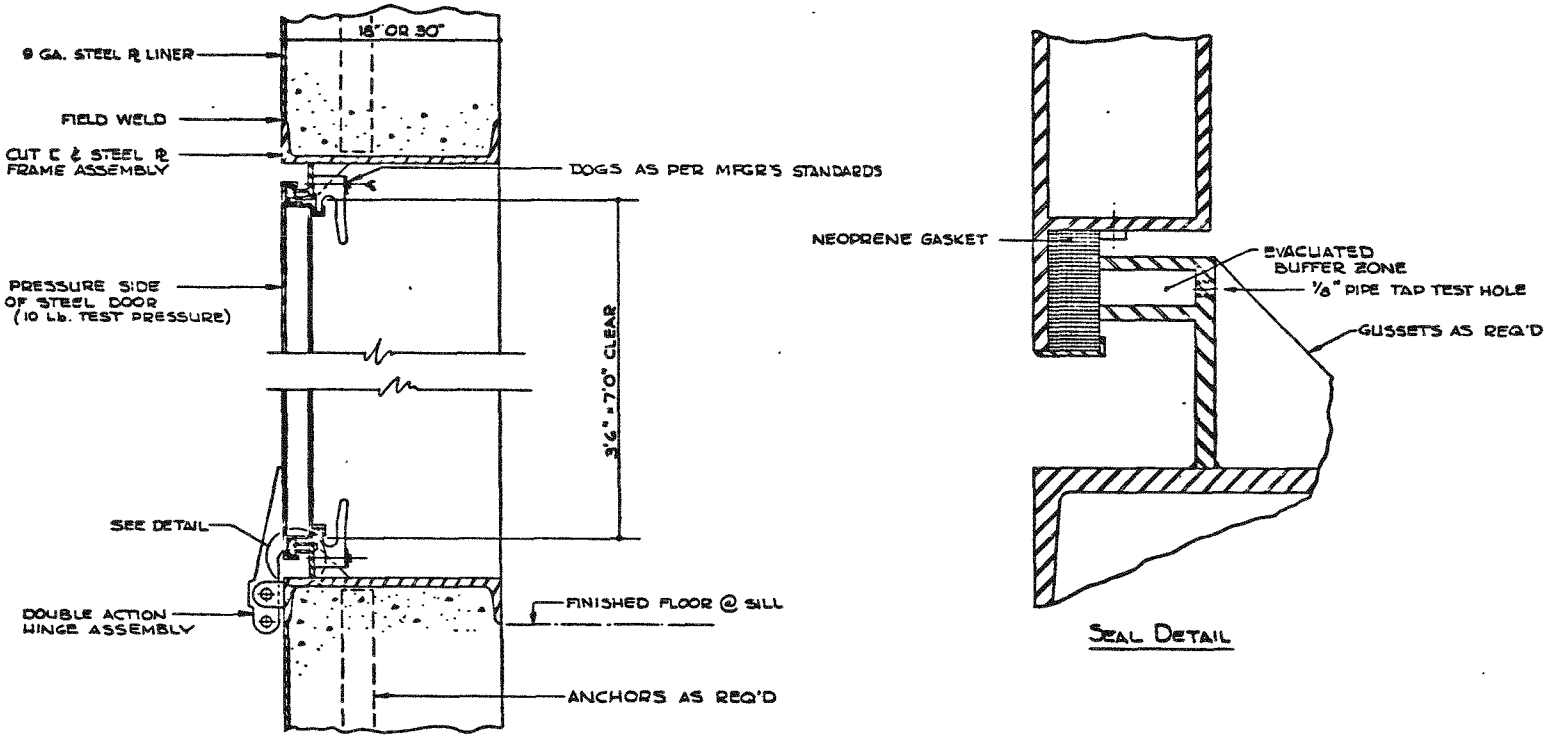

Fig. 9.2.1 Access door seals

Pneumatic Tube Boxes - The tubes that carry control air pass through manifold boxes that are cast into the concrete walls or are bolted to a penetration plate that covers a cast-in sleeve. The latter type of tube manifold box is shown in Fig. 9.2.2. Inside the box, the tubes are joined to the front and rear faceplates. Containment is maintained by the gasketed joints between the faceplates and the cast-in enclosure flange or cover. Each tube is closed with a solenoid valve and hand valves.

Electrical Conduits - Electrical cables or wires penetrate the containment through compression gland seals of two types, illustrated in Fig. 9.2.3. The plate connector is used for cables that pass through multiple-hole penetration plates bolted to cast-in enclosures. The bushing connector passes single cables through cast-in conduits.

Because the compression gland seals only the outside of multi-conductor cables, two other types of seals are made on each cable beyond the gland on the inside of the containment. First, the free space between the individual conductors and the cable jacket is filled with an epoxy compound. Then, each wire in the cable is dipped in solder and terminated in a solid connector, and the insulation-to-connector gap is closed with shrunk-on polyvinyl chloride tubing.

Pipe Sleeves - Where a containment wall is penetrated by a pipe that contains fluids at near-ambient temperatures, the pipe is joined directly to a pipe sleeve of the same size which is cast into the wall. Pipes containing hot or cold fluids pass through an oversize sleeve. A concentric bellows, joined to the pipe at one end and to the sleeve at the other, makes the seal. All pipes can be closed with isolation valves near the penetrations.

9.3 Secondary Containment Ventilation

For ventilation of the secondary containment during reactor operation, one of two parallel, in-line blowers moves the air in a closed

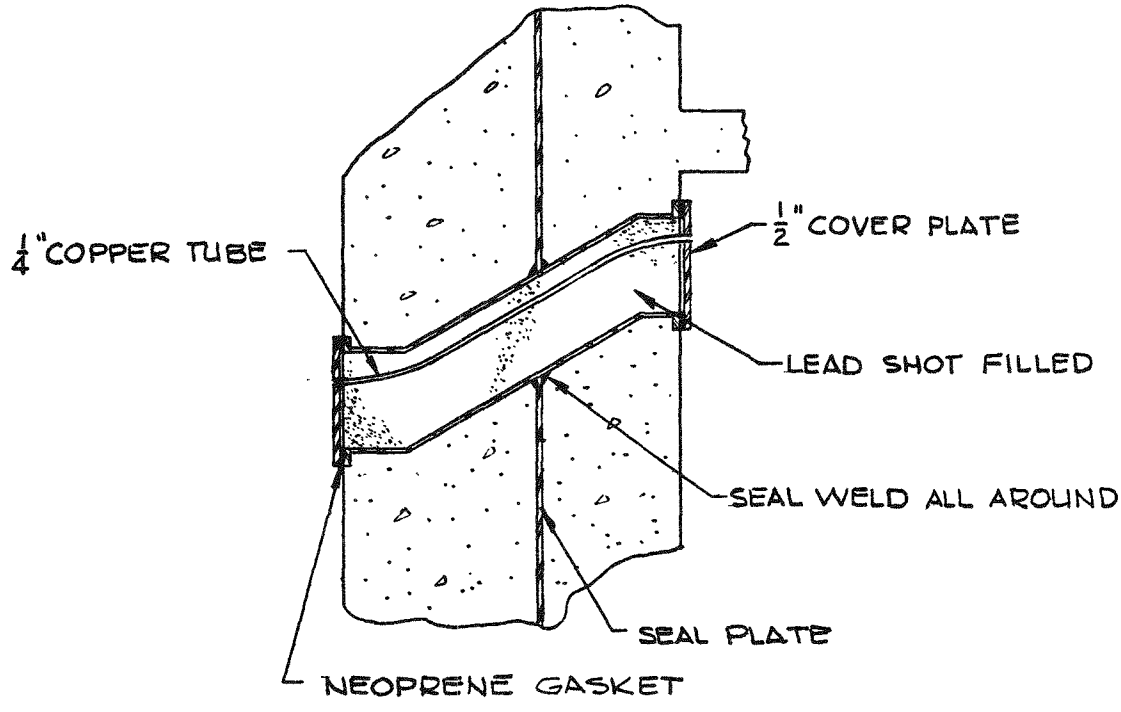

Fig. 9.2.2 Pneumatic tubing penetration box

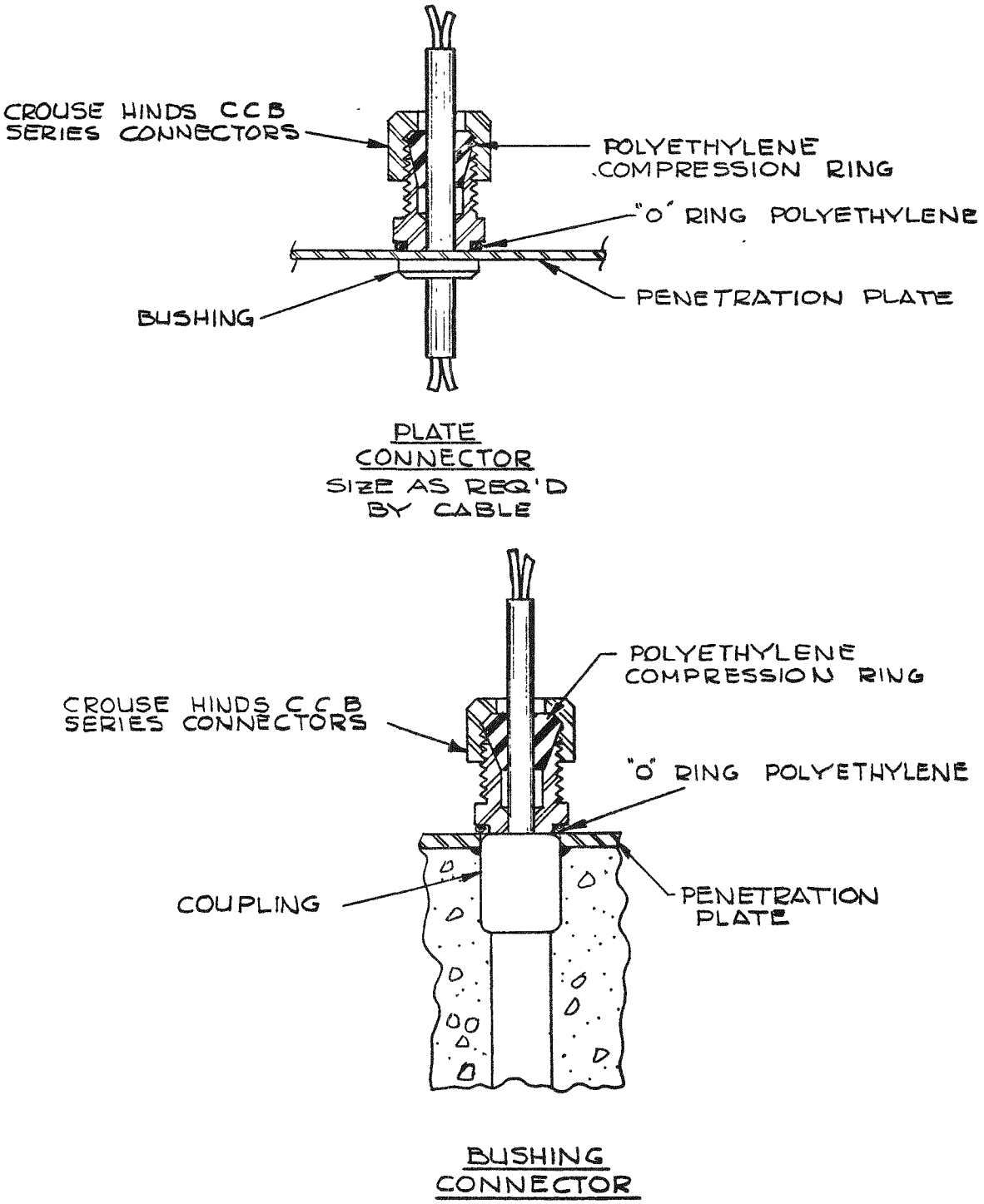

Fig. 9.2.3 Electrical penetration connectors

cycle through a system designed to withstand 7.5-psi internal pressure. This system, an extension of the secondary containment, is depicted in Fig. 9.3.1. The full air flow, 9700 cfm, circulates through absolute and activated carbon filters and heating and cooling coils. Pressure inside the containment structure is maintained at 0.5 in. w.g. below atmospheric by a 25-ft^3/min continuous bleed of filtered air to the stack through one of two parallel bleed fans. Within the rooms, air moves from the regions least likely to be contaminated to regions where contamination is more likely and then returns to the filters before recirculation. The flow rate is sufficient to provide 15 air changes per hour in the regions where equipment contains fission products.

When personnel are inside the secondary containment structure, the ventilation system brings in fresh air, draws it through roughing and Aerosolve filters, passes the filtered air once through the rooms, and exhausts it through the absolute and carbon filters to the stack.

The exhaust filters in this system are very likely to become contaminated should leaks develop in the helium systems. Therefore, these filters are located in a separate shielded pit outside the building.

If an accident should occur that vents the primary loop inside the secondary containment, automatic control circuits detect the accident and close isolation valves in the ventilation and coolant system. The circuits and their functions are described in Sec. 11.4.1. An activity release due to some other accident would be detected by monitors described in Sec. 13.6.1. The response to the resulting alarm would be made by an operator whose actions would depend on the circumstances.

Analyses of potential accidents and discussions of the steps to be taken to control them appear in Chapter 16.

After a day's operation of the reactor at design power, the ^{41}Ar activity within the secondary containment will have reached an equilibrium level of approximately 9 curies or an average concentration of 2×10^{-3} C/m^3. As is shown in Sec. 13.3.2, personnel would not be prevented from

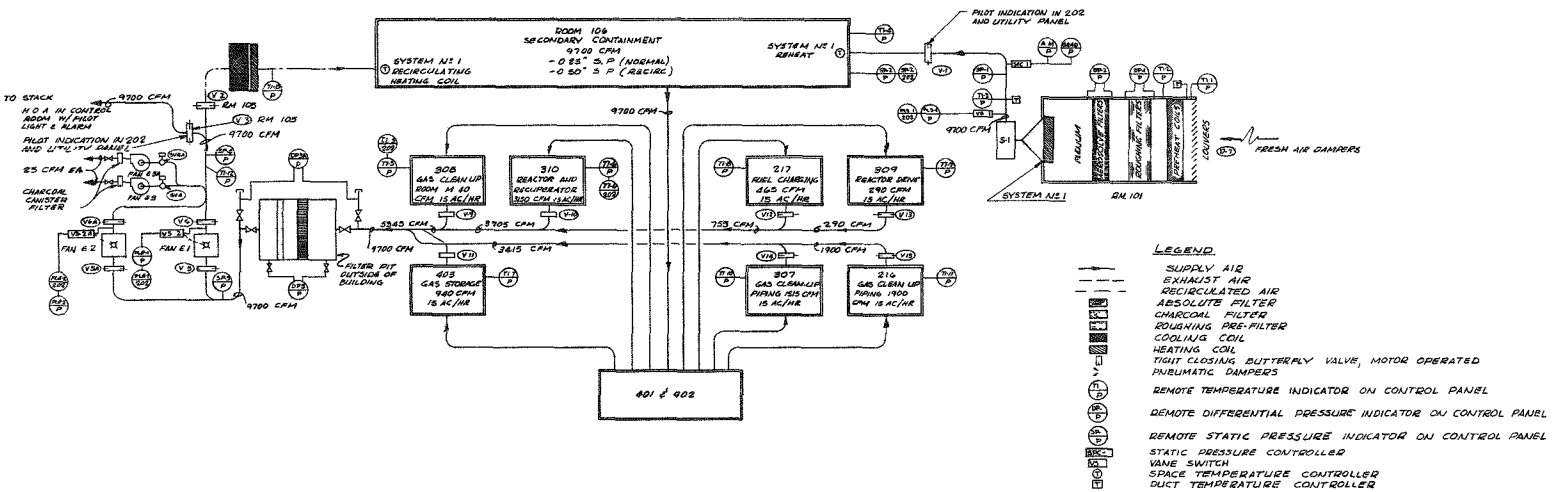

Fig. 9.3.1 Secondary containment ventilation system

entering the secondary containment by this source density. However, several complete changes of the secondary containment air will normally be made before personnel go in. Furthermore, access to the secondary containment is prohibited until the absolute pressures in the coolant and purification loops have been reduced to near atmospheric, a procedure that takes a minimum of about 24 h following operation at design pressure.

During the period of venting and purging of the secondary containment enclosure before personnel entry, the ^{41}Ar discharged to the stack produces in adjacent, uncontrolled areas maximum dose rates that are well within tolerance levels.

9.4 Design Pressure Calculations

The requirement for a 5-psi maximum, internal, positive pressure capability in the containment structure was derived from a maximum credible accident analysis that was reported in Sec. 9.3.1 of the UHTREX Hazard Report.[1] Subsequent analyses, presented in Chapter 16 of this report, predict that the maximum internal pressure generated in the course of an accident will be considerably less than the 5-psi design pressure.

9.5 Testing

A series of pneumatic tests have been made to determine the leak rate of the secondary containment structure. When construction work had been completed, a final test was run in which the internal air pressure of the structure was raised to 5.00 psig, and the pressure decay was observed over a 2-day period. Readings of temperatures,

[1]Los Alamos Scientific Laboratory Report LA-2689, March 1962, p. 124.

differential pressure, barometric pressure, and humidity were recorded every 30 min. From these data, the calculated leak rate was found to be 3% of the contained volume per day at 5-psig internal pressure. Subsequently, the leak rate was confirmed in another test.

When equipment installation is complete inside the containment structure, a leak test will be made with permanently mounted apparatus to establish a standard leak test procedure. The standard procedure will be used at suitable intervals to confirm the leak tightness of the containment structure.

10. EMERGENCY ELECTRICAL SYSTEM

Power for the safe shutdown of the UHTREX reactor and for the maintenance of critical facility functions is ensured, despite the failure of external power sources, by on-site generators and automatic switch gear.

10.1 General Description

Electrical power for the UHTREX facility comes from the Los Alamos power distribution center over two separately routed, 13.2-kV power lines. A load center in the ground-level electrical equipment room feeds the facility distribution system, shown schematically in Fig. 10.1.1.

Normally, each of the 13.2-kV lines carries about half of the facility load, but either line with its associated 750-kVA transformer is capable of carrying the full load for 30 min. If power from one of the lines should be interrupted, the main breaker for that line opens, and a normally open tie breaker closes, connecting the two sides of the load center. Upon restoration of the main-line power, the breakers return to their normal positions.

Loads that are critical for safe shutdown of the reactor are supplied continuously from two generators located near the facility load center. One generator, which supplies 20 kW to instrumentation and critical motor loads through Motor Control Center (MCC) No. 4, is driven, normally, by a load-center-supplied ac motor or, on line failure, by a diesel engine. The second generator, which feeds 10 kW to critical instrumentation through Distribution Panel X, is driven, normally, by an ac motor on MCC No. 2 or, on line failure, by a battery-supplied dc motor. If the 20-kW generator

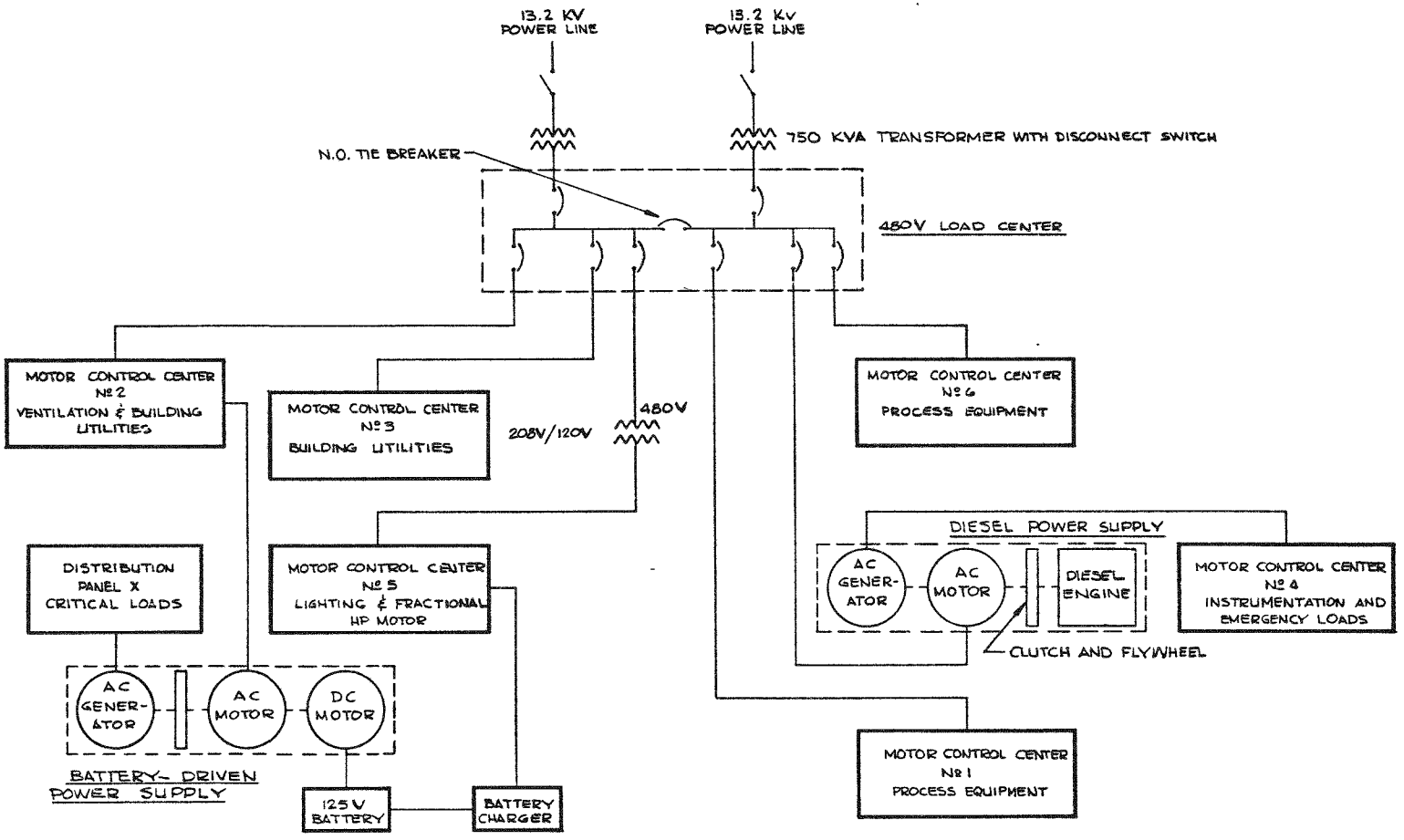

Fig. 10.1.1 Electrical power distribution system

should fail while in normal operation, its load transfers to MCC No. 5. On failure of the 10-kW generator, at any time, its load transfers to MCC No. 4.

10.2 Design Details

10.2.1 Distribution System

A 1500-kVA load center substation, built by General Electric Company, serves the facility. The substation includes two 750-kVA, liquid-immersed, askarel-filled transformers mounted outside the building. Inside the building, the low voltage switchgear section has an incoming bus, a main breaker, and five feeder breakers for each 13.2-kV power line. A tie breaker connects the two buses when one line fails.

The two electrically operated main breakers and the tie breaker are controlled by individual control switches, in conjunction with a manual-automatic selector switch. When the selector switch is in the manual position, any of three breakers can be operated or tripped in any sequence, except after a main breaker has tripped on overcurrent. Then, a lockout relay must be reset manually before either the tripped breaker or the tie breaker can be closed electrically. When the selector switch is set in the normal, automatic, position, an adjustable, three-phase, undervoltage relay detects undervoltage conditions in any phase of either incoming line, and, after a time delay, trips the corresponding main breaker. As soon as the main breaker opens, the tie breaker closes. When normal conditions are restored on the incoming line, the main breaker closes, after a time delay to insure that the line condition is stable. When the main breaker is closed, the tie breaker opens. As it does in the manual mode, a lock-out relay prevents closure of the main or tie breaker when a main breaker trips on overcurrent.

The low voltage switchgear distributes the power load as shown in Fig. 10.1.1. Continuous power loads on the two on-site generators are listed in Table 10.2.1.1.

TABLE 10.2.1.1

ELECTRICAL LOADS SUPPLIED BY ON-SITE GENERATORS

Diesel Generator through MCC No. 4

1. Critical loop control systems
2. Secondary containment bleed fans
3. Diesel fuel pump
4. Emergency control room ventilation blower
5. Emergency demineralized water pump
6. Emergency control room lighting
7. Facility paging system
8. General instrumentation power supplies
9. Annunciator system
10. Area monitoring system and stack monitor
11. Miscellaneous recorders, logging typewriters, lamps
12. Panel X loads on failure of battery-powered generator

Battery-Powered Generator through Panel X

1. On-line computer
2. Nuclear and loop safety systems
3. Reactor control rod clutches
4. Reactor neutronic instrumentation

10.2.2 Diesel Power Supply

In case of line power failure, the instrumentation and power loads on MCC No. 4 are assumed, without interruption, by a Consolidated Diesel Electric Corporation Model UPS 20-60 MG uninterrupted power supply. The power supply unit consists of a diesel engine, a magnetic clutch, a flywheel, an induction motor, and an ac generator.

When the power supply is in normal, standby condition, the induction motor, running on line power, drives the generator and flywheel. The

generator supplies a maximum of 20 kW to the load. When line power fails, relays in an associated control cubicle open the starter on the induction motor and energize the magnetic clutch. Inertia of the turning flywheel starts the diesel engine and supplies enough energy to power the generator during the transition period. The diesel engine assumes the generator load, and power continues to flow from the generator.

While the diesel is running, control systems constantly monitor the line power quality. After proper voltage and frequency have been re-established on the line circuits, the control systems check the stability of the line power for a time and then close the starter on the induction drive motor. The magnetic clutch is then automatically de-energized, and the diesel engine shuts down. The line-fed induction motor continues to turn the generator and flywheel, and the power supply is again in standby condition.

10.2.3 Battery-Driven Power Supply

A 10-kW uninterrupted power supply system, built by Allis-Chalmers Manufacturing Company, assumes the instrumentation loads on Panel X in case of line power failure. The power supply system consists of an induction motor, a synchronous generator, a dc motor, and a flywheel, all direct-connected and mounted on a common base.

During the normal mode of operation, the induction motor, running on line power, drives the generator and flywheel. The fields of the dc motor are energized, but its armature circuit is interrupted by solenoids that hold the brushes away from the commutator. The brush-lifting solenoids are energized by line power. When the line power fails, a control circuit disconnects the ac motor from the line. Simultaneously, the solenoids release the brushes, and the dc motor begins to drive the generator, which has been powered in the interim by the inertia of the spinning flywheel. Power for the dc motor flows from a bank of 60, Exide-Tytex, Type EOP-21, lead acid batteries, which are maintained by a trickle charger. The batteries can drive the motor-generator set for 4 h under full load.

After the line power is restored, control circuits return the system to its normal mode of operation.

10.3 Tests and Inspections

The capabilities of both emergency power supplies have been demonstrated in acceptance and operational tests. Inspection of both units is a part of the operators' routine during periods of reactor operation. Operational tests are made periodically of the ability of each unit to function when line power is interrupted. Maintenance work is performed routinely according to written schedules.

11. INSTRUMENTATION AND CONTROL

11.1 General

11.1.1 Control Room

The control room (see Fig. 3.3) is located on the operating level, well separated from the reactor and accessible directly from the outside and through the operating area via the main entrance stairway. In the control room are the main operations console, the on-line computer, the display and operating panels, and their auxiliary electronics racks. A plan of the control room appears in Fig. 11.1.1.1.

Main Operations Console - While the reactor is operating, the principal control point is the main operations console, which consists of seven control panels. On these panels are the controls and display instrumentation for the reactor and both coolant loops and the computer operator console, all easily accessible to the reactor operator who sits at the console. Directly behind him are the logging and alarm typewriters for the computer. Panel 31 is an eight-channel continuous trace recorder. Important variables, such as reactor power, coolant flow rates, or system temperatures and pressures, can be displayed on the recorder. Three panels, 32, 33, and 34 are associated with the reactor. There are two panels, 35 and 36, for the primary and secondary coolant loops.

A description of the individual panels of the main operations console follows.

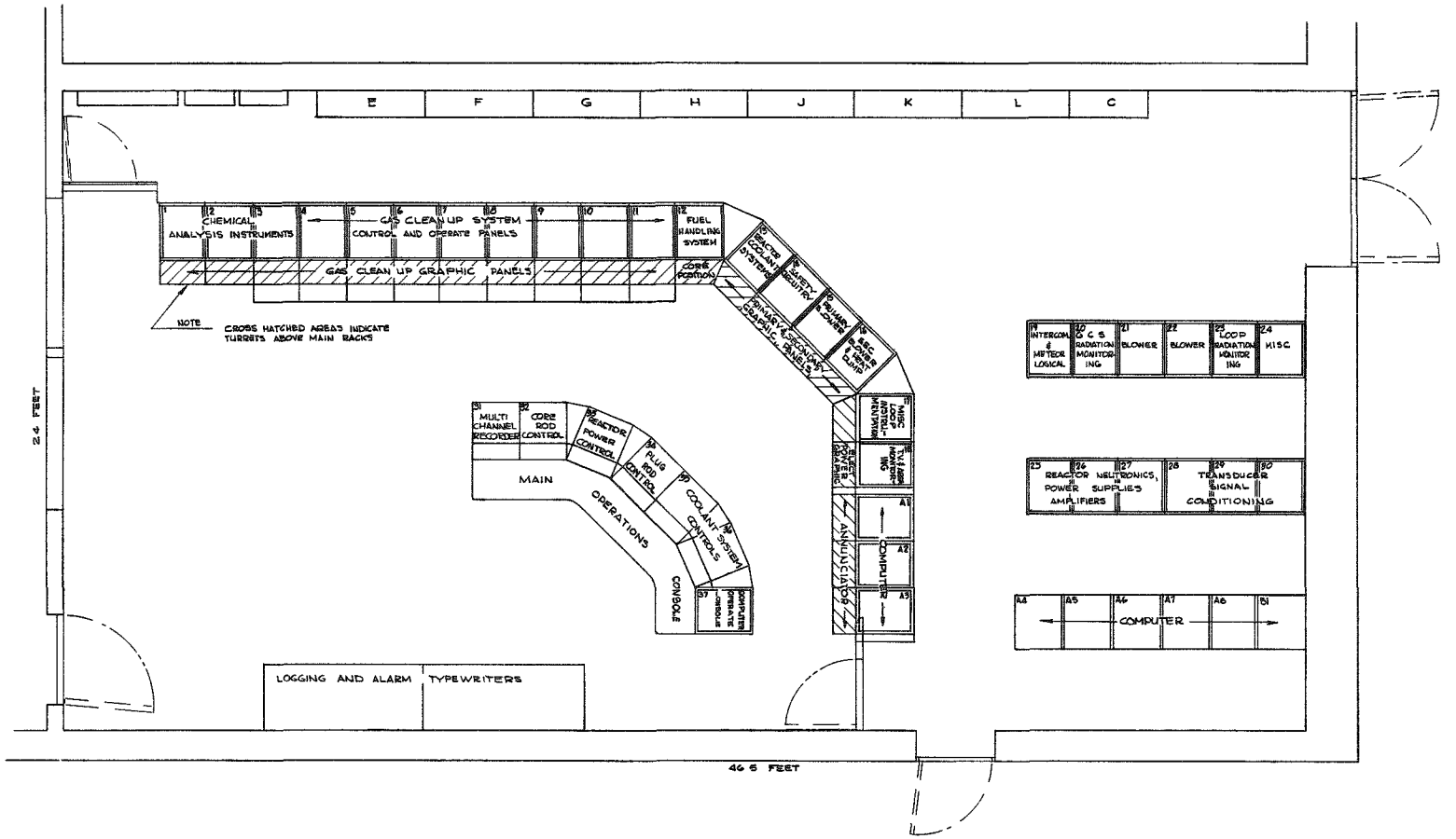

Fig. 11.1.1.1 Control room

1. Panel 32 (Core Control Rods) - The four core control rods are controlled from this panel. Rod position indication is displayed for each rod. Other variables displayed are the clutch current of each scram rod and a log gamma flux indication.

2. Panel 33 (Reactor Power) - All of the neutron level information that is required to operate and monitor the reactor is available from this panel. The following neutron flux measurements are displayed.

2 Log count rate indications

2 Reactor period signals (derived from log count rate)

2 Log power indications

2 Reactor period signals (derived from log power)

2 Linear power indications.

3. Panel 34 (Plug Control Rods) - The eight plug rods are controlled from panel 34, and rod position is displayed here. Manual scram and manual trip of automatic rundown system are initiated and reset from this panel.

4. Panels 35 and 36 (Coolant System) - The two coolant system panels include a display of the following variables.

$Q_{thermal}$	calculated thermal power from the reactor
T_{avg}	measured or calculated reactor temperature indicative of average reactor solid temperature
T_o	reactor exit gas temperature
T_i	reactor inlet gas temperature
T_{xhi}	heat exchanger hot inlet gas temperature
T_{xho}	heat exchanger hot outlet gas temperature
$\dot{W}_1$	primary loop gas flow rate
BS_1	primary loop blower speed
P_1	primary loop pressure
X_b	recuperator bypass valve stem position
%B	% bypass around recuperator
ΔP_{21}	pressure difference between primary and secondary loop

T_{xco}	heat exchanger cold outlet gas temperature
T_{dho}	heat dump hot outlet gas temperature
$\mathring{W}_2$	secondary loop gas flow rate
BS_2	secondary loop blower speed
P_2	secondary loop pressure
FS_1, FS_2	heat dump fan speeds

A variety of controls are included on the system panels. In particular, the system "independent" variables can be adjusted from here to achieve desired values of other variables as described in Sec. 5.2.1. As currently constituted, the panel provides the means for manual control of the reactor and coolant loops system. However, the design is compatible with projected automatic control systems that may be developed after operating experience is accumulated.

5. Panel 37 (Computer) - The computer console can be used to perform the following functions.

a. Demand logs

b. Enable and disable typewriters

c. Display alarm limits

d. Display or trend transducer outputs in engineering units

e. Enter new limits; delete analog input points from scan, or put them back on scan

f. Demand sequencing programs such as fuel loading

g. Inhibit computer (puts computer on stall)

h. Select outputs to be printed on all-purpose recorder.

Gas Cleanup System Panels - Racks 1 through 11 contain the controls and instrumentation used in the operation of the gas cleanup system. An elevation and a side view of three typical racks appear in Fig. 11.1.1.2. At the top of each rack is an inclined graphic panel which depicts a portion of the system. The condition of each valve in the system is shown by colored lights on the graphic panels, which also

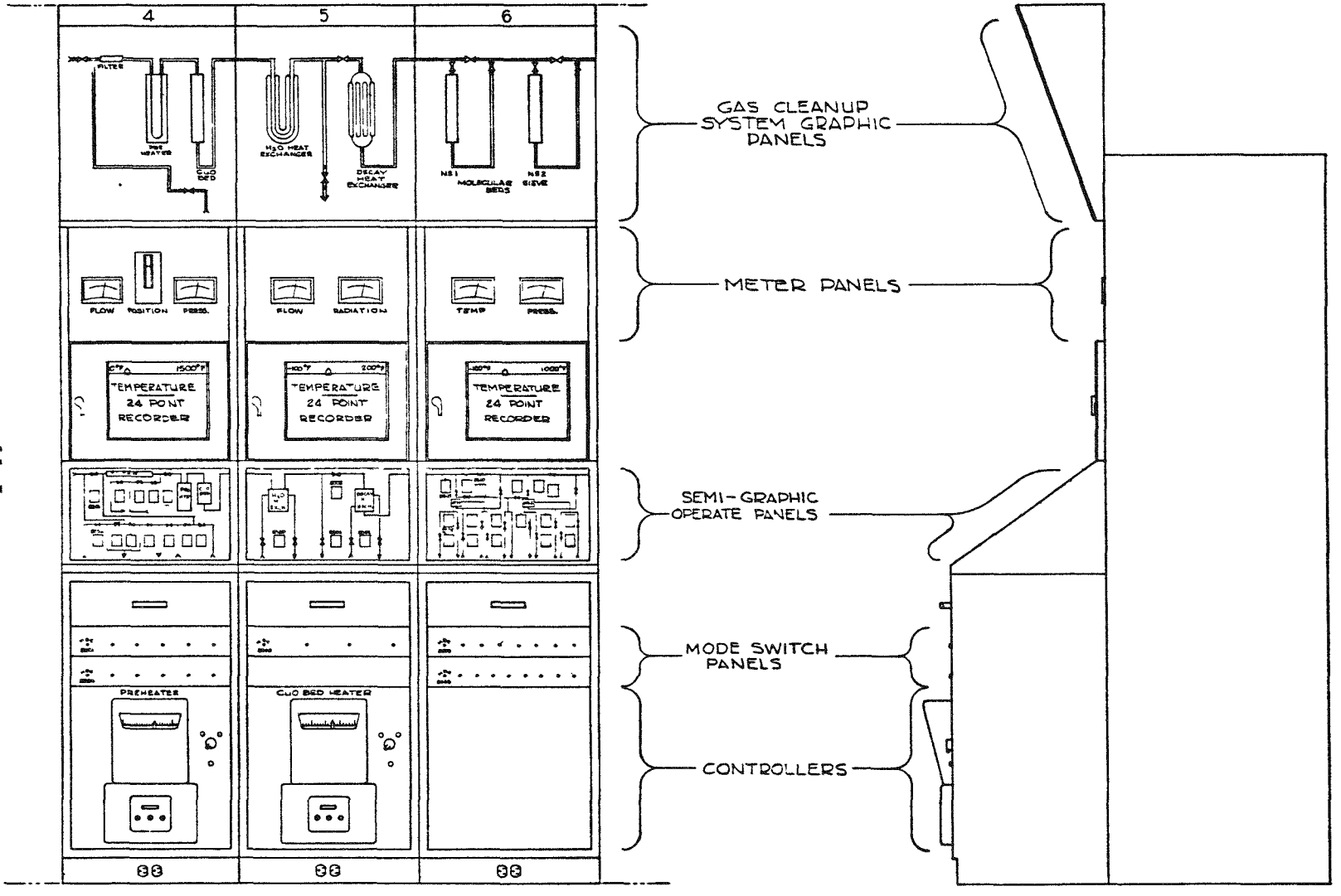

Fig. 11.1.1.2 Three typical control room panels for gas cleanup system

display the location of system transducers. Below the graphic panels are meters which indicate, and multipoint recorders which print out, the values of system parameters, and the controls for the blower and compressors. On inclined surfaces below the recorders are semigraphic panels on which are arranged the control switches for system valves. Next lower on the racks are panels that contain mode switches, which are wired into the valve operating switch circuits for future use, in conjunction with the computer, with semiautomatic or automatic control circuits. Initially, the mode switches are set for manual control of the entire system. At the bottoms of the panels are located the control units for the heaters and air.

Fuel Handling System Panel - A graphic panel on rack 12 displays the condition of the fuel handling system as it operates under computer control. On this rack are located manual switches with which gas lock valves can be closed and the core can be rotated, independent of the computer.

Coolant System Panels - At the top of racks 13, 14, 15, and 16 is an inclined panel on which appears a flow chart of the reactor and both coolant loops. This panel shows the location of the transducers that monitor the coolant system. Below the panel are located the controls for both coolant loop blowers and for the heat dump fan and the safety circuits' meters and controls. In rack 17 are a general purpose recorder and test meters.

Facility Monitoring Panels - Rack 18 contains the instrumentation for the facility area monitoring system. Also, on rack 18 is mounted a television monitor connected to a camera which is located inside the secondary containment structure. Above the rack is an inclined graphic panel that shows the condition of the facility electrical power load center, described in Sec. 10.2.1.

11.1.2 Instrumentation and Measurements

General Considerations - The instrumentation for the UHTREX facility is grouped, for channel designation and listing reasons, into nine function categories: temperature, pressure, flow, position, nuclear, electrical, stress, analysis, and control. In most of these classes, the basic transducer elements are conventional. In certain critical areas, however, special techniques and transducers are required. To satisfy the stringent sealing requirements necessary in the coolant systems, and to accommodate the restricted availability of the loops once operation has started, very special care was used in the design and installation of the instrumentation components to insure a high degree of reliability and maintenance-free operation.

The selection of transducers was guided by careful analyses of the radiation and temperature environments, and by considerations of high seal integrity, reliability, long-term performance, ruggedness, and minimum maintenance. Where possible, duplicate detectors are used and replaceable primary elements are employed to provide control backup and to simplify the maintenance of the system.

Except for the valve operators associated with the gas cleanup and helium handling systems, the control and data transmission channels are electrical. Pneumatic valve operators are used because of their proven reliability in operation and relative freedom from maintenance problems.

The instrumentation and control systems are designed to provide a major degree of protection to personnel and plant equipment by means of a system of electrical interlocks, sensing elements, relays, warning devices, and instruments. In the event of a component malfunction or failure, appropriate protective circuits are actuated and alarms are initiated to provide the automatic actions necessary to eliminate potential accidents or to give the operator time to take the required corrective action. Redundant channels are included in critical control

areas, and coincidence circuits are employed for initiating emergency procedures in order to reduce the occurrence of false actions due to instrument malfunctions.

Temperature Measurements - There are 278 channels of temperature measurement in the UHTREX systems. Except for two temperatures inside the reactor pressure vessel, all measurements are made with thermocouples. The other two temperatures are measured with acoustic thermometers developed by General Atomic. The large majority of the thermocouples are chromel-alumel; the only other type used is tungsten-5% rhenium/tungsten-26% rhenium. The following tabulation shows the distribution of transducers in the various UHTREX subsystems.

	Chromel-Alumel	W5Re/W26Re	Acoustic
Reactor	66	36	2
Primary loop	32	--	-
Secondary loop	34	--	-
Gas cleanup and storage	100	--	-
Stack	8	--	-
Total	240	36	2

Of the totals shown, about 45% measure the temperature of helium coolant or internal reactor and bed components, i.e., graphite, carbon, tubes, etc. The remainder are associated with either surface or utility stream temperatures. In the former category, only those inside the reactor pressure vessel, the recuperator, and the main heat exchanger cannot be replaced during the experiment. These thermocouples are wholly contained within the primary coolant system, and their signals are brought through leak-tight electrical connectors in the associated instrument pipes. Many of the others, e.g., in the cleanup system beds, can be replaced with great difficulty, but replacement is possible without disrupting the integrity of the major system components. These thermocouples are installed inside wells, and a secondary seal is made with compression glands and a seal-welded fitting.

Most of the chromel-alumel thermocouples are locally fabricated. Used in positions where the maximum temperature is 1600°F, the thermocouple units employ premium grade thermoelement wires, grounded junctions, 1/8-in.-o.d. stainless steel sheaths, and MgO insulation. All units are subjected to visual, electrical, dye-penetrant, and radiographic inspection and are calibrated against melting point standard equipment.

Because of physical size limitations and time-response considerations, chromel-alumel units that are installed in thermocouple wells use 1/16-in.-o.d., ungrounded junction assemblies of standard commercial quality, which have been subjected to a rigorous series of tests designed to detect physical or electrical deficiencies. A three-point calibration is run prior to their assembly into the system.

Temperature cycling and life tests were conducted with chromel-alumel prototype units. A maximum of 2600 h for any one unit and a total of 50,000 thermocouple-hours with 22 units were accumulated during these tests. No failures were observed, nor were any shifts detected in junction emf characteristics.

Thermocouples used for the measurement of temperatures above 1600°F have tungsten-5% rhenium/tungsten-26% rhenium junctions. This combination of thermoelements was chosen after extensive testing at LASL and the consideration of related information from other sources. Life tests at LASL with units of this type were run at temperatures up to 2500°F for over 2100 h. No adverse results attributable to the test conditions were observed. Features of the thermocouple unit design, illustrated in Fig. 11.1.2.1, include a 1/8-in.-o.d. niobium sheath, beryllia insulation, and a floating 1/4-in.-o.d. junction assembly. Designed to prevent failures caused by differential expansion stresses between the thermocouple wires and the sheath, the junction assembly also prevents undue stress on the welded junction, which may be weakened by embrittlement. All weld areas that are exposed to the embrittling environment of graphite are mechanically reinforced.

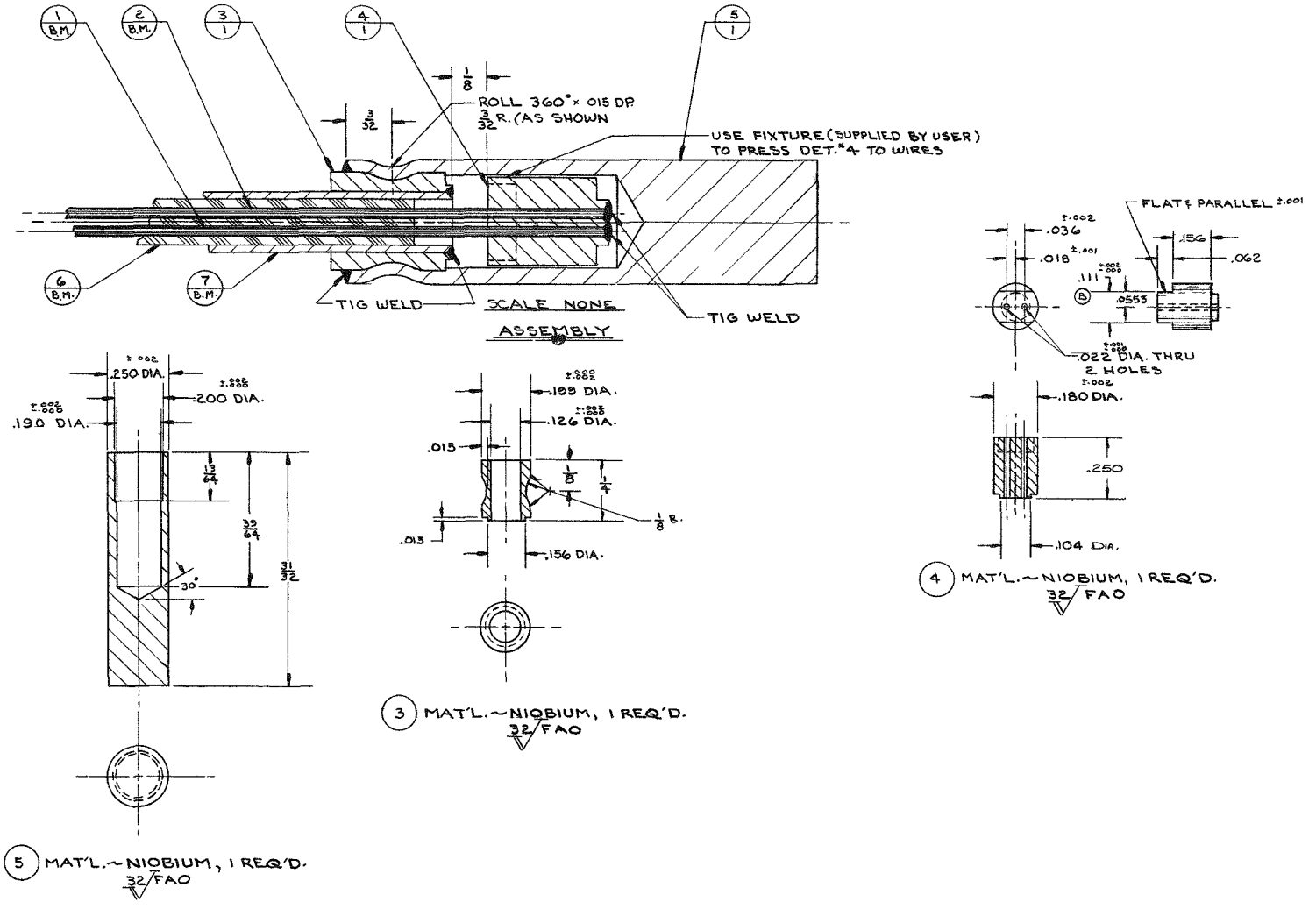

Fig. 11.1.2.1 Floating junction thermocouple assembly

Ten thermocouples, all W-5Re/W-26Re, measure temperatures in the movable core. Lead wires from each thermocouple junction run to the plate upon which the core is supported, and there the wires are connected to a set of two molybdenum contacts held in a ceramic block. The 10 contact blocks move as the core is rotated. Fixed to the bottom forging of the reactor vessel are two other contact blocks which are connected, in parallel, through the reactor thermocouple pipe to readout circuits. To read the output of a core thermocouple, an operator shifts the core until the proper movable contact block slides into position on either of the two fixed contact blocks. For an estimate of the reliability of the sliding contacts in the core environment, tests were run with a prototype sliding block assembly at 500°F in an atmosphere of helium contaminated with graphite dust. After 1600 h of operation, about 30,000 make-break contact cycles, the first transmission failure occurred, due to an oxide formation on a contact surface. Subsequent operation of the assembly removed the oxide, and the transmission of the 15-35-mV signal resumed.

Two acoustic thermometers measure the temperature of the helium stream at the reactor exit and the temperature of the fixed graphite reflector adjacent to the movable core. For each thermometer, a small acoustic cavity located at the point of interest is connected to two remote acoustic transducers with small diameter, gas-filled tubes. One transducer, serving as the transmitter, emits an acoustic signal into the cavity, which resonates. The other transducer detects the resonant signal, whose frequency is proportional to the square root of the mean temperature of the cavity. This system has excellent long-term stability and life because the acoustic cavity is inherently simple and can be made from niobium which is not susceptible to damage in the high temperature environment of the UHTREX reactor.

Cavities, tubing, and acoustic transducers are all completely contained within the primary gas system and operate at primary loop pressure. The transducers are located inside the bottom end of the reactor

instrumentation pipe in Room 402, out of severe temperature and neutron radiation environments. Electrical connections are fed through primary containment via penetration connectors. Access to the transducers for replacement or maintenance, although not a simple operation, is possible during shutdown. Each channel has its own automatic servo balance and readout chassis in the control room. A slave signal is available to the computer to facilitate raw data interpretation and logging.

The cavities are simple, but not the rest of the equipment required for operational use of the system. This fact, together with the poor time response and spatial resolution of the cavity, resulted in the relegation of acoustic thermometry to use as a backup to, and as an installed calibration system for, the less stable thermocouples installed in the reactor.

An acoustic thermometer, operated for an extended period in a LASL laboratory, was calibrated at temperatures up to 2600°F with excellent correlation between calculated and measured values of temperature.

Pressure Measurements - There are 105 channels of pressure and differential pressure measurements, distributed through the various subsystems as follows.

	Pressure		Differential Pressure	
	Helium	Service	Helium	Service
Reactor and primary loop	12	1	13	2
Secondary loop	7	5	11	--
Gas cleanup and storage	22	11	11	10
Totals	41	17	35	12

All transducers that are installed on the helium loops are designed to withstand the severe environment. Signals produced by the transducers are all electrical, to satisfy the requirements for remote operation and for leak-tight seals around the signal conduits where they penetrate the secondary containment. Units are designed for use at locations where estimated maximum radiation dosages are 10^{12} nvt neutrons

(thermal and fast) and 10^6 R gamma, and maximum temperatures are 200°F. Where higher radiation levels or temperatures prevail, transducers are located in adjacent, shielded rooms and connected to the point of measurement with stainless steel tubing.

All absolute pressure units in helium service are designed for proof test at 50% above their full-scale range and for diaphragm burst pressures at least 100% above full-scale range. In the event of diaphragm failure, the all-welded transducer cases provide secondary back-up capability far in excess of any pressures available in any of the helium systems. Helium pressure transducers employ four-active-arm strain gage bridge sensors and have full-scale outputs of approximately 25 mV dc.

Two different types of differential pressure transducers are used to satisfy different service requirements. For applications where large differential pressures cannot be generated, e.g., across flow meters, the transducers have light duty diaphragms and strain gage sensors of the sort used in the absolute transducers. For those locations where high transient pressure surges can occur, differential pressure transducers are used that are capable of taking full line pressure, 500 psi, without diaphragm failure or calibration shift. The transducers have variable reluctance sensors which require external demodulation circuitry, use a 3-kc power source, and produce raw dc output signals of about 0.2-0.3 volt. Another version of the same units, incorporating a double diaphragm as backup protection against cross leakage, is used for the measurement of primary-secondary loop differential pressure across the main heat exchanger. All parts of all units exposed to system helium are metallic, and all connections are welded.

A testing program for pressure transducers was undertaken to verify conformity with specifications and to develop long-term histories of calibration shifts, leak integrity, reliability, and overall transducer performance characteristics. Performance tests were run dynamically with a pressure cycling system, in which one unit of each type and

range was cycled over its full-scale range. Differential units were cycled at 500-psi line pressure. Each transducer was subjected to 200,000 cycles of operation, over a 4000-h period, at temperatures that reached 200°F. When the transducers were rechecked at the end of the performance tests, no leaks were found and calibration shifts were all < 1%. One of the double-diaphragm, differential pressure transducers was cycled for 5000 h, 250,000 full-scale cycles, without a seal failure or calibration shift.

Flow Measurements - The measurement of helium flow in the coolant loops and gas cleanup system (GCS) is made with Gentile flow tubes. These are impact-type head meters designed for accurate measurement with low head loss. The differential pressure signal developed by the tube is converted to a 0-to 25-mV dc signal with a Dynisco transducer and is fed, with absolute pressure and temperature data, to the on-line digital computer for the calculation of helium flow. The flow information, in engineering units, is indicated by meters on the control panels and is logged on typewriters by the computer data system.

The measurement of air, water, and glycol flows in the gas cleanup system is made with orifice plates connected to differential pressure transmitters. The 1-to 5-mA dc signal from the transmitter is conditioned to 0-1 V dc, and fed to meters on the GCS panels and to the data system for logging.

Oxygen flow to the copper oxide bed in the GCS is monitored with a thermopile mass flowmeter. The generated signal is a dc voltage proportional to the rate of mass flow through the tube. The information is presented on a meter at the GCS control panel and is sent to the computer system for logging.

Position Measurements - Valve limit positions throughout the piping systems are derived from snap-acting switches. Magnetic proximity devices are used to signal similar information from the fuel conveyors and the control rod drives. These signals are used to drive lamps and relays in the control room racks and are fed to the computer where the signals are scanned once per second.

Analog position measurements are derived either from potentiometers or from selsyns attached to the monitored device. Selsyns are used to transmit position information from the control rods, the reactor core, and the fuel conveyors. Where auxiliary signals are required to duplicate the selsyn position, a multiturn potentiometer is ganged through a gear train to the selsyn receiver.

Stress Measurements - High temperature weldable strain gages are mounted on the reactor pressure vessel and on the recuperator pressure vessel. The strain gages, designed to withstand temperatures up to 600°F and a moderate amount of radiation for a limited period of time, should continue to function for a period well into the first high temperature, full power cycle of reactor operation.

Power for the strain gages comes from signal conditioning equipment located outside the secondary containment area. In addition to power supplies, the conditioning equipment consists of span and zero adjustment potentiometers and bridge completion resistors, the outputs of which are fed to the computer system for monitoring and data recording.

Sound Monitors - Carbon microphones are mounted in contact with sound producing units of each control rod drive, the core indexing mechanism, each coolant blower, the fuel handling system, and both heat dump fans. The signal from each audio transmitter is fed to individual preamplifiers. A single signal output from the preamplifiers is selected for further amplification and drives a speaker on the main operations console.

Audio monitoring is, of course, a qualitative measurement used to complement existing instrumentation and not as a substitute. The monitoring of equipment sounds has proved to be useful in the early detection of abnormal operating conditions. Furthermore, a more orderly operation results when audio feedback is available to operations personnel.

Analytical Measurements - Analytical measurements in the gas clean-up system are described in detail in Sec. 7.4.1. The control room

instrumentation for these measurements is located in racks 1, 2, and 3. All readout and control functions are centered at these locations and are under the direct surveillance of the control room operator. Auxiliary equipment concerned with helium sampling is located within the secondary containment area and is operated remotely from the control room. The status of the sample valves associated with these operations is displayed on the graphic panel on racks 4 through 11.

Meteorological Instrumentation - There are eight temperature measurements of the outside air made at four different locations along the stack at elevations of 25, 50, 75, and 100 ft. These data are fed to the computer system for logging.

Wind direction and velocity information is transmitted from a tower located on the roof of the secondary containment structure to indicators in the control room.

Additional outside air temperature and humidity measurements made in the plant ventilation systems are displayed at the utility control board in the electrical equipment room.

Signal Conditioning System - The signal conditioning system, which provides the means for conditioning transducer outputs into useable, calibrated signals, is composed of rack-mounted units each containing 12 individual modules of signal conditioning circuitry. The units are located in racks 28, 29, and 30 in the control room where they are easily accessible. The signal conditioning circuits provide the capability of adjusting the zero and span of each transducer. Solid-state operational amplifiers are used to isolate meters and relays so that they do not disturb the transducer output signals. Test jacks are provided for monitoring channel output and for adjusting zero and span as required by the transducer calibrations. Each channel has a fuse to prevent the overloading of the power supply by electrical shorts in the transducer or associated wiring. An additional feature of the signal conditioning units are test buttons that connect artificial full-scale signals for tests of the proper operation of the electronics and equipment associated with transducer channels.

The signal conditioning circuits are grouped by type of transducer served. Each group has its separate set of two power supplies wired in parallel. Each of the pair of power supplies is isolated from the other. If a failure toward zero output or an internal short develops in one power supply, the load is assumed by the other power supply without interruption.

11.1.3 On-Line Process Computer

An on-line process computer aids in the operation of the reactor, the reactor coolant loops, and the gas cleanup system. The computer monitors a large number of variables to ensure that they are within their safe operating limits, monitors changes in the status of components such as valves, and prepares typewritten logs of data and activities. Control of the fuel handling system is another function of the computer as are the associated tasks of fuel inventory and history preparation. The computer has the capability for control of reactor power, coolant flow, and coolant temperatures. Basic control and safety of the reactor is under the surveillance of the operating personnel, aided by automatic alarm and protection circuits, described in Sec. 11.4. Meters, recorders, instruments, and manual controls allow the operator to safely hold the reactor at steady state or shut it down in the event the computer is not functioning properly.

The central processor is a small solid-state, general purpose computer supplemented with features that make it suitable for on-line process use. Equipment included in the central processor is listed in Table 11.1.3.1. A large number of analog and digital inputs and outputs afford a considerable capability for monitoring and controlling. The special equipment makes feasible the on-line use of the system.

Twenty system interrupts, ordered as shown in Table 11.1.3.2, facilitate "time sharing" of input/output to enable immediate recognition of special external or internal conditions. The computer automatically scans the interrupts after executing each instruction, with

TABLE 11.1.3.1

PROCESS COMPUTER COMPONENTS

General Purpose Computer Equipment

Arithmetic unit	24-bit word plus parity bit 16 μsec to add 32 μsec to multiply
Magnetic core storage	4096 words
Drum storage	31,680 words
Input-output typewriter	10 characters/sec
Paper tape punch	60 characters/sec
Paper tape reader	300 characters/sec

Process Computer Equipment

Visual display	
4 logging and alarm typewriters	10 characters/sec
608 analog inputs	Scanned at 200/sec (max)
516 digital inputs	Scanned at 190,000/sec
24 analog outputs	Updated twice/sec
444 digital outputs	20 to 4000 outputs/sec

Special Equipment

20 interrupts

Automatic safe shutdown on power failure

Stall warning

Watchdog timer

Real time clock

TABLE 11.1.3.2

UHTREX INTERRUPT ORDER

1. Power on
2. Power outage
3. W-buffer, end of word } Drum-core transfers
4. W-buffer, end of block }
5. Watchdog timer
6. Real time clock
7. Analog to digital converter complete
8. Elapsed time counter complete
9. UHTREX system
10. UHTREX system
11. UHTREX system
12. UHTREX system
13. Relay output (matrix) complete (digital output matrix)
14. Analog output complete
15. Punch (on EOM-POT lines) complete
16. Alarm typewriter complete
17. Log typewriter complete
18. Computer console
19. Main system operations } from UHTREX system operation panels
20. Auxiliary system operations }

three exceptions, and either transfers control to the program associated with the highest order interrupt that is present, or continues the current sequence of instructions if no new interrupt has occurred. On completion of an interrupt program, control returns to the sequence of instructions from which it was transferred. However, after this return, the interrupts are again scanned, to insure that the program associated with the highest order of interrupt is executed. The computer neither forgets an interrupt nor gets lost if multiple interrupts occur.

Most of the time, there are no active interrupts and the computer is in the "executive" program or a program controlled from the executive. In the executive the computer constantly loops through a list of about 30 programs to see if it is time to run one of them. These programs include the input scans, which are done once per second; two logs, which are done once per hour; and operator console programs; which are done only on request of the operator.

Some interrupts originate in the input/output equipment, and indicate either that information is ready to be transferred into memory, every 5 msec during an analog scan, for example; or that an output operation has been completed and another output may be started, every 100 msec in the case of a log. The executive program and the ordering of the interrupts ensure that computer programs are handled in a sensible sequence, with priority given to the most important activity. Interrupts 9 through 12 are reserved for special reactor system signals, at least some of which are associated with emergency conditions. For example, interrupts are activated by neutronic signals from the reactor or signals concerning pressure changes in the coolant secondary loops.

The stall warning equipment which automatically prevents the computer from making system changes, operates upon receipt of the following signals: memory parity error, manual operation of the "Inhibit Computer" pushbutton, failure of certain power supplies, or a watchdog timer interrupt. Except for parity error and some power supply failures, the

computer does not stop operating during stall, but the computer cannot make changes in any of the analog or digital outputs that are connected to process equipment. The computer has no control capability in the stall condition, but, depending on the source of the stall signal, may continue to monitor inputs, run typewriters, and operate lights and recorders. The net effect of the stall warning equipment is to transfer all operating systems from computer operation to manual when a computer malfunction is detected.

The watchdog timer is a safety device that has a high position on the interrupt list. It is a 5-sec alarm clock that is ordinarily reset to zero many times per second by the executive routine. However, if the computer stops, if an endless loop is encountered, or if the computer does not return to the executive program and reset the watchdog timer at least once every five sec, the timer generates interrupt No. 5, and puts the computer in stall.

The real-time clock generates an interrupt (No. 6) every second, which transfers the computer to a program that increments the real time count stored in the computer, does several other short jobs, and returns the computer to the interrupted program. The executive program needs real time to identify programs that are run periodically.

Computer Jobs - Some of the computer jobs, which are all passive in the sense that they do not involve any control functions, are described below.

1. Monitor and Alarm - About 50 vital analog signals are sampled, linearized, and compared with high and low limits each second. If any signal is found to be out of limits, a message is typed on the alarm typewriter and, for critical variables, an annunciator is operated. A second set of 50 analog signals is sampled every 3 sec and treated in the same way. The remaining 508 signals are sampled once every 15 sec.

All digital inputs are scanned once per second, changes in the condition of system components are recorded, and comparisons are made with acceptable configurations. An alarm is initiated if an unacceptable or inconsistent configuration is found.

2. Calculations - A small number of process variables, such as flow rates and blower coefficients are calculated each second and compared with limits in the same manner as the analog signals. Some of the calculated variables are displayed on the main operations console. Calculations such as heat balances and reactivity balance are made once a minute and any unusual results printed as an alarm message. A large number of calculations, such as heat balances, blower efficiency, heat transfer coefficients, helium inventories, and molecular sieve bed loading, can be calculated when needed or when requested by the operator.

3. Hourly and Demand Logs - The computer prepares and types two hourly logs, with 40 entries each, on paper with preprinted headings in engineering units. Two of the four typewriters are used for these logs. In addition, the operator can request as many as 20 demand logs that are typed on a third typewriter. The fourth typewriter is reserved for alarm messages. The demand logs include the current values of all analog points, a summary of points currently on alarm, a summary of limits, a summary of points which are not being scanned, a summary of all surface or internal temperatures, a summary of strain gage readings, and the results of special calculations. The fuel history log, which is discussed below, is the longest demand log.

4. Operation Monitoring - The control switches on the system operating panels are connected to a computer digital input matrix and to interrupt No. 19 or 20. Every time an operator actuates one of the momentary control switches to open a valve, the computer receives an interrupt and scans the digital inputs related to that interrupt, to identify the control switch that has been actuated. In its minimum response, the computer types a message on the alarm typewriter to

record the switch action and the time. In some cases the computer may check the action to see if it is acceptable, based on the current status of other valves, rod positions, and analog signals. The computer may take action if the check reveals that the operator made a mistake; the computer can initiate an alarm or can prevent, through an interlock, the completion of the action initiated by the operation of the switch.

5. System Histories - The computer keeps a number of histories, e.g. the number of MW days of operation, number of days of operation, quantity of contaminants removed in the gas purification system, and number of revolutions of the core. The one large job of this type is the compiling of a history of the 1248 fuel elements in the core. The fuel history program includes a record of each fuel element's serial number, its loading, and its position in the reactor as a function of time. These data, when combined with a computer record of reactor power and operating time, allow the computer to produce each fuel element's history. The history is available to the operator on demand and is logged each time an element is discharged from the computer.

The computer-maintained histories of fuel elements, power, temperature, and flow are logged on the paper tape punch once per week in a format that is compatible with other LASL data processing equipment. Thus, historical data from the reactor will be available in convenient form for later analysis.

Testing - A 3-month, 24-h per day, reliability demonstration run of the computer system was completed on June 22, 1966. During the run, programs continually exercised and checked the computer systems. Where feasible, actual on-line process programs, e.g., the executive, analog scan, linearization, and log programs, were used. Over the 3-month period of continual operation, the computer system experienced three failures and 6.5 h of down time, all of which occurred in input or output equipment. There were no failures in the central processor.

Computer Control - In the design and construction of the computer and of the instrumentation for the various operating systems, the

capability was included to permit computer control of system variables through closed loop feedback systems. During the initial phases of reactor operation, the only system that will be under direct computer control is the fuel handling system. As operating experience accumulates and the dynamic characteristics of each operating system are established, other systems will operate under computer control. Table 11.1.3.3 lists computer control systems for which the instrumentation is installed on the main operations console. None of these control systems will be put to use until all steps of the design and test procedures described in Item 4 below are completed. Computer control of the control rod drives will not be attempted until a program for the switch to computer control has been reviewed by the Division of Reactor Development and Technology of the AEC.

1. Control Outputs - The computer has 24 analog outputs and 44 digital outputs. Twelve of the analog outputs are 0 to +20 V, and 12 are 0 to 20 mA. The digital outputs include 288 magnetically latching relays, one-hundred and two 48-V single shots of various durations, and 54 flip-flop type outputs producing 48-V signals. Some of these outputs are used to run recorders, panel lights, and console meters. Many outputs are available to operate valves and motors in the reactor, the coolant system, and the gas purification system.

2. Control Modes - Many of the control switches for valves or motors in the operating systems have associated mode selector switches. The mode selector has three positions: Manual, Computer, and Both. When the mode selector is in the Manual position, and the operator actuates a control switch, the signal is transmitted directly to the controlled device, as is normal for manual control. The computer can monitor this action, but does not have any active control over the device. If the selector switch is in the Computer mode, actions originate in a computer program and the computer output is transmitted to the device. In the Both mode, the control circuit requires simultaneous signals from both the operator and the computer before a signal is transmitted to the system.

TABLE 11.1.3.3

CLOSED LOOP COMPUTER CONTROL SYSTEMS CURRENTLY AVAILABLE

System Number	Demanded Variable	Physical Variable Adjusted to Achieve Demand
1A* or	Primary Coolant Flow Rate ($\dot{W}_1$)	Primary Blower Speed (N_1)
1B	Reactor Thermal Power (Q_t)	Primary Blower Speed (N_1)
2A* or	Secondary Coolant Flow Rate ($\dot{W}_2$)	Secondary Blower Speed (N_2)
2B	Temperature of Coolant at Heat Exchanger Cold Side Outlet (T_{xco})	Secondary Blower Speed (N_2)
3	Temperature of Coolant at Heat Exchanger Hot Side Outlet (T_{xho})	Heat Dump Fan Speed (FS)
4	Temperature of Coolant at Reactor Inlet (T_i)	Bypass Valve Position (X_b)
5	Reactor Neutronic Log Power (LOG Q_n)	(Selected) Reactor Plug Rod Position (X_p)

*Neither 1A and 1B nor 2A and 2B run concurrently.

The mode selection feature provides flexibility in dividing authority between the computer and operator. It also supplies the means for interlocking control circuits and checking out computer programs.

3. Sequencing and Interlocking - The computer can operate valves and motors in a system and can be programmed to operate them in fixed sequence. An example of a sequential operation is the loading of a fuel element. After receiving, through the computer console, the fuel element's identification number, its fuel load, and the channel to which it is to be loaded, the computer operates in sequence the core indexing motor, the two secondary gas lock valves, the charge conveyor, three more gas lock valves, six pressure equalization valves, the elevator, and a loading ram. A

similar sequence of operations is performed to remove the discharged fuel element. Checks on valve positions, loader positions, and system pressures are made throughout the loading and unloading sequence.

Until confidence in the computer is established and the programs are thoroughly tested, many of the mode selector switches in a sequence of operations will be in either the Both or Manual position. Then the sequence of computer-controlled operations always stops until the operator actuates the correct switch. If most switches are placed in the Manual position and a few in Both, the computer can check a sequence of operations done by an operator. Thus, the computer can provide interlocks on the operator actions, just as it is possible for the operator to check the computer operation.

All of the devices that can be controlled by the computer are described in Tables 11.1.3.4 through 11.1.3.7. Table 11.1.3.4 is a list of the valves that have on-off manual switches and associated mode switches and are actuated through latching relays. Those valves that have a computer interlock and those that are included in plans for computer-controlled systems are identified. Devices listed in Table 11.1.3.5 have momentary manual switches, associated mode switches, and "toggle" outputs for computer control. The "toggle" is a 48-V output from a solid state power supply which the computer switches on or off. The advantage of the toggle is that the signal is set to "off" in the event of a computer or power supply failure. The devices described in Table 11.1.3.6 do not have manual controls or mode switches, and can be operated only by the computer through latching relays. Finally, Table 11.1.3.7 lists devices that have potential uses in computer control systems, but for which the control wiring is not installed.

Although they are not planned for use under direct computer control, the valves described in Table 11.1.3.8 send digital inputs to the computer when the valves are operated by independent automatic control systems.

4. Control System Design and Testing - A considerable understanding of the dynamics of the reactor and coolant system has been obtained from

TABLE 11.1.3.4

VALVES WITH MANUAL AND MODE SWITCHES AND LATCHING RELAY CONTROLS

Designator	Function	Computer Interlocked	Computer Control
8406 to 8417	Helium-Auxiliary Gas Lock Valves	Yes	Yes
8501 & 8520	Helium-GCS Isolation Inlet-Outlet (1)	Yes	
8502	Helium-Filter Isolation Outlet		
8503	Helium-Decay Heat Exchanger Block	Yes	
8504	Helium-Decay Heat Exchanger Bypass Block		
8505	Helium-Blower Block on Exhaust		
8508 & 8509	Helium-Molecular Sieve - 1 Block on Inlet-Outlet	Yes	
8510	Helium-Molecular Sieve - 1 Block on Bypass		
8511 & 8512	Helium-Molecular Sieve - 2 Block on Inlet-Outlet	Yes	
8513	Helium-Molecular Sieve - 2 Block on Bypass		
8514 & 8516	Helium-Delay Bed Block on Inlet-Outlet		
8515	Helium-Delay Bed Block on Bypass		
8517	Helium-Side Stream Adsorption Bed Block on Inlet	Yes	
8518	Helium-Side Stream Adsorption Bed Block on Bypass	Yes	
8519	Helium-Side Stream Adsorption Bed Block on Outlet	Yes	
8524	Oxygen-Block on Inlet	Yes	
8525	Helium-Molecular Sieve - 1 Purge Inlet	Yes	
8526	Helium-Molecular Sieve - 2 Purge Outlet	Yes	
8527	Helium-Side Stream Adsorption Bed Purge Inlet	Yes	

TABLE 11.1.3.4 (Continued)

Designator	Function	Computer Interlocked	Computer Control
8528	Helium-System Pressure Bleed		
8529	Helium-System Pressure Makeup		
8530	Helium-High Pressure Working Tank Outlet		
8531	Helium-High Pressure Working Tank Inlet	Yes	
8532	Helium-High Pressure Compressor Bypass	Yes	
8535	Helium-High Pressure Storage Inlet	Yes	
8536	Helium-High Pressure Storage Outlet	Yes	
8538	Helium-System Recycle Inlet	Yes	
8542	Helium-Low Pressure Storage Inlet	Yes	
8543	Helium-New Helium Inlet		
8544	Helium-Low Pressure Receiver Outlet	Yes	
8545	Helium-Low Pressure Comp. - 1 Stage 1 Bypass		
8548	Helium-Low Pressure Comp. - 2 Stage 1 Bypass		
8553	Helium-Stack Vent		
8554	Helium-High Pressure Storage Vent		
8555	Helium-Side Stream Adsorption Bed Vent	Yes	
8556	Helium-Vacuum Pump Bypass		
8559	Helium-Jacking Gas Block		
8560	Helium-Molecular Sieve - 1 Vent	Yes	
8561	Helium-Molecular Sieve - 2 Vent	Yes	
8562	Helium-High Pressure Storage Isolation	Yes	
8563	Helium-Jumper Stack to Low Pressure Receiver		
8564	Helium-Low Pressure Receiver from Fuel Load System		

TABLE 11.1.3.4 (Continued)

Designator	Function	Computer Interlocked	Computer Control
8565	Helium-Side Stream Adsorption Vent to Receiver	Yes	
8566	Helium-Block for Valve 8529		
8571	Oxygen-Line Vent		
8572 & 8573	Glycol-Cooler Inlet-Outlet		
8574 & 8575	Glycol-Delay Bed Inlet-Outlet		
8576 & 8577	Glycol-Sidestream Adsorption Bed Inlet-Outlet	Yes	
8578	Air-Secondary Containment Test		
8580 & 8581	Water-Cooler Inlet-Outlet		
8582 & 8583	Water-Decay Heat Exchanger Inlet-Outlet		
8588	Air-Side Stream Adsorption Bed - 2 Jacket Vent	Yes	
8589	Air-Side Stream Adsorption Bed - 1 Jacket Vent	Yes	
8590 & 8591	Water-Low Pressure Compressor Precooler Inlet-Outlet		
8592 & 8593	Water-High Pressure Compressor Cooler Inlet-Outlet		
8594 & 8595	Water-Low Pressure Compressor - 2 Cooler Inlet-Outlet		
8596 & 8597	Water-Low Pressure Compressor - 1 Cooler Inlet-Outlet		
8600	Air-Heater Inlet		
8601	Air-Molecular Sieve Bed - 1 Cold Inlet		
8602	Air-Molecular Sieve Bed - 1 Hot Inlet		
8603	Air-Molecular Sieve Bed - 2 Hot Inlet		
8604	Air-Side Stream Adsorption Bed Hot Inlet	Yes	

TABLE 11.1.3.4 (Continued)

Designator	Function	Computer Interlocked	Computer Control
8605	Air-Molecular Sieve Bed - 2 Cold Inlet		
8606	Air-Side Stream Adsorption Bed Cool Inlet	Yes	
8612	Helium-Secondary Loop Makeup Inlet		
8613	Helium-Secondary Loop Vent		
8614	Helium-Helium Dock Filter Outlet		
8623 & 8624	Water-Blower Inlet - Outlet		
8625	Air-Molecular Sieve - 2 Jacket Vent		
8626	Air-Molecular Sieve - 1 Jacket Vent		
8627	Air-Molecular Sieve - 1 Jacket Exhaust		
8628	Air-Molecular Sieve - 2 Jacket Exhaust		
8629	Air-Side Stream Adsorption Bed Jacket Exhaust	Yes	
8630	Glycol-Side Stream Adsorption Bed - 1 Line Drain	Yes	
8631	Glycol-Side Stream Adsorption Bed Jacket Drain	Yes	
8632	Glycol-Side Stream Adsorption Bed - 2 Line Drain	Yes	
8641	Helium-Copper Oxide Sample		
8643 to 8648	Helium Sampling Valves		

TABLE 11.1.3.5

DEVICES WITH MOMENTARY MANUAL AND MODE SWITCHES AND TOGGLE CONTROLS

Designator	Function	Computer Interlocked	Computer Control
8400 to 8405	Helium - Gas Lock Valves	Yes	Yes
8441	Core Index Drive	Yes	Yes

TABLE 11.1.3.6

DEVICES UNDER COMPUTER CONTROL THROUGH LATCHING RELAYS

Designator	Function	Computer Interlocked	Computer Control
8425 & 8439	Load Rams	Yes	Yes
8441	Dislodger		Yes
8442	Preloader	Yes	Yes
8443	Elevator	Yes	Yes

TABLE 11.1.3.7

DEVICES PLANNED FOR POTENTIAL COMPUTER CONTROL

Designator	Function	Computer Interlocked	Computer Control
5007	Primary Blower Speed Control		Yes
5002	Secondary Blower Speed Control		Yes
5004 & 5005	Heat Dump Fan Speed Control		Yes
3276	Bypass Valve Position		Yes
8351 to 8362	Plug and Control Rods	Yes	Yes

TABLE 11.1.3.8

VALVES UNDER AUTOMATIC CONTROL WITH INPUTS TO COMPUTER

Designator	Function	Computer Interlocked
8475	Helium - Secondary Isolation No. 1	
8476	Helium - Secondary Isolation No. 2	
8477	Helium - Secondary Bypass	
8533	Helium - High Pressure Compressor Inlet	Yes
8534	Helium - High Pressure Compressor Outlet	Yes
8537	Helium - High Pressure Compressor Vent	Yes
8539	Helium - Emergency Blowdown	
8540	Helium - Blowdown	
8546	Helium - Low Pressure Compressor - 1 Inlet	Yes
8547	Helium - Low Pressure Compressor - 2 Inlet	Yes
8549	Helium - Low Pressure Compressor - 1 Interstage	
8550	Helium - Low Pressure Compressor - 2 Interstage	
8551	Helium - Low Pressure Compressor - 1 Outlet	Yes
8552	Helium - Low Pressure Compressor - 2 Outlet	Yes
8557	Helium - Vacuum Pump Inlet	
8558	Helium - Vacuum Pump Outlet	
8567 & 8569	Helium - Low Pressure Compressor - 1 Vent	Yes
8568 & 8570	Helium - Low Pressure Compressor - 2 Vent	Yes

the studies, described in Sec. 5.2.1, that produced the digital simulation program, UHXCOM. To test the suitability of system control programs, each will be tried in the UHXCOM simulation under a variety of operating conditions. The control loop gain, timing, etc. will be varied to determine optimum design. Then, the optimized control system designs will be investigated by operating the real control hardware and program with a simulated physical system. The simulated systems vary in complexity from a simple gain term to a sophisticated, 100-amplifier, analog computer model of the reactor, recuperator, heat exchanger, and heat dump.

As each component of the system becomes operational, its static and dynamic characteristics will be determined and compared with those predicted by the UHXCOM program. If there are significant discrepancies between anticipated and actual behavior, the computer control system design and the various system simulations will be reviewed and necessary design changes will be made.

Computer control loops will not be used routinely until they are completely debugged, thoroughly understood, and have gained the complete confidence of design and operating personnel. The computer control loops will be closed with considerable care; the performance of each control loop will be monitored continuously by an operator during the initial period of control loop operation. An operator can disable any loop instantly at any time by switching to Manual.

11.2 Reactor

11.2.1 Nuclear Instrumentation

The reactor nuclear instrumentation system consists of 11 channels:

1. Two neutron counting channels
2. Two log power channels
3. Two linear power channels
4. Four safety level channels (reactor safety system)
5. One log gamma flux channel.

The dynamic range of each neutron flux measuring channel is plotted in Fig. 11.2.1.1.

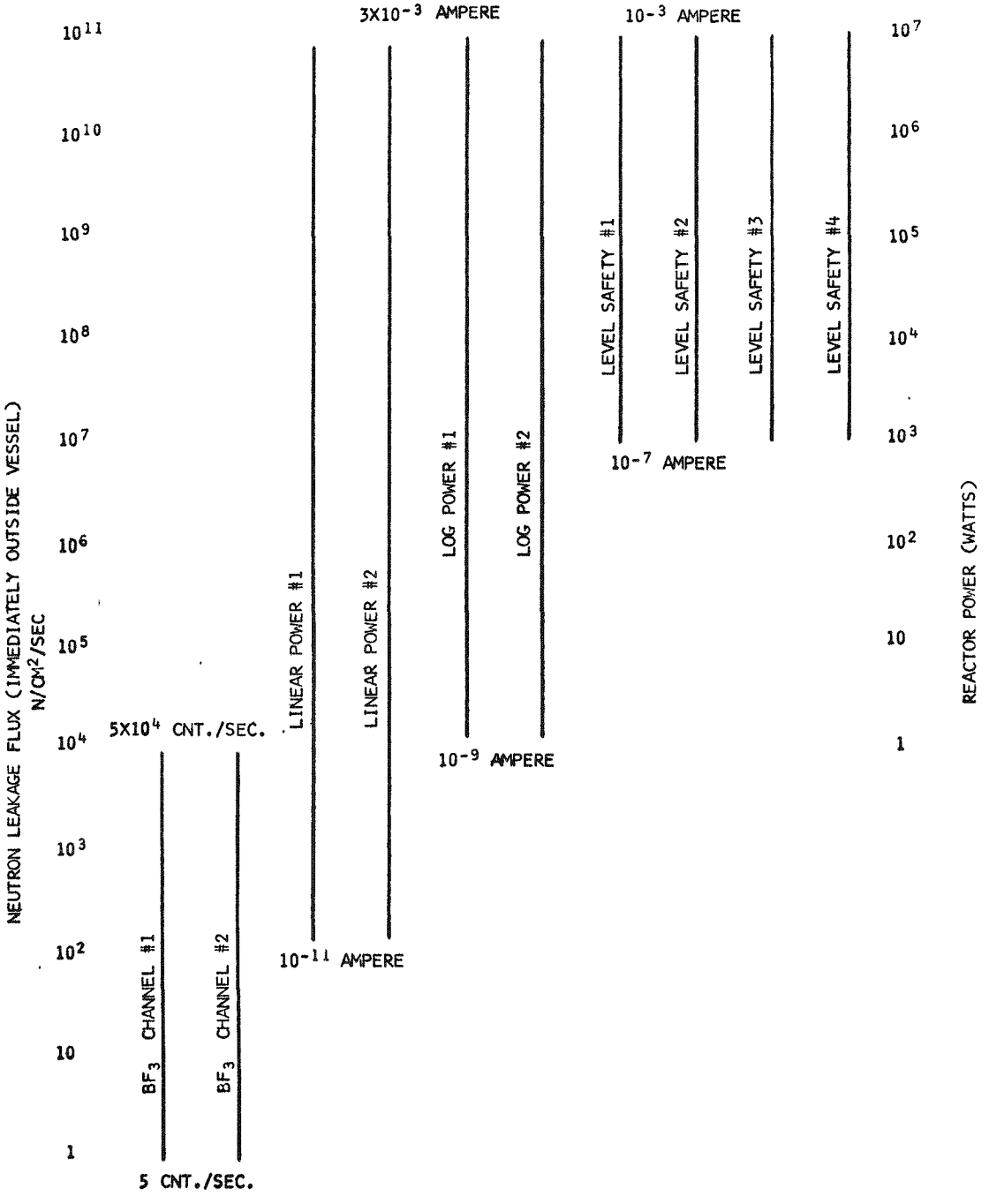

Fig. 11.2.1.1 Dynamic ranges of neutron flux measuring channels

All neutron detectors are located outside the reactor pressure vessel. Measurements made during UCX[1] showed that the leakage neutron flux immediately outside the vessel should be $\sim 10^4$ n/cm^2-sec per W of reactor power.

Neutron Counting Channels - Two neutron counting channels are used to monitor the reactor when it is shut down, and to provide multiplication data for reactor startup. A block diagram of the channels appears in Fig. 11.2.1.2. Figure 11.2.1.3 shows a typical shield for the startup detectors which are located adjacent to the reactor. The shield, made of high purity lead, has been designed to improve the neutron-to-gamma ratio by a factor of 100. Cooling of the shield is accomplished with a flow of 0.1 gal/min water through aluminum tubing within the lead.

To prevent radiation damage, the BF_3 detectors are removed from the high flux region of the reactor vessel during high power operation by individual actuators which withdraw the detectors into the shield slabs above the reactor.

Reactor Startup - An external neutron source is used for reactor startup. The source, 10^8 n/sec ^{238}PuBe, is positioned immediately outside the reactor vessel at the core midplane. The BF_3 startup detectors are located directly across the reactor at the same radial distance from the center as the source. The UCX source-detector experiments demonstrated that this geometry yields satisfactory core multiplication for reactor startup. A minimum of 5 counts per second is expected from each BF_3 detector when core multiplication equals 10.

Log and Linear Power Channels - All of the log and linear power channels diagrammed in Fig. 11.2.1.2 are conventional nuclear instrumentation which supplies neutron level information above the source range. The neutron detectors are shielded in the same manner as the BF_3 detectors to improve the neutron-to-gamma ratio.

---

[1]Appendix D.

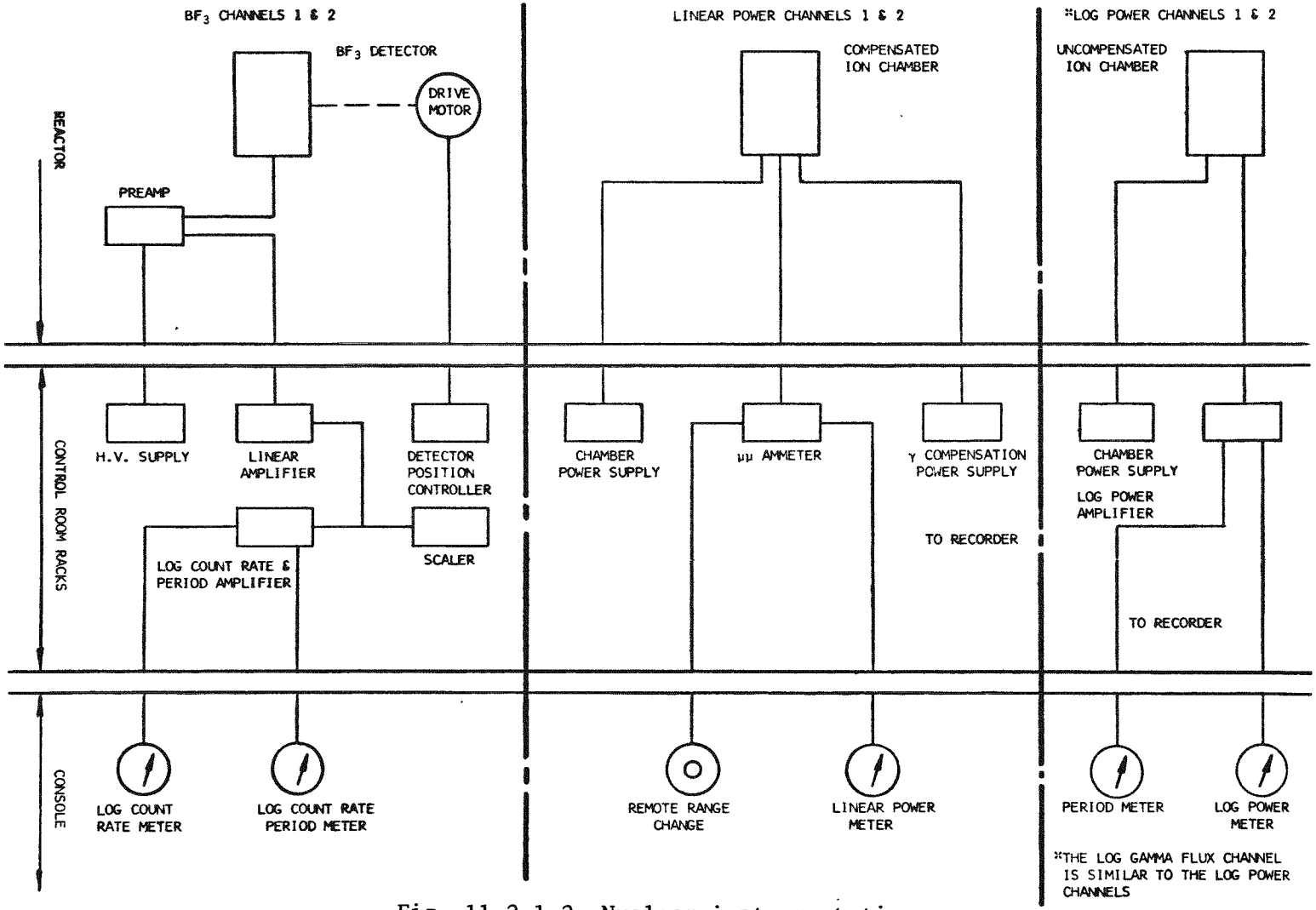

Fig. 11.2.1.2 Nuclear instrumentation

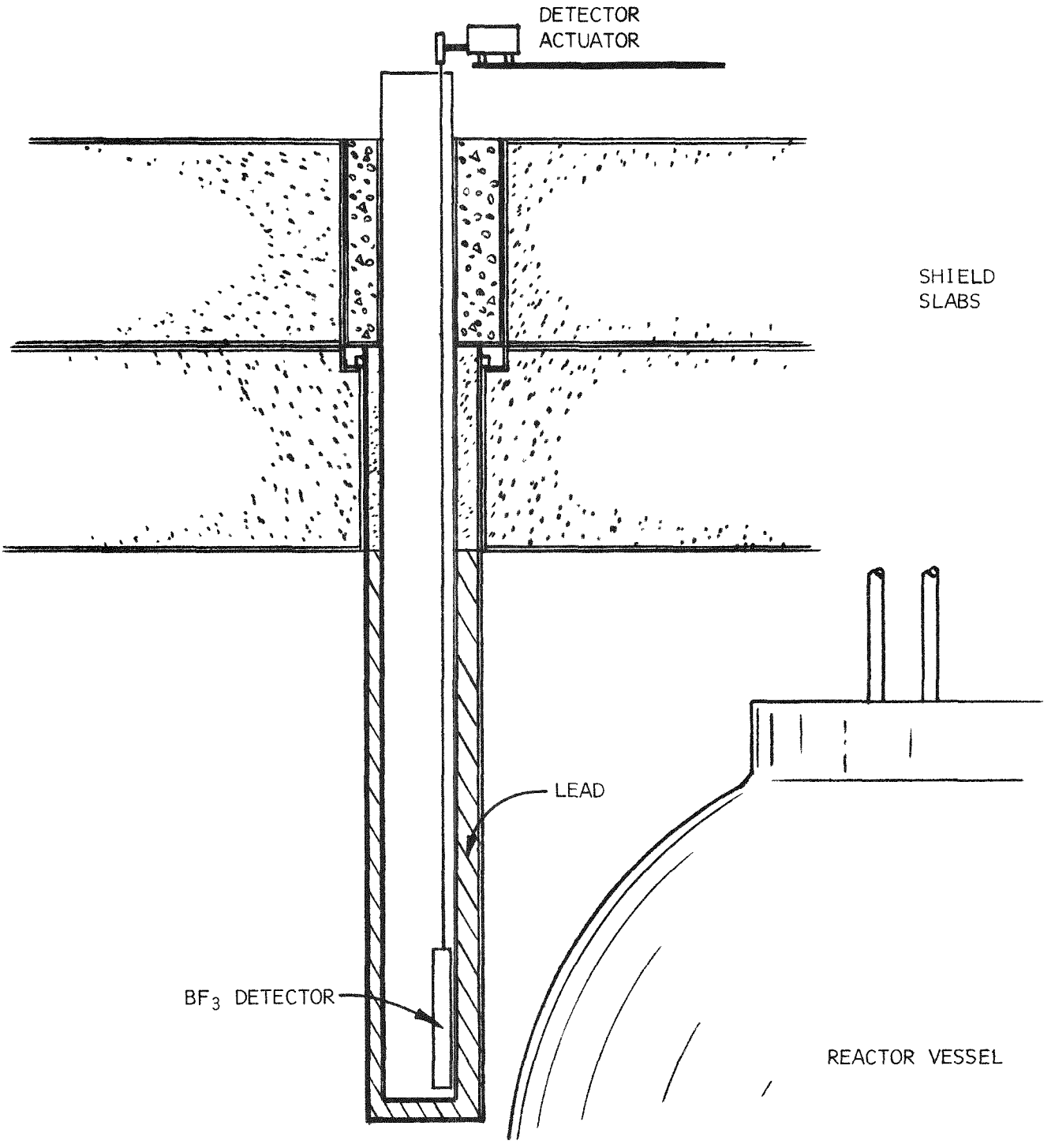

Fig. 11.2.1.3 Typical detector shield and actuator

Log Gamma Flux Channel - The log gamma flux channel is similar to the log power channels except for the replacement of the neutron-sensitive ion chamber with a gamma-sensitive chamber. There is no period signal derived from the log gamma function.

Nuclear Safety System - Sole purpose of the nuclear safety system is to initiate a fast automatic scram. Four, independent, neutron flux measuring channels continually monitor the reactor. A trip or a high flux level on two or more channels automatically scrams the reactor. A schematic diagram of the safety system appears in Fig. 11.2.1.4, and the four sections of the system are discussed below.

Section I of each channel incorporates a neutron ion chamber, chamber power supply, and electrometer circuit. From the ion chamber, current that is proportional to reactor power flows to the input of the electrometer which has two linear current measuring ranges. When S_1 is open, an input of 10^{-6} A, generated by the ion chamber, produces an electrometer circuit output of 10 V. With S_1 closed, the electrometer output is 10 V at a 10^{-3}-A input.

The reactor scram level can be set at any point within a 1- to 10-kW power range while the electrometer is switched to its 10^{-6}-A input range. The scram level range increases to 1 to 10 MW when the electrometer is set for a 10^{-3}-A input.

The ion chamber power supply is monitored for high voltage failure.

In Section II, the output of the electrometer circuit, Eo_1, is compared to reference voltage, E_{R_2}. When $Eo_1 < E_{R_2}$, the output of the comparator circuit is -9 V. When Eo_1 becomes an infinitesimal amount greater than E_{R_2}, the comparator output swings to +9 V. To adjust the scram level of each channel, the reference voltage, E_{R_2}, is varied.

Section III is a passive adder used as a logic circuit. The potential at the scram voltage monitor, Eo_3, varies according to

$$Eo_3 = \frac{(E_1 + E_2 + E_3 + E_4)}{5} . \qquad (1)$$

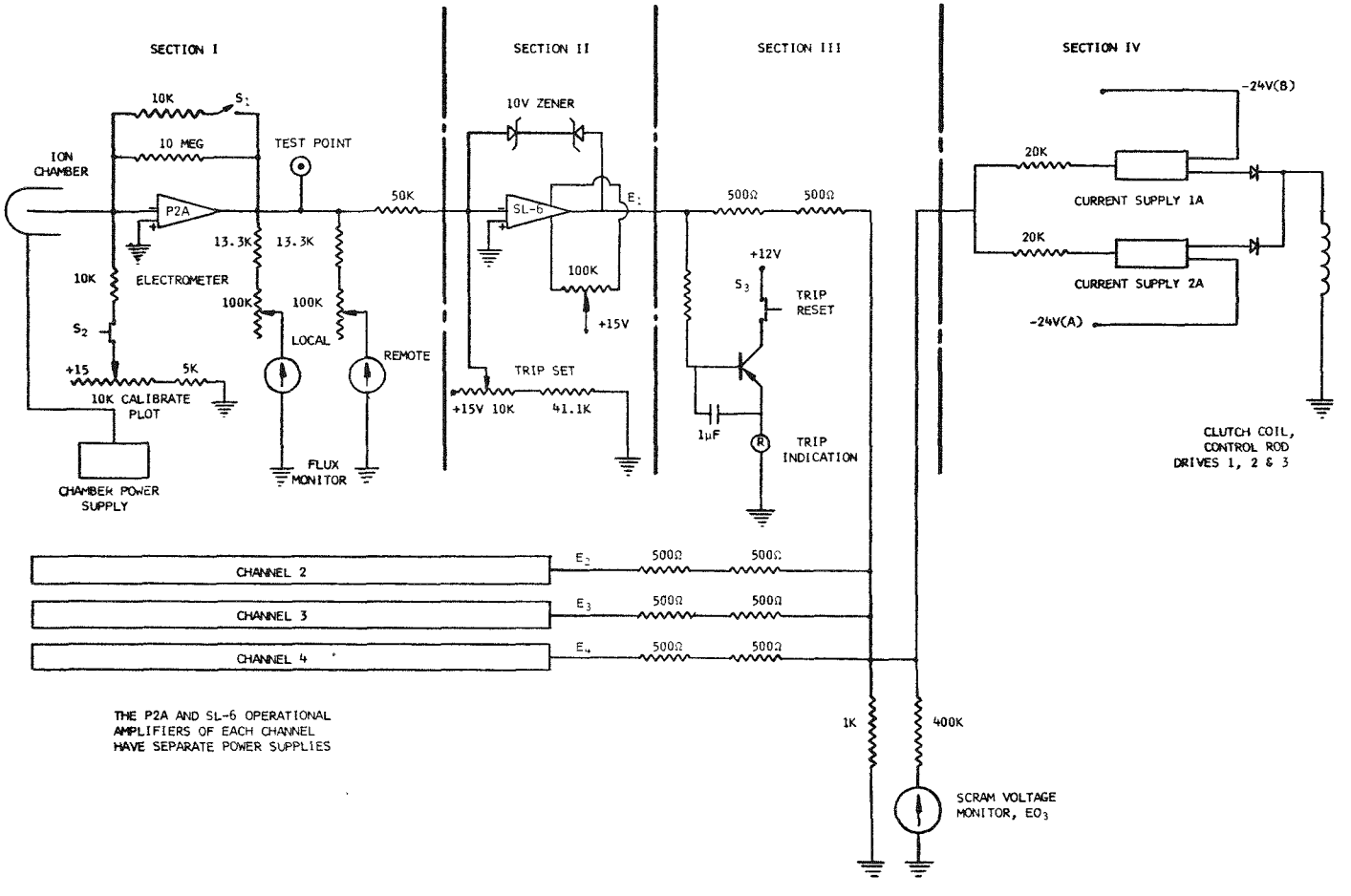

Fig. 11.2.1.4 Nuclear safety system circuits

This equation is valid because E_1, E_2, E_3, and E_4 are low impedance voltage sources, and a high impedance voltage sensor is used to measure Eo_3.

The voltage summed at Eo_3 indicates the status of the four flux measuring channels. A scram is initiated when $Eo_3 \geq -2$ V. Under normal conditions, according to Eq. (1), $Eo_3 = -7.2$ V. If a high flux at the ion chamber of a single channel produces an electrometer voltage higher than the reference voltage, the input to the logic circuit rises to 9 V and Eo_3 to -3.60 V. When the scram level of two channels is reached, the logic circuit has an output voltage of 0 V, and a reactor scram occurs. A short or open circuit associated with the logic circuit output voltage, Eo_3, produces a scram.

Section IV consists of two current supplies, acting in parallel, that deliver current to the electromagnetic clutches of the scrammable control rod drives. Each supply furnishes a current of 0.5 A. The clutches are magnetically saturated by a 1-A current. However, each clutch has more than adequate torque to hold its control rod at one-half of the rated current. For this reason, a false scram will not result if one of the current supplies should fail. Silicon controlled switches in each current supply interrupt the output when a scram signal is received. The operator must reset the scram to regain clutch current.

Safety System DC Power - Figure 11.2.1.5 shows the power arrangement that furnishes 24-V dc to the reactor safety system current supplies, and the circuits that energize clutches of the scrammable control rod drives.

11.2.2 Rod Drive Control Systems

Plug Rod System - Figure 11.2.2.1 is an electrical schematic of the plug rod drive system. One plug rod at a time can be withdrawn, after the interlocks of Table 11.2.2.1 are all satisfied.

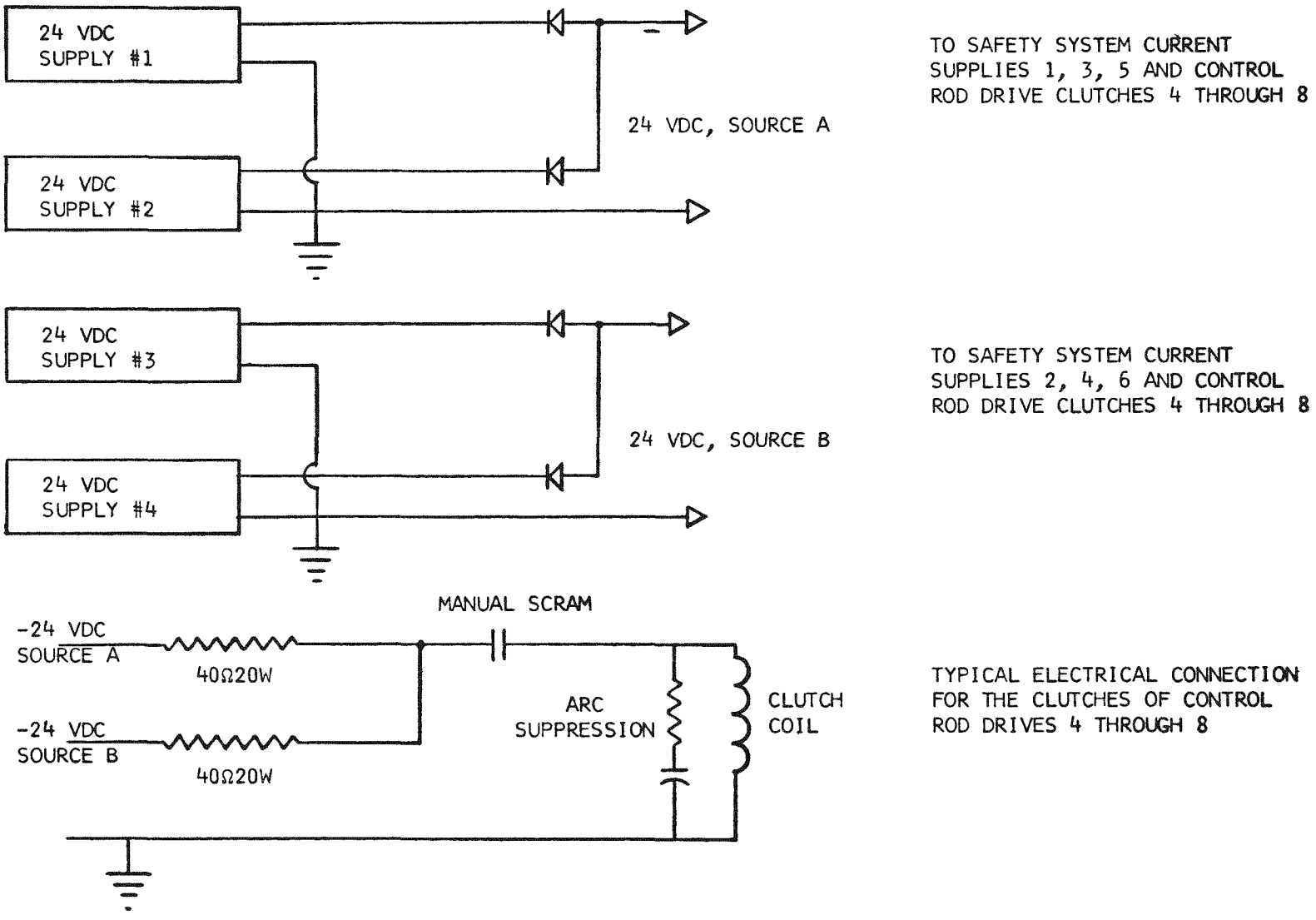

Fig. 11.2.1.5 Nuclear safety system dc power circuits

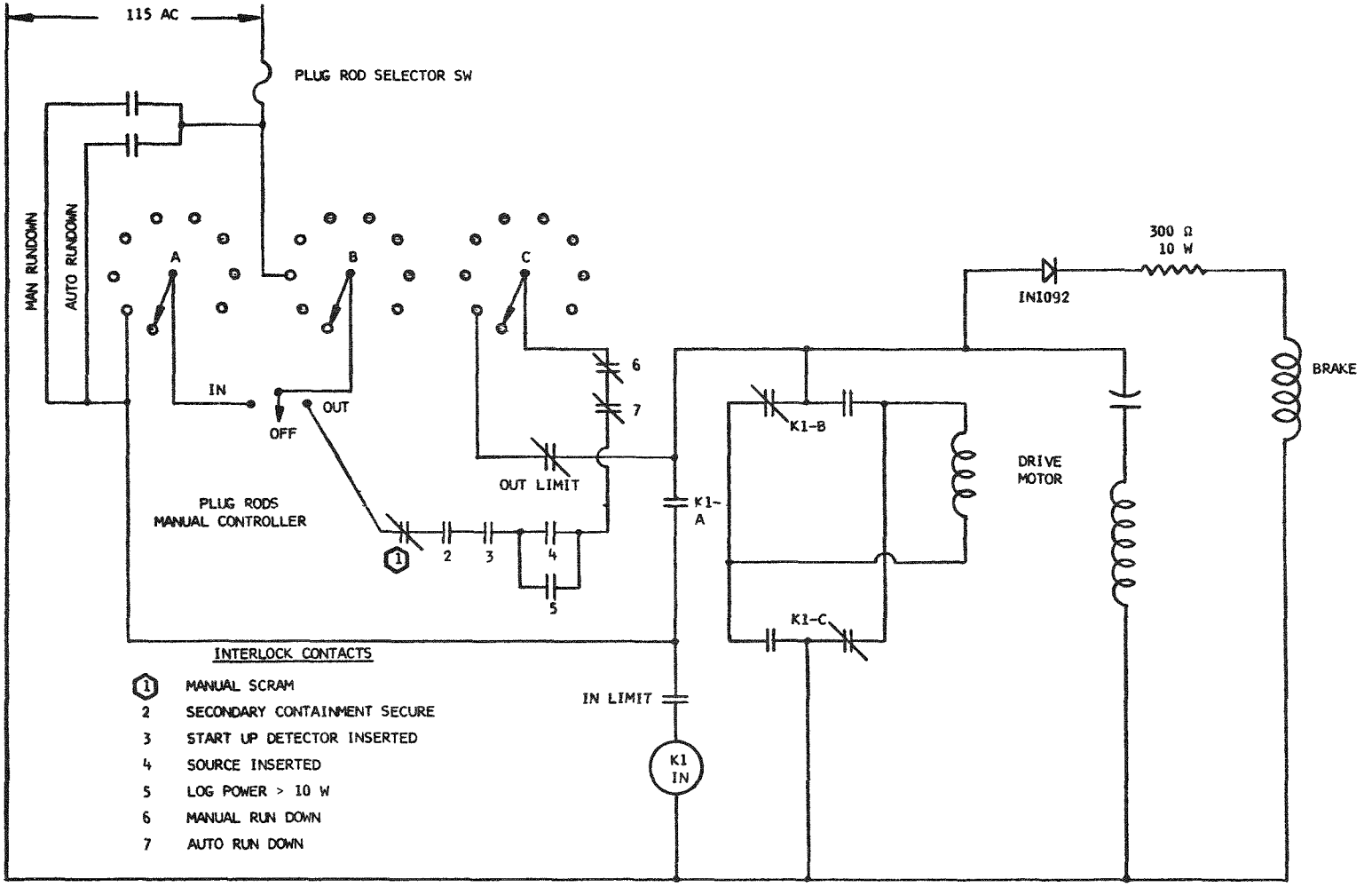

Fig. 11.2.2.1 Plug rod drive electrical circuits

TABLE 11.2.2.1

INTERLOCKS ON PLUG ROD WITHDRAWAL

1. The key to the plug rod drive manual controller inserted and turned to the "on" position.
2. The rod to be withdrawn selected with the plug rod selector.
*3. The neutron source inserted to the "in" limit.
*4. Startup detectors inserted to the "in" limit.
5. Both log count rate meter calibration switches in "operate" position.
6. Two plug rods from among rods 1, 2, and 3 fully withdrawn to the "out" limit if rods 4 through 8 are to be withdrawn.
7. Manual and automatic reset.
8. Automatic rundown reset.
9. Selected rod's manual rundown switch not in "insert" position.
10. Secondary containment secured.

---

*Interlocks 3 and 4 are not required when log power exceeds 10 W.

When a plug rod is to be withdrawn, the proper rod is first selected with the plug rod selector switch, then the rod drive controller is turned to the "out" position, and the selected rod moves out of the core. The rod drive controller is a manual, pistol-grip switch that is spring returned to the "off" position from either the "in" or "out" position.

Insertion of plug rods can be initiated through either manual or automatic controls, the response to which can be either a free-fall rod drop or a controlled rundown. The various methods of insertion are discussed below.

1. Automatic Scram - When the reactor safety system detects a scram condition, the system circuitry interrupts the current to the electromagnetic clutch coils in the drives for plug rods 1, 2, and 3, and the rods fall into the core.

2. Manual Scram - If an operator decides to scram the reactor, he presses the scram button located on the operations console. In response, holding relays, protected with arc suppression, interrupt the current to the clutches in the five plug rod drives that do not respond to automatic scram.

3. Automatic Rundown - When any of the following situations occur, an automatic rundown system closes a contact in each of the eight plug rod drive circuits, and the eight rods run down to their "in" positions.

a. Heat exchanger tube temperature > 1200°F
b. Reactor inlet pipe temperature > 650°F
c. Primary loop rupture
d. Secondary loop rupture
e. Loss of secondary loop coolant flow
f. Loss of heat dump air flow
g. Loss of primary loop coolant flow
h. Reactor automatic scram.

In addition to inserting the rods, the rundown system shuts down the primary loop blower.

4. Manual Rundown - Individual plug rods can be driven into the core by two methods. In the first method, the desired rod is chosen with the control rod selector switch, and the manual rod drive controller is turned to the "insert" position. The second method involves the use of manual rundown controller switches, eight of which are mounted on the operations console. Each manual rundown switch, when moved to the "insert" position, closes a contact that is wired in parallel to the automatic rundown contact in the rod drive circuit. By either method, the rundown continues only as long as the controller or

switch remains in the "insert" position. In all cases, an "in" command overrides an "out" command.

Core Rod System - Since the core rod drives do not have an electromagnetic clutch, the rods must be driven into, as well as out of, the core. The core rod system has its own rod selector switch and manual rod drive controller, but the two rod systems cannot be operated simultaneously. Each rod drive controller has a lock, but there is only a single key, which cannot be withdrawn unless the controller is locked in the "off" position.

The electrical features of the core rod drive control system are nearly identical to those of the plug rod system shown in Fig. 11.2.2.1. The two exceptions are as follows.

1. Power to drive a core rod in or out is supplied only through the rod selector switch and the rod drive manual controller.

2. There is no automatic core rod rundown system nor any individual manual rundown switches for the core rods.

Core rod insertion is subject to satisfaction of the following interlocks.

1. The key to the core rod drive manual controller inserted and turned to the "on" position.

2. The average core temperature < 1200°F. (This interlock can be manually overridden.)

For withdrawal, core rods are subject to the same interlocks as the plug rods.

11.3 Coolant System Controls

11.3.1 Coolant Blowers

A schematic diagram of one of the two identical helium blower control systems is shown in Fig. 11.3.1.1. The systems are operated under manual control from the control room. Circuits are designed for eventual automatic control of the blower speeds through the computer.

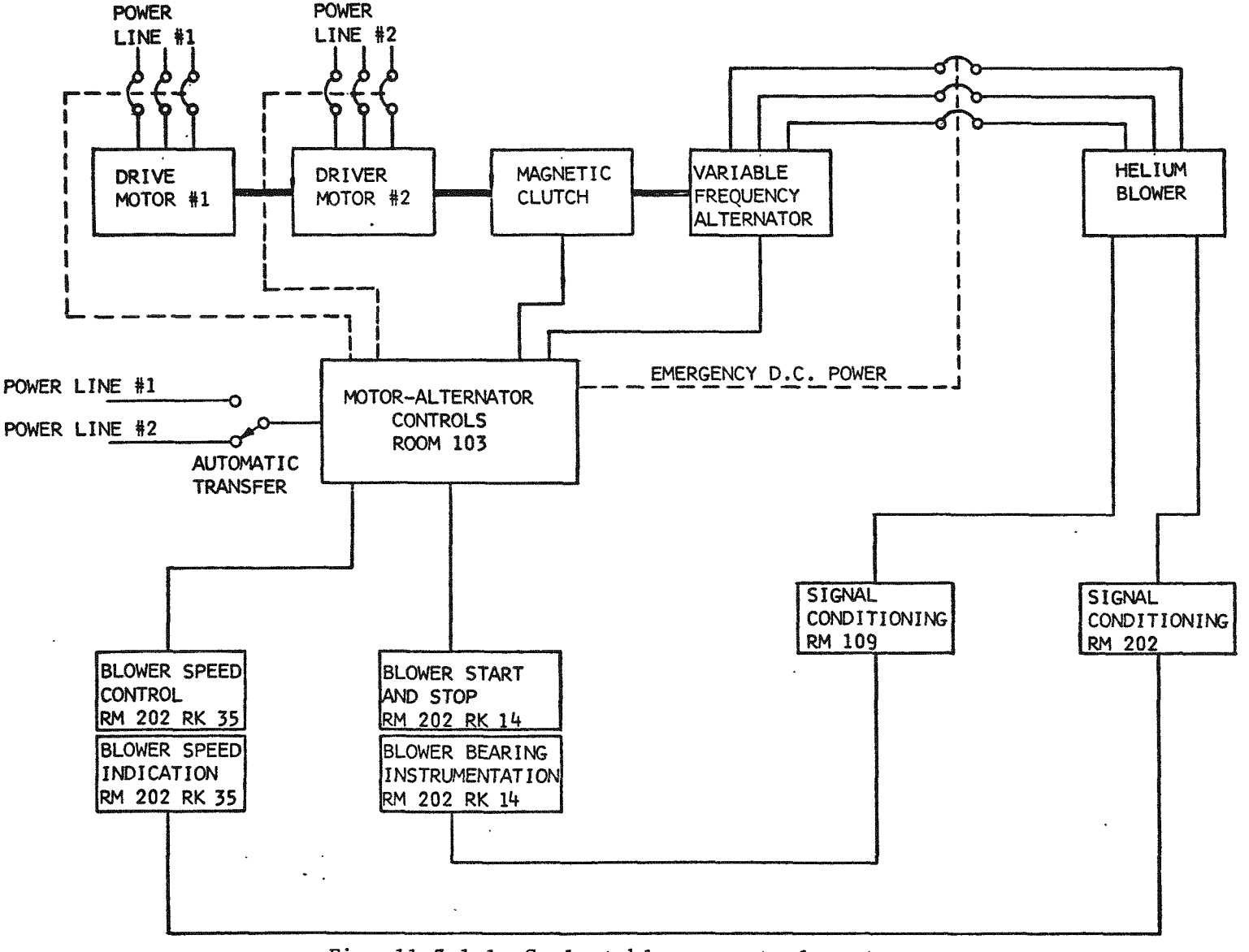

Fig. 11.3.1.1 Coolant blower control system

Both blowers are started with manual controls that are mounted on racks 15 and 16. A blower cannot be started until the following interlocks are satisfied.

1. Water is flowing in the coolant loop to the blower.
2. Jacking gas valve is open, allowing helium to flow to the journal bearings in the blower.
3. Motor-alternator frequency control is set for minimum frequency.

Once the blower is started, the operator brings it to speed while monitoring the blower bearing clearance on an oscilloscope mounted on the rack. Manual speed controls for both coolant loop blowers are located on the main operations console, near the blower speed indicators.

A coolant blower shutdown can be initiated by any one of the following.

1. Manual shutdown by operator in control room
2. Automatic rundown of the reactor
3. Loss of water coolant flow to the blower
4. Loss of power to both power lines driving the motor-alternator set for the blower.

If a shutdown is initiated by any of these conditions, jacking gas flow to the blower automatically starts and continues for a predetermined time, sufficient for the blower to coast to a stop without damage to the gas bearings.

11.3.2 Recuperator Bypass Valve

The recuperator bypass valve is driven by a geared-down synchronous motor at a speed of about 1/8 rpm. To rotate the valve either clockwise or counterclockwise through 360°, the operator manipulates a spring-loaded switch located on the console panel. Position indication is shown on the same panel by a meter which is driven from a potentiometer located in the valve operator housing.

11.3.3 Secondary Loop Isolation Valves

A rupture of the secondary coolant loop is detected by a system that is sensitive to a rapid rate of pressure decrease in the loop. The sensing system, called the trigger, is depicted in Fig. 11.3.3.1. An accumulator, made from a 32-in. length of 4-in. pipe, is welded to a tee in the secondary loop piping near the heat dump outlet. The principal volume of the accumulator is separated from the secondary loop by a 1/4-in.-thick plate welded just below the joint between the tee and the accumulator. A 1/64-in.-diam hole drilled through the plate creates an orifice between the loop and the accumulator, and, therefore, the pressures on both sides of the plate are normally balanced.

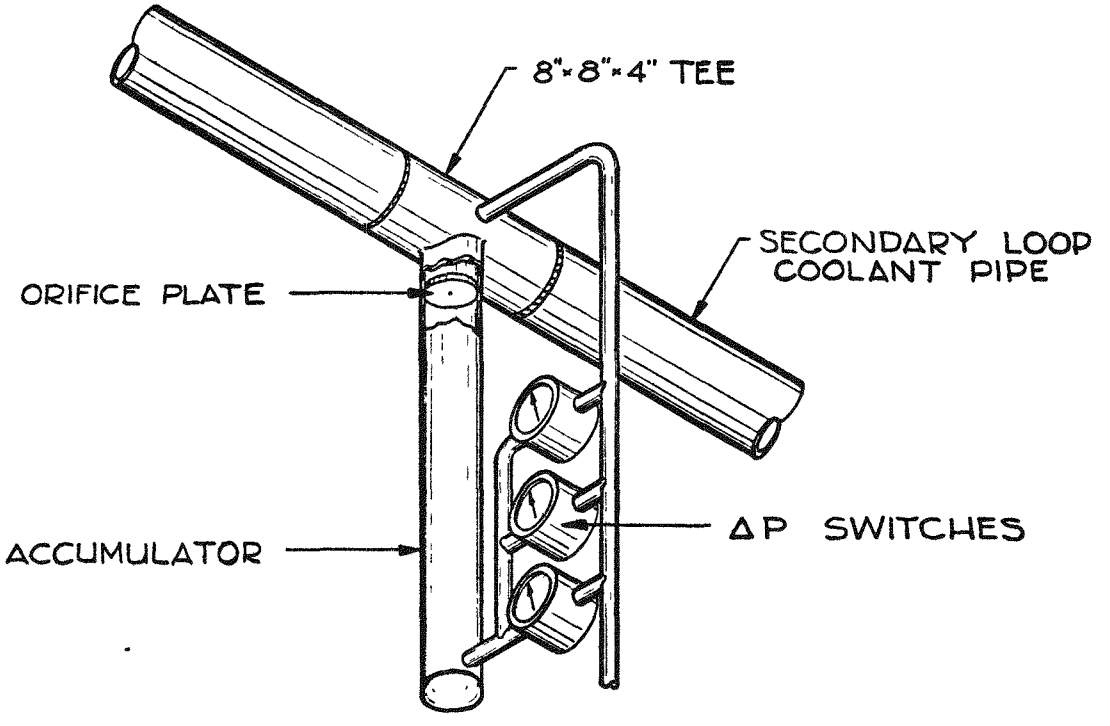

Fig. 11.3.3.1 Isolation valve trigger

If a rupture were to occur in the secondary loop, the coolant helium would vent and loop pressure would decline rapidly. However, the small orifice in the accumulator plate would restrict the venting of accumulator pressure to a much slower rate, and a differential pressure would develop across the plate. Any pressure differential across the accumulator plate is sensed by three pressure transducers connected in parallel across the accumulator. Each transducer has a mechanical switch with two normally open contacts that close when a preset differential pressure is reached. The switches are set to close at 2/3 of the 400-psi differential that would develop in the case of a loop rupture. This set point is well above the pressure differentials that are created by normal loop operations. When two of the three switches close, they actuate the secondary loop loss of coolant emergency system, described in Sec. 11.4.2, and the loop valves operate.

The electrical circuits include features which permit a complete system test of the valve operating circuits. Valve positions are indicated with lamps on the coolant loop graphic panel. Pneumatic system pressures are monitored, and out of limit pressures are annunciated. The system can be actuated manually from the main console.

11.3.4 Heat Dump

Speed of the heat dump fans can be varied with controls located on the main operations console. Operation of the heat dump is under manual control, but automatic control through the computer is planned.

Start controls, condition indicator lights, and pitch controls for the heat dump shutter blades mounted in rack 16 for each of the fans, make possible independent operation of the two fans. Positive action switches restart the fans immediately when power is restored after an interruption. However, a power loss is improbable; each fan is supplied from a separate power line at the facility load center, described in Sec. 10.2.1.

A speed indicator for each fan is located on panel 35 of the console, near a common speed control for both fans. The speed control can be used to regulate a single fan when only one is being operated.

11.4 Safety Systems

Ten independent safety systems are installed to protect the reactor and its associated coolant loops. The UHTREX facility has been designed to operate without the aid of backup or emergency systems. However, it is possible for failures to occur that have serious consequences. Therefore, safety systems have been included to detect malfunctions and take corrective action. Each safety system consists of independent, redundant instrument channels which sense the abnormal condition. Control circuits act to prevent or minimize the damage that can result when failures occur. The safety systems are:

1. Primary loop loss of coolant emergency system
2. Secondary loop loss of coolant emergency system
3. Primary loop coolant flow monitor
4. Secondary loop coolant flow monitor
5. Reactor inlet pipe temperature monitor
6. Heat exchanger tube temperature monitor
7. Primary loop pressure relief system
8. Secondary loop pressure relief system
9. Secondary loop radiation contamination detection system
10. Heat dump air flow monitor

In the discussion of the safety systems that follows, the instrumentation and control circuits of the primary loop loss of coolant emergency system are discussed in detail. For the remaining safety systems, which follow the same design and operating philosophy, only operating characteristics are described.

11.4.1 Primary Loop Loss of Coolant Emergency System

A rupture of the primary coolant loop would release contaminated helium into the secondary containment with consequences that are described in Sec. 16.3.1. A rupture would be sensed as a fall in loop pressure below 300 psia, detected by three, independent, pressure measuring channels. The fall in loop pressure triggers the emergency system which automatically acts as follows:

1. The secondary containment is isolated by closing the solenoid valves and stopping the fans in the pressure bleed lines. (See Fig. 9.3.1.)

2. The primary loop blower is turned off.

3. The gas cleanup system is isolated by closing valves 8501, 8502, and 8520. (See Fig. 7.1.1.)

4. The gas cleanup system blower is turned off.

5. The reactor is shut down by driving the rods in with the auto rundown system.

Figure 11.4.1.1 shows the detection and control circuits used in the loss of primary loop coolant emergency system. Each pressure transducer has an associated resistance bridge that furnishes an electrical signal proportional to pressure; a pressure change of 0 to 600 psia produces a 0- to 30-mV transducer output.

Section I - Section I consists of the resistance bridge of the pressure transducer, the signal conditioning amplifier A_1, and the transducer excitation power supply. The transducer excitation voltage, nominally 6-V d.c., is delivered through transistor Q_1, which, with its related components, forms a simple regulator circuit. The regulator circuit is normally supplied by S_1, a conventional power supply. If this supply should fail, battery B_1 automatically takes control, and the transducer continues to receive its normal excitation voltage. The battery has a life of 1000 h.

Amplifier A_1 serves to increase the transducer output signal to a suitable level for the comparator. The power supplies of amplifier A_1 have battery backup.

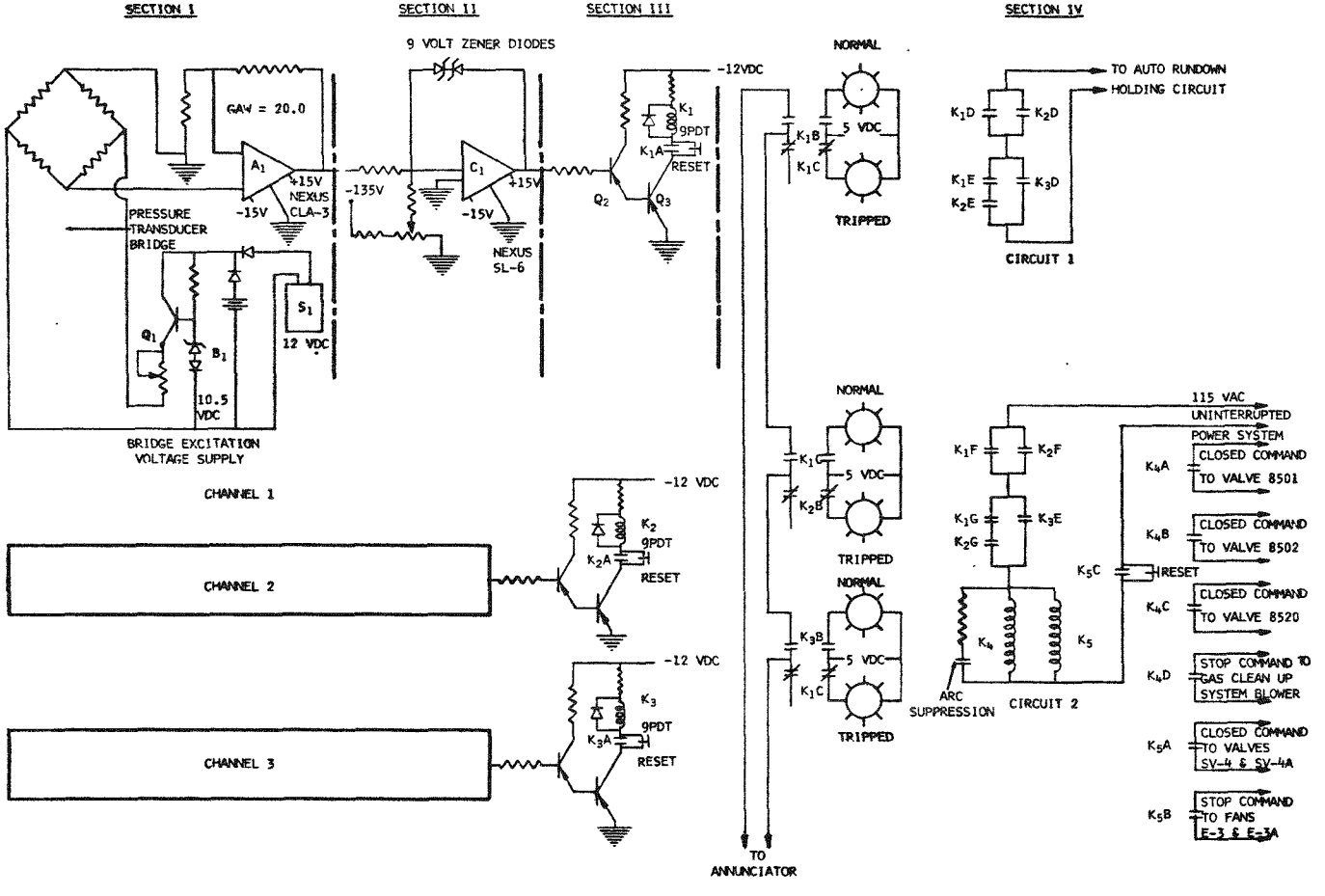

Fig. 11.4.1.1 Primary loop loss of coolant emergency system

Section II - Section II is the comparator circuit or decision making element. It has two stable states. When $|E_S| > |E_R|$ the comparator's output is -9 V. When $|E_S|$ becomes an infinitesimal amount less than $|E_R|$, the comparator's output flips to +9 V. Battery backed-up power supplies furnish voltage to the comparator.

Section III - Section III consists of relay drivers Q_2 and Q_3 plus a 9-pole, double-throw relay. The relay is normally energized by a -9-V comparator output signal. When the comparator flips up to +9 V, the driver transistors are turned off and the relay is de-energized. Failure of power to the relay driver circuit would result in the same action; therefore, the relay driver power is backed up with batteries.

Section IV - Section IV shows the control circuits that are made up with the contacts from the output relays of each instrument channel. Each channel has an indicating light to show its status. Signals are sent to the annunciator when one or more channels have tripped.

Circuit 1 uses contacts from relays K_1, K_2, and K_3 in 2/3 logic to form a closure in the auto rundown holding circuit. The auto rundown system, described in Sec. 11.2.2, shuts off the primary loop blower and drives the eight reactor plug control rods to their full "in" position.

Circuit 2 uses the same 2/3 logic to form a holding circuit for relays K_4 and K_5. These relays are energized with the 115-V ac uninterrupted power system. When K_4 is deenergized, the gas cleanup system is isolated and the gas cleanup system blower is turned off. (Valves 8501, 8502, and 8520 are closed.) Deenergizing relay K_5 closes the secondary containment bleed valves (SV-4 and SV-4A) and stops bleed fans E-3 and E-3A. Loss of the 115-V ac uninterrupted power system also initiates the above action. The system must be reset by the operator after power has failed or two or more channels have tripped.

11.4.2 Secondary Loop Loss of Coolant Emergency System

A rupture of the secondary coolant loop is detected by three differential pressure switches mounted on the isolation valve trigger, described in Sec. 11.3.3. Upon receipt of a digital signal from two or more of the three differential pressure switches, the following action is initiated by the emergency system.

1. Secondary loop isolation valves are closed.
2. The secondary loop blower bypass valve is opened.
3. The secondary loop blower is stopped.
4. The primary loop blower is stopped.
5. The reactor is shut down by driving the eight plug rods to their "in" limit.

The emergency action can also be initiated by the operator through a manual trip. An alarm occurs if secondary loop pressure is less than primary loop pressure, but the emergency system will not function if secondary loop pressure reduction takes place slowly.

11.4.3 Primary Loop Coolant Flow Monitor

Coolant flow through major primary loop components produces a pressure differential across each unit. The coolant flow monitor measures the differential across three of the components, the reactor, the hot side of the recuperator, and the hot side of the main heat exchanger. If the ΔP across one of the components falls below the safe level, defined by the experimental plan, the safety system trips and automatically takes the following action.

1. The primary loop blower is stopped.
2. The reactor is shut down by driving the plug control rods to their "in" limit.

Loss of coolant flow in the primary loop can be caused by loss of power to the primary loop blower, or abnormal blower operation. If the loss of flow is caused by abnormal blower operation, it is desirable to quickly stop the blower to reduce the probability of mechanical damage to the blower or its housing.

The reactor is shut down by driving all plug control rods to their "in" limit with the automatic rundown system. The reactor remains shut down until the reason for loss of coolant flow is determined and the problem is corrected.

11.4.4 Secondary Loop Coolant Flow Monitor

Three transducers measure the pressure differential across the cool side of the main heat exchanger for the secondary loop flow monitor. If the ΔP drops below a safe level, the safety system automatically takes the following action.

1. The secondary loop blower is stopped.
2. The primary loop blower is stopped.
3. The reactor is shut down by driving the plug rods to their "in" limit.

The secondary loop blower is stopped to minimize damage that might occur if it operated abnormally. The primary loop blower is stopped to prevent excessive temperature in the heat exchanger, and the reactor is shut down to stop power production until coolant flow in the primary and secondary loops is restored.

11.4.5 Reactor Inlet Pipe Temperature Monitor

Three temperature measuring channels sense the reactor inlet pipe temperature. If the pipe temperature exceeds the safe operating temperature, the monitoring system initiates the following action.

1. The primary loop blower is stopped.
2. The reactor is shut down by driving the plug control rods to their "in" limit.

Stopping the primary loop blower interrupts the flow of hot gas within the reactor inlet pipe, thus preventing any damage that might occur.

11.4.6 Heat Exchanger Tube Temperature Monitor

Three thermocouples measure the temperatures of three tubes in the heat exchanger. (See Fig. 5.1.1.7.) If a tube temperature exceeds 1200°F, the tube temperature monitor initiates the following action.

1. The primary loop blower is stopped.
2. The reactor is shut down by driving the plug control rods to their "in" limit.

Stopping the primary loop blower decouples the heat exchanger from the reactor and prevents overheating.

11.4.7 Primary Loop Pressure Relief System

Three instrument channels continuously monitor helium pressure at the blower discharge, at the main heat exchanger outlet, and at the low temperature side of the recuperator. Where necessary, battery power backup is provided to guarantee the availability of pressure signals, even though all conventional and emergency power in the facility has failed. The hysteresis comparator circuits of each channel are set to trip at 505 psia and reset at 475 psia. The output relays of each channel are wired in 2/3 logic to operate valve 8540. (See Fig. 8.3.1.1.) If two or more pressure measuring channels trip, power is interrupted and valve 8540 opens. There are manual controls available to open either 8539 or 8540. Valve 8540 opens upon power loss. Valve 8541 may be closed when the primary loop is being pumped down with the low pressure compressors, but a key is required since this action overrides the pressure relief system's ability to function.

11.4.8 Secondary Loop Pressure Relief System

Helium pressure in the secondary loop is automatically relieved if it exceeds 545 psi. Three pressure measuring channels sense secondary loop pressure. The instrument channels have battery backup which provides pressure signals even if primary and secondary power

sources fail. Each channel drives a relay whose contacts form a 2/3 logic circuit for opening and closing the secondary loop vent valve, which fails open upon loss of power.

11.4.9 Secondary Loop Radiation Contamination Detection System

Two photomultiplier tubes with attached NaI crystals serve as detectors for the secondary loop radiation contamination detection system. The detectors and their preamplifiers are located at the heat dump. The output signals of the preamplifiers are sent to rate meters in the control room. The rate meters have adjustable trip settings and are set to alarm if secondary loop contamination occurs.

If the secondary loop becomes contaminated, the reactor and coolant systems are shut down by the reactor operator.

11.4.10 Heat Dump Air Flow Monitor

The speed of each heat dump fan is monitored as a check on heat dump air flow. If the speed of both fans falls below a preset level, the following action is initiated.

1. The reactor is shut down by driving the plug control rods to their "in" limit.
2. The primary loop blower is turned off.

This action protects the heat exchanger from excessive temperature and prevents overpressure in either of the coolant loops.

11.4.11 Annunciator System

The annunciator system is composed of 72 annunciator stations which are arranged on rack turrets in the control room within the direct view of the main operations console. The annunciator, made by Rochester Instrument Systems, Inc., has back-lighted name plates that flash an alarm. All stations of the annunciator are of the first-in visual sequence type; the first-in alarm is identified by an additional red glow on the appropriate annunciator window. The stations are capable of being divided into independent groups of not less than 12 stations.

The annunciator stations can be acknowledged and reset from the main operations console. Momentary alarms may be locked in to permit the operator to examine the cause of the alarm and be forewarned of possible sources of trouble. The audible and lamp portions of the annunciator can be tested by means of pushbuttons located on the annunciator panels.

11.5 Communications Systems

11.5.1 Telephones

There are 24 telephones at the site, all but one of which are serviced through the Ten-Site (TA-35) switchboard. There is one direct line into the site.

11.5.2 Paging System

The UHTREX facility and surrounding areas are covered by a paging system that can be used from any of the telephones at the site. Power for the paging amplifier is supplied from the 20-kW diesel system.

11.5.3 Audio Intercommunication System

A site intercom system facilitates equipment installation, checkout, calibration, and general operations. The system consists of a central control panel in the control room and 48 plug-in stations for telephone head sets throughout the working areas. Through the central panel in the control room, any station may be interconnected with as many as five others. Four trunks make possible as many as four simultaneous, but separate, conversations at any one time.

11.5.4 Emergency Alarm System

The emergency alarm system includes an array of Klaxon horns, audible in all facility and outside areas, that are automatically initiated by radiation monitors covering the secondary containment area. This system, completely separate from the paging system, is powered from the 20-kW diesel supply, and can be manually actuated from the control room.

11.5.5 Closed Circuit Television

Closed circuit television systems monitor the secondary containment areas. Two cameras are mounted on the Minotaur remote maintenance machine for closeup views of components of the reactor, coolant loop, and gas cleanup rooms. Another camera is installed for overall area surveillance of the secondary containment. All cameras have remote control pan and tilt devices and zoom lenses. Monitors for the secondary containment system are located on the Minotaur control console in the remote maintenance corridor. Another slave monitor is mounted in the control room in direct view of the main operations console.

12. AUXILIARY SYSTEMS

12.1 Gas Sampling System

A sample loop carries a stream of primary coolant helium to the fuel charging room, near the fuel transfer lock where apparatus will be set up for the collection of gas samples. The sample loop, made of 1/4-in. stainless steel tubing with welded joints, taps into the primary loop at the same place where the gas cleanup system inlet line is connected, downstream from the blower. From there the loop passes, through the reactor room and the reactor drive room, into the fuel charging room, and returns to the primary loop at the point where the gas cleanup system outlet line connects. The pressure drop across the blower maintains a flow of helium through the sample loop.

In the fuel charging room, a series of remotely operated, bellows-sealed valves, shown in Fig. 12.1.1, controls the flow of helium from the sample loop, through the secondary containment wall, into the fuel transfer lock. When a sample is to be taken, valves 8454 and 8455 close and trap a sample between them. Then valve 8456 opens, and the sample flows into the line through the wall. Finally, 8456 closes, 8458 opens, and the sample flows into collection equipment operated with the master-slave manipulators in the transfer lock. At all times, two or more valves isolate the primary coolant loop from the collection apparatus. Interlocks prevent the opening of valve 8456 when either 8454 or 8455 is open, and the opening of 8458 when 8456 is open.

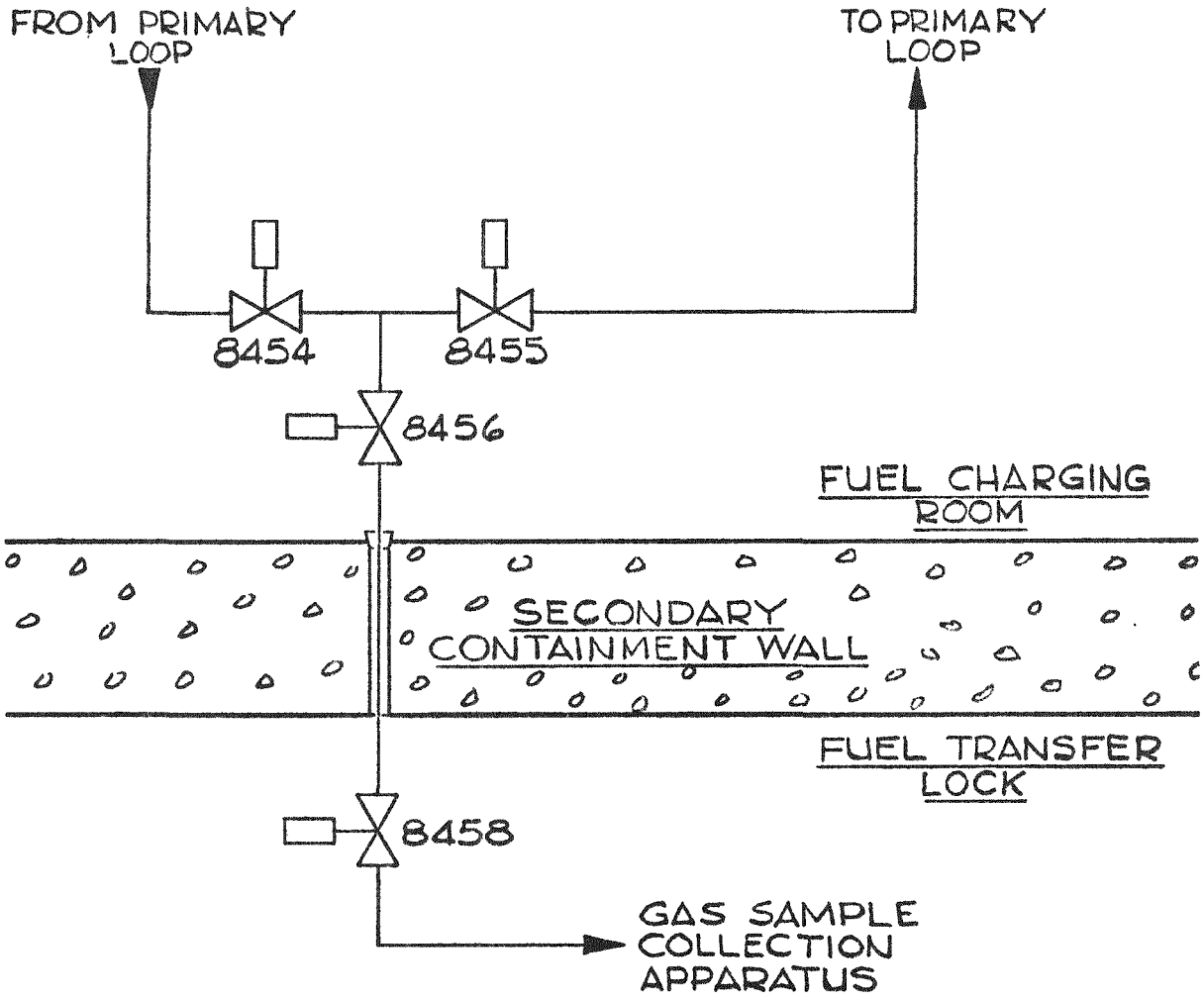

Fig. 12.1.1 Gas sampling system

12.2 Cooling Water Systems

12.2.1 General Description

Two closed-loop water systems carry away the heat from water-cooled components. Figure 12.2.1.1 is a schematic diagram of the systems and of the supply from Los Alamos water mains. Heat is dissipated to the atmosphere from two evaporative coolers that function in the cooling

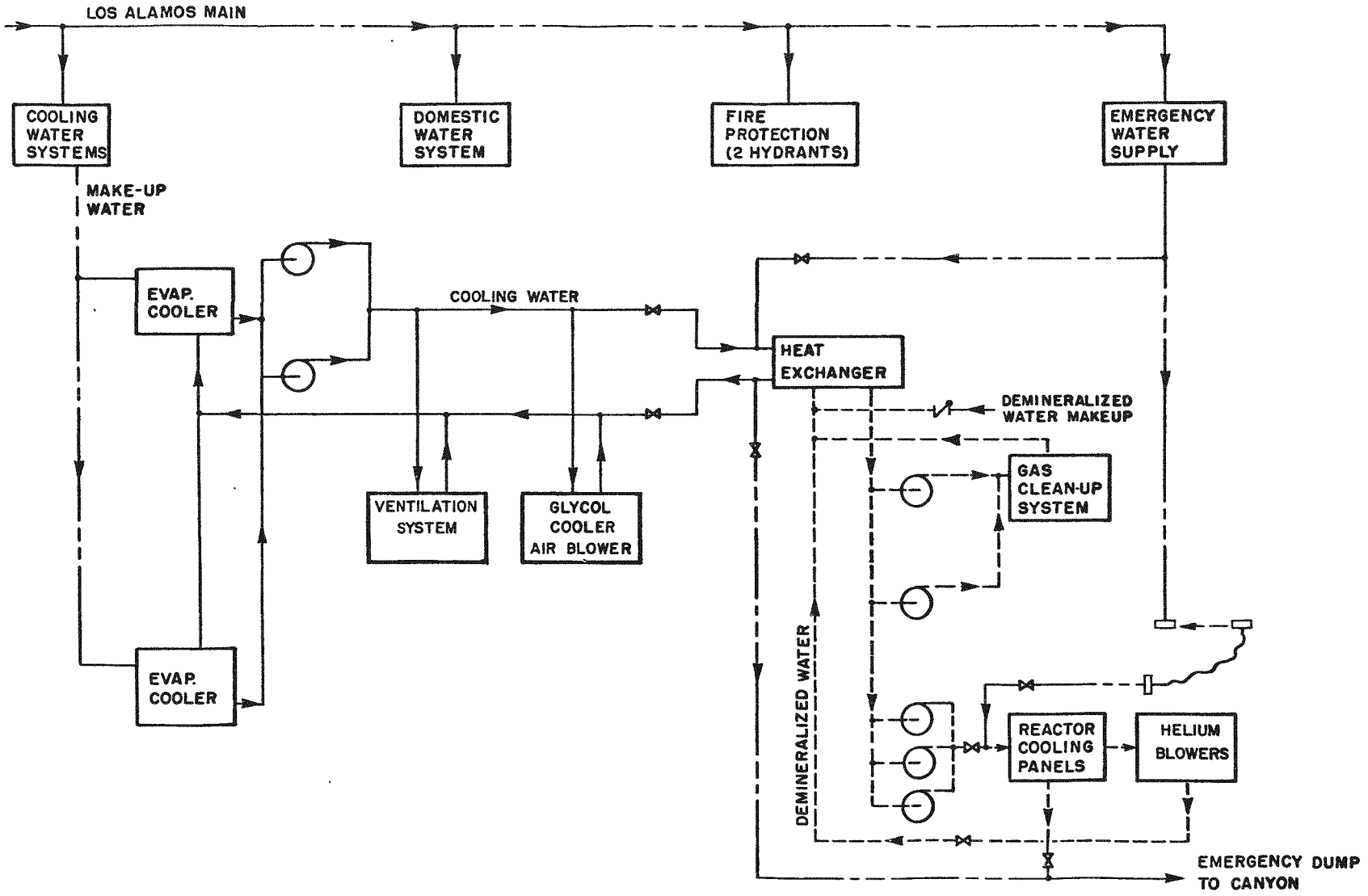

Fig. 12.2.1.1 Water flow diagram

water system, which circulates untreated water. An isolation heat exchanger transfers heat from the second closed system, which circulates demineralized water to components inside the secondary containment structure.

12.2.2 Design Details

Water from the Los Alamos distribution system flows to the UHTREX site in an 8-in. main, which reduces to 6-in. size to feed directly two fire hydrants and the facility water systems. Inside the building the water line reduces to 3-in. size and passes through a pressure regulator set at 60 psig. The 3-in. main supplies domestic water, cooling systems fill and makeup water, and emergency cooling water for the demineralized water system. A reduced pressure backflow preventer separates the domestic water and emergency cooling water systems.

Cooling Water System - Untreated water circulates at the rate of 490 gal/min against a 54-ft head through the closed loop of the cooling water system. One of two identical centrifugal pumps moves the water; the other is on standby. Power for both comes from a line-fed motor control center.

Each of the two evaporative coolers, where the circulated water gives up its heat, is capable of cooling 245 gal/min from 87° to 78°F, a heat load of 1.1×10^6 Btu/h. A 15-hp blower moves 25,000 ft^3/min of air through each of the coolers to evaporate water sprayed on the outside of the cooler tubes by a recirculating pump system at a maximum rate of 64 gal/min. Thermostats control dampers in the air intake ducts to regulate the outlet cooling water temperature.

Water flows from the coolers to the pumps and then to a distribution system with 6-in.-diameter steel supply and return loops. The supply loop feeds cooling coils in the facility ventilation systems, condensers and Freon compressors in refrigeration systems for control room air conditioning and the gas cleanup system glycol cooler, an aftercooler on the cleanup system process air blower, and the isolation heat

exchanger that cools the water in the demineralized system. The 6-in. return loop delivers the heated water directly to the evaporative coolers.

Demineralized Water System - A purification unit, which consists of a deoxygenator and a mixed bed deionizer in series, treats the initial fill and makeup water for the demineralized system. The pH of the circulating water is continuously monitored and is maintained between 10.25 and 10.75 by a control system that directs a sidestream flow through either a hydrogen cycle cation exchanger or a lithium-7 cycle mixed-bed deionizer.

In the circulating system, depicted schematically in Fig. 12.2.2.1, heat is transferred from the demineralized water in the shell to cooling water in the tubes of the isolation heat exchanger. The exchanger is designed to cool 470 gal/min of water in the shell from 96° to 89.6°F, a heat load of 1.5×10^6 Btu/h. Working pressure of the exchanger is 125 psig.

From the heat exchanger, demineralized water flows to a manifold that feeds five pumps (Fig. 12.2.1.1): two that serve the gas cleanup system and three that serve the reactor cooling panel and coolant blower cooling systems. One of the cleanup system pumps is on-line, the other is on standby, and both are driven by line power. Either can circulate 170 gal/min against an 80-ft head. Of the three other pumps, one is on-line, one is on standby, and the third is for emergency use. Either of the first two can circulate 300 gal/min against a 90-ft head and are driven by line power. The third, rated for 150 gal/min against a 50-ft head and driven by power from the 20-kW emergency supply, is started only if both power lines are lost.

If both power lines to the facility were to fail, the normal and standby water pumps in the cooling water system would shut down and the isolation heat exchanger would cease to function. To provide cooling capacity for reactor heat removal via the cooling water panels, valves in the emergency water supply line would be opened to allow untreated water from the mains to flow through the tube side of the isolation heat

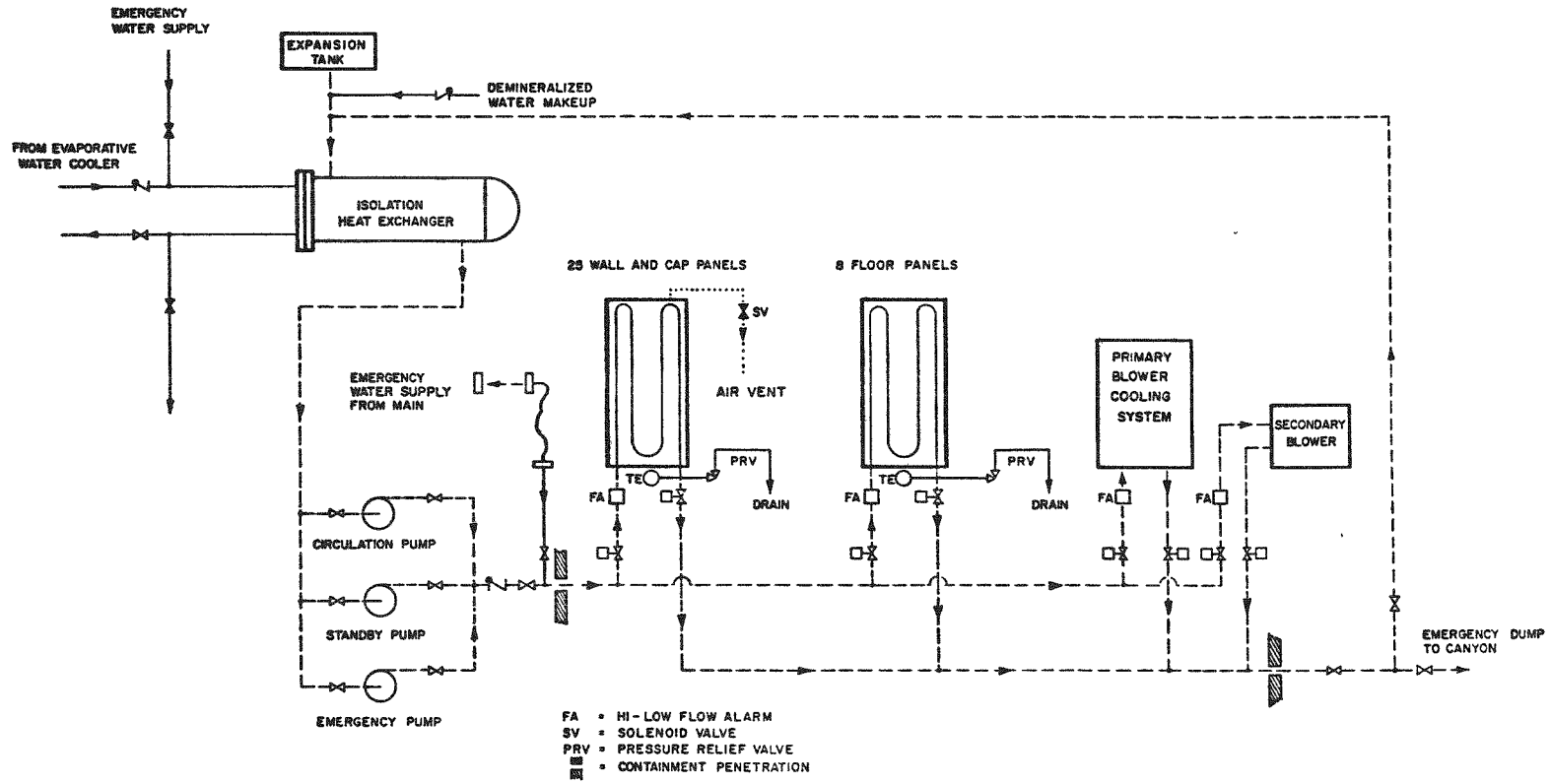

Fig. 12.2.2.1 Demineralized water flow

exchanger and out to the canyon south of the facility. Meanwhile, the emergency pump would have come on the line, and its full 150-gal/min flow would circulate through the panels and back to the heat exchanger. Should the 20-kW, diesel-driven, emergency power supply also fail, the emergency water would be connected, with a fire hose, directly to the water panel circuit. In this case, untreated water would flow through the panels and out to the canyon.

Water-Cooled Panels - The walls in the reactor-recuperator room are covered with 24 vertical, water-cooled panels, three of which appear in Fig. 5.1.1.10. On the floor are eight more panels; a single, round panel rests on legs above the reactor vessel cap, and panels enclose the secondary loop pipes where they penetrate the containment walls. Demineralized water flows through channels in the panels, which are made of an embossed steel plate welded to a flat base plate. Each panel is on a separate water circuit that can be isolated from the demineralized water supply and return loop. A high-low flow alarm indicates in the control room if flow abnormalities should develop in any panel.

Blower Cooling Systems - Finned tube heat exchangers in the two coolant loop blowers use demineralized water to keep the blower motor windings cool. The secondary loop blower, which circulates clean helium, is supplied with demineralized water directly from the water system, but the primary loop blower, which circulates contaminated helium, has an isolated water supply.

For the primary blower, water from the demineralized system flows through the tubes of dual isolation heat exchangers at a rate of 14 gal/min. On the shell side of the exchanger, water flows in a closed loop to a pair of pumps, one on standby, that circulate 10 gal/min through the blower's internal heat exchanger. The isolation exchanger is designed to remove 60,000 Btu/h and to operate at a pressure of 160 psig.

If the primary loop blower's internal heat exchanger were to fail, the helium pressure would force water out through a rupture disk, which vents at 65 psi, in the blower cooling water piping system. Then the

helium would vent inside the secondary containment structure. Should the secondary loop blower heat exchanger fail in the same manner, helium pressure would rupture glass flow meters in the water lines and, once again, the helium would vent inside the secondary containment structure.

12.2.3 Instrumentation

Standard pressure, temperature, and flow instruments monitor the performance of the water systems and transmit signals to the utilities graphic panel in the ground-level electrical equipment room. Critical flow and temperature sensors are connected to the Scanalarm system, which activates a control room annunciator when a malfunction occurs.

The utilities graphic panel, which includes instrumentation for the ventilation and other systems as well as the water systems, shows flow diagrams for all of the utility circuits. Power switches for the system components are on the panel, as are pilot lights that show system status. A recorder and a temperature indicator can be connected with plugs or switches to determine trends or current temperatures throughout the facility. Meters continuously indicate critical pressures. The panel is in a clean area that is always accessible.

Each of the reactor cooling panel and blower cooling water circuits has an independent control system on the utilities panel. At the panel, the inlet, outlet, and vent valves for each circuit can be operated, and the position of each circuit's high-low flow switch is indicated. A pH recorder on the panel shows the condition of the demineralized water system.

12.2.4 Design Analysis

The design features that provide cooling capacity for safe reactor shutdown after loss of power are described in context in Sec. 12.2.2. Emergency cooling water from city mains can be admitted to the cooling water systems only through hand-operated valves near the isolation heat exchanger in the basement-level, mechanical equipment room. This area

of the facility has controlled access, but is shielded against the reactor and is habitable at all times. Heat capacities in the reactor cooling panel systems are adequate to allow time for manual operation of the valves in case of power failure.

The isolation heat exchanger in the cooling water system maintains the integrity of the secondary containment where it is penetrated by cooling water lines. If an accident were to cause simultaneous release of fission products and the rupture of water lines in the containment structure, the water system on the shell side of the exchanger would become the backup containment boundary.

Direct connection of the primary and secondary coolant loops through the blower cooling water piping is prevented by the isolation heat exchanger in the primary blower cooling system.

12.2.5 Tests and Inspections

Cooling water system components are inspected daily as a part of the operator's routine. The standby pump is started, and the condition of the evaporative cooler controls is checked weekly.

Daily checks are made of the demineralized system functions that are recorded or indicated on the utilities panel. Visual inspections of the accessible portions of the system are made routinely. The system standby and emergency pumps are operated weekly.

The procedures for admitting emergency cooling water are performed periodically as a part of the emergency drill for operators.

12.3 Facility Ventilation Systems

12.3.1 General Description

Figure 12.3.1.1 is a schematic air flow diagram for the building. There are four independent ventilation systems, one for each of the following regions: the secondary containment structure, the fuel handling and gas sampling cells and their adjacent operating areas, the

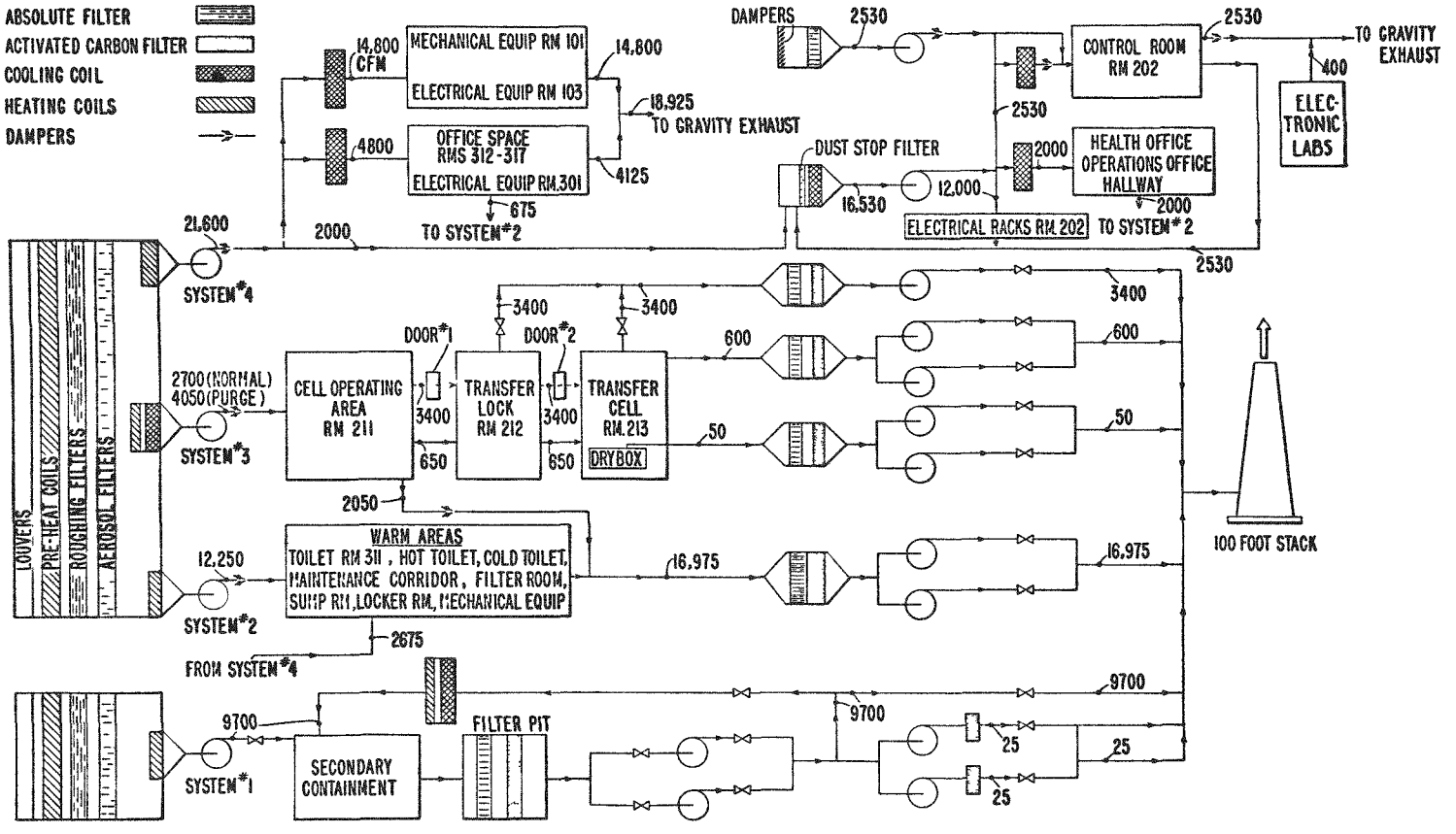

Fig. 12.3.1.1 Building ventilation flow diagram

change rooms and other "warm areas" that might become contaminated during normal operations, and the control room and other clean areas. The secondary containment ventilation system, System No. 1, is described in Sec. 9.3; the other three systems are the subject of this section.

Ventilation air is not recirculated, except to the air-conditioned electronics racks in the control room. All intake air passes through preheat coils, roughing filters, and aerosol filters designed to remove particles as small as 20 μ in diameter. Exhaust air from areas that might be contaminated is passed through absolute and activated carbon filters and vented through a 100-ft stack. Air from clean areas exhausts through rooftop vents. Throughout the facility, air moves from areas that are clean toward those that might become contaminated.

12.3.2 Design Details

System No. 2, which ventilates the potentially contaminated areas, takes in outside air from a filter bank shared with Systems No. 3 and No. 4, heats the air, moves it through the warm areas, and exhausts it through absolute and charcoal filters to the stack. System No. 2 changes the air 10 times per hour in the warm areas. An additional 10 changes per hour are produced in the locker room, toilets, and mechanical equipment room by air that enters through door louvers from the clean areas served by System No. 4.

System No. 3 serves the cell operating area and the two hot cells, the fuel transfer lock and the fuel handling cell. When the cell doors are closed, the intake blower, operating at low speed, supplies 2700 ft^3/min of air to the cell operating area. Most of the air, 2050 ft^3/min, passes through the operating area and exhausts in a duct to the System No. 2 exhaust filter plenum. A small flow, 650 ft^3/min, enters the cells via a duct and exhausts through two sets of independent blowers and filter banks that maintain the cells at a pressure below the operating area pressure. A 150-ft^3/min blower-filter set is installed for use as a drybox ventilation system.

If the outer cell door is opened, the drive on the System No. 3 intake blower shifts into high speed to supply 4050 ft^3/min of air, and a 3400-ft^3/min cell exhaust blower starts up. The major airflow, then, is through the operating area, into the cells, and out to the stack through the cell exhaust blower and filter bank.

System No. 4 serves the clean areas: the office and laboratory areas, the ground level equipment rooms, and the control room. The majority of the air passes through offices and equipment rooms to roof-top vents. However, air that ventilates the operations and health offices and the adjacent hallway passes into System No. 2 through the locker room and hot toilet. Some of the exhaust air from the lower level offices also enters System No. 2, through the sump pump room and the adjacent toilet.

In the control room, 85% of the air flow enters the electronic racks, via a plenum formed by the suspended floor, and is recirculated through an independent system, which filters dust from the air and recools it with a coil served by a refrigerated, chilled water system. A second independent system makes the control room habitable if an accident should result in the release of fission products inside or from the facility. In this emergency system, a blower driven by the emergency power supply, takes in outside air through an absolute filter, and discharges into the control room, from which the air exhausts to the atmosphere.

The electronics laboratories have an independent, conventional, ventilation system. Its only tie to the other facility systems is a connection through which 400 ft^3/min of air discharge into the System No. 4 gravity exhaust duct.

All absolute filters in the ventilation systems are designed for minimum efficiency of 99.95%, i.e., dioctyl phthalate penetration of 0.05% for 0.3-μ-diameter homogeneous particles. Each filter is inspected and tested, independently of the manufacturer, for conformance to the specification of AEC Accident and Fire Prevention, Issue No. 104, December 11, 1959, "Recommended Minimal Specifications for Fire Resistive

High Efficiency Particulate Air Filter." The charcoal filters are Barnebey-Cheney Type 7-FE-A, which meet the requirements for activated charcoal, radioactive iodine adsorptive filters, as generally described in AEC Report DP-778, for use in series after absolute filters.

12.3.3 Instrumentation

Operation of the ventilation systems is monitored with the aid of the usual instrumentation: pressure and differential pressure transducers, temperature sensors, flow switches, and valve position indicators. Conventional control systems regulate temperatures and maintain pressure differentials.

Meters, recorders, and indicators for the ventilation systems' instrumentation and controls are located on a panel in the ground level electrical equipment room, together with the control switches for system components. A Scanalarm system on the panel indicates irregular performance, sensed by flow switches, of the intake and exhaust fans in each ventilation system. An alarm on the equipment room panel is indicated also on the control room annunciator panel, but the source of the alarm is not identified there.

12.3.4 Design Analysis

The air flow in all four facility ventilation systems is designed to limit the spread of contamination. Loss of any one of the facility ventilation systems during reactor operation would not create an emergency situation of an immediate nature. Precautionary measures, such as more frequent air sample analysis and cessation of fuel transfer cell operations, would be taken. If the cell area system were lost, the cells would be isolated by closing a slide valve in the duct from the operating area into the transfer lock.

In the unlikely event that all normal ventilation were to be interrupted simultaneously by a power failure, the control room would be provided with ventilating air automatically by the emergency supply fan.

12.3.5 Tests and Inspections

Filter differential pressures are checked monthly in order to anticipate the need for filter replacement. The automatic start circuit for the control room emergency supply fan and the cell door interlock circuit are tested monthly to insure operability.

12.4 Compressed Air Systems

12.4.1 General Description

Two systems distribute compressed air throughout the facility from compressors located in the ventilation equipment room on the ground level. One system supplies control systems and the pneumatic operators on valves in the helium systems and in the ventilation systems. The second, house air, system supplies outlets to which power tools may be attached at locations inside the building.

12.4.2 Design Details

The source of control air is a unitized dry air system capable of supplying 100 std ft^3/min of air at 100 psig, dried to -40°F dew point. A 15-hp compressor supplies two, heatless, automatically regenerated, dryer towers that have prefilters, traps, and afterfilters. Air is stored at 100 psig in a 57-ft^3 storage tank. Pressure switches on the tank start the compressor at 90 psig and stop it at 100 psig.

For the house air supply, another identical, 15-hp compressor feeds a 25-ft^3 storage tank through a centrifugal separator and dual cartridge filters.

The two compressors are piped to a common header, but ordinarily operate independently, separated by a closed manual valve. While maintenance or repairs are being made on one compressor, the second one can supply both systems, if the use of house air is curtailed.

Mains of 1-1/4-in. copper tubing carry air to points of use. One air line penetrates the secondary containment to supply valve operators.

Just outside the containment wall, this air supply line passes through a ball valve with a fail-closed pneumatic operator supplied by line air from the downstream side. In case of compressor failure or rupture of the supply line inside the containment structure, a spring in the operator closes the ball valve to maintain containment.

Operating air is supplied from 3-way solenoid valves in cabinets outside the containment to all of the valves that have critical functions and are located inside the containment. Each solenoid valve can be isolated with hand valves for repair or replacement, and all vent into the containment structure.

12.4.3 Design Analysis

Because pneumatic operators control valves in the helium handling and other critical systems, the reactor must be shut down if a complete failure of the compressed air system should occur. However, all pneumatic operators fail safe, and no hazards would arise from a loss of the compressed air system.

12.4.4 Tests and Inspections

The air compressors are inspected daily as a part of the operators' routine. Function of the pressure regulation system is tested, and water is drained from filters, dryers, silencer, and receivers.

12.5 Door Seal Vacuum System

12.5.1 General Description

A standard, oil-sealed vacuum pump maintains a reduced pressure in a copper tubing system that serves the two gas-tight doors into the secondary containment and the shielding doors at the hot cells.

The seal arrangement on the gas-tight doors appears in Fig. 9.2.1. A pipe connects the seal's buffer zone to the vacuum system. After a door is closed and dogged, the buffer zone is evacuated, and atmospheric

pressure forces the neoprene gasket on the door against the sealing surfaces on the door frame.

On the shield doors, an inflated gasket seals each door around its periphery. The vacuum system is used to pull the deflated seals away from the doors when they are to be opened.

12.5.2 Design Details

The pump in the door seal vacuum system is a Kinney, Model CVM 556, rotary compound type, which discharges to the stack. It has a capacity of 3 ft^3/min at 0.2-μ pressure. Just upstream from the pump is a 20-gal receiver.

A pressure switch on the receiver starts the pump at 20-in. Hg pressure. If the pressure in the receiver rises above 20 in. Hg, an alarm is triggered on the Scanalarm at the utilities panel and on the control room panel. A pressure rise indicates either a leak in a seal or an open access door. Local valves and gauges permit the testing of individual door seals. Functional tests of the pump pressure switch and alarm are made weekly.

12.6 Contaminated Liquid Waste System

12.6.1 General Description

Although contaminated liquid wastes will not be generated routinely in the facility, the possibility exists that liquids could be released in contaminated areas. Therefore, the floor drains in the secondary containment structure and in the hot cells are connected to a contaminated waste system that discharges to the LASL low level waste treatment plant.

Liquid waste flows in 3-in. steel pipe from the floor drains to a 2300-gal tank located under the floor of the basement-level sump room. Waste also flows to the tank from the vacuum cleaning system's cyclone separator, which has water spray nozzles in its hopper. From the tank,

duplex centrifugal pumps, operated by an electrode level control, move the waste to a ground-level treatment station in a building about 120 ft north of the facility. The waste is neutralized there with sodium hydroxide to 7.0 pH and can be stored in two 5000-gal storage tanks. Eventually the waste is pumped through the contaminated sewer to the TA-50 waste treatment plant.

12.6.2 Design Analysis

The contaminated waste system operates only intermittently and is not essential for reactor operation. Normally, a hand valve near the sump tank closes off the drain lines from the secondary containment. High liquid level in the sump tank is indicated on the Scanalarm at the utilities graphic panel.

12.7 Facility Service Systems

12.7.1 Vacuum Cleaning System

For picking up potentially contaminated dust in the exhaust ventilation filter room and the secondary containment, there is a 13-outlet vacuum cleaning system. Air moves through 2-in. stainless steel ducts from the outlet hose connections to a cyclone separator, absolute filter, and multistage centrifugal blower, all located in the sump room. Dust removed in the separator is washed to the contaminated waste tank through a rotary vane valve. Any dust remaining in the air is collected on the absolute filter before the air enters the blower, which discharges to the outlet filter plenum of ventilation system No. 2.

When the blower is turned on, a water spray in the dust separator also starts. A liquid-level controller on the separator's hopper maintains a water seal above the rotary valve, actuates the valve motor to empty the hopper, and initiates an alarm in the Scanalarm system if the water level in the hopper rises too high.

Spring loaded covers keep the vacuum system outlets closed unless a hose is connected. A plug cock, normally closed, isolates the secondary containment portion of the system.

12.7.2 Breathing Air System

If contamination should be released in the secondary containment structure, people entering there might be required to use air-supplied face masks. Clean air at regulated pressure is supplied for this use by a water-sealed rotary compressor located in the ground level ventilation equipment room. The compressor feeds six outlets inside the containment structure. An isolation valve near the compressor closes off the system during reactor operations.

12.7.3 Air Sampling System

A multistage centrifugal blower, located in the exhaust filter room, pulls air through a 20-outlet system and discharges to the stack. The outlets, located throughout the facility operating areas, are designed to accommodate standard filter paper holders that collect airborne particulates for the radioactivity monitoring program described in Sec. 13.7.6. System blower operation is monitored by the Scanalarm.

13. RADIOACTIVITY CONTROL

13.1 Fuel Handling

13.1.1 New Fuel

UHTREX fuel elements are transported from the CMR building, where they are fabricated, to the UHTREX facility in aluminum cans 5.5-in. in diameter and 58-in. long. Each can contains as many as 15 aluminum tubes, 1.05-in. i.d., each of which holds as many as 10 fuel elements. The largest mass of uranium which could be concentrated in a single can of fuel elements is 2 kg.

The cans are stored in horizontal array on high-rise, safe-geometry racks in Room 104, a ground-floor room above the fuel transfer lock and cell. Each rack permits storage of 14 cans (seven cans per column, two cans per row). Configuration of each rack establishes a 4-in. separation between cans in a column and 9 in. between cans in a row. Administrative controls limit the amount of fuel stored in Room 104 to 15 kg of uranium.

Calculations confirm that the fuel storage arrangements are safe. Table 13.1.1.1 lists the limiting number of fuel elements which may be safely accumulated in a close-packed spherical array. Consideration was given to both bare, dry assemblies and to water flooded and reflected assemblies. While the elements are in storage cans, a close-packed array cannot be made, and the flooding of Room 104 with water cannot occur.

During loading operations, a few storage cans at a time are moved to the cell operating area and unloaded there by hand. The leaching

process to which all elements are subjected (see Sec. 4.1.4) effectively removes all exposed uranium and makes the new elements safe for use in manual operations. People who handle the elements wear cotton gloves, primarily to keep the elements clean.

TABLE 13.1.1.1

FUEL STORAGE SAFETY CALCULATIONS

Gram ^{235}U per Fuel Element	Condition	Critical Radius (cm)	Critical Mass, Kg ^{235}U	Number of Fuel Elements
9.8	Dry	86.3	313.0	32,000
9.8	Flooded	21.7	4.9	510
4.0	Flooded	24.3	2.9	715
1.5	Flooded	32.9	2.7	1,790
1.5	Dry	96.2	67.5	45,000

13.1.2 Spent Fuel

The methods for handling individual spent fuel elements are described in Section 6.1. Briefly, not more than 21 spent fuel elements, sealed in an alpha can, are placed with manipulators in a cart-mounted cask for transport out of the fuel cell to the loading dock at the rear of the facility. At the dock, a 10-ton crane lifts the cask from the cart to the bed of a truck. The truck carries the cask to hot cell facilities at Wing 9 of the CMR building. There the alpha can is removed from the cask and stored in a shielded pit until fuel processing begins.

Twenty-one spent fuel elements have the potential for producing a source of approximately 20,000 C. Shielding in the casks limits contact radiation levels to 100 mR/h. The casks used to move UHTREX spent fuel elements are standard transfer casks used extensively by radiochemistry and metallurgy groups at LASL. The body of each cask is

constructed of depleted uranium with a minimum wall thickness of 7 in., and the top of the cask is shielded by a Meehanite plug 22-in. thick. A cask basket, which contains the radioactive material, hangs from the Meehanite plug on two bayonet-lock pins. A door in the base of the cask slides open to allow lowering of the plug-basket assembly from the cask directly into a storage pit at the CMR facility.

13.2 Liquid Wastes

Contaminated liquid wastes are not generated routinely in the UHTREX facility. Limited quantities of contaminated water would be produced if a decontamination washdown were done inside the secondary containment structure. This water, and any other liquid turned free inside the structure, is routed by floor drains to the collection and treatment facilities described in Sec. 12.6. No radioactive liquid wastes are expected from laboratory facilities on the site. All active wastes are carried by a separate contaminated sewer to TA-50, a treatment site which receives active waste liquids from many other technical areas at LASL.

13.3 Gaseous Wastes

The two radioactive gases that are released during normal operations are ^{41}Ar, produced in the air inside the reactor cell, and ^{3}H, produced in the primary coolant and released as water by the gas cleanup system. The intensities of these sources are evaluated in Sec. 13.3.2.

13.3.1 Dilution Factors for Stack Release

Expressions for the calculation of minimum dilution factors, for instantaneous and continuous stack release and for distances from the stack to points of maximum concentration, are quoted below from AECU-3066[1] for two modes of release.

[1]Sutton, "Meteorology and Atomic Energy," AECU-3066, July 1955.

For instantaneous release

$$d_{max} = \left(\frac{2h^2}{3C^2}\right)^{1/(2-n)},$$

$$K_{max} = \frac{X_{max}}{Q} = \frac{2}{(2/3\ e\pi)^{3/2}\ h^3}.$$

For continuous release

$$d_{max} = \left(\frac{h^2}{C^2}\right)^{1/(2-n)},$$

$$K_{max} = \frac{2}{e\pi\bar{u}h^2},$$

where

d_{max} = downwind distance in meters from the stack to the point of maximum ground level concentration, X_{max}
K_{max} = dilution factor at distance d_{max} downwind, sec/m^3
h = stack height, m
n = dimensionless meteorological parameter related to stability
C^2 = dispersion parameter dependent on h and n, $(m)^n$
$\bar{u}$ = wind velocity, m/sec.

The meteorological parameters selected and the calculated values of d_{max} and K_{max} are listed in Table 13.3.1.1. Values for n and C^2 are from Sutton.[1] Values for $\bar{u}$ were selected after an examination of wind velocity data presented in Sec. 2.4 of this report.

TABLE 13.3.1.1

METEOROLOGICAL PARAMETERS FOR STACK RELEASE

	Instantaneous		Continuous
Parameter	Large Inversion	Large Lapse	Typical Inversion
$\bar{u}$ (m/sec)	1	1	2.2
C^2 (m^n)	0.004	0.043	0.006
n	0.5	0.2	0.33
d_{max} (m)	2800	200	1300
K_{max} sec/m^3	5.19×10^{-6}	5.19×10^{-6}	1.14×10^{-4}

13.3.2 Source Intensities

^{41}Ar Within the Secondary Containment - The production rate of ^{41}Ar can be calculated from the expression

$$\frac{dN}{dt} = N_o \sigma \phi A \ell,$$

where

N = total number of ^{41}Ar atoms

N_o = number of atoms of ^{40}Ar per cm^3 in the air = 3.02×10^{17} cm^{-3}

σ = thermal neutron capture cross section = 0.53 b

ϕ = thermal neutron flux outside of the reactor vessel = 2×10^{10} cm^{-2} sec^{-1}

A = area of the reactor vessel = 5×10^5 cm^2

ℓ = average neutron path length in the air = 2×10^2 cm.

Using the given values of the variables, $dN/dt = 3.2 \times 10^{11}$ sec^{-1}. The decay constant of ^{41}Ar is $\lambda = 1.05 \times 10^{-4}$ sec^{-1}, so the source production rate is 9.1×10^{-4} C/sec.

For closed-cycle operation of the ventilation system, the equilibrium source within the secondary containment is

$$\frac{3.2 \times 10^{11}}{3.7 \times 10^{10}} = 8.65 \text{ C},$$

and the concentration in the 4200-m^3 containment structure is 2.06×10^{-3} C/m^3. To derive the equilibrium source dose rate, the structure is treated as a hemisphere of 10-m radius. The gamma flux at the center of a sphere, according to Rockwell,[2] is

$$\phi = \frac{BS_v}{\mu_s}\left(1 - e^{-\mu_s R_o}\right),$$

where

B = dose buildup factor = 1

S_v = source per unit volume

μ_s = macroscopic energy absorption cross section of air for 1.3-MeV γ rays = 3×10^{-5} cm^{-1}.

For a hemisphere the flux is $\phi/2$.

Argon-41 emits a 1.3-MeV γ ray 99% of the time (none the other 1%), and the end-point energy of the principal β particle is 1.2 MeV. Therefore, for calculating dose rate, the mean energy per disintegration is assumed to be 1.8 MeV. The photon flux at the center of curvature of the hemisphere, is 3.8×10 cm^{-2}/sec^{-1}, which produces a whole-body dose rate of about 0.16 R/h. Although the secondary containment structure will be flushed with outside air before personnel enter, this dose rate would permit limited access without flushing.

---

[2]Theodore Rockwell, III, Reactor Shielding Design Manual (D. Van Nostrand Co., Princeton, N. J., 1956, p. 371).

^{41}Ar in Stack Effluent - Assuming that typical inversion conditions prevail in the Los Alamos area, a continuous release of the ^{41}Ar at its production rate would produce the maximum ground concentration at a distance of about 1300 m, and the dose rate at that point would be about 10^{-4} R/h. A consideration of the frequency and duration of such inversions (none has been recorded as lasting through a 24-h period) and the variability of wind direction over any extended operating time, leads to the conclusion that the average dose rate at any one point would be less, in actuality, by at least an order of magnitude. Closed-cycle operation of the secondary containment ventilation system, coupled with the short half-life of ^{41}Ar, reduces greatly the total activity released for the arbitrary case of a venting of the containment structure after a 26-h operating period. The total released activity is only 1/10 of the amount liberated in a continuous release over the same period. The reduction due to closed-cycle operation increases linearly with operating time. A combination of actual wind conditions and closed-cycle operation reduces the average integrated dose from ^{41}Ar to persons in unrestricted areas to no more than a few mR/yr, and the production of even this dose requires unreasonably frequent shutdown and venting operations.

Tritium Production and Release - Tritium is produced in the primary coolant by the ^{3}He (n,p) ^{3}H reaction. The fractional concentration of ^{3}He in natural He is about 1.3×10^{-6}. The (n,p) cross section of ^{3}He is about 2.1×10^{3} b at the operating temperature of 0.14 eV. There are about 7×10^{2} g He in and near the core in an average neutron flux of less than 3×10^{13} cm^{-2}/sec^{-1}. Therefore, the tritium production rate is no greater than

$$\frac{dN}{dt} = 1.3 \times 10^{-6} \times \frac{7 \times 10^{2}}{4} \times 6 \times 10^{23} \times 2.1 \times 10^{-21} \times 3 \times 10^{13}$$

$$= 7.4 \times 10^{12} \text{ sec}^{-1}$$

which amounts to approximately 4×10^{-7} C/sec.

Normally ^{3}H is removed in the gas cleanup system by oxidation to water in the copper oxide bed and adsorption of the water in the molecular sieve beds. Periodically the molecular sieve beds are regenerated and the water vented to the stack. Averaged over the production time, the ^{3}H release rate can be no greater than the production rate of 4×10^{-7} C/sec. Assuming a typical inversion for the Los Alamos area, the maximum ground concentration, averaged over the production time, is about 4.6×10^{-11} C/m^3, which is far below the concentration of 2×10^{-7} C/m^3 permitted in uncontrolled areas.[3]

13.3.3 Gas Cleanup System Vent Gas

Radioactivity can be vented to the stack in gas streams that come from three sources in the gas cleanup system: the sample gas discharge of the gas chromatograph, the discharge of the vacuum pump during molecular sieve bed regeneration, and the purge gas outlet of the sidestream beds during their regeneration. Of the three, only the sidestream bed purge represents a real source of concern, but analysis shows that it can be discharged safely through the stack.

Sample gas is discharged continuously from the gas chromatograph, while it is operating, at a flow rate of about 100 cm^3/min at atmospheric pressure. Since samples can be taken from points throughout the cleanup system, the purity of the sample discharge gas can range from that of raw primary loop coolant to that of the fully treated helium returning to the primary loop. How much activity exists in any of these streams depends on the history of the reactor operations preceding the time at which the sample is taken. Early in the life of UHTREX, activity in the primary loop coolant will be nonexistant or at very low levels. It is during this period that the gas chromatograph will be used most frequently, to follow the course of outgassing in the reactor and recuperator. Later on, when activity levels in the raw coolant prohibit its

---

[3]"Standards for Protection Against Radiation," Title 10, Code of Federal Regulations, Part 20, (10 CFR 20), November 17, 1960.

release to the stack, the use of the chromatograph will be confined to the analysis of treated helium streams whose activities will be lower than that of the sidestream purge gas, described below.

Gas discharged from the vacuum pump during molecular sieve bed regeneration contains high concentrations of water and carbon dioxide, and therefore must be vented to the stack instead of being recirculated through the low pressure receiver. Happily, the regeneration of the molecular sieve bed will occur most frequently during the early, high outgassing rate period of reactor operations when the activity levels in the primary coolant are low. The volatile isotopes that do exist in the coolant can reach the molecular sieve beds only after passing through the decay heat exchanger, where halogens will be trapped. What remains in the coolant at the sieve beds are essentially the noble gases, which are not strongly adsorbed on molecular sieves, and are purged out of the bed in the first step of the regeneration process. Thus, in the early period of operation when regeneration of the sieve bed is certainly necessary, there will be no residual activity to be discharged when the beds are evacuated. If regeneration should be necessary later, when residual activity might be present in a sieve bed, the frequency of regeneration will be so low that long purge periods could be used to ensure removal of entrained activity from the beds, and the evacuation step could be scheduled for periods when favorable meteorological conditions exist for the discharge of activity. The isotopes that would be discharged are the same as those described below for the sidestream bed purge gas.

The sidestream adsorption beds must be regenerated throughout the life of the experiment, and the purge gas from the beds will be discharged through the stack. Helium from the primary loop enters these beds only after passing through the delay beds, and therefore the only radioactivity in the bed is that of the long-lived isotopes of krypton and xenon. An upper limit can be established for the hazards that might be created if these isotopes were vented from the stack, by assuming that the radioactive gases are vented at their rate of elution from the delay beds.

Under this assumption, the sidestream beds receive the full flow of coolant from the delay beds for 4 h, before breakthrough occurs, and are regenerated immediately thereafter. No credit is taken for the decay that occurs during normal operations, when the sidestream beds may remain on-line for weeks at a time. The results of calculations based on these worst-case conditions are presented in Table 13.3.3.1. An examination of the table shows that the only isotope that may cause concern is ^{85m}Kr. In reality, this isotope, with a half-life of 4.36 h, would undergo 4 h of decay in the sidestream beds and in the coolant loop as the beds reach saturation and another 5 h of decay as the beds are isolated and heated. Furthermore, there is no compelling reason for venting the beds during any period when adverse meteorological conditions exist. In practice, the venting would be delayed at least until inversions had dissipated.

TABLE 13.3.3.1

CONCENTRATIONS PRODUCED BY WORST-CASE VENTING OF SIDESTREAM BED PURGE GAS

Isotope	Delay Constant (sec^{-1})	Fission Yield (%)	Elution Rate from Delay Beds (C/sec)	Concentration in Nearest Uncontrolled Areas* (C/m^3)	MPC^3 (C/m^3)
^{85m}Kr	4.41×10^{-5}	1.5	1.7×10^{-3}	1.7×10^{-7}	1×10^{-7}
^{85}Kr	2.14×10^{-9}	0.3	2.0×10^{-5}	2.0×10^{-9}	3.10^{-7}
^{131m}Xe	6.68×10^{-7}	0.03	7.9×10^{-6}	7.9×10^{-10}	4.10^{-7}
^{133}Xe	1.52×10^{-4}	6.5	2.0×10^{-5}	2.0×10^{-9}	3×10^{-7}

* Assumes 5-mph wind, typical inversion, ~1-mile distance.

13.4 Primary Shielding

Shielding requirements were specified for the UHTREX facility in accordance with the following criteria.

1. Operating and control areas and, in general, all areas outside the secondary containment regions should be fully accessible during normal full power operation of the reactor. The design radiation level for these regions is 1 mrem/h. In addition, the control room proper is designated as a refuge for operating personnel in the event of a major disaster, such as the rupture of the primary containment system and consequent release of fission products to the secondary containment system. The shielding is specified to limit the dose rate in the control room to about normal working tolerance level.

2. Areas inside the secondary containment system will be accessible normally only when the reactor is shut down. After extended operation, radiation levels in most of these areas may be above the 40-h week tolerance level, and working times will have to be adjusted accordingly. Radiation levels in the reactor cell proper will probably be so high as to preclude access to that room even after long cooling times.

13.4.1 Reactor and Gas Cleanup Rooms

The calculated fluxes incident on the reactor biological shield for 3-MW operation, together with some of the values used in specifying shield thicknesses, are tabulated in Table 13.4.1.1. The basic assumptions and the calculational methods used in obtaining those values are discussed in detail by Bergstein and Battat.[4] The configuration of the main shielding is shown in Figs. 3.2 - 3.6 of this report.

Between the reactor room and the control room, there are shield walls of 3.5 ft of magnetite concrete and 7 ft of ordinary concrete.

---

[4]J. Bergstein and M. E. Battat, "Turret Shielding Report," Los Alamos Scientific Laboratory report LAMS-2557, February 1961.

TABLE 13.4.1.1

DATA FOR SPECIFICATION OF SHIELD THICKNESSES

Source	Flux Incident on Bulk Shield (per cm^2-sec)	Decade Length in Ordinary Concrete (in.)	Decade Length in Magnetite Concrete (in.)	Decade Length in Tuff (in.)
Thermal neutrons	2.2×10^{10}	6.4	2.2	30
Nonthermal neutrons	2.4×10^{9}	12	8.7	23.4
Gamma rays E_{av} = 2 MeV	3.1×10^{10}	12	8	26
Gamma rays E_{av} = 8 MeV	2.0×10^{10}	18	12.5	48

Further protection for the control room is provided by the 4-ft magnetite concrete wall of the fuel transfer cell and transfer lock, which are situated between the control room and the biological shield. The change rooms and operating floor hallway are shielded from the reactor by 5 ft of magnetite concrete and 5 ft of ordinary concrete. The remote maintenance corridor, to which full-time access is not required, is shielded from the reactor by 5 ft of magnetite concrete and 2.5 ft of ordinary concrete. The exterior walls of the reactor room are of ordinary concrete, 5-ft thick. Because the reactor room is below grade, advantage is taken of the shielding properties of the surrounding earth and rock (tuff).

The components of the gas cleanup system, located in the gas cleanup room, are expected to accumulate a significant portion of the fission products generated in the reactor. The intensity of this source is difficult to determine. However, the position of the gas cleanup cell between two layers of the reactor biological shield provides a minimum

of 2 ft of magnetite concrete and 5 ft of ordinary concrete between this source and the operating areas.

The top shield for the reactor room and the gas cleanup room consists of 5 ft of magnetite concrete, sufficient to maintain near-tolerance levels inside the secondary containment above-grade structure when the reactor is shut down. Radiation levels in areas immediately outside the structure will be held near tolerance values during reactor operation by the ordinary concrete walls of the structure, 1.5-ft thick on three sides and 3-ft thick on the side facing the control room.

13.4.2 Other Areas Inside the Secondary Containment

As noted above, these areas are accessible only during shutdown, so the fission product inventory is the source of concern. Shielding requirements for these areas were determined using a method developed by Ashley.[5,6] In this method, valid for spent fuel surrounded by thick shields, only those fission products that emit photons of energies greater than, or equal to, 1.6 MeV are considered. From Ashley's data, the hard gamma power, following 1 yr of operation and 24 h of cooling time, is 1.1×10^{16} MeV/sec. Based on an effective energy of 2 MeV, the shutdown source is 1.5×10^{5} C.

Shield thicknesses of magnetite concrete between these areas and the reactor cell are as follows:

Upper gas cleanup piping room	5 ft
Reactor drive room	4 ft
Fuel discharge room	4 ft
Fuel charging room	3.5 ft

---

[5]R. L. Ashley, "Graphical Aids in the Calculation of the Shielding Requirements for Spent U-235 Fuel," NAA-SR-1992, 1957.

[6]R. L. Ashley, "Effective-Energy Method for Spent-Fuel Shielding," Nucleonics 16, No. 10, 78 (1958).

13.4.3 Fuel Transfer Cell and Lock

Accessibility of the fuel transfer cell and lock to personnel will be limited by the presence of spent fuel within the rooms rather than by reactor power level. Analysis by Ashley's method predicts a storage capacity, without exceeding tolerance levels outside the cell, of at least 100 spent fuel elements, delivered from the reactor at the maximum discharge rate.

13.4.4 Shielding Materials

The basic shield materials used in the facility are magnetite concrete and ordinary concrete. As most of the facility is below grade level, the shielding properties of soil and porous rock (tuff) were calculated and taken into account in specifying the external shield wall thickness. The mixes specified for magnetite and ordinary concrete were as follows:

	Ordinary	Magnetite
H_2O	260 lb/yd^3	300 lb/yd^3
Fine aggregate	3300 lb/yd^3	2747 lb/yd^3
Coarse aggregate	---	2747 lb/yd^3
Cement	318 lb/yd^3	470 lb/yd^3
Plastiment	---	30 fl. oz.

Cross sections for gamma absorption in the shields were calculated from the elemental compositions listed in Table 13.4.4.1.

13.4.5 Thermal Shield

A 2-in.-thick lead, thermal shield lines the inside wall of the reactor room to reduce the energy current delivered to the primary concrete shield. Table 13.4.5.1 shows the effect of the thermal shield

TABLE 13.4.4.1

ELEMENTAL COMPOSITION OF SHIELD MATERIALS (g/cc)

Element	Ordinary Concrete	Magnetite Concrete	Tuff
C	0.004	---	---
Fe	0.0625	2.011	0.0131
H	0.0117	0.0088	0.0014
Si	0.6334	0.0993	0.3453
Al	0.2570	0.0012	0.0694
Na	0.0472	---	0.0288
K	0.0705	---	0.0379
O	1.0955	1.013	0.4890
Mg	---	0.0757	---
Density	2.35	3.5	1.0

TABLE 13.4.5.1

ENERGY CURRENT IN MAIN CONCRETE SHIELD (mW/cm^2)

	No Thermal Shield	Two-In. Lead Shield
Gamma rays (E = 2 MeV)	10	1
Gamma rays (E = 8 MeV)	26	3
Thermal neutrons	3.9	3.9
Nonthermal neutrons	0.5	0.5
Totals	40.4	8.4

in reducing the current to the main shield. Rockwell[2] and Price et al.[7] give maximum allowable values of 20-30 mW/cm^2. Calculations were based

[7]B. T. Price, C. C. Horton, and K. T. Spinney, Radiation Shielding, (Pergamon Press, New York, N. Y., 1957).

on the fluxes of Table 13.4.1.1. In computing the neutron energy currents shown, the average binding energy per neutron, and hence the energy deposited per neutron capture, was taken to be 5.5 MeV. This value was used for both thermal and nonthermal neutrons; i.e., the kinetic energy of the neutrons was neglected in comparison with the binding energy. For the gamma rays, the energy current was assumed to be equal to the product of flux and energy.

13.5 Shielding of the Secondary Containment

The secondary containment structure of the UHTREX facility has inside dimensions of 56 ft x 46 ft x 37 ft high. There is a 2-ft thickness of concrete in the roof and 1.5 ft in three of the walls. To provide additional shielding in the direction of the control room and approach road, a 3-ft-thick concrete shield forms the fourth wall. Shielding calculations were made for the source that would exist if all of the volatile fission products were to escape from the primary coolant loop into the structure, as in case of primary containment failure. The volatile fission product activity, after long-term operation at 3 MW and at the instant of fission product release, was computed to be 1.7×10^6 C, using the data of Kerr and Walton.[8] One photon of 1.5-MeV energy per disintegration was assumed, and the source was assumed to be uniformly distributed in the containment volume. Results are presented for zero shutdown time; between 0 and 2 h after shutdown, the activity is reduced by only a factor of two or three.

In evaluating the dose rates outside the secondary containment, both the direct and scattered (sky-shine) radiation were considered. The calculation of the direct dose rate is straightforward for simple

[8]T. B. Kerr and R. B. Walton, "Results Obtained Using an IBM 704 Program for Computing U-235 Fission Product Populations, Activities, and Powers," AFSWC-TN-59-19, August 1959.

geometrical configurations--sphere, cylinder, or slab--containing uniformly distributed sources. The calculation of the scattered dose rate is both difficult and time-consuming. However, Geller and Epstein[9] have made extensive calculations for the direct and scattered dose rates from fission products contained in a 96-ft-radius spherical vessel half-buried in the ground. Although they are not directly applicable to our problem, use was made of the results of Geller and Epstein in the present calculations.

The containment shell was approximated by a 50-ft-diam cylinder to simplify the dose rate calculation, the successive steps of which are enumerated below.

Step 1: An analytical expression was derived for the dose rate at points outside a nonabsorbing finite cylinder containing a uniformly distributed source. (The derivation is presented in Appendix E.) Dose points were chosen along a radial line at the midheight of the cylinder. The volumetric source was computed assuming a total source strength of 1.7×10^6 C and a cylinder 50-ft diam x 34-ft high.

Step 2: The direct unshielded dose rate (G_{du}), as a function of the distance (D) from the axis of the cylinder was then computed. In computing G_{du}, no side or top shield was used; however, the attenuation of the gamma rays in air was included. G_{du} is plotted in Fig. 13.5.1.

Step 3: The direct shielded dose rate (G_{ds}) was then computed as $G_{ds} = (G_{du})/(\text{Attenuation in side shield})$. The attenuation for 1.5-MeV gammas, with buildup included, was taken as 37 for 1.5 ft of ordinary concrete and 4000 for 3 ft.

Results of these calculations are displayed in Figs. 13.5.2 and 13.5.3. For the 1.5-ft concrete shield, the surface dose rate is approximately 1000 R/h; at distances of 70 and 1000 ft from the structure, the dose rates are 100 and 0.1 R/h, respectively.

---

[9]L. Geller and R. Epstein, "Evaluation of Containment Shielding," Proceedings of the Second United Nations Conference on the Peaceful Uses of Atomic Energy, Geneva, 1958, P/435, 11, 21.

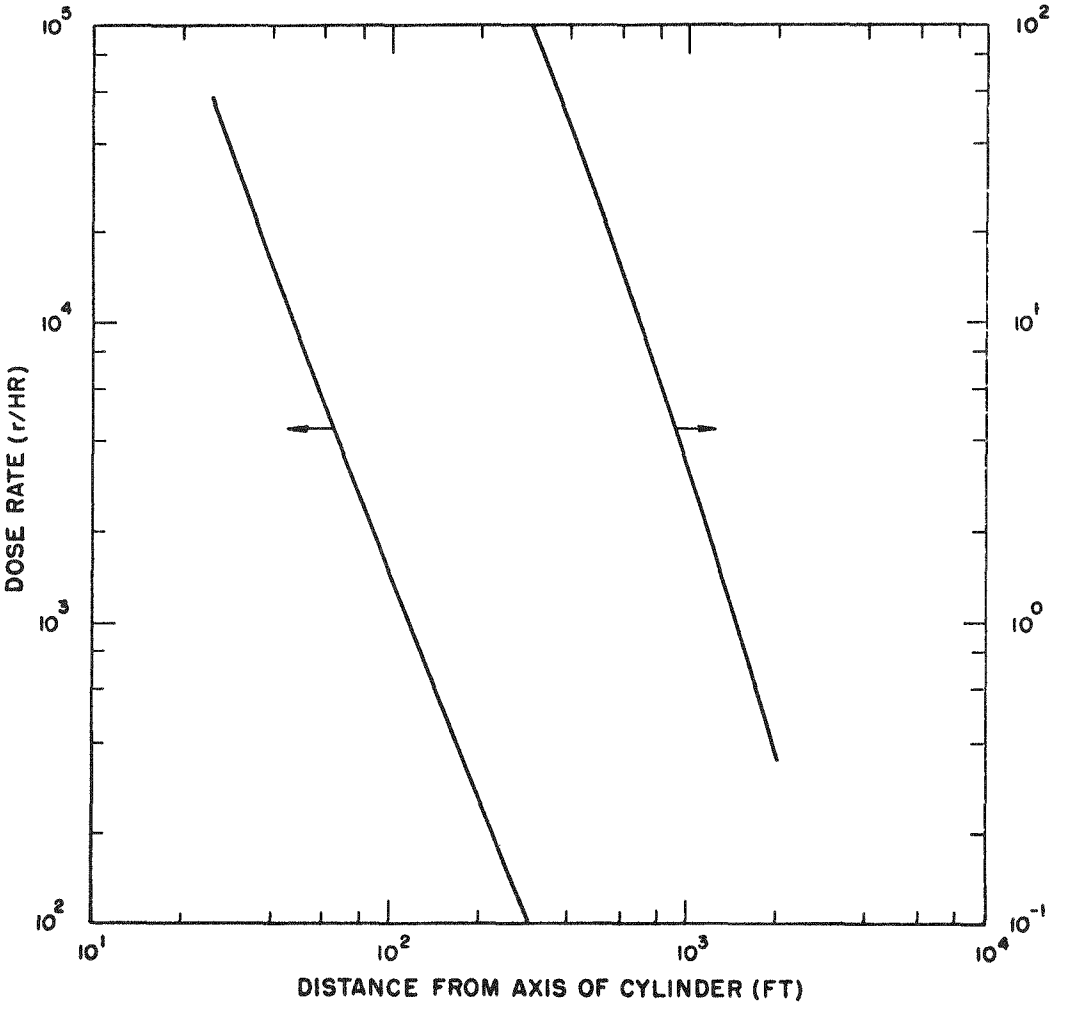

Fig. 13.5.1 G_{du}: Direct unshielded dose rate from cylinder (50-ft diam x 34-ft high) containing a 1.7×10^6-C source of 1.5-MeV gammas

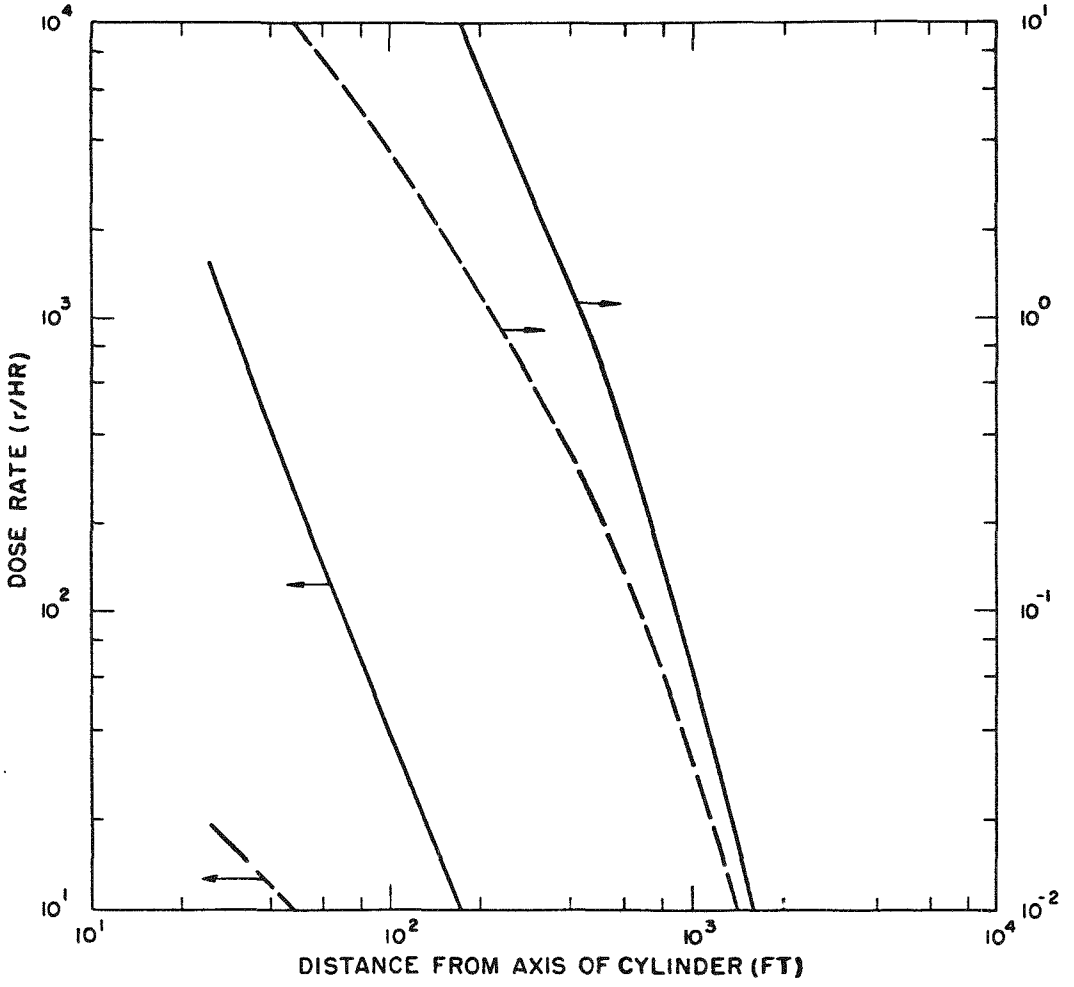

Fig. 13.5.2 Solid line: Dose rate from radiation which penetrates 1.5-ft-thick side walls of cylinder containing a 1.7×10^6-C source of 1.5-MeV gammas. Cylinder is 34-ft high and 50 ft in diam.

Dashed line: Dose rate from air-scattered radiation (sky shine) with 2-ft top shield

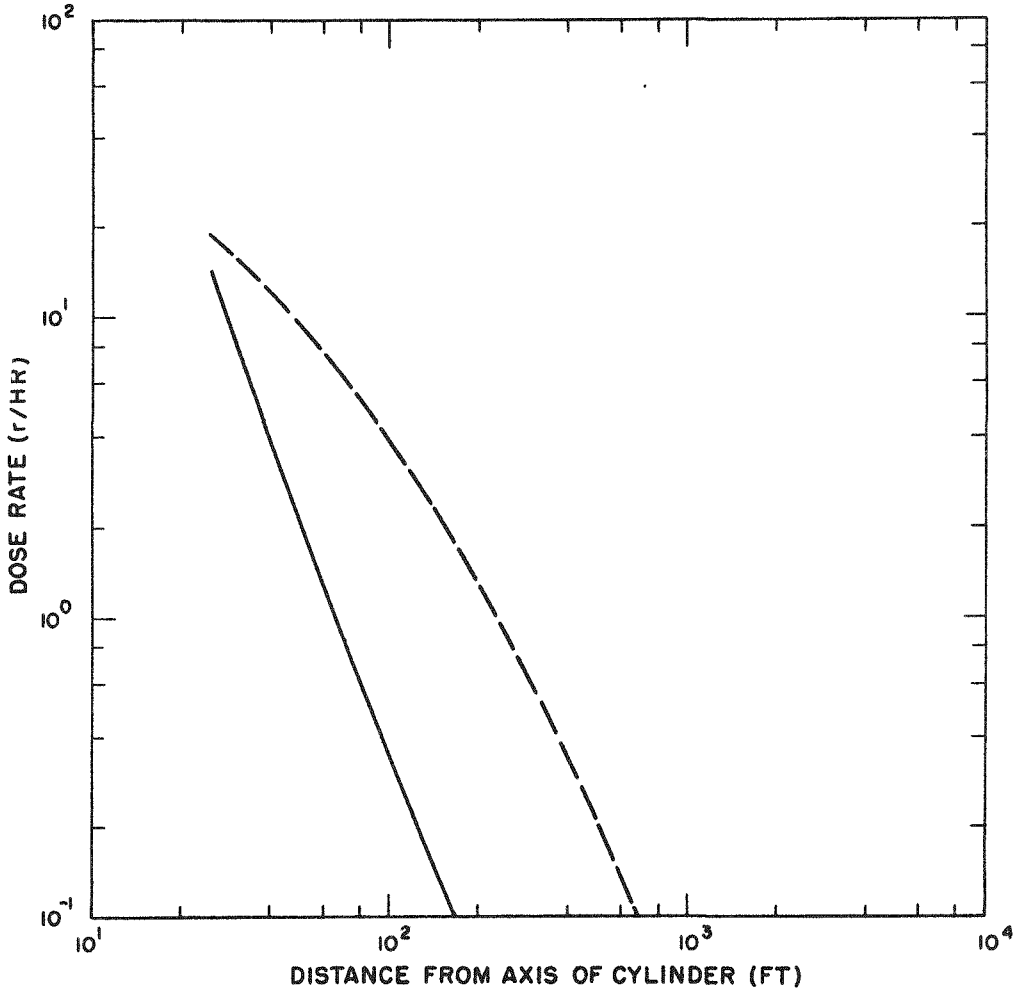

Fig. 13.5.3 Solid line: Dose rate from radiation which penetrates 3-ft-thick side walls of cylinder

Dashed line: Dose rate from sky shine with 2-ft top shield

Step 4: The starting point for the scattered dose-rate estimates was the information given in Fig. 8 of Kerr and Walton.[8] In this figure a plot of the scattered and direct dose rates versus distance D from the center of the containment vessel is shown for an unshielded spherical vessel (96-ft radius) at the instant of fission product release. For the present calculation, the following terms are defined.

G_{su} = scattered unshielded dose rate
F = $(G_{du})/(G_{su})$; G_{du} is defined in Step 2
R_s = radius of sphere.

From Fig. 8 of Reference 9, it can be seen that for $D/R_s = 1$, $F = 15$; as the value of D/R_s increases to 9, the value of F decreases monotonically to 1. For D/R_s between 9 and 21, F decreases from 1 to about 2/3. All of this is for the case where half of the sphere is below ground level. If all of the sphere were above ground level, it seems reasonable to assume that the direct dose rate would be doubled, and the scattered dose rate would remain substantially unchanged. Under these assumptions, as D/R_s increases from 1 to 9, F should decrease from 30 to 2; and as D/R_s increases from 9 to 21, F should decrease from 2 to 4/3. The preceding statements are valid for a containment vessel with no side or top shielding, but the UHTREX secondary containment has a 2-ft concrete top shield. Therefore, an estimate is needed of the attenuation of the scattered radiation by the top shield.

Step 5: In Figs. 12 and 17 of Kerr and Walton,[8] curves are plotted for the direct and scattered dosage versus D for a spherical containment vessel with (1) a 4-ft concrete side shield, and (2) a 4-ft concrete side shield plus a 1.55-ft concrete top shield. From these data, the ratio of the scattered dosage without the top shield to the dosage with the top shield is 100 when $D/R_s = 1$. This ratio increases to 180 when $D/R_s = 21$. For the attenuation of the scattered radiation by the 2-ft concrete roof of the secondary containment structure, the lower ratio, 100, was chosen. Note that for the direct dose calculations, Step 3, an attentuation factor of 37 was used for the 1.5 ft of concrete. The

reason for this difference in attenuation of the direct and scattered radiation, for the same shield thickness, is not obvious from a comparison of the analytical expressions used to compute the dose rates. Complexity of the scattered dose rate formulae precludes any rigorous comparison. However, it is apparent that the radiation leaving a shield differs from the incident radiation, not only in intensity, but also in energy and angular distribution. It can be argued, then, that the component of source radiation that reaches the dose point via air scattering is more strongly affected by this change in energy and angular distribution than the direct component and, therefore, the effective attenuation of the scattered radiation is the greater.

Step 6: A new ratio was defined.

$$F' = (G_{du})/(G_{ss}),$$

where

G_{ss} = scattered dose rate with 2-ft top shield.

From Step 4, it follows that F' = 100 F. The recipe used for estimating the scattered dose rates (G_{ss}) can then be stated as follows.

$$D/R_s = \quad 1 \qquad 9 \qquad 21,$$

$$F' = 3000 \qquad 200 \qquad 130.$$

Step 7: The scattered dose rate (G_{ss}) was computed using the relationship $G_{ss} = (G_{du})/F'$; G_{du} was calculated by the method outlined in Steps 1 and 2; and F' was obtained from Step 6. Under the assumption that the scattered dose rate is the same whether the source is contained in a sphere or a cylinder, the symbols R (radius of cylinder) and R_s were used interchangeably. In the tabulation below, the scattered dose rates (G_{ss}) are shown as a function of D/R.

D/R	D = distance from axis of cylinder (ft)	G_{ss} = scattered dose rate (R/h)
1	25	19
9	225	1.0
20	525	0.2

13.6 Health Monitoring Systems

13.6.1 Area Monitoring System

Gamma radiation levels are measured by 20 area monitors located throughout the facility. Any person working in an area being monitored may read at a glance the current level in mR/h, may see that the monitor is functioning properly, and will be warned by audible and visible alarm if the high level setpoint is exceeded. The same information is indicated on a central panel in the control room.

Table 13.6.1.1 lists the 20 channels of area monitoring, the monitor locations, and their ranges. Figures 13.6.1.1 - 13.6.1.3 show health monitoring equipment locations on plan views of each level of the facility.

Four of the 20 area monitoring detectors are located inside the secondary containment, to serve as health monitors during shutdown periods and as operational monitors during reactor operation. Three detectors are located outside the building: in the heat dump area, at the stack, and at the east wall of the secondary containment. The high level alarms of four of the detector channels are connected by a "three out of four" coincidence circuit to the emergency alarm system. These four detectors are widely separated, in peripheral locations outside the secondary containment. An alarm condition on three of them indicates a major release of fission products to the containment. All four of these channels are equipped with built-in auxiliary power supplies to ensure continued operation despite loss of all facility power.

The detectors in the area monitoring system are Nuclear Measurements Corporation Model GA-2T, all-transistorized, gamma-scintillation detectors, using NaI crystals (low range) and activated plastic crystals (high range). Scintillation detectors of this type show good stability and sensitivity and are not susceptible to jamming in high radiation fields. Each detector has two levels of alarm: (1) a low level, fail-safe alarm that indicates failure of the unit, and (2) a high level radiation alarm. The level of both alarms is set with an electronic control

TABLE 13.6.1.1

AREA MONITORING SYSTEM

Channel Identification	Area Monitor Location (Room No.)	Range (mR/h)
H-4001	Ventilation equipment room (101)	$0.1 - 10^2$
H-4002	Electrical equipment room (103)	$0.1 - 10^2$
H-4003	Exhaust filter room (105)	$0.1 - 10^2$
H-4004	Exhaust filter room (105)	$0.1 - 10^2$
H-4005	Heat dump area (outdoors)	$0.1 - 10^2$
H-4006	Stack survey (outdoors)	$10 - 10^4$
H-4007	Inside secondary containment (106)	$10 - 10^6$
H-4008	Inside secondary containment (106)	$10 - 10^6$
H-4009	Control room (202)	$0.1 - 10^2$
H-4010	Cell operating area (211)	$0.1 - 10^2$
H-4011	Cell operating area (211)	$0.1 - 10^2$
H-4012	Fuel transfer lock (212)	$10^2 - 10^7$
H-4013	Fuel transfer cell (213)	$10^2 - 10^7$
H-4014	Remote maintenance corridor (215)	$0.1 - 10^2$
H-4015	Electrical equipment corridor (301)	$0.1 - 10^2$
H-4016	Mechanical equipment room (305)	$0.1 - 10^2$
H-4017	Maintenance corridor (306)	$0.1 - 10^2$
H-4018	Gas cleanup piping room (307)	$10 - 10^4$
H-4019	Subbasement (401)	$10 - 10^4$
H-4020	East wall (outdoors)	$10^2 - 10^7$

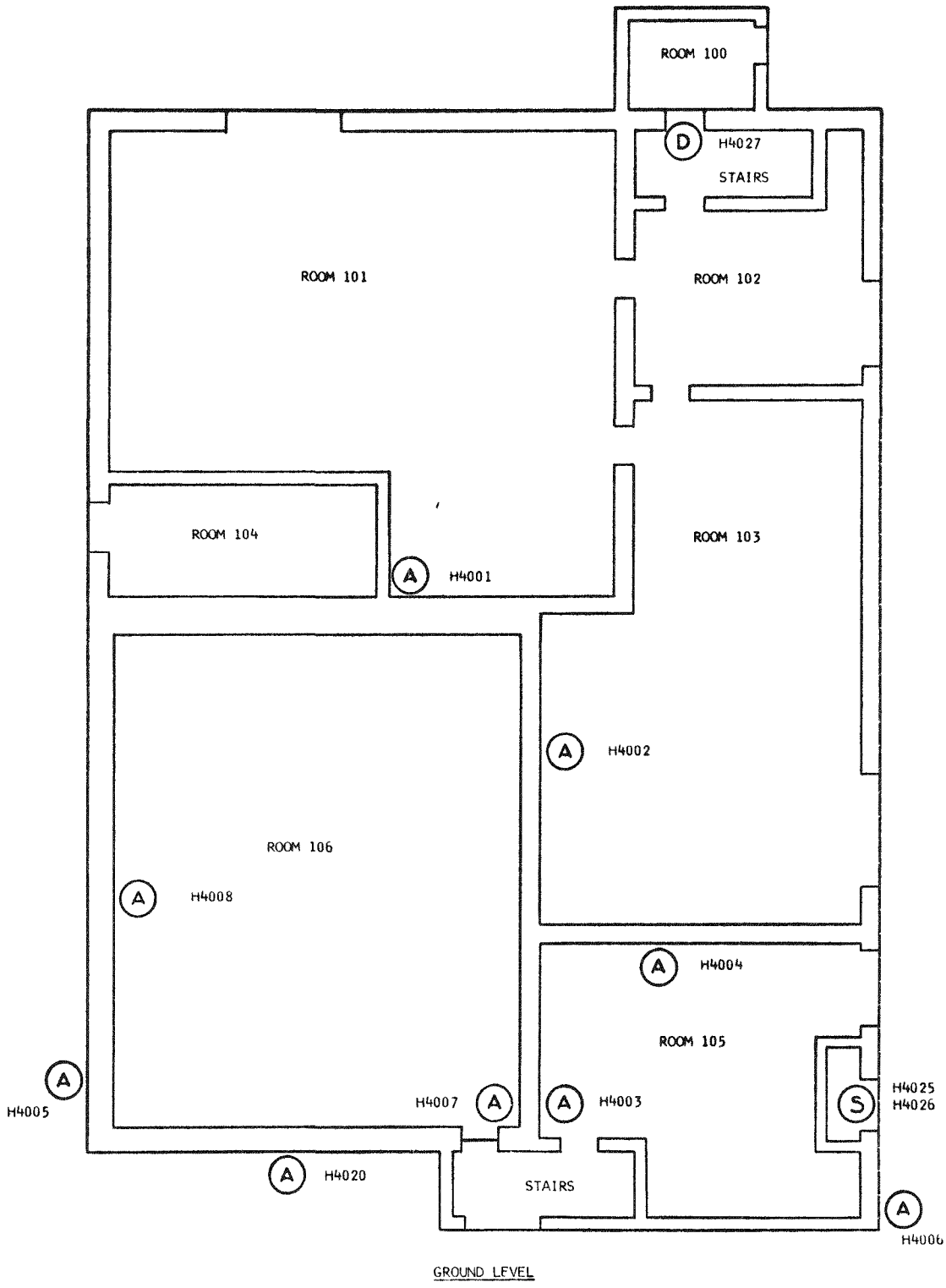

Fig. 13.6.1.1 Ground level health monitor locations
Legend: A, gamma area; P, air particle; S, stack
D, portal (door); H, hand and foot

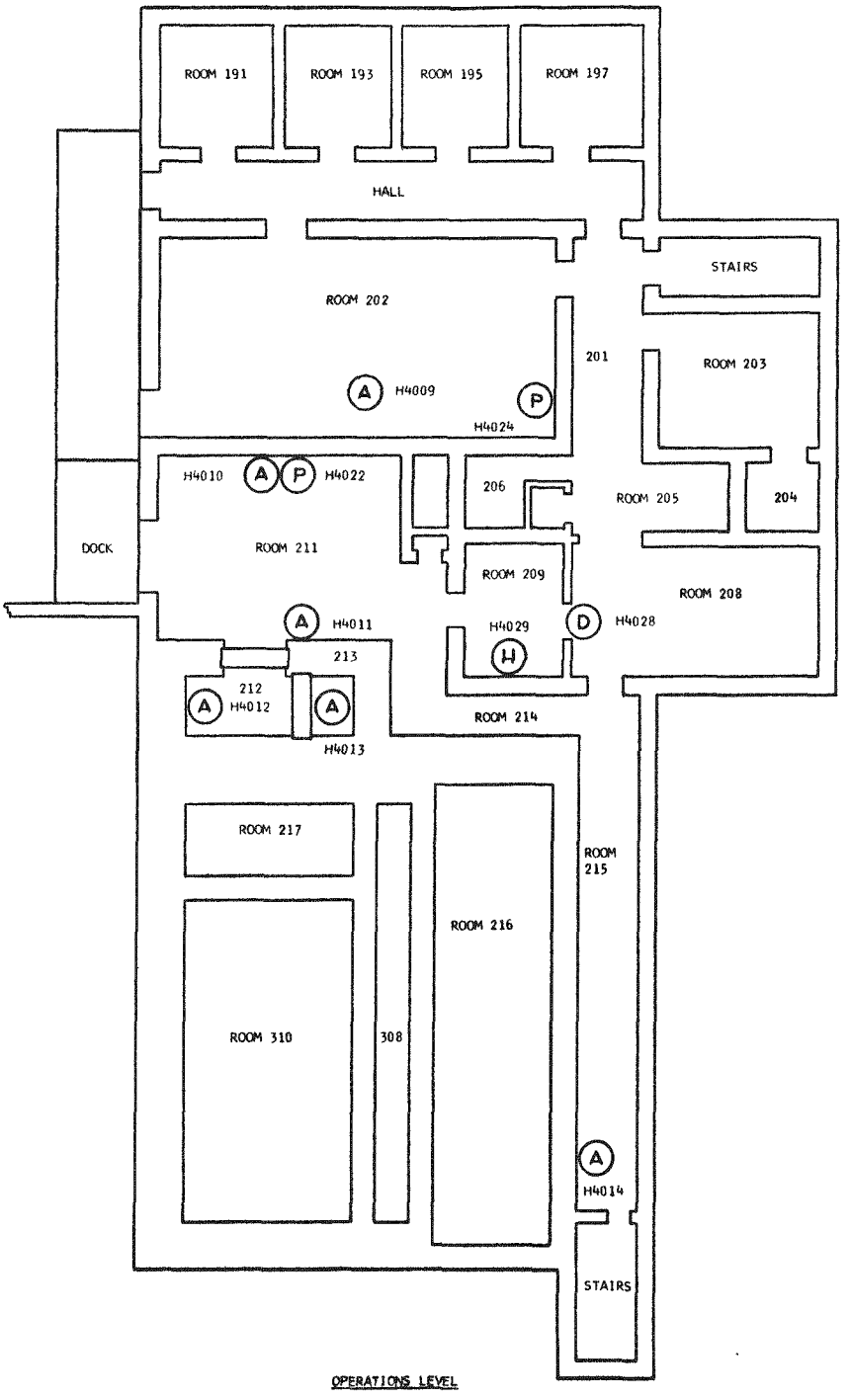

Fig. 13.6.1.2 Operations level health monitor locations
Legend: See Fig. 13.6.1.1

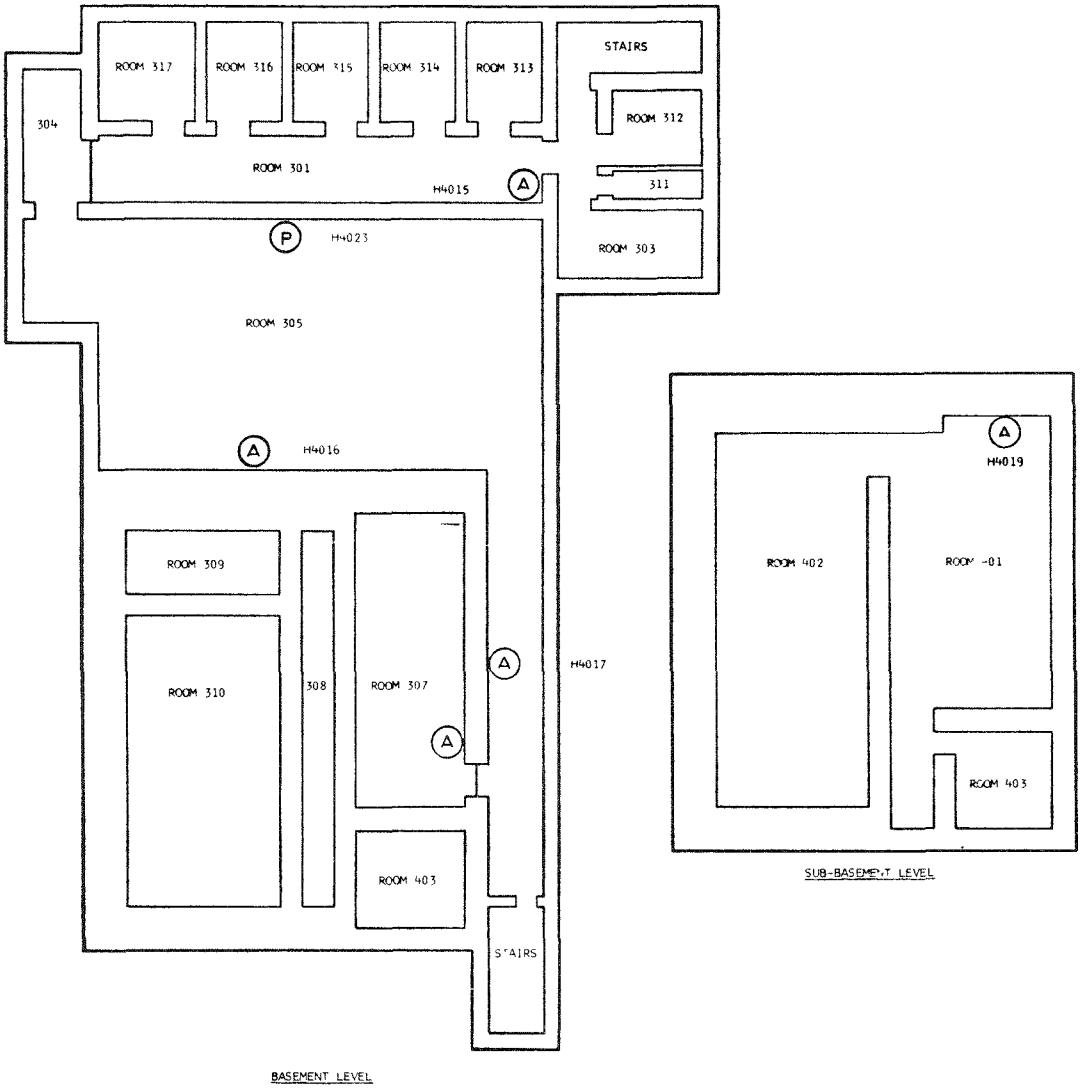

Fig. 13.6.1.3 Basement levels health monitor locations
Legend: See Fig. 13.6.1.1

circuit that includes a light source. The light source allows a check of detector and alarm circuitry without a radioactive check source. Power is supplied from the diesel generator-backed power supply. Each channel emits a 0- to 50-mV dc signal to the on-line computer for periodic logging of levels.

13.6.2 Air Particle Monitoring System

Three, fixed-filter, air particle monitors continuously sample for radioactive particles in the air of the cell operating area (Room 211), the exhaust filter room (Room 105), and the mechanical equipment room (Room 305). The monitors are Eberline Instrument Corp. Model AIM 3BL, which use β-γ end window GM detectors. The air particle monitors draw a 10-ft^3/min sample and indicate a rise $\geq$ 40 C/min above background in an atmosphere of 10^{-9} $\mu C/cm^3$, with a collection time of 1 min. The monitors are large stand-mounted units, with shielding around the detector for background rejection. Each air particle monitor is equipped with a recorder, a local meter, and local failure and high level alarms. Alarm signals and a 0- to 50-mV dc signal, for computer logging, are transmitted to the control room.

A fourth particle monitor is intended for intermittent use in the control room. The unit, an Eberline Instrument Corp. Model AIM3, uses a scintillation detector, and draws a 2-ft^3/min sample. Alarm and computer logging signals are identical to those of the other three air particle monitors.

13.6.3 Stack Monitoring System

In the stack monitoring system, a sidestream, isokinetic sampling loop delivers stack effluent to a Tracerlab MAP-1B/MGP-1A combination air particulate and radiogas monitor, which uses all solid-state circuitry, except for the photomultiplier tubes in the detectors. The system is shown schematically in Fig. 13.6.3.1.

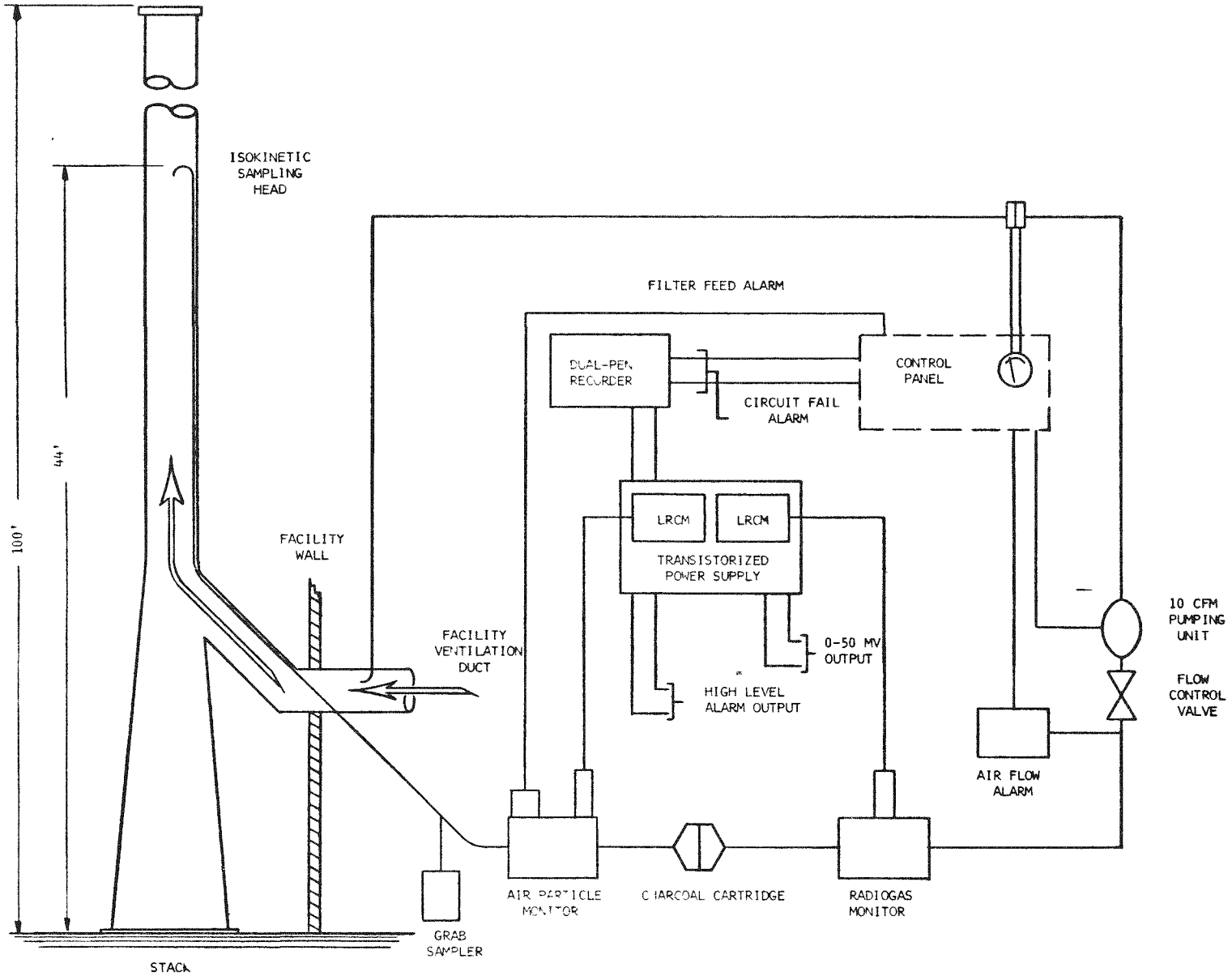

Fig. 13.6.3.1 Stack monitoring system

An isokinetic sampling head, located inside the stack, draws a 10-ft^3/min sample at a point 44 ft above the base of the stack. The sample moves through a stainless steel pipe, with a minimum number of bends, to the stack monitor, located in a small room near the stack base. Just inside the room is a tap where grab samples can be taken.

First in the line of flow is the air particle monitor in which a shielded, plastic phosphor, beta-scintillation detector scans a moving filter tape. The detector and an integral, solid-state preamplifier are contained in an aluminum housing sealed with an o-ring. A log rate meter, mounted in a nearby chassis, indicates the detector output over a 10- to 10^6-cpm range and has single-threshold discrimination. Outputs from the meter are high level alarm signals to local and control room warning devices and two data signals: a 0- to 10-mV output to a nearby strip chart recorder and a 0- to 50-mV output to the on-line computer for logging purposes.

From the air particle monitor, the sample stream moves to a charcoal cartridge where iodine is adsorbed. The stack monitoring system cannot detect gaseous radioiodine at very low levels in the sample stream. Therefore, the cartridge is a removable iodine concentrator that can be examined periodically in a more sensitive multi-channel analyzer located elsewhere in the facility.

Past the charcoal cartridge, the sample stream enters the radiogas monitor. There a Tl-activated NaI, scintillation crystal, photomultiplier detector extends through a wall recess into a shielded gas sampler. The log rate meter connected to the detector has single channel analyzer capability derived from spectrometer input circuitry and adjustable gain, window, and threshold. There are local and control room high level alarms. A 0- to 50-mV dc analog signal to the on-line computer is recorded periodically as a data log entry. The monitor output is also recorded on a strip chart recorder mounted at the stack monitor. In coordination with the continuous radiogas monitor analysis, grab samples will be taken throughout the reactor lifetime for gamma counting of gross activity

and for the determination of the contributions of specific isotopes to the gross activity. The grab samples will be run on an on-site multichannel analyzer.

Beyond the radiogas analyzer, a sealed, sliding-vane, positive displacement pump returns the sample to the stack. The pump and an associated control valve produce a maximum flow of 10 ft^3/min, regulated to ±5%. Flow, measured by an in-line meter, is indicated on the local control panel and monitored by a high-low flow alarm.

Detection Capabilities - Maximum permissible concentrations (MPC's) for many isotopes in unrestricted areas are so low that the count rates produced are not detectable, above background, by most commercially-available stack monitors. Therefore, the design of the stack monitor takes advantage of an atmospheric dilution factor which may be applied to MPC's to arrive at average tolerable levels in the stack. These "stack MPC's" generally fall within the range of detection of the stack monitor.

Table 13.6.3.1 lists important isotopes, generally noble gases, thyroid seekers, or bone seekers; the expected form of each isotope; and their MPC's in unrestricted areas. When a stack dilution factor, $K = 1.14 \times 10^{-4} sec/m^3$, is taken into account, the result is the tolerable discharge rate, Q. Dividing each of the tolerable discharge rates by the stack flow rate (8.5 m^3/sec) results in a tolerable stack concentration, TSC. Response of the stack monitor to each of these concentrations is shown as approximate net count rates above expected background (NCR).

Early in the operation of the reactor, the stack monitor will be used in the gross counting mode with maximum sensitivity and low alarm setpoint. When the isotopes or groups of isotopes normally released to the stack are identified by gamma-spectrum analysis of grab samples, optimum discriminator and spectrometer window settings will be determined, and the monitors will be set for minimum background and more effective detection of isotopes of particular interest.

TABLE 13.6.3.1

STACK MONITOR DETECTION CAPABILITIES

Isotope	Form	Maximum Permissible Concentration MPC* ($\mu C/cm^3$)	Tolerable Discharge Rate, Q (C/sec)	Stack Concentration TSC ($\mu C/cm^3$)	Net Count Rate NCR** (counts/min)
^{41}Ar	Gas	4×10^{-8}	3.5×10^{-4}	4.1×10^{-5}	1.6×10^{4}
^{82}Br	Gas	4×10^{-8}	3.5×10^{-4}	4.1×10^{-5}	1.1×10^{4}
^{85}Kr	Gas	3×10^{-7}	2.5×10^{-3}	3×10^{-4}	216
^{131}I	Part	3×10^{-10}	2.5×10^{-6}	3×10^{-7}	1.2×10^{6}
^{131}I	Gas	3×10^{-10}	2.5×10^{-6}	3×10^{-7}	N.A.
^{133}Xe	Gas	3×10^{-7}	2.5×10^{-3}	3×10^{-4}	1.8×10^{4}
^{89}Sr	Solid	1×10^{-9}	8.8×10^{-6}	1×10^{-6}	8.8×10^{6}
^{90}Sr-^{90}Y	Solid	1×10^{-11}	8.8×10^{-8}	1×10^{-8}	5.6×10^{4}
^{91}Y	Solid	1×10^{-9}	8.8×10^{-6}	1×10^{-6}	8.8×10^{6}
^{144}Ce-^{144}Pr	Solid	3×10^{-10}	2.5×10^{-6}	3×10^{-7}	1.8×10^{6}

* Concentrations in unrestricted areas based on 168-h/week exposure.

** Net count rate at equilibrium (assumed background 500 cpm).

The count rate signals from the air particle channel and radiogas channel are recorded on a two-pen recorder built into the stack monitor. One detector of the area monitoring system is mounted on the stack to transmit a gross indication in the event that a major accident drives the stack monitor off-scale. The range of the detector is 0.01 to 10 R/h.

13.7 Health Physics

13.7.1 Los Alamos Scientific Laboratory Radiation Safety Policies

The duties and responsibilities of individuals and groups who work with radioactive materials are defined by Laboratory policies described below.

Individual - Individuals at the Los Alamos Scientific Laboratory who have any contact with radioactive materials or radiation are responsible for:

1. Keeping their own exposures to radiation and also those of others as low as possible and, specifically, below the maximum permissible levels. Exceptions are exposures received in medical examinations and treatments and, with prior approval by the Health Division, cases where urgent situations require exposures in excess of the recommended levels.

2. Wearing the prescribed monitoring equipment (pocket dosimeters, film badges) in radiation areas. Requesting that neutron films be read when exposure to 0.1 rem is suspected.

3. Surveying hands, shoes, and body for radioactivity and removing loose contamination to the tolerance levels, in accordance with the recommended decontamination procedures, before leaving a contaminated area.

4. Wearing appropriate protective clothing whenever clothing contamination is possible, and not wearing such clothing outside the hot laboratory areas. Using gloves, hoods, and respiratory protection (respirators or supplied-air masks, as recommended by the Health Division)

when necessary. Using proper techniques and facilities in operations involving radioactive materials.

5. Observing the recommended procedures in regard to eating and smoking in contaminated areas.

6. Reporting injuries and ingestion or inhalation accidents promptly to the Health Division and carrying out the recommended corrective measures. Cooperating in any and all attempts to evaluate exposures, particularly by promptly returning requested urine specimens.

7. Carrying out recommendations of the Health Division in roping off hazardous areas, posting warning signs, and otherwise controlling special hazards for which they are responsible. Contacting the Health Division (Group H-1) about recommended procedures for high level radiation areas or when conditions are altered significantly.

8. Cleaning up contamination for which they are responsible. Arranging for a survey by Group H-1 and carrying out the decontamination recommended for the area when changing locations or ending an operation.

9. Properly storing and labeling radioactive materials for which they are responsible.

10. Properly packing, in sealed containers whenever possible, and labeling with origin and date, all contaminated waste materials.

Supervisors - Supervisors are responsible for ensuring that the above individual responsibilities are discharged by those under their control, and are further responsible for:

1. Instructing those employees for whom they are responsible in the use of safe techniques and in the application of approved radiation safety practices.

2. Providing such staff as is required for packaging contaminated waste and for decontaminating anything for which they are responsible.

3. Furnishing information to the Health Division concerning individuals and activities in their areas, particularly additions to or deletions from their personnel rosters.

4. Contacting the Health Division whenever they anticipate major

changes in operational procedures, new techniques, alterations in physical plant, or new operations that might lead to personnel exposures.

5. Preparing written Standard Operating Procedures for all operations involving hazardous amounts of radioactive materials.

Monitoring Group, H-1 - This group is responsible for:

1. Furnishing consulting services on all aspects of radiation protection.

2. General surveillance of all radiation activities, including assistance to individuals and supervisors in discharging their responsibilities.

3. Distribution and processing of personnel monitoring equipment, including keeping of personnel exposure records, notifying individuals and their supervisors of exposures greater than the permissible levels for their situation, and recommending appropriate restrictions.

4. Supervision and coordination of the waste disposal program, including keeping of waste storage records.

5. A continuous program of environmental hazard evaluation and hazard elimination.

6. Storage, leak testing, issue, and disposal of radioactive sources; supervising the shipping of radioactive material. Further, the inspection of requests for sources to assure standardization of capsules for general utility.

7. Scheduling urinalysis measurements when required.

8. Decontaminating large pieces of equipment (e.g., motor vehicles) and assisting personnel decontamination in cases of contaminated wounds or persistent personal contamination.

13.7.2 Facility Layout

Control Areas - A control area is considered to be any area that could become contaminated. The control areas (see Figs. 3.2 - 3.4) include on the ground level: the exhaust filter room; on the operating level: the hot toilet, the cell operating area, the two cells, the hall

and ajacent remote maintenance corridor, the loading dock, and the east stairwell; on the basement level: the mechanical equipment room and the maintenance corridor; and all four levels of the secondary containment structure. All accessible areas are routinely monitored and kept clean.

The only access between cold and control areas is the door to the change room near the Health Physics office. Anyone entering the control area will be required to wear protective clothing consisting of at least a smock and shoe covers.

Change Room - Personnel must pass through a locker room to enter the control areas. Here the person entering makes a complete change of clothing or merely puts on a smock and shoe covers, depending upon conditions or the work to be done in the control area.

A portal monitor, located between the change room and the hot toilet, detects any contamination before it is carried into the change room. Another portal monitor is located at the main entrance of the facility.

Decontamination Provisions - Adjoining the change room is a hot toilet which includes showers. Decontamination of personnel is possible here. Tools or other materials which cannot be decontaminated in place are sent to a LASL facility which specializes in decontamination.

13.7.3 Personnel Monitoring

Film Badges - Film badges are issued on a monthly basis to all personnel routinely located at the facility. Badges will be issued to visitors, when Health Physics personnel consider it necessary, before visitors are allowed to enter the control area.

Badges are constructed of brass and have an open window and a cadmium window. The areas under these two filters, brass and cadmium, are used to estimate the effective gamma-ray energy as well as the exposure; the open window area is used to estimate beta and soft gamma exposure. Each badge contains three films (low range gamma, high range gamma, and fast neutron) and a silver phosphate glass rod for measuring high level exposure. In certain areas where the probability of physical contamination

is high, an unsealed, removable plastic cover is placed on the film badge to prevent its contamination.

Dosimeters - Self-reading pocket dosimeters are issued to personnel working in a radiation field where it might be possible to receive as much as 100 mR within a week. Pocket dosimeters are read at least daily, more often if the radiation levels warrant it.

Reporting - Two copies of each of the facilities' exposure reports are sent to the Division Leader's office for distribution at the end of each calendar quarter. These quarterly reports are cumulative over the year. An annual exposure is calculated for each individual and is added to the previous accumulated exposure total recorded in his medical folder.

Form letters are sent to an individual and his supervisor when the individual's monthly exposure record indicates that, should he continue to be exposed at the same rate for the remainder of the year, he would receive more than 5 rem, the present LASL administrative yearly acceptable exposure.

Should an individual too closely approach a cumulative exposure of 3 rem in any one calendar quarter, his area Health Physicist is notified. An informal investigation, usually by phone call to the man and his supervisor, is then initiated by the Health Physicist.

Should an individual actually receive an exposure greater than 3 rem in any one calendar quarter, a formal investigation is conducted by the area Health Physicist. Within 72 h of the time that H-1 learns of the exposure, the Health Physicist must submit a report of his findings and recommendations to the H-1 Group Office. The H-1 Group Leader, in turn, must submit the report to the AEC, Division of Operational Safety, in Washington. A copy of the report is sent to the Group Office or supervisor of the individual involved.

13.7.4 Protective Equipment

Face Masks - Before the UHTREX reactor reaches initial criticality, all operating personnel will be fitted for full-face respirators by the

Industrial Hygiene Group, H-5. The respirators are equipped with combination canisters that will protect against organic vapors, acid gases, ammonia, and hydrocyanic acid gases; radioiodine, and radioactive aerosols; and other toxic particulates. At the same time these respirators are fitted, the personnel are instructed in the use of the respirators and tested in a chamber for proper respirator fit. All respirators are inspected at least once a year. If they are used, they are sent to a group which decontaminates or renews the respirators before they are returned.

Air Packs - Self-contained breathing apparatus is placed in cabinets at emergency stations throughout the facility. Periodic personnel training and apparatus maintenance is provided by Group H-5.

Protective Clothing - Protective clothing, consisting of smocks, coveralls, shoe covers, head covers, and surgical gloves is available in the change room at all times.

13.7.5 Monitoring Equipment

Portable Survey Equipment - The Laboratory has a large supply of survey instruments of all types readily available at all times. The instruments kept at the UHTREX facility are listed in Table 13.7.5.1.

These instruments are routinely sent out every 6 months for maintenance and recalibration unless repair is necessary before this time. Batteries are replaced by the health monitor when necessary, and proper operation is routinely checked with either an internal or external source.

Laboratory Equipment - The facility is equipped with a gas-flow proportional counter plus a scaler and associated electronics. This unit can be used on either the alpha or the beta plateaus for counting swipes, air samples, etc.

A multi-channel analyzer equipped with a NaI crystal will be available to aid in identifying and measuring gamma-emitting isotopes in samples of any kind.

TABLE 13.7.5.1

PORTABLE SURVEY INSTRUMENTS

Type	Number	Range	Scales
Geiger-Müller	3	0 - 20 mR/h	3
Ion chamber	3	0.1 mR/h - 10^3 R/h	3
Alpha	2	0 - 10^5 cpm	3
Neutron	1	0 - 5×10^5 events/min	4
Neutron	1	0 - 250 m rem/h	4

Portal Monitors - Two portal monitors are installed in the building; one at the main entrance to the building, and the other in the door between the hot toilet and the change room. Anyone passing from a control to a cold area must pass through the portal monitor. The sensitive unit located at the main entrance can be set to detect small amounts of beta-gamma contamination.

Hand and Foot Monitor - A hand and foot monitor is located inside the hot toilet room. The monitor detects any hand or foot contamination and has a frisker for the rest of the body. The alarm levels on this unit are set very low in order to keep any contamination from getting into the change room.

Floor Monitors - A beta-gamma floor monitor is normally used daily in the control areas and only weekly in the cold areas unless a significant amount of contamination is found in the control area.

An alpha floor monitor is used during periods when fresh fuel is loaded or at any other time when there is a possibility of alpha contamination.

13.7.6 Routine Surveys

Smear Surveys - Surface contamination is surveyed by using an appropriate instrument. If a contaminated area is found, swipes are taken to

aid in localizing contamination and removing it.

Material to be moved from the site is surveyed by instrument and smear. The material is then tagged with activity information by the monitor who made the survey. A laboratory counter is available at the site for alpha and beta counting of any smear tests that are made.

Air Sampling - In addition to the four air particle monitors described in Section 13.6.2, the UHTREX facility has a vacuum system with 20 outlets to which air sampling heads may be attached. Each outlet has its own valve which may be used to adjust the entering air flow or to shut it off completely. The normal procedure is to use a 2-1/8-in. HV-70 filter paper on as many units as is found desirable. The units sample the air at 2 cfm during the time the area is occupied, and the filters are counted the next day with automatic counting equipment for both alpha and beta activity.

Daily reports are issued to the Health Physicist for the facility. If any air concentrations are found to be over the LASL action levels (66 dpm/m^3 for ^{235}U and 6.7×10^3 dpm/m^3 for fission products), an investigation is made to discover the reason for the high air counts, and a recommendation follows on how to prevent a recurrence.

13.7.7 Bioassay

At LASL, urine samples are collected routinely from personnel working with materials considered hazardous. In the event of an incident, accident, or emergency, further urine sampling is carried on to furnish detailed information about actual exposure. If the need exists for rapid estimation of exposure, analytical procedures may be abridged, shortening the time required for analysis, with a consequent loss of sensitivity and specificity.

Two whole-body counters are available at all times to determine the amount of, and to identify, any gamma-emitting nuclides that may have been taken internally.

13.7.8 Medical Examinations

A complete physical examination is made of every person before he is hired. At three-year intervals thereafter everyone is re-examined. For those who work with radioactive materials, blood samples are taken every 6 months, particularly for a white cell count, and other routine blood tests are also performed.

14. CONDUCT OF OPERATIONS

Operations within the UHTREX facility are conducted by LASL staff members and technicians well-experienced and qualified in reactor operation. Normal operation following startup is on a 24-h, 7-day per week basis. Initial reactor startup and subsequent reactor operation are performed by the same organization, although initial startup is covered more extensively by design engineers and physicists on a consulting basis. The rules of standard practice, procedures, and operating information by which facility operations are conducted, are contained in the UHTREX Operating Manual.

14.1 Organization and Responsibility

14.1.1 Organization Structure

The organization responsible for safe and productive operation of the reactor has been structured to give firm lines of authority and responsibility while retaining the flexibility essential to a project experimental in nature.

The UHTREX project has been from its inception the responsibility of K-Division (Reactor Development), one of 12 technical divisions of Los Alamos Scientific Laboratory. Overall responsibility for its operation lies with the K-Division Leader. The K-Division Leader is advised by two LASL committees, the Nuclear Criticality Safety Committee and the Reactor Safety Committee, appointed by the Laboratory Director, who review reactor operations and operating policies at LASL.

K-4 Group Leader - Responsibility for the design, development,

construction, testing, and operation of UHTREX is assigned to Group K-4 within K-Division. The K-4 Group Leader is directly responsible to the Division Leader and actively reviews the experimental program by direct surveillance, by attending operations staff meeetings, as chairman of the UHTREX Steering Committee, and by reading regular written reports from the operations staff.

Operations Superintendent - The Operations Superintendent, who reports to the K-4 Group Leader, is responsible for day-to-day scheduling and coordination of reactor operations. The Operations Superintendent is assisted in his duties by one full-time staff member. Technical support is available to him from K-4 engineers and Group K-1 physicists. He is authorized to approve and carry out modifications that, in his judgement, do not affect safety. He may authorize changes in the UHTREX Operating Manual, except to the sections (Vols. I and IV) that relate to safety and require UHTREX Steering Committee approval. All experimental plans, once approved by the Steering Committee, are coordinated by the Operations Superintendent.

Shift Crew - Shift crews of three men each provide the coverage for 24-h-per-day, 7-days-per-week operation. A crew consists of a Shift Supervisor, who is a LASL-qualified reactor senior technician and two LASL-qualified experimental reactor technicians, one of whom mans the main operations console while the other mans the system control panels. The reactor technicians operate the reactor and its associated systems under the direct supervision of the shift supervisor. The shift supervisor reports to the Operations Superintendent and carries responsibility for operational activities in an 8-h shift period.

Fuel Manager - The Fuel Manager maintains records of fuel accountability and checks computer logging of fuel element data. The Fuel Manager directs loading of new fuel and ensures proper handling and storage of spent fuel within the facility. He is responsible for safe-configuration storage of all fuel inside the facility. The Fuel Manager is responsible to and submits regular reports to the Operations Superintendent.

Instrumentation and Maintenance Staff - The instrumentation and maintenance staff consists of one reactor senior technician who is in charge, and one or more technicians, classified either as experimental reactor technicians or electromechanical technicians. The senior technician in charge reports to the Operations Superintendent and is responsible further for coordinating instrumentation alignment and equipment maintenance or repair activities with the Shift Supervisor.

Health Physics - A health physics team is provided by Group H-1, the group within Health Division that performs health monitoring for the entire Laboratory. One health physics monitor normally covers each of the three daily shifts. The monitors are supervised by health physicists who work day shifts. The health physics team is responsible to the Operations Superintendent, but maintains necessarily close communication with each Shift Supervisor. Requests by a Shift Supervisor for nonroutine services are directed to the health physics team via the Operations Superintendent.

14.1.2 UHTREX Steering Committee

The UHTREX Steering Committee is responsible to the K-Division Leader for:

1. Long range planning of experiments to be undertaken.
2. Review and approval of experimental plans.
3. Periodic review of operations with particular attention to safety aspects.
4. Review and approval of original UHTREX Operating Manual.
5. Review and approval of changes to specific sections of the UHTREX Operating Manual that relate to safety (Vols. I and IV).

The Steering Committee is composed of five to eight members and is chaired by the K-4 Group Leader. Members, appointed from K-Division Groups, have been involved in the design, development, or operation of UHTREX. The operating staff is represented on the Committee by the Operations Superintendent, who provides the direct liaison required to

give the Committee an active voice in reactor operations. Safety audits by the Steering Committee are performed at the request of the Division Leader, Group Leader, or the Operations Superintendent. Meetings of the Committee are called at least once every 3 months or more often if required to fulfill the objectives stated above.

14.1.3 Operating Staff Qualifications

Operations Superintendent and Assistant - The same general qualifications apply to both positions: degree in engineering or physics, experience in reactor-associated fields, participation in design, development, and construction phases of UHTREX, and appropriate supervisory experience.

Fuel Manager - Qualifying requirements for the Fuel Manager include a degree in engineering or physics, experience in health physics procedures, and special knowledge of UHTREX fuel chemistry and development program.

Reactor Senior Technician - The general requirements applied to the selection of senior technicians are as follows:

High School diploma or military "certificate of equivalence."

Passing of LASL personnel employment tests in upper quartile.

Specialized training in fields relevant to reactor operation.

Five years directly applicable reactor experience.

One year reactor experience in supervisory capacity.

Experimental Reactor Technician - The general requirements applied to the selection of experimental reactor technicians are identical to those of the senior technician with these exceptions:

Four years directly applicable reactor experience.

Supervisory experience not required.

14.2 UHTREX Operating Manual

Operations of UHTREX are conducted in accordance with the UHTREX Operating Manual. The basic rules, practices, operational limits, normal

and emergency procedures, experimental plans, instrumentation and control information, and maintenance and repair practices are included in the multivolume Manual. Identical sets of the Manual are maintained for ready availability in three locations: the reactor control room, the operations office in the facility, and in the Group K-4 office. The routine for making changes in the Manual varies among the volumes; the routine for changing particular volumes is described in the discussions that follow.

14.2.1 Operating Standards

The contents of this volume serve as the guidelines which the operations staff establishes to direct itself through the experimental program. These guidelines are consistent with statements made in the Safety Analysis Report and the Operating Limits. The Operating Standards state administrative controls and policies governing: (1) use of and revision of the UHTREX Operating Manual, (2) experimental and operational objectives, (3) log keeping, record keeping, and reporting, (4) continuity during shift changes, (5) organization structure, (6) manning requirements for various reactor conditions, and (7) radiation safety policy.

The Operating Standards further state limits on operation, such as reactivity addition limits, system parameter limits, and scram set points. Maintenance or modification restrictions, postshutdown recalibration requirements, and requirements for periodic tests and inspections are specifically stated as guides to operating personnel. The Operating Standards volume may be changed only by approval of the UHTREX Steering Committee.

14.2.2 Standard Operating Procedures

This volume contains system procedures and facility procedures. System procedures list the steps to be followed in operating each system and major component. Facility procedures list the sequence of operations to be performed in the course of an overall facility operation (such as

startup), using system procedures and other supporting material as references.

The Standard Operating Procedures volume is prepared by the operating staff and reviewed initially for content and completeness by the UHTREX Steering Committee. SOP's may be revised on the authority of the Operations Superintendent, or he may choose to request Steering Committee review of any change if the change affects safety.

14.2.3 Emergency Operating Procedures

Emergency Operating Procedures include a discussion of symptoms and consequences of each credible accident or casualty and provide procedures for remedial or suppressive action.

Each procedure is initially reviewed and approved by the UHTREX Steering Committee. Subsequent changes may be made on the recommendation of the Operations Superintendent and concurrence of the Steering Committee Chairman.

14.2.4 Operating Plans

Operating Plans are devised by various K-Division staff members. The plans express the general order in which operational steps are taken to achieve the experimental objectives of the facility. Each plan generally contains: (1) description and purpose of the operation, (2) safety analysis of the operation, (3) sequence of operations, and (4) nonroutine data-taking requirements.

For all Operating Plans, review and approval by the UHTREX Steering Committee is required for the initial edition and for any subsequent change.

14.2.5 Instrumentation and Control

This volume contains six sections as follows: (1) elements of reactor control, with details of console and control room layout, interlocks, annunciators, etc., (2) on-line digital computer, covering data

acquisition, control functions, and programming, (3) nuclear instrumentation, (4) radiation monitoring, (5) nonnuclear instrumentation, and (6) nuclear characteristics information required for control of the reactor.

This volume is reviewed for content and completeness by the UHTREX Steering Committee, but changes need be approved only by the Operations Superintendent, within the limits defined in the operating standards.

14.2.6 Maintenance and Repair

Maintenance and Repair procedures guide the operating staff in the maintenance of contaminated equipment. Methods are detailed for the use of the MINOTAUR remote maintenance machine and the bridge crane for work on major components of each potentially contaminated system. Radiation safety procedures shall apply in the cases of some equipment. Preventive maintenance schedules are presented in this volume. Changes and appropriate additions to the volume may be made when authorized by the Operations Superintendent.

14.3 Training and Qualification Program

14.3.1 Classroom Review and Instruction

The training program is organized for presentation to reactor technician candidates who already have a good background of training and experience in reactor operation. Its chief aim is to familiarize the operations personnel with the special features of UHTREX. A review of the basic principles of reactor design and operation is included in the program, but on a limited basis.

The training program runs in two phases. In attendance during the first phase are all prospective reactor technicians and a number of K-4 staff members. Curriculum for the first phase includes:

Principles of reactor operation

Facility design and operating characteristics

Instrumentation and control

Standard and emergency operating procedures

Radiological safety

The second phase of the training program prepares the reactor senior technician candidates for their supervisory roles. The subjects covered are:

Reactor theory and operating characteristics

Operating standards and operating limits

Administrative controls

Radiation hazards

Waste disposal

Maintenance procedures

Hazards evaluation and reactor safety

Record keeping

Organization

Instructors for the program are (1) engineering and physicist staff members with special knowledge in particular areas of reactor or system development and operation, and (2) reactor technician candidates who have acquired special knowledge in certain areas of reactor operation.

14.3.2 On-the-Job Training

The time not occupied in classroom work is spent in on-the-job training, on checkouts in the facility of the information presented in lectures, or in normal electromechanical technician activity. Work assignments are made with the object of distributing time equally among activities so that each person receives a balanced background of experience.

14.3.3 Qualification

The qualification program by which the competence of a candidate is determined is conducted as follows:

1. All candidates are required to take brief exams at intermediate

points in the first phase of the training program. These exams are used as an indication of progress made and effectiveness of instruction.

2. At the end of the first phase, all candidates are required to take an experimental reactor technician qualifying exam which consists of a written exam (4 to 8 h), an oral walk-through exam (2 to 4 h), and an operating exam (simulated startup).

3. Reactor technician candidates who successfully pass these exams go directly into electromechanical technician activity. Candidates who fail to pass enter retraining, a supervised study schedule on an individual basis. Reactor senior technician candidates who successfully pass the exam enter the second phase of the program.

4. Reactor senior technician candidates are given a written qualifying exam covering the additional subject matter required of supervisory personnel. Candidates who fail to qualify enter retraining.

14.4 Records

14.4.1 Operations Log Book

The official record of operations performed by the shift crews is maintained in book form by the Shift Supervisor.

14.4.2 Periodic Test and Inspection Record

A permanent record of the performance of periodic tests and inspections, to meet the requirements of the Operating Standards, is made by the Shift Supervisor.

14.4.3 Instrumentation Record

Calibration data, performance data, and maintenance and repair details are entered in a permanent log by the Instrumentation and Maintenance Crew Supervisor.

14.4.4 On-Line Computer Data File

A chronological file of the printout of each of the five computer typewriters is maintained.

14.4.5 Fuel Management Records

The Fuel Manager maintains fuel accountability and inventory records, supplementary to on-line computer printout records of fuel data.

14.4.6 UHTREX Operating Manual Change Record

Subject and chronological listings of revisions to the Operating Manual are maintained by the Operations Superintendent.

14.4.7 Facility Modification Record

Full documentation of any field changes to the facility or systems is available to the operations staff from a file kept by the Operations Superintendent.

14.4.8 Health Physics Record

Standard files of personnel exposure, results of daily surveys, waste discharge, and other subjects related to health physics are maintained by the Health Physicist.

14.4.9 UHTREX Steering Committee Meeting Minutes

Minutes of Committee meetings, starting with review of the first experimental plan, are kept in a file that is readily accessible to the operating staff.

15. INITIAL TESTS AND OPERATIONS

After tests on individual components and subsystems of the UHTREX reactor are completed, testing of the reactor as in integrated unit will commence. This phase of the operations will include:

1. Integral tests to be performed prior to the fueling of the reactor.
2. Initial fueling and low power operations at ambient temperature, and
3. Initial power and temperature ascension.

The aim in these tests is to verify the predicted performance and interactions of system components. Commensurate with this objective, the tests are further designed to minimize the buildup in fission product inventory and the thermal cycling and stressing of components during the initial temperature ascension. The operations are paced conservatively to allow time for removal from the helium coolant of the contaminants that are emitted from the reactor and coolant loop components during the temperature ascension.

15.1 Tests Prior to Reactor Operation

The ability of each system in the reactor facility to function properly will be checked during test programs that precede the initial operation of the reactor. As each system is completed, it undergoes functional tests described in previous chapters of this report. For the final preoperational test program, all of the systems will be operated as one integrated reactor system to demonstrate that the reactor system meets all design requirements and is ready for a safe startup.

Reactor system tests will be performed by the reactor operators, from their normal control stations and according to written procedures that parallel as nearly as possible the normal operating procedures. Particular attention will be given to tests of reactor operation and safety systems.

15.2 Initial Fueling and Low Power Tests at Ambient Temperature

The initial fueling and critical operations of the reactor will be performed at room temperature. The tests to be conducted during this phase of the operations include:

1. Partial proof testing of fuel loading apparatus and procedures.
2. Evaluation of the effectiveness of the neutron source and integral testing of nuclear instrumentation.
3. Measurement of the critical mass at room temperature with all control rods withdrawn.
4. Calibration of one plug rod in terms of critical mass and reactivity versus the position of the rod.
5. Initial power calibrations.
6. Measurement of the pressure coefficient of reactivity.
7. Measurement of the coolant flow coefficient of reactivity.
8. Measurement of critical masses with successively greater numbers of plug rods inserted.

15.2.1 Initial Fuel Loading

Initial fueling will be performed under open system conditions.

1. The reactor and fuel handling system will be at atmospheric pressure and ambient temperature.
2. Both primary gas locks will remain open.
3. The drybox, secondary gas locks, and conveyors in the fuel

handling system will not operate. In the charging operation, fuel elements will be dropped, by hand, directly into the inlet primary gas lock through an inspection plate opening in the charge conveyor housing. (The plate will be welded in place after initial fueling is complete.) The fuel loading crew will work in the fuel charging room (see Fig. 3.3) instead of in the cell operating area. Discharged fuel elements will fall out of the open outlet primary gas lock into a container in the place of the trap cask.

4. An abridged on-line computer program will operate the fuel loader.

The general schedule for loading elements into the reactor will be similar to that used in the UCX, described in Appendix D. The fuel element loadings for UHTREX are given in Table 4.1.4.1. This loading schedule permits critical mass measurements to be made either with all channels containing the same fuel loading or with different channel loadings distributed symmetrically within the core in UHTREX.

Procedures during the initial fueling will be governed by the following rules:

Rule 1 - All eight plug control rods shall be inserted.

Rule 2 - Fuel in the core shall not exceed that loading which is critical with six plug rods inserted.

Since rotation of the core is necessary during fuel loading operations, all core control rods will remain withdrawn.

15.2.2 Low Power Tests

For the initial reactor loading, a neutron source of 2×10^7 n/sec will be centrally located in the core plug. Later, the central neutron source will be replaced with an external source of 10^8 n/sec. Measurements made during UCX show that an external source of 10^8 n/sec will permit satisfactory neutron multiplication data for reactor startup. Experiments will be performed to confirm that the UHTREX source detector geometry is satisfactory for subcritical monitoring and reactor startup.

Each nuclear instrument channel will be tested with appropriate calibration equipment to determine that it is operating properly. Particular attention will be given to the neutron counting channels that are used for reactor startup and to the nuclear safety system. Interference from other electrical equipment will be eliminated in the neutron counting channels. The safety system will be checked for stability, time response, and freedom from false scrams.

The critical mass measured at room temperature will be compared with the critical mass observed in UCX. Because in UHTREX additional reflector material exists which was not present in UCX, it is expected that the UHTREX critical mass will be approximately 20% less than that observed in UCX.

After criticality has been attained, instrumentation channels will be compared to determine that all channels correlate and signals are proportional to reactor flux level. A flux mapping of the core will be performed and a power calibration of the nuclear instrumentation obtained.

Following the critical mass measurement at room temperature, a portion of a plug rod will be calibrated, both in terms of incremental mass additions and by period measurements. This calibration will be used in subsequent tests for determining the temperature, pressure, and flow coefficients of reactivity.

Experiments will be done to measure the reactivities of single fuel element additions and the effect on reactivity of the rotation of the core. The effects in both cases are expected to be small.

The following general rule will govern all UHTREX critical operations:

Rule 3 - During critical operations at least two plug rods shall be fully withdrawn and available for scramming the reactor.

15.3 Initial Power and Temperature Ascension

The objectives of the initial system operation at significant powers and temperatures are:

1. To determine the actual temperature coefficient of reactivity, which will be used to predict the final loading.

2. To gain operating experience with the whole system while extensive checks on the system are made at each of one or more successively higher temperature plateaus.

3. To bring the reactor and its cooling systems to operation at design temperatures and design powers.

Unnecessary reactor temperature cycling will be avoided, and activation of the reactor pressure vessel and other components will be held as low as is reasonably practical.

To reach the first objective, the reactor will be started up and brought to stable operation at an average core temperature of about 600°C. Data gathered at this point will allow a calculation of the temperature coefficient of reactivity and an accurate prediction of the amount of fuel required to operate at design conditions. This first operation at temperature will also allow the exercise of the coolant loops and a significant check of their operation.

Next, the reactor will be scrammed, and additional fuel will be loaded. After loading is complete, the plug rods will be withdrawn part way to establish a temperature plateau. The primary and secondary blowers will be operated at their lowest speeds to minimize reactor power. Primary and secondary loop coolant pressures will be maintained near 500 psi.

After thorough checks of the entire system at the first temperature plateau, the plug rods will be withdrawn further to establish a second, and perhaps a third, temperature plateau. When the rods are fully withdrawn, the temperatures of the reactor and its cooling system should be near design conditions. The reactor power and coolant flow rates will be about half their design values.

Final ascension to full power will be made by increasing the speed of the primary and secondary blowers.

Figure 15.3.1 shows, in profiles, the variation of system parameters during the initial ascension. Neither time, along the abscissa, nor the

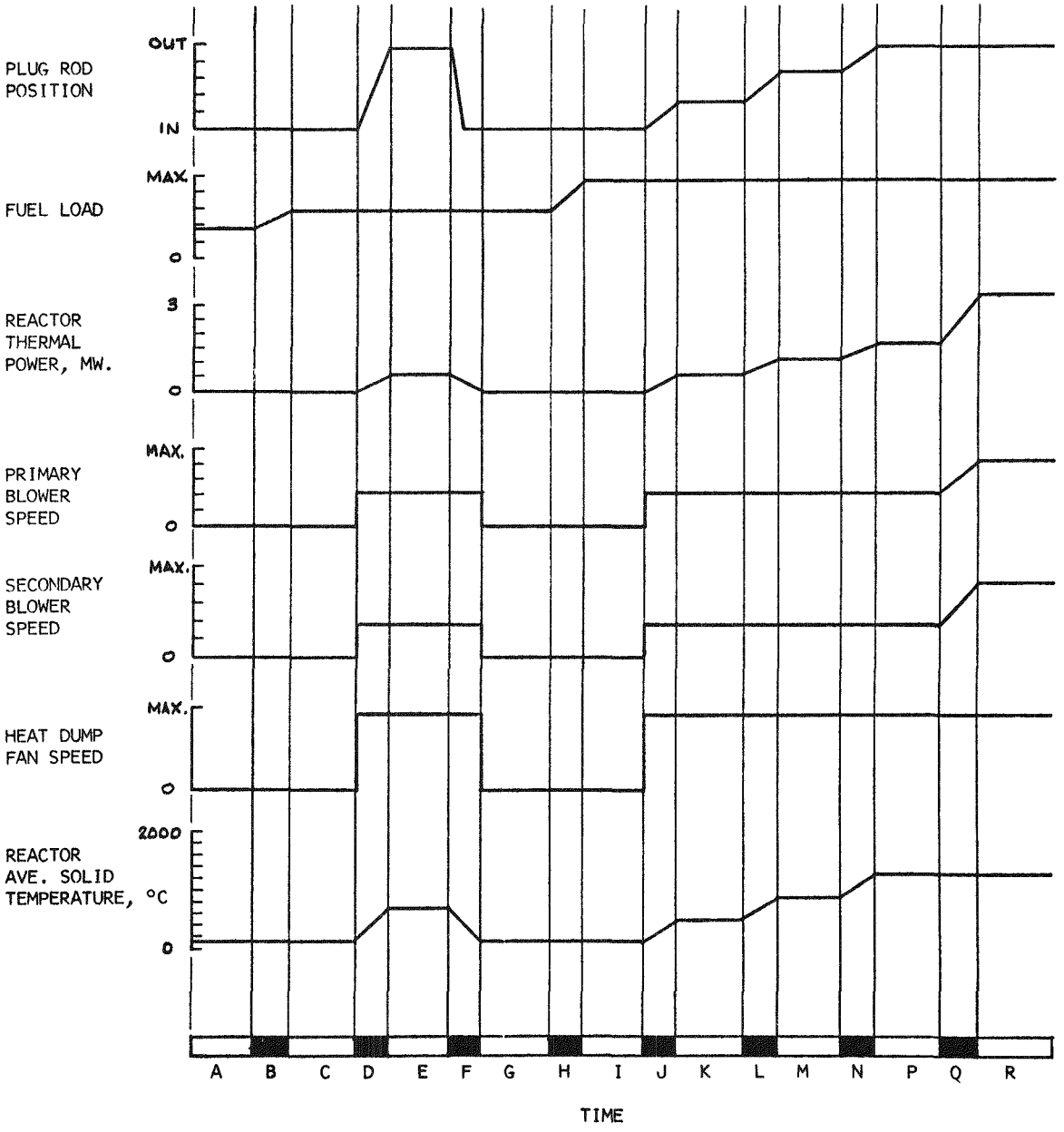

Fig. 15.3.1 Initial power and temperature ascension

ordinate variables are to scale. The duration and number of plateaus, e.g., K and M, are representative. There may be one, two, or more such plateaus in the actual startup. Fine details of the operation of control rods and other system components are not shown in Fig. 15.3.1.

Major changes in operating conditions such as those shown at D, F, J, L, N, and Q ordinarily will be made during the day shift and will require about 6 to 8 h. Operating plateaus will be maintained at least overnight and for whatever additional time is required for a thorough check of system operation.

At each plateau, a variety of steady-state measurements and oscillation and perturbation tests will be made. None of these tests will disturb the system significantly. Examples of standard measurements, tests, and checks made at each plateau are:

1. Steady-state measurements of system temperatures, pressures, and coolant flow rates.
2. Oscillation tests at various frequencies on primary and secondary blower speeds, recuperator bypass flow fraction, heat dump fan speed, plug rod position, and coolant loop pressures.
3. Perturbation (small step) tests on primary and secondary blower speeds, recuperator bypass flow fraction, heat dump fan speed, plug rod position, and coolant loop pressures.
4. Heat balance checks.
5. Out-of-limit checks.

Each time fuel is loaded, i.e., at Times B and H in Fig. 15.3.1, careful consideration will be given to maintaining an adequate reactivity shutdown margin at room temperature. Checks of the shutdown margin will require reactor control rod movements that do not appear in Fig. 15.3.1.

15.3.1 Fuel Loading

During the ascension phase of operations, fuel elements will be loaded with the reactor and fuel handling system closed and filled with

helium. The operation of the fuel handling system will be under the control of the on-line computer as described in Chapter 6.

While the first fuel increment is being loaded, Time B in Fig. 15.3.1, the reactor pressure will be atmospheric and both primary gas locks will be open. Under these conditions, the wear on seals that would accompany numerous operations of the gas locks will be avoided. When the reactor is pressurized the gas locks will be operated as described in Chapter 6.

With the fuel handling system closed, Rules 1 and 2 no longer apply. Instead, the following rules will govern loading operations:

Rule 4 - No more than six plug rods shall be inserted during closed-system loading operations.

Rule 5 - Fuel in the core shall not exceed that loading which is critical at room temperature with six plug rods and four core rods inserted.

Closed system fuelings may be performed with the reactor either critical or subcritical. Rule 5, in effect, means that a shutdown margin equivalent to two plug rods shall always be maintained.

15.3.2 Initial Ascension

The progress of the initial ascension is discussed below in terms of the time increments that appear in Fig. 15.3.1.

Time A - Before the beginning of the initial ascension, the cold critical tests and the pressure and cold-flow reactivity tests will be complete. The reactor will be loaded to cold critical, and the plug rods will be in.

Time B - The fuel load will be increased by an increment, ΔM_1, chosen to permit operation of the reactor at an average solid temperature of about 600°C when all rods are removed. Following completion of the loading, the coolant loops will be pressurized to near 500 psi with helium.

Time C - Plateau for standard measurements, tests, and checks.

Time D - Primary and secondary blowers will be operated at their minimum speeds. Heat dump fans will be operated at their design speeds. Reactor control rods will be withdrawn almost entirely.

Time E - At this plateau the reactor core temperature will be about 600°C. Other system solid and gas temperatures will rise about one-third of the difference between room temperature and their design values. An average core temperature will be calculated. This temperature, combined with information obtained at cold critical and knowledge of the load ΔM_1, will allow a realistic calculation of the reactor temperature coefficient of reactivity and a prediction of the loading required to achieve design conditions. A tentative value of the incremental loading, ΔM_2, will be chosen to allow operation of the reactor at a point just short of design operating conditions, without compensation for xenon poisoning.

System temperatures will have risen enough to provide good data for comparisons of actual operations with predicted operations.

Time F - Rods will be scrammed in a test of the nuclear safety system, and, as the thermal power decline permits, blowers and fans will be stopped.

Time G - Progress to this point will be checked.

Time H - The primary loop will be depressurized, and the second increment of fuel, ΔM_2, will be loaded. This loading will be made while the reactor and the fuel loading system are filled with helium at a pressure slightly above one atmosphere. All components of the fuel handling system will operate, except the inlet and outlet primary gas locks, both of which will remain open until the loading is complete.

Time I - Plateau for checks on progress.

Time J - Primary and secondary blowers will be operated at their minimum speeds, and the heat dump fans at their design speeds. The reactor control rods will be partially withdrawn. Under these conditions, heat generation in the core and heat removal in the coolant loops will be restricted. The reactor thermal power and core temperatures will rise to an intermediate level and remain there.

Time K - Plateau for system checks at intermediate power level.

Time L - Control rods will be withdrawn another increment of length to allow the power level and core temperatures to rise to a higher level.

Time M - Plateau for systems checks at higher power level.

Time N - Control rods will be withdrawn until reactor design temperatures are achieved.

Time P - Plateau for system checks at reactor design temperatures. Since the reactor fuel loading will be low, the rods will have been completely withdrawn, but the reactor temperatures will be somewhat below their design values. Additional fuel will be loaded. The particular course of action taken during Time P cannot be specified until the system is operated, measurements are taken, and careful consideration is given to the results.

Time Q - By raising blower speeds, heat removal will be increased and the reactor power level will rise to near design level.

Time R - Final plateau for systems checks. Reactor and other systems will be operating at or near design values. Fuel load and rod adjustments will be made to maintain temperatures as poisoning and fuel burnup occur.

General - At Times J through Q, the primary and secondary coolant flow rates will decrease as the coolant temperatures increase. Thus, at Time P, the system will be operating at roughly design temperatures, half-flow, and half-power. Full power will be achieved by increasing the flow rates to their design values. This type of system operation has been studied with the use of a computer code that solves a mathematical model of the UHTREX system. The mathematical models, the computer code, and various reactor startup and restart results have been reported elsewhere.[1]

---

[1]H. B. Demuth, K. H. Duerre, F. P. Schilling, and C. E. Stiles, "System Dynamics Study for the Ultra High Temperature Reactor Experiment," Los Alamos Scientific Laboratory report LA-3561, in preparation.

As noted previously, the startup discussed above is representative of a procedure that will be used. The planned startup will be improved and defined in more detail as better understanding of the system is obtained through analysis and through actual operating experience.

16. SAFETY ANALYSES

Particular care has been taken throughout the design and construction phases of UHTREX to ensure that the reactor and its auxiliaries can be operated with a maximum degree of safety. In the preceding descriptions of components and systems, safety aspects of the designs were discussed in context. Below, the principal safety features of the overall design are reviewed briefly, and detailed discussions are presented of accidents that have been postulated to demonstrate the soundness of the UHTREX design.

It is conceivable that accidents could arise from two different sets of circumstances: the inadvertent commission of operational errors, and the unforeseen mechanical failure of major system components.

All UHTREX systems are designed to withstand the effects of operational errors until corrective actions are taken, usually automatically. The effects of credible mechanical failures are limited by design to acceptable proportions, or are controlled within tolerable limits by automatically actuated devices.

16.1 Safety in the Design

16.1.1 Reactor

Many hazards associated with conventional reactor fuel elements do not apply in UHTREX. The dispersion of uranium in a refractory matrix precludes a nuclear explosion due to rapid critical reassembly following a core meltdown. Small, discrete units of fuel, one added and another discharged simultaneously, make impossible the sudden

addition of reactivity through failure of fuel-loading mechanisms or the inadvertent addition of excess fuel in massive quantities. Fuel damage, in the usual sense of rupture of the cladding, cannot occur. The release of fission products from the fuel is anticipated in the coolant system design.

A solid moderator that encloses the fuel and serves as a structural part of the reactor limits the hazards that can arise from a sudden change in moderation. No experimental channels complicate the nuclear aspects of core design.

The plug rods are constructed of refractory, chemically stable materials that can withstand the core environment when the rods are inserted for shutdown. During full power operation, the rods are raised from the core into the upper, cooler part of the reactor. There, the rods do not need to be cooled to prevent thermal distortion and cannot initiate an excursion caused by their abrupt withdrawal. Since there is no need for coolant flow around the rods, buoyancy effects do not influence rod insertion or withdrawal.

All mechanical components that enter the reactor pressure vessel, and the mechanisms that drive those components, are enclosed in extensions of the pressure vessel. There are no penetrations of moving parts through seals. Junctions with the pressure vessel are made with welds, test-proved Conoseal couplings, or bolted flanges with seal welds.

16.1.2 Control Systems

Nuclear safety circuits initiate automatic rundown when preset conditions occur, operating procedures are limited by interlocks, and annunciators give audible and visual indication of abnormal conditions. The control room instruments have indication and recording capabilities adequate for diagnosis of incidents to be expected in an experimental reactor. An on-line process computer constantly monitors the status of all systems, alarms when unsafe conditions are approached, performs sequential and repetitive operations, and aids operating personnel by

verifying their conformance to procedures. The computer also frees the operators for closer attention to critical work by logging data and keeping fuel element records and histories.

Control system designs for auxiliaries, including the gas cleanup system, have the general safety characteristics of the nuclear controls described above.

Health physics requirements are met with ample instrumental systems tied into pertinent alarm systems.

16.1.3 Coolant Loops

Direct junction of the reactor vessel to the recuperator vessel and of the recuperator vessel to the main heat exchanger shell creates essentially one pressure vessel for these three major components, lowers thermal stresses among them, reduces the need for high temperature piping, and minimizes the number of joints in the loop. Again, all joints are welds, seal-welded bolted flanges, or Conoseals. The one valve used in the loop is completely enclosed.

Recuperator heat exchange conditions can be varied with a simple bypass. The main heat exchanger is designed to withstand multiple exposures to abnormal conditions. Its design minimizes internal thermal stresses. Blowers are canned and have gas bearings to eliminate shaft seals. All blowers have backup power supplies.

Secondary containment is provided by the secondary loop, built to the same stringent specifications as the primary loop, and by a gas-tight portion of the building. The secondary loop dissipates its heat to an ever-present supply of air.

Much of the equipment located in parts of the building that are inaccessible during reactor operation can be inspected by means of the television cameras mounted on MINOTAUR, the remote maintenance machine. MINOTAUR can be used to make minor repairs or adjustments found to be necessary on inspection, or to verify the existence of serious difficulties, indicated on control instruments, that justify a reactor shutdown.

16.1.4 Auxiliaries

Operation of the reactor is not strongly dependent on the gas cleanup system, whose function is to limit rather than to eliminate the concentrations of mobile oxidants and fission products in the primary loop. Under some conditions, the reactor can operate indefinitely without the gas cleanup system; under others, the reactor must be shut down within a reasonable time after loss of the cleanup system.

Ample capacity exists in the helium storage system to contain all of the coolant helium inventory after an emergency shutdown. Compressors are duplicated to ensure a means for moving helium into storage.

All utilities have a reserve capability. Electrical power can be supplied from two independent lines or can be generated on the site. Cooling water, for auxiliary systems that include pumps, can flow under main pressure or by gravity at reduced flow rates.

16.2 Effects of Operational Errors

For UHTREX to fulfill its primary purpose, the design of the reactor and its auxiliary systems must include the means for operation of the experiment under a variety of conditions. Inevitably, this design flexibility introduces the possibility that, inadvertently, a series of operations may produce an accident. To test the safety of proposed designs, a large number of operational error accidents were postulated as a part of the design process. In most instances, the possibility of the postulated accident was eliminated by redesign. In certain cases the possibility remains, but the probability of the occurrence of an accident is reduced and the final design includes features that mitigate the consequences of an accident.

Analyses are present below of possible, but not necessarily credible, accidents that might evolve from operational errors. The consequences of each accident were assessed with computer programs, principally UHXCOM, that simulate system operations.

16.2.1 Reactivity Insertions

Positive reactivities can, in principle, be induced in UHTREX by:

Adding fuel,

Filling voids with graphite,

Cooling the core,

Heating the reflector,

Removing fission product poisons,

Dispersing fuel, or

Withdrawing control rods.

Rapid reactivity insertions by fuel addition are not possible. The insertion of a fuel element consumes several minutes time, and involves at most, a few cents gain in reactivity.

No mechanisms have been discovered for introducing materials from the environment of UHTREX into voids in the vicinity of the core. The introduction of common materials other than graphite would cause reactivity losses. Water, for example, would act primarily as a poison. Filling the voids with graphite would require a general collapse of the core support structure. This is not credible.

Because of the large heat capacity of the core, cooling of the core occurs relatively slowly, even with full coolant flow. From studies using the UHXCOM code, described in Chap. 5, the reactivity insertion rate due to cooling of the core was determined to be less than 1¢ per second under all conditions. The reflector temperatures rise as heat is generated in the core, but the negative core temperature coefficients always nullify the positive reflector coefficients.

The loss of the fission product poisons from the core, or significant dispersal of the fuel in the core, could occur only under extreme transient conditions. An indication of the type of transient that would produce these effects is given below in the discussion of rod withdrawal accidents.

For purposes of analysis, two excursions caused by control rod withdrawal are postulated below. The starting conditions for each excursion are listed in Table 16.2.1.1.

TABLE 16.2.1.1

INITIAL CONDITIONS FOR ROD WITHDRAWALS

	Case I	Case II
Power	1 watt	3 MW
Temperature	293°K	1714°K
Rods inserted	1 plug rod	1 plug rod
Worth of rod	2.4% ΔK	3.2% ΔK

In each case, the rod is considered to be fully inserted initially, and then withdrawn fully at the design speed of 18 in./min. The driving reactivity function generated by the rod withdrawals is plotted in Fig. 16.2.1.1. The calculational model assumed for the high temperature case, Case II, is described in Sec. 4.2.2. The same model was used for the room temperature case, Case I, except that coolant flow was deleted, and heat transfer from the fuel to the moderator was assumed to occur only by radiation.

The effects of the excursions on reactor power and fuel temperatures are plotted in Figs. 16.2.1.2 through 16.2.1.5, and the significant parameters of the excursions appear in Table 16.2.1.2.

TABLE 16.2.1.2

PARAMETERS OF EXCURSIONS

Parameter	Case I	Case II
Time to peak power (sec)	49	75
Peak power (MW)	50	39
Energy to peak (MW-sec)	64	1600
Maximum fuel temperature (°K)	1660	2740
Maximum moderator temperature (°K)	380	1940

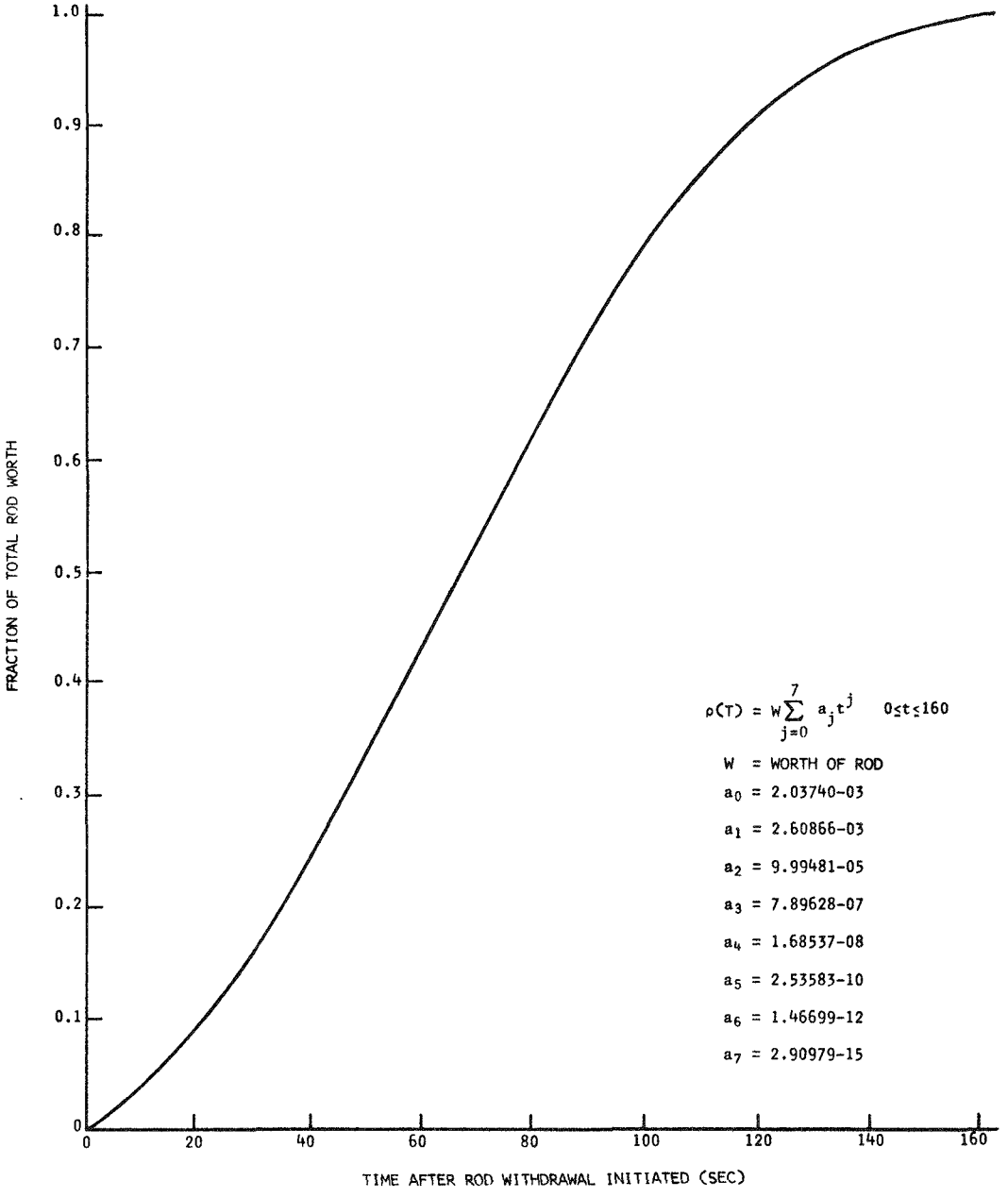

Fig. 16.2.1.1 Reactivity insertion for control rod withdrawal at the rate of 18 in./min

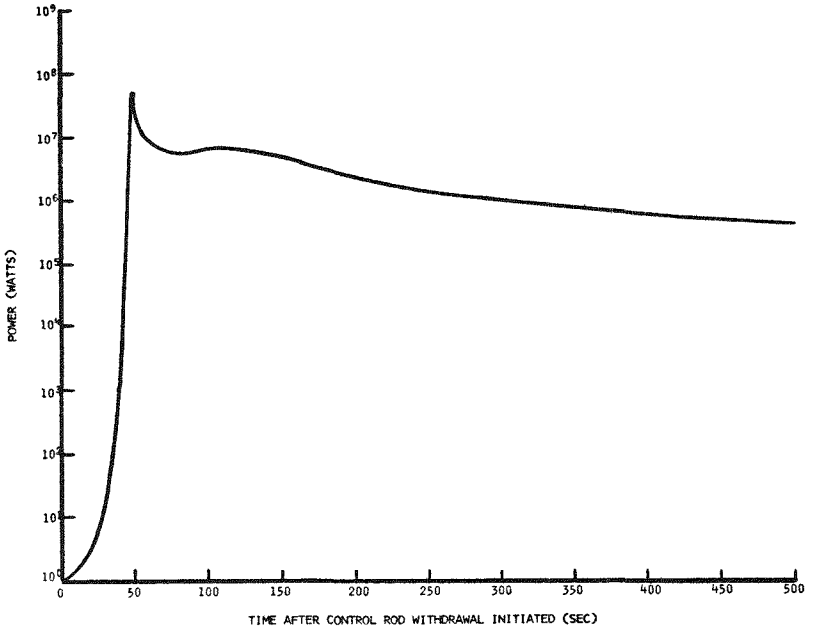

Fig. 16.2.1.2 Power transient during Case I excursion

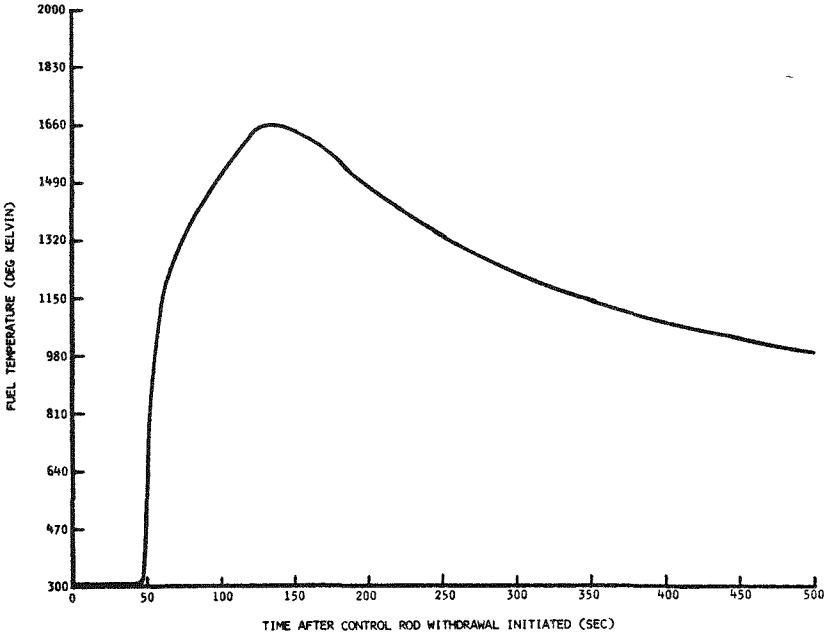

Fig. 16.2.1.3 Fuel temperature transient during Case I excursion

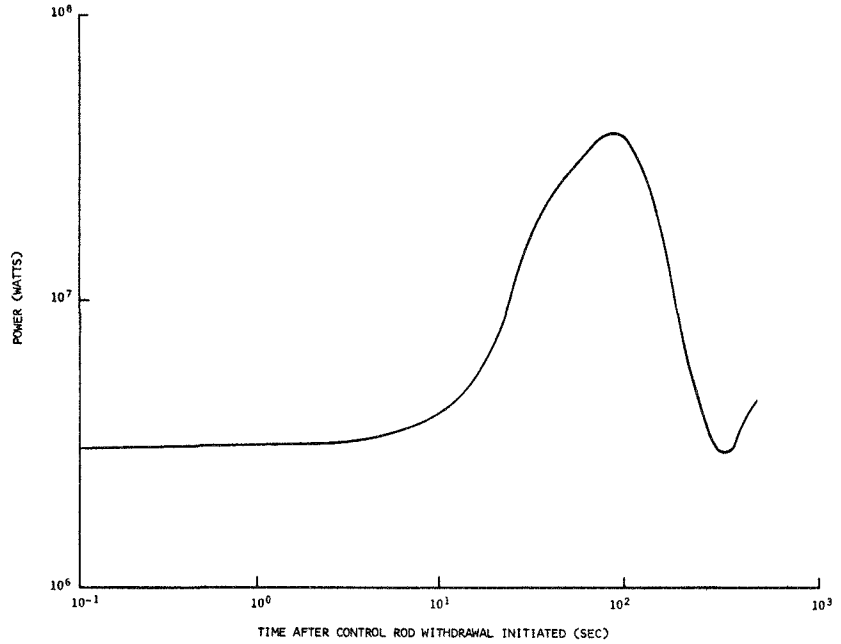

Fig. 16.2.1.4 Power transient during Case II excursion

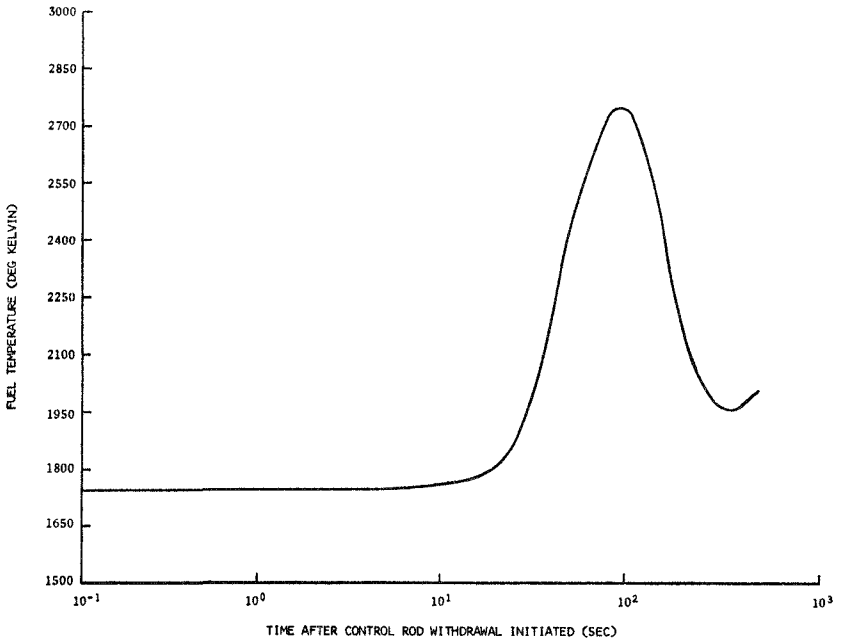

Fig. 16.2.1.5 Fuel temperature transient during Case II excursion

No damage to the fuel or to the system would result from the thermal effects of the Case I transient. In Case II, however, there is a possibility that some damage to the coated particles might occur, since the maximum in the average fuel temperature, 2740°K, is near the melting point of the particle cores, 2750°K. A test of the capabilities of UHTREX fuel to resist temperature transients was made as a part of the KIWI-TNT test in Nevada on January 12, 1965. During the test, the coated particles in the fuel samples experienced a very rapid temperature transient, which reached a level near the melting point of the UC_2 cores. Radiochemical analysis of the tested fuel indicated that only 0.1% of the ^{133}Xe was lost from the particles. Furthermore, no failed particles were discovered in the metallographic examinations of the fuel.

The rod withdrawals postulated in the two calculated transients are scarcely credible. The withdrawals cannot occur unless at least two independent scram channels fail simultaneously and the control room operator fails to take any corrective action during the 2-min period required to withdraw a rod.

16.2.2 Coolant Blower Shutdowns

Heat moves from the core to the atmosphere in flowing helium that is circulated by electrically driven blowers and finally cooled with forced-draft air. When the operation of a single coolant blower or of the heat dump fans is interrupted, heat transfer throughout the coolant systems is affected. The effects and their consequences are discussed below for the primary loop blower, the secondary loop blower, and the heat dump fans. In every case, there is ample time for taking corrective or preventive action before loop components reach their design limits.

Primary Loop Blower - An inadvertent shutdown of the primary loop blower leads to a mild rise in core temperatures, which is not transmitted to coolant loop components that are vulnerable to high temperature damage. No immediate counteraction is necessary, but the loss of

flow initiates an automatic insertion of the plug rods, which ensures a monotonic decline in reactor power.

An UHXCOM analysis of a primary blower shutdown was made, under the assumptions that the reactor is operating at design conditions and that no immediate corrective action is taken when the blower power is interrupted. The results of the analysis show that, 10 sec after the blower starts its coastdown, primary loop coolant mass flow rate drops to < 0.5 lb/sec and the reactor thermal power falls to about 0.6 MW. There is a 50°F rise in the reactor inlet gas temperature in the first 5 sec, and another rise of 25°F in the following 20 sec. At the reactor outlet, the gas temperature rises 400°F in 50 sec. The temperature of the hottest fuel element zone rises 150°F, in 25 sec, to about 3150°F, but moderator temperatures increase < 25°F. None of these temperature rises are transmitted outside the reactor because the mass flow rate of the coolant drops so rapidly to a very low level. Generally, gas temperatures decrease in the heat exchanger and heat dump. At the hottest point in the heat exchanger, the tube temperature decreases > 300°F in 50 sec.

Increase in the fuel and moderator temperatures decreases the system reactivity, and the neutronic power falls linearly to 1454 Btu/sec (1.5 MW) within 50 sec after the start of blower coastdown. The concurrent decreases in thermal, neutronic, and heat dump powers are plotted in Fig. 16.2.2.1.

Secondary Loop Blower - Interruption of power to the blower and closure of an isolation valve can stop flow in the secondary coolant loop. If, for the worst case, flow is stopped short by a closed isolation valve, a general rise occurs in temperatures around the main heat exchanger, which continues to receive heat from the flowing primary loop coolant but cannot dissipate heat to the stagnant secondary loop. The average rate of rise in temperature, 4-6°F/sec, allows ample time for shutdown of the primary loop blower before loop components become overheated.

If an isolation valve is closed while the reactor is operating at full-power, steady-state conditions, there is little change in

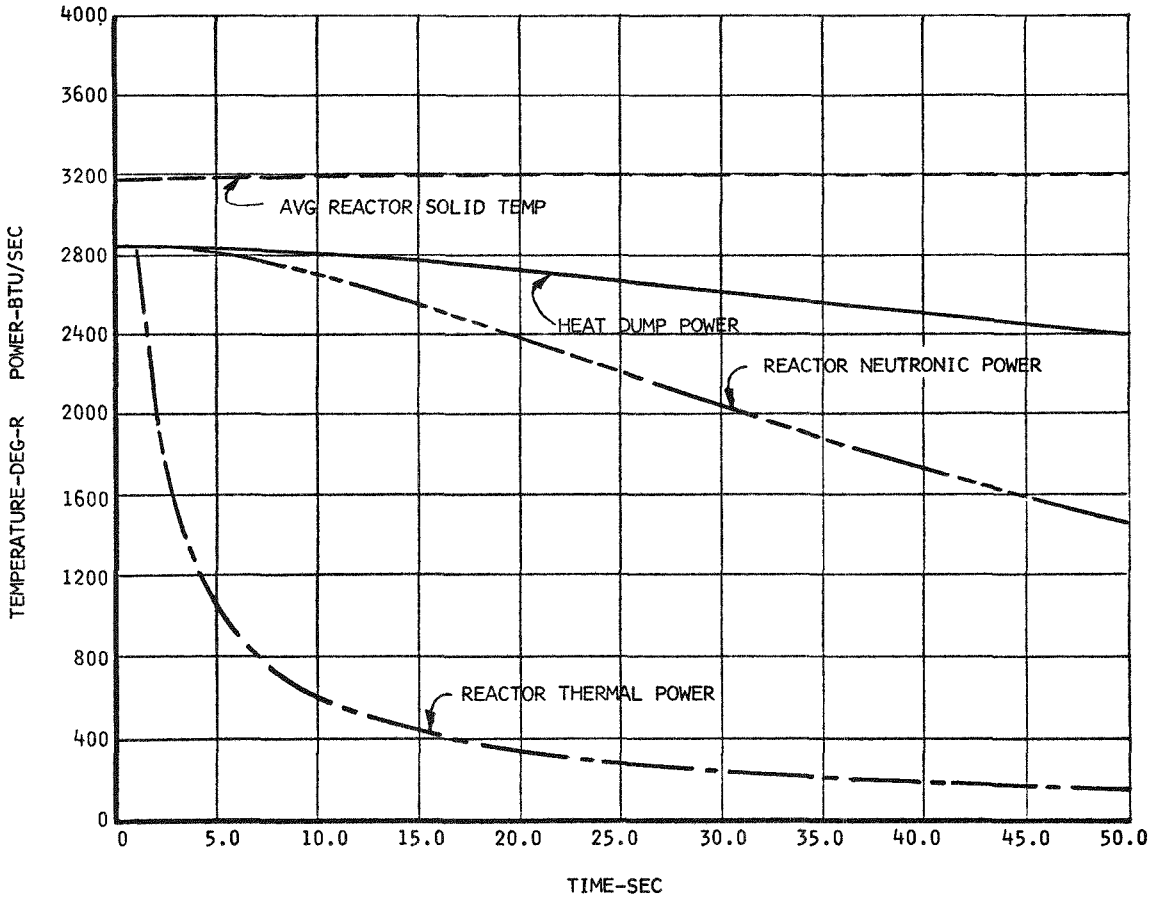

Fig. 16.2.2.1 System power responses to primary blower shutdown

reactor power or coolant system temperatures during the first 50 sec after closure, except at the heat exchanger. There, the highest tube temperature rises 210°F, and the gas temperature at the heat exchanger outlet to the primary loop rises 300°F in 50 sec. The latter temperature reaches 600°F in 32 sec after secondary flow stoppage. The blower motor would overheat if corrective action were not taken within 3-4 min. However, an automatic safety system, triggered by loss of secondary loop flow, immediately shuts down both coolant loop blowers and runs down the control rods. After this corrective action is taken, the system response is similar to that described above for primary blower shutdown.

Heat Dump Fans - If the heat dump fans are stopped while the reactor is operating at design conditions, the immediate effect is a general rise in temperature throughout the secondary loop. The heat capacity of the loop components resists a rapid temperature rise and allows corrective measures to be taken in time to prevent damage. A loss of air flow at the heat dump automatically initiates a shutdown of both coolant loop blowers, and a reactor control rod rundown.

An UHXCOM analysis shows that about 350 sec elapse, after a heat dump fan shutdown, before the first design limit is reached. At that time, if no corrective action has been taken, the inlet coolant to the primary loop blower reaches its maximum operating temperature, 600°F, and the blower begins to overheat. Another 200 sec pass before other component temperatures rise to their limits.

16.2.3 Opening of Recuperator Bypass Valve

Heat exchange conditions within the primary loop are adjusted with a bypass flow of coolant around the cool side of the recuperator. The flow is regulated by a throttling valve in the bypass line. Valve position, normally partially open, is set to adjust the inlet gas temperature to the reactor. Through a controller malfunction or an operator error, the valve can be opened wide in 90 sec. The effects of a sudden opening of the nearly closed valve are the admission of an 800°F stream of helium to the bottom of the reactor and the loss of the coolant to the recuperator. The consequences of both effects develop slowly enough that automatic safety systems can shut down the reactor and stop the coolant blower before damage occurs.

In an analysis of the most severe consequences of this incident, two UHXCOM simulation runs were made in which the bypass flow fraction was stepped from its normal 0.20 to its maximum value of 0.80. The system responses were assessed first under the assumption that the safety systems fail and there is no shutdown. As shown in Fig. 16.2.3.1, the reactor thermal power rises as the bypass valve is opened, and reactor

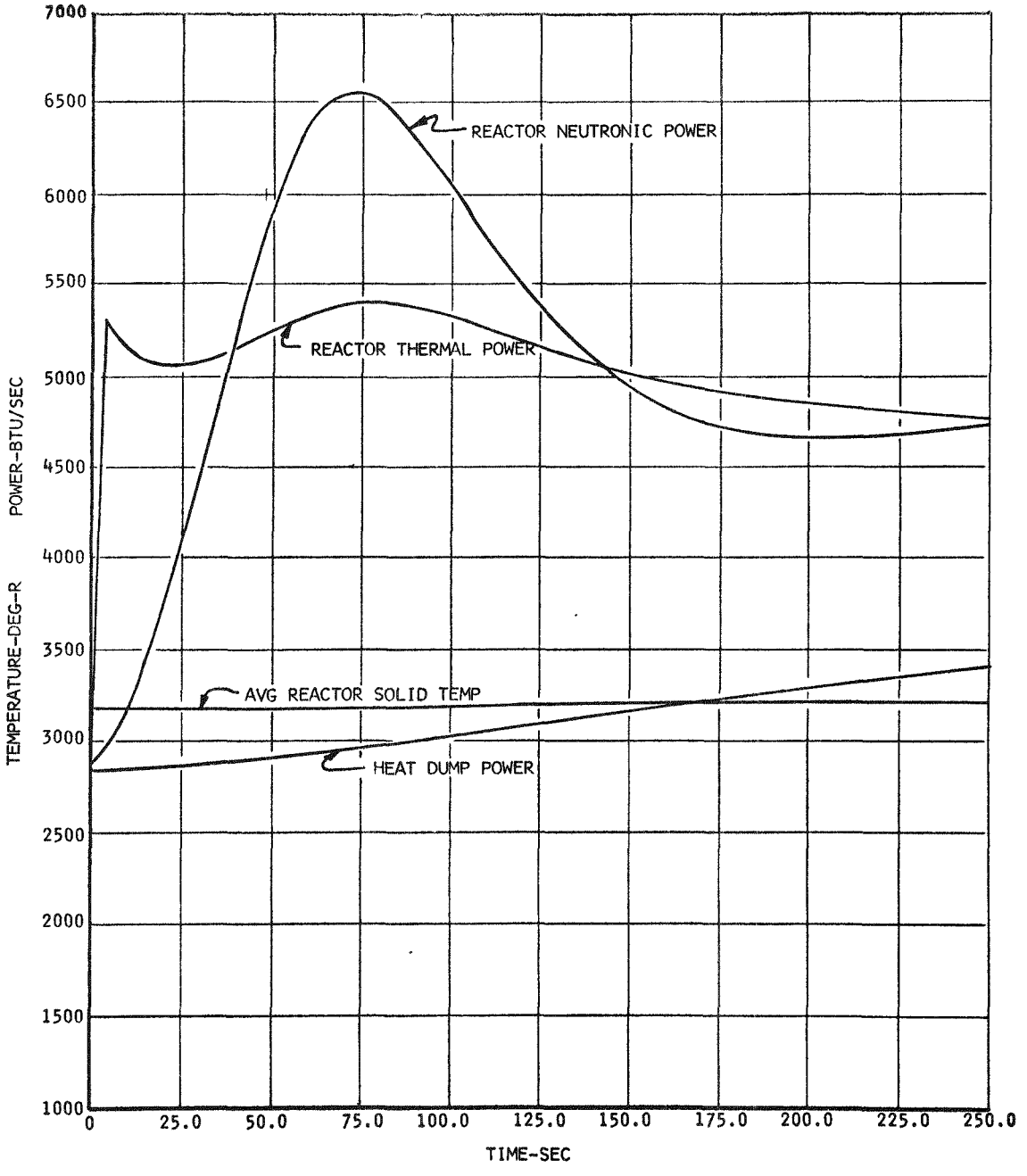

Fig. 16.2.3.1 Response of reactor and coolant system to opening of bypass valve without shutdown

neutronic power follows afterwards, reaching a peak of 6.9 MW in about 75 sec. The heat dump power rises slowly, and, at steady state, all three powers settle to 4.38 MW, almost 50% above the initial power level. During the power transient, the maximum net reactivity is 12¢ and the minimum period is 57 sec. Fuel element temperatures oscillate and spread, as do the moderator temperatures. The recuperator hot outlet gas temperature rises at about 2°F/sec and exceeds the allowable heat exchanger hot inlet temperature in 100 sec. The heat exchanger tube temperature rises more slowly, at a maximum rate of 1°F/sec, and does not exceed tolerable limits.

The second UHXCOM run includes reactor scram and primary blower shutdown. Both of these corrective actions are assumed to start when the reactor neutronic power reaches 150% of its standard value. The temperature of the hot gas entering the heat exchanger rises more rapidly than it does in the uncontrolled case, owing to the reduction in primary flow. However, at the lower flow rate, less heat is transmitted to the heat exchanger, and the heat exchanger tube temperature rises less than 50°F, reaching a maximum of 815°F at about 32 sec. Thus, the corrective actions taken by the safety systems are more than adequate to protect the loop components, and the core components do not exceed tolerable limits.

16.2.4 Malfunctions in the Gas Cleanup System

Coupling is not close between the primary loop and the gas cleanup system, which processes helium at a flow rate only 1% of the primary loop flow rate. If a malfunction or operational error were to occur in the gas cleanup system, there would be ample time to take corrective action and prevent the transmission of effects to the primary loop. To affect the primary loop, a malfunction or error must result in the rapid injection of a harmful material into the circulated helium stream at a point where subsequent removal is impossible. Such an accident is conceivable, but incredible when the duplication of temperature, analytical and sensor elements, and their interlocks is considered.

There are no combustion or explosive reaction hazards associated with the cleanup system. Oxygen for combustion exists only in the vicinity of the copper oxide bed. At the maximum operating temperature of that bed, the dissociation of CuO is so slow that oxygen introduced into the helium stream does not produce a concentration that is detectable on an instrument sensitive to 1 ppm of oxygen. There is a faint possibility that oxygen introduced during the regeneration of the CuO bed might cause the combustion of a minute portion of the sidestream adsorption beds if the oxygen were to be adsorbed in the cold sidestream beds and combustion were to be initiated when the sidestream beds are heated for regeneration. However, operation of the CuO regeneration loop at a reduced pressure prevents flow from the loop to any of the carbon beds. Furthermore, at the low oxygen concentration used for regeneration, only a very small mass of free oxygen exists in the loop at any time.

Loss of coolant flow to any of the gas cleanup system components does not lead to an unsafe condition. Flow switches in the coolant streams initiate the shutdown of the blower when coolant ceases to circulate. The massive beds which contain fission products could warm up slowly if coolant were lost, but the result would be no more than a redistribution of the desorbed fission product gases, which are present in such small quantities that their desorption would not add significantly to system pressures.

16.3 Effects of Component Failures

As it may in any system that consists of many related parts, the mechanical failure of a single component in a UHTREX reactor system may affect the entire complex. In UHTREX, because the reactor is designed to be used for experimental purposes and not for the generation of power, the response to a mechanical failure would most often be a reactor shutdown to permit repairs. There are few backup systems whose function it is to keep the reactor operating; instead, backup systems ensure that

the reactor can be shut down safely and that the consequences of mechanical failures are limited within safe bounds. The most vulnerable UHTREX subsystems are the coolant loops and the fuel-handling systems. Failures, not necessarily credible, in these systems are postulated below, and the effects of the failures are discussed.

16.3.1 Rupture of the Primary Coolant Loop

Contaminated helium, released by rupture of a primary loop component, is confined inside the secondary containment under the most rigorous conditions. Mobile fission products carried in the released helium create a radiation field around the superstructure, but do not produce an intolerable hazard to site personnel or to the general public. Two accidents are described and analyzed here. The first, barely credible, is a failure of the reactor vessel at the elevator housing. The second, purely hypothetical, is a double-ended failure of the pipe that connects the recuperator to the reactor inlet. After the initial failure, the course of each accident is the same: quick release of primary loop coolant into the reactor room, reaction of the core graphite with air from the containment structure, and dissipation of sensible and decay heat of the reactor to its surroundings. Each of the accidents, whose results differ only slightly in the degree of severity of off-site hazards, was analyzed according to the calculational methods described in Appendix F. A description of each accident is presented below. Following the description of the hypothetical accident, an assessment is presented of the resultant radiobiological hazards, based on calculations that are discussed in Appendix G.

Reactor Vessel Failure - For the credible case of rupture in the primary coolant loop, a ductile failure in the reactor pressure vessel is assumed to form a crack at the center of the elevator housing cover. The crack propagates to the top and bottom edges of the housing and terminates where the stresses are low in massive sections.

The elevator housing, which is shown in cross section in Fig. 4.1.5.1, is a boxlike structure welded into a reinforced section at the side of the reactor vessel. The cover is a 2-in.-thick flat steel plate into which are screwed 14 fuel loader tubes, each 2-1/2-in. o.d. x 1-1/2-in. i.d. The cover is highly stressed, but overall stress conditions are satisfactory under the operating conditions of the reactor. At all other points in the reactor vessel, stresses are much lower than allowable.

Strain readings obtained during pressure tests indicated a maximum principal stress, on the outside surface of the cover, of 26,600 psi in compression at the center of the plate and a 30,800 psi compressive stress concentration near the point of insertion of the tube that is nearest the center. At the ends of the plate the principal stress value was only 3700 psi in compression. The temperature distribution in the housing, plotted in Fig. 4.3.1.6, reduces these stresses by decreasing the bending moment exerted in the cover plate by the expansion of the pressure vessel shell.

Before the vessel failure postulated here can occur, two consecutive failures must occur in fuel loader mechanisms or in the computer program that operates the fuel loader rams. First, a loader ram must be inserted into the core and must remain there until the end of the ram reaches 2500°F. (Under normal conditions, the computer program initiates retraction of a rod within 2 sec after it reaches its innermost position.) Second, a failure must occur to allow the ram to be retracted past its normal rest position to a position where the hot end of the rod is adjacent to the junction of the fuel loader tube and the elevator housing cover plate. There, the heat from the rod causes a temperature rise in the tube and a concomitant loss of strength in the tube wall. The internal pressure then causes the tube to deform until helium begins to leak through the tube threads. Hot helium, moving directly from the core through the graphite loader tube, flows through the leak, causing more overheating. Finally, a crack forms between two of the loader tube holes in the cover plate and progresses, from hole to hole, to the edges of the plate.

A general failure of the pressure vessel does not occur, even though the pressurizing medium is a gas, for the following reasons:

1. The tube insertion holes toward which the cracks in the cover progress, tend to slow down, if not completely stop, the propagation.

2. On reaching the edge of the cover, a crack can proceed only through the wall of the housing and into the 3-in.-thick shell of the pressure vessel. However, these two components are under low stress, they are well above the NDT temperature for ASTM 212B steel, and the arch action of the spherical shell reduces any bulging effect. Therefore, the crack stops at the edge of the cover plate.

After the cover plate fails, coolant helium escapes into the reactor-recuperator room through the opening, estimated to be about 40 $in.^2$ in area. From the reactor room, the liberated helium and its load of mobile fission products move into the remainder of the secondary containment. The pressure inside the reactor room rises slightly until flows into and out of the room become equal. The internal force due to pressure differential is insufficient, by a factor of more than 3, to raise the loose shielding slabs that cover the reactor room.

Meanwhile, the pressure inside the primary loop drops rapidly, within 1 sec, to 300 psi. The pressure drop initiates, 1 sec after the rupture, a rundown of control rods, a shutdown of both coolant loop blowers, and the closure of valves in the ventilation system bleed from the secondary containment.

About 10 sec after the rupture, the pressures inside and outside the reactor become essentially equal, and the coasting blower begins to introduce a mixture of air and helium into the hot reactor core and recuperator. There, the oxygen reacts with graphite to form carbon monoxide at a reaction rate limited by the mass transfer of oxygen through the gas film on the graphite surfaces. Mass transfer decreases as the blower speed falls, until the transfer rate is controlled by natural convection, 24 sec after the shutdown of the blower. There is no runaway oxidation of the core graphite. Instead, the reaction proceeds so slowly

that the core temperature soon begins to fall and then declines rapidly after about 3 hours.

The pressure inside the secondary containment structure, driven upward by the release of the coolant helium, rises within 10 sec to 1.75 psig. The gas is contained within the structure, which was designed to withstand 7.5-psig internal pressure and has been tested to 5.0 psig. Once free, the hot coolant helium begins to lose heat to its surroundings and the temperature inside the containment falls (see Fig. 16.3.1.1). As a result of the temperature drop, there is a concurrent decrease in containment pressure. The pressure decline is plotted in Fig. 16.3.1.2. The production of carbon monoxide and heat in the core combustion reaction, $2C + O_2 \rightarrow 2CO$, which liberates two moles of CO per mole of O_2 consumed, makes a negligible contribution to the pressure. The net result of these two effects, plus that of leakage from the structure, is a plateau in the containment structure pressure curve at about 0.75 psig, starting about 30 min after rupture.

During the whole period of time after the postulated rupture, gas escapes from the containment structure, at rates commensurate with an assumed building leak rate of 7.5% per day at 5-psig internal pressure. (This assumed leak rate, 2.5 times the building leak rate measured during tests prior to installation of equipment in the building, was set high to include the effects of any general deterioration in structure integrity that may occur during the lifetime of UHTREX.) The combined effects of the cooling of the contained gas and leakage from the structure cause a decline in containment pressure to 0 psig after 16 days.

If the automatic safety systems do not act immediately after the rupture to shut down the reactor and the coolant blowers, a manual shutdown can be made without an aggravation of the accident. According to the results of an UHXCOM-calculated simulation run, the reactor thermal power falls to 116 kW in 10 sec after the rupture, though the reactor is not shut down, and neutronic power drops 50% in 50 sec. Moderator temperatures show little change. The maximum fuel element temperature

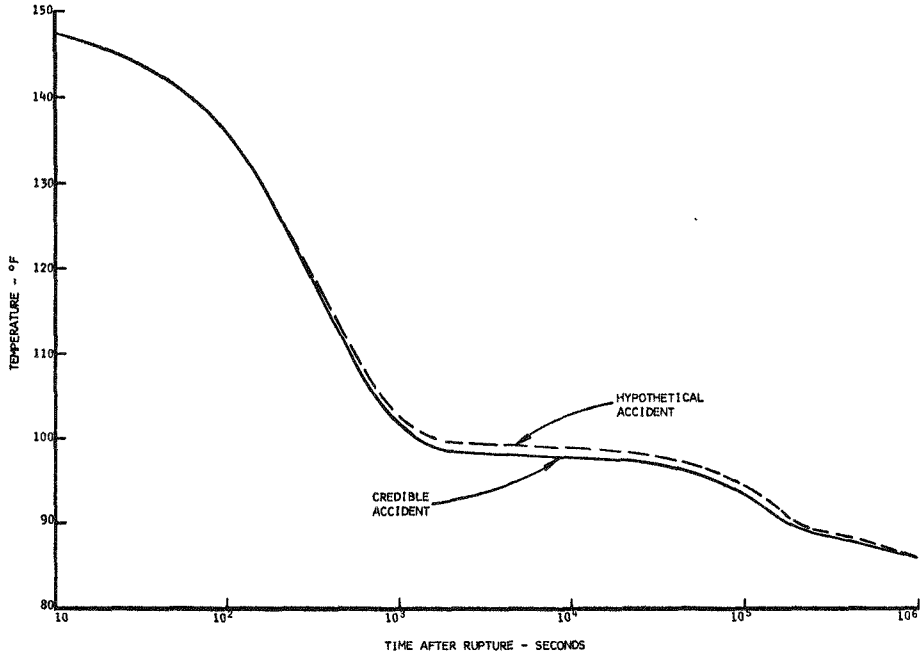

Fig. 16.3.1.1 Air temperature inside secondary containment after primary loop rupture

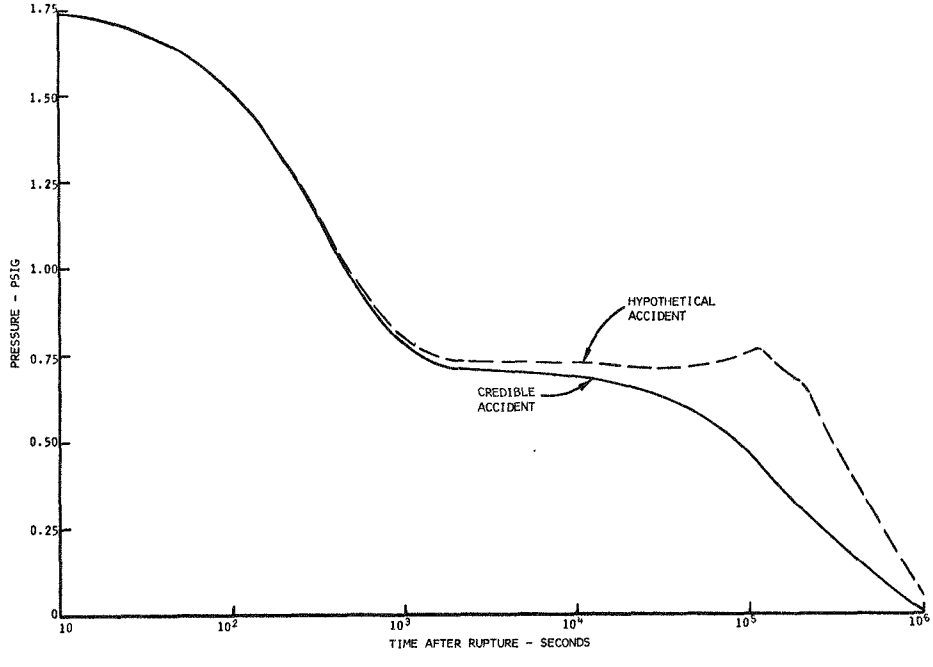

Fig. 16.3.1.2 Containment pressure after primary loop rupture

rises about 15% in 30 sec and then starts to fall. An abrupt rise of about 400°F occurs in the reactor outlet gas temperature, but the effect is not transmitted downstream because the helium flow rate falls so rapidly. In the main heat exchanger, the tubes continue to be cooled by the secondary loop flow. The only adverse effect of a slightly delayed shutdown would be a deferment of the primary blower coastdown period, which might lead to a small increase in the amount of air introduced into the core.

Double-Ended Pipe Rupture - To determine the upper limit on hazards that could be created, a hypothetical accident, more severe than the vessel failure described above, has been analyzed. In the hypothetical accident, a fracture occurs at each end of the pipe that carries the 1600°F helium stream from the outlet of the recuperator to the inlet of the reactor, and the pipe falls away, leaving two openings.

The results of this accident are more severe than those of the vessel rupture because two openings at different elevations increase the natural convective flow of air through the core after the helium coolant has escaped. Although more carbon is oxidized, the effect is slight on gas temperatures in the secondary containment, plotted in Fig. 16.3.1.1. However, the continued oxidation does sustain the secondary containment pressure plateau at 0.75 psig, shown in Fig. 16.3.1.2. and does release more fission products as a result of the combustion of 45.5% of the fuel, versus 0.8% consumed in the pressure vessel failure accident. These two effects combine to increase the level of radiobiological hazards, which are analyzed below.

Aside from the oxidation, the course of this accident closely parallels that of the vessel failure accident. The venting of helium from the core is somewhat faster, but does not cause a material increase in the peak pressure inside the reactor room.

Radiobiological Hazards - Because the activity release associated with the double-ended pipe rupture accident is more severe than that resulting from the reactor vessel failure accident, the radiological

hazards were evaluated only for the former case. The significant hazards that are consequences of the postulated accident consist of direct gamma radiation from fission products inside the containment structure, internal radiation following inhalation of fission products in the air-borne effluent, and external radiation from gamma-emitting fission products in the air-borne effluent. Calculations that were made to assess these hazards are discussed in Appendix G, and the results of the calculations are presented below.

Doses associated with direct gamma radiation from the secondary containment structure are ploted in Fig. 16.3.1.3 for the first 2 h after the accident and for 30 days later. In the dose calculations, the shielding effect of the 1.5-ft-thick walls of the structure was taken into account.

The results of calculations are listed in Table 16.3.1.1 for doses due to fission product leakage from the secondary containment structure. Doses were computed for the first 2 h and the first 30 days at 2000 m, the distance to the nearest residence. Inhalation doses to nine critical organs are tabulated, as well as the whole-body inhalation and the whole-body gamma dose due to immersion in the effluent cloud.

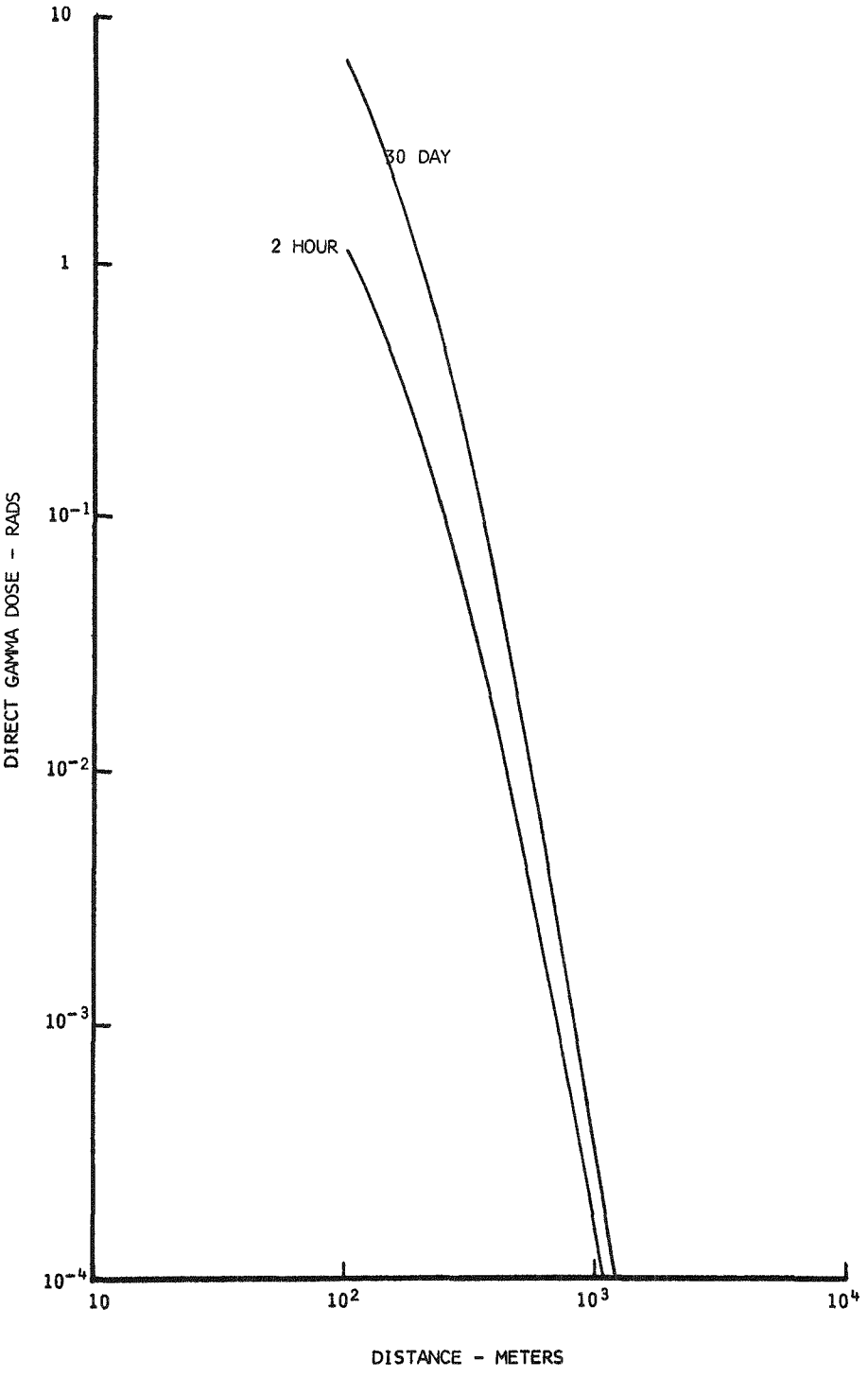

Fig. 16.3.1.3 Doses due to direct gamma radiation from secondary containment structure after primary loop rupture

TABLE 16.3.1.1

LIFETIME DOSE IN REM AT 2000 METERS DUE TO
PRIMARY COOLANT LOOP DOUBLE-ENDED PIPE RUPTURE

	2 Hour Exposure				
Critical Organ	Noble Gases	Halogens	Volatiles	Solids	Total
Bone			0.002	0.007	<0.1
G.I.	0.2	0.018	0.013	0.025	0.26
Kidney			0.001	0.034	<0.1
Liver			0.002	0.007	<0.1
Lung	0.346	0.023	0.020	0.089	0.48
Muscle					<0.1
Spleen					<0.1
Testis			0.001		<0.1
Thyroid		0.78			0.78
Whole body (Inhalation)			0.001	0.002	<0.1
Whole body (Immersion)	0.05	0.005	0.005	0.002	<0.1
	30 Day Exposure				
Critical Organ	Noble Gases	Halogens	Volatiles	Solids	Total
Bone			0.37	0.232	0.27
G.I.	3.19	0.18	0.151	0.502	4.0
Kidney			0.029	0.708	0.74
Liver			0.033	0.137	<0.17
Lung	7.1	0.38	0.41	3.05	10.9
Muscle			0.013		<0.1
Spleen			0.014	0.015	<0.1
Testis			0.014		<0.1
Thyroid		13	0.004		13.0
Whole body (Inhalation)		0.03	0.021	0.045	<0.1
Whole body (Immersion)	0.19	0.04	0.021	0.031	0.28

16.3.2 Rupture of the Secondary Coolant Loop

Isolation valves close immediately to maintain secondary containment after a major rupture of the secondary coolant loop. If the rupture occurs beyond the valves, the pressure regulating controller restores pressure in the shell side of the heat exchanger, now isolated from the remainder of the loop. The effects of this sequence of events are those described above for an operational loss of flow in the secondary loop. When a rupture occurs inside the isolation valves, the pressure in the main heat exchanger cannot be restored, and the effects are equivalent to those described for an inadvertent venting of the secondary loop.

Wherever the rupture occurs, safety circuits described in Sec. 11.4.2 initiate action to prevent the overheating and consequent rupture of the main heat exchanger. If these circuits should fail and a path develop between the primary and secondary loop inside the exchanger, the isolation valves maintain secondary containment.

If a small leakage path were to develop in the main heat exchanger tubes, the flow of helium, by design, would be inward from the secondary to the primary loop. Operational procedures require a higher pressure in the secondary loop; the pressure regulation system maintains this differential. A slow leak, either to the primary loop through the heat exchanger or to the atmosphere, would be indicated by the continual operation of the pressure control system and a steady drop in the pressure at the makeup helium manifold. The immediate action to be taken in response to a slow leak would depend on its magnitude, but an eventual shutdown of the reactor would be necessary.

The possibility exists, in the case of a small leak in the main heat exchanger, that fission products could diffuse through the hole to the secondary loop. There, the radioactivity would be sensed by detectors that continually monitor the loop, and an alarm would sound in the control room. The reactor operator's response to the alarm would depend on the activity level in the secondary loop and would range from a triggering of the isolation valve safety system to an orderly shutdown of the reactor.

16.3.3 Failure in the Fuel Loader and Core Indexing Mechanisms

The principal effects of failures in the fuel loader and core indexing mechanisms are limitations on future reactor operations, rather than the creation of immediate hazards. When a component fails, in many cases the ability to load or unload fuel is lost until the reactor can be shut down and depressurized to permit correction of the failure. In other cases, all or part of the fueling capability is permanently lost.

For an example of a serious credible failure, the halting of a loading ram can be assumed to occur while the ram is moving a fuel element into the movable core. When the ram is partially inserted, it bridges the gap between the loader and the core, and a partially discharged element projects into the stationary core plug. The choice of what to do next lies between shutting down the reactor to effect immediate repairs or temporarily abandoning this loading position by rotating the core to shear off the protruding ram and element. If the choice is to proceed with loading, the graphite ram and hollow graphite fuel element can be readily sheared with minimal damage to the core. The short piece of ram and the fragments of fuel element, in the worst case, fall into the annuli at the edges of the core. There, the pieces either ride around the bottoms of the annuli as the core rotates, or are ground between the movable and stationary parts. The pieces do not have size or structural strength enough to bind the movable core. The capability of the core to shear fuel elements was demonstrated during the UHTREX critical experiment. On two occasions, the core was moved when a fuel element was partially displaced, with about 1/3 of its length projecting into the stationary core plug. The only damage to the core structure was a slight chipping of the sharp outer edge of the slot in the plug.

Reparable components of the loader extend into rooms shielded from the reactor. In these rooms, repairs can be made under controlled conditions after a reactor shutdown and decay period. However, one vital component, the elevator inside the loader, is enclosed in an integral part of the pressure vessel. The elevator itself and all but the

uppermost length of its actuating rod are inaccessible. For this reason, the elevator design is simple and conservative.

Three types of failures can happen in the core-indexing mechanism: drive breakdown, support bearing seizure, and sequence controller malfunction. If the drive stops while the core is in a position between index stations, loading operations are impossible until repairs are made under the conditions described above. A core support bearing seizure would result in permanent loss of loading capability. However, since the results of the bearing test described in Sec. 4.1.6 became known, no credible event that leads to bearing seizure has been postulated. The sequence controller prevents the movement of the core unless all loading rams are withdrawn; a malfunction can allow movement of the core and consequent shearing of a loader ram and fuel element.

No credible sequence of events that leads to the plugging of a fuel channel has been postulated without structural failure of the core as a prerequisite. Heat transfer calculations show that the plugging of a channel does not, in itself, introduce additional hazards. When coolant flow is stopped in a single channel, heat generation continues and the fuel elements reach an equilibrium temperature of less than 3500°F. Heat flows from the elements to the moderator graphite by radiation and is conducted to adjacent active channels. In those channels, the additional heat flow from the moderator to the coolant reaches equilibrium after a 175°F rise in local moderator temperatures. The local temperature increases in the moderator can be tolerated without mechanical failure of moderator parts.

16.3.4 Failure in the Fuel Handling System

Nuclear criticality hazards are eliminated in the fuel handling system design by two characteristics: the inability of the conveyors to handle more than one fuel element at a time, and the long operating cycle for the charging and removal of fuel. Failures in system components can limit future operation of the reactor, but the failures do not

create nuclear criticality hazards. Hazardous conditions can arise, however, through failure of the gas locks at the entrance to the fuel loader or at the bottom of the reactor.

Each of the conveyors consists of a single vessel, large enough to contain a single fuel element or its fragments, moved inside a housing by continuous cable drives. Electrical switching circuits and interlocks ensure that the conveyors and their corresponding gas locks are operated in proper sequence. In the loading cycle, a single new element moves from a dry box in the fuel handling cell through gas locks and a conveyor to the fuel loader. The fuel loader charges the single new element and concurrently discharges another single element. Only when the cycle is completed by the visible arrival of the spent element in the cell, does a new loading cycle start. The cycle is not completely automatic; new fuel elements must be fed into the first conveyor with a hand-operated manipulator. If an equipment failure interrupts the loading cycle, no emergency is created except in the case described below.

A series of valves, operated in proper sequence, closes the chambers in the gas locks that pass fuel elements into and out of the reactor pressure vessel. If, in an incredible circumstance, all three valves in a gas lock should be open concurrently, full coolant pressure would burst the rupture disk where the gas lock joins its adjacent conveyor. The result, provided that the valves could not be closed again, would be the release of the primary loop coolant into the secondary containment. Consequences would be similar to those described above for rupture of the pressure vessel, except that core combustion would not be promoted by the induction of air during blower coastdown. The valves are operated only by an on-line computer program which precludes simultaneous gas lock valve operation while the reactor is pressurized. Wiring interlocks prevent the accidental application of power to both the inner and outer valve of a gas lock set. The gas lock valves cannot be opened manually.

APPENDIX A

METEOROLOGICAL DATA FOR LOS ALAMOS

TABLE A.1

AVERAGE WIND DIRECTION, LOS ALAMOS

(PERCENT OF TIME)

1953 - 1957

Surface	Dir.	Jan.	Feb.	Mar.	Apr.	May	June	July	Aug.	Sept.	Oct.	Nov.	Dec.	Annual
	S	27.9	21.6	21.4	27.9	29.3	26.9	20.2	19.2	24.5	32.0	23.3	17.5	24.5
	SW	16.2	13.0	16.0	18.0	16.9	19.5	20.5	15.5	20.3	19.0	14.4	12.0	16.9
	W	13.8	16.0	21.3	21.7	18.5	22.3	16.6	21.0	20.2	15.2	15.3	15.5	18.7
	NW	7.7	10.5	10.9	8.2	7.4	7.3	8.5	8.5	7.3	7.2	9.4	10.6	6.9
	N	13.8	13.5	10.9	6.9	8.4	5.6	11.2	10.1	7.0	8.4	14.6	17.1	10.9
	NE	6.3	8.7	6.0	5.2	6.3	6.0	8.0	10.1	6.9	5.9	7.8	12.2	7.6
	E	7.7	8.9	8.5	7.8	8.9	7.6	9.2	10.1	8.2	6.6	8.7	7.4	8.6
	SE	6.6	7.8	5.0	4.3	4.3	4.8	5.8	5.5	5.6	5.7	6.5	7.8	5.9
Upper Air*	Dir.	Jan.	Feb.	Mar.	Apr.	May	June	July	Aug.	Sept.	Oct.	Nov.	Dec.	Annual
	S	11.9	5.7	10.7	13.8	18.4	30.6	17.7	26.7	22.8	20.9	8.9	6.5	16.2
	SW	18.6	16.1	22.1	14.4	25.0	20.2	24.2	20.0	18.8	22.1	15.0	15.9	19.4
	W	29.0	27.1	30.7	29.3	26.8	20.2	9.2	15.9	14.3	14.4	22.5	27.9	22.3
	NW	27.5	38.7	28.3	26.1	17.8	12.1	12.9	8.3	16.9	23.4	33.3	37.2	23.5
	N	8.6	9.2	4.5	8.6	7.0	8.9	6.9	10.1	8.6	8.6	15.0	9.4	8.8
	NE	1.1	0.3	0.0	2.8	0.0	3.2	4.6	3.7	4.0	1.6	2.7	0.3	2.0
	E	2.2	0.0	1.6	0.6	1.6	1.6	8.5	7.4	6.0	2.8	1.6	1.9	3.0
	SE	1.1	3.0	2.0	4.3	3.3	3.2	17.5	7.9	8.6	6.2	0.9	0.9	4.9

* About 1,000 ft above terrain; based on morning wind soundings at Albuquerque, data from three years of observation.

TABLE A.2

AVERAGE SURFACE WIND SPEED, LOS ALAMOS

(PERCENT OF TIME)

1953 - 1957

MPH	Jan.	Feb.	Mar.	Apr.	May	June	July	Aug.	Sept.	Oct.	Nov.	Dec.	Annual
0	5.4	5.3	2.3	1.7	1.2	1.3	2.4	3.8	3.7	3.1	3.1	4.6	3.2
1-5	54.7	49.3	32.2	29.9	31.1	25.3	40.9	43.1	26.7	33.8	43.1	49.7	38.2
6-10	26.5	28.5	33.4	32.6	35.4	37.2	37.7	38.9	40.2	38.0	35.0	33.5	34.9
11-15	7.7	9.9	16.9	18.7	17.2	21.4	13.5	10.9	20.1	16.9	12.5	7.9	14.5
16-20	3.4	5.0	9.9	10.7	10.1	11.0	4.6	2.8	7.2	5.4	4.2	3.0	6.5
21-25	1.7	1.2	3.2	3.8	3.4	2.8	0.9	0.4	1.9	1.8	1.4	0.9	2.0
26-30	0.4	0.5	1.3	1.8	1.2	0.8	0	<0.1	0.2	0.8	0.6	0.3	0.6
31-35	0.1	0.2	0.5	0.5	0.3	0.2	0	0	<0.1	<0.1	<0.1	<0.1	0.1
36-40	<0.1	<0.1	0.2	0.1	0	0	0	0	0	<0.1	0	<0.1	<0.1
41-45	<0.1	<0.1	<0.1	<0.1	0	0	0	0	0	0	0	0	<0.1
46-50	0	0	<0.1	0	<0.1	0	0	0	0	0	0	0	<0.1
51-55	0	0	0	0	0	0	0	0	0	0	0	0	0
56-60	0	0	0	0	0	0	0	0	0	0	0	<0.1	<0.1

TABLE A.3

PRECIPITATION, LOS ALAMOS

1952 - 1959*

	Jan.	Feb.	Mar.	Apr.	May	June	July	Aug.	Sept.	Oct.	Nov.	Dec.	Annual
Days of Precipitation													
Average	9.9	10.1	11.8	10.9	14.6	10.9	20.0	20.9	8.9	7.7	7.0	7.3	140.0
Maximum	18.0	13.0	23.0	16.0	23.0	18.0	24.0	27.0	19.0	20.0	14.0	11.0	
Minimum	5.0	4.0	2.0	3.0	7.0	2.0	16.0	16.0	3.0	0.0	2.0	3.0	
Days of Snow													
Average	9.6	9.6	11.1	6.0	1.6	0.0	0.0	0.0	0.0	1.1	5.9	6.7	51.6
Maximum	16.0	13.0	23.0	12.0	4.0	0.0	0.0	0.0	0.0	3.0	10.0	11.0	
Minimum	5.0	4.0	2.0	0.0	0.0	0.0	0.0	0.0	0.0	0.0	2.0	3.0	
Days of Thunderstorms													
Average	0.0	0.3	0.1	1.8	7.6	7.4	16.3	17.9	4.9	2.6	0.4	0.0	59.3
Maximum	0.0	1.0	1.0	4.0	12.0	15.0	25.0	23.0	11.0	8.0	2.0	0.0	
Minimum	0.0	0.0	0.0	0.0	3.0	2.0	7.0	16.0	1.0	1.0	0.0	0.0	
Snowfall (inches)													
Average	9.0	8.7	11.1	4.4	0.1	0.0	0.0	0.0	0.0	0.3	4.8	7.7	46.1
Maximum	18.8	18.0	35.5	33.6	4.0	0.0	0.0	0.0	0.0	0.3	34.5	11.5	100.0
Minimum	0.0	0.5	0.5	0.0	0.0	0.0	0.0	0.0	0.0	Tr	Tr	2.5	25.2
Precipitation (Since 1910) (inches)													
Average	0.90	0.66	0.95	1.07	1.46	1.34	3.24	3.64	1.95	1.44	0.67	0.83	18.15
Maximum	6.57	2.44	3.27	4.64	4.47	5.57	7.98	11.18	5.79	6.77	3.30	2.27	30.34
Minimum	0.0	Tr	Tr	0.0	0.0	0.0	0.72	0.51	Tr	0.0	0.0	0.05	6.80

* Except for last stub which covers the period 1910 to 1959.

TABLE A.4

WIND DIRECTION WITH PRECIPITATION, LOS ALAMOS

(PERCENT OF TIME)

Direction	Jan.	Feb.	Mar.	Apr.	May	June	July	Aug.	Sept.	Oct.	Nov.	Dec.	Annual
N	6.7	7.8	3.6	3.4	7.1	9.5	8.9	8.5	7.2	6.8	5.0	4.7	6.6
NNE	1.6	4.4	2.8	3.2	3.8	2.3	1.1	2.1	3.7	2.5	2.0	2.6	2.7
NE	2.8	4.7	5.5	4.4	6.0	3.6	3.7	3.6	0.8	1.1	2.2	4.1	3.5
ENE	2.0	2.3	2.1	3.0	2.7	4.0	4.8	2.9	5.8	0.2	1.6	2.2	2.8
E	2.1	1.9	1.3	2.0	3.3	3.7	4.6	4.2	2.9	1.6	1.4	3.2	2.7
ESE	6.1	3.4	2.5	1.7	3.0	1.8	3.2	3.3	3.9	1.8	1.7	5.0	3.1
SE	6.0	1.4	4.7	2.5	1.2	2.5	3.8	4.5	3.5	4.6	0.7	3.4	3.2
SSE	17.6	5.8	5.6	3.8	3.3	5.6	1.9	3.7	7.8	7.1	6.0	8.9	6.4
S	25.0	32.5	28.7	30.5	25.4	23.6	16.8	15.9	25.9	37.4	31.7	37.4	27.6
SSW	9.5	6.8	14.3	9.3	6.7	8.3	8.9	7.2	6.9	13.1	10.4	10.5	9.3
SW	9.1	6.2	7.8	12.8	9.3	5.9	7.9	6.0	5.7	5.7	11.5	5.6	7.8
WSW	3.6	5.6	6.2	11.7	9.7	6.3	9.3	12.8	6.3	8.0	6.9	3.4	7.5
W	2.0	4.7	4.5	4.0	5.5	6.2	7.9	9.3	4.3	2.9	4.3	3.3	4.9
WNW	2.2	2.2	4.8	1.8	5.0	6.8	5.5	8.2	5.2	2.4	5.1	1.2	4.2
NW	0.9	1.3	2.1	2.4	5.4	5.0	5.1	4.4	3.5	1.6	2.4	1.2	2.9
NNW	0.8	1.9	0.9	1.9	1.7	1.7	2.8	2.4	3.3	1.4	1.4	0.7	1.7
Calm	2.0	7.2	2.7	1.7	0.9	3.2	3.7	1.2	3.4	1.8	5.5	2.7	3.0

TABLE A.5

TEMPERATURES, LOS ALAMOS

1919 - 1965

	Jan.	Feb.	Mar.	Apr.	May	June	July	Aug.	Sept.	Oct.	Nov.	Dec.	Annual
Average Maximum	39	43	49	59	68	78	80	78	73	62	49	41	60
Average Minimum	18	22	26	34	43	52	55	54	48	38	26	20	36
Extreme Maximum	64	68	71	80	93	93	95	92	94	82	69	69	95
Extreme Minimum	-18	-14	13	5	24	28	37	4	23	17	-4	-10	-18

APPENDIX B

GEOLOGY AND HYDROLOGY OF THE UHTREX SITE*

The following information was compiled from data collected during the course of ground-water investigations in cooperation with the Atomic Energy Commission.

The area selected for the UHTREX facility is about a half mile east-southeast of the site of the waste-treatment plant (TA-50), and is slightly more than 1,500 ft south-southeast of the present Ten-Site facilities (TA-35). The reactor facility is located south of Ten-Site Canyon, which is immediately south of the Ten-Site facilities and is a tributary of Mortandad Canyon. The topographic relief in the upper part of Ten-Site Canyon is about 70 feet in the vicinity of the proposed site. The area is on the western half of the Pajarito Plateau which has been dissected into a number of finger-like mesas by eastward flowing intermittent streams tributary to the Rio Grande. Mortandad Canyou and its tributaries drain the immediate area.

The site of the UHTREX facility is in the area investigated recently by the Geological Survey for the proposed waste-treatment plant. This part of the Pajarito Plateau is capped by the Bandelier Tuff of Pleistocene Age. The Bandelier is a welded rhyolite tuff consisting of crystal fragments, tuff breccia, and pumiceous material. The Bandelier is about 700-ft thick near Ten-Site. The base of the Bandelier was encountered at

---

* W. E. Hale, District Engineer, U.S. Geological Survey, Ground Water Branch, Albuquerque, New Mexico. Compiled by J. H. Abrahams and E. Baltz.

an altitude of about 6,380 ft at Test Well 8 in Mortandad Canyon, three-quarters of a mile east of the UHTREX site which is at an altitude of about 7,160 ft. No bodies of water were found in the Bandelier at Test Well 8.

In the subsurface the Bandelier Tuff is underlain by the Puye Conglomerate of Pliocene (?) Age. The Puye consists of silt, sand, and gravel composed of pebbles to boulders of volcanic rocks. Basalt flows are interbedded with Puye sediments in the eastern part of the Pajarito Plateau. Test Well 8 was drilled through 575 ft of the Puye Conglomerate but did not reach the base of the formation. Water was not found in the upper part of the Puye, but was encountered in the lower part at a depth of about 985 ft below the floor of the canyon. The water rose about 25 ft in the well. This body of water, which is the main aquifer in the Los Alamos area, is at an altitude of about 5,960 ft in the vicinity of the UHTREX facility.

Studies indicate that little of the precipitation falling on the mesa tops filters into the Bandelier Tuff where it is overlain by soil. Probably clay in the alluvium in the canyons also inhibits or retards infiltration into the Bandelier. Data concerning the movement of water through tuff are scanty, but because the upper part of the Bandelier is moderately welded and jointed, some infiltration may occur along joints when water flows on bare rock. These joints commonly extend across and along the canyons.

Generally there is flow in Ten-Site Canyon only during spring snowmelt or during summer thundershowers. Radioactive liquids discharged accidentally into Ten-Site Canyon would flow eastward across the Bandelier Tuff for several hundred yards, then presumably infiltrate into the alluvium in the lower part of Ten-Site Canyon and in Mortandad Canyon. However, if the accident occurred during spring runoff or during a heavy summer thundershower, the wastes could be carried as a "slug" into Mortandad Canyon or conceivably to the Rio Grande. Observation wells already constructed in Mortandad Canyon below the mouth of Ten-Site Canyon would serve to monitor the liquids in the alluvium.

APPENDIX C

MANUFACTURING AND INSTALLATION

OF UHTREX PRESSURE VESSEL

1. Materials

1.1 Plate

Carbon steel plate was purchased to ASTM Specification SA212, Grade B, made to ASTM Specification SA300, and manufactured in accordance with fine grain melting practice. The plate material was subjected to an ultrasonic inspection per Lukens Specification UT-5 and was reinspected over 100% of the surface area by the vessel fabricator with a LASL inspector as witness. Both inspections were performed after the plate material had been formed to the spherical contour. A plate was rejected if it had any defect that gave an indication exceeding that obtained from a 3/8-in.-diam, flat-bottom hole in a similarly produced and finished reference plate.

The prepared edges of the plate were subjected to a magnetic-particle inspection for defects exceeding 3/8 in. in any direction, or any defect which reduced the thickness of sound metal, perpendicular to the plane of the plate, to less than the specified design thickness.

Two sets of impact strength tests were run on plate samples. The first set was run by the manufacturer of the plate to satisfy the Charpy test requirements of ASTM Specification SA300. For the second set, the vessel vendor prepared specimens of the base plate and weld materials

with a Charpy V-notch, Type A, per ASTM Specification E23. Plate specimens were welded, with the standard filler materials and according to standard procedures, to specimens of each major forging. The specimens were then passed through the same heat-treatment operations as the corresponding welds on the vessel. Finally, impact tests were run at 10°F in both the transverse and longitudinal directions. The minimum average impact strength of three specimens was established to be 15 ft-lb, and the minimum for an individual specimen was 10 ft-lb.

1.2 Forgings

Forgings were purchased to ASTM Specification SA105, Grade II, made to ASTM Specification SA350 Grade LF-2, and manufactured in accordance with fine grain melting practice. The forgings were ultrasonically inspected and magnetic-particle inspected in accordance with MIL-STD 271 B procedure with the acceptance standards of MIL-S-23194 applying for the ultrasonic test.

Impact strength tests were made as described above for plate material.

1.3 Tubing

All tubing is alloy-steel, seamless tube made to ASTM Specification SA334, Grade 3, cold-drawn and annealed. The tubing was ultrasonically inspected over 100% of the surface, in two passes in opposite circumferential directions. The calibration and acceptance standard was a longitudinal notch, on the inner or outer walls, equal to 3% of the nominal wall thickness.

Outside surfaces were checked with liquid penetrant in accordance with Babcock and Wilcox Specification NDT-2. Visible defects were explored and removed to the tube wall minimum thickness limits.

Charpy testing was performed at 10°F, using the values of Table IV of ASTM Specification SA334 for a 10-mm x 5-mm specimen. Minimum average strength of three specimens was established to be 10 ft-lb, and the minimum value for an individual specimen was 7 ft-lb.

1.4 Bolts

Bolting material was purchased to ASTM Specification SA320, Grade L-43, with a minimum yield strength of 105,000 psi at 600°F. Impact tests were performed at 10°F using a Charpy V-notch, Type A, of ASTM Specification E-23. The minimum average strength of three specimens was established to be 35 ft-lb, and the minimum for an individual specimen was 30 ft-lb.

1.5 Weld Materials

Welding supplies, including coated electrodes, automatic welding wire, and flux, were purchased with the stipulation that the vendor furnish the heat numbers for all coated rod and automatic wire, and information regarding the flux material. Mill test reports were required to demonstrate that the materials met the chemical and physical requirements of pertinent ASTM Specifications. An excess of materials was ordered to eliminate the possibility of a change of rod materials within a weld.

2. Fabrication

Fabrication of the vessel was performed according to a detailed overall procedure, written by the vendor and approved by LASL, which limited the number of post-weld heat treatments and called for the performance of all finish machining after the final post-weld heat treatment. Some of the details of the procedure are described below. Any deviation from the procedure required LASL written permission. Check points were designated at several stages of fabrication so that work could be inspected and corrected, if necessary, before fabrication was continued.

2.1 Welding

A welding procedure was written for each weld. All welding procedures and welders were qualified per the requirement of ASME Code

Section IX. The welding procedures covered process, filler metal, welding position, weld preparation and cleaning, welding technique, interpass cleaning and inspection, preheat and interpass temperature, in-process testing (consisting of X-ray, magnetic-particle, and dye-penetrant tests), weld repair, and post-weld heat treatment. Included in the details of the procedures were the following requirements.

1. All flame-cut surfaces were machined or ground to remove a minimum of 1/32 in. of material from the flame-cut surface.

2. All welds of 3/4-in. or greater width were preheated to a minimum of 250°F and a maximum of 350°F. The minimum interpass temperature was 250°F, and the maximum was 550°F.

3. All root passes were ground smooth and checked by the magnetic-particle method for cracks or other defects.

4. All pressure containment welds were 100% radiographically inspected after completion.

5. All nonfull penetration welds, such as fillet welds on the support structure of the vessel, were magnetic-particle checked after each weld layer.

6. All welds were heat treated.

Control over welding materials was established and enforced as follows.

1. All materials were checked upon receipt against the mill test reports to prove that the material received was that described in the purchase order.

2. All welding materials for the vessel fabrication were kept in a separate locked room and were dispensed only upon the written order of the welding foreman in charge of the project or of his immediate supervisor.

3. All coated rods were placed in a drying oven for a period of 12 h prior to use. All unused coated rods, at the end of each day, were returned to the drying oven. All unused automatic welding wire was tagged and returned to the storage room. After a flux bag was opened and a

portion of its content was removed, the bag was resealed. Any unused flux remaining in the welding machine hopper was discarded.

2.2 Heat Treatment

Post-weld heat treatments were generally conducted in an enclosed furnace fired by natural gas. All surfaces were degreased prior to heating. Chromel-Alumel thermocouples were placed on outside and inside surfaces to monitor the temperatures, particularly at all extremities of the vessel. Thermocouple temperatures were plotted on a multipoint, strip-chart, potentiometric recorder and the plots reproduced for LASL records.

Salient points of the heat treatment procedures are:

1. When a part was placed in the furnace, the temperature was controlled below 600°F.
2. The rate of temperature increase did not exceed 300°F/h.
3. The hold temperature was 1100-1200°F for a time equal to 1 h/in. of thickness, with a minimum hold time of 1 h.
4. The cooling rate was less than 300°F/h until the part reached 600°F, from which point the part was air cooled.
5. Throughout the process, temperature differentials between extreme monitored points did not exceed 100°F.

3. Inspections

Inspections were made according to procedures written by the vendor and approved by LASL. Throughout most of the fabrication period, a LASL inspector stationed at the vendor's plant witnessed the fabrication and inspections. Reports were prepared for each inspection and submitted to LASL.

All pressure containment welds were radiographed to a 2-1T quality level in accordance with Section 12 of NAVSHIPS 250-1500-1 and the acceptance standards of Section 10 of NAVSHIPS 250-1500-1. All X-ray films were reviewed for acceptance by LASL personnel.

Magnetic-particle and dye-penetrant procedures closely paralleled those of MIL-STD-271B. A final magnetic-particle inspection of all welds was performed after the hydraulic and pneumatic pressure tests, following a drying operation and prior to the sand blast operation.

Dimensional inspections were performed at all check points in the fabrication procedure and also at the completion of the vessel.

4. Tests

The finished vessel was subjected to a hydraulic test, a pneumatic test, and a helium mass-spectrometer leak test.

4.1 Hydraulic

In preparation for the hydraulic test, 92 strain gages were mounted on the inner and outer surfaces and on studs. The gage sites were points at which calculated stresses were at their highest levels or where the stress calculation results were least certain. The strain measurements were recorded on a 96-channel strain gage analyzer. During the initial phase of the test, water and vessel temperatures were equalized at 92°F and then the vessel was subjected to three pressure cycles, each of which consisted of a pressure rise from 0 to 400 psig, a 5-min hold period, and a pressure drop to 0 psig. After the final cycle, strain gage readings were zeroed. Then, pressure was increased in 100-psi increments to 400 psig, followed by 50-psi increases to 800 psig, and a final rise to 825 psig. At each step the strain gages were read. The 825-psig pressure was held for 1 h.

4.2 Pneumatic

After the hydraulic test, a pneumatic test was run with air and vessel at 90°F. Following a slow pressure rise to 345 psig, the air pressure was increased in 68-psi increments to the maximum test pressure, 685 psig, Pressure was then reduced to 550 psig, and the vessel was inspected.

4.3 Helium Leak

A helium mass-spectrometer leak test was performed on all pressure containment welds. The vessel was pressurized to 500 psig with a mixture of 90% helium and 10% air. The weld areas were encapsulated, and the enclosed volume was evacuated and tested directly with a CEC Model 24-120A mass-spectrometer leak detector. Where it was not convenient to encapsulate a weld area, the area was enclosed in a plastic bag sealed with masking tape, allowed to soak for 8 h, and then checked, using a reverse sniffer technique with a CEC sniffer probe. Sensitivity was demonstrated to be $\sim 1 \times 10^{-10}$ atm cc/sec. No significant leakage was observed during the test.

5. Installation

During the lowering of the vessel into position in the reactor cell, the final nine feet of descent were relatively uncontrolled because the electric motor burned out in the bridge crane and the friction brake failed to arrest the load. Very fortunately, the initial vertical alignment was relatively good and the rate of descent sufficiently slow so that no damage was done to the vessel itself. The small Y-shaped fuel discharge tube was bent as the vessel tilted slightly before coming to rest, but the tube was straightened satisfactorily and installation was completed without further incident.

5.1 Procedure

A temporary cradle bearing the vessel was rolled into the building, and the vessel was lifted and rotated into an upright position using the 30-ton bridge crane and a portable crane from which a cable extended through a temporary hole in the roof. The vessel was temporarily positioned on I-beams spanning the top of the cell, and the final lowering onto the permanent support columns was performed with the bridge crane. Although the 37-ton weight exceeded the nominal rating of the

crane, prior structural analysis and physical testing had indicated that the crane was adequate for this one-time operation in the required bridge/trolley positions.

After being raised a few feet to permit the I-beams to be moved to one side, the vessel slowly began its descent. Until the vessel was about nine feet above its final position, no trouble was apparent, but then the brake began to slip and the vessel began to settle in a retarded but uncontrolled manner. Analysis of a 16-mm movie film which recorded the operation indicates that, although the action of the brake was erratic, it still was effective in reducing the rate of motion of the vessel. Several times the brake appears to have checked the descent momentarily, and about 1/2 sec before the vessel contacted the stand, a pause of about 1 sec is observed.

The exact cause and sequence of internal events leading to the functional failure of the bridge crane cannot be definitely established. However, the critical factor is believed to have been improper adjustment of the brake shoes which has since been corrected.

5.2 Damage

As illustrated in Fig. 4.1.2.2, the vessel is built with projecting support brackets that rest on four vertical columns, with an intervening bearing plate to accommodate thermal expansion and fabrication tolerances. Each of the four bearing plate assemblies has a central bolt fitted in oversize holes to aid in installation alignment and to limit lateral motion of the vessel. For the vessel installation, pointed guide pins were placed in the bolt holes in the tops of the columns. During the terminal phase of uncontrolled descent, the brackets on the vessel were fairly well positioned over the vertical support columns, but, alignment was not quite good enough to center the bracket holes over their respective pins. Therefore, the two brackets on the south side of the vessel came to rest on top of their pins while the two north brackets missed their pins and came to rest on the support bearing assemblies.

Hence, the south pair of brackets were held by the pins 5 in. higher than the north brackets, causing a rolling motion of the vessel just before it stopped. Meanwhile, the Y-shaped fuel discharge tube entered the recess in the concrete floor, and the final motion of the vessel caused forceful contact of the tube with the side of the concrete recess. The tube was bent as shown in Fig. C.1.

That the vessel was moving slowly when it contacted the support stand was evident from analysis of the movie film and from visual inspection of the pins, brackets, and stand. Minor deformation of the conical tip occurred on the first pin to be contacted, but there was nothing else detectable to suggest an impact force significantly greater than the static loads. On the north side, where the slightly inclined support brackets contacted the bearing plates, no damage could be found along the edges of the brackets. From these considerations, it was concluded that damage was limited to bending of the discharge tube.

5.3 Repair of Bent Tube

After the vessel had been repositioned properly, an initial effort was made to straighten the fuel discharge tube in place by heating it with an induction coil to 1100-1200°F and applying lateral force with hydraulic jacks. Although satisfactory realignment was achieved, subsequent radiography showed cracks in the former bend region.

It was then decided not to attempt further repairs in place, and the fuel discharge tube was saw-cut from the vessel at a point approximately 3/4-in. below the pipe's junction with the 24-in.-diam cap. The stub-end was beveled and then radiographed to prove that the remaining material was sound. Shop repairs made to the "Y" section of the nozzle were removing the cracks by grinding, building up with weld metal, and remachining. Bore alignment was ensured by inserting a mandrel while the steel was heated to 1100-1200°F. Radiographs showed that all regions affected by straightening or welding operations were sound.

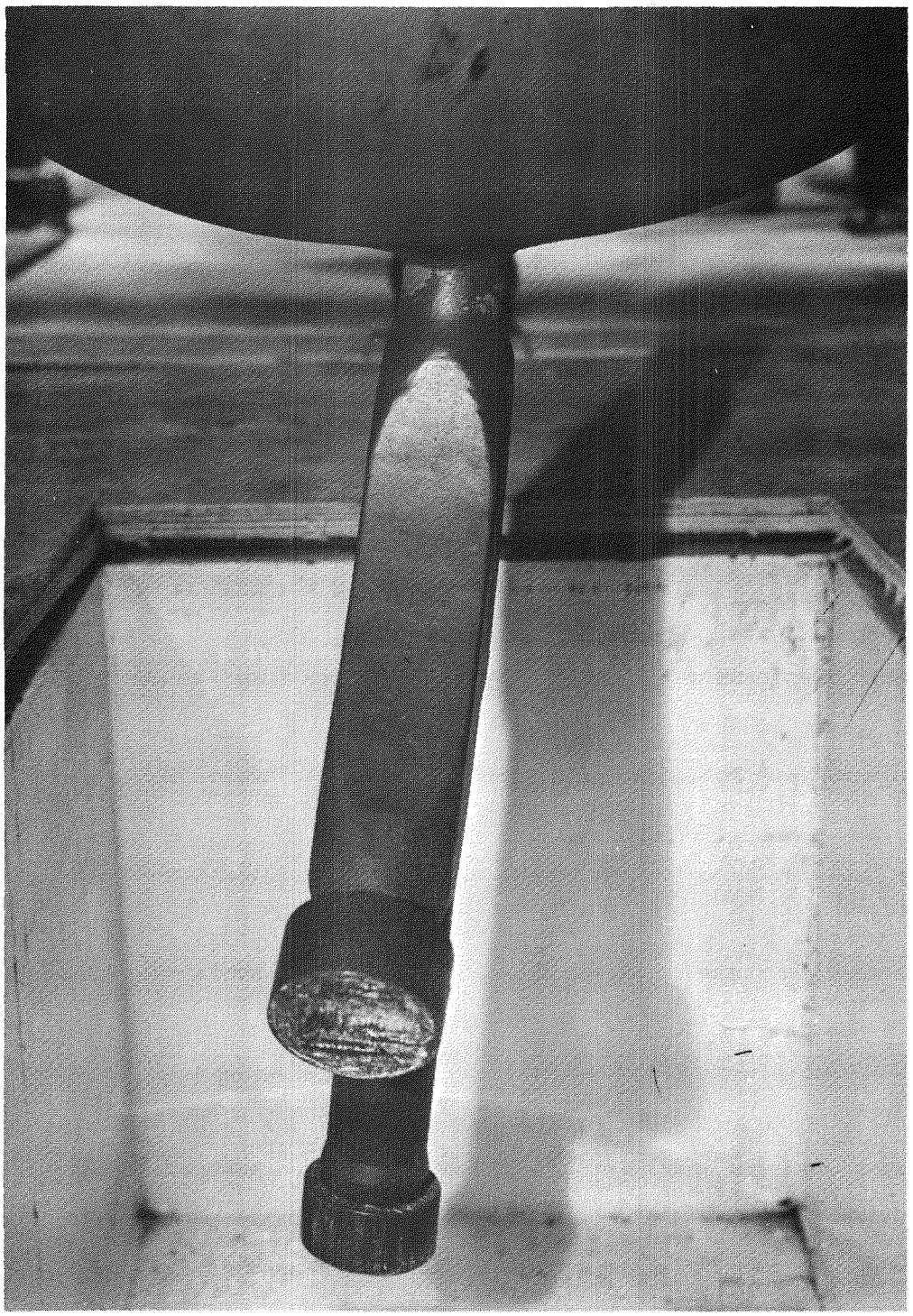

Fig. C.1 Damage to fuel discharge tube

The "Y" section was realigned in position beneath the vessel, rewelded, and radiographed. A local stress relief was performed with induction heating, using a hold time of 1 h at 1100-1200°F. Closure plugs were temporarily installed on the three openings of the "Y" section, and a hydrostatic test was performed at 825 psig for 30 min. Subsequently, the weld regions were tested with a dye penetrant and no defects were found.

6. Final Tests

Following the completion of other components of the primary cooling system, the system was pressure tested with helium at 688 psia and leak tested at 500 psia.

APPENDIX D

RESULTS FROM UHTREX CRITICAL EXPERIMENT

The graphite components of the core and immediate reflector of the Ultra High Temperature Reactor Experiment were assembled in early 1965 at the Los Alamos Scientific Laboratory for engineering tests. At the completion of the engineering tests, a temporary aluminum stand was placed on top of the assembly as a support for control rod drives and nuclear instrumentation, and the entire apparatus, which is illustrated in Figs. D.1 and D.2, was then used in a preliminary critical experiment for UHTREX.

A complete description of the facilities and a general outline of the experimental program are presented in the "Ultra High Temperature Reactor Critical Experiment (UCX) Safety Analysis Report."[1] Chapters 1 and 4 of the report are the bases for the present discussion. In the following text, the UCX Safety Analysis Report is referred to as the UCX SAR.

1. Critical Masses and Control Rod Worths

The critical mass measurements made in UCX are summarized in Table D.1. The critical masses, listed in the right-hand column of the table, were measured for the various control rod configurations cited in the first column. An explicit description of the critical loading for

[1] LA-3279, March 31, 1965.

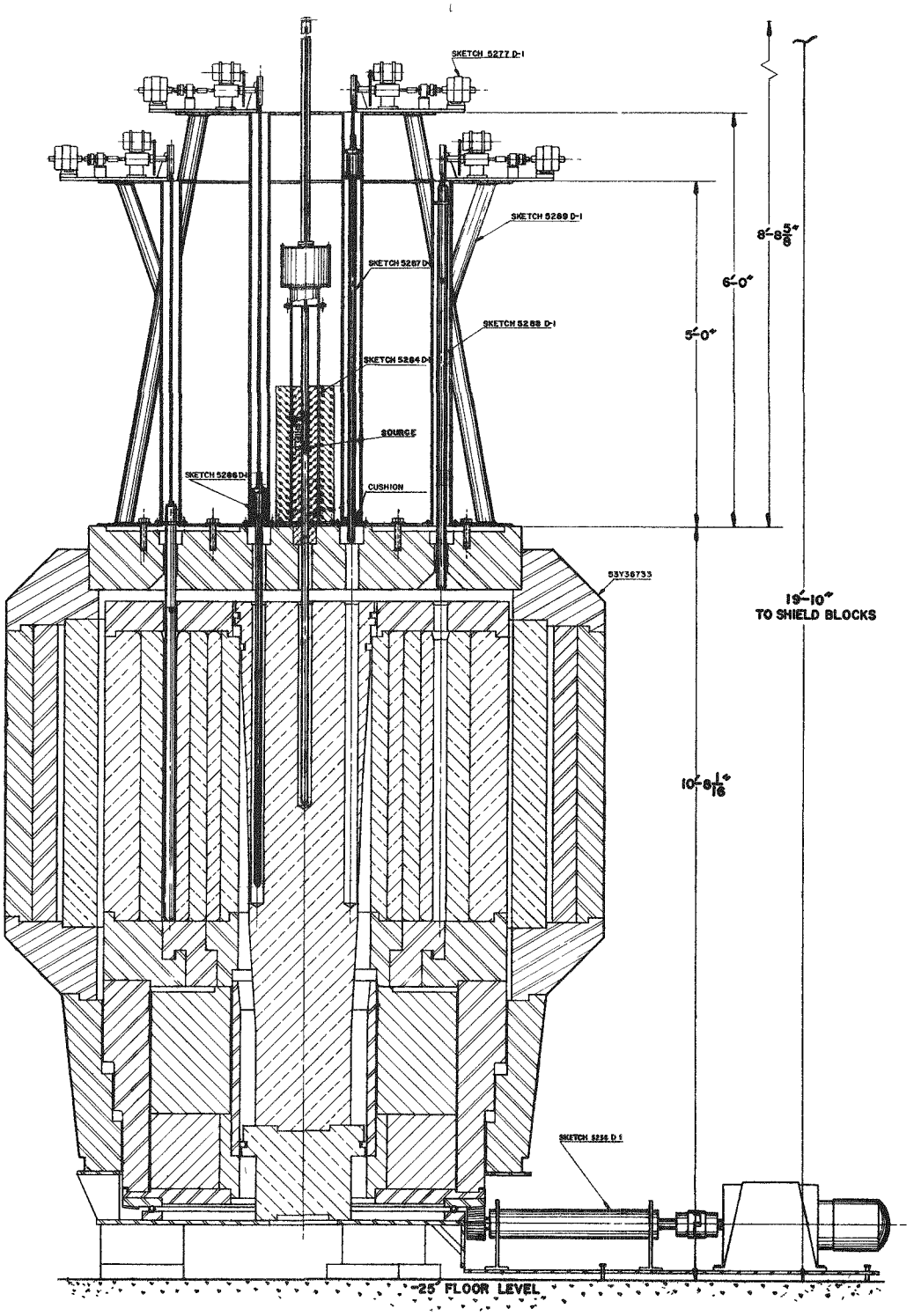

Fig. D.1 UCX assembly, vertical section

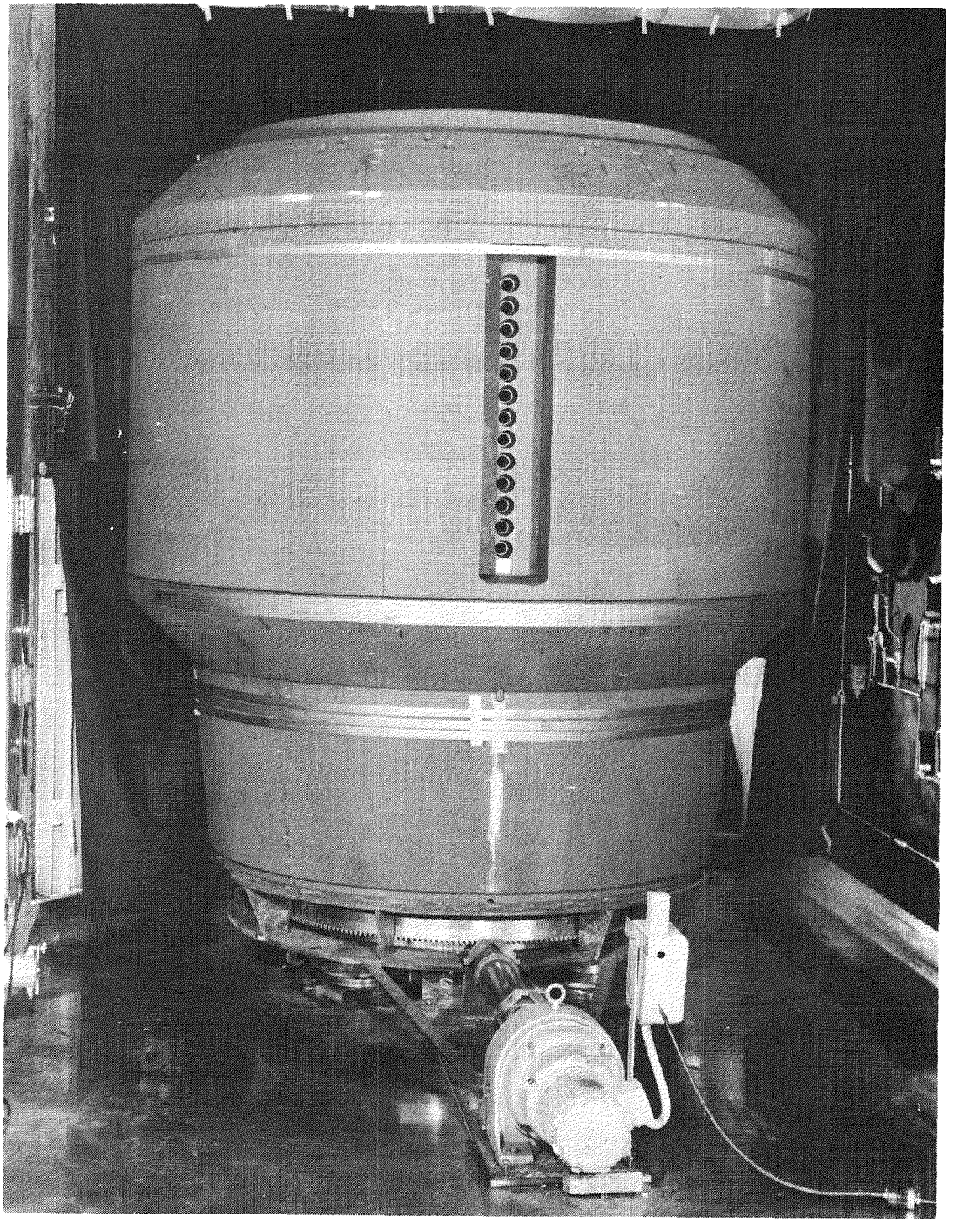

Fig. D.2 UCX core and reflector assembly, side view

TABLE D.1

CRITICAL MASS MEASUREMENTS

Control Rod Configuration	Group 1 Channels			Group 2 Channels (All Channels Not in Group 1) Loading	Critical Mass (Grams Highly Enriched Uranium)
	Loading	Vertical Channel Positions	Radial Channel Positions		
24 core rod holes filled with graphite	c	Even	1, 5, 9, 13, 17, 21	xc	6,513
All rod holes empty	x^2c	All	2, 4, 8, 12, 14, 16, 20, 24	xc	7,003
1 core rod (C1)	xc	All	5, 11, 23	x^2c	7,604
1 plug rod (P1)	x^3c	All	24	x^2c	7,813
2 core rods (C1 + C5)	x^3c	All	1, 3, 6, 9, 12, 15, 18, 21, 24	x^2c	8,219
1 plug rod + 1 core rod (P1 + C5)	x^3c	All	1, 3, 6, 7, 9, 12, 13, 15, 18, 19, 21, 24	x^2c	8,397
2 plug rods (P1 + P5)	x^2c	All	2, 5, 8, 11, 14, 17, 20, 23	x^3c	8,646
2 plug rods + 1 core rod (P1 + P5 + C1)	x^4c	All	12, 14	x^3c	9,184
4 core rods (C1 + C3 + C5 + C7)	x^3c	All	2, 5, 8, 11, 14, 17, 20, 23	x^4c	9,952
4 plug rods (P1 + P2 + P5 + P7)	x^3c	All	8, 11, 17, 20, 23	x^4c	10,206
5 plug rods (P1 + P3 + P5 + P7 + P8)	x^4c	All	All (Loading = 10,470 g)	None	10,955 (Extrapolated)
4 plug rods + 1 core rod (P1 + P3 + P5 + P7 + C1)	x^4c	All	All (Loading = 10,470 g)	None	11,103 (Extrapolated)

each case is presented in the intervening columns. Details of the rod configurations and the general loading procedures are amplified in the discussion following.

The configuration of potential rod positions in UCX is illustrated in Fig. D.3. Two rings of rods are represented, each containing eight rods. The central ring is called the "plug" ring, and rods in this ring are designated as P1, P2, etc. The outer ring is the "core" ring with positions denoted by C1, C2, etc. Actually, there are 24 rod holes provided in the UHTREX core. This redundance in rod holes accommodates insertion of the core ring at any core rotational position. (See Sec. 4.1.3 for further discussion of this feature.) For the first case in Table D.1, the critical mass was measured when the 24 core holes were filled with plain graphite rods. A comparison of the first two cases in the table, then, shows the effect on critical mass of removing the moderating graphite from the 24 rod holes. The remaining cases in the table show the increases in critical mass that are required to compensate for the insertion of various combinations of control rods. The boron loading in the rods made them essentially black to thermal neutrons.

The general procedures for loading fuel elements in the fuel channels in UCX are described in the UCX SAR. Specific channel loadings that were utilized in critical mass measurements for UCX are shown in Table D.2.

The fuel elements were loaded approximately according to the prescription, f, xf, x^2f, etc., where f is the smallest fuel element loading in grams of uranium, enriched to 93.1% ^{235}U, and x is the factor, 1.17, by which each loading is multiplied to obtain the next higher loading in the sequence. Channel loadings follow the same type of sequence. For the first entry in Table D.1, each Group 1 channel contains four elements. The total mass of uranium in these four elements is "c" grams, where $c = f + xf + x^2f + x^3f$. The fuel element at the innermost position in the channel contains f or 3.54 grams, the next innermost element contains xf or 4.16 grams, etc. When an element containing x^4f, 6.57 g, of fuel is inserted into a channel that contains

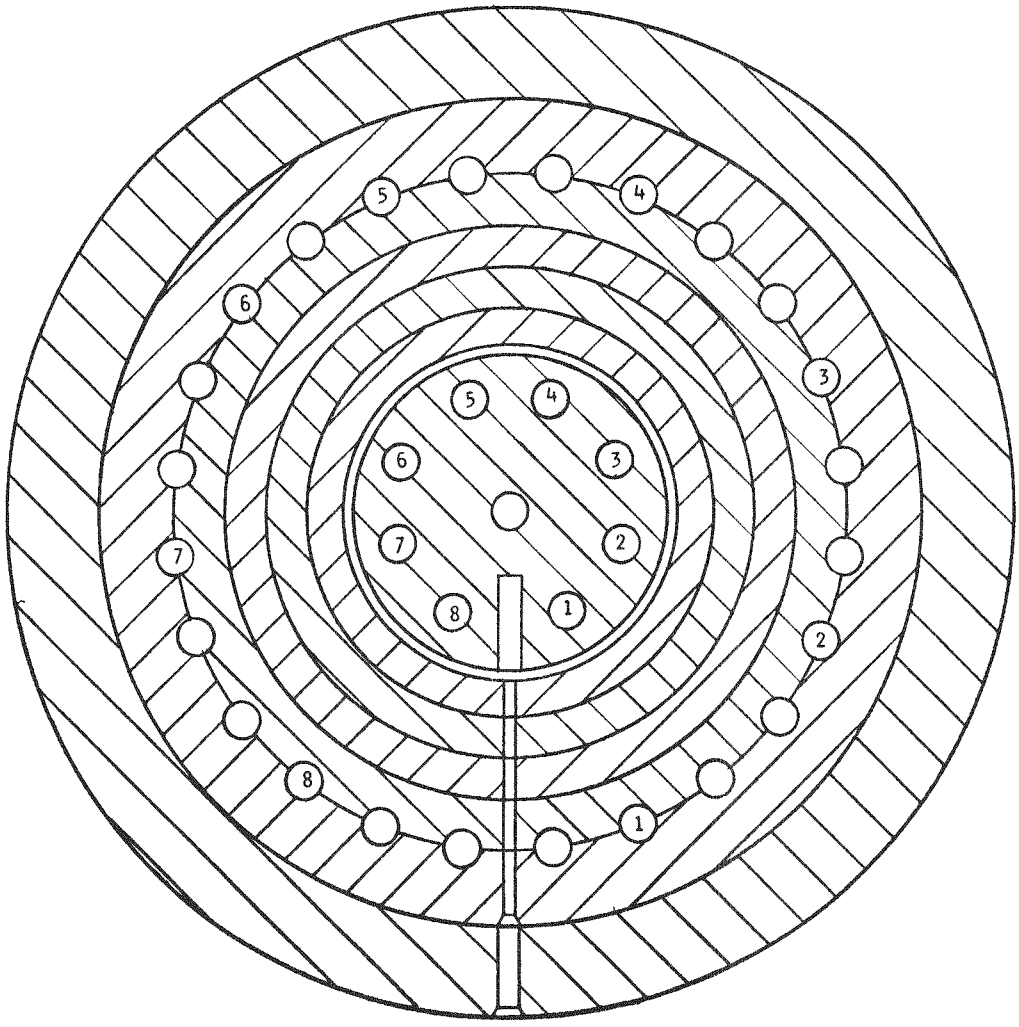

Fig. D.3 Rod positions in UCX

TABLE D.2

CHANNEL LOADINGS

Channel Loading Identification	Fuel Element Loadings in the Channel (grams, highly enriched U)
c	3.54, 4.16, 4.82, 5.67
xc	4.16, 4.82, 5.67, 6.57
x^2c	4.82, 5.67, 6.57, 7.76
x^3c	5.67, 6.57, 7.76, 9.15
x^4c	6.57, 7.76, 9.16, 10.08

$c = f + xf + x^2f + x^3f$ g of fuel, the innermost element, f, drops out of the core. The new channel loading, then, becomes $xf + x^2f + x^3f + x^4f = x(f + xf + x^2f + x^3f)$, which is xc, the second channel loading in Table D.2. Subsequent channel loadings in the table follow the same pattern.

In all the cases in Table D.1, it was necessary to use two different channel loadings to obtain the experimental critical masses. In each case the two different loadings were distributed over the 24 radial channel positions in a manner that preserved radial symmetry and minimized the local interactions between channels with different loadings.

The second case in Table D.1, in which all the rod holes were empty, is the reference UCX configuration. Results for rod configurations are compared to this case to obtain the worth of the configurations in terms of incremental mass changes. To obtain data for the conversion of mass changes to reactivity, period measurements were made at intervals. From the period measurements, the worth of mass changes, in ¢/g, was determined as the loading in the assembly was increased. Rod worths determined according to this procedure are plotted in Fig. D.4.

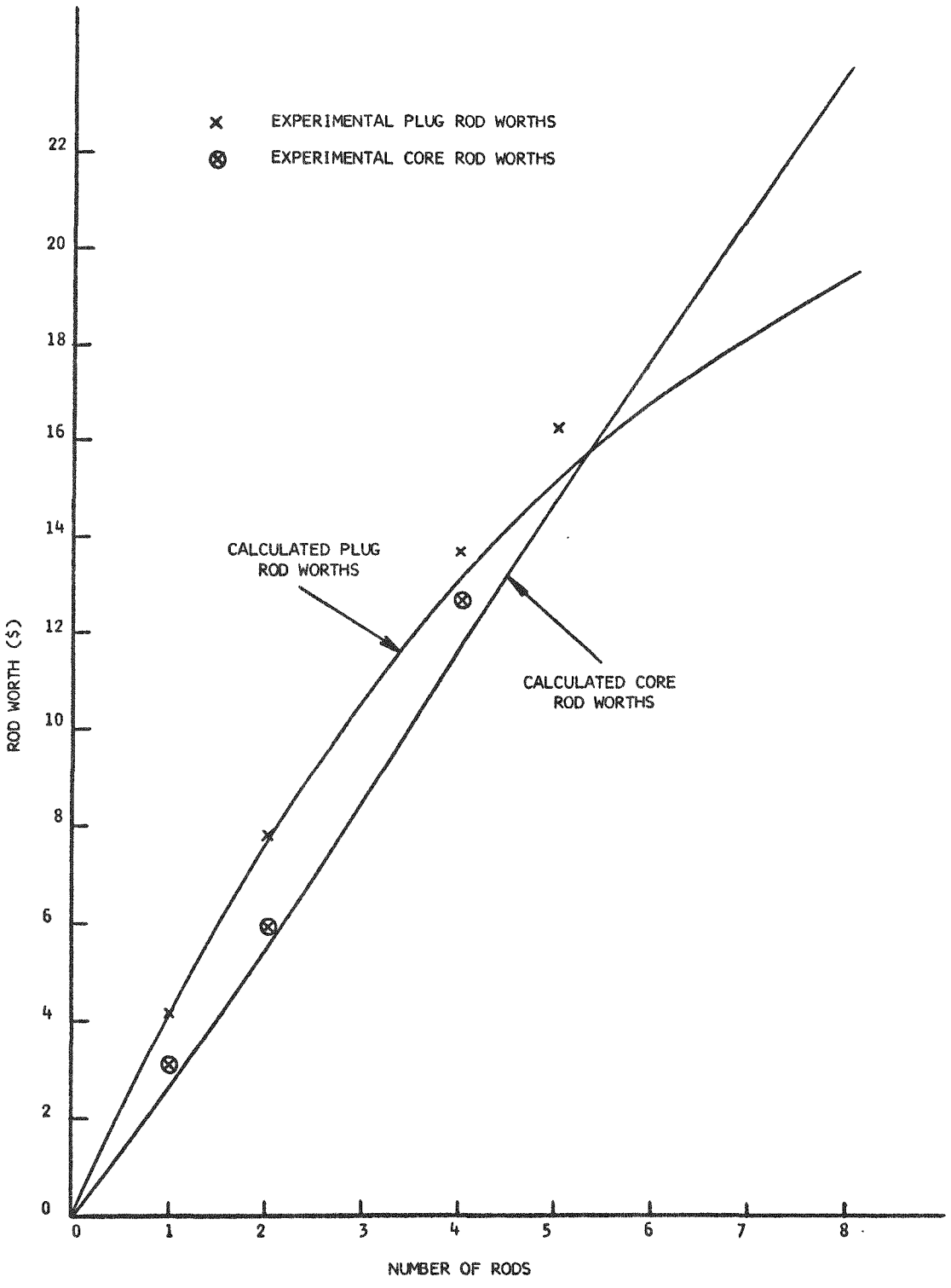

Fig. D.4 Worths of rods in UCX

2. Loading Change Reactivities

With reference to Table D.2 and the discussion above, a general channel loading of $x^n c$ grams is increased to $x^{n+1} c$ grams by inserting an element containing $x^{n+4} f$ grams of fuel. The innermost element of $x^n f$ grams of the original channel loading is displaced out of the core, and the other three original elements are advanced one position inwards. The net change in loading is $x^n(1+x^4)f$ grams. Thus, the changes in channel loadings follow a progression similar to the channel loadings; i.e., each succeeding change in mass is a factor of x larger than the preceding change.

As the loading in the assembly increases, however, the ¢/g of fuel added decreases. Since the two effects, increase in channel mass change and decrease in ¢/g, are compensating, the net result is that the reactivity associated with an average fuel element insertion remains nearly constant and independent of the total mass of fuel in the assembly. Reactivities associated with channel loading changes in UCX are summarized in Table D.3.

TABLE D.3

AVERAGE REACTIVITIES OF FUEL ELEMENT INSERTIONS

Channel Loading		Mass Change	Average	Fuel Element Insertion
Before Insertion	After Insertion	(g)	¢/g	Worth (¢)
c	xc	3.03	0.61	1.85
xc	x^2c	3.60	0.52	1.87
x^2c	x^3c	4.33	0.43	1.86
x^3c	x^4c	4.41	0.37	1.63

Thus, the average worth of a fuel element insertion is ∿1.8¢. However, the actual worth of an individual fuel element is affected by its vertical position in the core and by its proximity to inserted control rods.

3. Measurements of Void Worths

Worths of the voids in UCX were measured by filling the accessible holes with specially machined pieces of graphite. Measurements were made in the configuration that contains no control rods (critical mass = 7003 g, see Table D.1). The results are summarized in Table D.4.

TABLE D.4

WORTHS OF VOIDS IN UCX

Voids	Worth	
	Reactivity ($)	Fuel Mass (g)
24 core rod holes	2.82	490
16-in. exit coolant hole in radial reflector	0.56	97
Fuel loading slot	0.44	77
Cooling holes in 1248 fuel elements	0.70	121
Enlarged sections of 312 fuel channels	0.25	43

Although all of the accessible voids were filled in UCX to produce a maximum amount of experimental data, most of the holes listed in Table D.4 are open in UHTREX. The core rod holes must be open to receive the core rods. Helium coolant flows to the recuperator through the 16-in. hole in the reflector. The outer void at the fuel loading slot contains the fuel loader for UHTREX. Cooling holes in the elements pass the main flow of

coolant across the UHTREX core. Enlarged sections facilitate the insertion of fuel into the channels at the outer edge of the core.

4. Source Studies

Experiments were conducted to investigate the practicability of a startup on the inherent source, which is mainly the few hundred neutrons that are produced each second in C(α,n) reactions induced by alpha particles from uranium decay. With all rods inserted and extraneous neutron sources removed, the counting rate was about 1-2 counts/min, at a multiplication of 8. At a multiplication of 2500, the count rate increased to 30-50 counts/min, and at a multiplication of about 30,000, the count rate was 73-100 counts/min. The results indicate that it is possible to start up the reactor in this fashion, but the startup would be extremely slow and tedious.

To aid in estimating the neutron levels at detectors in the UHTREX geometry, UCX experiments were performed in which the source and detector were oriented on opposite sides of the core at approximately the radius of the UHTREX pressure vessel. The detector was enclosed in a steel container to approximate the shielding effect of the pressure vessel. With a source strength of 2×10^7 n/sec, the following counting rates were observed.

Counts per Minute	Multiplication
190	20
300	40
2400	500

These counting rates could be increased by a factor of five through an increase in source strength, and, if necessary, about one order of magnitude could be gained in detector sensitivity. A centrally placed source will be used for preliminary experiments in UHTREX, but the above experiments show that it will not be necessary to use a refractory central source for restarting at high temperatures.

5. Flux Measurements

In Fig. D.5, calculated thermal fluxes in the core are compared with experimental flux data. The experimental data were obtained from individual fuel elements in 13 channels that lie in one vertical plane of the core. Fluxes were plotted for four, imaginary, nested annuli. Each annulus is a vertical, hollow cylinder that is formed when a radial row of fuel elements is enclosed inside two circles about the core's vertical axis, and the circles are projected from the top to the bottom of the core. The innermost row of fuel elements lie in annulus 1. Discrepancies between calculated and experimental fluxes are attributed to asymmetries in the UCX assembly that were not taken into account in the calculations.

From the plotted data it is apparent that the vertical experimental flux shape at the innermost core annulus is not symmetric about the mid-plane of the core, while the experimental fluxes in the other three core annuli are almost symmetric. This anomaly may be due to neutron streaming through the inlet coolant plenum, which is wider at the bottom of the core than at the top because the lower part of the plug is tapered. Such streaming would cause the observed asymmetry in the innermost core annulus, which is adjacent to the central coolant plenum, but would not affect the other core annuli. The calculated flux in the innermost core annulus shows no asymmetry, which probably indicates an inaccurate computation of neutron streaming through the central coolant plenum. Another difference appears in the fluxes in the outermost core annulus where experimental fluxes are lower than computed fluxes. This discrepancy is attributed to the effect of the fuel loader slot, which was in line with the elements chosen for analysis. The agreement between experiment and calculation is good in core annuli 2 and 3, where there are no possible perturbations due to voids.

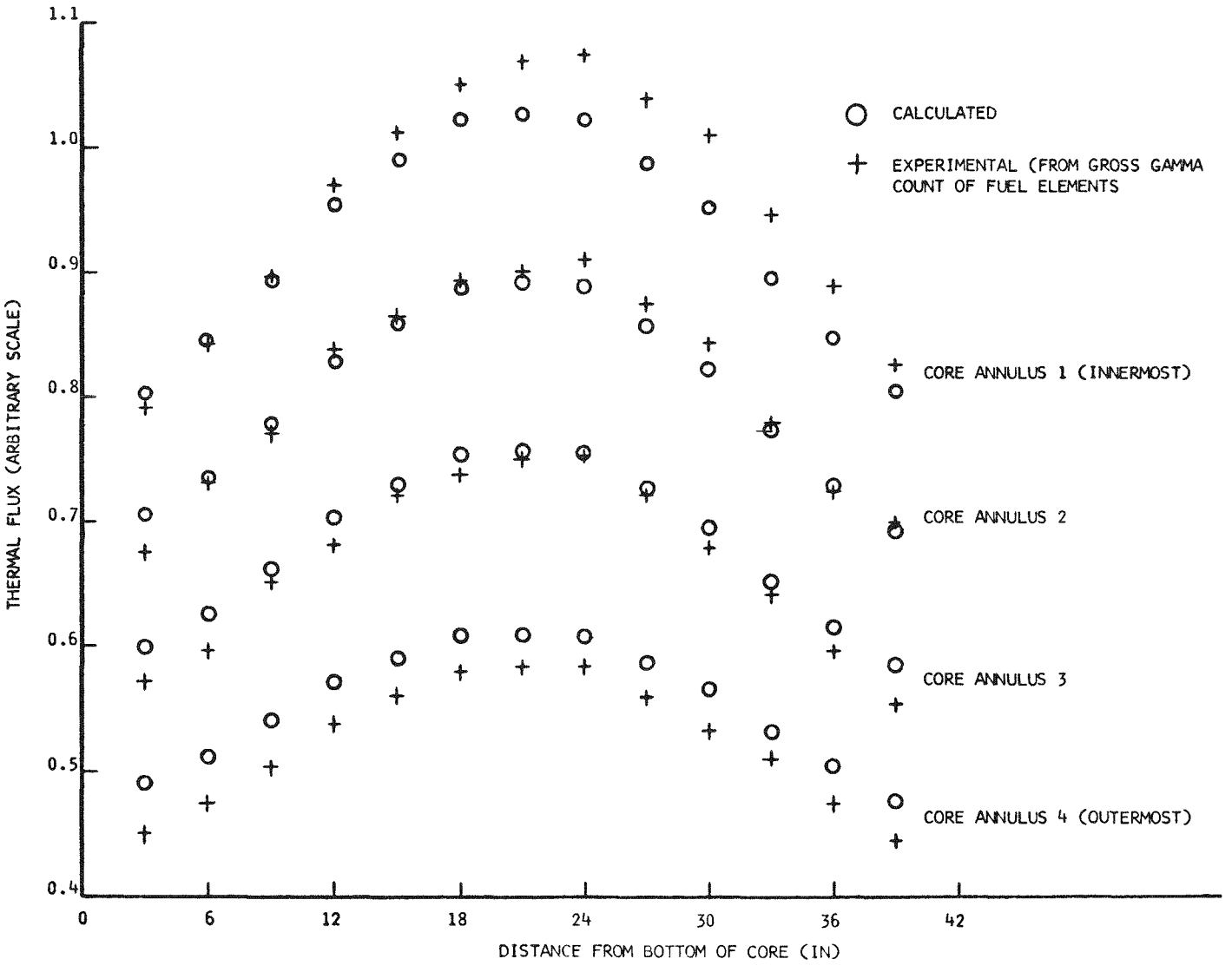

Fig. D.5 Comparison of experimental and calculated thermal flux distribution in the UCX core

APPENDIX E

DOSE RATE DERIVATION

The derivation of an expression for the dose rate at points outside a nonadsorbing finite cylinder that contains a uniformly distributed source is as follows.

Exterior on side

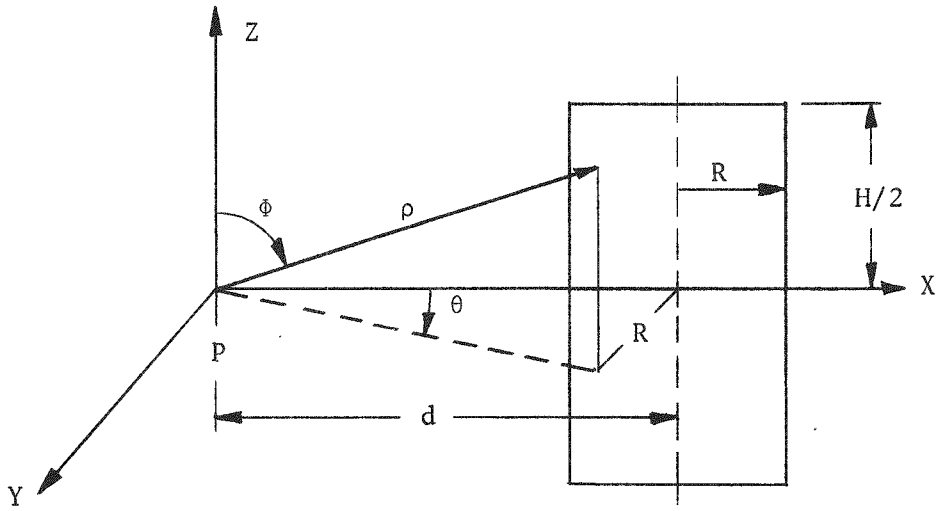

$$\Psi = \text{flux at point P} = S_V \int_V \frac{dV}{4\pi\rho^2} ,$$

where S_V is the source per unit volume.

$$dV = \rho^2 \sin\Phi \, d\rho \, d\Phi \, d\theta \qquad \therefore \quad \Psi = \frac{S_v}{4\pi} \int d\theta \int \sin\Phi \, d\Phi \int d\rho .$$

Limits of $\rho = \dfrac{d\cos\theta}{\sin\Phi} \pm \dfrac{\sqrt{R^2 - d^2\sin^2\theta}}{\sin\Phi}$.

Limits of $\Phi = \dfrac{\pi}{2}$ and $\tan^{-1}\dfrac{2(d-R)}{H}$. Multiply by 2 for whole cylinder.

Limits of $\theta = 0$ and $\sin^{-1}\dfrac{R}{d}$. Multiply by 2 for whole cylinder.

$$\Psi = 2 \times \frac{2S_v}{4\pi} \int_0^{\sin^{-1}(R/d)} d\theta \int_{\tan^{-1}\frac{2(d-R)}{H}}^{\pi/2} \sin\Phi \, d\Phi \int_{\frac{d\cos\theta}{\sin\Phi} - \frac{\sqrt{R^2-d^2\sin^2\theta}}{\sin\Phi}}^{\frac{d\cos\theta}{\sin\Phi} + \frac{\sqrt{R^2-d^2\sin^2\theta}}{\sin\Phi}} d\rho .$$

$$\Psi = \frac{2S_v}{2\pi} \int d\theta \int \sin\Phi \, d\Phi \left(\frac{1}{\sin\Phi} \times 2\sqrt{R^2 - d^2\sin^2\theta} \right),$$

$$= \frac{2S_v}{\pi} \left[\frac{\pi}{2} - \tan^{-1}\frac{2(d-R)}{H} \right] \int_0^{\sin^{-1} R/d} \sqrt{R^2 - d^2\sin^2\theta} \, d\theta,$$

$$= \frac{2S_v R}{\pi} \left[\frac{\pi}{2} - \tan^{-1}\frac{2(d-R)}{H} \right] \xi,$$

where

$$\xi = \int_0^{\sin^{-1} R/d} \sqrt{1 - \frac{d^2}{R^2}\sin^2\theta} \, d\theta$$

Now let

$$\sin \gamma = \frac{d}{R} \sin \theta \quad \therefore \quad d\theta = \frac{\cos \gamma \, d\gamma}{\frac{d}{R} \cos \theta}$$

for

$$\left.\begin{aligned} \theta &= 0, \qquad \gamma = 0 \\ \theta &= \sin^{-1} \frac{R}{d}, \qquad \gamma = \frac{\pi}{2} \end{aligned}\right\}.$$

Let

$$\frac{R}{d} = \kappa \quad \therefore \quad d\theta = \frac{\kappa \cos \gamma \, d\gamma}{\sqrt{1 - \kappa^2 \sin^2 \gamma}}$$

$$\therefore \quad \xi = \kappa \int_0^{\pi/2} \frac{\cos^2 \gamma \, d\gamma}{\sqrt{1 - \kappa^2 \sin^2 \gamma}} = \kappa \left[\frac{\overline{F\left(\kappa, \frac{\pi}{2}\right)} \times \left(\kappa^2 - 1\right) + \overline{E\left(\kappa, \frac{\pi}{2}\right)}}{\kappa^2} \right],$$

where

$F\left(\kappa, \frac{\pi}{2}\right)$ = complete elliptic integral of first kind,

$E\left(\kappa, \frac{\pi}{2}\right)$ = complete elliptic integral of second kind.

$$\therefore \quad \Psi = \frac{2 S_v R^2}{\pi d} \left[\frac{\pi}{2} - \tan^{-1} \frac{2(d-R)}{H} \right] \left[\frac{F\left(\frac{R}{d}, \frac{\pi}{2}\right) \times \left(\frac{R^2}{d^2} - 1\right) + E\left(\frac{R}{d}, \frac{\pi}{2}\right)}{\frac{R^2}{d^2}} \right].$$

$$\therefore \quad \Psi = \frac{2}{\pi} S_v d \left[\frac{\pi}{2} - \tan^{-1} \frac{2(d-R)}{H} \right] \left[F\left(\frac{R}{d}, \frac{\pi}{2}\right) \times \left(\frac{R^2}{d^2} - 1\right) + E\left(\frac{R}{d}, \frac{\pi}{2}\right) \right].$$

APPENDIX F

ANALYSIS OF PRIMARY LOOP RUPTURE ACCIDENTS

As a part of the safety analysis of the UHTREX facility, two accidents were postulated in which ruptures occur in the primary coolant loop. The course and consequences of both accidents, described in Sec. 16.3.1, were predicted from the results of the analyses presented here. Calculational methods used and the assumptions made for the analyses are described in the chronological order of the accidents. The calculations were made with the use of an IBM-7094 FORTRAN code, UHTMCA, in which all the phenomenal equations (heat balances, core combustion, blower coastdown, loop blowdown, etc.) are included. The transients are calculated by the finite difference technique using time increments beginning with 0.1 sec and increased an order of magnitude at the end of each decade.

1. Abbreviations

Symbols and abbreviations used in the analysis are as follows:

a_H = cross sectional flow area through rupture (ft^2)
a_R = cross sectional flow area out of reactor cell (ft^2)
A = surface area (ft^2)
C_i = oxygen concentration (moles O_2/total moles of gas)
C_p = specific heat (Btu/lb-°R)
C_v = flow coefficient
d = diameter (in)
D = diameter (ft)
D_e = equivalent diameter (ft)

f = friction factor

g_c = gravitational constant

h = heat transfer coefficient (Btu/ft^2-hr-°R)

H = height of air column for natural convection (ft)

ΔH_R = heat of reaction (Btu/lb mole)

k = thermal conductivity (Btu/ft^2-hr-°R/ft)

$K = \sum_i^n \frac{K_i \Delta_i}{dr_i}$ = 286 Btu/h-°R (evaluated grossly from results of relaxation calculations of the temperature distribution throughout the reactor)

L_h = length of transfer area (ft)

L_x = depth of oxidation reaction (in)

M = molecular weight (lb/lb mole)

n = number of lb moles

$\dot{N}_A$ = molal rate of transport (lb moles/hr)

P = absolute pressure (psia)

P_R = absolute pressure in reactor cell (psia)

ΔP = pressure differential (lb/ft^2)

ΔP_R = pressure differential between reactor cell and remainder of secondary containment (lb/ft^2)

q = heat rate (Btu/hr)

Q = total heat (Btu)

R = universal gas constant

t = wall thickness (ft)

T = absolute temperature (°R)

ΔT = temperature difference (°R)

ΔT_{io} = driving force for free convection (°R)

ΔT_{LM} = log mean temperature difference

v = velocity (ft/hr)

V = volume (ft^3)

$\dot{V}$ = volumetric flow (ft^3/hr)

W = weight (lb)

$\dot{w}$ = mass flow (lb/sec)

$\dot{W}$ = mass flow (lb/hr)

γ = ratio of specific heats (Cp/Cv)

ε = emissivity

θ = time (sec)

$\Delta\theta$ = time increment (hr)

μ = viscosity (lb/ft-hr)

ρ = density (lb/ft^3)

ρ_c = density of cool gas in column for natural convection

ρ_h = density of hot gas in column for natural convection

Subscripts

a = evaluated at bulk average temperature

A = pertaining to containment gas

c = pertaining to primary loop carbon surface

C = pertaining to primary loop carbon mass

cc = pertaining to building concrete

D = fission decay after shutdown

G = transfer to earth

k = transfer through reactor insulation

o = pertaining to steady state conditions prior to accident

p = pertaining to water panels

pc = transfer by convection between air and water panels

r = pertaining to oxidation reaction

s = pertaining to primary loop helium

vc = transfer by convection between air and vessels

vr = transfer by radiation between vessels and water panels

vs = pertaining to vessel surfaces

w = pertaining to water

Dimensionless Groups

N_{Gr} = Grashof number $\left(\frac{D^3 \rho^2 g_c \Delta T_{io}}{\mu^2 T_o} \right)$ (perfect gas)

N_{Gz} = Graetz number $\left(\frac{\dot{W}C_p}{kL_h}\right)$

N_{Pr} = Prandtl number $\left(\frac{\mu C_p}{k}\right)$

N_{Re} = Reynolds number $\left(\frac{D\rho_v}{\mu}\right)$

2. Initial Conditions

Each accident occurs while the reactor is operating at design conditions. The values of relevant parameters are:

Reactor power	= 3 MW for ∞ time
Primary loop flow rate	= 10,250 lb/h He
Primary loop pressure	= 495 psia
Reactor inlet temperature	= 1600°F
Reactor outlet temperature	= 2400°F
Average primary loop temperature	= 1100°F
T_A	= 100°F
T_c(core)	= 2600°F
T_{cc}	= 90°F
T_{vs}	= 492°F
T_p	= 80°F

3. Rupture of Primary Loop

Two different accidents are analyzed, both of which result in the release of the coolant from the primary loop. In the first accident, defined as the maximum credible accident, a 4-ft long, vertical crack forms in the elevator housing on the side of the reactor vessel. The second accident, purely hypothetical, arises from the complete, double-ended rupture and dislocation of the 14-in. o.d. pipe connecting the

recuperator with the reactor inlet. This accident is analyzed to evaluate the upper limit on hazards created by coolant-release accidents, regardless of their credibility. The mechanism of the failure that leads to the credible accident is discussed below. No mechanism for the failure in the hypothetical accident has been determined.

The elevator housing is a unique appurtenance to the reactor vessel, both from the standpoint of its stress pattern and its thermal environment. As discussed in Sec. 16.3.1, the operating temperatures and stress levels in the elevator housing have adequate margins under normal operating conditions, but an improbable sequence of operational errors could lead to local overheating and failure of the elevator housing. Although a crack thus initiated in the flat face of the elevator housing would probably terminate upon intersecting the adjacent loader tubes, for purposes of the analysis it is pessimistically assumed that the crack propagates to the top and bottom of the housing where the very low stress level ($\sim$ 3700 psi) is sure to arrest the rupture. For purposes of estimating the rate of air convection through the reactor core, the crack is assumed to be so wide that its flow impedance is negligible. It should be especially noted, therefore, that in the analysis of core oxidation presented in Sec. F.6, only the vertical length of the rupture influences the result, and the transverse width is not limiting.

4. Primary Loop Blowdown

When the primary loop helium vents adiabatically into the secondary containment, the immediate pressure rise there has two causes: (1) the added volume of helium and (2) the increase in the temperature due to the release of sensible heat from the helium. The rate at which the helium vents has no effect on the maximum temperature and pressure reached immediately after venting the confined gas mixture, but the rate has other important effects. It determines the length of the period between the beginning of venting and the entrance of air into the core, which

initiates oxidation of the carbon internals. Further, the rate of venting determines the magnitude of the pressure differential between the reactor room and the remainder of the secondary containment. This pressure differential reaches its maximum when the rate of molar flow from the cell (through the heat exchanger, fuel loader, water panel line, and ventilation duct penetrations) becomes equal to the rate of venting through the ruptured hole.

The venting rate from the reactor could be controlled either by the friction generated by flow through the primary loop internals or by the sonic velocity at the minimum flow cross section. For the credible accident case, the dominant frictional force develops in the 13 fuel loader ram passages, and the minimum flow cross section is the area of these passages, 22.4 in^2. For the hypothetical accident case, the frictional force is equal to one-half of the primary loop impedance, and the minimum flow cross section is the 38.0-in^2 area of the flow passage at the inlet to the central core plug. In both cases, calculations show that the venting rate is actually controlled by the frictional forces.

From the classical relation for friction loss[1], the Blasius friction factor[2], and the UHTREX fuel loader ram channel geometry, the blowdown flow for the credible case is

$$\dot{W} = 0.00361 \left[6.7876(10)^5 \, (P_s - P_r) \cdot \frac{P_f^2}{T_f^2} \right]^{0.5714} \qquad (1)$$

At the flow conditions, P_f and T_f are evaluated from the stagnation conditions according to[3]

---

[1]J. H. Perry, Chemical Engineers Handbook (McGraw-Hill, New York, 1950) p. 377.

[2]J. G. Knudsen and D. L. Katz, Fluid Dynamics and Heat Transfer (McGraw-Hill, New York, 1958) p. 171.

[3]U. A. Hall, Thermodynamics of Fluid Flow (Prentice-Hall, Inc., New York, 1951) p. 74.

$$P_f = \frac{P_s}{(1 + \frac{\gamma-1}{2} N_M^2)^{\gamma/\gamma-1}} \tag{2}$$

and

$$T_f = \frac{T_s}{(1 + \frac{\gamma-1}{2} N_M^2)} . \tag{3}$$

The blowdown flow for the hypothetical case is calculated by principles of similitude from the turbulent flow rates determined for the primary loop under a variety of normal operating conditions. It is

$$\dot{W} = \left[\frac{\rho_s}{\rho_o} \left(\frac{\mu_o}{\mu_s} \right)^{0.25} \frac{(P_s - P_R)}{\Delta P_o} \dot{W}_o \right]^{0.5714} .$$

Sonic velocities through the minimum cross sections are calculated from[4]

$$\dot{w} = \rho_f \, a_h \sqrt{\gamma g_c R T_f} \tag{5}$$

where $R = \frac{1544}{M}$.

Flow out of the reactor room is calculated from the following expression for orifice flow[5]

$$\dot{w} = C_v a_R \sqrt{2 g_c \rho_R \, \Delta P_R} \tag{6}$$

---

[4]Ibid., p. 75.

[5]J. H. Perry, op cit., p. 403.

The equilibrium condition is calculated at 0.001-sec intervals from zero time until the cell and system pressures are equal. At the end of each time interval, the system and room pressures are determined by a mass balance of the helium lost from the system and gained in the room, with a temperature correction for sensible heat gain in the room gas.

Results of the calculations for each case are plotted in Fig. F.4.1, which shows the loss of pressure in the primary loop, and Fig. F.4.2, which shows the resultant pressure peaks in the reactor cell and the overall rises in secondary containment pressure. Note that the final conditions are the same for both cases.

5. Blower Coastdown

The blower coastdown characteristic, which controls the amount of air that is forced through the core and is made available for oxidation, was determined by testing the actual blower that is installed in the loop. The results of these tests are plotted in Fig. F.5.1. Correlations of the data yielded the following relationship.

$$\dot{V} = \dot{V}_o \cdot 0.772/(0.26 + \theta). \qquad (7)$$

The test results indicate that the forced flow of air through the core is approximately 200 lb/h at the time the primary loop and reactor room pressures are essentially equal and then decreases to zero after 24 sec. Conservatism is introduced into the calculation by assuming that the gas flowing through the core is pure air after the blowdown period.

6. Oxidation of Graphite

The possible oxidation of the internal graphite components is an important consideration because of the increase in gas volumes that accompanies the chemical reaction at high temperatures and the release of

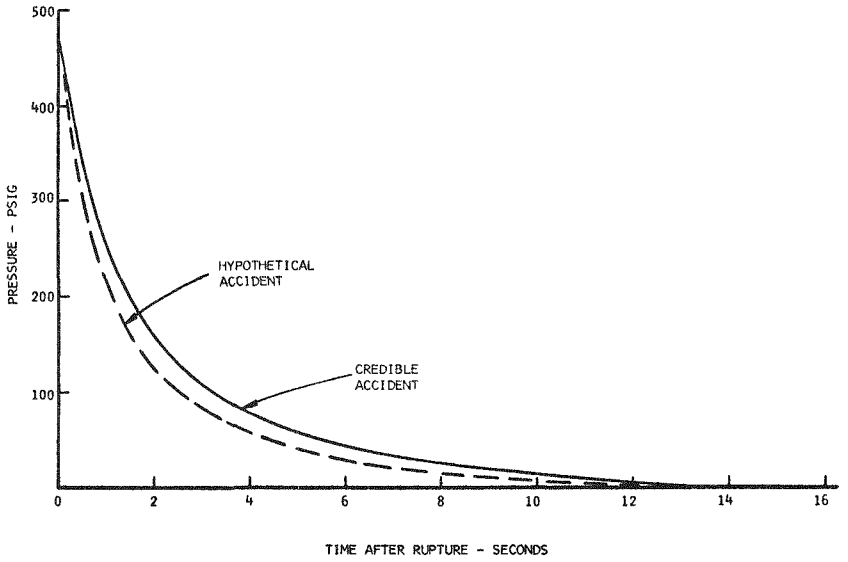

Fig. F.4.1 Primary loop blowdown following rupture

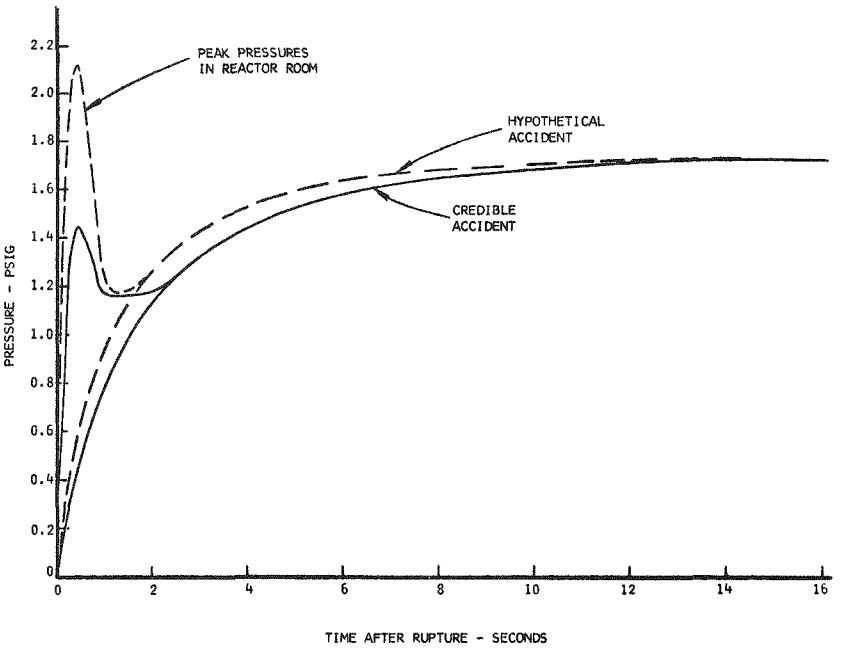

Fig. F.4.2 Containment pressure following rupture

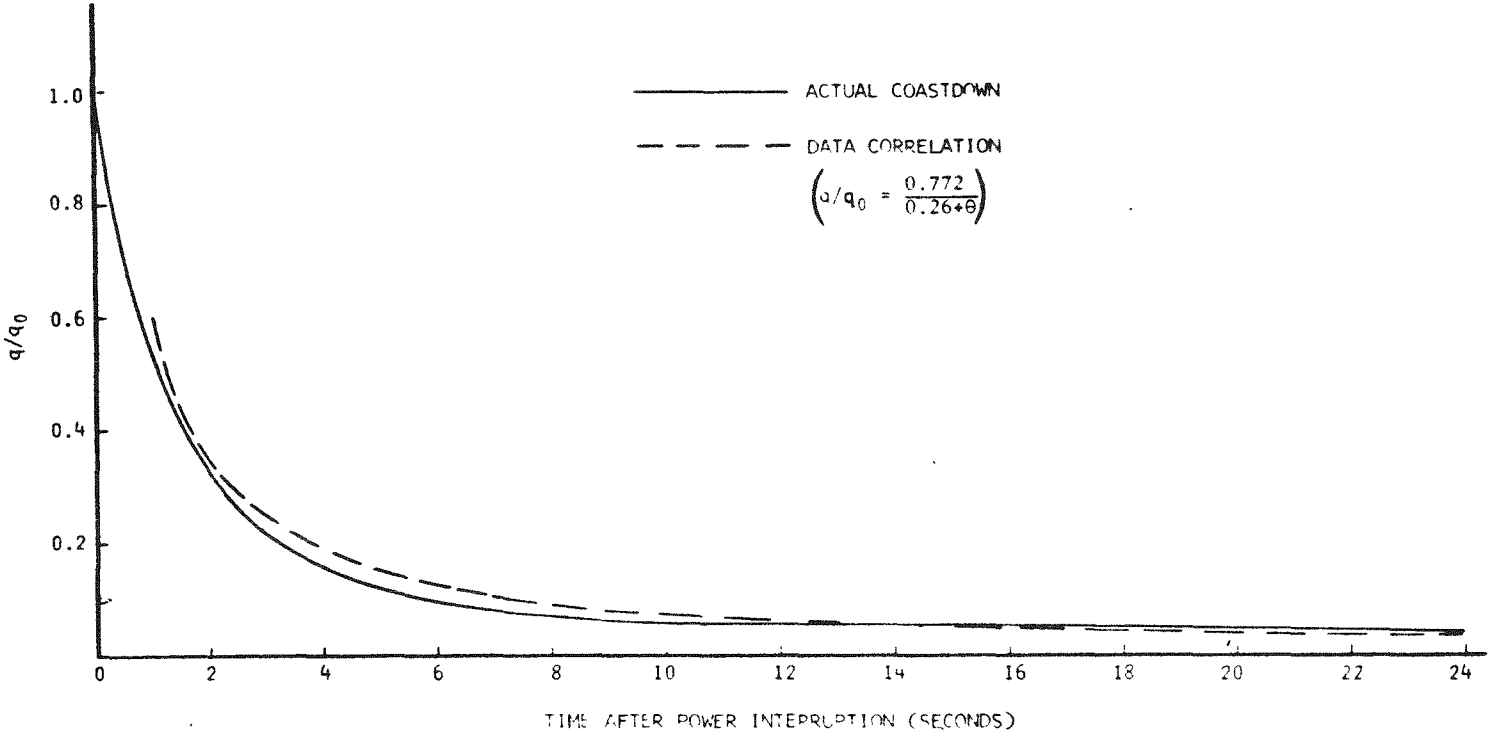

Fig. F.5.1 Coolant blower coastdown characteristic curve

fission products as fuel is consumed. Although the actual oxidation processes are too complex for exact analysis, simplifications can be made that yield conservative results. For the calculations reported here, the oxidation is assumed to proceed as follows:

1. At temperatures above 1200°F, the reaction produces only carbon monoxide: $2\ C + O_2 \rightarrow 2\ CO + 96{,}709$ Btu. Although this reaction produces less heat than the carbon dioxide reaction, $C + O_2 \rightarrow CO_2 + 170{,}179$ Btu, one more mole of gas is produced per mole of O_2. This excess gas has a greater effect on building pressure rise than the greater amount of heat produced in the CO_2 reaction. Furthermore, one mole of O_2 consumes two moles of C, in the form of fuel, liberating more fission products.

2. At temperatures between 750°F and 1200°F, 70% of the oxygen reacts to form CO_2 and 30% to form CO.[6]

3. At temperatures below 750°F, the O_2 that reacts produces only CO_2.

4. All O_2 that enters the core reacts with carbon there.

5. At temperatures above 2000°F, the oxidation reaction occurs at the graphite surface.[7] Fuel and other graphite are consumed in the same ratio as their available surface areas. Available surface areas include those of the reactor inlet passage in the core plug, the plenum around the core plug, and the walls of the fuel channels.

6. At temperatures less than 2000°F, the depth to which the reaction proceeds into the graphite is expressed by[8]

---

[6]J. B. Lewis, R. Murdoch, and P. Howtin, "The Effect of Temperature on the Manner of Oxidation of Large Blocks of Graphite in Air," CN-13/33, Chemical Engineering Division, UKAEA Research Group, Atomic Energy Research Establishment, Harwell, April, 1962.

[7]E. A. Gulbransen, K. F. Andrew, and F. A. Brassart, "Studies on the Oxidation of Graphite at Temperatures of 600°C to 1500°C and at Pressures of 2 to 76 Torr of Oxygen," WRL-SP-62-123-121-P2, March 28, 1962.

[8]L. J. Robinson, "The Effects of Diffusional Control of Oxidation of Graphite," Proceedings of the US/UK Meeting on the Compatibility Problems of Gas-cooled Reactors, Oak Ridge National Laboratory, Feb. 1964, 1, p. 414.

$$L_x = 0.01299 \left(\frac{T}{492}\right)^{0.38} K_x^{-0.5} \tag{8}$$

where T is assumed to be the average core temperature and K_x is the oxidation rate expressed in weight of carbon reacted per unit weight of carbon available for reaction. The rate at which the carbon reacts is determined by the rate at which oxygen is convected through the system. Available carbon is determined by the depth of reaction.

7. All oxygen is consumed before it reaches the reflector in the plenum around the core. This assumption is conservative because it increases the ratio of fuel consumption to bulk graphite consumption.

Changes in core temperature are calculated from heat balances described in Sec. 7.

The combustion heating rate is determined by the rate at which oxygen flows through the reactor core, i.e.,

$$q_r = \Delta H_R \cdot \dot{W} \cdot C_i/M_A \tag{9}$$

where ΔH_R = 96,709 Btu/lb mole for the $C + 1/2\ O_2 \rightarrow CO$ reaction
= 170,159 Btu/lb mole for the $C + O_2 \rightarrow CO_2$ reaction.[9]

The air flow rate during blower coastdown for both the credible and hypothetical cases is, according to Eq. (7),

$$\dot{W} = \frac{0.772}{(0.26 + \theta)} \cdot V_o \cdot \rho_a, \tag{10}$$

where V_o = 58,300 ft^3/hr.

After blower coastdown, the air flow rate through the core is controlled by natural convection caused by differences in gas densities

---

[9]H. Hunt, Physical Chemistry (Thomas Crowell Co., New York, 1947) p. 62.

in the flow systems. The flow systems for both the credible and the hypothetical cases are illustrated in Fig. F.6.1. The driving forces, which are analagous to chimney draft, arise from the differences in column pressures between the base and reference planes in each system. These pressure differentials are equal to the height of the column multiplied by the average density of the gas contained in the column.

For the credible case, the pressure differential is

$$\Delta P = H(\rho_a - \rho_c) \tag{11}$$

where H = 4 ft, the distance between the lowest and the highest loader tube penetration, assuming that an open crack extends between them. The air flows at a rate which produces a friction pressure loss equal to the pressure differential. The friction pressure loss is[10]

$$\Delta P = \frac{32 f L_n \dot{W}^2}{\pi^2 \rho g_c D_e^{\ 5}} \tag{12}$$

Since the natural convection air flow is laminar, the friction factor is expressed by[11]

$$f = \frac{16}{N_{Re}} = \frac{16\pi\mu D_e}{4W} \tag{13}$$

After substituting Eqs. (13) and (11) into Eq. (12) and rearranging, the air flow rate is calculated from

---

[10]J. H. Perry, op. cit., p. 377.

[11]J. H. Perry, op. cit., p. 382.

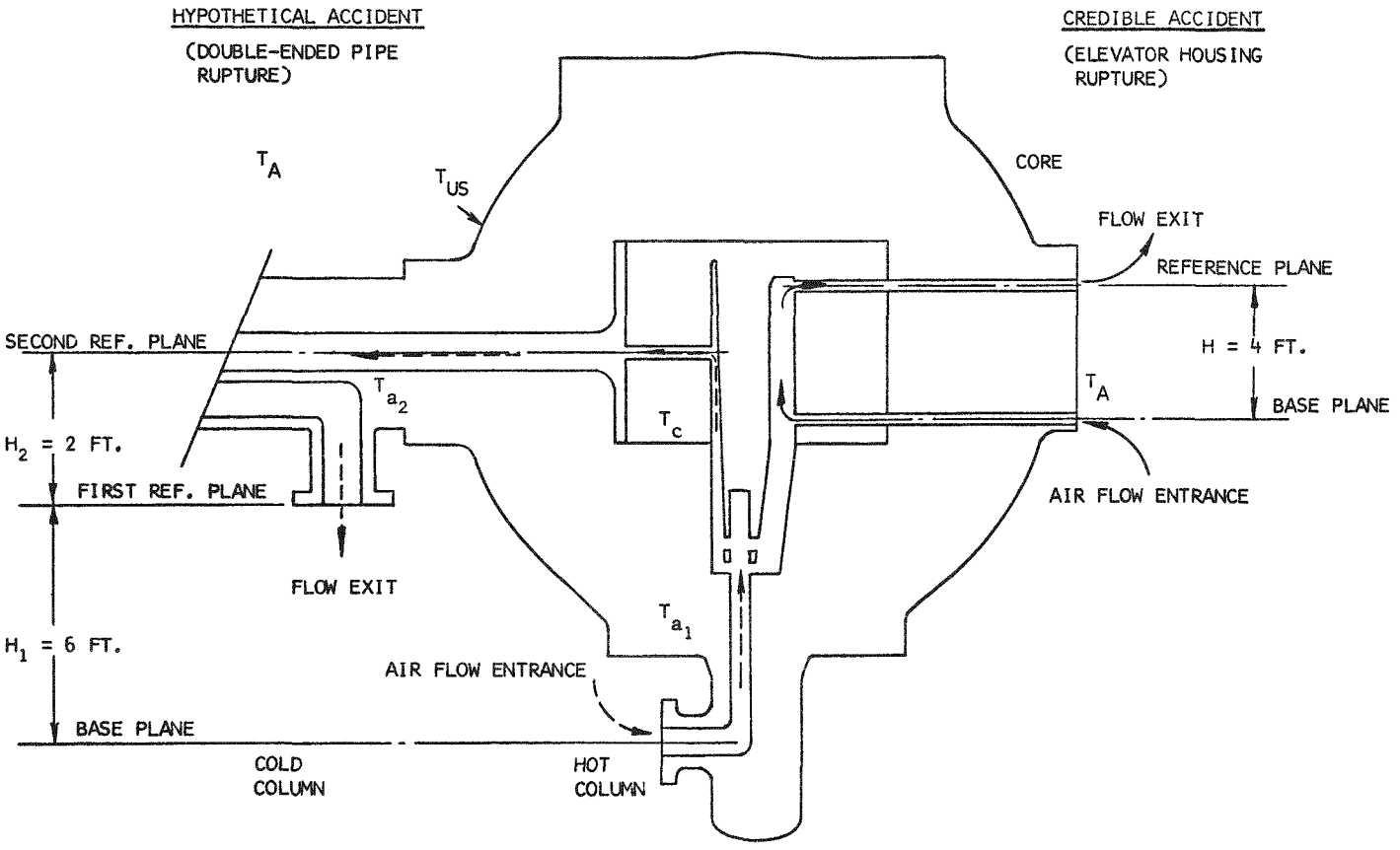

Fig. F.6.1 Natural convection flow systems through core

$$\dot{W} = \frac{\pi \rho_a g_c D_e^4 H(\rho_A - \rho_c)}{128 \mu_a L_h} \qquad (14)$$

where ρ = gas density calculated from the perfect gas law, $\rho = P_A M_A / RT$, using the relevant gas temperatures:

$T_a = \frac{T_c + T_A}{2}$ for ρ_a, T_A for ρ_A, and T_c for ρ_c.

D_e = equivalent diameter, that of a flow channel, 0.05 ft

H = column height, 4 ft

μ_a = gas viscosity, calculated from the Sutherland formula,[12]

$$\mu_a = 0.04136 \left(\frac{T_a}{492} \right)^{0.768} .$$

This flow calculation is based on a conservative assumption that the flow is impeded only inside the core flow channels. The air moves unrestricted through the opening in the elevator housing and through the loader ram tubes. In actuality, air would flow through all of the fuel channels adjacent to the fuel loader in a pattern determined by constantly changing flow impedances and temperature-induced pressure differentials. For a conservative estimate of this practically incalculable total flow, the result from Eq. (14), the flow into the bottom and out of the top channel, is multiplied by a factor of 13.

For the hypothetical case the determination of the pressure differentials in the flow system is more complex, since the air circulates through the entire primary loop. For simplicity, the flow system is divided into two zones, with two reference planes above the base plane (see left side of Fig. F.6.1). The base plane passes through the center line of the 14-in. pipe opening at the reactor inlet. The first reference plane passes along the flange face of the 14-in. recuperator nozzle. The second reference plane passes through the center line of the reactor exit

[12] J. H. Perry, op. cit., p. 370.

nozzle. These three planes divide the flow system into two zones of constant temperature. With the reference planes placed at these particular locations, the following simplifying assumptions can be made:

1. The gas in the upper zone, between the first and second reference planes, is isothermal and there is no net column pressure.

2. The gas is isothermal throughout the recuperator, heat exchanger, and piping system. All column pressures due to elevation cancel each other.

3. The hot column pressure at the base plane is $p = H_1 \rho_{a_1} + H_2 \rho_c$ where the densities, ρ_{a_1} and ρ_c, are calculated as in Eq. (14) from temperatures ρ_{a_1} and T_c. The average temperature is assumed to be $T_{a_1} = 2/3\ T_c + 1/3\ T_a$. This conservative assumption gives double effect to the core temperature, lessening the density of the gas in the hot column and increasing the net pressure differential.

4. The cold column base plane pressure is $p = H_1 \rho_A + H_1 \rho_{a_2}$. The average temperature of the gas here is assumed to be $T_{a_2} = 1/2(T_c + T_{vs})$. Because lower temperatures in the cold column cause higher base plane pressures and thus result in higher pressure differentials, conservatism dictates the use of the lowest realistic value of T_{a_2}. For compatibility with the calculational method, T_{a_2} must be defined as a function of calculated variables, i.e., some combination of T_c, T_A, and T_{vs}. The highest gas temperature is T_c, 2600°F in the initial stages of oxidation, and the lowest is T_A. A reasonable value of T_{a_2} must be near the average temperature of the graphite in the recuperator, because this is the largest mass in contact with the gas in the cold column. Furthermore, after coastdown, the temperature of the well-insulated remainder of the flow system should approach that of the recuperator graphite, which averages 1500°F at design conditions. The combination of variables that gives the nearest approximation of the average recuperator temperature is

1/2 ($T_c + T_{vs}$). At the beginning of oxidation, T_c is 2600°F, T_{vs} is 492°F, and 1/2($T_c + T_{vs}$) is 1546°F.

As the core and the vessel surfaces cool, the recuperator graphite temperature follows the assumed value of T_{a_2}.

The pressure differential for natural convection through the primary loop can then be calculated,

$$\Delta P = H_1(\rho_a - \rho_{a_1}) + H_2(\rho_{a_2} - \rho_c) \tag{15}$$

where H_1 = 6 ft and H_2 = 2 ft.

The matching flow system impedance (friction pressure loss) is calculated from the known steady state system impedance using principles of similitude. Therefore, from Eq. (12)

$$\frac{\Delta P}{\Delta P_o} = \frac{f\rho_o \dot{W}^2}{f_o \rho \dot{W}_o^{\,2}} . \tag{16}$$

The steady state, design flow is turbulent,[13] and $f_o = 0.079\ N_{Re_o}^{-0.25}$. However, the natural convection flow is laminar, and Eq. (13) defines f. Substituting these relations for friction factor in Eq. (16), the result is

$$\dot{W}_A = \frac{0.005922\rho_a \dot{W}_o^{1.75} \mu_o^{0.25} \Delta P}{\mu_a \rho_o D_e^{0.75} \Delta P_o} \tag{17}$$

---

[13] W. E. Browning, Jr., R. P. Shields, C. E. Miller, Jr., and B. F. Roberts, "Release of Fission Products on Inpile Melting or Burning of Reactor Fuels," ORNL-3483, September, 1963, pp. 24-26.

where, for steady state conditions,

ρ_o = 0.12 lb/ft^3

μ_o = 0.098 lb/ft-hr

$\dot{W}_o$ = 10,250 lb/hr

ΔP_o = 1065.6 lb/ft^2

D_e = "overall" equivalent diameter of the primary loop, 0.172 ft, estimated as follows:

1. From Eq. (17), the friction loss in each component of the primary loop is proportional to the product, $\Delta P_o \cdot D_e^{0.75}$, for both sets of flow conditions, turbulent design, and natural convection. The total friction loss in the primary loop, should be proportional to the sum of the losses in components, and, therefore,

$$\Delta P_o \cdot D_e^{0.75} = \sum_i (\Delta P_o \cdot D_e^{0.75})_i. \qquad (18)$$

2. The total ΔP_o and the ΔP_o of each component are calculated for design conditions. Values of ΔP_o for the components are 0.5 psi for the reactor, 4.0 psi for the recuperator, 1.9 psi for the heat exchanger, and 1.0 for the piping.

3. Each component D_e is estimated by substitution of the design conditions in Eq. (12), using the turbulent friction factor. The D_e values for the various components are 0.035 ft for the reactor, 0.065 ft for the recuperator, 0.083 ft for the heat exchanger, and 0.733 ft for the piping.

4. The value of the overall D_e is calculated with Eq. (18).

μ_a = average viscosity, and

ρ_a = average density, calculated as in Eq. (14) at the average temperature, $T_a = 1/2(T_{a_2} + T_{a_1})$. This average is based on the assumption that 1/2 of the gas volume in the flow system is at T_{a_2}, 1/3 is at T_c, and 1/6 at T_A.

The results of these calculations for the credible and hypothetical cases are presented in Figs. F.6.2 and F.6.3. In Fig. F.6.2 it is apparent that there is little difference between the two cases in the cooling rate of the core, although there is a great difference in the amount of oxygen reacted, as shown in Fig. F.6.3. The heat of oxidation does not drive the core temperature upward because the heat leak rate from the core is much greater than the heat generation rate.

For conservatism in the credible accident case, it is assumed that all of the oxygen, the convective flow of which is restricted, reacts with the fuel elements. Even so, only 0.8% of the fuel is consumed. For the hypothetical accident case, where more oxygen is available, the reaction proceeds according to assumptions 5 and 6 on p. F-11, and 45.5% of the fuel is consumed. Because the core cools below 2500°F during the 10^4-sec period before significant production of CO begins (see Fig. F.6.3),

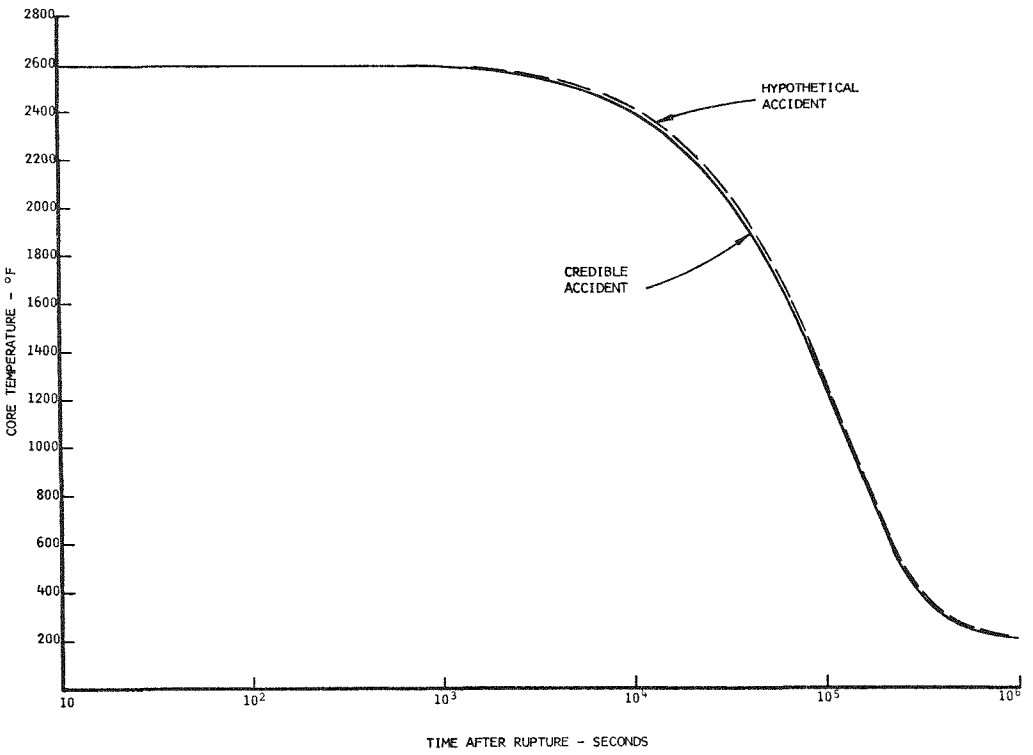

Fig. F.6.2 Cooling of UHTREX reactor core following primary loop rupture

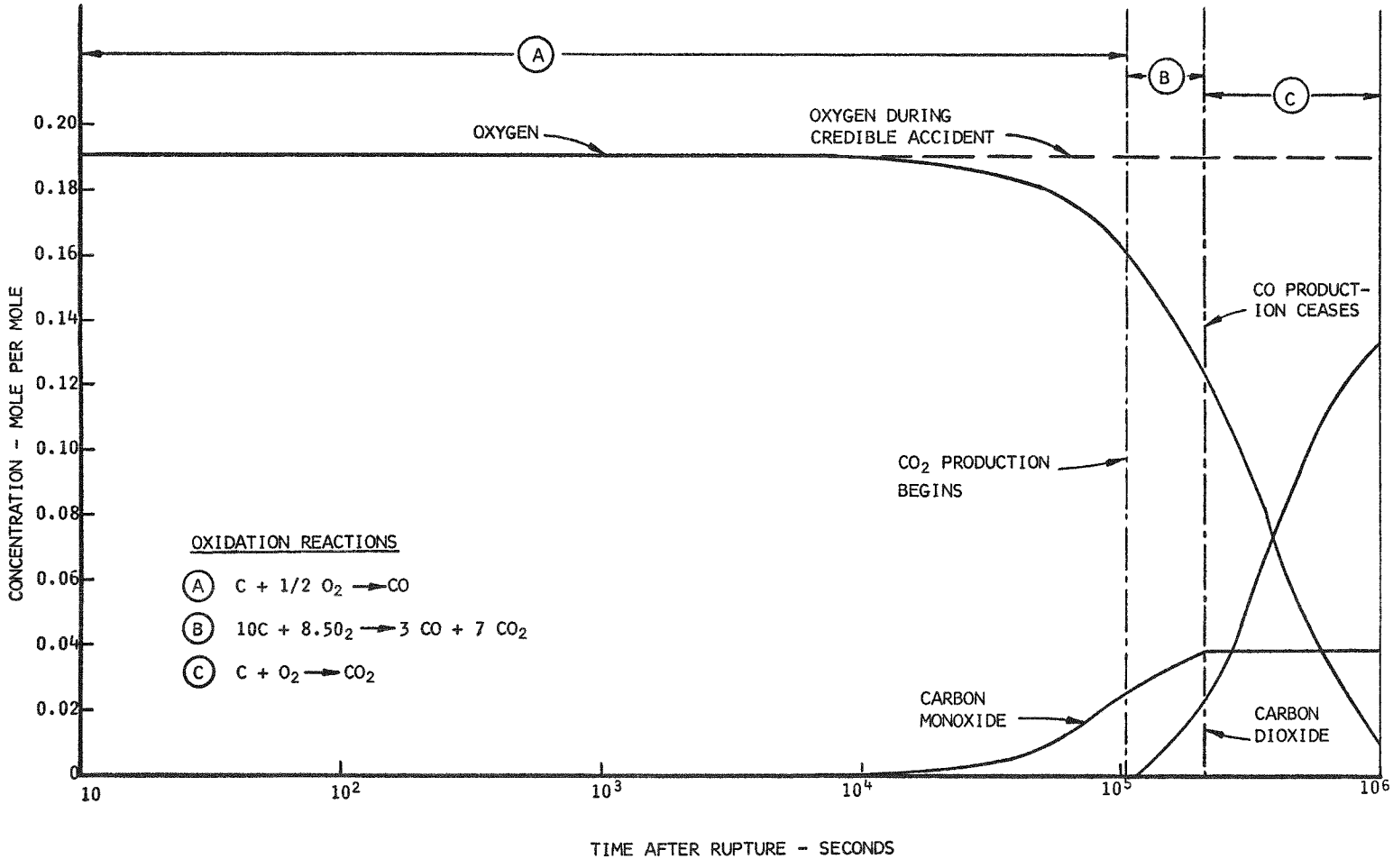

Fig. F.6.3 Change in gas concentrations following hypothetical accident

the data of Browning, et al,[13] are valid for the analysis of fission product release presented in Appendix G.

To verify the results of the combustion calculations, an experiment was performed in the UHTREX corrosion test loop[14] at the design temperature and full helium flow rate. The actual geometry and materials of a typical fuel channel were used in a full-scale model. Loop depressurization and the introduction of air by a coasting blower were simulated. All conditions associated with the combustion phase of the experiment were reproduced with great conservatism. Decay heat was modeled accurately with electric resistance heaters, but the heat leak from the well insulated experimental rig was less than the corresponding leak from a reactor fuel channel during the rupture accident. Air was introduced into the test channel over a much longer period and at a rate 1.5 times that of the maximum rate predicted for the blower coastdown period of the postulated accidents. Convective flow of air through the test channel was more than 3 times the convective flow calculated for the hypothetical accident case. Despite all of these conditions that would tend to increase the oxidation rate, the temperature in the test channel declined and runaway oxidation did not occur. Gas samples revealed that only 1/2 of the oxygen that entered the test channel reacted with the carbon there.

The low consumption of oxygen observed experimentally, along with the high temperatures and low flow rates, are characteristic of gas film control of the oxidation rate. Catalytic effects as a result of impurities in the graphite matrix, often observed in low temperature oxidation of carbon, are ineffective under conditions of gas film control, where the rate of oxidation is limited by the transfer of oxygen from the main gas stream to the surface of the graphite. If, as it is assumed here, all oxygen that reaches the carbon surface is consumed, no increase in the rate can be realized through catalysis.

---

[14] P. G. Salgado, "Graphite Corrosion Studies for the Ultra High Temperature Reactor Experiment," LAMS-3063, April, 1964.

7. Heat Balances

The change in the temperature of the gas inside the containment depends on an equilibrium between two heat transfer rates: (1) the rate at which heat is transferred to the gas from components at higher enthalpy levels (primary loop components, reactor core, etc.) and (2) the rate at which heat is transferred from the gas to components at lower enthalpy levels (building concrete and surrounding earth and air). Individual rate equations that describe heat transfer to and from all components are combined in the calculations to determine the equilibrium gas temperature.

Since the flow of air is laminar (N_{Re} <2100), the heat transfer coefficient (h) for heat removal from the core during blower coastdown is expressed by[15]

$$\frac{hD_e}{k} = 1.75\ (N_{Gz})^{1/3}, \tag{19}$$

where

$$N_{Gz} = \frac{\dot{W}C_p}{kL_h}.$$

When the flow decreases, on blower coastdown, to the point at which the temperature difference is the driving force for flow, the heat transfer coefficient is defined by[16]

$$\frac{hD_e}{k} = 0.4(N_{Gr} \cdot N_{Pr})^{0.25}, \tag{20}$$

---

[15]W. H. McAdams, Heat Transmission, 3rd Ed. (McGraw-Hill, New York, 1954) p. 232.

[16]Ibid., p. 176.

where

$$N_{Gr} = \frac{D_e^3 \rho^2 g_c \Delta T_{io}}{\mu^2 T_o} .$$

The rate of heat removal from the internal carbon surfaces by convection to the flowing gas is then

$$q_c = hA_c \Delta T_{LM}. \tag{21}$$

The rate of heat removal from the internal carbon parts by conduction to the surface of the vessel is

$$q_k = K(T_c - T_{vs}), \tag{22}$$

where

$$K = \sum_i^n \frac{k_i A_i}{dr_i} .$$

The decay heat is[17]

$$q_D = 312 \left[\frac{3282.4}{(10+\theta)^{0.2}} - \frac{2855.7}{(2x10^7+\theta)^{0.2}} \right]. \tag{23}$$

The increase in carbon temperature is then

---

[17] B. T. Price, C. C. Horton, and K. T. Spinney, Radiation Shielding (Pergamon Press, New York, 1957) p. 65, Fig. 2.10.2.

$$\Delta T_c = \frac{(q_r + q_D - q_c - q_k)\Delta\theta}{W_c C_{p_c}} . \tag{24}$$

The rate of heat transfer from the vessel surfaces to the water panels by radiation is[18]

$$q_{vr} = \frac{0.173\ A_{vs}\left[\left(\frac{T_{vs}}{100}\right)^4 - \left(\frac{T_p}{100}\right)^4\right]}{\frac{1}{\varepsilon_{vs}} + \frac{A_{vs}}{A_p}\left(\frac{1}{\varepsilon_p} - 1\right)} . \tag{25}$$

The rate of heat removal from the reactor and recuperator by natural convection is

$$q_{vc} = hA(T_{vs} - T_A), \tag{26}$$

where

$$h = 0.5\left(\frac{\Delta T}{D}\right)^{0.25} \text{ for the reactor (sphere),}$$

$$h = 0.5\left(\frac{\Delta T}{d}\right)^{0.25} \text{ for the recuperator (cylinder).}[19]$$

The rate of heat exchange between the air and the water panels by natural convection is

$$q_{pc} = hA(T_A - T_p), \tag{27}$$

---

[18]D. Q. Kern, Process Heat Transfer (McGraw-Hill, New York, 1950).

[19]Ibid., p. 215.

where

$$h = 0.27(\Delta T)^{0.25} \text{ for the walls,}$$
$$h = 0.38(\Delta T)^{0.25} \text{ for the floor.}^{19}$$

The rate of heat transfer between the air and concrete by natural convection is

$$q_{cc} = hA(T_A - T_{cc}), \tag{28}$$

where

$$h = 0.27(\Delta T)^{0.25} \text{ for the walls,}$$
$$h = 0.38(\Delta T)^{0.25} \text{ for the floor,}$$
$$h = 0.2(\Delta T)^{0.25} \text{ for the ceiling.}$$

The rate of heat removal from the air to the cooling coils in the ventilation system is

$$q_{ac} = \dot{V}_A \rho_A C_{pA} (T_A - T_{ao}) \tag{29}$$

T_{ao} is calculated by equating (29) to

$$q_{ac} = hA\Delta T_{LM} \tag{30}$$

where h = 912 Btu/hr-ft^2-°R and A = 18.3 ft^2, and $\dot{V}_A$ = 482,000 ft^3/hr.

The rate of heat transfer through the concrete walls is

$$q_G = \frac{k\ A_{cc}}{t} (T_{cc} - T_{wo}). \tag{31}$$

From the preceding rate equations, the increase in air temperature is then

$$\Delta T_A = \frac{(q_c + q_{vc} - q_{pc} - q_{cc} - q_{ac})\Delta\theta}{W_A C_{PA}} . \qquad (32)$$

The increase in concrete temperature is

$$\Delta T_{cc} = \frac{(q_{cc} - q_G)\Delta\theta}{W_{cc} C_{pcc}} . \qquad (33)$$

8. Pressure Change

At any time after the rupture, the number of moles of contained gas is the sum of (1) the initial volume of air, (2) the helium discharged, and (3) the excess volume of carbon monoxide produced over oxygen consumed, minus the accumulated leakage from the structure.

The secondary containment structure leakage rate for the pressure change calculations is assumed to be 7.5% per day at 5 psig, 2.5 times the rate measured prior to equipment installation. During the tests made to measure this leakage, data were obtained at pressures of 1.5, 2.0, 3.0, and 5.0 psig for use in direct interpolation of the actual leakage at any pressure between 0 and 5 psig. The results from these data indicate that the leakage is through laminar flow paths, and is, therefore, directly proportional to the pressure difference between the contained gas and the atmosphere. The factor of 2.5 in assumed leakage over the measured leakage was chosen to compensate for the general deterioration of the building during operation and the increased number of building penetrations made during equipment installation.

The internal pressure change is calculated from the perfect gas law as

$$P_A = \frac{RT_A\Sigma_n}{V_A} , \qquad (34)$$

where Σ_n is the summation of the number of moles of originally contained air, helium from the primary loop, and additional gas produced as carbon monoxide from carbon oxidation. The value for V_A is 149,700 ft^3.

9. Values of Parameters Used in Calculations

a_h = 0.2638 ft^2 (double pipe rupture)
= 0.1556 ft^2 (elevator housing rupture)

a_R = 30 ft^2

A_{cc} = 18,412 ft^2 (total)
= 12,440 ft^2 (walls)
= 3,326 ft^2 (floor)
= 2,646 ft^2 (ceiling)

A_p = 2,840 ft^2 (total)
= 2,160 ft^2 (walls)
= 680 ft^2 (floor)

A_{vs} = 890 ft^2
= 615 ft^2 (reactor)
= 175 ft^2 (recuperator)

C_{p_a} = 0.24 Btu/lb-°R (air)

C_{p_c} = 0.12 Btu/lb-°R (carbon)

$C_{p_{cc}}$ = 0.15 Btu/lb-°R (concrete)

C_{p_s} = 1.25 Btu/lb-°R (helium)

C_{p_w} = 1.0 Btu/lb-°R (water)

C_v = 0.6 (orifice)

V_A = 149,700 ft^2

V_R = 13,780 ft^3

V_s = 632 ft^3

$\dot{V}_A$ = 582,000 ft^3/hr

$\dot{V}_o$ = 58,300 ft^3/hr

W_A = 8,100 lb (air)

W_c = 30,000 lb (carbon)

W_{cc} = 9,760,000 lb (concrete)

W_s = 76.0 lb (helium)

γ = 1.667 (helium)

ε_{cc} = 0.6 (concrete)

ε_p = 0.7 (panels)

ε_{vs} = 0.7 (vessels)

APPENDIX G

CALCULATION OF RADIATION DOSES RESULTING FROM DOUBLE-ENDED PIPE RUPTURE ACCIDENT

1. Bases

The dose calculations are based on the following assumptions.

1. The reactor has operated continuously for 1 yr at 3 MW.

2. The release of radioactive species to the secondary containment atmosphere is complete in 100 sec. This assumption, made to simplify the dose calculations, is conservative because the only significant release is associated with fuel burning, which takes place over a period of about 1 day.

3. The composition of the released activity is based on the calculations described in Appendix H and on the results of ORNL experiments reported by Browning, et al.[1] The assumed composition is:

   a. 100% of the equilibrium activity circulated in the coolant.

   b. The activity released when 46% of the fuel is burned during the course of the accident. Of the activity in all of the fuel particles at the start of the accident, the following percentages are released to the secondary containment:

      (1) 100% of the noble gases

      (2) 27% of all isotopes of I and Br

      (3) 41% of all isotopes of Ru and Mo

---

[1]W. E. Browning, Jr., R. P. Shields, C. E. Miller, Jr., and B. F. Roberts, "Release of Fission Products on Inpile Melting or Burning of Reactor Fuels," ORNL-3483, September, 1963, pp. 22-26.

(4) 35% of all isotopes of Te

(5) 37% of all isotopes of Cs and Rb

(6) 6% of all isotopes of Ce, Y, La, Pr, Nd, Pm, Sm, and Gd

(7) 1% of all isotopes of Ba, Sr, Zr, Nb, Rh, and Pd

(8) 100% of all other isotopes (Ag, As, Cd, Ge, In, Sb, Se, Sn, Tc).

The above release values, with the exception of (1) and (8), are derived from Browning's UC_2-graphite fuel burning experiment in which 58% of the fuel was burned. Since the calculations discussed in Sec. F.6 indicate that less than 2% of the core oxidation occurs at temperatures higher than 2550°F, Browning's data were used without extrapolation to higher temperatures. Where possible, by comparing chemical and physical properties of the elements, their oxides, and their carbides, Browning's data were extended to other elements. Uncertain cases were placed in group (8) and given the most conservative release factor possible (100%). It is probable, for example, that Sn, Sb, and Ge would be released in no greater quantities than Te, and that In would be retained as effectively as Ce, but these elements were, nevertheless, placed in group (8). Likewise, Y is probably retained as efficiently as Sr or Zr, but it was grouped with Ce and the rare earths for conservatism.

4. Of all the activity, except the noble gases, released to the containment building atmosphere, 90% is removed from the airborne source by deposition on the interior building surfaces or on the high-efficiency particulate and activated charcoal filters in the ventilation system. The secondary containment atmosphere is constantly recirculated through the system at 9700 ft^3/min, a rate sufficient to process the entire volume every 15 min. The deposition assumption is conservative because (1) the filters are rated as 99.9% effective in retention of airborne particulate material and iodine vapor, (2) conditions in the containment

building do not favor formation of organic iodides,[2] and (3) coconut base charcoal filters are reasonably effective in retaining even the organic iodides at the relatively dry conditions anticipated in the containment structure (R.H. < 50% at 70°F).[3] For the purpose of computing the direct gamma dose from the activity inside the containment building, the activity removed by these processes is considered to contribute to the direct dose.

5. The leak rate from the secondary containment structure is 2.9% per day for the first 1000 sec following the accident, and 1.29% per day for the next 10^6 sec. These values are calculated for secondary containment pressures of 1.75 psig and 0.75 psig (see Fig. 16.3.1.2) and an assumed building leak rate of 7.5% per day at 5 psig. This assumed leak rate is 2.5 times the actual leak rate, which was experimentally determined at both 2 and 5 psig, from the secondary containment of the UHTREX facility. Extrapolations of the calculated leak rate values from the actual test pressures to the reference pressures are made with a relationship derived from the Hagan-Poiseuille equation.[4] Test results that confirm the validity of the extrapolation method are presented in Table G.1.

TABLE G.1

Test Date	Avg. Pressure (psig)	Leak Rate (%/day)	Leak Rate (%/day), Extrapolated 2.0 psig	5.0 psig
6/17/64	2.39	1.53	1.30	2.97
9/3/64	4.77	2.88	1.31	3.00
12/16/64	1.95	1.27	1.30	2.98

[2]G. W. Keilholtz, "Filters, Solvents, and Air Cleaning Systems as Engineered Safeguards in Nuclear Installations," ORNL-NSIC-13, October, 1966, pp. 90-92.

[3]Ibid, pp. 79-80.

[4]W. B. Cottrell and A. W. Savolainen, "U. S. Reactor Containment Technology," ORNL-NSIC-5, August, 1965, p. 10.33.

6. The leakage from the secondary containment structure constitutes a continuous, ground-level, point source.

7. The accident occurs during a strong inversion; wind velocity is 1 m/sec in the direction of the nearest uncontrolled land; and these conditions persist for 30 days. Because of diurnal variations in atmospheric stability, wind velocity, and wind direction, a factor of conservatism of at least 10 is introduced by this assumption.

Doses are calculated for 2 h and for 30 days. Whole-body gamma doses due to direct radiation from the secondary containment building are calculated as a function of distance from the structure, and doses due to the radioactive effluent are calculated at the boundary of the nearest uncontrolled land, 2000 m from the reactor building.

2. Dilution Factor

The atmospheric dilution factor at the 2000-m dose point is obtained from the relationship

$$K = \frac{2}{\pi C^2 \bar{u} x^{2-n}},$$

where

K = the dilution factor, $\frac{\text{Curies/m}^3}{\text{leak source Curies/sec}}$

x = downwind distance, m

$\bar{u}$ = mean wind velocity, m/sec

C^2 = 0.028, product of vertical and horizontal diffusion coefficients, m^n

n = 0.5, a dimensionless parameter related to atmospheric stability.

This is a special case, for a continuous point source at ground level, of Sutton's[5] equation for concentrations of airborne contaminants. For the defined assumptions, $K = 2.5 \times 10^{-4}$ sec/m^3.

3. Inhalation Dose

The Lockheed fission product inventory code (FPIC)[6] was modified to compute inhalation doses to 9 critical organs and the whole-body immersion dose. The code uses a library containing yield, half-life, energy, and biological-dose factor data for 200 nuclides.

The integrated dose, in rem, to the jth critical organ from the ith nuclide for the primary coolant loss accident is obtained from the relationship

$$D_{i,j} = \frac{0.01\ PKF_i RLH_{ij}}{G} \left\{ \frac{A_i}{\lambda_{1i}+L} \left[e^{-(\lambda_{1i}+L)t_1} - e^{-(\lambda_{1i}+L)t_2} \right] + \frac{B_i}{\lambda_{2i}+L} \left[e^{-(\lambda_{2i}+L)t_1} - e^{-(\lambda_{2i}+L)t_2} \right] \right\}$$

where

$$A_i = - \frac{(Y_{2i}-Y_{1i})\lambda_{2i}(1-e^{-\lambda_{1i}T})}{\lambda_{1i}-\lambda_{2i}} ,$$

$$B_i = \left[\left(\frac{Y_{2i}-Y_{1i}}{\lambda_{1i}-\lambda_{2i}} \right) \lambda_{1i} + Y_{1i} \right] \left(1 - e^{-\lambda_{2i}T} \right) ,$$

---

[5]"Meteorology and Atomic Energy," AECU-3066, July, 1955.

[6]K. O. Koebberling, W. E. Krull, and J. H. Wilson, "Lockheed Fission Product Inventory Code," ER-6906, May, 1964.

where

P = operating power, fissions/sec; 9.87×10^{16}

G = 3.7×10^{10}, d/sec-Curie

K = dilution factor, sec/m^3; 2.5×10^{-4}

F_i = fraction of the ith nuclide inventory available for leakage from the secondary containment structure

R = breathing rate, m^3/sec;

= 3.47×10^{-4} for the 2-h dose

= 2.31×10^{-4} for the 30-day dose

L = containment structure leak rate, sec^{-1}

= 3.36×10^{-7} for first 1000 sec

= 1.5×10^{-7} for next 10^6 sec

H_{ij} = dose factor, for the ith nuclide, jth critical organ, $\frac{\text{rem}}{\text{Curie inhaled}}$

λ_{1i} = disintegration constant for the parent of the ith nuclide, sec^{-1}

λ_{2i} = disintegration constant for the ith nuclide, sec^{-1}

Y_{1i} = yield of the parent of the ith nuclide, percent

Y_{2i} = yield of the ith nuclide

t_1 and t_2 = beginning and ending times for the dose integration, sec

T = reactor operating time, sec.

4. Immersion Dose

From WASH-740,[7] the dose rate in a semi-infinite cloud, corrected for air density at 7000-ft elevation, is

[7]"Theoretical Possibilities and Consequences of Major Accidents in Large Nuclear Power Plants," WASH-740, March, 1957.

$$d = 0.296\ CE_{\gamma}\ \text{rad/sec},$$

where

C = concentration of activity at the dose point, Curies/m^3,

E_{γ} = effective gamma-ray energy.

The relationship used to compute the integrated dose, in rads, for the ith nuclide is

$$D_i = \frac{0.296 \times 0.01\ PKF_i LE_i}{G} \left\{ \frac{A_i}{\lambda_{1i}+L} \left[e^{-(\lambda_{1i}+L)t_1} - e^{-(\lambda_{1i}+L)t_2} \right] + \frac{B_i}{\lambda_{2i}+L} \left[e^{-(\lambda_{2i}+L)t_1} - e^{-(\lambda_{2i}+L)t_2} \right] \right\}$$

where E_i is the total gamma-ray energy per disintegration for the ith nuclide, Mev.

The results of the foregoing calculations are tabulated in Table 16.3.1.1.

5. Direct Gamma Radiation from the Secondary Containment

The Lockheed fission product inventory code (FPIC)[6] was modified to compute the direct dose due to gamma emitting fission products inside the secondary containment. Attenuation coefficients and energy absorption coefficients for concrete are from ANL-5800.[8] The gamma ray activity is subdivided into seven energy groups and attenuation and absorption coefficients are taken for the top of each group.

---

[8]"Reactor Physics Constants," 2nd Edition, ANL-5800, July, 1963.

The integrated dose, in rads, from the ith nuclide, for the jth energy group, at a distance, d meters, from the secondary containment structure, from time, t, to t_2, is calculated as follows:

$$D_{i,j} = 0.985 \times 10^{-14} P_o F_i E_{i,j} B_j \mu_{aj} e^{-(\mu_j d + \mu_{cj} d_c)} \left\{ \frac{A_i}{\lambda_{1i} + L(t)} \left[e^{-[\lambda_1 + L(t)]t_1} - e^{-[\lambda_1 + L(t)]t_2} \right] + \frac{B_i}{\lambda_{2i} + L(t)} \left[e^{-[\lambda_{2i} + L(t)]t_1} - e^{-[\lambda_{2i} + L(t)]t_2} \right] \right\}$$

where

P_o = operating power, 9.87×10^{16} fission/sec

F_i = fraction of the ith nuclide inventory which is released to the secondary containment atmosphere

$E_{i,j}$ = gamma-ray energy, MeV, in the jth energy group, for the ith nuclide

B_j = buildup factor, for air and concrete, $1 + 0.8 k_j \mu_j d + k_{cj} \mu_{cj} dc$

μ_{aj} = energy absorption coefficient in air

μ_j = total attenuation coefficient in air, m^{-1}

μ_{cj} = total attenuation coefficient in concrete, cm^{-1}

d_c = concrete thickness, 45.72 cm

k_j = linear absorption constant in air, $\frac{\mu_j - \mu_{aj}}{\mu_{aj}}$

k_{cj} = linear absorption constant in concrete

$L(t)$ = containment structure leak rate, sec^{-1}

= $3.36 \times 10^{-7} sec^{-1}$ for $100 < t \leq 1000$ sec

= $1.50 \times 10^{-7} sec^{-1}$ for 1000 sec $< t \leq 10^6$ sec

= 0 for 10^6 sec $< t <$ 30 days.

The results of this computation, for 2 h and 30 days, are plotted in Fig. 16.3.1.3.

APPENDIX H

EQUILIBRIUM FISSION PRODUCT INVENTORY IN UHTREX

Equilibrium fission product inventories in UHTREX were calculated according to the following general assumptions:

1. The UHTREX primary coolant receives fission products from the fuel elements at a rate, R.

2. Fission products leave the coolant by deposition on the solid surfaces in contact with the flowing coolant and by removal in a side stream gas cleanup system. Flow rate in the gas cleanup system is 102 lb/h and holdup times are 1810 h for Xe, 44 h for Kr, and infinite for other fission products.

3. Iodine is considered to deposit with an effective half-life of 15 sec.

4. Other volatile and solid fission products deposit with an effective half-life of 5 sec. The average transit time around the UHTREX primary system is 2.7 sec.

5. The reactor is operating at 3 MW with the pyrolytic carbon-coated fuel described in Sec. 4.1.4.

6. A core temperature of 2600°F (1430°C) is defined for the purpose of estimating fission product release rates.

1. Estimation of the Release Rates of Fission Products from Fuel Particles

Release rates of fission products from the fuel are based on data taken from the following sources:

1. Fission product noble gas release rates for loose triplex particles were determined from experimental data measured in the Oak Ridge Research Reactor in-pile loop and reported by Reagan.[1] Temperatures of the irradiations were 2050°F and 2500°F. Burnups were as high as 19.8% of heavy metal. Estimates of the temperature dependance of the release rates are based on Kr^{88} data. Release rate dependance of Kr and Xe isotopes on half-life is shown in Fig. H.1.

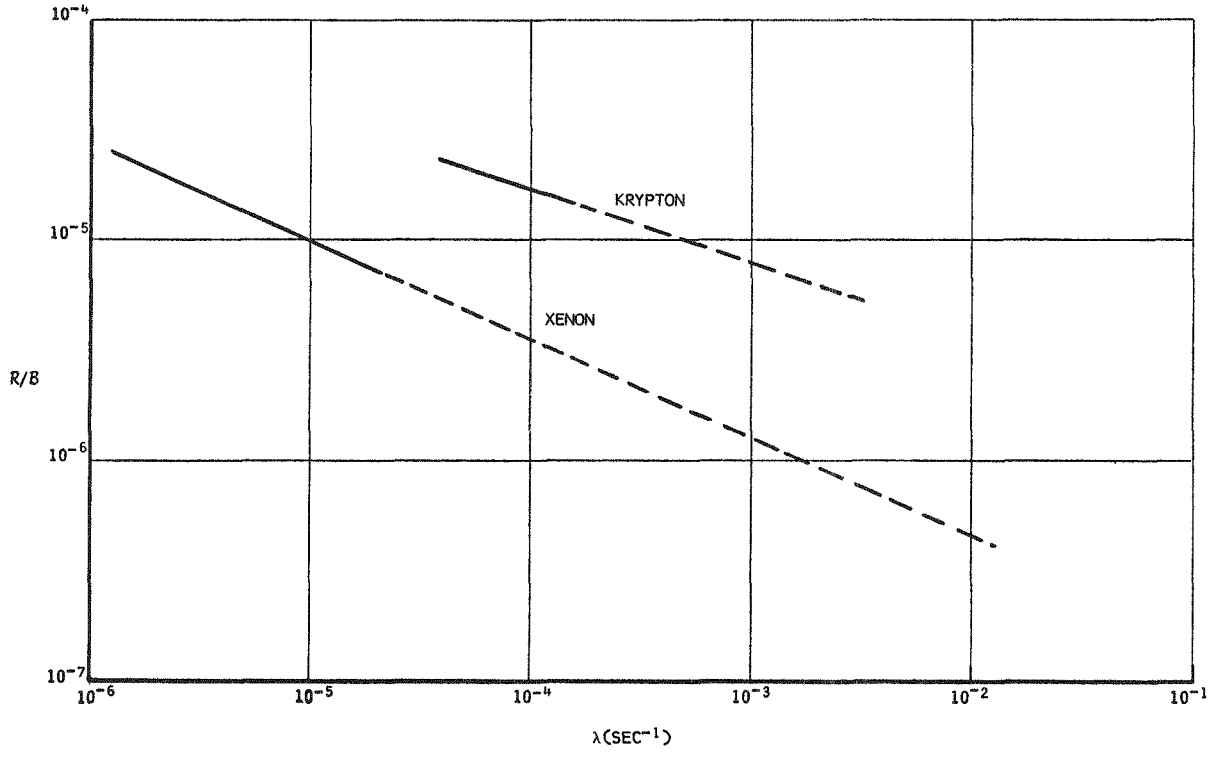

Fig. H.1 Noble gas release from triplex coated fuel at 2600°F

[1]P. E. Reagan, J. C. Morgan, O. Sisman, "Fission-Gas Release from Pyrolytic-Carbon Coated Fuel Particles during Irradiation at 2000 to 2500°F", Nucl. Sci. Eng., 23, 215-223 (1965).

2. Release characteristics of Cs, Ce, Ba, and Sr isotopes from triplex particles were estimated with data from post-irradiation examinations done at 2370°F. The data are reported by Goedel.[2] Release constants at 2370°F are shown in Table H.1 with estimated values for 2600°F. For the purpose of extrapolation, the release constant, R, is assumed to have the temperature dependance:

$$R = R_o \exp\left[-\frac{E_a}{2}\left(\frac{10^3}{T} - \frac{10^3}{T_o}\right)\right] \qquad (1)$$

where E_a is the activation energy in kcal/gmole and R_o is the release constant at T_o, °K. Values of E_a are taken from GA-6830.[3]

TABLE H.1

RELEASE CONSTANTS FOR TRIPLEX PARTICLES

Temperature (°F)	Release Constants (hr^{-1})			
	Cs^{137}	Ce^{144}	Ba^{140}	Sr^{89}
2370	6.4×10^{-5}	2.9×10^{-3}	4.4×10^{-3}	5.2×10^{-3}
2600	3.8×10^{-4}	1.5×10^{-2}	2.4×10^{-2}	1.4×10^{-2}

[2]Goeddel, W. V., C. S. Luby, and L. R. Zumwalt, "Coated-Particles Fuel Research at General Atomic from April 30, 1965, through October 30, 1965", GAMD-6817, November 8, 1965, Part I, p. 25.

[3]"Public Service Company of Colorado 330-MW(E) High-Temperature Gas-Cooled Reactor Research and Development Program, Quarterly Progress Report for Period Ending September 30, 1965", GA-6830, December 31, 1965, p. 75.

The ratio of the release rate of a fission product to its birth rate, R/B, is calculated from the release constants according to the expression

$$(R/B)_i = \frac{R_i}{R_i + \lambda_i} \qquad (2)$$

which is derived in Sec. H.2. The release rates for the isotopes of Se, Br, Sn, Sb, Te, I, and Sm are considered to be the same as rates for the isotopes of Xe. Therefore, release rates for these fission products are read from Fig. H.1. The value of R/B for the non-volatile isotopes of Y, Zr, Nb, Mo, Tc, Ru, Rh, La, Pr, Nd, and Pm is considered to be 10^{-5}. Estimates of R/B based on release from loose particles tend to be conservative for fuel in which the coated particles are held in a graphite matrix, because the graphite matrix is known to delay the release.[4]

Table H.2 lists, for the 107 significant fission product isotopes, the equilibrium gas-borne activity and equilibrium fuel activity attained after UHTREX has operated at 3 MW for one year using triplex coated particle fuel. The total inventory for any isotope is the sum of the gas-borne activity and the fuel activity, both listed in the table, and the activity deposited in the coolant loop or gas cleanup system.

2. Analysis of In-pile and Post-irradiation Fission Product Release Experiments

The following analysis relates fission product release rates calculated from measurements made after irradiation to the rates that prevail in the reactor core.

[4]Ibid. pp. 79-106.

TABLE H.2

FISSION PRODUCT INVENTORY: TRIPLEX PARTICLE FUEL

Isotope	Gas-borne Activity		Fuel Activity	
	Curies	Fraction of Total Inventory	Curies	Fraction of Total Inventory
Se 83	0.00004	0.72×10^{-8}	5,560	1
Br 83	0.0013	0.10×10^{-6}	12,700	1
Kr 83m	0.0055	0.43×10^{-6}	12,700	1
Se 84	0.00053	0.19×10^{-7}	27,800	1
Br 84	0.0064	0.23×10^{-6}	27,800	1
Br 85	0.0151	0.40×10^{-6}	38,200	1
Kr 85m	0.0096	0.25×10^{-6}	38,200	1
Kr 85	0.0026	0.49×10^{-5}	532*	1
Br 87	0.0209	0.30×10^{-6}	68,500	1
Kr 87	0.0384	0.56×10^{-6}	68,500	1
Kr 88	0.0329	0.35×10^{-6}	94,000	1
Rb 88	0.0043	0.46×10^{-7}	94,000	1
Kr 89	0.286	0.25×10^{-5}	116,000	1
Rb 89	0.0078	0.64×10^{-7}	122,000	1
Sr 89	0.128	0.10×10^{-5}	6,081	0.05
Rb 90	0.0427	0.29×10^{-6}	14,900	1
Sr 90	0.00082	0.20×10^{-6}	0	0
Y 90	0.00003	0.8×10^{-8}	3,760	1
Rb 91	0.0082	0.57×10^{-7}	144,000	1
Sr 91	3.24	0.22×10^{-4}	121,000	0.84
Y 91	0.000005	0.35×10^{-10}	144,000	1
Sr 92	4.05	0.26×10^{-4}	147,000	0.95
Y 92	0.0021	0.13×10^{-7}	155,000	1

*for 1 year operation at 3 MWth

TABLE H.2 (continued)

Isotope	Gas-borne Activity		Fuel Activity	
	Curies	Fraction of Total Inventory	Curies	Fraction of Total Inventory
Sr 93	4.43	0.27×10^{-4}	162,000	1
Y 93	0.00077	0.48×10^{-8}	162,000	1
Sr 94	3.41	0.23×10^{-4}	147,000	1
Y 94	0.0236	0.16×10^{-6}	147,000	1
Y 95	0.0121	0.75×10^{-7}	162,000	1
Zr 95	0.000001	0.6×10^{-11}	162,000	1
Nb 95	0.000003	0.2×10^{-10}	162,000	1
Zr 97	0.00012	0.76×10^{-9}	157,000	1
Nb 97	0.0017	0.11×10^{-7}	157,000	1
Nb 99	0.0500	0.32×10^{-6}	155,000	1
Mo 99	0.00003	0.2×10^{-9}	155,000	1
Tc 99m	0.00036	0.23×10^{-6}	1,550	1
Nb 101	0.0940	0.74×10^{-6}	127,000	1
Mo 101	0.0074	0.58×10^{-7}	127,000	1
Tc 101	0.0073	0.58×10^{-7}	127,000	1
Mo 102	0.0074	0.70×10^{-7}	106,000	1
Tc 102	0.527	0.50×10^{-5}	106,000	1
Tc 103	0.0475	0.65×10^{-6}	73,500	1
Ru 103	0.000001	0.14×10^{-10}	73,500	1
Rh 103	0.0011	0.15×10^{-7}	73,500	1
Tc 105	0.0018	0.79×10^{-7}	22,800	1
Ru 105	0.00007	0.31×10^{-8}	22,800	1
Rh 105	0.000008	0.35×10^{-9}	22,800	1
Ru 106	0.00000001	0.10×10^{-11}	9,650	1
Ru 107	0.0010	0.20×10^{-6}	5,080	1
Rh 107	0.00017	0.33×10^{-7}	5,080	1

TABLE H.2 (continued)

Isotope	Gas-borne Activity		Fuel Activity	
	Curies	Fraction of Total Inventory	Curies	Fraction of Total Inventory
Sb 127	0.0000002	0.61×10^{-10}	3,300	1
Te 127m	0.0000000001	0.7×10^{-13}	1,420	1
Te 127	0.0000009	0.14×10^{-9}	6,340	1
Sn 128	0.00065	0.69×10^{-7}	9,390	1
Sb 128m	0.00016	0.13×10^{-7}	12,690	1
Sb 129	0.00002	0.7×10^{-9}	25,300	1
Te 129m	0.00000007	0.8×10^{-11}	8,870	1
Te 129	0.00003	0.1×10^{-8}	25,300	1
Sn 130	0.0015	0.3×10^{-7}	50,600	1
Sb 130	0.00058	0.11×10^{-7}	50,600	1
Te 131	0.00024	0.31×10^{-8}	76,200	1
I 131	0.00004	0.52×10^{-9}	76,200	1
Xe 131m	0.00037	0.49×10^{-6}	760	1
Sb 132	0.0019	0.22×10^{-7}	86,300	1
Te 132	0.00004	0.4×10^{-9}	102,000	1
I 132	0.0027	0.26×10^{-7}	102,000	1
I 133	0.00030	0.17×10^{-8}	175,000	1
Xe 133	0.0014	0.80×10^{-8}	175,000	1
Xe 133m	0.0013	0.65×10^{-6}	1,500	1
Te 134	0.00062	0.37×10^{-8}	170,000	1
I 134	0.0033	0.17×10^{-7}	192,500	1
I 135	0.00052	0.35×10^{-8}	149,000	1
Xe 135m	0.149	0.33×10^{-4}	4,560	1
Xe 135	0.0069	0.44×10^{-7}	157,000	1
I 136	0.0022	0.28×10^{-7}	78,900	1
Xe 137	0.0518	0.35×10^{-6}	149,000	1

TABLE H.2 (continued)

Isotope	Gas-borne Activity		Fuel Activity	
	Curies	Fraction of Total Inventory	Curies	Fraction of Total Inventory
Cs 137	0.00087	0.22×10^{-6}	0	0
Ba 137m	2.46	0.63×10^{-3}	0	0
Xe 138	0.0330	0.24×10^{-6}	139,000	1
Cs 138	0.110	0.75×10^{-6}	147,000	1
Xe 139	0.0341	0.24×10^{-6}	139,000	1
Cs 139	0.101	0.68×10^{-6}	149,000	1
Ba 139	7.27	0.48×10^{-4}	145,000	0.95
Cs 140	0.104	0.68×10^{-6}	152,000	1
Ba 140	0.643	0.40×10^{-5}	12,400	0.08
La 140	0.00007	0.4×10^{-9}	12,400	0.08
Ba 141	7.08	0.48×10^{-4}	149,000	1
La 141	0.0031	0.20×10^{-7}	152,000	1
Ce 141	0.244	0.16×10^{-4}	6,490	0.043
Ba 142	6.57	0.46×10^{-4}	142,000	1
La 142	0.0084	0.56×10^{-7}	149,000	1
La 143	0.0066	0.42×10^{-7}	157,000	1
Ce 143	2.68	0.17×10^{-4}	91,200	0.58
Pr 143	0.00002	0.1×10^{-9}	91,200	0.58
Ce 144	0.297	0.33×10^{-6}	0	0
Pr 144	0.0073	0.81×10^{-7}	23,900	0.27
Ce 145	2.78	0.26×10^{-4}	106,000	1
Pr 145	0.00086	0.81×10^{-8}	106,000	1
Ce 146	2.33	0.29×10^{-4}	81,000	1
Pr 146	0.0104	0.12×10^{-6}	83,900	1
Pr 147	0.0044	0.29×10^{-5}	1,520	1
Nd 147	0.000003	0.5×10^{-10}	66,000	1

TABLE H.2 (continued)

Isotope	Gas-borne Activity		Fuel Activity	
	Curies	Fraction of Total Inventory	Curies	Fraction of Total Inventory
Pm 147	0.00000004	0.6×10^{-12}	66,000	1
Pr 148	0.0170	0.40×10^{-6}	43,000	1
Pm 149	0.000008	0.2×10^{-9}	33,000	1
Pm 151	0.000006	0.5×10^{-9}	12,700	1
Sm 151	0.000000005	0.4×10^{-11}	1,270	1
Sm 153	0.000002	0.5×10^{-9}	3,820	1
Total	49.3		8,574,000	

The rate of change, with time, of atoms of an isotope, i, in a fuel sample may be written:

$$\frac{dN_i}{dt} = B_i - \lambda_i N_i - R_i N_i \qquad (3)$$

where N_i is the number of atoms of isotope i in the fuel, t is time, B_i is the rate of birth of isotope i from fission, λ_i is the decay constant, and R_i is the release constant characteristic of isotope i. The value of N_i, from solution of Eq. (3), is

$$N_i = \left(N_{io} - \frac{B_i}{\lambda_i + R_i}\right) e^{-(\lambda_i + R_i)t} + \frac{B_i}{(\lambda_i + R_i)} \qquad (4)$$

where N_{io} is the amount of isotope i present when time, t, is zero.

During irradiation, the number of atoms of isotope i as a function of time is calculated from Eq. (4). When

$$t >> \frac{1}{(R_i + \lambda_i)}$$

an equilibrium is established where

$$N_i = \frac{B_i}{\lambda_i + R_i} . \tag{5}$$

The rate of release from the fuel during irradiation is defined by $\mathcal{R}_i = R_i N_i$ and the birth rate by $\mathcal{B}_i = B_i$. Therefore, the in-pile ratio of release rate to birth rate, $\mathcal{R}/\mathcal{B}$, is related to the release constant by

$$(\mathcal{R}/\mathcal{B})_i = \frac{R_i}{(R_i + \lambda_i)} \tag{6}$$

APPENDIX I

ANSWERS TO QUESTIONS OF DIVISION OF REACTOR DEVELOPMENT AND TECHNOLOGY FEBRUARY 1, 1967

The original version of this report, dated September 16, 1966, was submitted to the Division of Reactor Development and Technology for review. Revisions and additions to the main body of the original report have been made according to the suggestions of the reviewers. Questions that developed during the review are repeated below in the order used by the reviewers. Following each question or question subsection is the answer prepared by members of the LASL staff.

Question 1 Page 1-9, Item 32. The scram time indicated should be for the plug rods rather than the core rods.

The error is corrected in the revised text.

Question 2 Figures 3.2 to 3.6 (pages 3-2 to 3-7) should be clarified as to orientation (of sections) and location of the secondary containment boundary.

Secondary containment boundaries are marked on Figs. 3.2-3.6. The sections shown in Figs. 3.5 and 3.6 are intended to illustrate the relationship of the various rooms in the building; equipment details are not exact. Orientations of the two sections, referred to the plan views shown in Figs. 3.2 and 3.3, are as follows. The section for Fig. 3.5 is taken, in the south to north direction, along the pipe tunnel of the heat

dump facilities, and across the secondary containment. Then, after an offset to the west, the section line continues north across the electrical equipment room. For Fig. 3.6, the section line passes, in the east to west direction, directly through the building just south of the filter pit. The reactor and associated equipment are shown in side view, rather than in section.

Question 3 Page 3-8. What are the safety aspects of use of the building crane and Minotaur during reactor operation as related to any potential damage to equipment?

During reactor operations, the crane power is locked off at the motor control center in the electrical equipment room with a key that is attached to the same ring as the main operations console key. Therefore, the crane and reactor will not operate concurrently. Minotaur can be run during reactor operations, but interlocks controlled by limit switches prevent the movement of Minotaur into the vicinity of the control rod drives or the primary loop blower. The only remaining equipment that is both sensitive to damage and available to Minotaur is in the gas cleanup piping room. When Minotaur is in use there, the machine will be under visual control of an operator in the remote maintenance corridor.

Question 4 Page 4-1 and 4-29. If the fuel channels are simple 1.1 inch in diameter holes through the core cylinder graphite, an interference to insertion of 1.0 inch diameter fuel over the 3/16 inch step at the outer end of the fuel channels would occur. What provision is made to allow passage of the fuel over the 3/16 inch step?

The fuel loader discharges the fuel element into a 1-3/8-in.-diameter hole, bored on the same vertical centerline, parallel to, and 5/16 in. above the fuel channel. The element then drops into the fuel channel, past the step. Orientation of the loader, offset hole, step, and fuel channel is shown in Fig. 4.1.3.1 at the right-hand, outer edge of the core and in Fig. 4.1.5.1 at the left margin.

Question 5 Page 4-30. What is the diameter of the fuel loading ram rods? How deeply can they be inserted into the core cylinder? Can the fuel channels be loaded with less than 4 fuel elements per channel by deep insertion of the ram rod? If so, what plans have been made to use asymmetrical cores? Discuss any special safety considerations related to asymmetrical cores.

The loader rams are 1 in. in diameter along most of their length. At the end nearest the core, each ram necks down to a 5/8-in. diam x 2-in. long tip. The rams can be inserted 1-1/8 in. into the core cylinder.

A fuel channel cannot be loaded with less than 4 fuel elements by deep insertion of the ram. However, the same thing could be accomplished by loading one or more dummy fuel elements. No current plans exist for operation with asymmetrical cores, except that distributed asymmetries inevitably arise through the progressive introduction of more highly loaded fuel elements (see Table 4.1.4.1). Such effects will be minimized as far as practicable, although no special safety considerations arise as a consequence of asymmetrical arrangements.

Question 6 Page 4-37. What assurance is there that the embossed numbers on fuel elements will not disappear after exposure to the reactor environment? Does illegibility of fuel numbers have any safety significance?

The results of in-pile irradiation experiments indicate that the embossed numbers will remain legible. During the experiments, in which solution-impregnated elements were used, numbers embossed to a depth of 0.009 in. survived exposure to an impure helium atmosphere at 1500°C in a reactor where the elements were irradiated to 10% burnup. Details of the experiments are reported in LAMS-2814.[1] The UHTREX elements are embossed

[1]P. J. Peterson, J. A. Leary, and W. J. Maraman, "Reactor Irradiation of Uranium-Impregnated Graphite at 1500°C to 10% Burnup," Los Alamos Scientific Laboratory Report LAMS-2814, January 28, 1963.

to a depth of 0.020 in. and will be subjected to less damage than the experimental elements because fission recoil energy will be absorbed in the pyrocarbon coatings around the fuel particles, and oxidation of the elements will be reduced by the constant removal of impurities from the coolant by the gas cleanup system.

The legibility of the embossed numbers has a safety significance only when the element is new and unexposed. The number is used for inventory control and during fuel loading operations, to ensure that the proper element is loaded in the proper sequence. After the element is exposed, the number is used as a convenient method to identify the element for experimental purposes. If the number were to become illegible, the identity of an element could be established, at the time it is discharged from the reactor, by reference to inventory control records and the computer fuel loading logs.

Question 7 Page 4-33ff. What would be the safety implications of misplaced fuel elements in the core, if any?

The consequences are not grave. For example, an analysis shows that if 24 elements were misplaced the result would be no more than a moderate temperature rise.

To assess the effects of fuel element misplacements, the 7-channel HEATING code was used to calculate temperature profiles in the core. The normal fuel load in a channel is made up of elements, arranged in order from innermost to outermost, that contain the following masses of enriched uranium: 7.7 gU, 9.0 gU, 10.5 gU, 12.3 gU. The misplaced fuel element case considered here is for the 24 channels where $J = 7$, loaded with fuel elements containing the following masses of enriched uranium: 12.3 gU, 9.0 gU, 10.5 gU, and 12.3 gU. This misplacement of elements causes the power generation in the innermost fuel element to increase over the design loading at most by the ratio of 12.3 to 7.7. Temperature distributions in the moderator and fuel in Channel 7 are plotted in Fig. I.1 for the

misplaced element fuel loading and the design fuel loading. The maximum fuel temperature increases 40°F and the temperature gradient increases slightly in the moderator near the core plug.

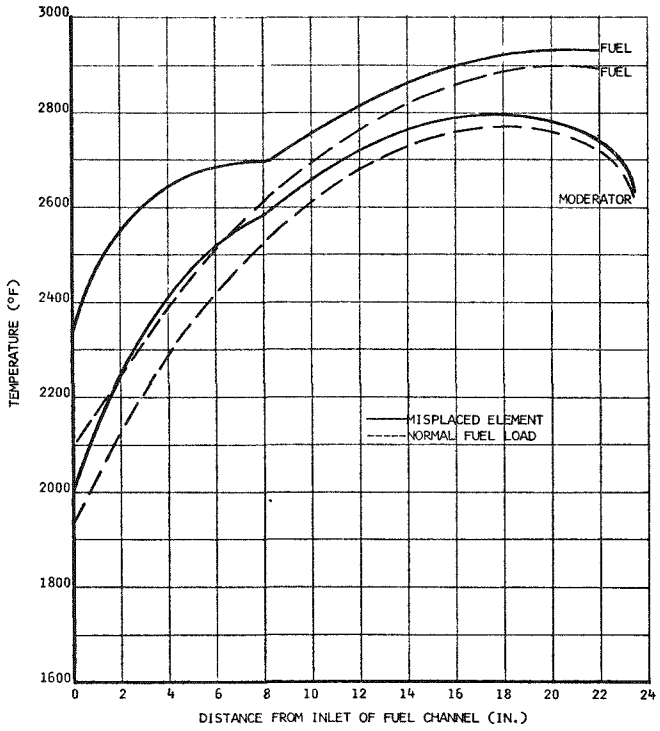

Fig. I.1 Effect of misplaced fuel element in Channel 7

Question 8 Page 4-37. Discuss the merits and difficulties in use of an interlock to prevent core rotation when one or more core rods is inserted.

Care must be used in rotating the core while core rods are inserted, since rotation through an angle greater than 18° would cause the articulated rods to bind against the sides of the holes through the reflector and in the core. Continued rotation could cause mechanical damage to the rods and to the upper part of the core and reflector.

When core rods are inserted, the only foreseeable need for core rotation would be related to fuel loading. The core might have to be rotated with core rods in place if fuel loading or unloading were performed

after a run at high temperature. Design provisions are made for the core to be rotated through a single 15° increment while core rods are inserted. This movement aligns a new row of fuel channels. To move the core to the next row of fuel channels, all of the core rods, in sequence, would be withdrawn and, on reinsertion, would move into new, vertically aligned rod holes. The core could then be rotated another 15° and the process could be continued until all the desired fuel channels were reached. If a positive ("hardwire") interlock prevented core rotation when a core rod is inserted, the above procedure could not be followed and the interlock could be unacceptably restrictive. Some method of overriding the interlock would be necessary.

Regardless of interlock provisions, all fueling operations will be carried out under close administrative control, according to written procedures and specific experimental plans. In general, fuel loading operations can proceed only through a complex sequence of events initiated by the computer digital outputs and by complementary manual actions. When the mode selector switch for the core indexing drive is in either the "Computer" or "Both" position, a programmed interlock in the computer prevents core rotation while core rods are inserted. Only by setting the selector switch to the "Manual" position and by holding down the operate switch can the core be rotated while the core rods are inserted. In this case, a programmed interlock is overridden, and the computer program consequently trips an annunciator and logs an alarm message on the typewriter. These programmed interlock features, together with proper training and administrative controls, will provide adequate safeguards against imprudent operator actions, and are preferable to the other alternatives considered.

Question 9 Page 4-37. What provisions assure that core rods will not be inserted during operation or before cooldown?

The core rods should not be exposed to the core environment for extended periods when the temperature is above 1200°F. Therefore, an

electrical interlock prevents the operation of the core rod drives when the core temperature, averaged from measurements made with three thermocouples, is greater than 1000°F. The interlock may be overridden, in case of necessity, by operating a switch on panel 32 of the main operations console.

Question 10 Page 4-37. Has the desirability and feasibility of providing dummy poisoned elements as a backup shutdown system been investigated?

Yes, this possibility has been considered from time to time, but was not previously adopted because of its obvious limitations. That is, if any essential feature of the fuel loading system happens to be inoperative when the occasion arises, then no backup shutdown capability is afforded. On the other hand, if the fuel loading system is operative, then the reactor can be shut down by the replacement of fuel elements with unloaded graphite dummy elements, and poisoned elements are not really necessary.

Despite these limitations however, the suggestion has considerable merit, since certain emergency contingencies could be covered at very little expense and without foreseeable difficulties. Approximately 60 boron nitride (BN) dummy elements will be kept on hand in the reactor facility for this purpose. The sharply contrasting appearance between the white BN and the black fuel elements makes it most unlikely that they would ever become interchanged. However, other appropriate precautions will be taken to prevent a BN dummy from being loaded into the reactor by mistake. The BN will be used only in the unlikely circumstance of complete failure of the primary shutdown mechanisms.

Question 11 Page 4-37, 4-41, 4-43, 4-52. There is a potential source of confusion as to the use of plug rods on these pages. Statements are made that these rods will be used for power regulation and also that they may remain out of the core. Some amplification of the planned use and temperature capabilities of the plug and core rods appears desirable.

Page 4-41 indicates that the core rods must be capable of "dropping" into the core. Aren't these rods only driven into the core?

The plug rods are used routinely for power regulation only during startups and shutdowns and during limited periods of time when significant changes are being made in the core loading. While the reactor is operating for long periods of time, the plug rods are withdrawn. Compensation for poison accumulation and burnup is made with fuel element changes. The plug rods are designed to withstand prolonged exposure to temperatures near 2400°F in the carbonaceous environment of the core plug.

The sole use for the core rods is to hold down the fully loaded core as it cools down after a run at elevated temperatures. These rods are designed for use at temperatures below 1200°F. They are driven into the core by rod drives that do not have a scram capability. The text on page 4-41 has been changed.

Question 12 Page 4-43. In scram tests of the plug rod drive, what has been the experience with rod insertion variations with scram height?

Data derived from scram tests on the prototype rod drive are plotted in Fig. I.2. The ordinate shows the height, above the zero or bottom stop position, at which the lower end of the rod was stopped by the decelerator after scrams were initiated at rod withdrawal heights plotted on the abscissa. At withdrawal heights above 18 in., the rod comes to rest at a position where it is at least 90% inserted. To avoid shock damage, the rod always stops no less than one inch above the bottom stop. At the end of the stroke, a difference of a few inches in position makes little difference in rod worth. (See Figs. 4.2.1.1 and 4.2.1.3.)

Because the rods are withdrawn one at a time and two rods are already in the fully withdrawn, ready-to-scram position before the reactor goes critical, a scram while one rod is partially withdrawn would not interfere

with complete shutdown of the reactor, even though the one rod did not reach its bottom position.

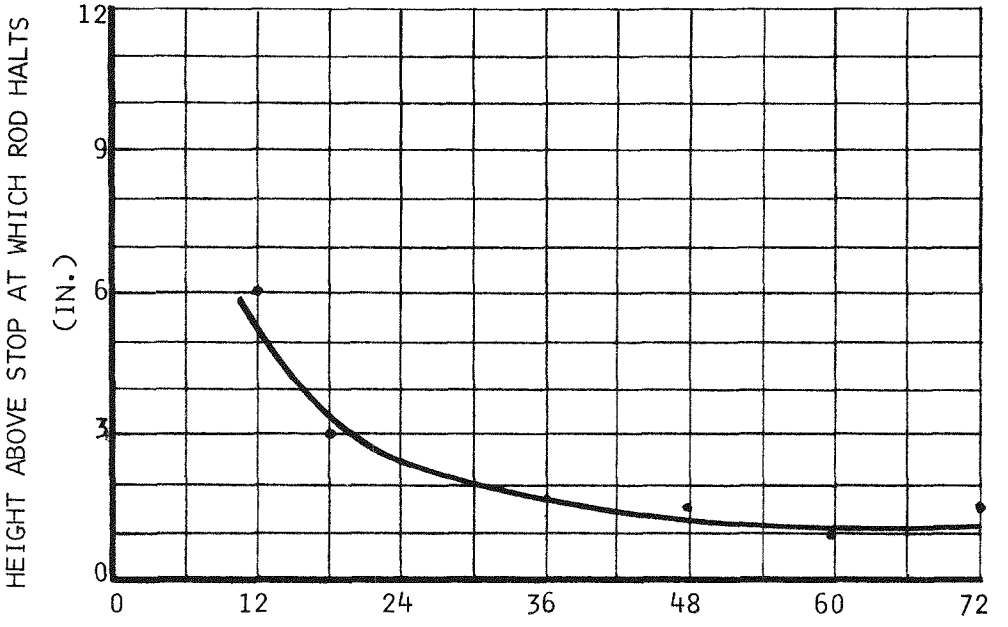

Fig. I.2 Effect of height at which scram occurs on final rod position

Question 13 Page 4-43. Is there any method for bleeding highly radioactive mixtures of helium and fission product gases from the tops of the rod drive tubes?

No. There is no trapped gas in the tops of the tubes, one of which is shown in cross section in Fig. 4.1.7.3. To bleed down or purge the tubes would involve the use of a complex system that would decrease the integrity of the primary containment without a compensating contribution to operational safety.

Question 14 Page 4-47. Some amplification of the description of rod position indication is needed. Is there more than one system of indication?

A schematic diagram of the rod position indicator is presented in Fig. I.3.

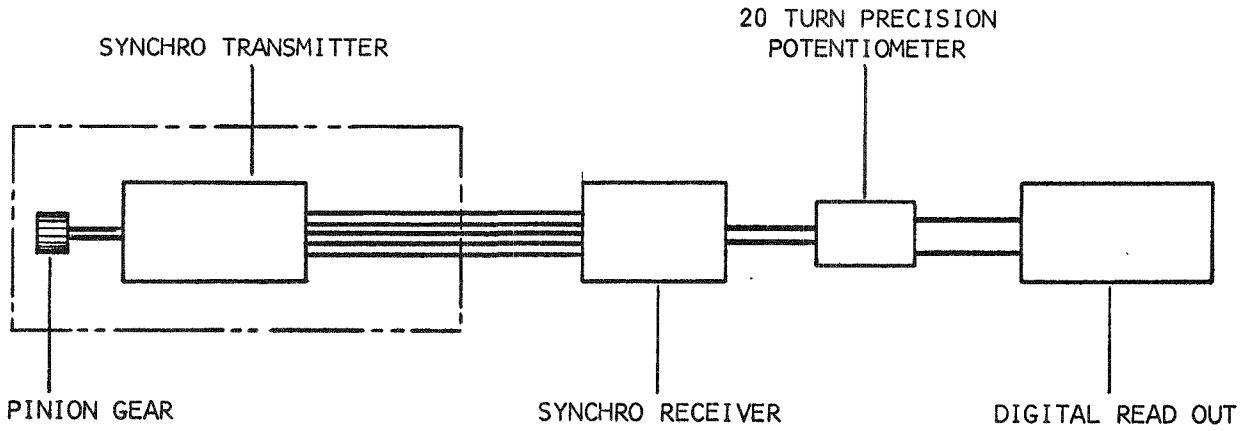

Fig. I.3 Rod position indicator system

A synchro transmitter is coupled to the pinion gear inside the control rod drive mechanism, shown in Fig. 4.1.7.3. The synchro receiver, located in the control room, drives a 20-turn precision potentiometer (0.1% linearity). The output of the potentiometer feeds a servo-driven, mechanical counter (digital volt meter), which reads directly in inches. It is mounted on the main operations console. This system permits reproducible control rod positioning to within ±0.05 in.

Independent indications of rod position at the "in" and "out" limits appear on the main operations console where lights turn on when the magnetic proximity switches, described in Sec. 4.1.7, sense the presence of the decelerator. If the synchro transmitter and receiver get out of synchronization, e.g., on a scram, the proximity switches are used to restore synchronization. If it is not already there, the rod is run down until the "in" light comes on. Then the synchro receiver is rotated until the

read out is zero. Because of the action of the decelerator (see Question 12) the innermost position of the rod is not precisely the same after each insertion. Therefore, the calibration of the rod position readout is rechecked the next time the rod is completely withdrawn. At its fully out position, the rod drive is restricted by a mechanical stop; consequently, this position is fixed and reproducible.

Question 15 Page 5-27. Reference is made to the secondary loop as acting as secondary containment in the event of a primary system rupture. This would be true only for an internal rupture in the heat exchanger.

This observation is correct.

Question 16 Page 6-7. The description of the discharge cycle indicates that the spent fuel element is held above each valve for a certain length of time to cool the element. No mention is made of just what this length of time is, but the whole load-unload cycle only takes 15 minutes so it cannot be very long. LASL does not show that a 2900°F fuel element can be cooled to 700°F in this short a time. Also, it has not been made clear why 700°F has been chosen as a cool enough fuel temperature. Why not 600°F or 400°F or why cool it at all?

Two analyses are presented below of the temperature history of spent fuel elements after they are unloaded from the reactor. The progress and temperature of each fuel element are determined primarily by the mechanics of the fuel handling system. A cooled element is desirable to avoid undue exposure of the conveyor components to high temperatures and to facilitate the handling of the elements in the drybox with the master-slave manipulators.

The basis for the cycle described on page 6-7 was a minimum period of 15 minutes for one fuel element loading cycle. The "holdup time" at each gas lock valve was arbitrarily chosen to satisfy two criteria: (1) no unnecessary delay in the cycle and (2) minimized heating and

radiation of the gas lock valves. The analysis of this cycle was made before the development of the fuel loading cycle computer program was begun. Since then, the fuel loading program was completed and it became clear that the minimum loading period could be decreased to 10 minutes. In the new program, the holdup time at each gas lock valve is equal to the time allowed in the program for pressure equalization and purging of the intervalve chamber. The conditions defined for both the initial analysis and for a recent one are as follows.

At start of unloading:

1. Fuel element temperature = 1800°F (element at outlet gas lock).
2. Reactor power = 3 MW for ∞ time.
3. Gas lock valve, drybox, alpha can temperatures = 100°F.

During unloading:

1. Reactor is shut down.
2. Core is assumed to be adiabatic.
3. Fuel elements decay at rate calculated according to Price.[2]
4. Heat transfer to gas lock valves is by radiation and conduction through end of element resting on valve snubber gate.
5. Heat transfer to conveyor is by radiation and conduction to transport boat.
6. Heat transfer in drybox is by radiation and convection to drybox helium atmosphere.
7. Heat transfer in alpha can is by radiation to walls and convection to contained helium.
8. When alpha can is placed in transfer cask, heat transfer from alpha can to cask is by radiation. There is sufficient heat capacity in the cask to absorb the fuel element decay energy, including gamma absorption in the depleted uranium shield. Cask temperature increases approximately 0.5°F/24-h day.

---

[2]B.T. Price, C. C. Horton, and K. T. Spinney, Radiation Shielding (Pergamon Press, New York, 1957), p. 65, Fig. 2.10.2.

9. After the alpha can is transferred to storage at CMR Building, heat transfer from the alpha can is by radiation and convection to the walls of the water-cooled storage pits.

The results of the analyses, made with FORTRAN code ELCOOL, are listed in Table I.1.

TABLE I.1

TEMPERATURE HISTORY OF SPENT FUEL ELEMENTS

	Initial Analysis	Recent Analysis
Number of elements unloaded	21	21
Loading cycle, min	10*	10
Hold-up time at 1st valve, sec	30	16
Maximum temperature of 1st valve, °F	185	160
Hold-up time at 2nd valve, sec	90	47
Maximum temperature of 2nd valve, °F	175	169
Hold-up time at 3rd valve, sec	210	44
Maximum temperature of 3rd valve, °F	164	136
Maximum temperature of 21 elements when transferred into drybox, °F	533	741
Maximum fuel element temperature when loaded into cask, °F	344	344
Time after start when alpha can is loaded in cask, min	250	250
Maximum fuel element temperature while in cask, °F	531	531
Maximum pressure inside alpha can during cask transport and storage at CMR Building, psig	8.6	8.6
Time after start when alpha can is transferred from cask to storage in CMR Building, h	6	6

*Assuming that a new element progresses through inlet locks while a spent element moves through outlet locks.

Question 17 Page 6-8. Inspection of the alpha-can for leakage should be part of the procedure.

Because the cans are filled with helium, a helium leak test is a satisfactory method for detecting faults. The procedure includes a helium leak test after the can is sealed.

Question 18 Page 6-11. Evidently no special provisions have to be made for the dissipation of decay heat generated by the fuel elements in the alpha-can. However, the reason for this should be explained clearly and fully.

See the answer to question 16.

Question 19 Page 7-1. What was the design basis for the helium gas cleanup system? What fission product leakage rate can it handle?

The capacity of the gas cleanup system was originally sized to satisfy dual functional requirements: (1) to limit the concentration of chemically active gaseous species (CO_2, CO, O_2, H_2O, etc.) to acceptable levels, which depend on time and temperature; and (2) to prevent the buildup of longer-lived fission products in the coolant because of the effects that they would have in a coolant loop rupture accident.

Since large quantities of the chemically active gases are released by desorption when the reactor and recuperator heat up, the cleanup system capacity was made large enough to accommodate the expected outgassing rate without prolonging the heatup period. For removal of radioactive contaminants, the gas cleanup system was designed to handle complete release from the fuel at the design temperature and power levels. It was assumed that individual species of fission products are instantaneously released unless they are known to be refractory elements or to form refractory carbides. For conservatism in computing the heating load of volatile species deposited in the decay heat exchanger (see Sec. 7.2.5),

no credit was taken for delay or fractionation in the fuel, decay in transport, or plateout at intermediate points in the system.

The size of the cleanup system was limited by practical design and economic considerations, since at much higher flow rates the adsorption beds become too large for the available space and the cost of heating and cooling the process equipment exceed economic limits.

Question 20 Page 8-1. What are the potential safety implications of a rupture of the high pressure helium storage tank?

There are no serious safety implications of a postulated storage tank rupture, either as a separate occurence or in conjunction with rupture of the primary loop. The secondary containment is capable of withstanding the internal pressure associated with release of the entire helium inventory in the primary loop and the associated storage system. When the primary loop is pressurized, the pressure in the storage tank will not exceed 350 psi, which represents about 19 lb/moles of helium. Release of this gas, concurrent with the other circumstances described in the maximum credible accident analysis, would initially increase the secondary containment pressure (Fig. 16.3.1.2) by about 0.85 psi. This would cause an increase of about 50% in the leakage rate from the secondary containment.

Rupture of the high pressure storage tank is quite unlikely. There is not enough helium in the entire cooling system to raise the tank pressure to its 1000-psig design limit, much less to its test pressure of 1500 psig. The tank is of simple design and was manufactured and inspected according to ASME code requirements. In its isolated location in the gas storage room (see Fig. 3.4) it is invulnerable to secondary damage by rupture of the primary cooling system. Conversely, shock or fragmentation from rupture of the storage tank would not jeopardize the integrity of either the primary coolant system or the secondary containment system.

Question 21 Pages 9-3 and 8. The electrical cable penetrations appear to allow leakage through the cables. Has this been checked and, if so, how serious is this source of leakage? How much control room contamination results from this leakage after a primary system rupture?

All leakage paths through the cables are blocked. The voids inside the cable jackets are filled with epoxy in-line blocks. Flow paths between the insulation and the conductor of individual wires are closed at the ends of the wires by solid connectors, crimped onto the conductor and joined to the insulation with shrunk-on polyvinyl chloride tubing. Leakage along the fine wires of stranded conductors is prevented by dipping the end of each conductor in molten solder before the connector is crimped on.

To check the efficacy of a typical cable seal, a test was run on a sealed 76-conductor cable. For the first test, 15 psig air pressure, triple the maximum service test pressure, was applied to the open end of the cable. Then the sealed end of the cable, complete with solid connectors, was immersed in water. No air bubbles formed, either between wires in the cable jacket or at the end of any individual wire. In another test, the leak rate through the seal was measured with a helium leak detector. At a pressure differential of one atmosphere, the leak rate was less than 10^{-5} std cc/sec.

Leakage along cables from the secondary containment to the control room is not a significant source of contamination. The 35 cables that join the two locations are 100 to 175 ft in length. Under the assumptions that each cable leaks at the measured rate and that there is no holdup in any cable, the upper limit estimate of the rate at which contamination could be delivered to the control room after a primary system rupture is 1 mC/day.

Question 22 Page 9-6. List and describe the containment isolation valves and describe the procedures and automatic devices that assure closure of these valves either before or immediately after a severe accident. What back-ups are available if an isolation valve fails to operate?

Valves in piping which penetrates secondary containment may be grouped in two categories: (1) valves in high pressure, closed-loop piping systems, and (2) valves which could, if open, provide a direct path from inside secondary containment to atmosphere or to inhabited areas inside the facility.

Valves included in the first category are normally-open valves located in the utility systems: auxiliaries cooling water system, glycol system, process air system, and compressed air system. Automatic closure of these valves has not been provided because the highest secondary containment pressure is too low to rupture any point in these systems. The utility systems can be isolated by closure of remotely-operated valves that control flow to individual system components or by manual closure of valves at the containment wall.

Valves in the second category are discussed in detail below. Table I.2 contains a description of these valves, locations, position indication, status control, and backup.

Valves V-1 and V-3 - Valves V-1 and V-3 are normally-closed valves which are opened only when the secondary containment may be opened and containment purge is desired. Valves V-1 and V-3 open when the secondary containment ventilation system is switched to exhaust cycle.

When closed, each valve is sealed by an inflatable rubber gasket. Air pressure on the inflatable gasket is monitored continuously by a pressure switch which annunciates a low pressure condition.

To provide backup for these valves and greater convenience in routine leak checking, two butterfly valves are to be installed in series with V-1 and V-3. Designated V-1a and V-3a, these valves will be located on the secondary containment side of V-1 and V-3. This arrangement will permit

TABLE I.2

SECONDARY CONTAINMENT ISOLATION VALVES

Valve Number	Description	Location	Position Indication and Status Control	Backup
V-1	24" butterfly with inflatable gasket	Fresh air inlet to secondary containment	Open-closed limit switch Procedural control	V-1a
V-3	24" butterfly with inflatable gasket	Secondary containment purge valve to stack	Open-closed limit switch Procedural control	V-3a
SV-4	3" solenoid-operated	Secondary containment bleed fan E-3 suction valve	Open-closed limit switch Safety system interlock	SV-4b
SV-4a	3" solenoid-operated	Secondary containment bleed fan E-3a suction valve	Open-closed limit switch Safety system interlock	SV-4b
SV-4b	3" solenoid-operated	Secondary containment bleed closure valve	Open-closed limit switch Safety system interlock	SV-4, SV-4a
WD-1	3" hand-operated globe valve	Secondary containment drain valve (Room 303)	Stem-travel pointer Procedural control	WD-1a
VC-1	3" hand-operated butterfly valve	Vacuum-cleaning line shutoff at secondary containment wall	Stem rotation Procedural control	Gasketed blank
BA-10	1-1/4" hand-operated globe valve	Breathing air line shutoff at secondary containment wall	Stem rotation Procedural control	Quick-disconnect caps at outlets, valve BA-9

pressurization of the space between valves for routine leak testing while the secondary containment is closed.

Normally all four valves will be maintained closed. Open-close control of V-1a and V-3a will be separate, requiring two deliberate actions to open ventilation ducts into the secondary containment.

Valves SV-4, SV-4a, SV-4b - Valves SV-4, SV-4a, and SV-4b can be left open after secondary containment integrity is established. SV-4 and SV-4a control flow through the 25-cfm bleed fans that maintain a slight negative pressure inside secondary containment. SV-4b (not shown in Fig. 9.3.1) is installed in the common pipe through which the bleed fans discharge to the stack, to act as a backup for SV-4 and SV-4a. The solenoids of all three valves are de-energized and the valves close when the Primary Loop Loss of Coolant Emergency System (see Section 11.4.1) is actuated. Continuous filtration of the air protects the seats of all three valves from damage by solid particles.

Valve WD-1 - Valve WD-1 is a normally-closed, manual valve, opened periodically for very short periods, in case water collects in the secondary containment floor drains, which empty into the liquid waste tank in Room 303. Valve WD-1a has been added in series with WD-1 to act as backup. These valves are never opened unless secondary containment conditions are safe. Before WD-1 and WD-1a are closed, the line is flushed to remove solids from the valve seats.

Valve VC-1 - Valve VC-1 is a normally-closed valve immediately outside the secondary containment wall. When closed, VC-1 isolates a vacuum cleaning system with 9 outlets inside the secondary containment. Backup is provided by a gasketed blank plate installed in a flanged joint. This system will be opened only when secondary containment integrity is not required. When it is ready to be closed after usage, the valve can be inspected visually for dirt on the sealing surfaces.

Valve BA-10 - Valve BA-10 is a normally-closed valve immediately outside the secondary containment wall. When closed, BA-10 isolates the breathing air system, which has air outlets in six cabinets inside the

secondary containment. Backup is provided by a swing-check valve, BA-9, immediately upstream of BA-10, and by caps installed on each quick-disconnect hose coupling at the outlet cabinets. The breathing air system is placed in operation only if containment access is required while an air contamination hazard exists.

Question 23 Page 9-10. Will valves V-1 and V-3 of the ventilation system be closed anytime the reactor is at elevated temperatures? What interlocks or procedural controls assure this? How does the operator know that these valves are fully seated and their leak rates will not be so great as to invalidate the claimed containment integrity? What prevents foreign bodies lodging in the valve seats?

Secondary containment (closure of normally-closed containment isolation valves and access doors) will be maintained whenever the combination of core temperature, coolant system pressure, and total fission product inventory produces conditions that are sufficient to create a safety hazard if a rupture of the primary containment were to occur. These factors will be considered in the establishment of the standard operating procedures.

The remainder of the question is answered in the discussion of containment isolation valves in Question 22.

Question 24 Page 11-1. Since the computer plays an important role in data handling and control and is subject to failure at any time, an analysis should be included in the report showing the consequences of complete and instantaneous shutdown of the computer system during all phases of operation, such as steady state operation, power change, startup, shutdown, fuel handling, etc.

A complete and instantaneous shutdown of the computer has the following consequences involving the computer system:

1. Special computer equipment detects a power loss taking place, interrupts the computer program being executed, and halts. Thus, the computer cannot malfunction while it is experiencing the loss of power.

2. All passive functions of the computer such as monitoring, logging, and alarming are lost for the duration of the shutdown.

3. All active functions of the computer such as fuel loading and closed loop control are terminated immediately. As noted elsewhere, a shutdown initiates computer stall, and in stall the computer cannot change the positions of valves, etc. Thus, a computer shutdown leaves the UHTREX system in the hands of the operators.

If the computer is shut down, administrative procedures require that a variety of system operations be terminated or not started. For instance, fuel loading is not started or continued if the computer is not available; startup of the reactor is not initiated or continued if the computer is not available; and significant changes (other than shutdown) in operating conditions of the reactor and primary and secondary coolant loop are not made if the computer is not available.

Reactor shutdown does not require the use of the computer. Shutdown may be initiated if the computer is lost, but there is no requirement for a shutdown. There is a substantial system of meters and recorders that do not depend on the computer, and the basic safety systems are independent of the computer. Therefore, steady state operation could be maintained under the conditions existing at the time of loss of computer function.

Computer programs and the most recent system data are stored on a magnetic drum and are available for computer restart at any time, even after a power failure. Restart of the computer takes less than one minute.

Question 25 Page 11-4. In addition to the above analysis, specific limited computer system failure should be analyzed such as:

a. Erroneous changing of set point limits.

The changing of limit points in the computer may be done from the computer panel by operating personnel. Any such change is automatically recorded by typewriter and is therefore available for review and confirmation. Typewriter logs are also available of all limit point settings. For important channels there are independently set limits for direct annunciation, for annunciation by the computer, and for typewriter alarm messages. Generally, the typewriter alarm limit is set lower than the annunciator limit to serve as a preliminary warning for the operator.

Erroneous setting of limits would result in either failures to detect an out-limit condition or false out-limit messages or annunciation. Since rundown or scram can be initiated only by operator action or by a safety system, false rundown cannot be initiated by the computer, except indirectly, i.e., in a case where the operator has acted in response to erroneous out-of-limit information. The automatic safety systems are independent of the computer.

b. Demand of control programs at the wrong time, either by operator error or machine failure.

If the operator demands a control program by pushing an AUTO switch at the "wrong time," that control program runs until the associated MANUAL switch is pushed or until the program terminates itself because of the failure of a self-check. Some of these self-checks prevent the control program from running at the wrong time.

Whenever the computer operates, a typewriter message is generated and a light on the main console comes on when any control program starts; each adjustment made by a control program is accompanied by a corresponding short term light on the main console; and the control programs make small enough changes and proceed at slow enough speeds that their progress can be monitored by an operator. Thus, it would be unlikely that an operator

would demand a control program and then not realize that it was running. Even if the wrong program were allowed to continue to run, it would move the controlled parameter slowly towards the value set on a manual potentiometer on the main operations console. If these set values are completely unreasonable, the control programs terminate themselves.

A control program that is started through a computer failure terminates itself before it makes a single output. Each control program reviews its own AUTO-MANUAL switch and stops if this switch is not in AUTO. In any case, a control program cannot make a field change, even if it runs, unless the operator puts its associated AUTO-MANUAL switch in AUTO. Thus, control programs cannot make field changes without the knowledge and cooperation of the operator.

> c. The possibility of damaging or altering, in some manner, the calibration of the sensors that are scanned by the computer system, either by excessive loading or any possible scan system malfunction.

The input multiplexing and analog-to-digital conversion equipment in the computer system has a very large input impedance, is isolated from the transducers by capacitors, and does not have any means for inducing voltage into the transducers. The sensors and signal conditioning are protected from overload or damaging voltage or current because of the high input impedance and capacitor isolation.

Question 26 Page 11-7, last paragraph. How will component (parts, subassemblies, and assemblies) malfunctions or failure be detected and annunciated? How often will tests be performed? How will test intervals be established and kept appropriate?

Malfunctions and failures of components and systems in critical parts of the UHTREX loops are annunciated directly in the control room. For example, a failure of a compressor diaphragm actuates an oil-leak detector in the line; failure of the bellows seal on a valve in a helium system

actuates a pressure switch in the air line; loss of any of the critical power supplies that serve the safety systems, neutron detectors, or transducer circuits closes a relay contact; loss of water flow in a reactor room panel actuates a flow switch; malfunctions in the stack or other radiation monitor closes a relay contact; and so on, through a list of hundreds of safety devices. Where it is not feasible to provide direct annunciation of a malfunction, associated changes in system parameters are sensed and out-of-limit conditions actuate current sensitive relays, the contacts of which actuate appropriate annunciators. In many cases, computer output relays are used in parallel with direct parameter measurement signals to actuate annunciators. Finally, building service equipment and functions are monitored with a "Scanalarm" system located in the electrical equipment room. Actuation of any of the channels in this system causes a remote signal to the control room annunciator system.

Checks of all vital equipment will be made routinely once each 8-hour shift. Tests, by check list, of all operating instrumentation and equipment will be made once a day.

Question 27 Page 11-8. The number and locations of reactor vessel and recuperator metal temperature monitoring thermocouples should be discussed.

See Fig. 4.1.3.9.

Question 28 Page 11-9, third paragraph. What tests have been conducted to determine the reliability of the thermocouples under prototypical conditions of radiation and temperature extremes? What were the results of these tests? Has the possibility of transient neutronic effects on thermocouple readings been considered? (Some information on these effects at low temperatures was presented at the 1966 Winter Meeting of the American Nuclear Society by J. H. Leonard and J. S. Crutchfield of the University of Cincinnati.)

Since the temperature and radiation levels in which chromel-alumel thermocouples are used in UHTREX fall well within the conventional range

of study and application in many other reactors, no extensive environmental test program was conducted. Because experience indicates that thermocouple failure generally results from mechanical breakage near the junction, probably from cold-work stresses induced by thermal expansion differences, the temperature testing program was concentrated on thermal cycling (see Sec. 11.1.2). These cycling tests were run between approximately 700 and 900°F. The temperature vs. emf characteristics of the thermocouples were rechecked about midway through each cycle test, and also at the end of the test, over a range of temperatures up to 1500°F. There was no detectable shift in calibration, which remained at all times within the ISA standards for chromel-alumel. No radiation testing was performed.

Some thought has been given to possible transient neutronic effects, particularly in the light of the recent results reported by Leonard and Crutchfield. In the operation of Kiwi and Phoebus reactors in the Rover program, LASL has observed no recognizable effects of large power changes upon chromel-alumel thermocouple output. However, the possibility of such a phenomena will be considered during the operation of UHTREX, and other investigations will be made if conditions warrant. There is a conservative temperature design margin in all materials and components equipped with these thermocouples, and no difficulties would arise if a change in UHTREX reactor power does cause an erroneous thermocouple response of 10 to 20°F (as might be expected from the report of Leonard and Crutchfield).

Question 29 Page 11-11, second paragraph. How often is the resonant frequency of the transducer determined? If a continuous measurement of resonant frequency is provided, how is the continuous readout of temperature accomplished?

The resonant frequency of each acoustic thermometer is continuously tracked by means of an electronic servo unit connected electrically to the transducer. This unit also controls the excitation frequency of the cavity. An output signal proportional to resonant frequency drives a

front panel meter and is also sent to the computer. From this signal, which is proportional to the square root of the absolute temperature, the computer calculates the temperature and can print out or display it on demand. When a temperature determination is desired which is more accurate than is available from the meter indication, the actual oscillator frequency at resonance is determined with a precision counting instrument.

Question 30 Page 11-16, last paragraph. Test signals of 1/3 and 2/3 full scale value in addition to full scale signals would provide a much better indication of the status of the electronics and equipment associated with transducer channels. Has the use of such test signals been considered?

The use of more than one calibrate signal was considered at the time the signal conditioning circuitry was designed. However, because of space limitations and the desire to keep the circuitry as simple as possible, it was decided instead to provide only one calibrate signal, but one which could be varied easily. This was accomplished with the use of a variable potentiometer in a simple divider or bridge circuit. Since the time of writing of the material on page 11-16, it has been decided to set and lock this calibrate signal potentiometer at 0.8 of full scale. However, if other values are ever desired and prove useful, it is a simple matter to change this signal to a new value.

Question 31 Page 11-17, first paragraph. Has consideration been given to annunciating the fact that a power supply has failed or assumed total circuit load?

All power supply banks serving the signal conditioning circuitry trip an annunciator if their voltage output goes to zero. However, loss of function in any one of two power supplies in parallel is not annunciated but is detected during instrumentation checks made at the beginning of each shift.

Question 32 Page 11-17. What is the test philosophy regarding the computer? For example, are checking routines other than purity check or the "watch dog" time check used during operation?

The regular on-line program is superior to special diagnostic tests in checking overall computer functioning.

The on-line program contains self-checks which are made by programming and are in addition to the parity checks and the watch dog timer check, which are made automatically by hardware. A partial list of these program checks is given below:

1. Every transfer of a program from drum to core is checked by the executive program. The executive program examines the last word of the transferred information. This last word should be the number of the beginning drum track from which the transfer was made. If the last word is not the proper one, the transfer is repeated immediately. If the computer fails on nine successive tries, it puts a stop identification bit in the B register and halts. If the test is passed after less than 9 tries a typewriter message giving the number of failures is printed and the computer proceeds. This check is made many times each second. (The drum transfer parity checks, which are made by hardware but are detected by the executive program, are handled in a similar manner. A check failure is followed by repeated tries and, eventually, by either a typewriter message or an identified stop. No drum transfer failure of any kind has been recorded since the start of the three-month computer reliability test on March 16, 1966.)

2. The analog and digital scan programs both check at least two known fixed inputs each second. A priority typewriter message is typed and an annunciator is sounded if any of these inputs are not correct.

3. Many subordinate parts of the on-line program contain their own self-checks. For instance, if the GET subroutine does not find a

designator on the track where it should be, the subroutine loads bit 23 into the B register and halts. The computer programs have many checks built into them to verify that all the control hardware, transducer inputs, and other programs needed for control are working properly.

Question 33 Page 11-21. What specific administrative action will be taken in regard to the functions delegated to the computer? Will the alarms be checked before taking corrective action; and if a discrepancy is evident, which conclusion will be overriding?

Whenever an alarm condition is found by the computer, an alarm message and the time of the alarm are printed on the alarm typewriter. The control room operator reads the message, evaluates the situation, and takes the necessary action according to established policies. If his response involves the manipulation of monitored equipment, the change in equipment status and the time at which the change was made are printed on the demand log typewriter. Therefore, a record of alarms and responses is kept automatically.

If the alarm condition is immediately hazardous, safety systems automatically take corrective action, independent of the computer or the operator. These conditions drop an annunciator, which is cleared by operator action only, and cause the printout of an alarm message. Again any change in monitored equipment is recorded on the demand log typewriter.

When an alarm typewriter message requires no immediate response, the operator can verify the existence of the out-of-limits condition and check its trend on recorders before he decides what to do. He records any abnormalities in a written control room log.

Question 34 Page 11-24. Control Modes - For the case of the "Both mode," is an annunciation that the computer signal is present provided in close proximity to the associated control switch so that the fact that an action will occur when the control switch is actuated is known?

In the "Both mode," within one second after the operator depresses the "open" or "close" pushbutton, a white light flashes within the pushbutton to show that the computer output pulse is transmitted. Depressing the pushbutton interrupts the computer, which then checks interlocks and sends the output pulse if no interlock will be violated.

Question 35 Page 11-24. The function of the computer "Correct Switch," to check the sequence of control functions initiated by an operator, should be discussed further. For example, can the computer inhibit initiation of a control function at a time that could result in an unsafe condition?

There is no "Correct Switch" associated with the computer controls. The "correct switch" referred to in the quoted text is simply the switch on the system operations panel that must be pressed to initiate the next step in a sequence of operations. If the control circuit for the device actuated by this switch is in the Both mode, the computer verifies the fact that operation of the device at this particular time does not violate any interlocks or program sequences, before the control circuit is energized to operate the device. The verification occurs within a one-second period after the operate switch is pressed.

An operator can always override the computer by turning the mode selector switch to Manual. Both the operate and the mode selector switch for each device are located in the same rack, three of which are illustrated in Fig. 11.1.1.2.

Question 36 Page 11-27, paragraph 4, - Reactor Startup. Since the limits of sensitivity of the counting channels are shown in Figure 11.2.1.1 to be 5 CNT/SEC and 5 x 10^4 CNT/SEC,

it is not apparent what instrumentation will provide neutron flux information from source level (<5 CNT/SEC) to the point where core multiplication equals 10. How is this flux level monitored at reactor startup?

During the period when the multiplication is less than 10, i.e., during the initial loading of UHTREX at room temperature, a source of 10^8 neutrons per second will be installed in the reactor core plug. This source will be positioned near the center of the central plug region. Experience with sources during the UHTREX Critical Assembly (UCX) indicates that the central source in UHTREX should provide a strong flux of neutrons at detectors situated outside the primary vessel even when there is no fuel in the reactor.

After the initial approach to critical at room temperature is completed, the source will be removed from the central plug and placed at a position just outside the vessel near the horizontal midplane of the reactor. At that time, the actual effectiveness of the source and counter system will be determined at various shutdown multiplications.

A source experiment, described on page D-11, was conducted to determine the effectiveness of the source positioned outside the vessel. In that experiment, 6 counts per second were observed at a multiplication of 20. The UHTREX source-detector arrangement will be increased in efficiency by a factor of 50 over that used in UCX by increasing the source strength by a factor of 5 and by increasing detector sensitivities by a factor of 10. This would increase the detector response to 300 counts per second, mutatis mutandis. However, in UHTREX there will be additional materials, mainly carboniferous, interposed between the source and counters. These materials, which were not present in the UCX configuration, will reduce the efficiency of the source-detector system somewhat. The effect of these additional materials is really inestimable. A conservative guess is that counting rates of at least 5 counts per second will be available at multiplications of the order of 10. This should be adequate for starting up the reactor, since data accurate to a few percent

can be obtained during 5- to 10-minute counting periods.

After the initial room temperature loading, the reactor will not be shut down below a multiplication of 10.

Question 37 Page 11-27. Why are uncompensated rather than compensated ion chambers used for the log power channels?

The ion chambers of the log power channels deliver current to log amplifiers that have six decades of dynamic range. These instrument channels are calibrated for a 10-MW reactor power indication at full scale on the logarithmic range. The start of the lowest decade on the log scale is 10 W reactor power. This minimum power indication is produced by an ion chamber current of about 3×10^{-9} A. Because the ion chambers are shielded with lead, the neutron to gamma ratio at 10-W reactor power should yield a satisfactory signal without requiring compensated detectors.

The linear power channels have electrometer circuits with a wider dynamic range than the log power channels. The linear electrometers are capable of minimum current measurements of 10^{-11} A. The ion chambers of the linear power channels are of the compensated type to make possible the lower level neutron flux measurements.

Question 38 Pages 11-31 and 33. Are meters provided to monitor clutch coil current supply output currents so that failures can be detected and repairs made?

Yes, meters are provided to monitor the clutch current of the plug control rod drives.

Question 39 Page 11-31. How is the operator alerted to an open circuit in the signal lead from the ion chamber to the electrometer?

There is no provision for detecting an open circuit in the signal lead of the electrometer.

Prior to the initial loading, each chamber is source tested and a sensitive electrometer is used to determine that the cable and ion chamber are properly connected. The chamber cable is then reconnected to the safety system electrometer. While the reactor is being brought up in power the operator checks to determine that all safety channels in each power range are functioning properly and yielding the proper output signals.

Question 40 Page 11-32, line 5. Is not the scram point minus 2 volts?

Yes. The error is corrected in the text.

Question 41 Page 11-32. What happens if one channel of the safety system suffers an open circuit and another channel shows a scram condition?

$$Eo_3 = \frac{0 + 9 - 9 - 9}{5} = -1.8V$$

A scram might be initiated or it might not be, depending on what combination of channels is involved. The value of $\geq$-2V for scram trip is nominal. Slight differences in the components that make up the separate current supplies result in some variation in the trip levels. In addition, there is a variation in trip level with current supply temperature. The total deviation might be $\pm$0.4V. For the situation described in the question, the reasonable implication is that the scram condition in only one channel arises from a spurious signal. If a high flux actually existed, the three remaining active channels would detect it, the output would be 5.4V, and a scram would be initiated.

How is the operator alerted to open circuit faults and short circuit faults in the safety system?

Each channel of the safety system can be tested, without a scram, to

determine that it is functioning properly. For the test a current is fed to the electrometer circuit through a press-to-test switch. The voltage of the logic circuit is then indicated by a meter on the front panel of the safety system. In addition, a selector switch and voltmeter on the front panel of the safety system permit all power supplies within the system to be checked. The above tests are performed periodically to determine if the safety system is behaving normally.

Question 42 Pages 11-34 and 35. Since interlocks 3 and 4 are not required when the log power exceeds 10W as stated in Table 11.2.2.1, interlock contact "5" should parallel interlock contacts 3 as well as 4 as shown in Figure 11.2.2.1.

No. Paralleling interlock 5 with 3 and 4 does not increase safety. The wiring of contact 5 in the present design minimizes the chance of the log count rate meters being left in the "Calibrate" position. The log count rate channels are required to monitor the reactor when it is shut down.

Question 43 Page 11-36, items 1 and 3. The reasons for providing the automatic scram and rundown functions listed should be outlined here and reference should be made to the reasons for selecting these (and not selecting others).

The automatic scram is provided to shut the reactor down immediately on the occurrence of a high flux level in the reactor or of any intolerable fault in the nuclear safety system.

The automatic rundown is provided to shut the reactor down in an orderly manner on the occurrence of a condition that might damage the reactor or coolant systems if the reactor were to continue to operate.

These functions were selected after detailed analyses were made of the effects of out-of-limit conditions on the various systems. Some of these analyses are discussed in Sec. 5.2.1 and Chapter 16.

Question 44 Page 11-42. Is there a high pressure trip on the reactor? If not, why not?

There is no reactor trip or shutdown signal from the primary loop pressure relief system. The primary loop pressure is automatically reduced when it reaches 505 psia, well within the design pressure of 550 psia. When the primary loop pressure relief system trips, an annunciator warns the reactor operator who then monitors primary loop pressure to confirm that it is decreasing. If primary loop pressure is not automatically relieved, the operator shuts down the reactor.

Question 45 Page 11-44. Although the final control relays are wired in a two out of three configuration, the failure of two or more transistors (Q_3) could result in a "no scram" condition. This situation would remain unless circuit tests are performed to confirm their (Q_3) operability and malfunctions repaired as they occur. What testing program, if any, is planned in this regard?

Each system has a calibrator that will permit the trip level and the output relay of each channel to be checked. Each channel will be tested separately, with a press-to-test button, once per day initially and thereafter, on a schedule based on operating experience.

Question 46 Page 14-6. At what radiation levels and air contamination levels do the emergency procedures call for building and control room evacuation? If evacuation of the entire building is not called for, what maximum radiation levels and air contamination levels are anticipated in any area expected to be habitable after the MCA? How were these levels calculated? Was consideration given to leakage of fission products from the containment to the control room through the electrical cables?

It is a LASL policy to limit personnel radiation exposure to as low a level as possible. Upper limits on exposure rates and air contamination levels depend on circumstances. It is the responsibility of the person

in charge of the site to decide on the course of action. The advice of Health Physics Division personnel is available at all times. The guide lines listed below are followed:

1. Personnel should not be allowed to remain in areas where the exposure rate is above 100 mR/h or the air contamination is 10 times the MPC. In general, when either of these limits is exceeded, all unnecessary personnel shall be evacuated from the facility. Only the few people whose presence is required to prevent further damage to the facility or to prevent release of radioactivity, shall be allowed to remain.

2. If the air contamination level is > 10 times the MPC, all exposed personnel shall wear full face respirators.

3. If the exposure rate is greater than 100 mR/h, close health physics supervision shall be used to ensure that no one receives a dose in excess of the 3 rem per quarter limit.

4. As set forth in AEC Manual Appendix 0524, Part III: "When the person in charge of emergency action onsite deems it essential to reduce a hazard potential to acceptable levels or to prevent a substantial loss of property, a planned exposure up to but not to exceed 12 rem for the year or 5 (N-18), whichever is more limiting, may be received by individuals participating in the operation. However, the person in charge of emergency action at the incident may elect under special circumstances to waive limits and permit volunteers to receive an exposure up to but not to exceed 25 rem". Even this is not limiting if a hazard to life or public safety is involved.

As stated in Sec. 13.4, the control room is designated as a refuge for operating personnel. The shielding is designed to limit dose rate in the control room to about normal working tolerance in the event of a major accident, such as the rupture of the primary coolant system and consequent release of fission products to the secondary containment. Protection from air-borne contamination is provided in the control room by an independent ventilation system described on page 12-12. Leakage paths through cables

running from secondary containment to control room are closed by cable sealing techniques discussed in the answer to Question 21.

Question 47 Page 15-4, Rule 3. What is meant by "critical operations"?

The term "critical operations" applies to all circumstances in which the reactor is in a critical (or supercritical) state, i.e., with $k_{eff} \geq 1$. By implication, Rule 3 would also require that two plug rods be available for scramming in approach-to-critical operations even though $k_{eff} < 1$.

Question 48 Page 16-5. Can an accidental drop of a shielding block onto the reactor vessel be ruled out completely? If not, what are the possible consequences?

There is no foreseeable reason for disturbing the shielding blocks above the reactor vessel after the commencement of critical operations. These particular blocks were made "removable" primarily to facilitate installation of reactor components. However, if the necessity arises for their removal, the reactor will be shut down and depressurized.

Since the control rod drives protrude above the shielding blocks, they are vulnerable to accidental damage that could render them inoperative. Consequently, shielding blocks (or other massive objects) will not be lifted or handled at any time when inadvertent contact with the control rod drives might jeopardize reactor safety.

Question 49 Page 16-11. Discuss the possibility and consequences of a primary loop blower shutdown and restart in a few seconds with no reactor scram. Assume the operator accomplishes some rod withdrawal or bypass valve adjustment in his efforts to hold reactor temperature constant.

The primary loop blower shuts down automatically in the following circumstances:

1. Power failure,

2. Blower failure, as detected by the loss of primary coolant flow safety circuit, or

3. Run down of reactor plug rods.

In each of these three cases the blower power is shut off and the reactor rods run in automatically. The blower cannot restart automatically, and it cannot be started manually until several safety circuit trips are reset. Reactor restart is carefully controlled by administrative procedures and is not initiated until reasons for shutdown have been determined, and plans for restart are made. In any case, restart cannot be initiated in less than a few minutes after blower shutdown.

The general problem of hot restart of the reactor has been studied.[3] It has been shown that hot restart is safe even if the operator does not manipulate rods or the bypass valve. However, some rod manipulation is planned to moderate the maximum power on restart.

Question 50 Figure 16.2.2.1. What would be the temperature versus time response of the reactor vessel wall after a loss of coolant flow accident? What portions of the reactor vessel internals are included in "Avg. Reactor Solid Temp."? What is the heat conductivity for the various forms of graphite used in the reactor vessel?

The time-temperature response of the vessel wall was calculated with the aid of a heat conduction computer code in spherical geometry. The response is shown in Fig. 1.5.

Only the core moderator and fuel are included in the "Avg. Reactor Solid Temp".

The conductivities are given on page 4-82.

---

[3]H. B. Demuth, K. H. Duerre, F. P. Schilling, and C. E. Stiles, "System Dynamics Study for the Ultra High Temperature Reactor Experiment," Los Alamos Scientific Laboratory Report LA-3561, August 30, 1966, pp. 5-32 to 5-39.

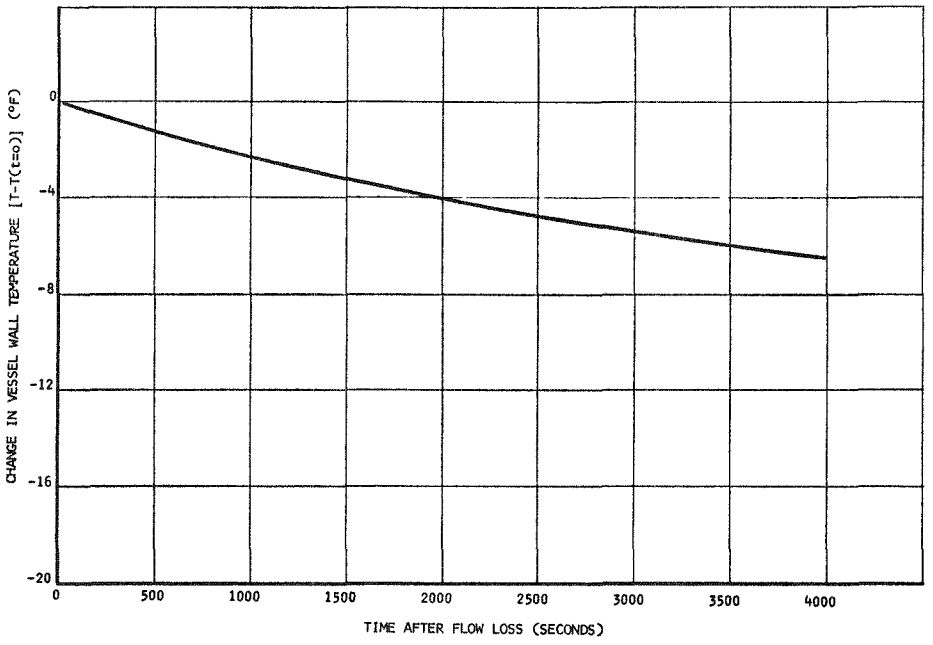

Fig. I.5 Response of reactor vessel wall temperature to loss of coolant flow accident

Question 51 Pages 16-10 to 16 consider the effects of several failures, such as blower shutdown. In each case detection and corrective action is accomplished before serious consequences result. What are the "second line of defense" detection means and corrective actions for these events, and what consequences, if any, would result from failure of the "first line" protection?

The effects of failures that have serious consequences are detected by safety systems that are defined here as "first line" defenses. "Second line defenses" or secondary indications that are available to the reactor operator are listed in Table I.3. In many cases these secondary indications warn the operator and allow him to take corrective action before a safety system is tripped. The third column in the table lists the responses that the operator would make if a system parameter exceeded its

TABLE I.3

BACKUPS FOR SAFETY SYSTEMS

Safety System	Sources of Secondary Indications	Operator Response
High Power Scram	1. 2 log meters on console 2. 2 linear power meters on console 3. Annunciator drop through computer	Initiate manual scram
Primary Loop Loss of Coolant	1. Primary loop pressure meter on console 2. Primary-secondary ΔP meter on console 3. Alarm typewriter message, pressures out-of limits 4. Annunciator drop tripped by pressure transducers 5. Annunciator drop through computer 6. Area monitor indication of activity in secondary containment, followed by annunciator drop 7. Alarm typewriter message, above normal secondary containment pressure	Initiate auto rundown Close secondary containment bleed fan valves Close cleanup system inlet and outlet valves
Secondary Loop Loss of Coolant	1. Secondary loop pressure meter on console 2. Primary-secondary ΔP meter on console 3. Alarm typewriter message, pressure out-of-limits 4. Annunciator drop tripped by pressure transducers 5. Annunciator drop through computer	Initiate auto rundown Operate isolation valves close button on panel 14 Stop secondary loop blower at panel 16

TABLE I.3 (Continued)

Safety System	Sources of Secondary Indications	Operator Response
Primary Loop Coolant Flow	1. Blower speed and flow meters on console 2. Alarm typewriter message, low flow level 3. Annunciator drop through computer 4. Decrease in power on console meters, followed by annunciator and alarm typewriter message	Initiate auto rundown
Secondary Loop	1. Blower speed and flow meters on console 2. Alarm typewriter message, low flow level 3. Annunciator drop through computer 4. Heat exchanger outlet temperature meter on console 5. Annunciator drop tripped by T_{xho} transducer 6. Trip in high heat exchanger tube temperature safety system	Initiate auto rundown Stop secondary blower at panel 16
Reactor Inlet Pipe Temperature	1. Annunciator drop tripped by any of 3 thermocouple outputs 2. Alarm typewriter message and annunciator drop tripped by any of 4 thermocouples through computer	Initiate auto rundown
Heat Exchanger Tube Temperature Monitor	1. Annunciator drop tripped by thermocouple signal of high inlet blower temperature 2. Annunciator drop, high blower temperature, through computer 3. Annunciator drop, tripped by any of 3 thermocouple signals of high tube temperature	Initiate auto rundown

TABLE I.3 (Continued)

Safety System	Sources of Secondary Indications	Operator Response
Primary Loop Pressure Relief	1. Primary loop pressure meter on console	Initiate manual vent
	2. Secondary loop pressure meter on console	
	3. Alarm typewriter message, high pressure limit exceeded	
	4. Annunciator drop tripped by pressure transducer	
Secondary Loop Pressure Relief	1. Secondary loop pressure meter on console	Initiate manual vent
	2. Primary-secondary ΔP meter on console	
	3. Alarm typewriter message, high pressure limit exceeded	
	4. Annunciator drop tripped by pressure transducer	
Heat Dump Air Flow	1. Alarm typewriter message, exit air temperature out-of-limits	Initiate auto rundown
	2. Annunciator drop tripped by blower inlet temperature transducer	
	3. Annunciator drop, high blower temperature, through computer	
	4. Secondary loop temperature meter on console	

trip point and the corresponding safety system failed to take automatic corrective action. The consequences of failure of the "first line" protection are described in detail in Secs. 16.2.2-16.2.4.

Question 52 The following statement is made on page 16-21: "The only adverse effect of a slightly delayed shutdown would be a deferment of the primary blower coast down period which might lead to a small increase in the amount of air introduced into the core."

a. How long a delay could be tolerated before this increase in air introduction into the core would be significant?

The blower could continue to run for 50 sec before a 1% increase in oxidation would occur. However, within 1 sec after rupture, the primary loop loss of coolant emergency system shuts down the blower. This system is backed up, 2.5 sec later, by the primary loop coolant flow monitor which detects the loss of flow and shuts down the blower. Both safety systems are backed up by annunciators, an alarm typewriter, and meter indications which warn the operator to take action. Therefore, it is highly unlikely that the blower could continue to operate more than a few seconds after rupture.

b. How much of an increase of the air in the core coming about either from a delayed shutdown of the primary blower or by a much larger leak in the primary system could be tolerated before "runaway oxidation" of the core graphite would take place, assuming such a limit exists?

Runaway oxidation of the core graphite would not take place. The maximum flow of air that the blower can circulate through the core is about 3200 lb/h. At this flow rate, 615 kW of heat would be generated by oxidation and 550 kW would be removed by the forced convection of the air and combustion products. Decay heat would add another 110 kW, but the heat leak from the reactor by conduction and radiation would be 180 kW.

Therefore, there would be a net flow of heat out of the reactor, the core would cool, and combustion would cease.

Question 53 Section 16. There is no indication in this particular section of how sensitive the accident condition is to various parameters in the analysis.

a. To what extent will an increase of rupture size change the conclusions?

An increase of rupture size has no effect on the conclusions because flow out of the primary loop is restricted by the flow impedance of the loop not of the hole.

b. To what extent will a delayed shutdown of the blower change the conclusions?

See the answer to question 52a.

c. To what extent would reaction of the graphite have to occur (and over what time period) in order that the pressure in the system could significantly deviate from the curve presented in Figure 16.3.1.2?

The only method of significantly changing the pressure curve in Fig. 16.3.1.2 would be to continue forced air circulation, producing carbon monoxide at the rate of 45 moles/h. The worst condition would arise if forced convection were continued for about 150 min, when all oxygen would be consumed. Since the overall heat loss rates are about the same as the heat generation rates during this period, the air temperature would remain at 147°F. The volume of contained gas will increase by about 57 lb moles. The resulting building pressure rise, to about 4.1 psig, would be caused by the additional formation of carbon monoxide not by increased heat generation.

d. To what extent would combustion of the graphite have to take place and over what time period to cause the average temperature of the reactor core to increase above the steady state condition as presented in Figure 16.3.1.1?

The core temperature cannot increase unless the sum of all heat generation rates in the core (heat of oxidation, decay heat, and continued nuclear reaction) is greater than the rate of heat removal from the core (cooling by the air flow and conduction through the internal insulation to the vessel surface). After the nuclear reaction and forced convection from the blower are stopped, the only contributions to heat generation are the fission decay and oxidation reaction heating rates. Even under forced convection these are not enough to sustain the core temperature. (See answer to Question 52b.) As is shown in Appendix F, the natural convection flow diminishes at higher core temperatures because the increased gas viscosities have a greater effect than the decreased gas densities.

e. If the chemical reaction were to occur to an extent great enough to cause temperatures to increase, would the increase in temperature be the more catastrophic effect or would the possible increase in pressure and its decay be more critical?

See the answer to part c above for the pressure-temperature effects. If the pressure were to rise to 4.1 psig, the structure would not fail, but the leakage rate from the structure would increase in proportion to the difference between internal and external pressures.

Question 54 Appendix F. The experiment performed in the UHTREX corrosion test loop indicated that under simulated conditions of loop depressurization and introduction of air, the runaway oxidation of graphite does not occur and that fuel channels indicated an increase in temperature of about 100°F during the first 30 minutes. More detail should be given in the description of the experiment which provided data for Figure F.6.1.

a. Was the increase in temperature due only to the combustion of the graphite or was this a loop which had decay heat present?

Decay heat was simulated by a predetermined power input to the heater rod of the corrosion test loop.

b. If the oxygen level were increased in this experiment, what would be the associated temperature increase?

A temperature rise could be generated by an increase in reaction rate. The experimental evidence indicates that the reacting surfaces were in a region of gas film control, where the rate of reaction is limited by the rate at which O_2 can reach the carbon surface. Therefore, the reaction rate should increase in proportion to the increase in O_2 partial pressure. However, because air supplied the O_2, the maximum possible partial pressure of O_2 was 0.21 atm.

An increase in the air flow rate, however, does increase the reaction rate, for two reasons. First, the "film thickness" decreases, i.e., the nominal O_2 concentration of the main gas stream exists closer to the carbon surface. Second, a smaller fraction of the O_2 concentration is depleted as the gas flows through the channel, which has the effect of increasing the average O_2 partial pressure throughout the channel. By increasing the flow rate, the experiment was conducted with an excess of O_2. In the postulated reactor accident, the flow rate of air after 24 sec would be 30 lb/h. In the experiment a flow equivalent to 112 lb/h was used.

c. Was the reaction essentially uniformly distributed throughout the channel or was it preferential?

Visual examination of the rod after the experiment showed uniform loss of carbon.

d. Were the graphite walls clean or did they contain catalytic materials such as fission product barium, iron, or other metals? It is known that graphite oxidation may be quite sensitive to the presence of catalytic materials such as those mentioned.

The graphite walls were not impregnated with simulated fission products but were composed of material similar to the virgin carbon in the moderator (National Carbon Type ATJ). Simulated fission products were not used because the experimental conditions would have obscured any catalytic effects. Only when the mechanism of reaction shifts from gas film control to chemical reaction rate control, does the catalytic reaction rate become important. The temperature at which this shift occurs is probably below 1650°F for high velocity (>1700 ft/min) air and even lower for flow rates expected from natural convection.[4] If catalytic effects were to occur in the postulated reactor accident, the analyses still would be valid, because of the assumption that all of the oxygen that enters the core is consumed.

e. What was the effect of radiant heat loss on the maximum temperature reached?

The radiant heat loss from the experimental rig was sufficiently small to cause very little drop in rod temperature. To ensure a conservative experiment, the heat loss from the experimental rig was designed to be lower than that expected from a reactor channel in the event of air introduction.

---

[4]T. J. Clark, R. E. Woodley, and D. R. DeHalas, "Gas-Graphite System", Nuclear Graphite (Academic Press, New York, 1962), p. 414.

Question 55 Have the potential effects of nitrogen-carbon reactions (in the presence of whatever water vapor might be expected) been evaluated as contributing to the consequences of a primary system rupture?

An extrapolation of experimental data[5] indicates that carbon reacts in N_2 at the rate of 2.9×10^{-9} gm/cm -sec. At this rate, approximately 10^{-4} of the air oxidation rate, the formation of nitrogen-carbon reaction products would have a negligible effect. On a purely speculative basis, if it could be assumed that a nitrogen-carbon reaction were to proceed, the reaction should be endothermic and the moles of gaseous reaction products should balance the moles of gaseous reactants. The net effect would be a cooling of the reactor and no increase in secondary containment pressure.

[5]A. Maimoni, "Corrosion of Graphite by Nitrogen, A Summary of Blowpipe Data", RTN No. 205, Document Number UCID-4135, March 10, 1958.